EPRI
Electric Power
Research Institute

Keywords:
Boiling water reactor
Electrochemical corrosion potential (ECP)
Hydrogen water chemistry
Stress corrosion cracking
Vessel and internals

EPRI TR-106068
December 1995

BWR Vessel and Internals Project

Modeling Hydrogen Water Chemistry for BWR Applications—New Results (BWRVIP-13)

Prepared by
GE Nuclear Energy

Effective October 1, 2008, this report has been made publicly available in accordance with Section 734.3(b)(3) and published in accordance with Section 734.7 of the U.S. Export Administration Regulations. As a result of this publication, this report is subject to only copyright protection and does not require any license agreement from EPRI. This notice supersedes the export control restrictions and any proprietary licensed material notices embedded in the document prior to publication.

PROPRIETARY INFORMATION

NOTICE: This report contains proprietary information that is the intellectual property of BWRVIP utility members and EPRI. Accordingly, it is available only under license from EPRI and may not be reproduced or disclosed, wholly or in part, by any Licensee to any other person or organization.

REPORT SUMMARY

BWRVIP Vessel and Internals Project

Modeling Hydrogen Water Chemistry for BWR Applications—New Results (BWRVIP-13)

The Boiling Water Reactor Vessel and Internals Project (BWRVIP), formed in June 1994, is an association of utilities focused exclusively on BWR vessel and internals issues. This report, thirteenth in a series of several, provides the results of radiolysis/ECP model calculations applied to estimate H_2, O_2 and H_2O_2 concentrations and ECP as a function of feedwater hydrogen addition rate for 10 BWR plants.

INTEREST CATEGORIES

Piping, reactor, vessel & internals
Licensing and safety assessment

KEYWORDS

Boiling water reactor
Electrochemical corrosion potential (ECP)
Hydrogen water chemistry
Radiolysis modeling
Stress corrosion cracking
Vessel and internals

BACKGROUND Studies have shown a strong relationship between ECP and the occurrence of stress corrosion cracking (SCC) in BWR reactors. SCC initiation and propagation is substantially inhibited when coolant ECP is maintained below –230 mV_{SHE}. Intentional reduction of ECP by addition of hydrogen to the feedwater is a mitigation remedy that is being applied or seriously considered at a number of BWR plants. ECP varies significantly with location in reactor depending on many factors including localized coolant flow rate, radiation level and water chemistry. Knowledge of the ECP at specific component locations provides an important measure of the relative aggressiveness of the reactor coolant and the degree of SCC protection that has been achieved with hydrogen injection. Radiolysis/ECP modeling is the primary means of estimating ECP at various reactor locations for which direct measurement is impractical.

OBJECTIVE To calculate H_2, O_2 and H_2O_2 concentrations and ECP at various BWR plants and reactor regions as a function of feedwater hyrdrogen addition rate in order to determine hydrogen addition requirements for SCC mitigation.

APPROACH Complex models describing radiolysis reactions were developed to help predict H_2, O_2 and H_2O_2 levels in the BWR primary circuit. Empirical correlations describing relationships between ECP, flow rate, H_2, O_2 and H_2O_2 were also developed based on results of rotating cylinder electrode laboratory tests. Empirically developed correlations were combined with radiolysis model predictions to generate ECP estimates for the BWR primary circuit. Radiolysis/ECP calculations were performed for ten BWR plants assuming feedwater hydrogen addition rates ranging from 0 to 3.0 ppm.

RESULTS Results show that the reduction of O_2 and H_2O_2 in response to H_2 addition is dependent on the region in the BWR circuit and the location within the region. ECP calculations for various reactor regions showed the amount of H_2 needed to reduce ECP below –230 mV_{SHE} also varied with reactor region and BWR plant.

Model calculations showed H_2 required to achieve SCC protection ranged from 0.35 to 1.8 ppm for recirculation system piping, and from 0.7 to 2.2 ppm for the reactor pressure vessel bottom. The amount of H_2 required for ECP reduction in the jet pump region varied from 0.8 to 2.2 ppm near the jet pump outlet to very high

levels ranging from 1.5 to 3.0 ppm at the jet pump inlet. The amount of H_2 required to achieve ECP <–230 mV_{SHE} at the shroud support to vessel weld region was 0.3 to 0.4 ppm. Higher H_2 addition levels were needed at the upper regions of the core bypass and outer bypass as compared with the lower regions near the bottom of the active fuel. ECP<–230 mV_{SHE} was achieved with 0.3 to 1.0 ppm feedwater H_2 addition in the upper regions of the core and outer bypass, whereas 1.0 to 2.0 ppm was needed for protection of the lower core and outer bypass regions. Results showed that ECP was not reduced below –230 mV_{SHE} in the in channel, mixing plenum, steam separator, upper plenum and upper downcomer regions for H_2 addition rates up to 3 ppm.

EPRI PERSPECTIVE This study, a continuation and expansion of previous work, has provided additional insight into the chemistry of the primary BWR system. Improvements and additions to radiolysis and ECP models have enabled more reliable calculations of H_2, O_2 and H_2O_2 concentrations and ECP levels throughout the BWR primary circuit. The results of this 10-plant study are useful for estimating feedwater H_2 addition requirements for SCC mitigation at various BWR plants and reactor regions. However, utilization of more accurate plant specific dose profiles that reflect varying conditions that occur during an operating cycle would yield additional useful information about how H_2 addition requirements vary with reactor operating state point. Continuing BWRVIP Mitigation Committee work on the development and application of cost effective dose estimation capabilities and model benchmarking with in-reactor measurements will enable more accurate estimation of H_2 addition requirements for SCC mitigation.

PROJECT
RPB401
EPRI Project Manager: K. Ramp
Nuclear Power Group
Contractor: GE Nuclear Energy

For ordering information about this report, call the EPRI Distribution Center (510) 934-4212.

For membership information, call (415) 855-2514.

BWR Vessel and Internals Project

Modeling Hydrogen Water Chemistry for BWR Applications - New Results (BWRVIP-13)

TR-106068
Research Project B401

Final Report, December,1995

Prepared by

GE NUCLEAR ENERGY

Prepared for

BOILING WATER REACTOR VESSEL & INTERNALS PROJECT and
ELECTRIC POWER RESEARCH INSTITUTE
3412 Hillview Ave.
Palo Alto, California 94304

DISCLAIMER OF WARRANTIES AND LIMITATION OF LIABILITIES
This report was prepared by the organization(s) named below as an account of work sponsored or cosponsored by the BWR Vessel and Internals Project (BWRVIP) and the Electric Power Research Institute, Inc. (EPRI). Neither BWRVIP, EPRI, any member of EPRI, any cosponsor, the organization(s) named below, nor any person acting on behalf of any of them:

(a) makes any warranty or representation whatsoever, express or implied, (i) with respect to the use of any information, apparatus, method, process or similar item disclosed in this report, including mechantability and fitness for a particular purpose, or (ii) that such use does not infringe on or interfere with privately owned rights, including any party's intellectual property, or (iii) that this report is suitable to any particular user's circumstance, or

(b) assumes any responsibility for any damages or other liability whatsoever (including any consequential damages, even if BWRVIP, EPRI or any EPRI representative has been advised of the possibility of such damages) resulting from your selection or use of this report or any information, apparatus, method, process or similar item disclosed in this report.
Organization(s) that prepared this report:

GE NUCLEAR ENERGY

EPRI (Appendix A)

ORDERING INFORMATION

Requests for copies of this report should be directed to the BWRVIP Program Manager, 3412 Hillview Ave., Palo Alto, Ca. 94304, (415) 855-2340.

ABSTRACT

Radiolysis and ECP calculations were performed for ten BWR plants assuming feedwater hydrogen addition rates ranging from 0 to 3.0 ppm. Concentrations of H_2, O_2 and H_2O_2 and ECP levels were estimated for ten reactor regions at each BWR modeled. Calculations were made using Version 4 of the GE-Harwell radiolysis model and ECP correlations empirically derived based on EPRI-sponsored rotating cylinder electrode studies.

Results showed that the reduction of O_2 and H_2O_2 concentrations and ECP levels in response to hydrogen addition is dependent on reactor region and location within the region. Comparison of available measured recirculation and steam line hydrogen and oxygen concentrations with radiolysis model calculation results showed reasonable agreement.

ACKNOWLEDGMENTS

The important contributions by Drs. W.G. Burns and J. Henshaw (AEA, Harwell) to the development of the computer radiolysis simulation model, and the ECP measurements of Dr. Y.J. Kim (GE CRD), are gratefully acknowledged by the authors.

Credit is given to R.N. Robinson for his involvement in the early stages of model development.

The work of G. E. Petersen, S.J. Bellows and M.J. Wood in the compilation of input data for the model is sincerely appreciated. Dr. M.E. Indig has provided useful suggestions.

The authors are pleased to acknowledge the support and encouragement in the course of this study of. K.S. Ramp (EPRI), Dr. R.L. Cowan and Dr. R.M. Horn, and the help of D.G. Crawford, C.B. Kincaid and David E. Delwiche in the preparation of this report.

EPRI-sponsored GE/Harwell radiolysis modeling work was started at GE Nuclear Energy under the supervision of Dr. Carl P. Ruiz. Although his premature death in July 1993 prevented him from seeing it through to completion, Dr. Ruiz's expertise and dedication to his work earned him respect and recognition at GE Nuclear Energy and throughout the industry. This report is dedicated to his memory.

TABLE OF CONTENTS

Section			Page
Summary			**1**
Introduction			**5**
2	**Model Description**		**9**
	2.1	Radiolysis Model	9
	2.2	Input Data	13
		2.2.1 G Values of Radiolytic Products	14
		2.2.2 Reaction Rate Constants	14
		2.2.3 Reactor Specific Data	16
		2.2.4 Radiation Dose Profiles	16
3	**Results and Discussion**		**21**
	3.1	Radiolysis Model	21
		3.1.1 Channel Region	22
		3.1.2 Core Bypass Region	22
		3.1.3 Outer Bypass Region	23
		3.1.4 Upper Plenum Region	23
		3.1.5 Steam Separator Region	24
		3.1.6 Mixing Plenum Region	24
		3.1.7 Downcomer Region	25
		3.1.8 Recirculation Region	25
		3.1.9 Jet Pump Region	26
		3.1.10 Lower Plenum Region	23
	3.2	Comparison of Measured and Calculated Values	26
4	**Chemistry in the Modified LPRMs**		**79**
	4.1	LPRM Model	79
	4.2	Effect of Flow Rate and Feedwater H_2 on LPRM Chemistry and ECP Sensors	80
	4.3	Differences in Concentrations and ECP Inside and Outside LPRM	81

TABLE OF CONTENTS (continued)

Section		Page
5	**Calculation of ECP Values**	**125**
5.1	Development of ECP Models	125
5.2	Calculated ECP Values	126
6	**Conclusions**	**132**
6.1	Conclusions	132
6.1.1	Modified LPRMs	132
6.1.2	ECP Calculations	133
7	**Future Work**	**134**
7.1	Projected Developments	134
7.2	ECP Correlation Upgrade	134
7.3	Effect of Copper Impurities	134
7.4	Radiation Fields	134
7.5	Liquid/Gas Transport	134
7.6	Velocity Mapping	134
7.7	Sensitivity Studies	135
7.8	Two Dimensional Modeling	135
8	**References**	**136**

Appendix A: Model results for ten BWRs represented as charts depicting ECP, H_2, O_2 and H_2O_2 concentrations as a function of feedwater H_2 addition and vessel region length fraction (EPRI-generated charts based on GE supplied model calculation results)

A-1 In-Channel Region ECPs at 0.5 Length Fraction

A-2 Core Bypass Region ECPs at 0.5 Length Fraction

A-3 Outer Bypass Region ECPs at 0.5 Length Fraction

A-4 Upper Plenum Region ECPs at 0.5 Length Fraction

A-5 Steam Separator Region ECPs at 0.5 Length Fraction

A-6 Mixing Plenum Region ECPs at 0.5 Length Fraction

A-7 Downcomer Region ECPs at 0.5 Length Fraction

TABLE OF CONTENTS (continued)

A-8 Recirculation Region ECPs at 0.5 Length Fraction

A-9 Jet Pump Region ECPs at 0.5 Length Fraction

A-10 Lower Plenum Region ECPs at 0.5 Length Fraction

A-11 In-Channel Region ECPs with 0 ppm Feedwater H_2 Addition

A-12 In-Channel Region ECPs with 0.6 ppm Feedwater H_2 Addition

A-13 In-Channel Region ECPs with 1.5 ppm Feedwater H_2 Addition

A-14 In-Channel Region ECPs with 3.0 ppm Feedwater H_2 Addition

A-15 In-Channel Hydrogen Levels with 0 ppm Feedwater H_2 Addition

A-16 In-Channel Hydrogen Levels with 0.6 ppm Feedwater H_2 Addition

A-17 In-Channel Hydrogen Levels with 1.5 ppm Feedwater H_2 Addition

A-18 In-Channel Hydrogen Levels with 3.0 ppm Feedwater H_2 Addition

A-19 In-Channel Oxygen Levels with 0 ppm Feedwater H_2 Addition

A-20 In-Channel Oxygen Levels with 0.6 ppm Feedwater H_2 Addition

A-21 In-Channel Oxygen Levels with 1.5 ppm Feedwater H_2 Addition

A-22 In-Channel Oxygen Levels with 3.0 ppm Feedwater H_2 Addition

A-23 In-Channel Peroxide Levels with 0 ppm Feedwater H_2 Addition

A-24 In-Channel Peroxide Levels with 0.6 ppm Feedwater H_2 Addition

A-25 In-Channel Peroxide Levels with 1.5 ppm Feedwater H_2 Addition

A-26 In-Channel Peroxide Levels with 3.0 ppm Feedwater H_2 Addition

A-27 Core Bypass Region ECPs with 0 ppm Feedwater H_2 Addition

A-28 Core Bypass Region ECPs with 0.6 ppm Feedwater H_2 Addition

A-29 Core Bypass Region ECPs with 1.5 ppm Feedwater H_2 Addition

A-30 Core Bypass Region ECPs with 3.0 ppm Feedwater H_2 Addition

A-31 Core Bypass Hydrogen Levels with 0 ppm Feedwater H_2 Addition

A-32 Core Bypass Hydrogen Levels with 0.6 ppm Feedwater H_2 Addition

A-33 Core Bypass Hydrogen Levels with 1.5 ppm Feedwater H_2 Addition

A-34 Core Bypass Hydrogen Levels with 3.0 ppm Feedwater H_2 Addition

A-35 Core Bypass Oxygen Levels with 0 ppm Feedwater H_2 Addition

TABLE OF CONTENTS (continued)

A-36 Core Bypass Oxygen Levels with 0.6 ppm Feedwater H_2
A-37 Core Bypass Peroxide Levels with 0 ppm Feedwater H_2 Addition
A-38 Core Bypass Peroxide Levels with 0.6 ppm Feedwater H_2 Addition
A-39 Core Bypass Peroxide Levels with 1.5 ppm Feedwater H_2 Addition
A-40 Core Bypass Peroxide Levels with 3.0 ppm Feedwater H_2 Addition
A-41 Outer Bypass Region ECPs with 0 ppm Feedwater H_2 Addition
A-42 Outer Bypass Region ECPs with 0.6 ppm Feedwater H_2 Addition
A-43 Outer Bypass Region ECPs with 1.5 ppm Feedwater H_2 Addition
A-44 Outer Bypass Region ECPs with 3.0 ppm Feedwater H_2 Addition
A-45 Outer Bypass Hydrogen Levels with 0 ppm Feedwater H_2 Addition
A-46 Outer Bypass Hydrogen Levels with 0.6 ppm Feedwater H_2 Addition
A-47 Outer Bypass Hydrogen Levels with 1.5 ppm Feedwater H_2 Addition
A-48 Outer Bypass Hydrogen Levels with 3.0 ppm Feedwater H_2 Addition
A-49 Outer Bypass Oxygen Levels with 0 ppm Feedwater H_2 Addition
A-50 Outer Bypass Oxygen Levels with 0.4 ppm Feedwater H_2 Addition
A-51 Outer Bypass Peroxide Levels with 0 ppm Feedwater H_2 Addition
A-52 Outer Bypass Peroxide Levels with 0.6 ppm Feedwater H_2 Addition
A-53 Outer Bypass Peroxide Levels with 1.5 ppm Feedwater H_2 Addition
A-54 Outer Bypass Peroxide Levels with 3.0 ppm Feedwater H_2 Addition
A-55 Upper Plenum Region ECPs with 0 ppm Feedwater H_2 Addition
A-56 Upper Plenum Region ECPs with 0.6 ppm Feedwater H_2 Addition
A-57 Upper Plenum Region ECPs with 1.5 ppm Feedwater H_2 Addition
A-58 Upper Plenum Region ECPs with 3.0 ppm Feedwater H_2 Addition
A-59 Upper Plenum Hydrogen Levels with 0 ppm Feedwater H_2 Addition
A-60 Upper Plenum Hydrogen Levels with 0.6 ppm Feedwater H_2 Addition
A-61 Upper Plenum Hydrogen Levels with 1.5 ppm Feedwater H_2 Addition
A-62 Upper Plenum Hydrogen Levels with 3.0 ppm Feedwater H_2 Addition
A-63 Upper Plenum Oxygen Levels with 0 ppm Feedwater H_2 Addition

TABLE OF CONTENTS (continued)

A-64 Upper Plenum Oxygen Levels with 0.6 ppm Feedwater H_2 Addition
A-65 Upper Plenum Oxygen Levels with 1.5 ppm Feedwater H_2 Addition
A-66 Upper Plenum Oxygen Levels with 3.0 ppm Feedwater H_2 Addition
A-67 Upper Plenum Peroxide Levels with 0 ppm Feedwater H_2 Addition
A-68 Upper Plenum Peroxide Levels with 0.6 ppm Feedwater H_2 Addition
A-69 Upper Plenum Peroxide Levels with 1.5 ppm Feedwater H_2 Addition
A-70 Upper Plenum Peroxide Levels with 3.0 ppm Feedwater H_2 Addition
A-71 Steam Separator Region ECPs with 0 ppm Feedwater H_2 Addition
A-72 Steam Separator Region ECPs with 0.6 ppm Feedwater H_2 Addition
A-73 Steam Separator Region ECPs with 1.5 ppm Feedwater H_2 Addition
A-74 Steam Separator Region ECPs with 3.0 ppm Feedwater H_2 Addition
A-75 Steam Separator H_2 Levels with 0 ppm Feedwater H_2 Addition
A-76 Steam Separator H_2 Levels with 0.6 ppm feedwater H_2 Addition
A-77 Steam Separator H_2 Levels with 1.5 ppm Feedwater H_2 Addition
A-78 Steam Separator H_2 Levels with 3.0 ppm Feedwater H_2 Addition
A-79 Steam Separator 0_2 Levels with 0 ppm Feedwater H_2 Addition
A-80 Steam Sparator 0_2 Levels with 0.6 ppm Feedwater H_2 Addition
A-81 Steam Separator 0_2 Levels with 1.5 ppm Feedwater H_2 Addition
A-82 Steam Separator 0_2 Levels with 3.0 ppm Feedwater H_2 Addition
A-83 Steam Separator H_20_2 Levels with 0 ppm Feedwater H_2 Addition
A-84 Steam Separator H_20_2 Levels with 0.6 ppm Feedwater H_2 Addition
A-85 Steam Separator H_20_2 Levels with 1.5 ppm Feedwater H_2 Addition
A-86 Steam Separator H_20_2 Levels with 3.0 ppm Feedwater H_2 Addition
A-87 Mixing Plenum Region ECPs with 0 ppm Feedwater H_2 Addition
A-88 Mixing Plenum Region ECPs with 0.6 ppm Feedwater H_2 Addition
A-89 Mixing Plenum Region ECPs with 1.5 ppm Feedwater H_2 Addition
A-90 Mixing Plenum Region ECPs with 3.0 ppm Feedwater H_2 Addition
A-91 Mixing Plenum Hydrogen Levels with 0 ppm Feedwater H_2 Addition

TABLE OF CONTENTS (continued)

A-92 Mixing Plenum Hydrogen Levels with 0.6 ppm Feedwater H_2 Addition
A-93 Mixing Plenum Hydrogen Levels with 1.5 ppm Feedwater H_2 Addition
A-94 Mixing Plenum Hydrogen Levels with 3.0 ppm Feedwater H_2 Addition
A-95 Mixing Plenum Oxygen Levels with 0 ppm Feedwater H_2 Addition
A-96 Mixing Plenum Oxygen Levels with 0.6 ppm Feedwater H_2 Addition
A-97 Mixing Plenum Oxygen Levels with 1.5 ppm Feedwater H_2 Addition
A-98 Mixing Plenum Oxygen Levels with 3.0 ppm Feedwater H_2 Addition
A-99 Mixing Plenum Peroxide Levels with 0 ppm Feedwater H_2 Addition
A-100 Mixing Plenum Peroxide Levels with 0.6 ppm Feedwater H_2 Addition
A-101 Mixing Plenum Peroxide Levels with 1.5 ppm Feedwater H_2 Addition
A-102 Mixing Plenum Peroxide Levels with 3.0 ppm Feedwater H_2 Addition
A-103 Downcomer Region ECPs with 0 ppm Feedwater H_2 Addition
A-104 Downcomer Region ECPs with 0.6 ppm Feedwater H_2 Addition
A-105 Downcomer Region ECPs with 1.5 ppm Feedwater H_2 Addition
A-106 Downcomer Region ECPs with 3.0 ppm Feedwater H_2 Addition
A-107 Downcomer Hydrogen Levels with 0 ppm Feedwater H_2 Addition
A-108 Downcomer Hydrogen Levels with 0.6 ppm Feedwater H_2 Addition
A-109 Downcomer Hydrogen Levels with 1.5 ppm Feedwater H_2 Addition
A-110 Downcomer Hydrogen Levels with 3.0 ppm Feedwater H_2 Addition
A-111 Downcomer Oxygen Levels with 0 ppm Feedwater H_2 Addition
A-112 Downcomer Oxygen Levels with 0.6 ppm Feedwater H_2 Addition
A-113 Downcomer Oxygen Levels with 1.5 ppm Feedwater H_2 Addition
A-114 Downcomer Oxygen Levels with 3.0 ppm Feedwater H_2 Addition
A-115 Downcomer Peroxide Levels with 0 ppm Feedwater H_2 Addition
A-116 Downcomer Peroxide Levels with 0.6 ppm Feedwater H_2 Addition
A-117 Downcomer Peroxide Levels with 1.5 ppm Feedwater H_2 Addition
A-118 Downcomer Peroxide Levels with 3.0 ppm Feedwater H_2 Addition
A-119 Recirculation System ECPs with 0 ppm Feedwater H_2 Addition

TABLE OF CONTENTS (continued)

A-120 Recirculation System ECPs with 0.6 ppm Feedwater H_2 Addition
A-121 Recirculation System ECPs with 1.5 ppm Feedwater H_2 Addition
A-122 Recirculation System ECPs with 3.0 ppm Feedwater H_2 Addition
A-123 Recirculation System H_2 Levels with 0 ppm Feedwater H_2 Addition
A-124 Recirculation System H_2 Levels with 0.6 ppm Feedwater H_2 Addition
A-125 Recirculation System H_2 Levels with 1.5 ppm Feedwater H_2 Addition
A-126 Recirculation System H_2 Levels with 3.0 ppm Feedwater H_2 Addition
A-127 Recirculation System 0_2 Levels with 0 ppm Feedwater H_2 Addition
A-128 Recirculation System 0_2 levels with 0.6 ppm Feedwater H_2 Addition
A-129 Recirculation System 0_2 Levels with 1.5 ppm Feedwater H_2 Addition
A-130 Recirculation System H_20_2 Levels with 0 ppm Feedwater H_2 Addition
A-131 Recirculation System H_20_2 Levels with 0.6 ppm Feedwater H_2 Addition
A-132 Recirculation System H_20_2 Levels with 1.5 ppm Feedwater H_2 Addition
A-133 Recirculation System H_20_2 Levels with 3.0 ppm Feedwater H_2 Addition
A-134 Jet Pump Region ECP Levels with 0 ppm Feedwater H_2 Addition
A-135 Jet Pump Region ECP Levels with 0.6 ppm Feedwater H_2 Addition
A-136 Jet Pump Region ECP Levels with 1.5 ppm Feedwater H_2 Addition
A-137 Jet Pump Region ECP Levels with 3.0 ppm Feedwater H_2 Addition
A-138 Jet Pump Region Hydrogen Levels with 0 ppm Feedwater H_2 Addition
A-139 Jet Pump Region Hydrogen Levels with 0.6 ppm Feedwater H_2 Addition
A-140 Jet Pump Region Hydrogen Levels with 1.5 ppm Feedwater H_2 Addition
A-141 Jet Pump Region Hydrogen Levels with 3.0 ppm Feedwater H_2 Addition
A-142 Jet Pump Region Oxygen Levels with 0 ppm Feedwater H_2 Addition
A-143 Jet Pump Region Oxygen Levels with 0.6 ppm Feedwater H_2 Addition
A-144 Jet Pump Region Oxygen levels with 1.5 ppm Feedwater H_2 Addition
A-145 Jet Pump Region Peroxide Levels with 0 ppm Feedwater H_2 Addition
A-146 Jet Pump Region Peroxide Levels with 0.6 ppm Feedwater H_2 Addition
A-147 Jet Pump Region Peroxide Levels with 1.5 ppm Feedwater H_2 Addition

TABLE OF CONTENTS (continued)

A-148 Jet Pump Region Peroxide Levels with 3.0 ppm Feedwater H_2 Addition

A-149 Lower Plenum ECP Levels with 0 ppm Feedwater H_2 Addition

A-150 Lower Plenum ECP Levels with 0.6 ppm Feedwater H_2 Addition

A-151 Lower Plenum ECP Levels with 1.5 ppm Feedwater H_2 Addition

A-152 Lower Plenum ECP Levels with 3.0 ppm Feedwater H_2 Addition

A-153 Lower Plenum Hydrogen Levels with 0 ppm Feedwater H_2 Addition

A-154 Lower Plenum Hydrogen Levels with 0.6 ppm Feedwater H_2 Addition

A-155 Lower Plenum Hydrogen Levels with 1.5 ppm Feedwater H_2 Addition

A-156 Lower Plenum Hydrogen Levels with 3.0 ppm Feedwater H_2 Addition

A-157 Lower Plenum Oxygen Levels with 0 ppm Feedwater H_2 Addition

A-158 Lower Plenum Oxygen Levels with 0.6 ppm Feedwater H_2 Addition

A-159 Lower Plenum Oxygen Levels with 1.5 ppm Feedwater H_2 Addition

A-160 Lower Plenum Peroxide Levels with 0 ppm Feedwater H_2 Addition

A-161 Lower Plenum Peroxide Levels with 0.6 ppm Feedwater H_2 Addition

A-162 Lower Plenum Peroxide Levels with 1.5 ppm Feedwater H_2 Addition

A-163 Lower Plenum Peroxide Levels with 3.0 ppm Feedwater H_2 Addition

Appendix B:Computer Model Studies of Quad Cities-2 Modified LPRM

B-1 Quad Cities-2 - Effect of flow rate through LPRM on H_2 concentration at sensor 1

B-2 Quad Cities-2 - Effect of flow rate through LPRM on H_2 concentration at sensor 2

B-3 Quad Cities-2 - Effect of flow rate through LPRM on H_2 concentration at sensor 3

B-4 Quad Cities-2 - Effect of flow rate through LPRM on H_2 concentration at sensor 4

B-5 Quad Cities-2 - Effect of flow rate through LPRM onH_2 concentration at sensor 5

B-6 Quad Cities-2 - Effect of flow rate through LPRM on H_2 concentration at sensor 6

B-7 Quad Cities-2 - Effect of flow rate through LPRM on O_2 concentration at sensor 1

B-8 Quad Cities-2 - Effect of flow rate through LPRM on O_2 concentration at sensor 2

B-9 Quad Cities-2 - Effect of flow rate through LPRM on O_2 concentration at sensor 3

B-10 Quad Cities-2 - Effect of flow rate through LPRM on O_2 concentration at sensor 4

TABLE OF CONTENTS (continued)

B-11 Quad Cities-2 - Effect of flow rate through LPRM on O_2 concentration at sensor 5

B-12 Quad Cities-2 - Effect of flow rate through LPRM on O_2 concentration at sensor 6

B-13 Quad Cities-2 - Effect of flow rate through LPRM on H_2O_2 concentration at sensor 1

B-14 Quad Cities-2 - Effect of flow rate through LPRM on H_2O_2 concentration at sensor 2

B-15 Quad Cities-2 - Effect of flow rate through LPRM on H_2O_2 concentration at sensor 3

B-16 Quad Cities-2 - Effect of flow rate through LPRM on H_2O_2 concentration at sensor 4

B-17 Quad Cities-2 - Effect of flow rate through LPRM on H_2O_2 concentration at sensor 5

B-18 Quad Cities-2 - Effect of flow rate through LPRM on H_2O_2 concentration at sensor 6

B-19 Quad Cities-2 - Effect of flow rate through LPRM on ECP at sensor 1

B-20 Quad Cities-2 - Effect of flow rate through LPRM on ECP at sensor 2

B-21 Quad Cities-2 - Effect of flow rate through LPRM on ECP at sensor 3

B-22 Quad Cities-2 - Effect of flow rate through LPRM on ECP at sensor 4

B-23 Quad Cities-2 - Effect of flow rate through LPRM on ECP at sensor 5

B-24 Quad Cities-2 - Effect of flow rate through LPRM on ECP at sensor 6

B-25 Quad Cities-2 - H_2 concentration inside and outside of LPRM for normal water chemistry

B-26 Quad Cities-2 - H_2 concentration inside and outside of LPRM for 0.1 ppm H_2 in feedwater

B-27 Quad Cities-2 - H_2 concentration inside and outside of LPRM for 0.2 ppm H_2 in feedwater

B-28 Quad Cities-2 - H_2 concentration inside and outside of LPRM for 0.5 ppm H_2 in feedwater

B-29 Quad Cities-2 - H_2 concentration inside and outside of LPRM for 1.0 ppm H_2 in feedwater

B-30 Quad Cities-2 - O_2 concentration inside and outside of LPRM for normal water chemistry

B-31 Quad Cities-2 - O_2 concentration inside and outside of LPRM for 0.1 ppm H_2 in feedwater

B-32 Quad Cities-2 - O_2 concentration inside and outside of LPRM for 0.2 ppm H_2 in feedwater

B-33 Quad Cities-2 - O_2 concentration inside and outside of LPRM for 0.5 ppm H_2 in feedwater

B-34 Quad Cities-2 - O_2 concentration inside and outside of LPRM for 1.0 ppm H_2 in feedwater

B-35 Quad Cities-2 - H_2O_2 concentration inside and outside of LPRM for normal water chemistry

B-36 Quad Cities-2 - H_2O_2 concentration inside and outside of LPRM for 0.1 ppm H_2 in feedwater

B-36 Quad Cities-2 - H_2O_2 concentration inside and outside of LPRM for 0.1 ppm H_2 in feedwater

TABLE OF CONTENTS (continued)

B-37 Quad Cities-2 - H_2O_2 concentration inside and outside of LPRM for 0.2 ppm H_2 in feedwater

B-38 Quad Cities-2 - H_2O_2 concentration inside and outside of LPRM for 0.5 ppm H_2 in feedwater

B-39 Quad Cities-2 - H_2O_2 concentration inside and outside of LPRM for 1.0 ppm H_2 in feedwater

B-40 Quad Cities-2 - ECP inside and outside of LPRM for normal water chemistry

B-41 Quad Cities-2 - ECP inside and outside of LPRM for 0.1 ppm H_2 in feedwater

B-42 Quad Cities-2 - ECP inside and outside of LPRM for 0.2 ppm H_2 in feedwater

B-43 Quad Cities-2 - ECP inside and outside of LPRM for 0.5 ppm H_2 in feedwater

B-44 Quad Cities-2 - ECP inside and outside of LPRM for 1.0 ppm H_2 in feedwater

LIST OF TABLES

Table No.		Page
2-1	Correlation Between Circuit Distances, Fraction of Region Lengths and Reactor Locations	12
2-2	Plant Characteristics	13
2-3	G Values of Primary Radiolytic Species in Water Measured at 285°C	14
2-4	Reactions and Rate Constants Used in the Simulation of Water Radiolysis	15
2-5	Radiolysis Model Main Input Variables for Ten BWRs	16

LIST OF FIGURES (continued)

Figure No.		Page
2-1	Computer Model of BWR Primary System	27
2-2	Radiolysis Model Region and Circuit Identification	18
2-3	Simplified Schematic of Steam Separator	19
3-1	H_2 Concentration at Region Inlet	28
3-2	H_2 Concentration at Region Outlet	29
3-3	O_2 Concentration at Region Inlet	30
3-4	O_2 Concentration at Region Outlet	31
3-5	H_2O_2 Concentration at Region Inlet	32
3-6	H_2O_2 Concentration at Region Outlet	33
3-7	Gamma and Neutron Dose Rates in the Channel Region	34
3-8	H_2 Concentration in the Channel Region	35
3-9	O_2 Concentration in the Channel Region	36
3-10	H_2O_2 Concentration in the Channel Region	37
3-11	Gamma and Neutron Dose Rates in the Core Bypass Region	38
3-12	H_2 Concentration in the Core Bypass Region	39
3-13	O_2 Concentration in the Core Bypass Region	40
3-14	H_2O_2 Concentration in the Core Bypass Region	41
3-15	Gamma and Neutron Dose Rates in the Outer Bypass Region	42
3-16	H_2 Concentration in the Outer Bypass Region	43
3-17	O_2 Concentration in the Outer Bypass Region	44
3-18	H_2O_2 Concentration in the Outer Bypass Region	45
3-19	Gamma and Neutron Dose Rates in the Upper Plenum Region	46
3-20	H_2 Concentration in the Upper Plenum Region	47
3-21	O_2 Concentration in the Upper Plenum Region	48
3-22	H_2O_2 Concentration in the Upper Plenum Region	49
3-23	Gamma and Neutron Dose Rates in the Steam Separator Region	50

LIST OF FIGURES (continued)

Figure No.		Page
3-24	H_2 Concentration in the Steam Separator Region	51
3-25	O_2 Concentration in the Steam Separator Region	52
3-26	H_2O_2 Concentration in the Steam Separator Region	53
3-27	Gamma and Neutron Dose Rates in the Mixing Plenum Region	54
3-28	H_2 Concentration in the Mixing Plenum Region	55
3-29	O_2 Concentration in the Mixing Plenum Region	56
3-30	H_2O_2 Concentration in the Mixing Plenum Region	57
3-31	Gamma and Neutron Dose Rates in the Downcomer Region	58
3-32	H_2 Concentration in the Downcomer Region	59
3-33	O_2 Concentration in the Downcomer Region	60
3-34	H_2O_2 Concentration in the Downcomer Region	61
3-35	Gamma and Neutron Dose Rates in the Recirculation Region	62
3-36	H_2 Concentration in the Recirculation Region	63
3-37	O_2 Concentration in the Recirculation Region	64
3-38	H_2O_2 Concentration in the Recirculation Region	65
3-39	Gamma and Neutron Dose Rates in the Jet Pump Region	66
3-40	H_2 Concentration in the Jet Pump Region	67
3-41	O_2 Concentration in the Jet Pump Region	68
3-42	H_2O_2 Concentration in the Jet Pump Region	69
3-43	Gamma and Neutron Dose Rate in the Lower Plenum Region	70
3-44	H_2 Concentration in the Lower Plenum Region	71
3-45	O_2 Concentration in the Lower Plenum Region	72
3-46	H_2O_2 Concentration in the Lower Plenum Region	73
3-47	Comparison of Calculated and Measured Steam Hydrogen Concentrations	74
3-48	Comparison of Calculated and Measured Steam Oxygen Concentrations	75
3-49	Comparison of Calculated and Measured Recirculation Hydrogen Concentrations	76

LIST OF FIGURES (continued)

Figure No.		Page
3-50	Comparison of Calculated and Measured Recirculation Oxidant Concentrations	77
4-1	Fitzpatrick - Effect of Flow Rate Through LPRM on H_2 Concentration at Sensor 1	84
4-2	Fitzpatrick - Effect of Flow Rate Through LPRM on H_2 Concentration at Sensor 2	85
4-3	Fitzpatrick - Effect of Flow Rate Through LPRM on H_2 Concentration at Sensor 3	86
4-4	Fitzpatrick - Effect of Flow Rate Through LPRM on H_2 Concentration at Sensor 4	87
4-5	Fitzpatrick - Effect of Flow Rate Through LPRM on H_2 Concentration at Sensor 5	88
4-6	Fitzpatrick - Effect of Flow Rate Through LPRM on O_2 Concentration at Sensor 1	89
4-7	Fitzpatrick - Effect of Flow Rate Through LPRM on O_2 Concentration at Sensor 2	90
4-8	Fitzpatrick - Effect of Flow Rate Through LPRM on O_2 Concentration at Sensor 3	91
4-9	Fitzpatrick - Effect of Flow Rate Through LPRM on O_2 Concentration at Sensor 4	92
4-10	Fitzpatrick - Effect of Flow Rate Through LPRM on O_2 Concentration at Sensor 5	93
4-11	Fitzpatrick - Effect of Flow Rate Through LPRM on H_2O_2 Concentration at Sensor 1	94
4-12	Fitzpatrick - Effect of Flow Rate Through LPRM on H_2O_2 Concentration at Sensor 2	95
4-13	Fitzpatrick - Effect of Flow Rate Through LPRM on H_2O_2 Concentration at Sensor 3	96
4-14	Fitzpatrick - Effect of Flow Rate Through LPRM on H_2O_2 Concentration at Sensor 4	97
4-15	Fitzpatrick - Effect of Flow Rate Through LPRM on H_2O_2 Concentration at Sensor 5	98
4-16	Fitzpatrick - Effect of Flow Rate Through LPRM on ECP at Sensor 1	99
4-17	Fitzpatrick - Effect of Flow Rate Through LPRM on ECP at Sensor 2	100
4-18	Fitzpatrick - Effect of Flow Rate Through LPRM on ECP at Sensor 3	101
4-19	Fitzpatrick - Effect of Flow Rate Through LPRM on ECP at Sensor 4	102
4-20	Fitzpatrick - Effect of Flow Rate Through LPRM on ECP at Sensor 5	103
4-21	Fitzpatrick - H_2 Concentration Inside and Outside of LPRM for Normal Water Chemistry	104
4-22	Fitzpatrick - H_2 Concentration Inside and Outside of LPRM for 0.1 ppm H2 in Feedwater	105

LIST OF FIGURES (continued)

Figure No.		Page
4-23	Fitzpatrick - H_2 Concentration Inside and Outside of LPRM for 0.2 ppm H_2 in Feedwater	106
4-24	Fitzpatrick - H_2 Concentration Inside and Outside of LPRM for 0.5 ppm H_2	107
4-25	Fitzpatrick - H_2 Concentration Inside and Outside of LPRM for 1.0 ppm H_2 in Feedwater	108
4-26	Fitzpatrick - O_2 Concentration Inside and Outside of LPRM for Normal Water Chemistry	109
4-27	Fitzpatrick - O_2 Concentration Inside and Outside of LPRM for 0.1 ppm H_2 in Feedwater	110
4-28	Fitzpatrick - O_2 Concentration Inside and Outside of LPRM for 0.2 ppm H_2 in Feedwater	111
4-29	Fitzpatrick - O_2 Concentration Inside and Outside of LPRM for 0.5 ppm H_2 in Feedwater	112
4-30	Fitzpatrick - O_2 Concentration Inside and Outside of LPRM for 1.0 ppm H_2 in Feedwater	113
4-31	Fitzpatrick - H_2O_2 Concentration Inside and Outside of LPRM for Normal Water Chemistry	114
4-32	Fitzpatrick - H_2O_2 Concentration Inside and Outside of LPRM for 0.1 ppm H_2 in Feedwater	115
4-33	Fitzpatrick - H_2O_2 Concentration Inside and Outside of LPRM for 0.2 ppm H2 in Feedwater	116
4-34	Fitzpatrick - H_2O_2 Concentration Inside and Outside of LPRM for 0.5 ppm H_2 in Feedwater	117
4-35	Fitzpatrick - H_2O_2 Concentration Inside and Outside of LPRM for 1.0 ppm H_2 in Feedwater	118

LIST OF FIGURES (continued)

Figure No.		Page
4-36	Fitzpatrick - ECP Inside and Outside of LPRM for Normal Water Chemistry	119
4-37	Fitzpatrick - ECP Inside and Outside of LPRM for 0.1 ppm H_2 in Feedwater	120
4-38	Fitzpatrick - ECP Inside and Outside of LPRM for 0.2 ppm H_2 in Feedwater	121
4-39	Fitzpatrick - ECP Inside and Outside of LPRM for 0.5 ppm H_2 in Feedwater	122
4-40	Fitzpatrick - ECP Inside and Outside of LPRM for 1.0 ppm H_2 in Feedwater	123
5-1	Channel ECPs	127
5-2	Core Bypass ECPs	128
5-3	Outer Bypass ECPs	129
5-4	Upper Plenum ECPs	130
5-5	Steam Separator ECPs	131
5-6	Mixing Plenum ECPs	132
5-7	Fitzpatrick - Downcomer ECPs	133
5-8	Recirc ECPs	134
5-9	Jet Pump ECPs	135
5-10	Lower Plenum ECPs	136

SUMMARY

GE Nuclear Energy, in conjunction with UKAEA Harwell Laboratory, has been continuously developing computer simulations of radiolysis in BWRs. The results of the simulation provide calculated concentrations of hydrogen, oxygen and hydrogen peroxide in various regions of the primary circuit, and also the concentration of labile species that contribute to the radiolytic phenomena. Hydrogen, oxygen and hydrogen peroxide are the relevant species involved in the stress corrosion cracking (SCC) of austenitic stainless steels. Calculated concentrations of these species provide a basis for estimating the susceptibility to failure of reactor components, especially in areas of the reactor where direct measurements are not feasible.

Previous versions of the computer model had provided the opportunity to observe the response of oxygen and hydrogen peroxide to feedwater hydrogen addition in several regions of the BWR primary circuit. The study herein reported is extended to more reactor regions and other BWR plants. Most of these plants had undergone HWC testing or implementation. The current version of the computer code incorporates a number of modifications and improvements that provide more reliable and detailed results. In addition, the results of a separate investigation of the electrochemical potential (ECP) of Type-316 SS have been used to generate ECP values pertinent to the BWRs object of this study.

This report contains a description of the model, calculated hydrogen, oxygen and hydrogen peroxide concentrations, a comparison of the model results with experimental data available for four plants, ECP values calculated on the basis of the chemistry results, and a comparison of chemistry and ECP results calculated for two modified LPRMs containing ECP electrodes.

Results

Radiolysis model calculations were performed for ten BWRs and for the following ten feedwater hydrogen concentrations: 0.0, 0.2, 0.4, 0.6, 0.8, 1.0, 1.5, 2.0, 2.5, and 3.0 ppm. In general, the following was observed:

(a) The reduction of oxygen and hydrogen peroxide in response to hydrogen addition varies, depending on the region in the BWR circuit and the location within the region. The oxygen response is more sensitive than the hydrogen peroxide response.

(b) The concentrations of oxygen and hydrogen peroxide decrease rapidly in the reactor recirculation line with increasing feedwater hydrogen concentration. Other non-boiling regions, including the downcomer and lower plenum, also exhibit decreasing oxygen and hydrogen peroxide concentrations with increasing feedwater hydrogen concentrations.

(c) In the core regions, the decrease in the oxygen and hydrogen peroxide concentrations with increasing feedwater hydrogen concentration is slower than in the recirculation region. The decreases are apparent up to the highest feedwater hydrogen concentration modeled and occur within the channel region and in the other core regions, as well as in the upper plenum and in the mixing plenum.

Experimental measurements of hydrogen and oxygen dissolved in the recirculation lines and condensed steam were compared with the corresponding values calculated with the radiolysis model. For this comparison, results of water chemistry measurements performed at four BWRs were used. In general, satisfactory agreement was found between experimental and calculated results for the hydrogen and oxidant[1] concentrations in the recirculation lines and the condensed steam.

The radiolysis model was extended to include LPRMs modified to contain ECP sensors. The results for two BWRs show that the concentrations of hydrogen, oxygen and hydrogen peroxide, and the corresponding ECP values, are generally different inside and outside the LPRM. Variation in these differences are dependent upon the flow rate. It was also observed that at the top of the core the ECP is not sensitive to sensor position. In other words, a slight misplacement of the sensors is not significant. On the other hand, the sensors are very sensitive to their position below the core plate, especially at high FW H_2 injection rates. No major difference in the response of the two types of modified LPRMs was attributed to their differences in design.

On the basis of oxidant concentrations and other parameters, ECP values were calculated for all the model regions of each BWR in this study. The corresponding charts included in Appendix A of this report provide an estimate of the degree of SCC mitigation, in each region. The results indicate that, in general, mitigation can be achieved at hydrogen levels of 1 ppm or less in the outer core bypass region (the outer core bypass region corresponds to the inner surface of the core shroud), in the lower section of the downcomer, in the recirculation lines, and in the lower plenum. In some other regions of the primary circuit mitigation can be achieved only with higher concentrations of feedwater hydrogen, or cannot be achieved within the range of hydrogen concentrations modeled. In the latter case, the concurrent application of other technologies presently under development, for example noble metal technology (NMT), may provide the required protection at acceptable hydrogen injection levels .

It should be emphasized that the radiolysis model is undergoing continuous revision. In-plant tests specifically designed to benchmark the model would provide the basis for further refinements. Improvements to the radiolysis model will allow more accurate

[1] The term "oxidant" signifies the combined dissolved oxygen produced by radiolysis and that produced by decomposition of the hydrogen peroxide. ($[O_2]+1/2[H_2O_2]$ = oxidant concentration.)

predictions of conditions leading to SCC. In particular, determining more accurately the concentration of oxidizing species and the corresponding ECP values at specific locations in the BWR primary system (for example, shroud welds) is part of the scope of future work. Future model developments are expected to incorporate surface chemistry effects, plant specific radiation fields, and mapping of coolant velocities for enhanced calculation of chemical species concentrations and ECPs.

SECTION 1

INTRODUCTION

Boiling water reactors (BWRs) use high purity water as the neutron moderator and primary coolant in the production of steam. As a result of water radiolysis, liquid-vapor phase equilibrium and recirculation, the coolant in the BWR recirculation line contains oxidant (oxygen plus half the concentration of hydrogen peroxide) in the concentration range from 150 to 300 ppb. This range of oxidant concentration under normal water chemistry (NWC) operation increases the susceptibility of austenitic stainless steel to stress corrosion cracking (SCC), when other requisite factors such as stress and sensitization are present.

It has been found that reducing the level of oxygen to the range of 1 to 10 ppb, which results in a decrease in the electrochemical potential to <-230 mV (SHE), can effectively mitigate SCC in austenitic stainless steels, when the water purity is sufficiently high[1], i.e., conductivity less than 0.3 μS/cm. Based on prior work in the laboratory and at reactors, it was determined that the oxidant concentration can effectively be reduced by the use of hydrogen and that SCC can be controlled.

In 1977 GE undertook a 4 year program to carefully evaluate the alternate water chemistry required to reduce the oxygen concentration[2-6]. This study, jointly sponsored by the US Department of Energy and Commonwealth Edison Company, indicated that an alternate water chemistry was feasible with hydrogen selected as the additive.

In 1982, GE with participation of the original two organizations and Electric Power Research Institute performed the first full scale implementation test at Dresden-2. [7,8] That test clearly demonstrated engineering feasibility and defined process parameters for HWC operation for mitigation of SCC in the reactor recirculation system piping. Since the first Dresden-2 test, GE has performed or has been directly associated with nearly 20 HWC tests at various plants. In the majority of these tests, hydrogen was added via the feedwater in amounts sufficient to suppress the oxygen in the recirculation system to the low value required to attain protection from SCC. In some of the HWC tests, the feedwater hydrogen concentration was raised to levels sufficient to guarantee protection not only to the recirculation lines but to the internal components. This was monitored in most instances by electrochemical potential measurements and constant extension rate tests conducted simultaneously. The results of these studies indicated successful operation without detrimental aspects, and have been reported elsewhere. [9-16]

It has been observed that the oxygen concentration and the N-16 concentration in the main steam vary approximately in the same manner with increasing feedwater hydrogen concentrations for all plants tested.[17] However, a significant variation exists among the plants in the recirculation oxygen response to given feedwater hydrogen concentration changes. This variability in the feedwater hydrogen concentration requirements for recirculation water oxygen suppression can be correlated with variations of the dose rate

in the downcomer region[18]. It has also been reported [17] that the presence of significant levels of soluble copper in the reactor water has a marked effect on the feedwater hydrogen requirements for recirculation oxygen suppression.

The majority of chemistry data from the HWC tests are obtained from samples of the recirculation water and the main steam. These two regions show quite a different response of the oxygen concentration to hydrogen addition. The steam phase oxygen, which is a measure mainly of the core exit oxygen concentration, decreases with increasing feedwater hydrogen concentration. The recirculation water oxygen also decreases, but more rapidly and with significantly greater variation. Samples obtained from the core bypass region also exhibited a different response, with oxygen showing an even larger decrease at feedwater hydrogen concentrations higher than 0.7 ppm. [19] These data indicate that each region in the primary circuit may behave differently in the response of its oxidant to feedwater hydrogen, and that the response is dependent on certain characteristics of the particular region. This difference has also been indicated in the results of computer simulation of radiolysis by other workers. [20,21]

Besides mitigation of SCC in the reactor recirculation system, it is of increasing importance to investigate the concentration of hydrogen and oxidizing species in other regions of the primary circuit, where it may be possible to reduce the oxidant concentration to levels sufficiently low for SCC mitigation. Two such regions are the in-vessel region below the fuel support plate (lower plenum) and the core bypass region. SCC has been observed in internals at various locations in the reactor vessel. One approach would be to install sample lines for each of the regions of each reactor and to measure the response in oxygen concentration to hydrogen addition, as has been done for the recirculation system in the HWC pre-implementation tests (mini-tests). Although possible, this approach would be very difficult and costly. In addition, it would not provide information for other areas outside the sampled region.

An alternate approach is computer simulation of water radiolysis in the BWR primary circuit. [20-23] During the past decade GE, in conjunction with UKAEA, Harwell Laboratory, has been continuously developing and improving a computer radiolysis model which describes the concentrations of hydrogen, oxygen, hydrogen peroxide and other labile hydrogen-oxygen species in the various parts of the BWR primary circuit and in the main steam.

Results of prior work [17] provide details of the model's parameters, a description of the previous three versions of the model, the input data, and mass balance calculations . The subject of this current report is work conducted under EPRI Research Project C101-12. The latest Version 4 of the model's code was applied to a study of 10 BWR plants which, with one exception, had undergone HWC tests or implementation.[24] Major differences between the previous and the latest versions are:

1. A new set of high temperature G values[2] is utilized, as listed in Table 2-2.
2. New chemical reaction rate constants, as well as detailed dose rate and velocity profiles in the various regions of the circuit, are used.
3. A region of inactive fuel between the top of the active fuel and the top of the fuel channel (see Figure 2-2), previously computed by the code only at the top of the channel region , has now been inserted at the top of the core bypass and of the outer bypass.
4. The internal region of modified LPRMs used at Fitzpatrick and at Quad Cities-2 for in-core ECP measurements has been modeled to compare the concentrations of hydrogen, oxygen and hydrogen peroxide next to the reference electrodes with the concentrations outside the LPRM. This calculation is optional, depending upon whether the plant being modeled has such a unit.
5. The steam separators have been modeled as a new separate region of the flow circuit.
6. Transport coefficients between steam and water have been modified.

The results of the radiolysis model have been compared with measurements of hydrogen and oxygen in the recirculation and the steam sample piping, performed at four plants having significantly different responses to HWC. The agreement between steam data and the model is within ~20% for three reactors (no steam data are available for the fourth reactor).

For the recirculation hydrogen, the measured concentrations are always higher than those calculated with the model. Underpredicting the hydrogen results in conservatively high calculated values of ECP. The measured recirculation oxygen is usually less than predicted by the model. Overpredicting the oxidant concentration also results in conservatively calculated values of ECP.

It should be emphasized that the radiolysis model is undergoing continuous revision and improvement. In-plant tests specifically designed to benchmark the model can provide the basis for further refinements.

[2] The number of molecules formed per 100 eV of absorbed dose.

SECTION 2

MODEL DESCRIPTION

2.1 Radiolysis Model

The radiolysis model uses the FACSIMILE program,[25] which calculates, from initial values of concentration, subsequent values resulting from a series of chemical reactions as affected by flow and transport. An input data program is required for FACSIMILE to provide the information from which the main program constructs a set of simultaneous differential equations. The radiolysis model code comprises the single input data program for FACSIMILE which includes parameters such as residence times and mass flows in different parts of the circuit, mean reactor power density, dose rates, carryunder fraction, feedwater hydrogen and oxygen concentrations, and the coefficients of polynomials for steam quality and void fraction, as functions of distance in the core channel region. A heat transfer program [26] is used to calculate the steam quality and void fraction from which the coefficients are obtained.

The flow characteristics and chemistry are linked through the velocity of the liquid, the radiation field, and the void ratio, which are all dependent on position. The void ratio influences the partitioning of hydrogen and oxygen between liquid and vapor, as well as the liquid velocity. The concentration of the chemical species in an element of liquid volume together with its associated vapor volume in those parts where steam quality is not negligible is followed by the program. Since the density of the vapor and therefore the radiation energy absorbed per unit volume is about one-twentieth that for the liquid, gas phase radiation chemistry is not considered in the current version of the model. In addition, the model considers only pure water, i.e., except for copper, the effect of impurities and nitrogen chemistry is not yet taken into account.

The circuit in the computer model now consists of 10 regions in the BWR primary system:

- channel
- core bypass
- outer bypass
- upper plenum
- steam separators
- mixing plenum
- downcomer
- recirculation
- jet pump
- lower plenum

A diagram of the circuit is shown in Figure 2-1 and the regions are defined in Figure 2-2. The core is divided into two parts, the "channel" region within fuel channels, where the boiling occurs; and the bypass region. The "channel" region comprises two subregions (not shown in Figure 2-2): the lower zone near the bottom of the fuel where the steam quality is less than 1%, and the upper zone where the steam quality is 1% or greater. The bypass region is also subdivided into two regions: "core bypass", i.e., the region outside the fuel channels but within the perimeter of the core, where boiling does not occur; and "outer bypass", i.e., the region bounded by the core and core shroud. The channel, core bypass and outer bypass regions terminate at the top of the fuel.

The upper plenum is the two-phase flow region under the shroud head dome. The channel, core bypass and outer bypass flows mix at the beginning of the upper plenum.

The steam separator region consists of 6 sub-regions, shown schematically in Figure 2-3, with different flow velocities and residence times for the fluid traversing them[3] :

1. The steam separator riser pipe, up to and including the region of the first stage vanes, where steam and water are a homogeneous mixture.
2. The region after the first stage vanes where water is separated as a film on the inner surface of the pipe.
3. The exit region of the water from the first stage of the steam separator. In this region a small fraction of the steam, highly enriched in dissolved gases, is "carried under" with the water returning to the mixing plenum as a homogeneous mixture.
4. The second stage of water separation.
5. The exit region of the water from the second stage, with virtually no steam carryunder.
6. The third stage of water separation and exit of the steam to the steam dryers.

The mixing plenum is treated by the code as consisting of two sub-regions, before and after the feedwater supply.

The downcomer region too is divided into an upper part and a lower part. In the lower part of the downcomer the flow splits into two portions. A portion of the flow, variable from plant to plant, enters the recirculation system; the second portion of the flow is sucked into the jet pumps. The composition of the flow in the jet pump region is calculated by the code separately. The downcomer annulus can be subdivided into separate concentric shells of equal length. The results herein reported are pertinent to the shell adjacent to the shroud wall.

The recirculation region is subdivided by the code into suction, discharge, header ring and riser pipe. The jet pump internal riser, up to the jet pump ram's head, is considered as the last segment of the recirculation line.

[3] For the sake of simplicity the 6 subregions of the steam separator have been combined into a single region in the plots of H_2 , O_2 and H_2O_2 vs. feedwater hydrogen.

Taking into account the variation in diameter of different segments of the jet pump, the jet pump region has been subdivided into throat, diffuser and tailpiece.

The lower plenum region corresponds to the last segment of the flow circuit. This is a non-linear region, because it extends from the exit of the jet pumps to the bottom of the active fuel region. Thus the length of the region does not correspond to a straight distance between two elevations, but rather to a curvilinear segment.

In parts of the circuit where the flow divides and merges later, each branch is treated separately in sequence from the point of separation to the point of recombination. The concentration at the junction is set as the sum of the product of concentration and liquid mass flow fraction for each branch. Concentrations are calculated as functions of distance along the flow path., which comprises all the branches placed end to end along a single line (see Figure 2-2).

Table 2-1 correlates for a BWR (in this case, Nine Mile Point-2), the distances of the circuit expressed in meters with the length fraction of each region and the corresponding reactor locations. This table summarizes the approximate location in the reactor corresponding to a given "fraction of region length" on the x-axis of the concentration plots described in a later section of this report. A more detailed list of the fractions of each region's length and the corresponding distances in meters is provided in Appendix A. Any location in the circuit can be estimated on the basis of known reference elevations in the reactor vessel.

Table 2-1
Correlation Between Circuit Distances, Fraction of Region Lengths and Reactor Locations
(EXAMPLE)

REGION	DISTANCE (m)	REGION LENGTH FRACTION (%)	REACTOR LOCATION
Channel Inlet	0.00	0	Bottom of Active Fuel
Channel Outlet	4.18	100	Top of Top Guide
Core Bypass Inlet	4.18	0	Bottom of Active Fuel
Core Bypass Outlet	8.35	100	Top of Top Guide
Outer Bypass Inlet	8.35	0	Bottom of Active Fuel
Outer bypass Outlet	12.53	100	Top of Top Guide
Upper Plenum Inlet	12.53	0	Top of Top Guide
Upper Plenum Outlet	14.00	100	Top of Shroud Head Dome
Steam Separators Inlet	14.00	0	Inlet of Steam Sep. (Region 6) Stand Pipe
Steam Separators Outlet	20.17	100	Outlet of Steam Sep. to Steam Dryer
Mixing Plenum Inlet	20.17	0	Equiv. Normal Water Level
Mixing Plenum Outlet	23.28	100	Top of Shroud Head Dome
Downcomer Inlet	23.28	0	Top of Shroud Head Dome
Downcomer Outlet	31.39	100	Top of J.P. & Shroud Support Plate
Recirculation Inlet	31.39	0	Recirc Inlet Nozzle
Recirculation Outlet	83.16	100	Recirc Outlet Nozzle
Jet Pump Inlet	83.16	0	Jet Pump Throat Entry
Jet Pump Outlet	88.19	100	Jet Pump Exit
Lower Plenum Downflow Inlet	88.19	0	Jet Pump Exit
Lower Plenum Downflow Outlet	89.90	30	*
Lower Plenum Upflow Inlet	89.90	30	*
Lower plenum Upflow Outlet	93.90	100	Bottom of Active Fuel

* - The direction of the circuit flow in the lower plenum is downward from the exit of the jet pump for approximately 30% of the region, then upward.

2.2 Input Data

With respect to its previous version,[27] the GE/Harwell BWR radiolysis model has been substantially refined by including detailed dose rate and velocity profiles, new chemical reaction rate constants and new high temperature G values.

A description of the pertinent characteristics of the 10 plants is given in Table 2-2 . Other input data used by the radiolysis model are described below.

Table 2-2
Plant Characteristics

	Monticello	Pilgrim	Quad Cities-2	Duane Arnold	Chin-shan-1	Hatch-2	Fitz-patrick	Peach Bottom-3	Nine Mile Point-2	Kuo-sheng-1
BWR Classification	3	3	3	4	4	4	4	4	5	6
Thermal Rated Power (MWt)	1670	1998	2511	1593	1775	2436	2436	3293	3323	2894
Reactor Pressure Vessel Int. Dia. (in.)	205	224	251	183	203	218	220	251	251	219
No. of Fuel Assem.	484	580	724	368	408	560	560	764	764	624
Active Core Length (m)	3.66	3.66	3.66	3.66	3.66	3.66	3.66	3.66	3.81	3.81
Core Average Rated Power Density (w/cc)	35.6	38.8	36.4	50.9	50.5	49.2	51.2	50.0	50.0	52.4
Core Average Heat Generation at Rated Power (kw/ft)	4.49	4.48	4.52	5.64	5.66	5.66	5.66	5.61	5.44	5.80
Core Shroud Outer Diam. (in.)	167	184	207	145	165	178	178	207	207	186
Downcomer Width (in.)	19	20	22	19	19	20	21	22	22	17
Core Shroud Thickness (in.)	1.75	1.50	2.00	1.25	1.50	1.50	1.50	2.00	2.00	2.00
No. of Recirculation Loops	2	2	2	2	2	2	2	2	2	2
No. of Jet Pumps	20	20	20	16	20	20	20	20	20	20
Jet Pump C_T, Distance from Core Center (in.)	86.4	99.9	113.3	80.6	90.3	96.9	97.3	113.3	113.2	99.9

2.2.1 G Values of Radiolytic Products

The latest high temperature G values used in the calculations are reported in Table 2-3.

Table 2-3
G Values of Primary Radiolytic Species in Water Measured at 285 °C

	e (aq)$^-$	H^+	H	H_2	OH	HO_2	H_2O_2
GAMMA	3.614	4.477	1.035	0.535	5.141	0.000	0.289
NEUTRON	0.0116	0.1473	0.2118	1.3274	0.9462	0.000	0.966

In contrast to what was reported previously[17], the G values of e^-_{aq} , H, H_2 and OH are higher than at room temperature. The value for H_2O_2 is lower than at room temperature.[27]

2.2.2 Reaction Rate Constants

The new set of reaction rate constants used is shown in Table 2-4. A major development in the determination of high temperature pertains to the decomposition of hydrogen peroxide into water and oxygen. A significant surface catalysis effect was found to influence this reaction. The rate of a heterogeneous catalyzed reaction is dependent upon both mass transfer and chemical activation processes. The observed rate constant (k_{obs}) is related to the individual rate constants by the equation [28,29]

$$\frac{1}{k_{obs}} = \frac{1}{k_{dif}} + \frac{1}{k_{act}}$$

or

$$k_{obs} = \frac{k_{act}\, k_{dif}}{k_{act} + k_{dif}}$$

where k_{obs} is the observed rate constant, k_{act} is the rate constant attributed to the chemical activation process that would be observed if there were no diffusion restriction on the reaction rate, and k_{dif} is the rate constant for complete diffusion (mass transfer) control.
Using the data available in the literature, mass transfer-controlled rate constants for the decomposition of hydrogen peroxide have been calculated and compared with the rate constants measured experimentally. [30] At temperatures lower than ca. 200 °C the decomposition reaction is mostly activation controlled, and above ca. 200 °C the mass transfer process becomes an important factor in determining the overall reaction rate.

Table 2-4
Reactions and Rate Constants Used in the Simulation of Water Radiolysis

Chemical Reactions	Rate Constant at 285°C (L/mole/sec)	Activation Energy (Kcal/mole)
$e_{aq}^- + H_2O \rightarrow H + OH^-$	1.71×10^2	3.0
$e_{aq}^- + H+ \rightarrow H$	3.5×10^{11}	0
$e_{aq}^- + OH \rightarrow OH^-$	2.13×10^{11}	3.0
$e_{aq}^- + H_2O_2 \rightarrow OH + OH^-$	1.3×10^{11}	0
$H + H \rightarrow H_2$	8.5×10^{10}	0
$e_{aq}^- + HO_2 \rightarrow HO_2-$	2.13×10^{11}	3.0
$e_{aq}^- + O_2 \rightarrow O_2-$	2.6×10^{11}	0
$2e_{aq}^- \rightarrow 2OH^- + H_2$	5.33×10^{10}	3.0
$2OH \rightarrow H_2O_2$	1.7×10^{10}	0
$OH + HO_2 \rightarrow H_2O + O_2$	8.6×10^{10}	0
$OH + O_2- \rightarrow OH^- + O_2$	8.6×10^{10}	0
$OH^- + H \rightarrow e_{aq}^- + H_2O$	6.96×10^8	4.5
$e_{aq}^- + H + H_2O \rightarrow OH^- + H_2$	2.67×10^{11}	3.0
$e_{aq}^- + HO_2- + H_2O \rightarrow OH + 2OH^-$	3.73×10^{10}	3.0
$H^+ + OH^- \rightarrow H_2O$	1.54×10^{12}	3.0
$H_2O \rightarrow H^+ + OH^-$	0.185	3.0
$H + OH \rightarrow H_2O$	5.5×10^{10}	0
$OH + H_2 \rightarrow H + H_2O$	1.20×10^9	4.31
$OH + H_2O_2 \rightarrow H_2O + HO_2$	3.49×10^8	3.11
$H + H_2O_2 \rightarrow OH + H_2O$	2.06×10^9	3.97
$H + O_2 \rightarrow HO_2$	8.6×10^{10}	0
$HO_2 \rightarrow O_2- + H^+$	2.74×10^5	3.0
$O_2- + H^+ \rightarrow HO_2$	5.33×10^{11}	3.0
$2HO_2 \rightarrow H_2O_2 + O_2$	6.29×10^7	5.46
$H + HO_2 \rightarrow H_2O_2$	2.13×10^{11}	3.0
$H + O_2- \rightarrow HO_2-$	2.13×10^{11}	3.0
$e_{aq}^- + O_2- \rightarrow HO_2- + OH-$	4.53×10^9	4.5
$OH + H_2O_2 \rightarrow HO_2 + H_2O$	6.27×10^9	0
$H_2O_2 \rightarrow H_2O + 1/2\ O_2$	Function of velocity	-

2.2.3 Reactor Specific Data

The reactor specific input variables used in the computer program for the ten BWRs are given in Table 2-5. Flow rates, power densities and chemistry data were obtained from Ref. 31 and from the GE Nuclear Energy database. The fraction of coolant going to the in-channel and core bypass regions were obtained from the GE Core Nuclear Design Group for the current fuel cycle for each reactor. The residence times in each region were calculated from the flow rates and from the fluid volumes and weights for each reactor.

2.2.4 Radiation Dose Profiles

The dose rate at a point in the reactor is determined by the location along the flow path. The neutron and gamma dose rate values were determined at Harwell for the core region on the basis of Monte Carlo calculations for a 50 W/cc standard plant and scaled to the power densities of each of the 10 BWRs. The radial average dose rates at the maximum axial node for gamma and neutron were 3.1 x 10^8 Rad/hr and 1.5 x 10^9 Rad/hr, respectively. The axial profile utilized was that typical of a BWR power distribution. The same dose rates in the channel and bypass regions were utilized. Other details of the dose rate calculations have been reported previously.[17]

Table 2-5
Radiolysis Model Main Input Variables for Ten BWRs

Variable	Monti-cello	Pilgrim	Quad Cities-2	Duane Arnold	Chin-shan-1	Hatch-2	Fitz-patrick	Peach Bottom-3	Nine Mile Point-2	Kuo-sheng-1
Core Flow (Te/s)[1]	7.26	8.69	12.35	6.17	6.68	9.70	9.70	12.91	13.67	10.65
Feedwater Flow (Te/s)	0.85	1.00	1.23	0.86	0.96	1.32	1.32	1.68	1.80	1.57
Fraction of Flow in Channel	0.888	0.898	0.896	0.873	0.882	0.885	0.877	0.888	0.898	0.897
Fraction of Flow in Bypass	0.1	0.1	0.1	0.1	0.1	0.1	0.1	0.1	0.1	0.1
Fraction of Flow in Jet Pump	0.573	0.504	0.651	0.631	0.564	0.556	0.556	0.666	0.671	0.709
Power Density (Watt/cc)	35.6	38.8	36.4	51.0	50.5	49.2	51.2	50.0	50.0	52.4
Residence Time (Sec)										
In Channel	1.29	1.28	1.13	1.18	1.19	1.12	1.13	1.15	1.12	1.17
Total Bypass	13.91	16.94	14.47	11.17	18.23	11.02	10.28	11.33	12.31	12.18
Upper Plenum	0.71	0.72	0.72	0.59	0.69	0.57	0.59	0.65	0.57	0.75
Mixing Plenum	3.96	3.96	3.64	4.69	5.75	4.30	4.47	4.11	3.86	3.44
Upper Downcmr (above JP)	2.49	2.28	2.26	2.38	2.62	2.03	2.13	2.08	1.97	1.85
Lower Downcmr(JP length)	10.02	5.54	6.59	8.16	7.44	4.07	6.12	7.34	6.98	5.66
Recirculation	6.71	4.90	4.74	4.96	4.52	5.14	5.55	5.01	3.38	3.37
Jet Pump	0.54	0.67	0.47	0.51	0.51	0.41	0.41	0.42	0.21	0.27
Lower Plenum	4.14	4.12	4.11	3.63	4.66	3.47	3.54	3.79	3.58	3.74
Region H (inactive fuel)	0.19	0.22	0.18	0.20	0.28	0.19	0.18	0.19	0.13	0.11
Gamma Dose Rate Factors (mRad/h)										
Upper Plnum/Upper Dwncmr	1.5	1.5	1.5	1.5	1.5	1.5	1.5	1.5	1.5	1.5
Downcomer	2.6	1.61	1.00	4.63	1.12	3.05	3.05	1.79	1.5	2.98
Lower Plenum	0.52	0.52	0.52	0.52	0.52	0.52	0.52	0.52	0.52	0.52
Other variables										
Fuel Length (m)	3.66	3.66	3.66	3.66	3.66	3.66	3.66	3.66	3.81	3.81
Feedwater H_2 (ppm)	1.5	1.5	1.5	1.5	1.5	1.5	1.5	1.5	1.5	1.5
Feedwater O_2 (ppm) [NWC]	0.044	0.032	0.029	0.036	0.024	0.025	0.030	0.021	0.032	0.031
Carryunder Fraction	0.001	0.001	0.001	0.001	0.001	0.001	0.001	0.001	0.001	0.001

[1]Metric tons per second

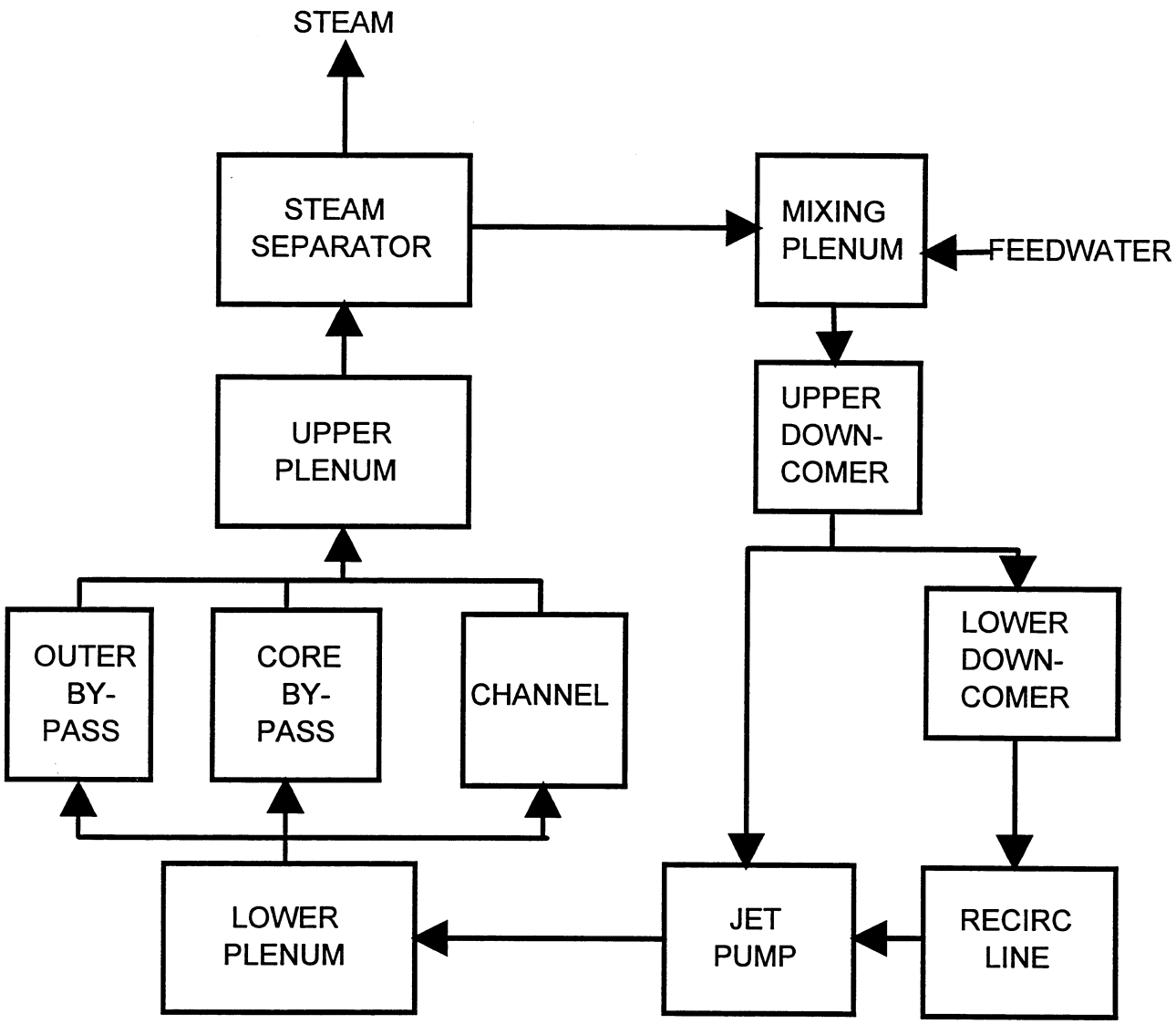

FIGURE 2-1. COMPUTER MODEL OF BWR (PRODUCT LINE 3 TO 6) PRIMARY SYSTEM

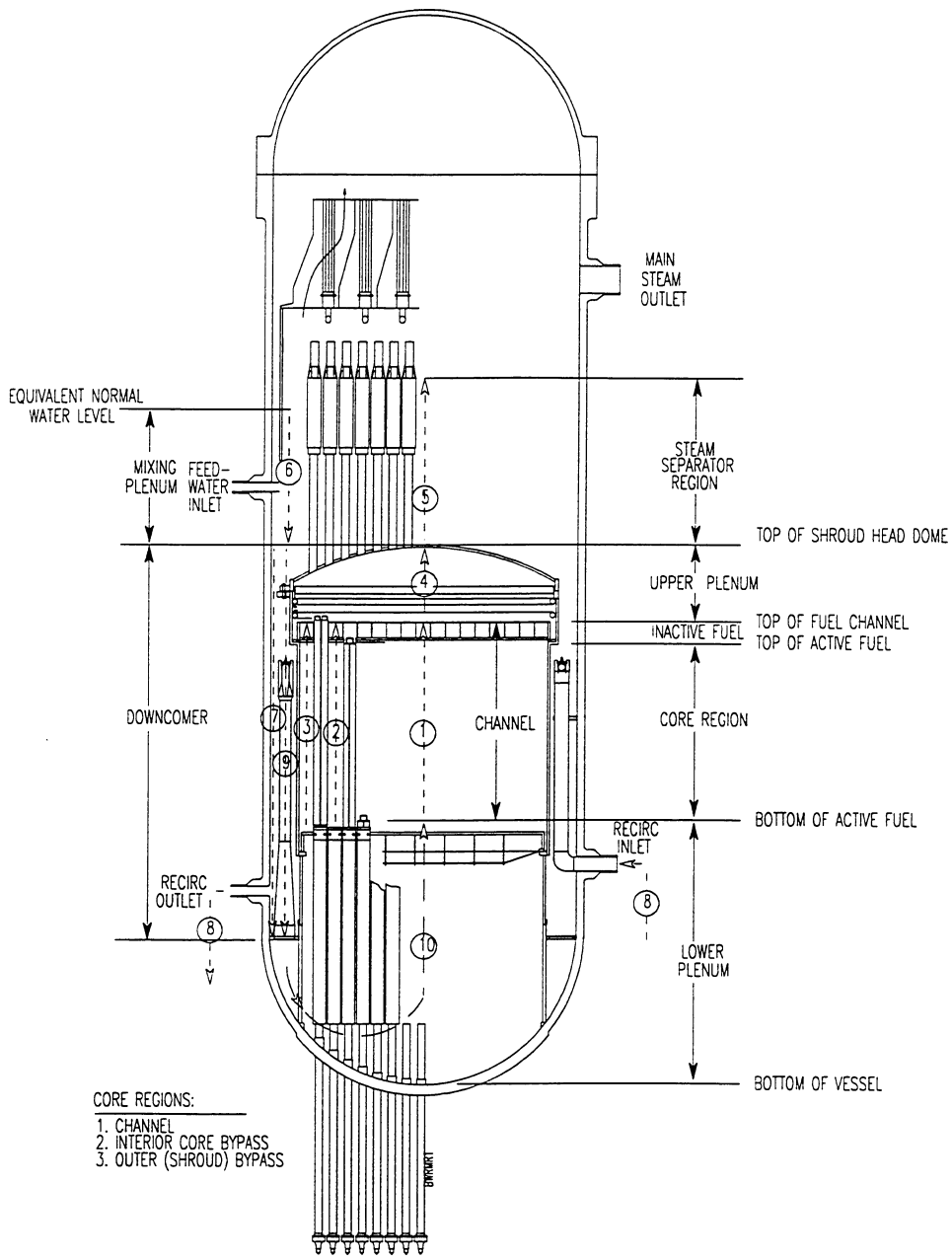

FIGURE 2-2. RADIOLYSIS MODEL REGION AND CIRCUIT IDENTIFICATION

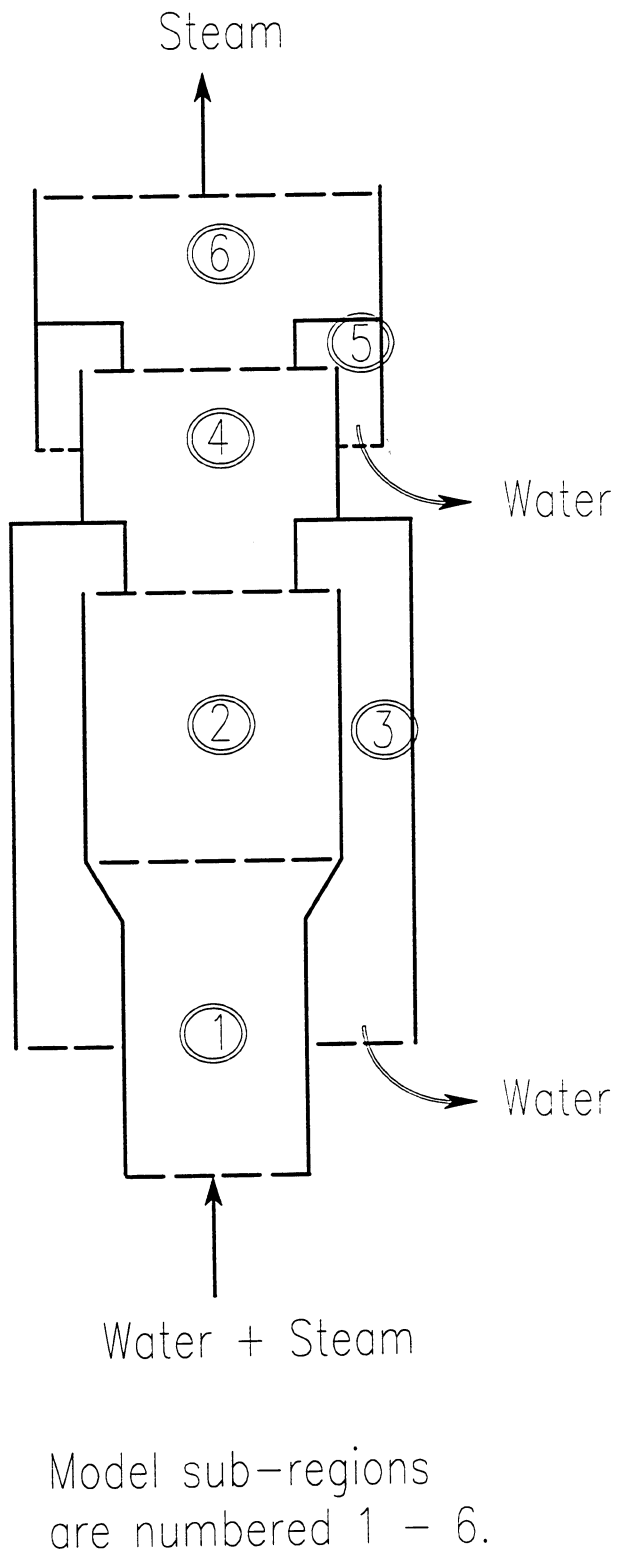

FIGURE 2-3. SIMPLIFIED SCHEMATIC OF STEAM SEPARATOR

SECTION 3

RESULTS AND DISCUSSION

3.1 Radiolysis Model

Calculations were performed for the ten BWRs and for the following ten feedwater hydrogen concentrations: 0.0, 0.2, 0.4, 0.6, 0.8, 1.0, 1.5, 2.0, 2.5 and 3.0 ppm. The choice of feedwater hydrogen concentrations is not limited to those herein reported, but can be varied at will by modifying the input data of the radiolysis code.

In general, the following is observed:

(a) The reduction of oxygen and hydrogen peroxide in response to hydrogen addition is dependent on the region in the BWR circuit and the location within the region. The oxygen response is more sensitive than the hydrogen peroxide response.

(b) The concentrations of oxygen and hydrogen peroxide decrease rapidly in the reactor recirculation line with increasing feedwater hydrogen concentration. Other non-boiling regions, including the downcomer and lower plenum, also exhibit decreasing oxygen and hydrogen peroxide concentrations with increasing feedwater hydrogen concentrations.

(c) In the core regions, the decrease in the oxygen and hydrogen peroxide concentrations is slower than in the recirculation lines, as feedwater hydrogen increases. The decreases are apparent up to the highest feedwater hydrogen concentration modeled, and occur within the channel region and in the other core regions, as well as in the upper plenum and in the mixing plenum.

Typical inlet and outlet hydrogen, oxygen and hydrogen peroxide concentrations at 100% power for each of ten regions of the primary circuit are plotted as bar charts in Figures 3-1 through 3-6 in correspondence to four feedwater hydrogen concentrations: 0.0 (the NWC condition), 0.6, 1.0 and 1.5 ppm. These bar charts provide a summary description of the variation in concentration of the relevant radiolytic species throughout the circuit.

Line charts corresponding to the ten regions and the ten feedwater hydrogen concentrations are shown in Figures A-11 through A-163 for the ten BWRs in Appendix A. The model-calculated concentrations (ppb) of dissolved hydrogen, oxygen and hydrogen peroxide are plotted across the length of each region, with the x-axis representing the fractional portions (0 to 100%) of the region length.

In addition, typical gamma and neutron dose rate profiles across each of the ten model regions are shown in Figures 3-7, 3-11, 3-15, 3-19, 3-23, 3-27, 3-31, 3-35, 3-39, and 3-43. These profiles can help with interpretation of the variations in the concentrations of

hydrogen, oxygen and hydrogen peroxide in the different regions. The dose rate at a given elevation in the reactor is determined by the distance along the flow path that has been traversed. In general, the neutron dose rate tends to generate oxidizing species by decomposition of the water molecules; the gamma dose rate tends to cause the recombination of hydrogen and oxygen into water.

Following is a region-by-region description of one typical set of results:

3.1.1 Channel Region

Figure 3-7 shows the gamma and neutron dose rate profiles in the boiling region inside the fuel channels. When no hydrogen is injected in the feedwater (FW H_2 = 0 ppm), water enters the core with substantial amounts of oxidant present, as shown in the oxygen and hydrogen peroxide plots of Figures 3-9 and 3-10. Under these oxidizing conditions there is a steady increase of radiolysis products, i.e. , an increase in hydrogen, oxygen and hydrogen peroxide between 0 and ~25% of the region length. This is apparent in the hydrogen plot of Figure 3-8 corresponding to FW H_2 = 0 ppm, and in the oxygen and hydrogen peroxide plots of Figures 3-9 and 3-10. The discontinuities (kinks) in the plots at ~25% of the region length correspond to the onset of boiling. Similar slight discontinuities can be seen at ~90% of the region length, in correspondence to the transition to the short zone of inactive fuel close to the fuel top guide.[4]

In HWC conditions, the profile of the curves shown in Figure 3-8 is nearly flat at 0.2 ppm feedwater hydrogen. As the feedwater hydrogen concentration increases, the hydrogen concentration shows a decreasing trend along the length of the channel region, due to the stripping action of the steam. Concurrently, the oxygen and hydrogen peroxide concentrations (Figures 3-9 and 3-10) increase along the length of the region because less hydrogen is available for recombination. Also, notice that the points of increase of oxygen along the length of the region are delayed with increasing available feedwater hydrogen (in Figure 3-9 the flat portion of the curves becomes longer).

Through approximately the first 25% of the region the oxidant is depressed by recombination with hydrogen. This effect is more marked for oxygen than for hydrogen peroxide, i.e., to reduce the concentration of hydrogen peroxide more feedwater hydrogen is required. In particular, Figure 3-10 shows that the level of hydrogen peroxide is reduced below the NWC level by increasing feedwater hydrogen through approximately 25% of the region length. The hydrogen peroxide level increases again, when, due to the stripping process, hydrogen is no longer available. Above ~40% of the region length not much hydrogen is available for recombination, as can be seen in the hydrogen plots of Figure 3-8.

[4] Sharp changes in slope (segment-like portions of the lines) are due to stepwise changes of the calculations along the length of the region. Calculated values are printed at incremental steps of 10 cm along the distance of the circuit. Changes in line slope are more evident when a region of shorter length is charted.

3.1.2 Core Bypass Region

The neutron and gamma dose rates profiles in the core bypass are essentially the same as those in the channel region (compare Figures 3-7 and 3-11). In the core bypass, however, no boiling occurs, and thus no stripping of hydrogen and oxygen takes place. The latter mechanism is predominant in the channel region.

Figure 3-12 shows little change in the hydrogen concentration across the region. The oxygen concentration in the core bypass is very sensitive to the hydrogen level. At feedwater hydrogen concentrations above 0.4 ppm the dissolved oxygen is virtually eliminated from the region (Figure 3-13). The minimum in oxygen concentration at ~3% of the region length and 0 ppm feedwater hydrogen reflects the transition from the oxygen concentrations of the lower plenum to the region of higher dose rate but lower flow of the core bypass. The minimum in the same oxygen curve at ~90% of the region length is probably due to two opposing effects: 1) the first effect is that of decreasing oxygen due to recombination with hydrogen, because the gamma dose rate is appreciable; the rate of recombination decreases rapidly along the length of the region as the gamma dose rate decreases; 2) the second effect is that of increasing oxygen due to the decomposition of hydrogen peroxide on the solid surfaces; the decomposition rate decreases gradually.

The hydrogen peroxide curves show trends similar to those of the oxygen curves, but hydrogen peroxide does not completely disappear from the region, as does the oxygen with increasing hydrogen injection (Figure 3-14).

3.1.3 Outer Bypass Region

The outer bypass is similar in behavior to the core bypass, but peak dose rates are lower by factors of ~7 for gamma and ~60 for neutrons (Figure 3-3), and so the concentrations of radiolytic species are lower. Note that in the core and core bypass regions, neutron dose rates dominate; in the outer bypass region, gamma dose rates are higher.

Outer bypass hydrogen concentrations are essentially constant over the total region length, as shown by Figure 3-16. In Figure 3-17, the oxygen curve at 0 ppm feedwater hydrogen shows the same minimum at ~3% of the region length, and some discontinuity at ~ 90% of the region length, in correspondence to the zone of inactive fuel similar to that of the plot for the core bypass region. The hydrogen peroxide drop at the start of the region (Figure 3-18) is due to the transition from the lower plenum to the outer bypass region. The trends of hydrogen, oxygen and hydrogen peroxide in this region are similar to those in the core bypass region. For a given feedwater hydrogen concentration, however, oxidant suppression is more easily reached in the outer bypass region (compare Figures 3-17 and 3-18 with Figures 3-13 and 3-14).

3.1.4 Upper Plenum Region

The upper plenum is a two-phase flow region, whose inlet streams are the output of the channel, core bypass, and outer bypass regions. As flow moves away from the core, the

neutron and gamma dose rates drop to very low levels. The neutron dose rate drops faster than the gamma dose rate due to the attenuation by the water (Figure 3-19).
Upper plenum hydrogen and oxygen concentrations decrease rapidly, then reach an approximately constant level, which indicates the species have reached equilibrium. The initial decreases are more pronounced at the higher feedwater hydrogen values (Figures 3-20 and 3-21). Hydrogen peroxide shows some decrease over most of the region length, but its concentration remains as high as ~230 ppb even at 3 ppm feedwater hydrogen (Figure 3-22).

3.1.5 Steam Separator Region

In the steam separator region the gamma dose rate decreases rapidly (Figure 3-23). Having reached equilibrium in the upper plenum, the hydrogen concentration remains constant across the steam separator region (Figure 3-24). The concentrations of oxygen and hydrogen peroxide, however, vary as a result of hydrogen peroxide decomposition over the large surface of the steam separator. A comparison of Figure 3-25 with Figure 3-26 shows that when oxygen increases, hydrogen peroxide decreases. The concentration of oxygen in the liquid phase is also affected by the stripping action of the steam.

The discontinuities in the oxygen and hydrogen peroxide curves of Figures 3-25 and 3-26 reflect the transitions between the six sub-regions of the steam separator model described in Section 2.1 of this report and shown in Figure 2-3. The plots show each of the six sub-regions of the steam separator in sequence, as if they were connected in series. In reality, the six sub-regions are not aligned sequentially (see Figure 2-3). Sub-region 2 feeds into sub-regions 3 and 4, and so a discontinuity can appear between sub-regions 3 and 4 on a linear plot. Similarly, sub-region 4 feeds sub-regions 5 and 6, so that a discontinuity appears between sub-regions 5 and 6.

In practice, the discontinuities are only large for oxygen and hydrogen peroxide, because these can change rapidly due to the decomposition of hydrogen peroxide and simultaneous formation of oxygen. Hydrogen only varies slowly in the last four sub-regions of the steam separator, and so discontinuities in the hydrogen chart of Figure 3-24 are not apparent.

3.1.6 Mixing Plenum Region

In the mixing plenum, feedwater with a relatively high hydrogen content mixes with the primary coolant, which is depleted in hydrogen. As the mixing plenum water flows in the direction of the core, the neutron and gamma dose rates, attenuated by the large volume of water and metal, are at a very low level throughout the region (Figure 3-27).

The sharp change in dissolved hydrogen shown in Figure 3-28 corresponds to the point in the region at which the mixing of feedwater with a relatively high hydrogen content and reactor water from the steam separator, which is depleted in hydrogen, occurs. The jump in hydrogen concentration is proportional to the feedwater hydrogen content. Because of the low dose rates, very little recombination of hydrogen and oxygen takes place in this

region, as indicated by the plots of Figures 3-28 and 3-29. Hydrogen peroxide levels also show very little change over the region length (Figure 3-30). Both oxygen and hydrogen peroxide levels are somewhat suppressed by increasing feedwater hydrogen (Figures 3-29 and 3-30).

3.1.7 Downcomer Region

The dose rate profiles in the downcomer have a shape similar to that found in the outer bypass. The peaks, however, are more pronounced (Figure 3-31). Higher dose rates are found in the center of the region, which corresponds roughly to the elevation of the active fuel mid-plane. In the downcomer, the gamma radiation is attenuated primarily by the shroud. On the other hand, the neutrons arriving from the core are attenuated by a large volume of water. Because the attenuation effect is greater for the neutrons, the gamma dose rate in the downcomer reaches levels approximately twice as high as those of the neutron dose rate.

The higher gamma dose rate favors the reaction of hydrogen with oxygen and hydrogen peroxide. Figures 3-32, 3-33 and 3-34 show the change in concentration of the three species due to recombination. The amount of hydrogen needed for recombination is in the mass ratio 1/17 to hydrogen peroxide and 1/8 to oxygen. Therefore a drop of ~250 ppb in hydrogen peroxide and ~ 150 ppb in oxygen would require approximately 15+19≅34 ppb of hydrogen. This mass balance explains why the variations in the downcomer hydrogen concentrations seen in Figure 3-32 are small as compared to the corresponding drops in oxygen and hydrogen peroxide of Figures 3-33 and 3-34. Thus a relatively low concentration of hydrogen in the feedwater entering the downcomer results in a large drop in downcomer oxygen in the section of the downcomer where the dose rate is higher. The effect on the hydrogen peroxide is less pronounced but equally significant.

The stepwise increase at the very beginning of the region in Figures 3-32 and 3-33 is due to collapse of the carryunder steam bubbles from the steam separators. The step is relatively small because, although rich in oxygen, carryunder amounts to only ~0.1% of the total flow.

The hydrogen peroxide curves of Figure 3-34 show an increase at between 20 and 30% of the region length at the lowest feedwater hydrogen concentrations, followed by a steep drop. This behavior, not observed in previous versions of the model, may indicate that SCC mitigation in the lower section of the downcomer is attained at low feedwater hydrogen concentrations, and is the subject of current investigation. In the lower part of the downcomer the flow is reduced by the amount educted into the jet pump, and recombination can occur more effectively due to increased residence time.

3.1.8 Recirculation Region

Dose rates in the recirculation region are extremely low (~ 50 R/hr of gamma). They climb toward a maximum only when the flow reaches the internal jet pump riser (Figure 3-35). At these low dose rates, there is no recombination reaction between hydrogen and

oxygen. The hydrogen concentration remains constant across the whole region (Figure 3-36).
Under NWC conditions, hydrogen peroxide decomposes into water and oxygen under the catalytic influence of the recirculation piping large surface area. The plots of Figures 3-37 and 3-38 show the increase in oxygen concentration and the decrease in hydrogen peroxide concentration across the recirculation region, due to this effect. The effect becomes less noticeable as soon as the feedwater hydrogen concentration increases.

3.1.9 Jet Pump Region

The dose rate profile in the jet pump region (Figure 3-39) shows a decreasing trend for both neutron and gamma dose rates to ~zero at approximately 60% of the region length. At low feedwater hydrogen, little oxygen or hydrogen peroxide decompose, because there is insufficient excess hydrogen to drive the recombination process (Figures 3-40 and 3-41). As the feedwater hydrogen increases to 0.4 ppm and onward, through 1.5 ppm, there is substantial recombination. At still higher feedwater hydrogen, there is little change in oxygen or peroxide, because they are very low at the entrance to the region. It is interesting to note that substantial changes can occur in the jet pump despite a residence time of only 0.5 seconds. This occurs in the first 60% of the jet pump, where the gamma dose rate is above 1 Mrad/hr.

3.1.10 Lower Plenum Region

The lower plenum is sub-divided into three zones: downflow away from the jet pumps, upflow towards the core but below the core plate, and upflow above the core plate.

The dose rates in the lower plenum are very important, especially in the zone immediately below the bottom of the active fuel (BAF), because they affect the chemistry in that zone significantly.

Dose rates are low in the area where flow enters the lower plenum from the jet pump exit (Figure 3-43). When the flow approaches the core plate, the dose rates begin to rise, the neutron dose rate faster than the gamma dose rate.

In the sub-region from the top of the core plate to the BAF, approximately 0.2 meters long, the dose rate increases very rapidly. No significant change in concentration of the radiolytic species occurs until the high dose rate zone is reached (Figures 3-44, 3-45 and 3-46).

3.2 Comparison of Measured and Calculated Values

Experimental measurements of hydrogen and oxygen dissolved in the recirculation lines and condensed steam were compared with corresponding values calculated with the radiolysis model. For this comparison, results of water chemistry measurements

performed at four BWRs (Duane Arnold, Fitzpatrick, Pilgrim and Quad Cities-2) were used. With the exception of Quad Cities-2, these results have been published. [32] Since the oxygen measured at the end of the sample lines is the sum of the oxygen dissolved in the stream and the oxygen generated by decomposition of hydrogen peroxide, the measured value is compared with the calculated concentration of oxidant, i.e., the sum of the calculated concentration of oxygen and half the calculated concentration of hydrogen peroxide.[5]

Figure 3-47 combines the comparison of calculated and measured hydrogen concentrations in the condensed steam, at various feedwater hydrogen concentrations. The maximum deviation between the two sets of values is ~26% at zero ppm feedwater hydrogen, but the agreement improves with increasing feedwater hydrogen, and is acceptable between 0.5 and 1.5 ppm feedwater hydrogen. The predicted minimum in the steam hydrogen occurs at approximately 0.3-0.4 ppm feedwater hydrogen, while experimentally the minimum occurs at ~0.6 ppm. The agreement is reasonable for the corresponding comparison of oxygen data of Figure 3-48. Note that the prediction of the model for the steam hydrogen and oxygen concentrations are virtually identical for the three plants.

The model predicts significant differences between the recirculation line hydrogen of different reactors (Figure 3-49). At high feedwater hydrogen, the slope of the calculated curves is determined by the ratio of the feedwater flow to the core flow. Hydrogen in the feedwater is diluted with the mixing plenum water. This mixture is the main source of hydrogen for the recirculation lines. At present, the model tends to undercalculate hydrogen, providing conservative predictions. As with the hydrogen, there are significant plant-to-plant differences in the oxygen. Figure 3-50 shows that the model tends to overcalculate the oxidant, producing again conservative results.

[5] For each decomposing molecule of hydrogen peroxide half a molecule of oxygen is formed, according to the reaction $H_2O_2 \rightarrow H_2O + 1/2\ O_2$.

FW H2 concentrations (ppm) are indicated above the In Channel bar set

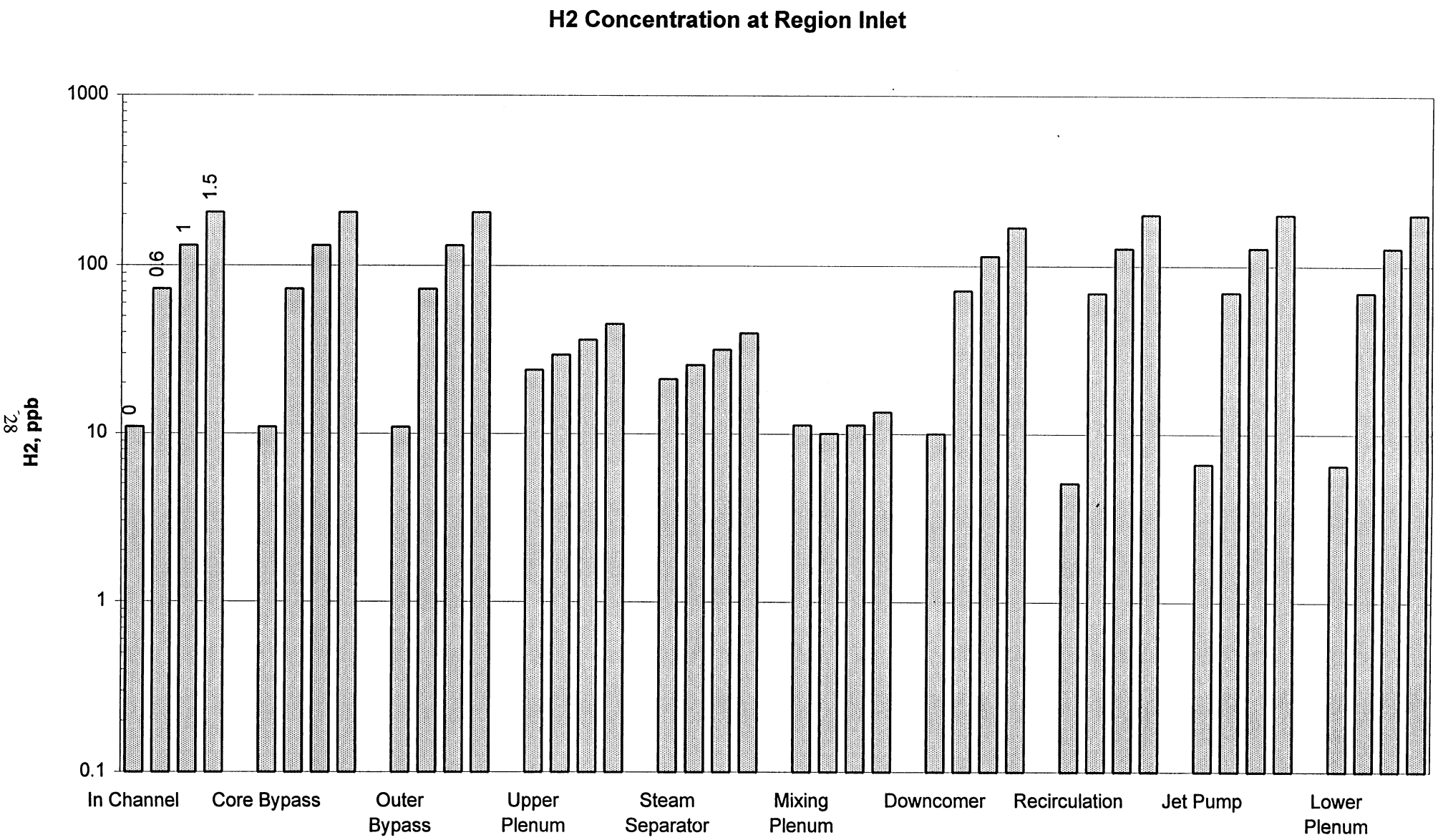

Figure 3-1

FW H2 concentrations (ppm) are indicated above the In Channel bar set

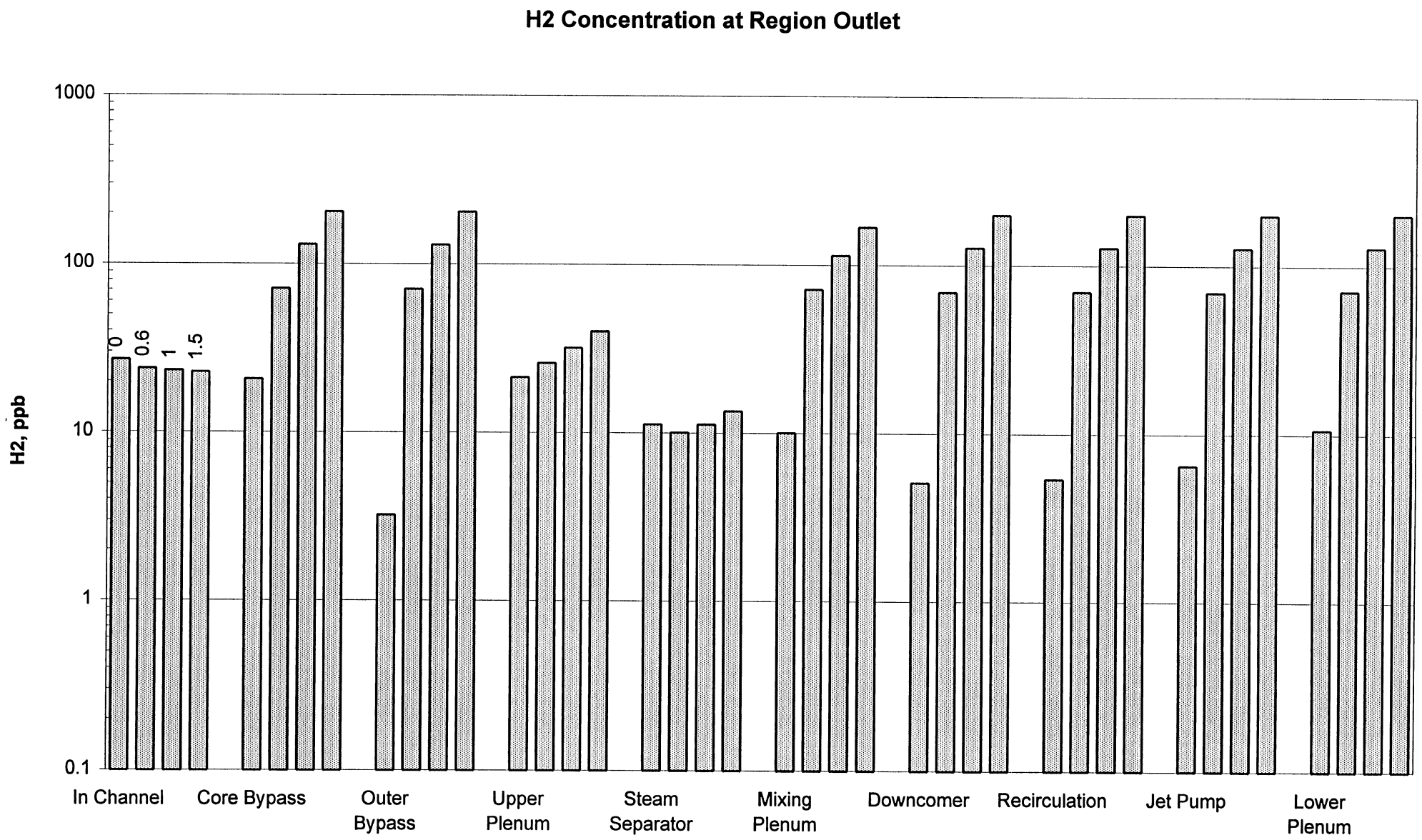

Figure 3-2

FW H2 concentrations (ppm) are indicated above the In Channel bar set

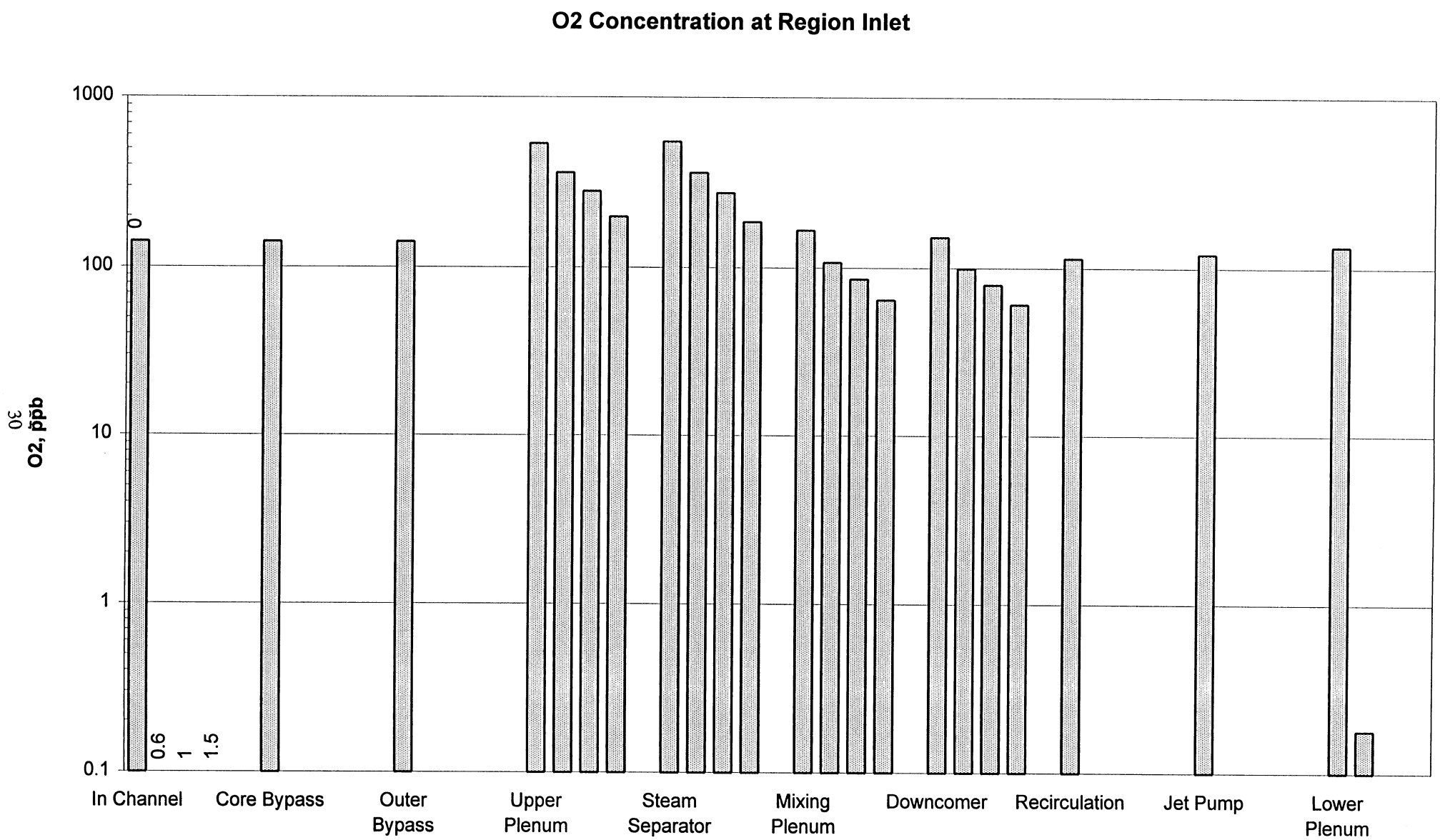

Figure 3-3

FW H2 concentrations (ppm) are indicated above the In Channel bar set

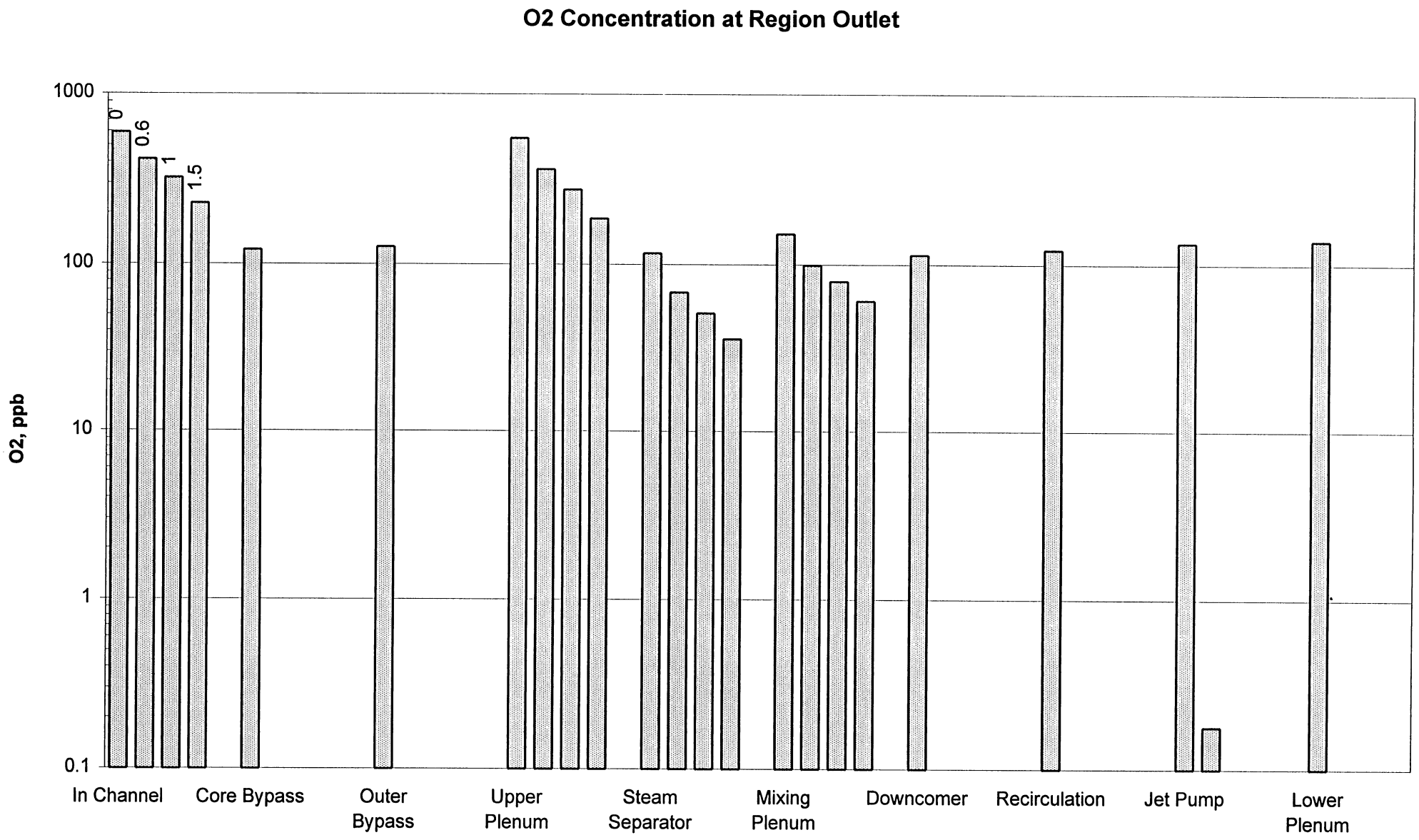

Figure 3-4

FW H2 concentrations (ppm) are indicated above the In Channel bar set

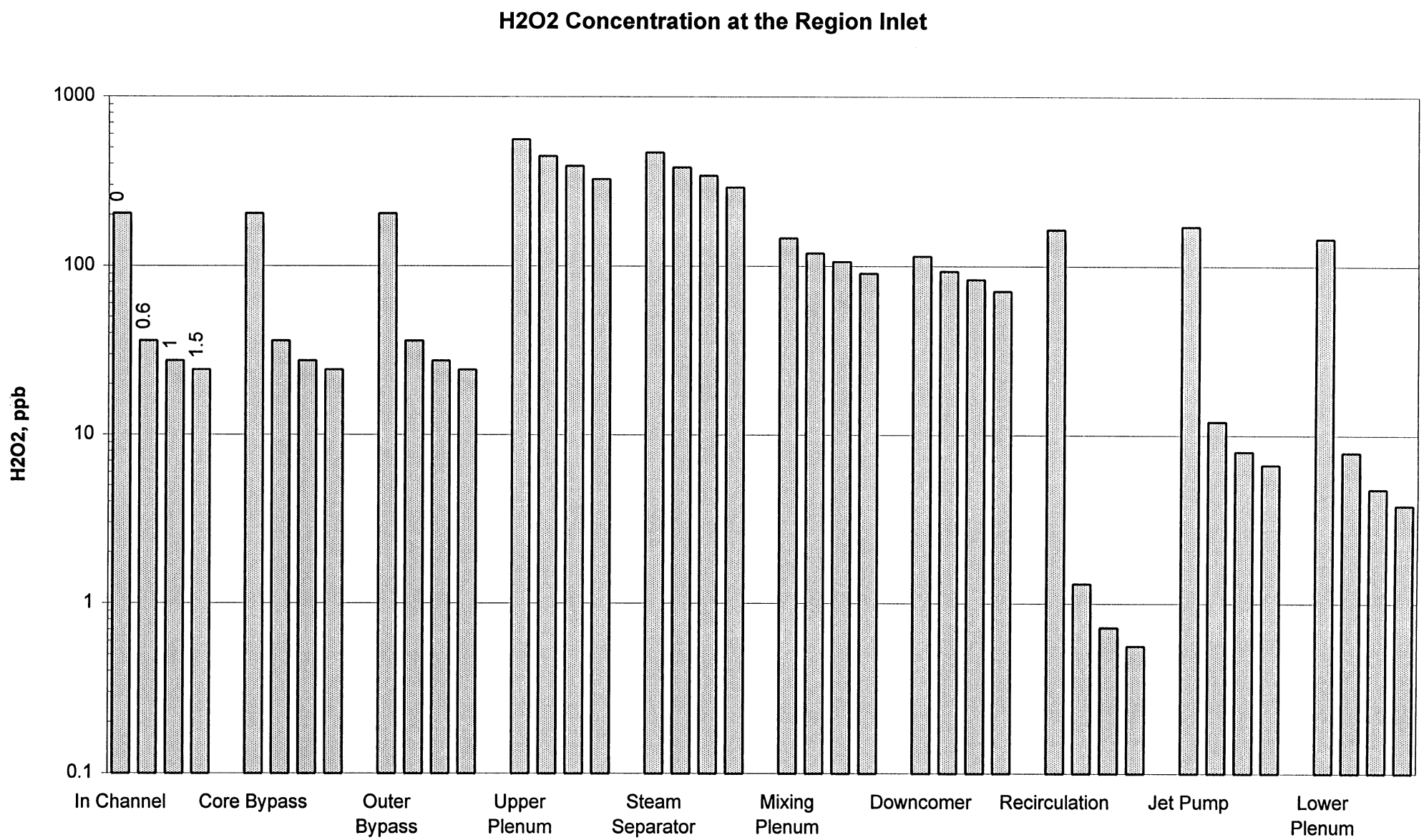

Figure 3-5

FW H2 concentrations (ppm) are indicated above the In Channel bar set

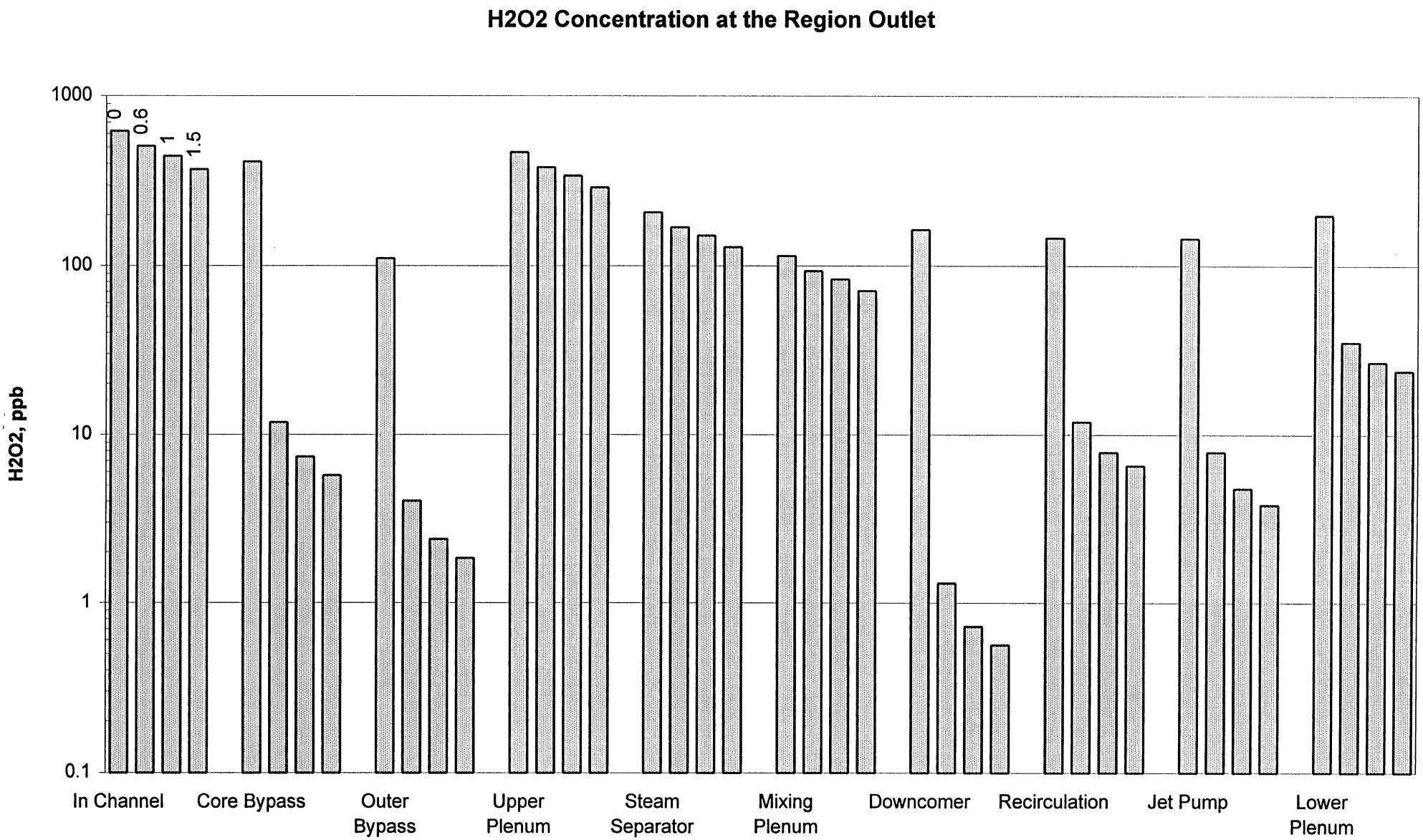

Figure 3-6

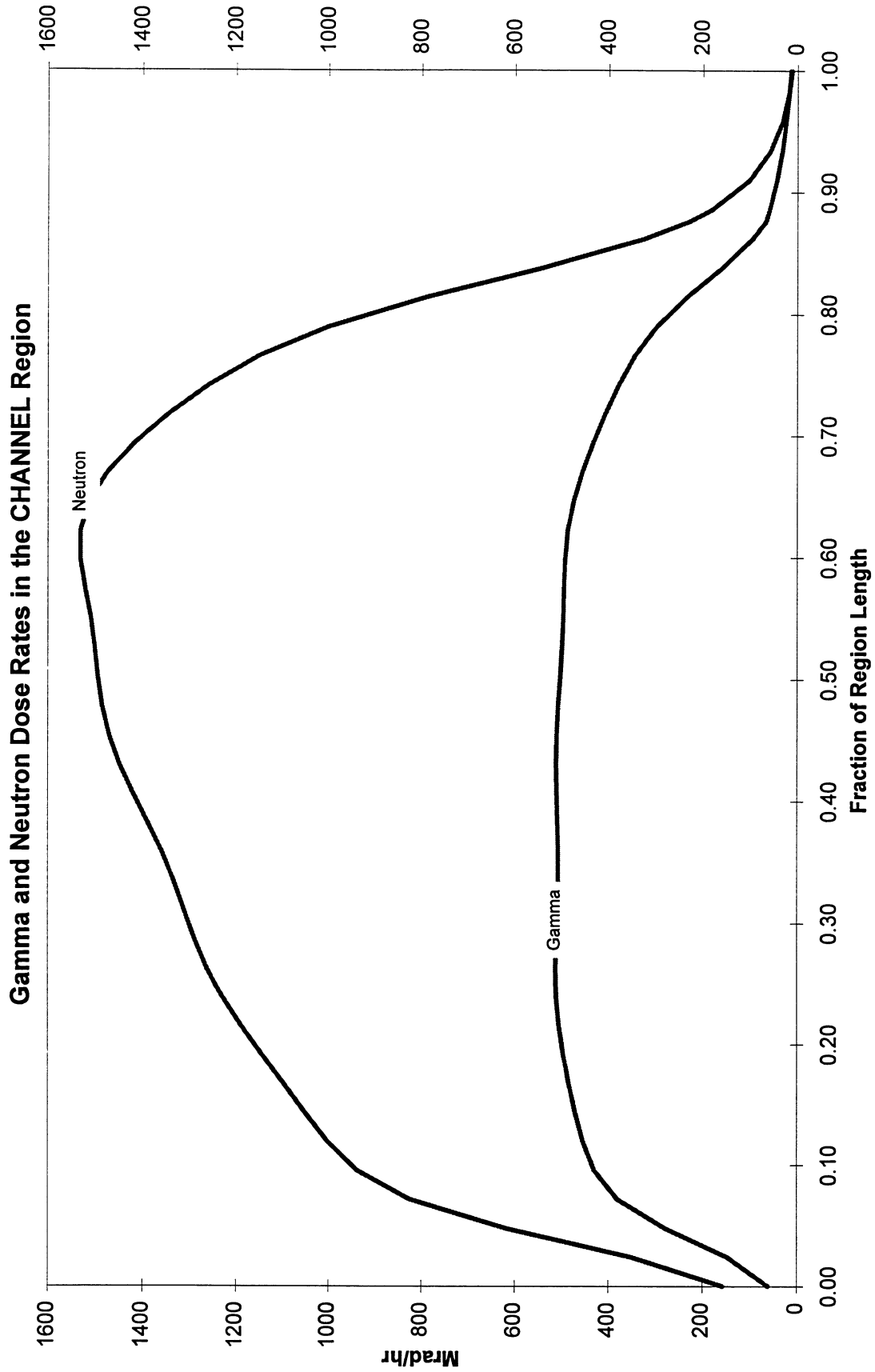

FITICRRG.xlc

BWRJP438 (VERSION 4.38.5)DATED 12/20/94

Figure 3-7

ALL VALUES ATTACHED TO CURVES INDICATE PPM OF FW H2

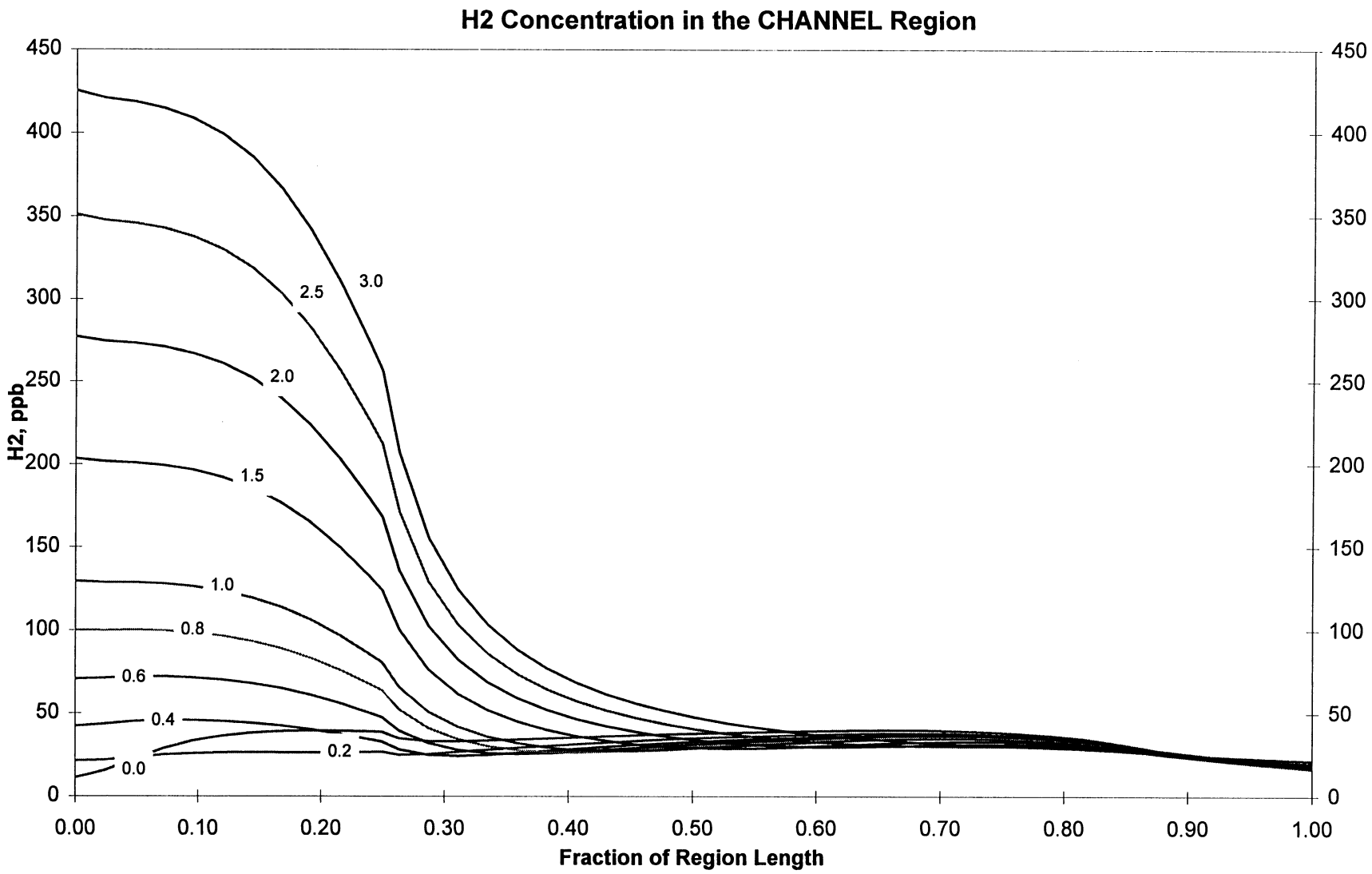

Figure 3-8

BWRJP438 (VERSION 4.38.5)DATED 12/20/94

FITICH2.xlc

EPRI Licensed Material

ALL VALUES ATTACHED TO CURVES INDICATE PPM OF FW H2

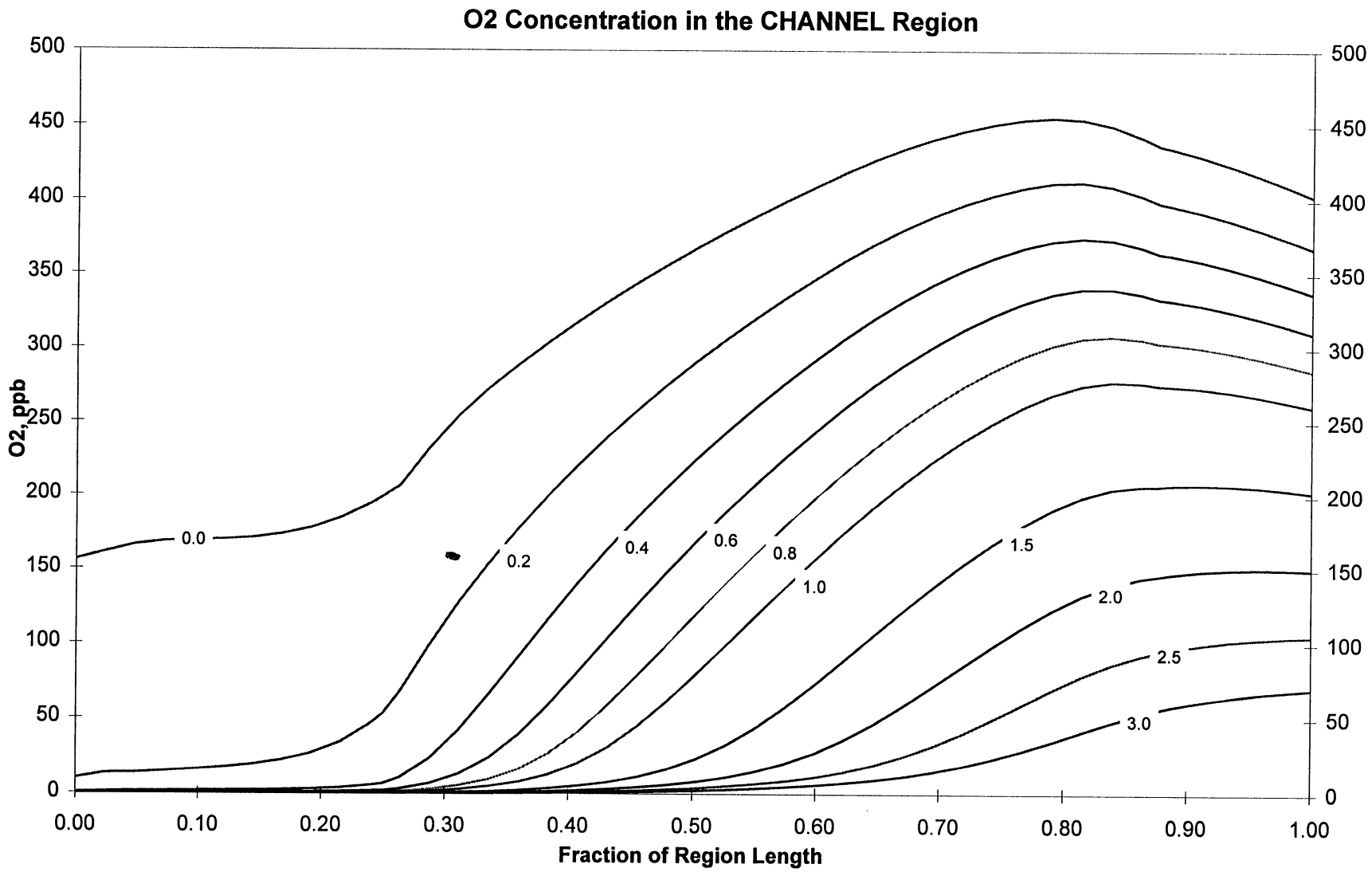

Figure 3-9

BWRJP438 (VERSION 4.38.5)DATED 12/20/94

FITICO2.xlc

EPRI Licensed Material

ALL VALUES ATTACHED TO CURVES INDICATE PPM OF FW H2

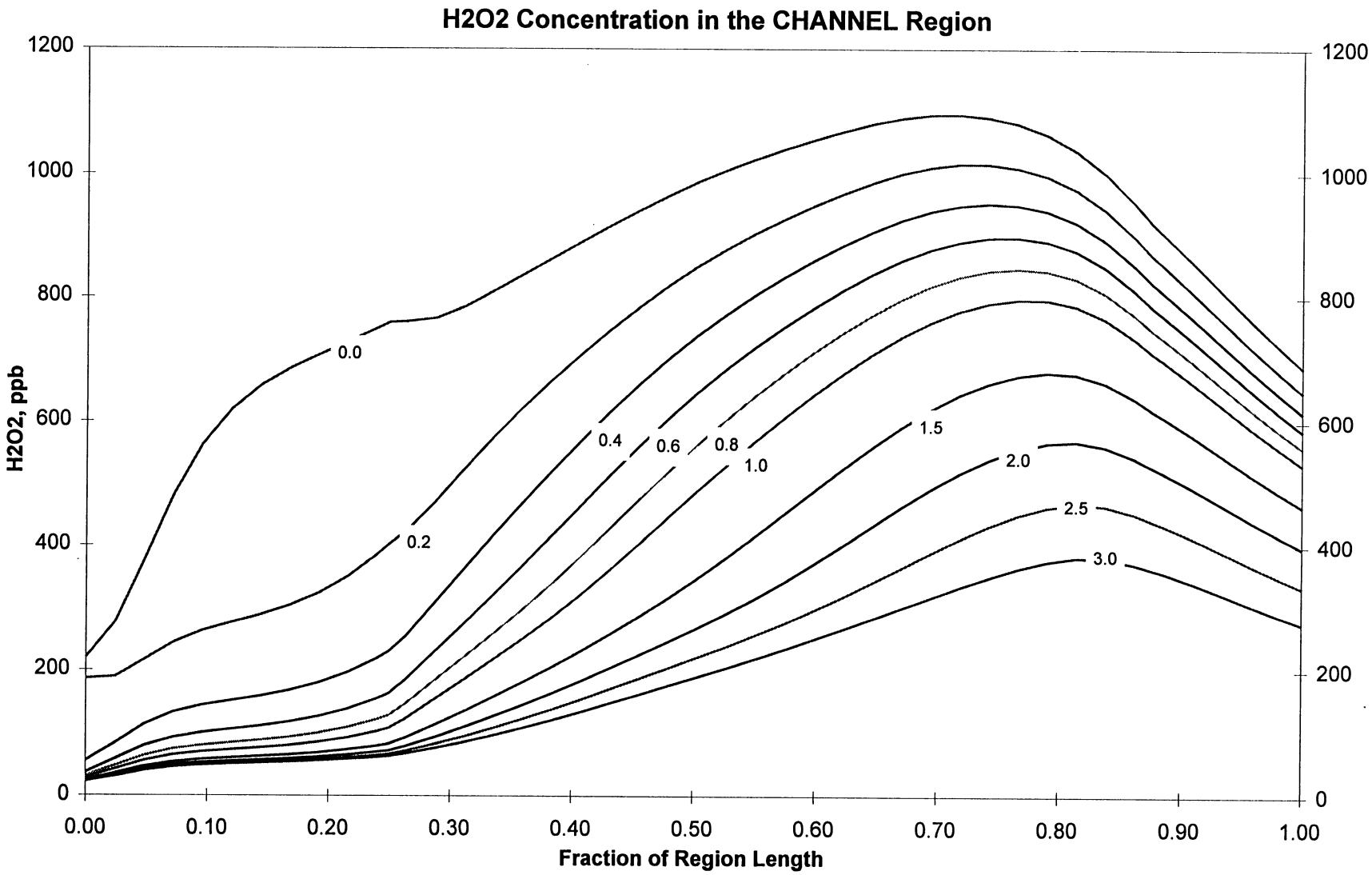

Figure 3-10

BWRJP438 (VERSION 4.38.5)DATED 12/20/94

FITICPER.xlc

EPRI Licensed Material

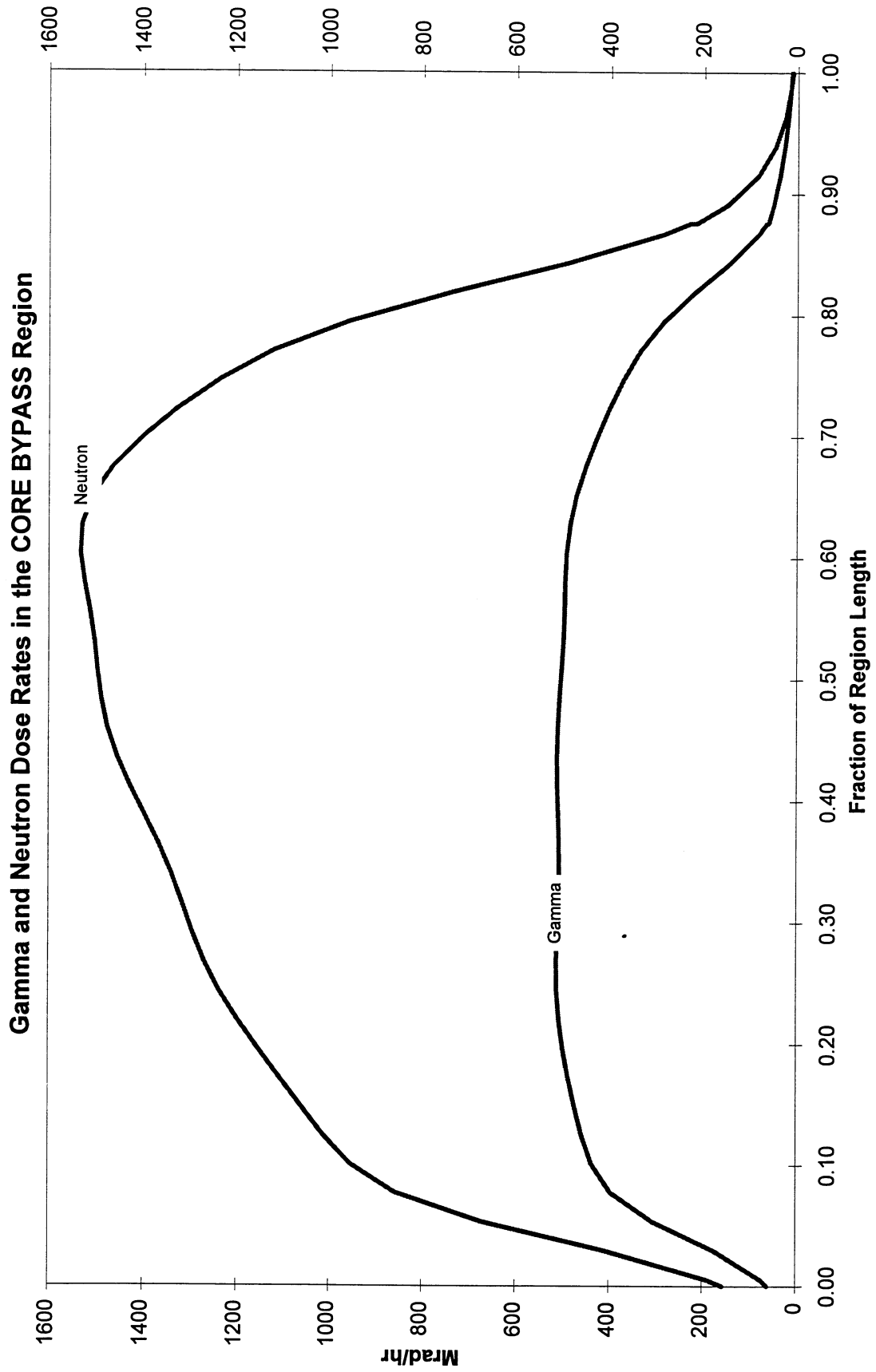

FITCBRRG.xlc

BWRJP438 (VERSION 4.38.5)DATED 12/20/94

Figure 3-11

ALL VALUES ATTACHED TO CURVES INDICATE PPM OF FW H2

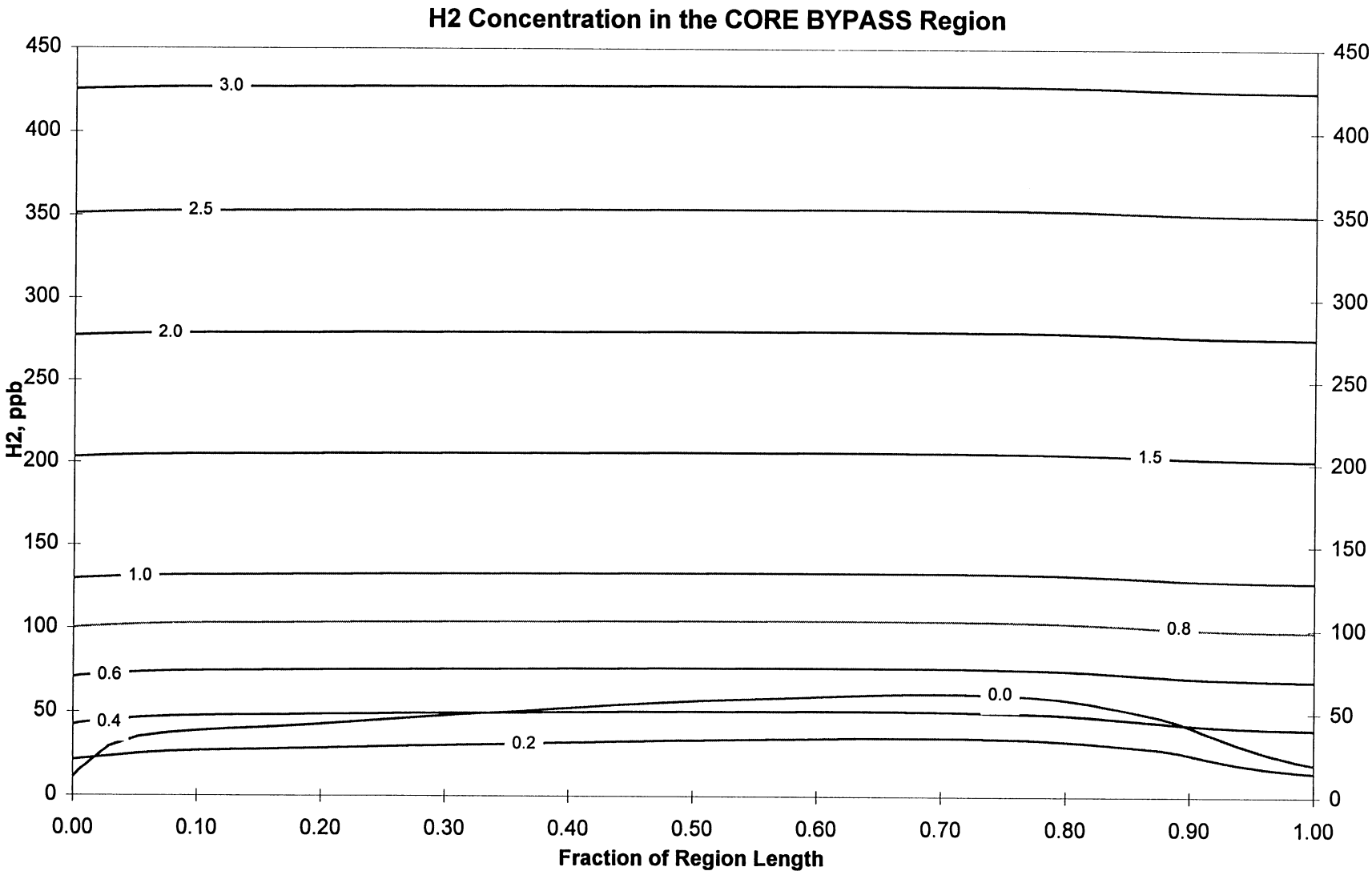

Figure 3-12

BWRJP438 (VERSION 4.38.5)DATED 12/20/94

FITCBH2.xlc

EPRI Licensed Material

ALL VALUES ATTACHED TO CURVES INDICATE PPM OF FW H2

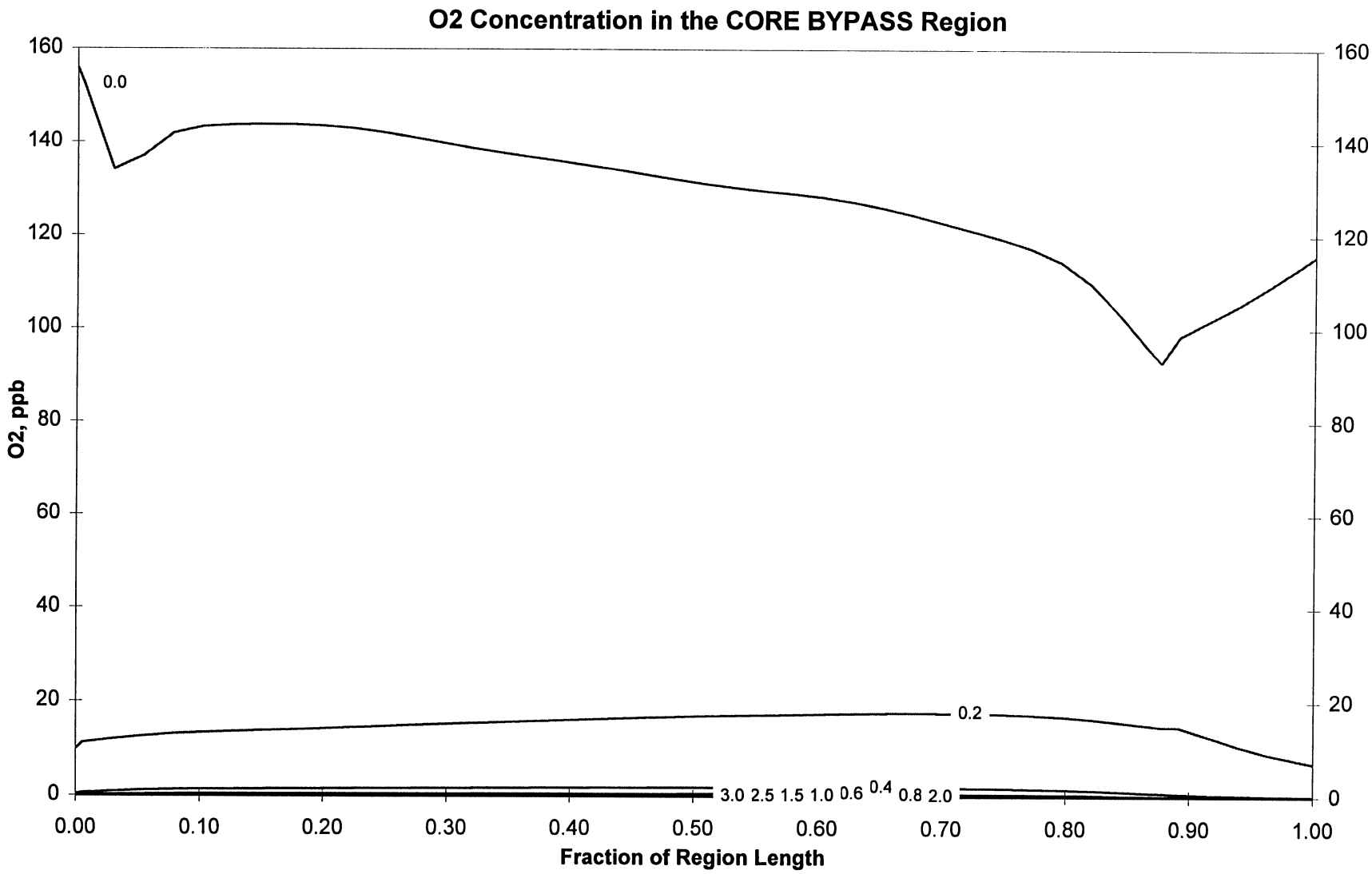

Figure 3-13

BWRJP438 (VERSION 4.38.5)DATED 12/20/94

FITCBO2.xlc

EPRI Licensed Material

ALL VALUES ATTACHED TO CURVES INDICATE PPM OF FW H2

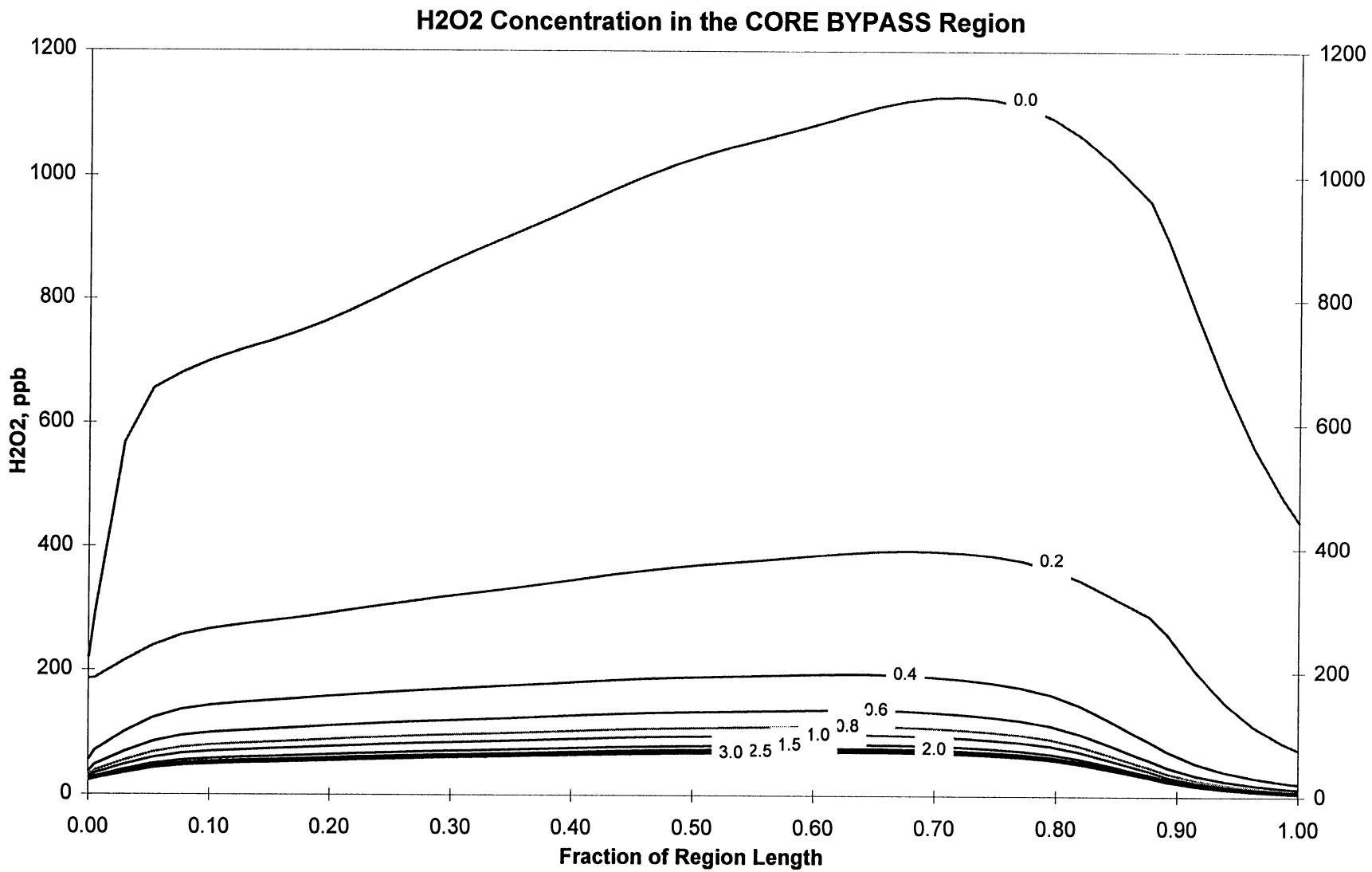

Figure 3-14

BWRJP438 (VERSION 4.38.5)DATED 12/20/94

FITCBPER.xlc

EPRI Licensed Material

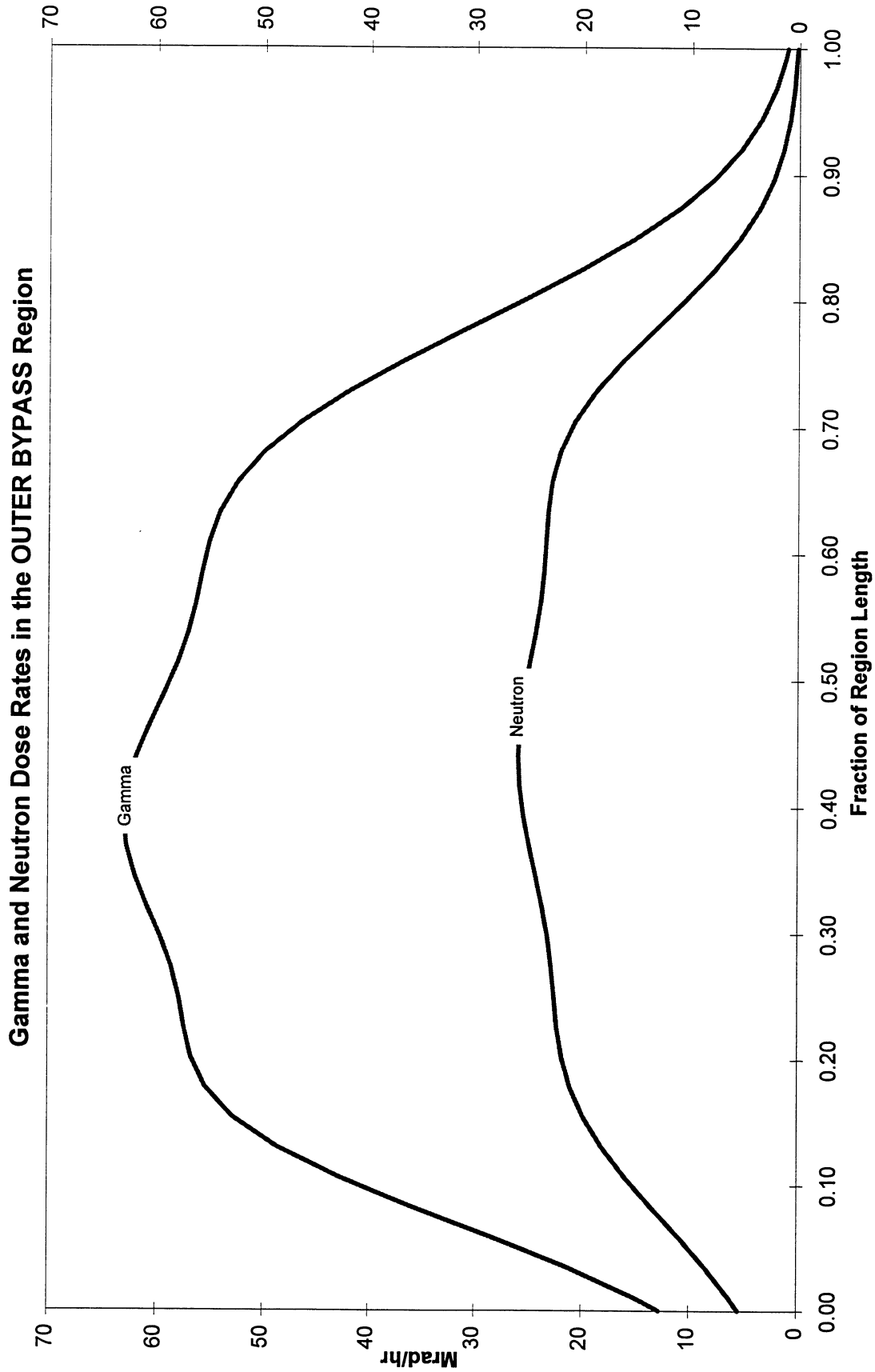

FITOBRRG.xlc

BWRJP438 (VERSION 4.38.5)DATED 12/20/94

Figure 3-15

ALL VALUES ATTACHED TO CURVES INDICATE PPM OF FW H2

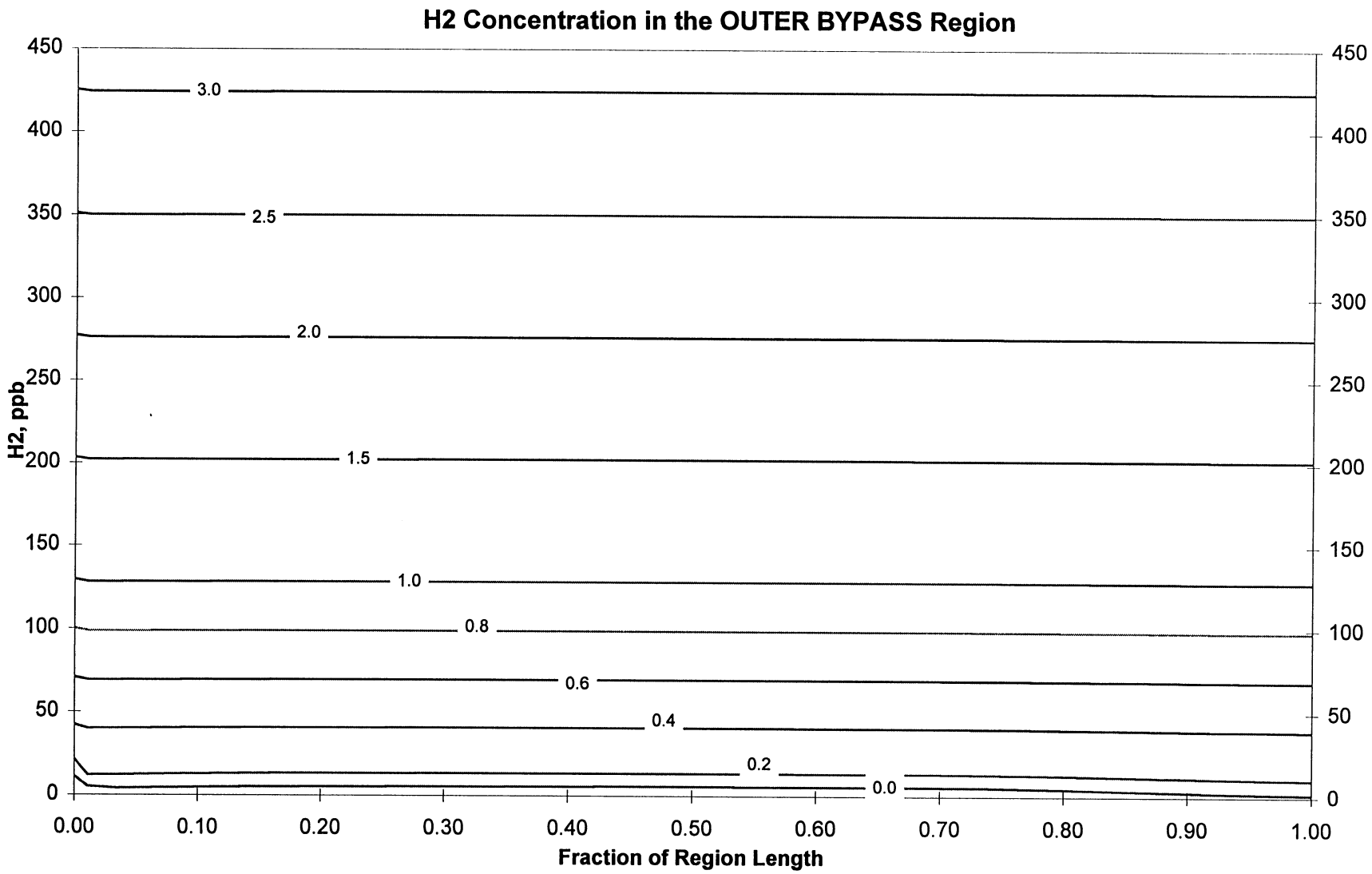

Figure 3-16

BWRJP438 (VERSION 4.38.5)DATED 12/20/94

FITOBH2.xlc

EPRI Licensed Material

ALL VALUES ATTACHED TO CURVES INDICATE PPM OF FW H2

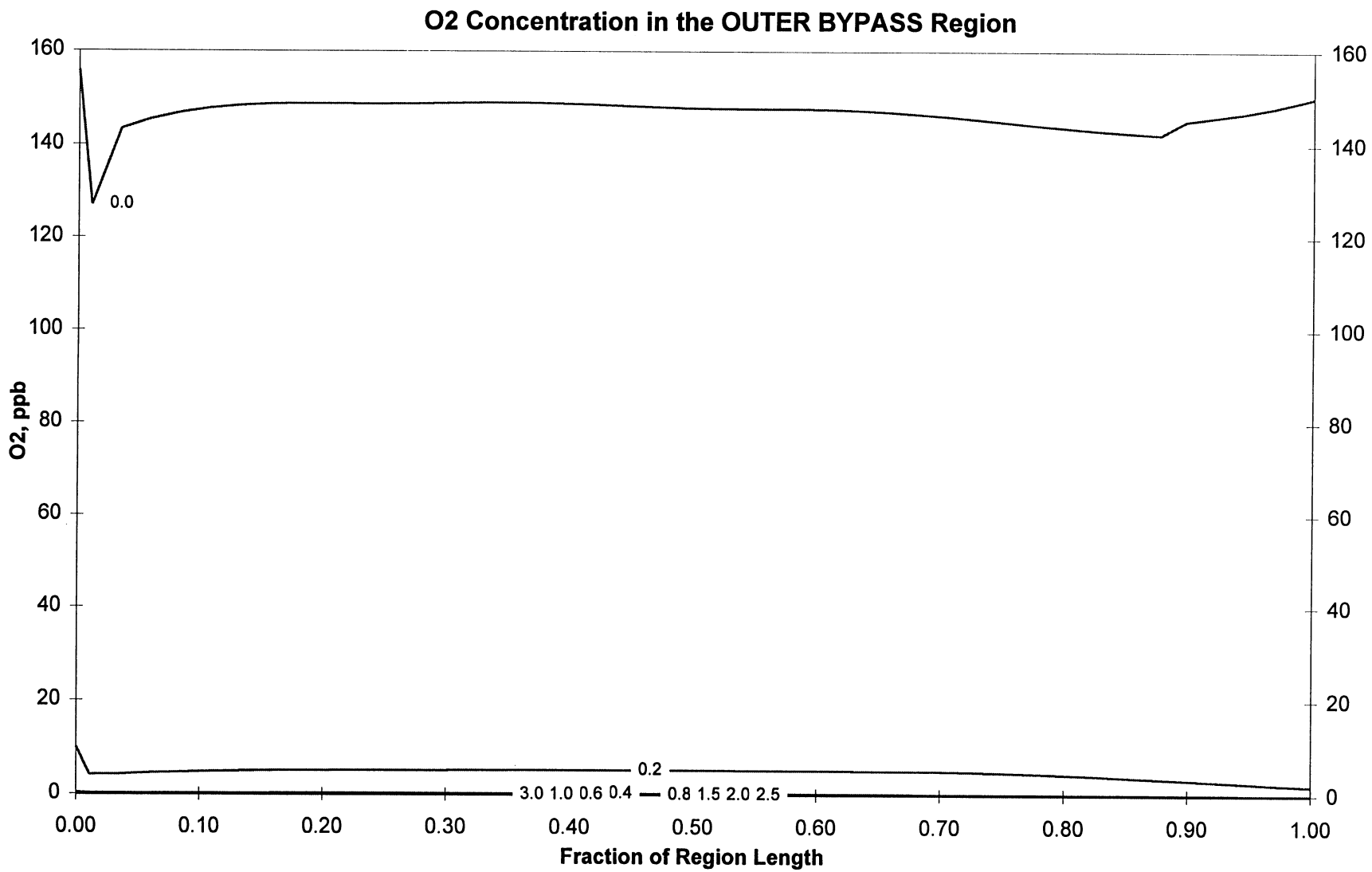

Figure 3-17

BWRJP438 (VERSION 4.38.5)DATED 12/20/94

FITOBO2.xlc

EPRI Licensed Material

ALL VALUES ATTACHED TO CURVES INDICATE PPM OF FW H2

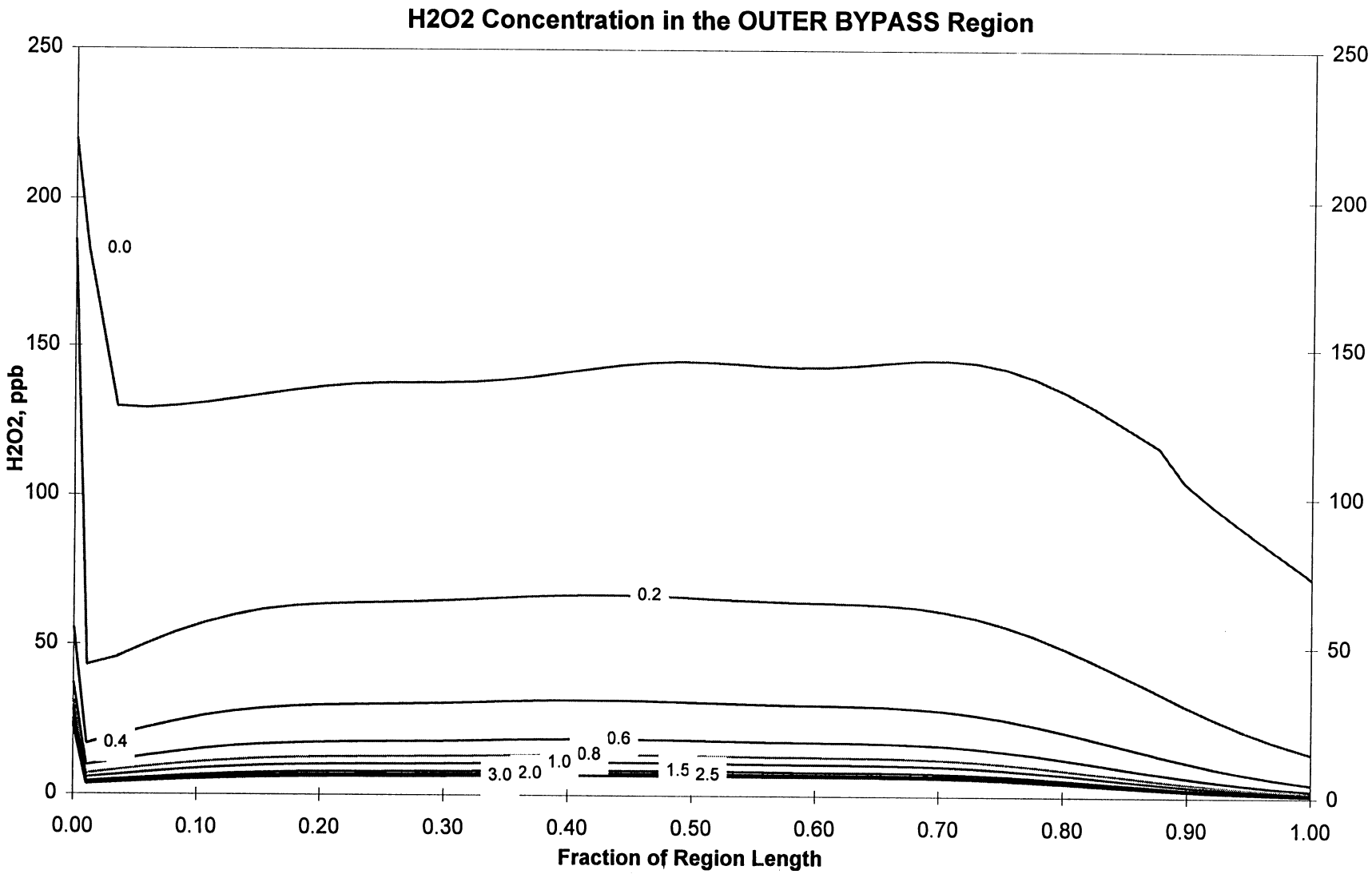

Figure 3-18

BWRJP438 (VERSION 4.38.5)DATED 12/20/94

FITOBPER.xlc

EPRI Licensed Material

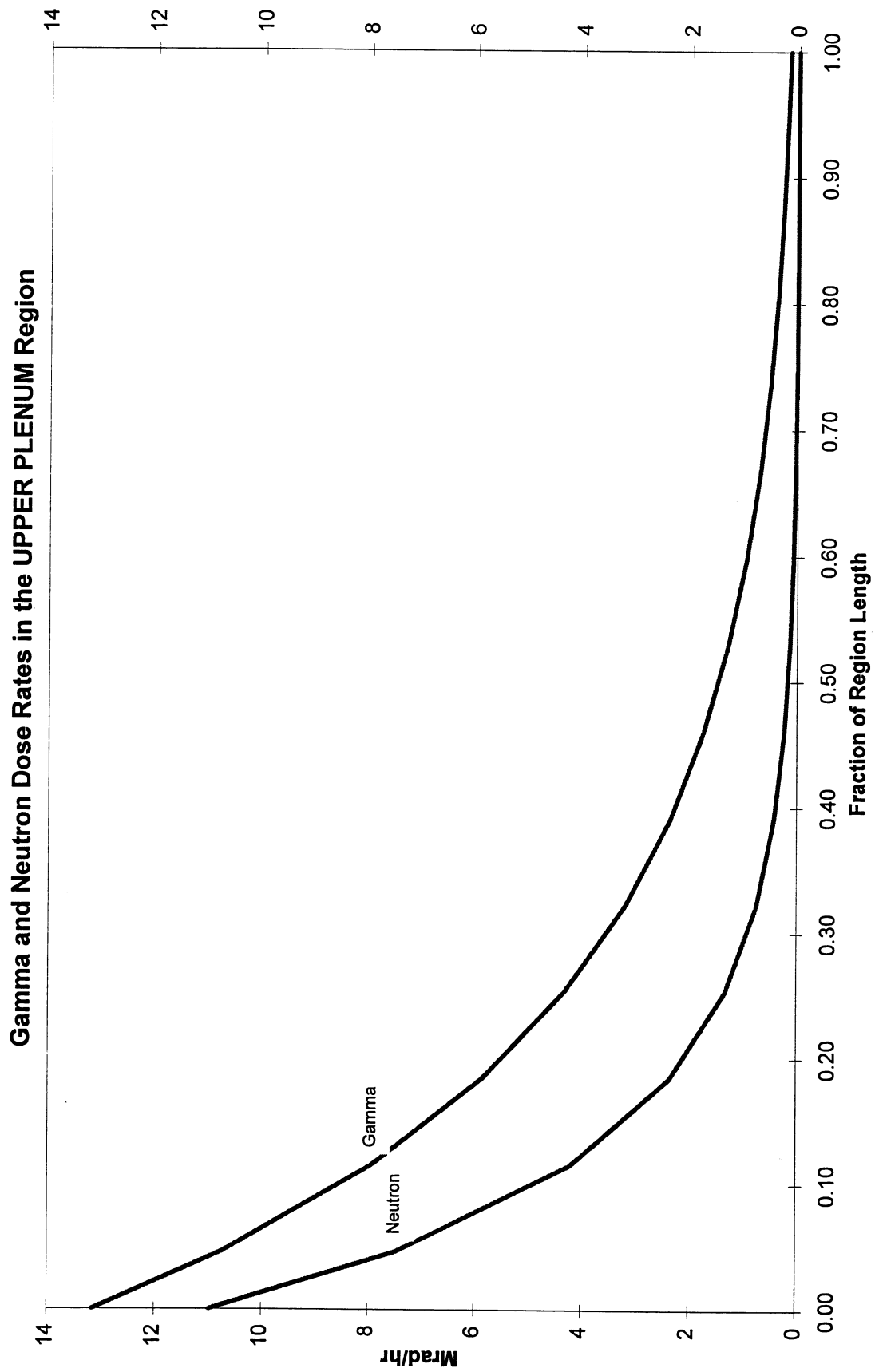

BWRJP438 (VERSION 4.38.5)DATED 12/20/94

FITUPRRG.xlc

Figure 3-19

ALL VALUES ATTACHED TO CURVES INDICATE PPM OF FW H2

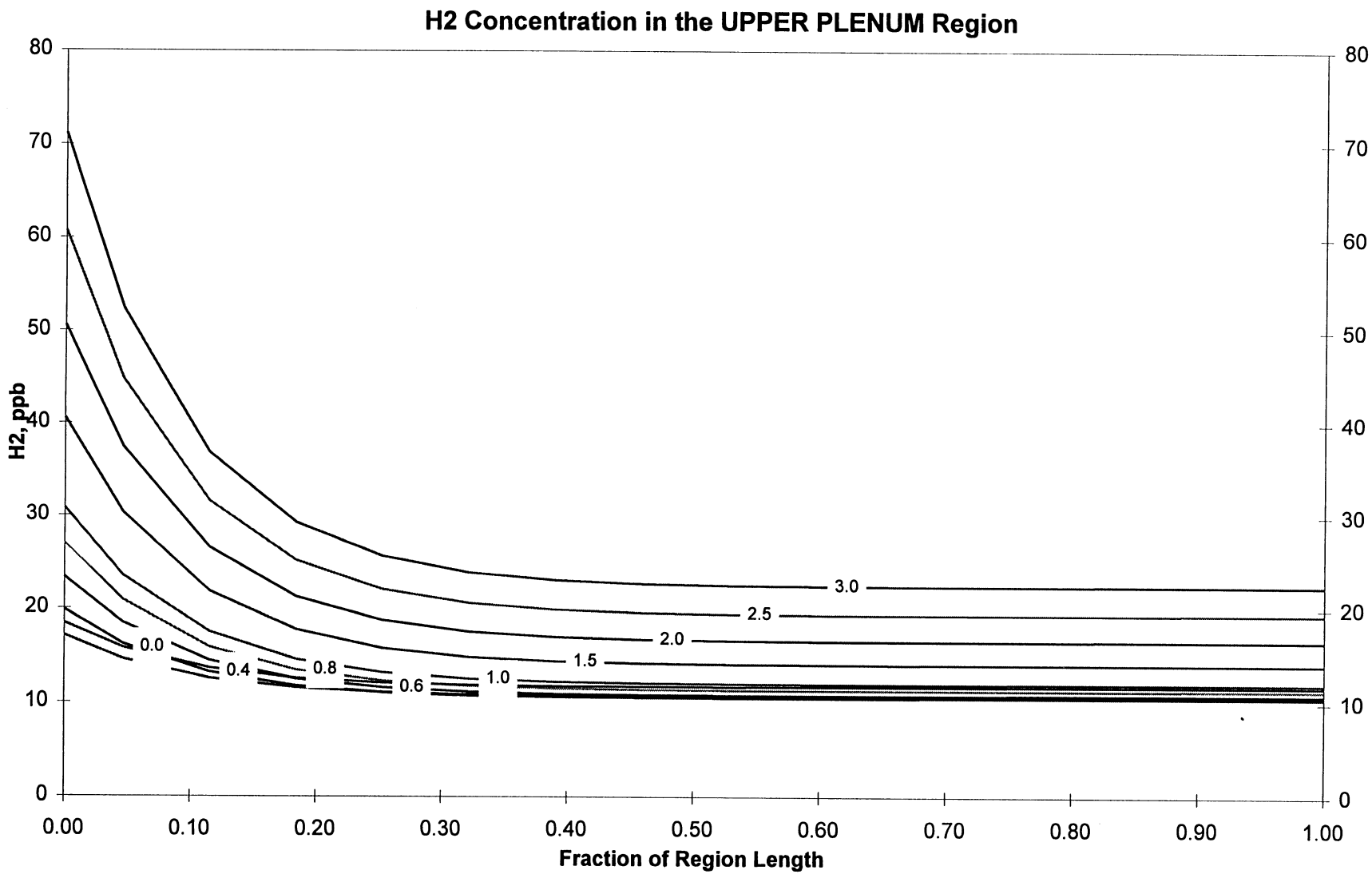

Figure 3-20

BWRJP438 (VERSION 4.38.5)DATED 12/20/94

FITUPH2.xlc

EPRI Licensed Material

ALL VALUES ATTACHED TO CURVES INDICATE PPM OF FW H2

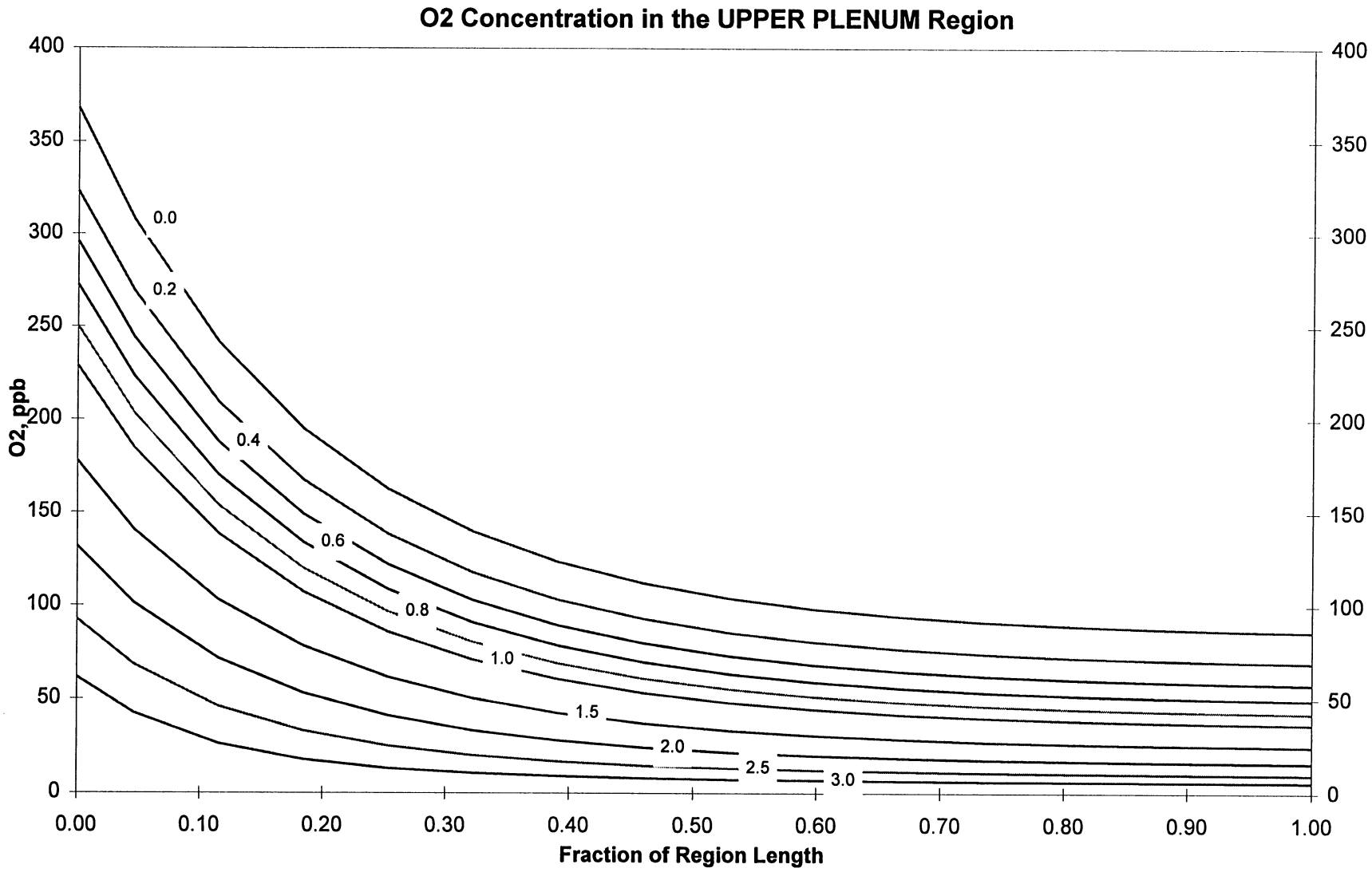

Figure 3-21

BWRJP438 (VERSION 4.38.5)DATED 12/20/94

FITUPO2.xlc

EPRI Licensed Material

ALL VALUES ATTACHED TO CURVES INDICATE PPM OF FW H2

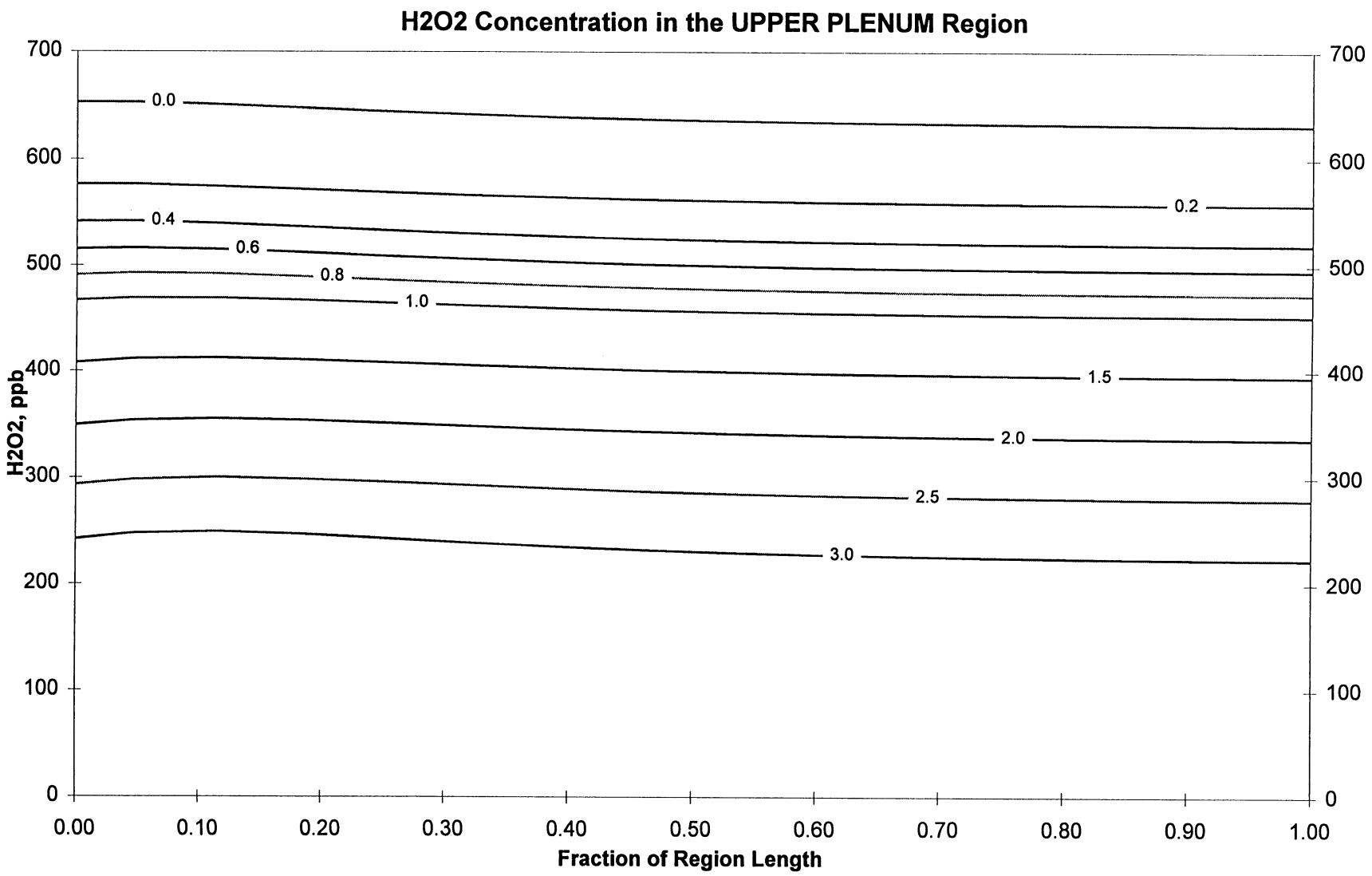

Figure 3-22

BWRJP438 (VERSION 4.38.5)DATED 12/20/94

FITUPPER.xlc

EPRI Licensed Material

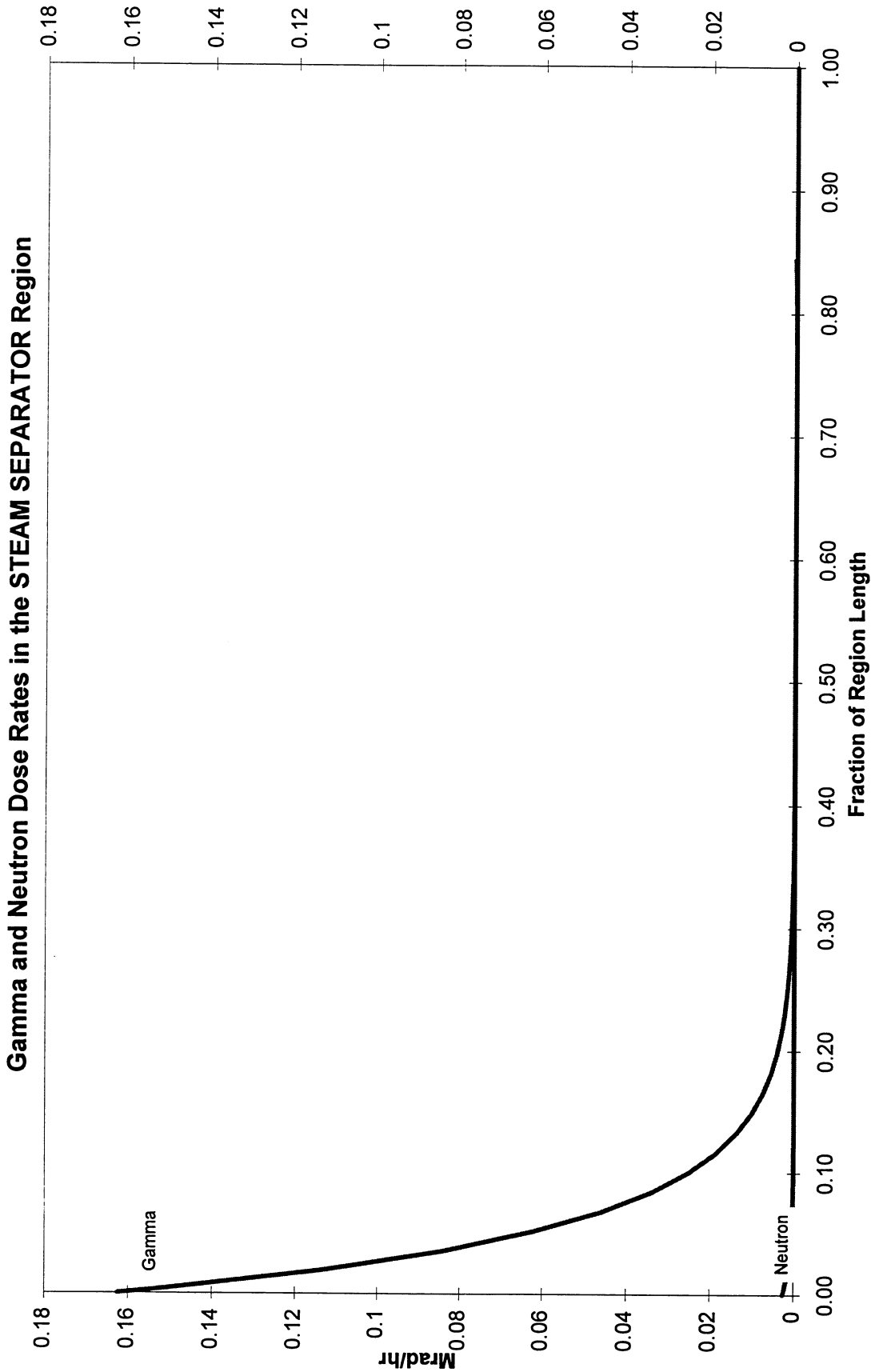

BWRJP438 (VERSION 4.38.5)DATED 12/20/94

FITSSRRG.xlc

Figure 3-23

ALL VALUES ATTACHED TO CURVES INDICATE PPM OF FW H2

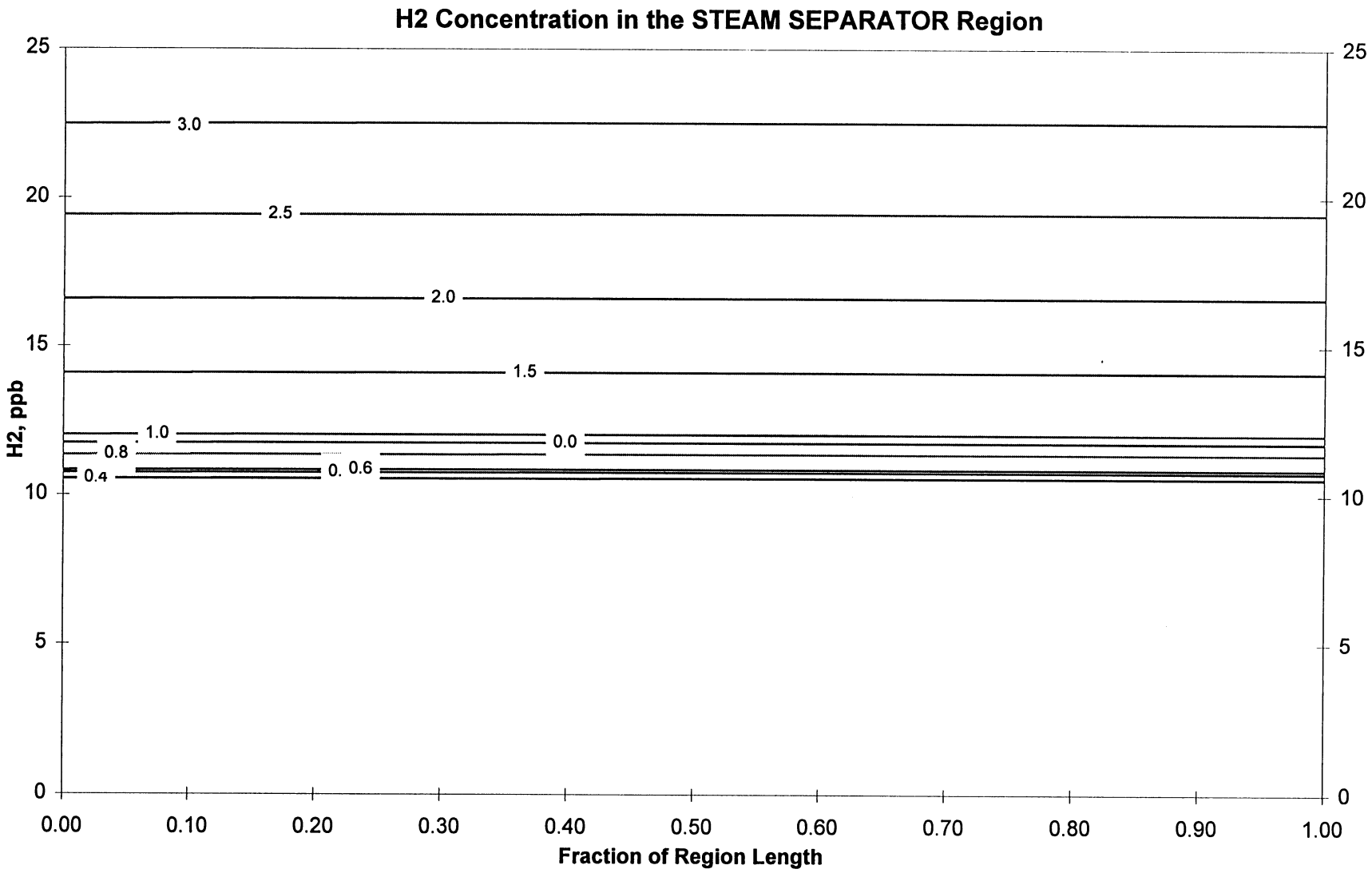

Figure 3-24

BWRJP438 (VERSION 4.38.5)DATED 12/20/94

FITSSH2.xlc

EPRI Licensed Material

ALL VALUES ATTACHED TO CURVES INDICATE PPM OF FW H2

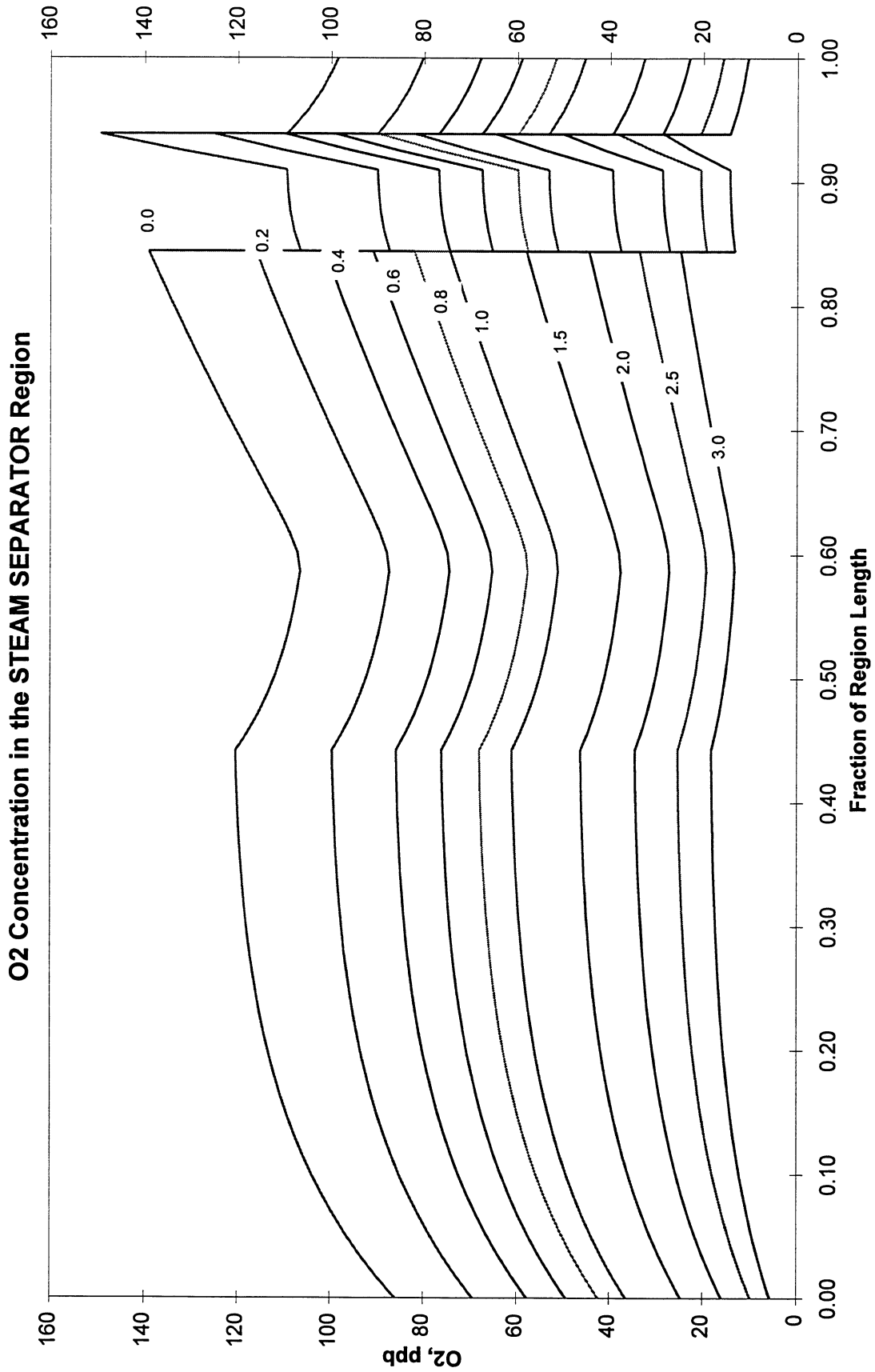

BWRJP438 (VERSION 4.38.5)DATED 12/20/94

FITSSO2.xlc

Figure 3-25

ALL VALUES ATTACHED TO CURVES INDICATE PPM OF FW H2

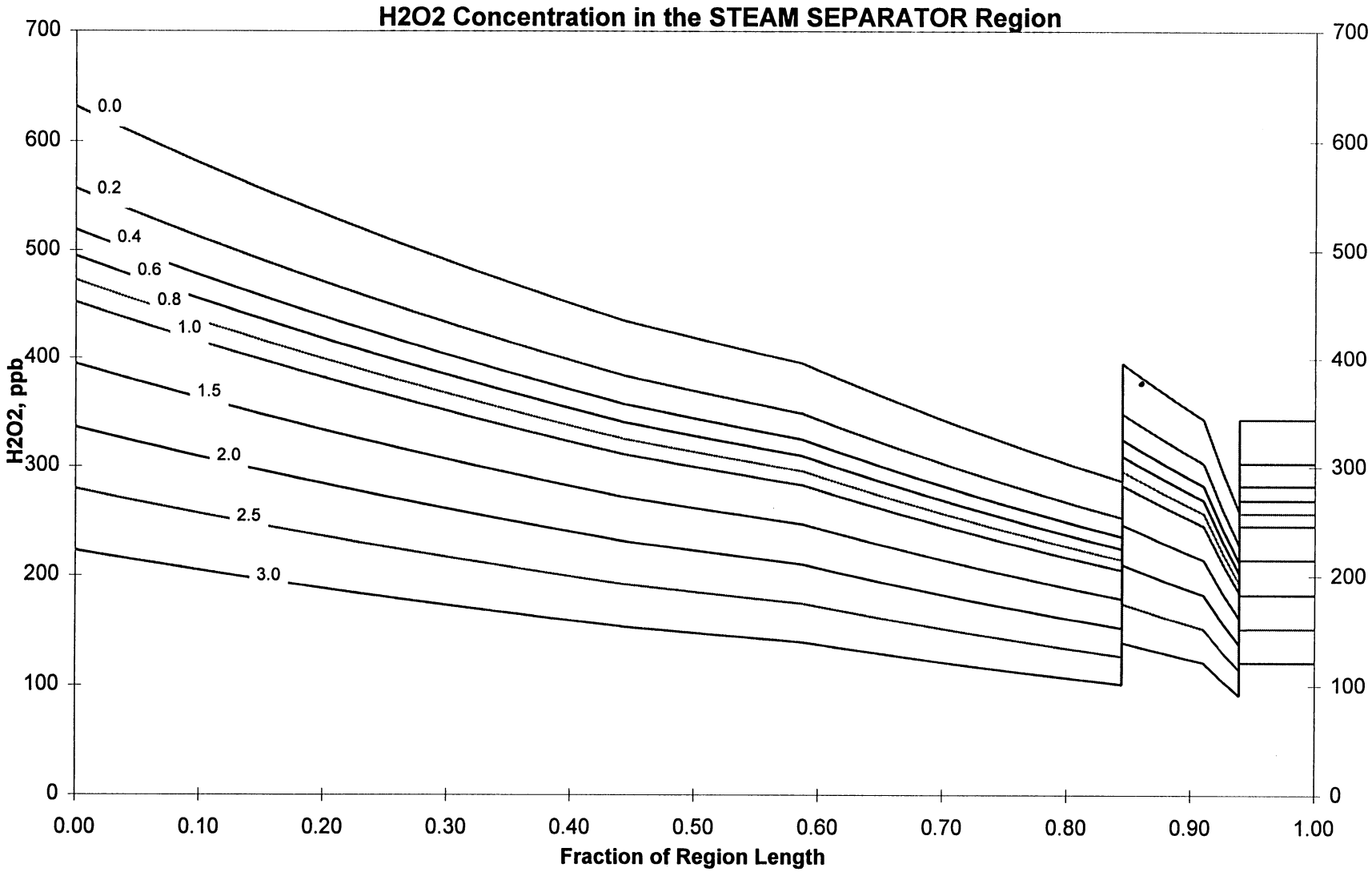

Figure 3-26

BWRJP438 (VERSION 4.38.5)DATED 12/20/94

FITSSPER.xlc

EPRI Licensed Material

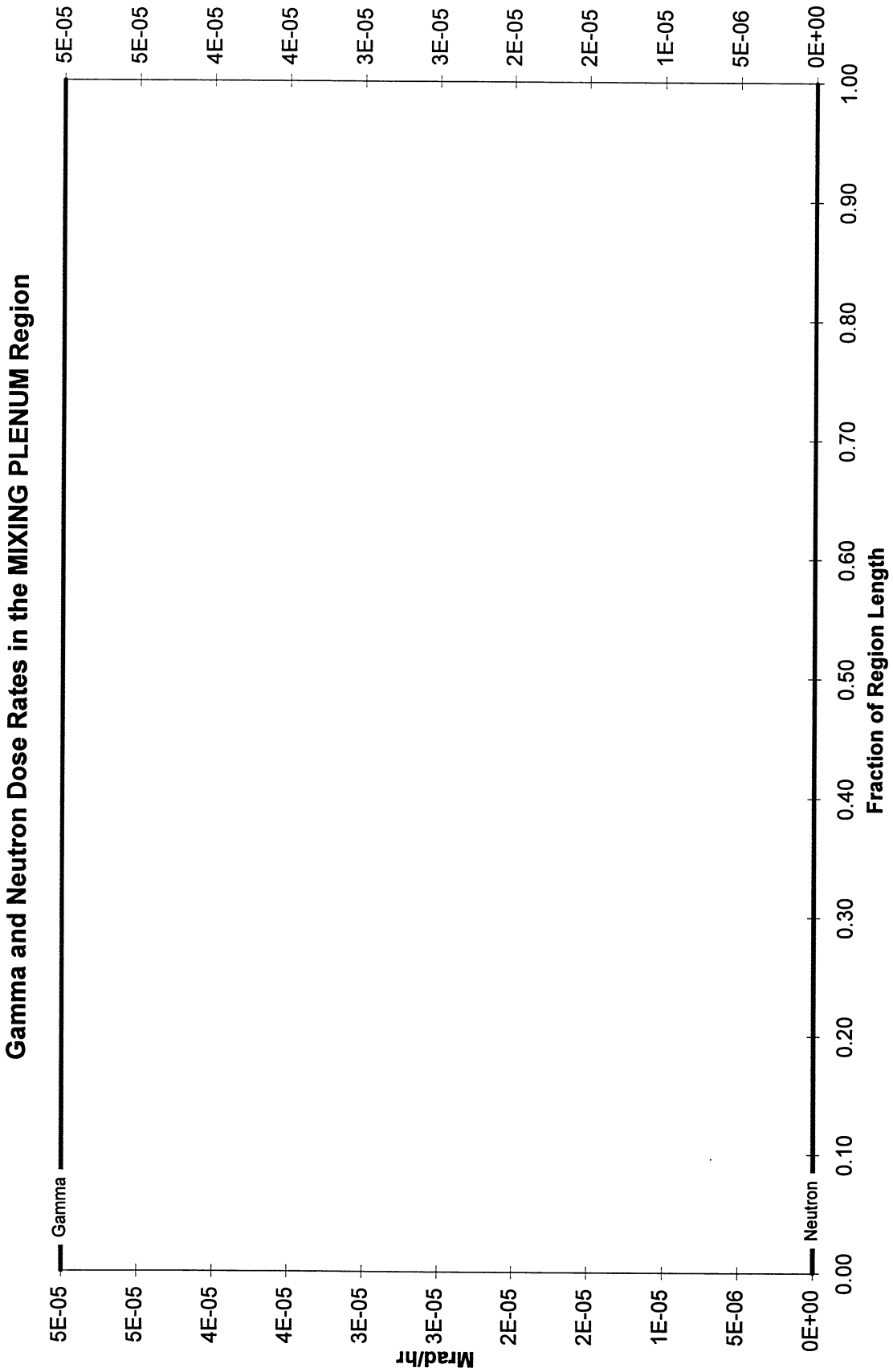

BWRJP438 (VERSION 4.38.5)DATED 12/20/94

FITMPRRG.xlc

Figure 3-27

ALL VALUES ATTACHED TO CURVES INDICATE PPM OF FW H2

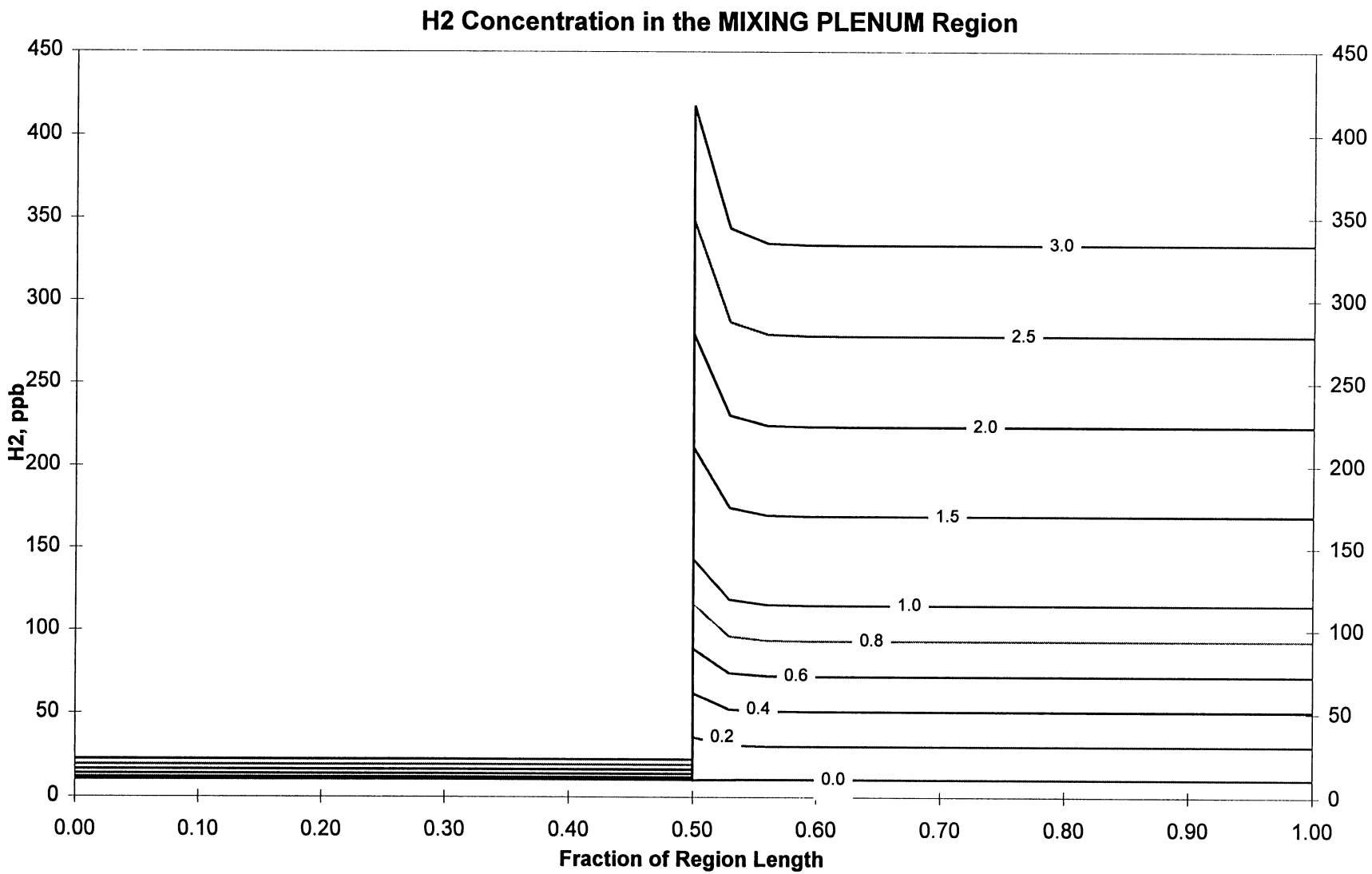

Figure 3-28

BWRJP438 (VERSION 4.38.5)DATED 12/20/94

FITMPH2.xlc

EPRI Licensed Material

ALL VALUES ATTACHED TO CURVES INDICATE PPM OF FW H2

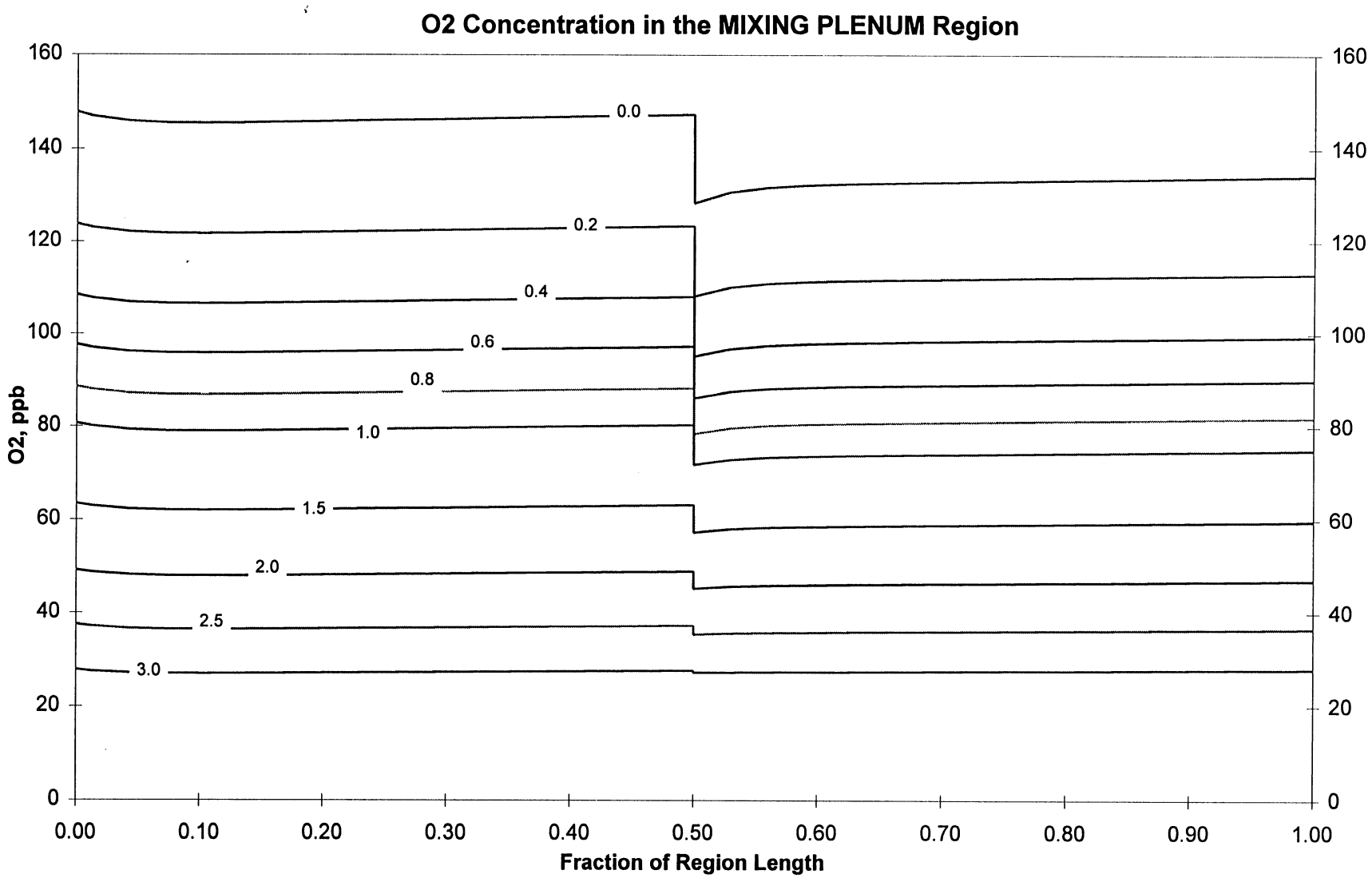

Figure 3-29

BWRJP438 (VERSION 4.38.5)DATED 12/20/94

FITMPO2.xlc

EPRI Licensed Material

ALL VALUES ATTACHED TO CURVES INDICATE PPM OF FW H2

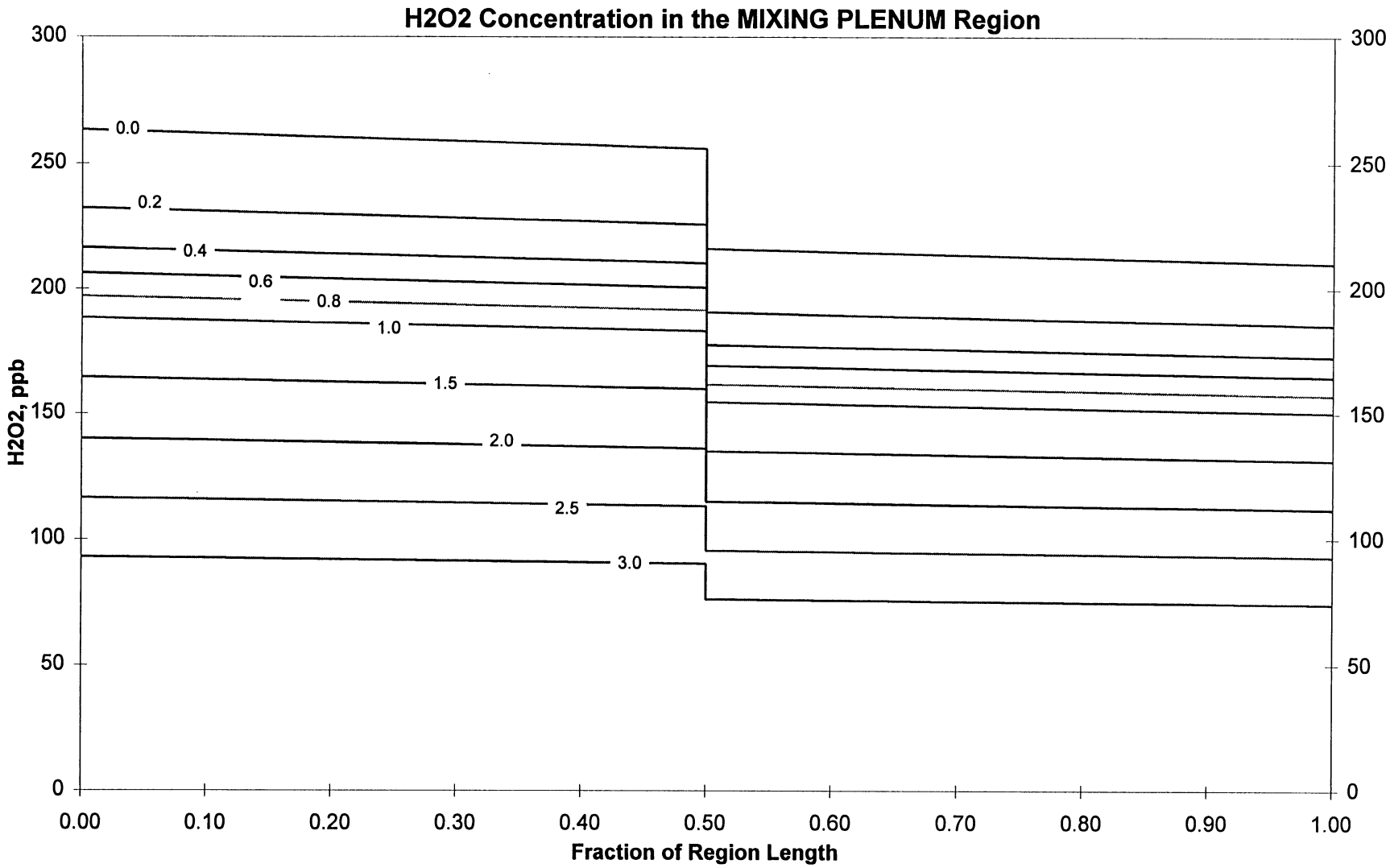

Figure 3-30

BWRJP438 (VERSION 4.38.5)DATED 12/20/94

FITMPPER.xlc

EPRI Licensed Material

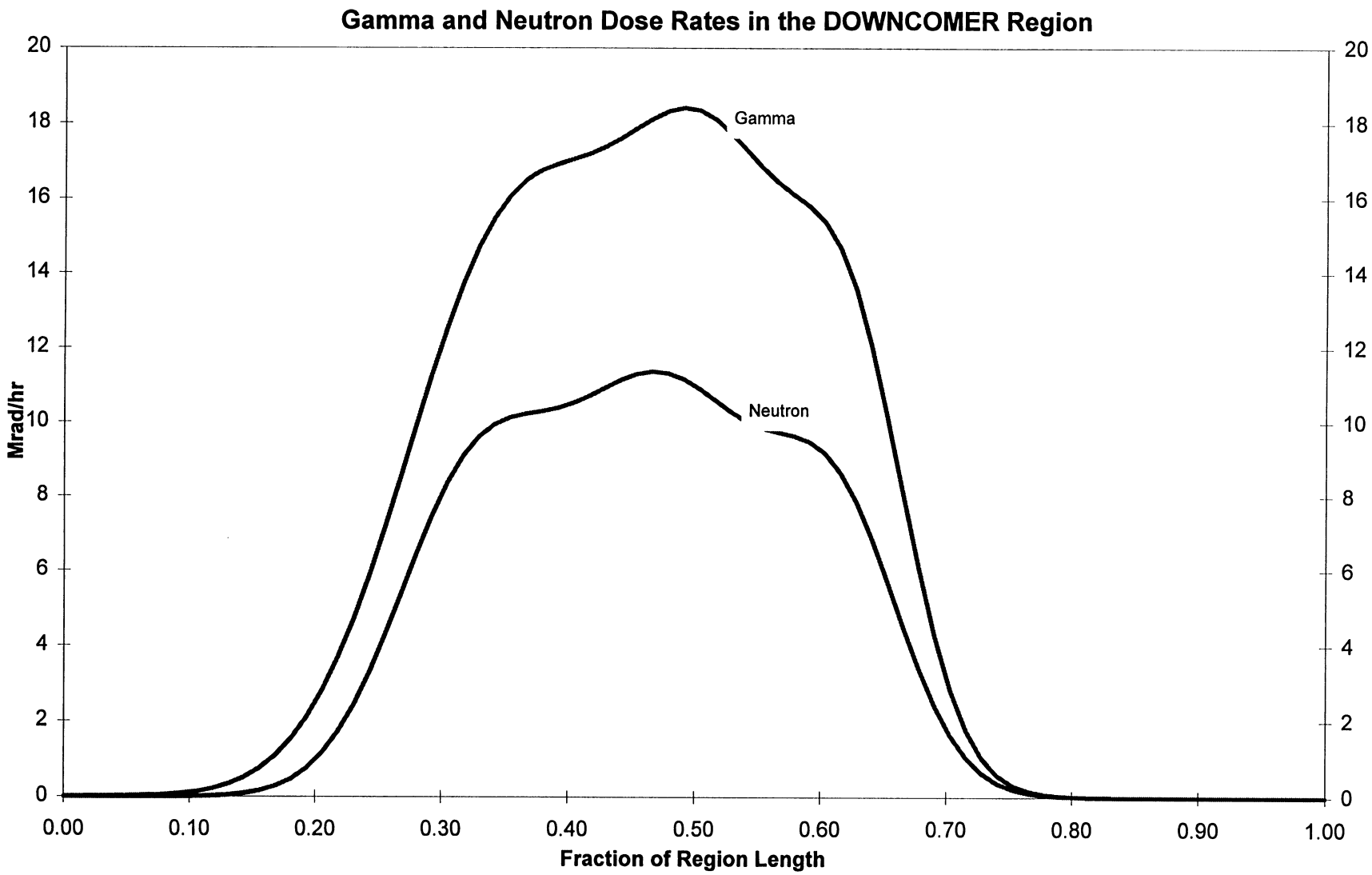

Figure 3-31

BWRJP438 (VERSION 4.38.5)DATED 12/20/94

FITDCRRG.xlc

EPRI Licensed Material

ALL VALUES ATTACHED TO CURVES INDICATE PPM OF FW H2

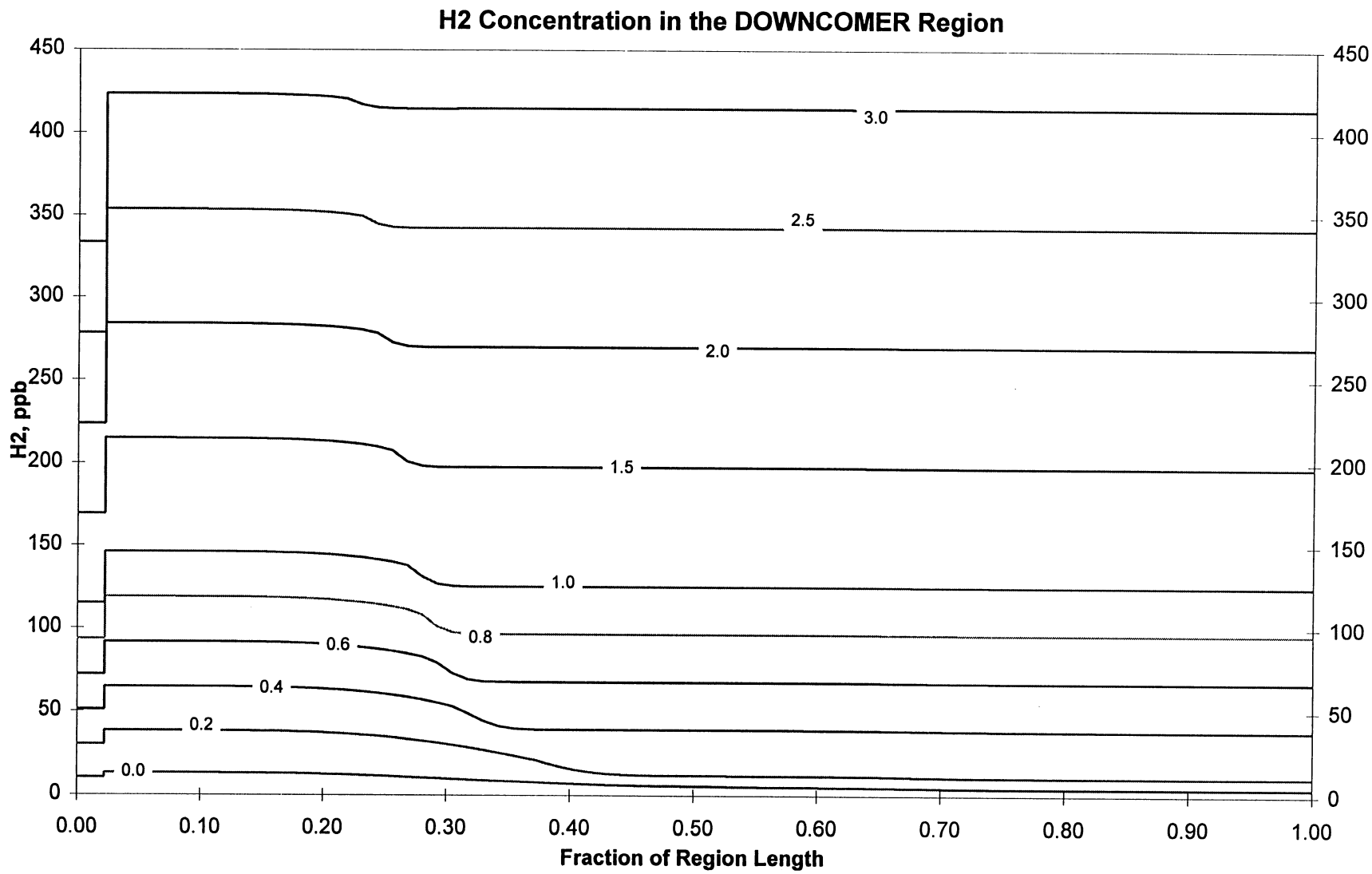

Figure 3-32

BWRJP438 (VERSION 4.38.5)DATED 12/20/94

FITDCH2.xlc

EPRI Licensed Material

ALL VALUES ATTACHED TO CURVES INDICATE PPM OF FW H2

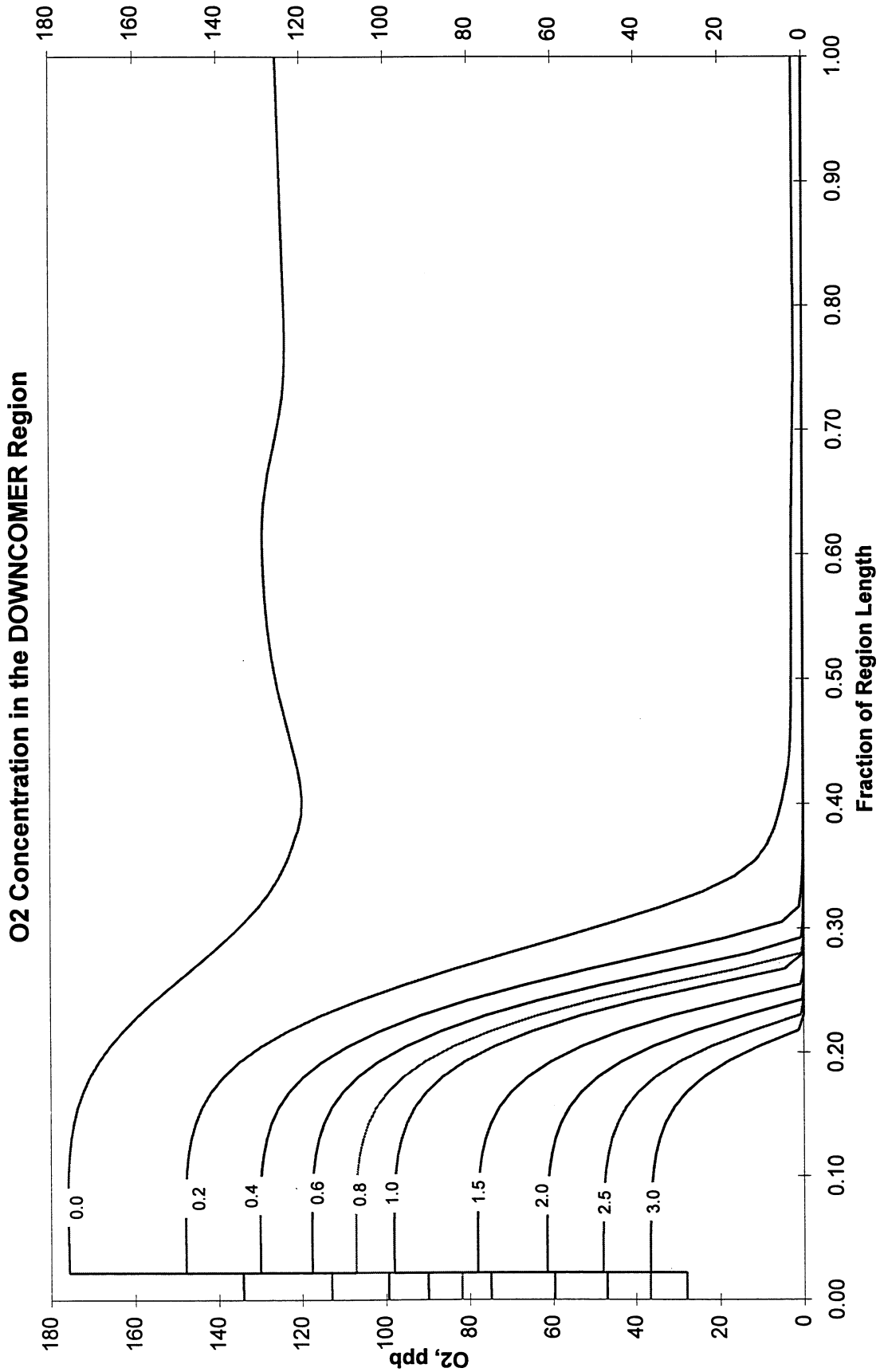

BWRJP438 (VERSION 4.38.5)DATED 12/20/94

FITDCO2.xlc

Figure 3-33

ALL VALUES ATTACHED TO CURVES INDICATE PPM OF FW H2

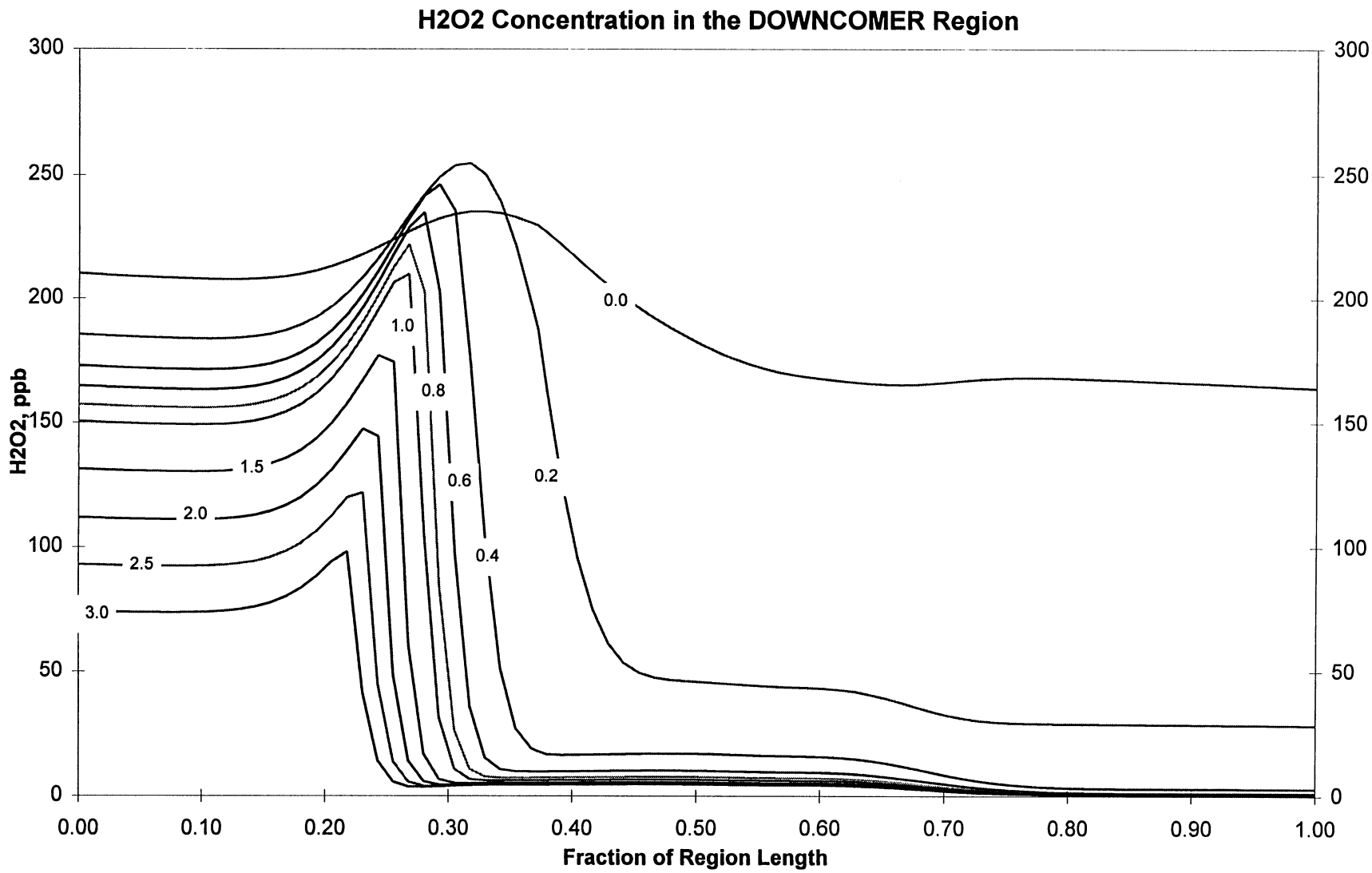

Figure 3-34

BWRJP438 (VERSION 4.38.5)DATED 12/20/94

FITDCPER.xlc

EPRI Licensed Material

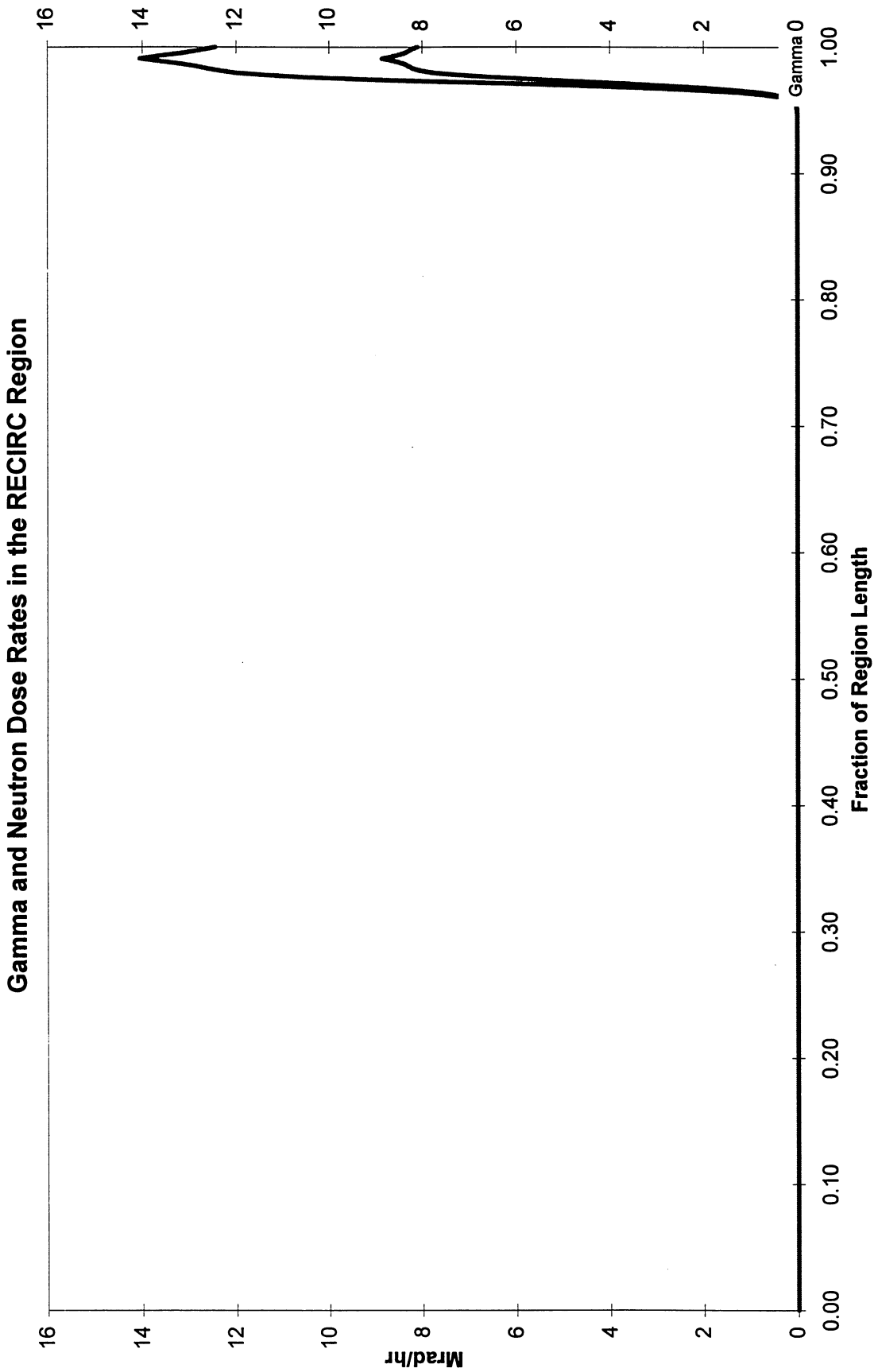

BWRJP438 (VERSION 4.38.5)DATED 12/20/94

FITRERRG.xlc

Figure 3-35

ALL VALUES ATTACHED TO CURVES INDICATE PPM OF FW H2

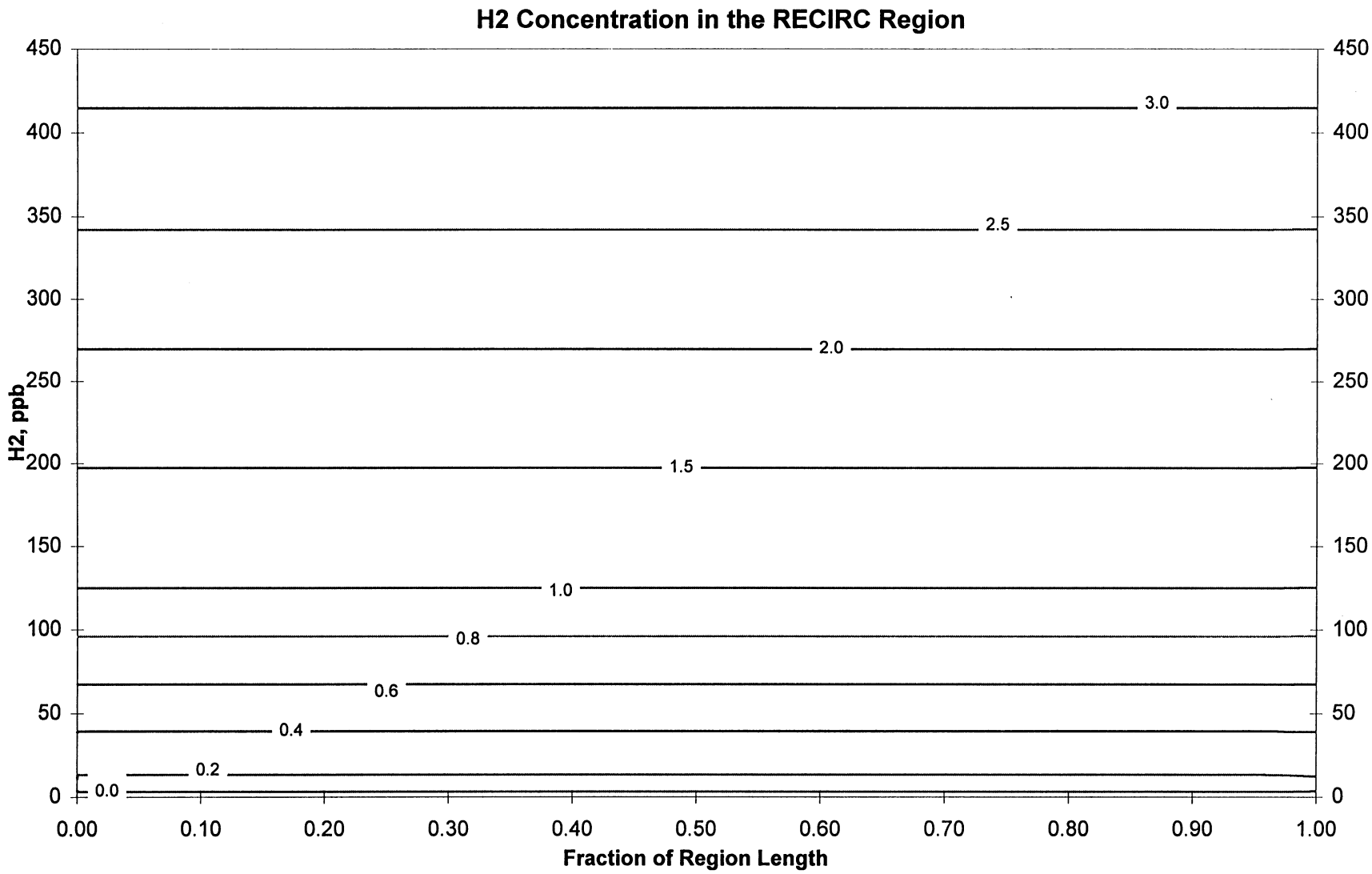

Figure 3-36

BWRJP438 (VERSION 4.38.5)DATED 12/20/94

FITREH2.xlc

EPRI Licensed Material

ALL VALUES ATTACHED TO CURVES INDICATE PPM OF FW H2

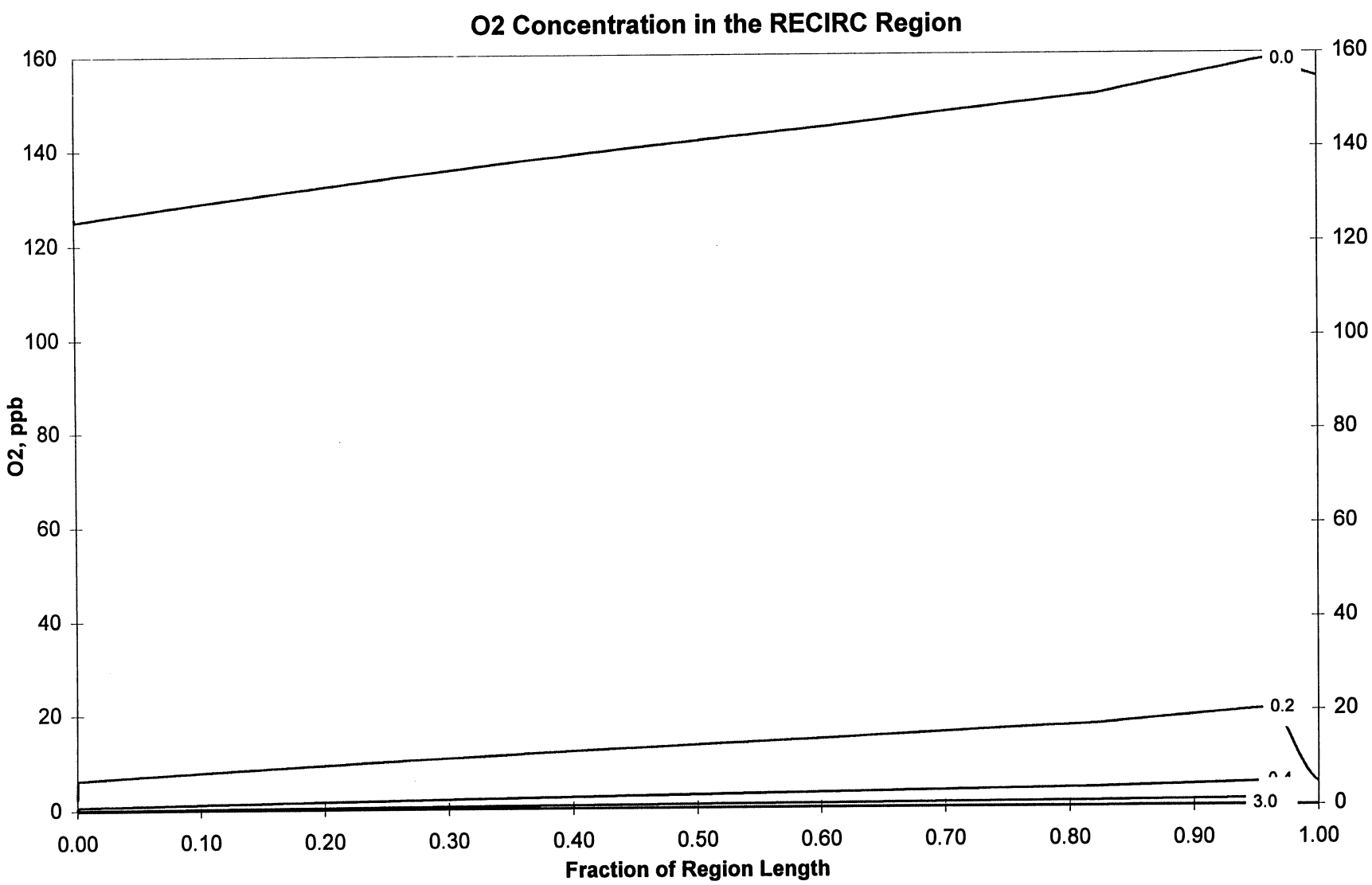

Figure 3-37

BWRJP438 (VERSION 4.38.5)DATED 12/20/94

FITREO2.xlc

EPRI Licensed Material

ALL VALUES ATTACHED TO CURVES INDICATE PPM OF FW H2

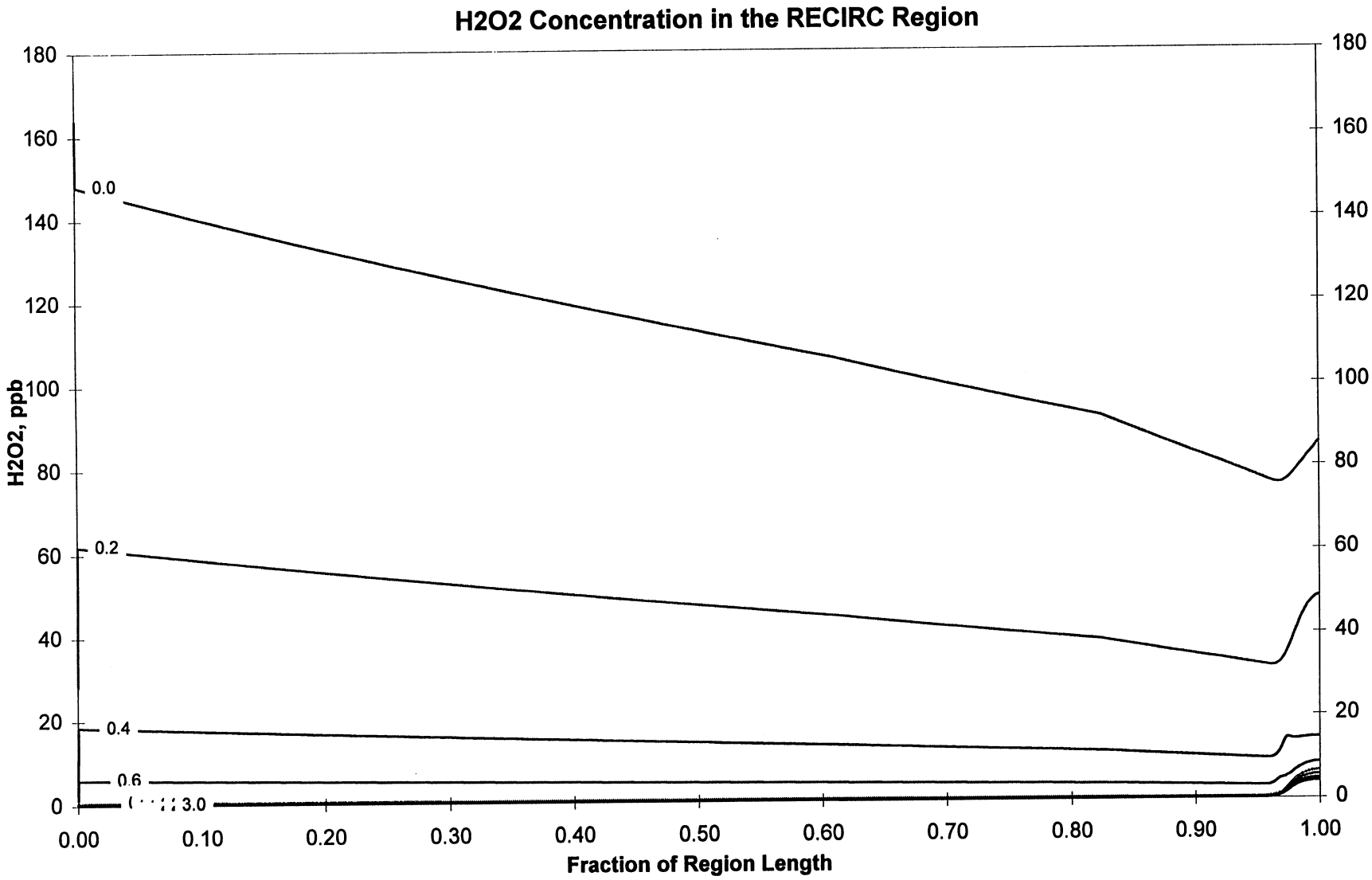

Figure 3-38

BWRJP438 (VERSION 4.38.5)DATED 12/20/94

FITREPER.xlc

EPRI Licensed Material

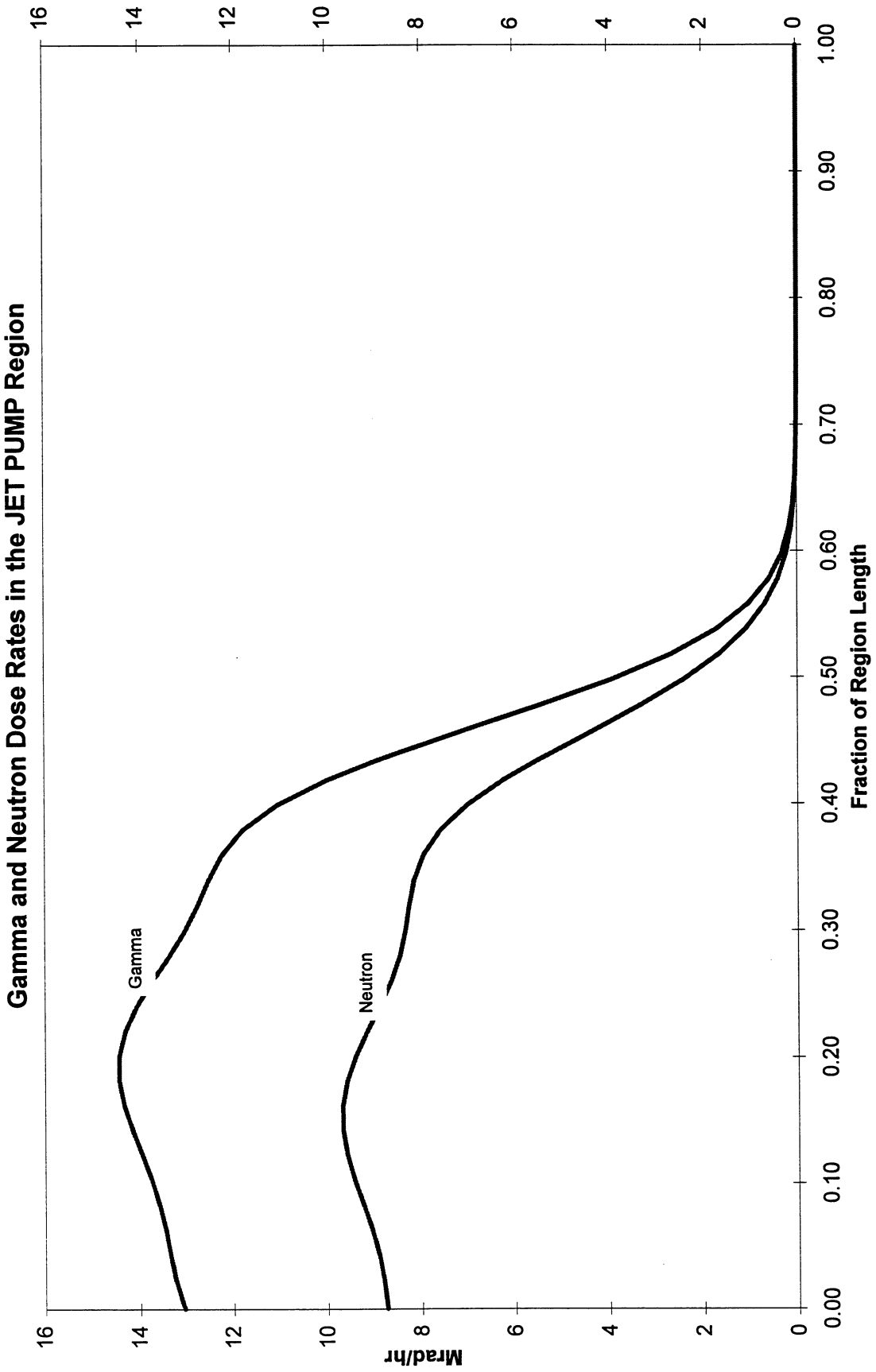

FIT:JPRRG.xlc

BWRJP438 (VERSION 4.38.5)DATED 12/20/94

Figure 3-39

ALL VALUES ATTACHED TO CURVES INDICATE PPM OF FW H2

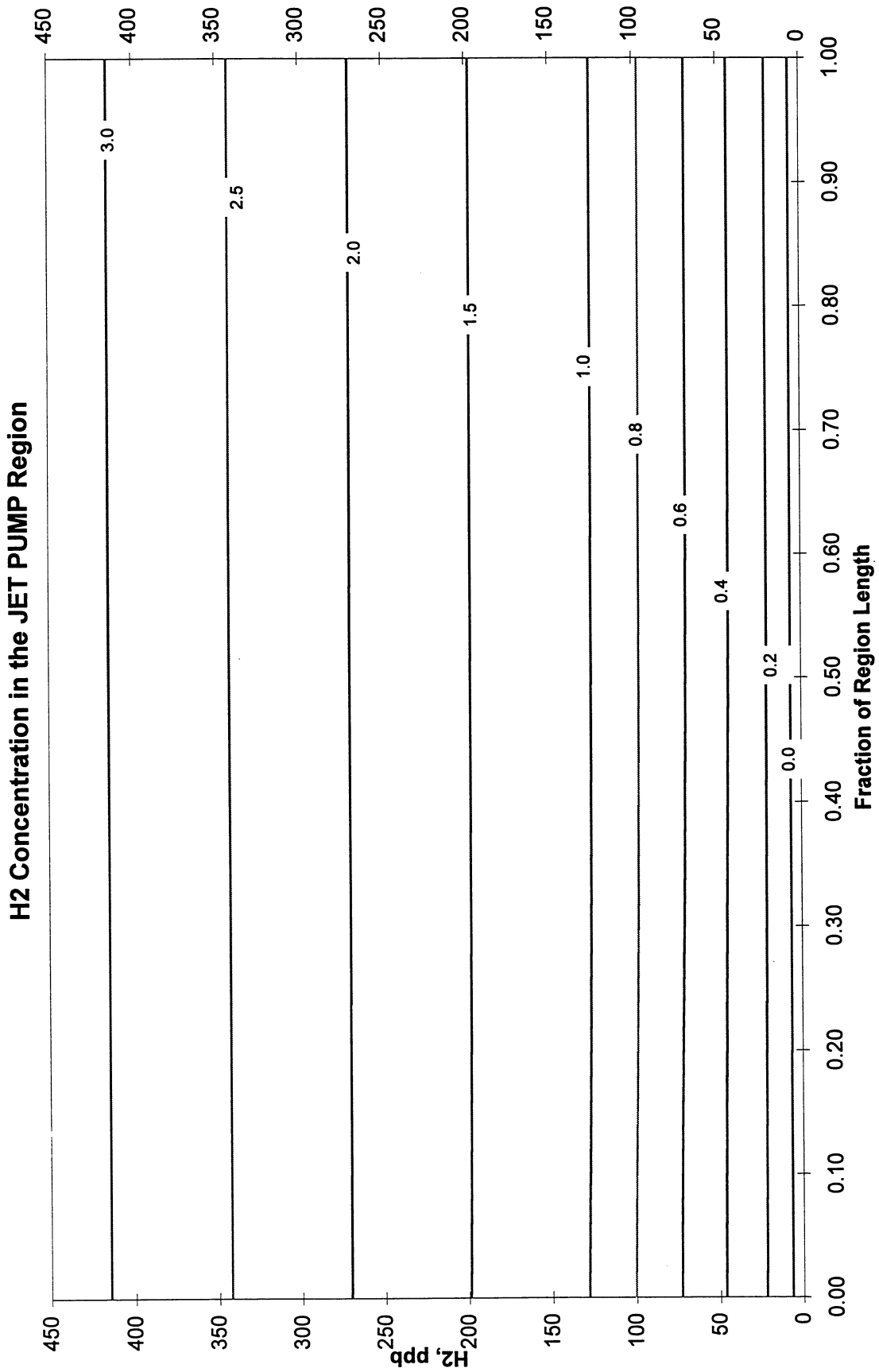

FITJPH2.xlc

BWRJP438 (VERSION 4.38.5)DATED 12/20/94

Figure 3-40

ALL VALUES ATTACHED TO CURVES INDICATE PPM OF FW H2

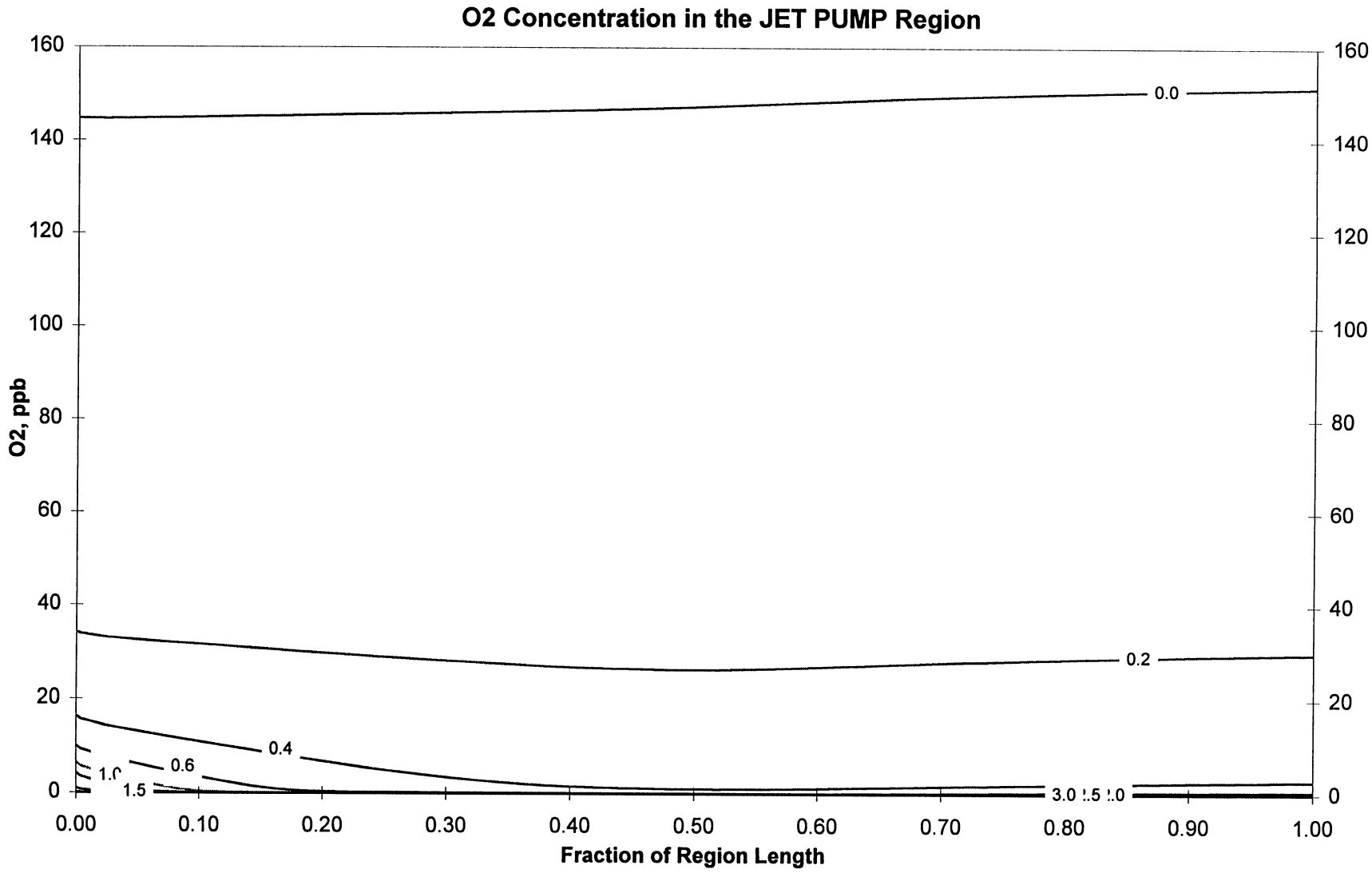

Figure 3-41

BWRJP438 (VERSION 4.38.5)DATED 12/20/94

FITJPO2.xlc

EPRI Licensed Material

ALL VALUES ATTACHED TO CURVES INDICATE PPM OF FW H2

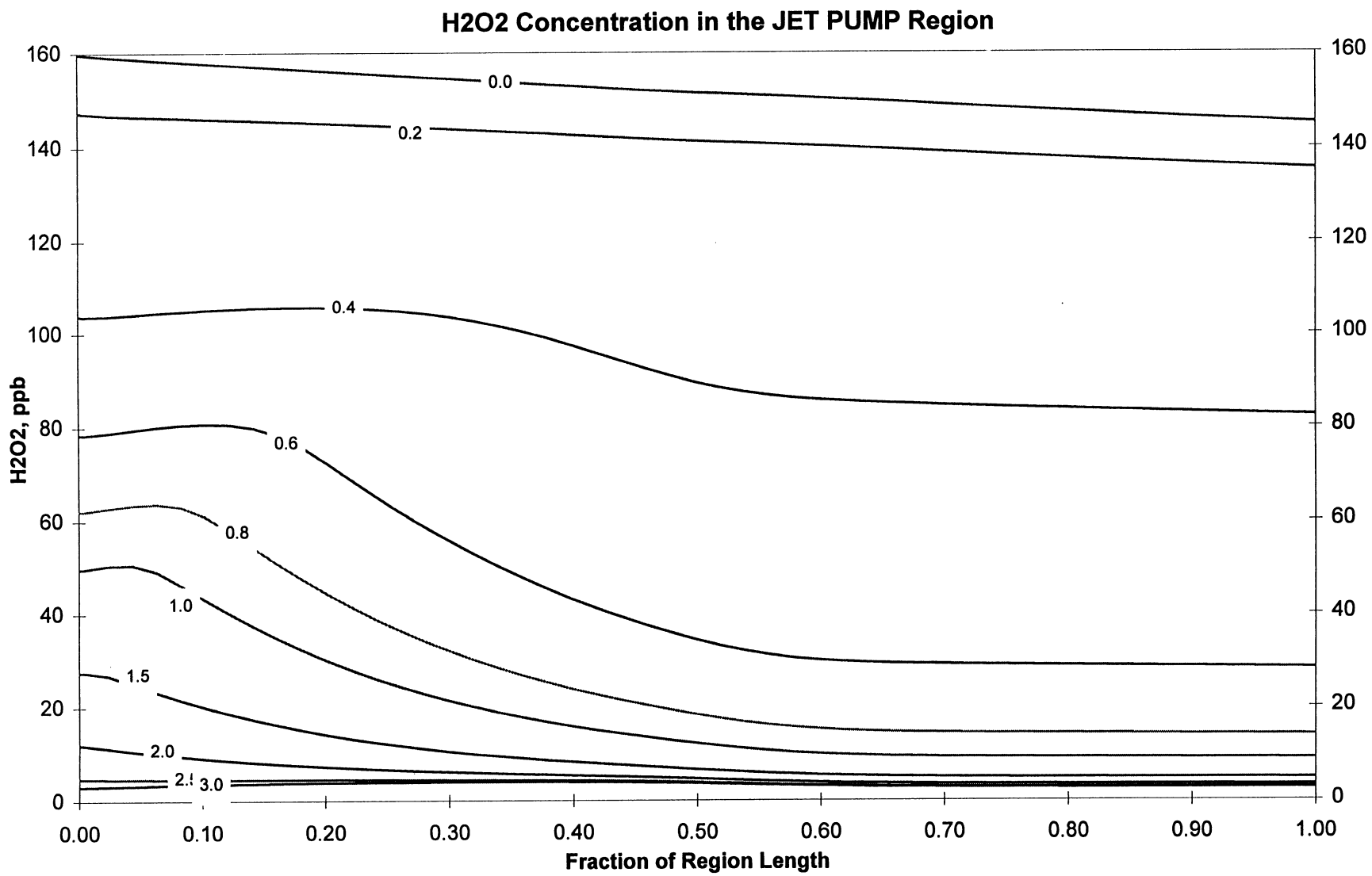

Figure 3-42

BWRJP438 (VERSION 4.38.5)DATED 12/20/94

FITJPPER.xlc

EPRI Licensed Material

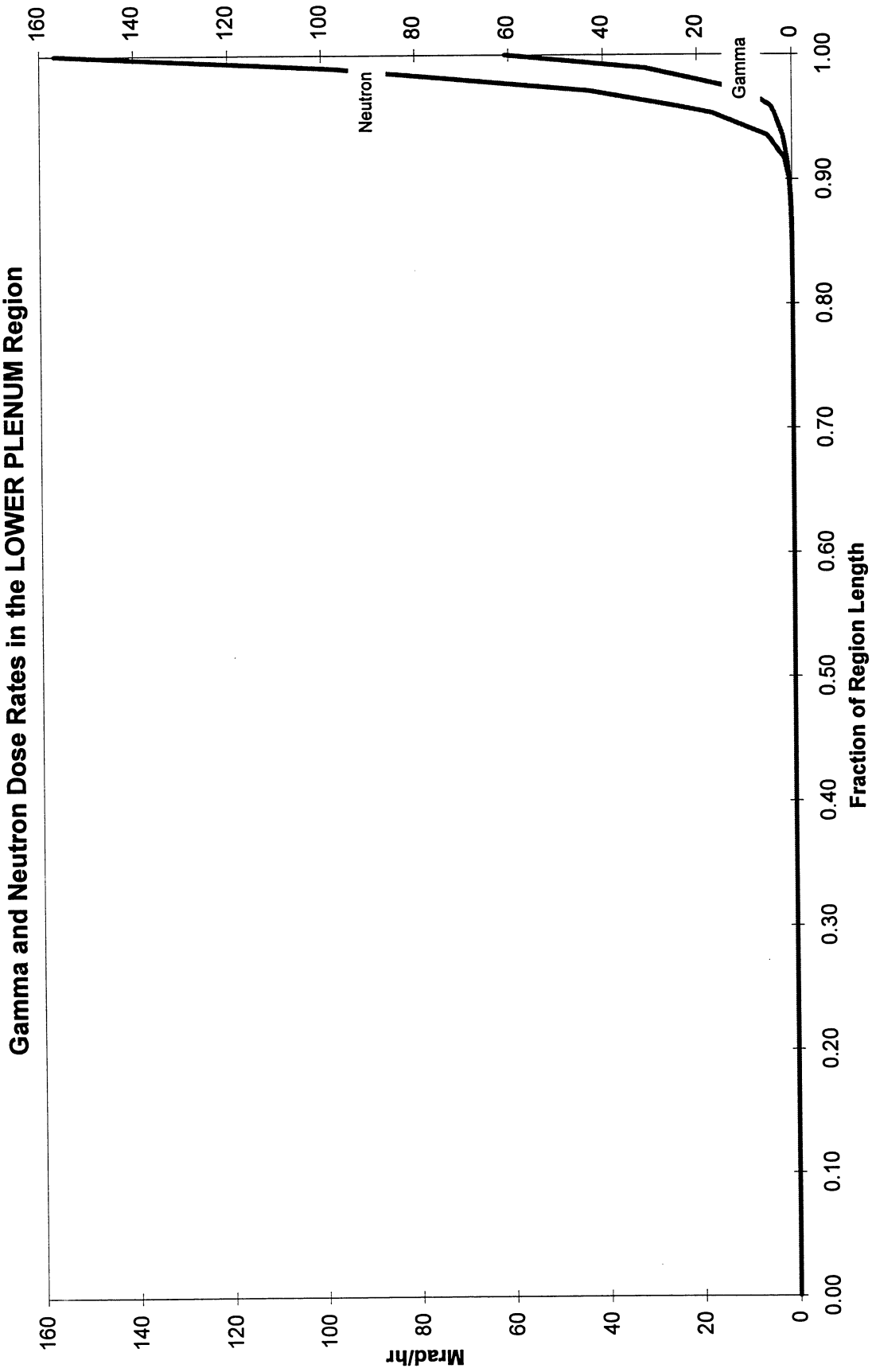

BWRJP438 (VERSION 4.38.5)DATED 12/20/94

FITLPRRG.xlc

Figure 3-43

ALL VALUES ATTACHED TO CURVES INDICATE PPM OF FW H2

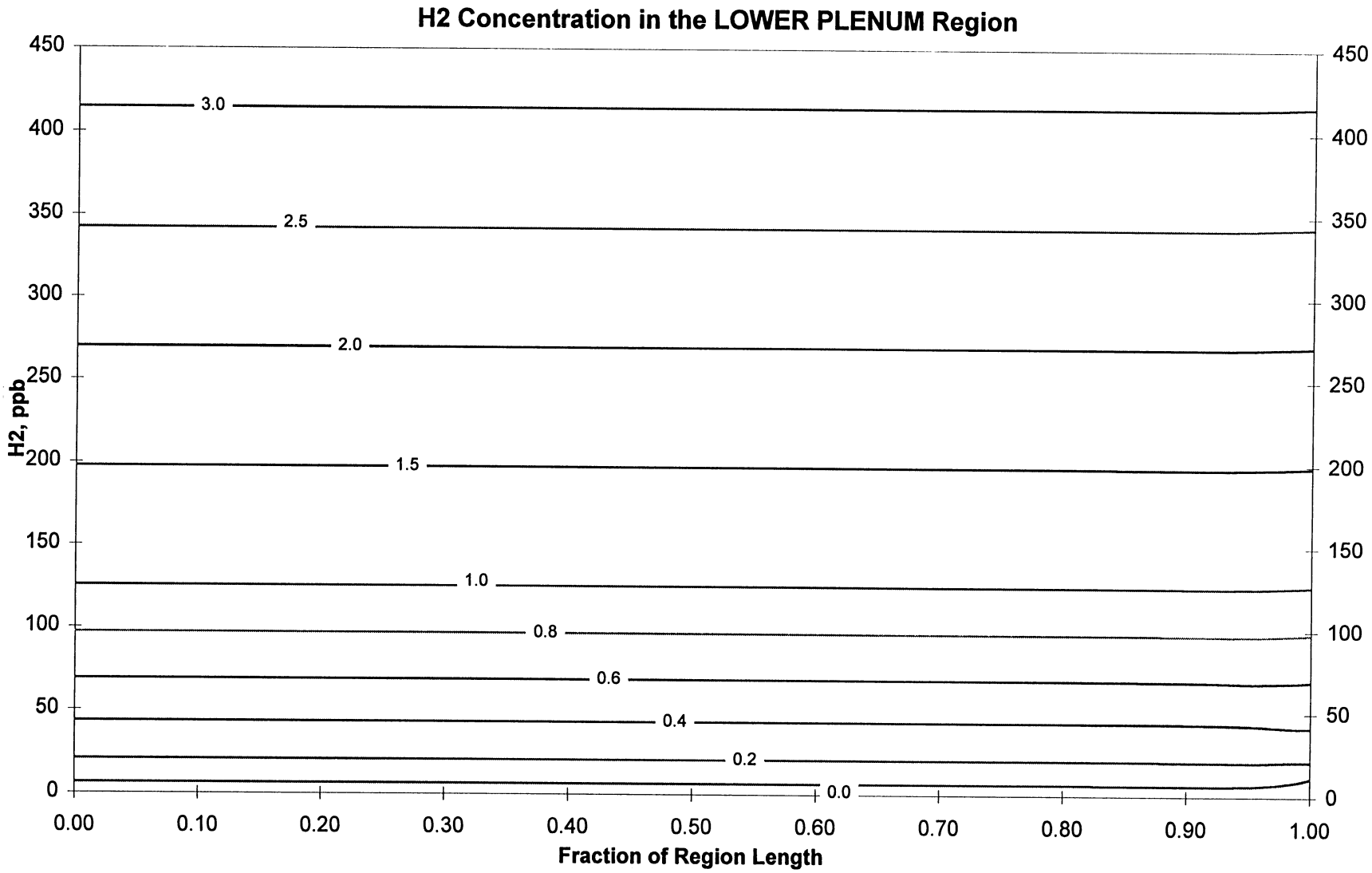

Figure 3-44

BWRJP438 (VERSION 4.38.5)DATED 12/20/94

FITLPH2.xlc

EPRI Licensed Material

ALL VALUES ATTACHED TO CURVES INDICATE PPM OF FW H2

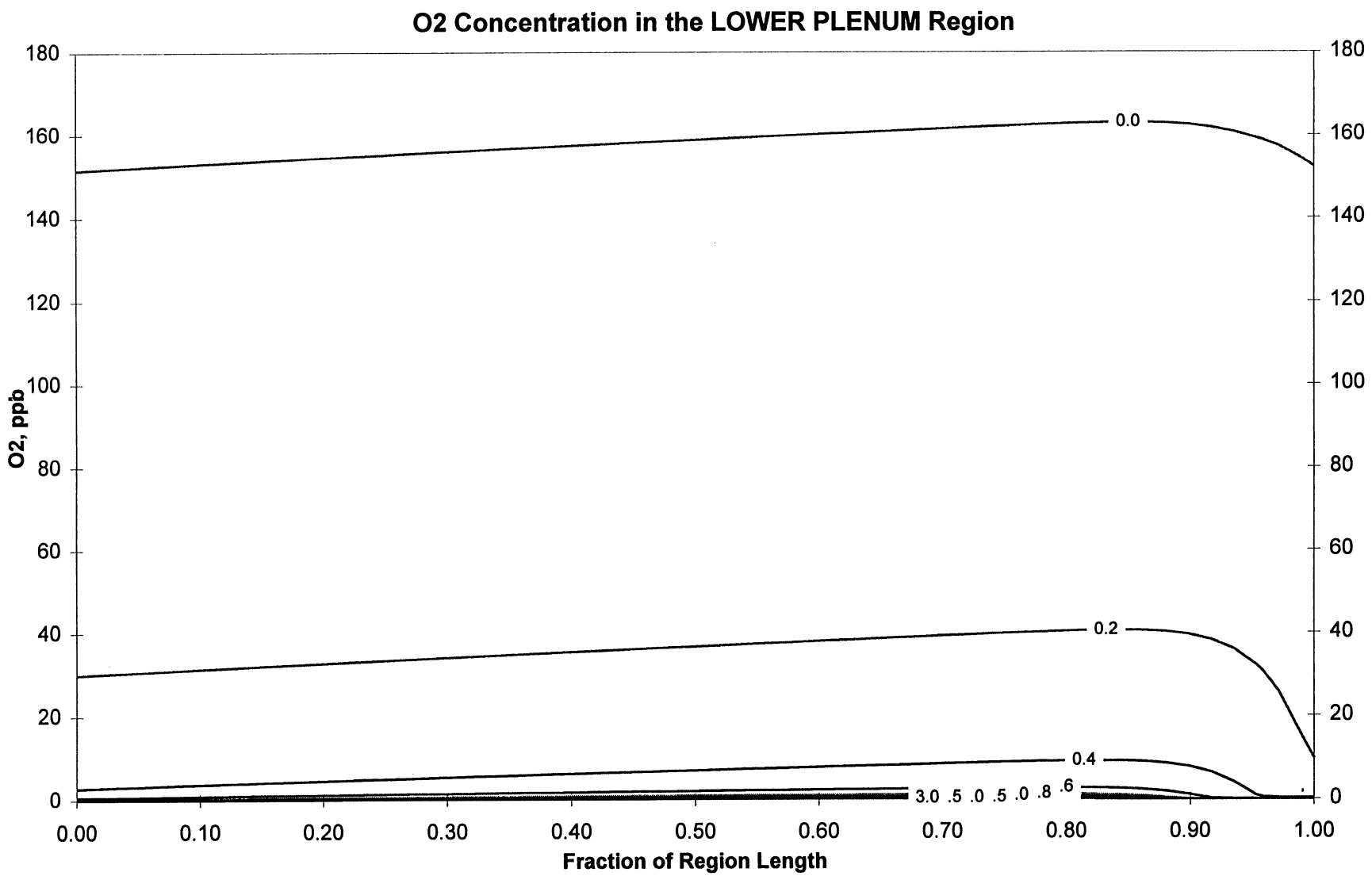

Figure 3-45

BWRJP438 (VERSION 4.38.5)DATED 12/20/94

FITLPO2.xlc

EPRI Licensed Material

ALL VALUES ATTACHED TO CURVES INDICATE PPM OF FW H2

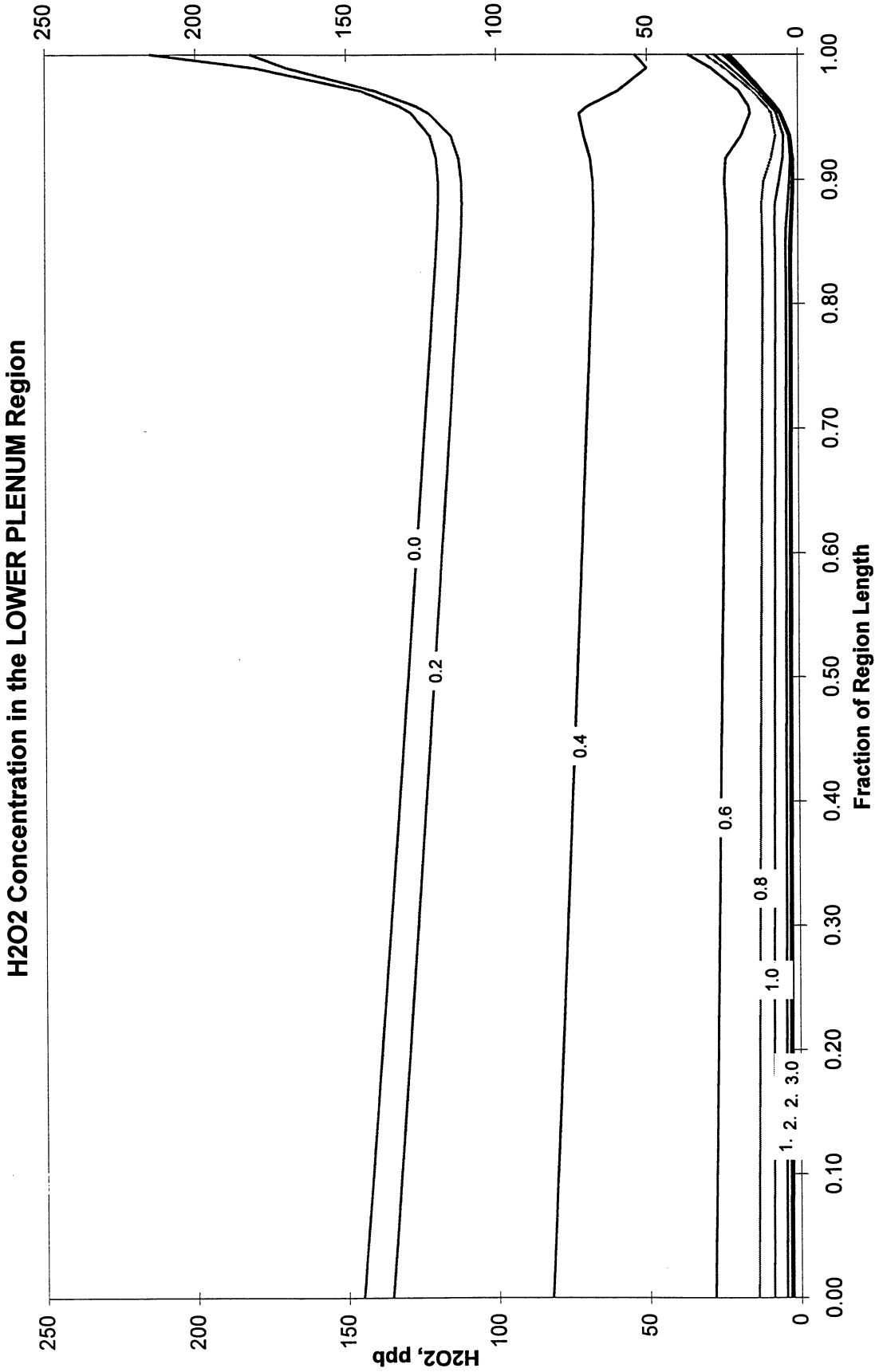

FITLPPER.xlc

BWRJP438 (VERSION 4.38.5)DATED 12/20/94

Figure 3-46

Comparison of Calculated and Measured Steam Hydrogen Concentrations

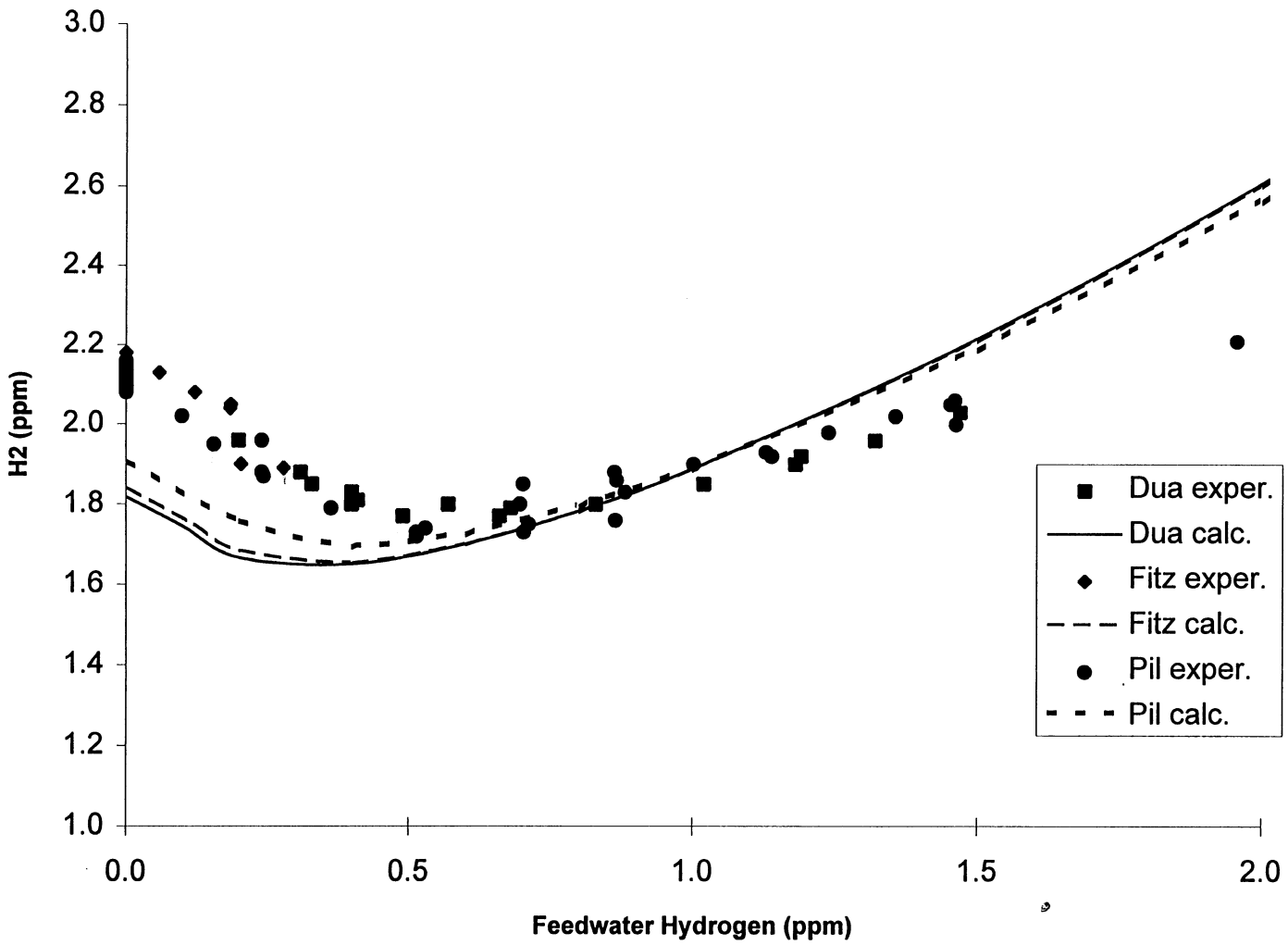

Figure 3-47

Comparison of Calculated and Measured Steam Oxygen Concentrations

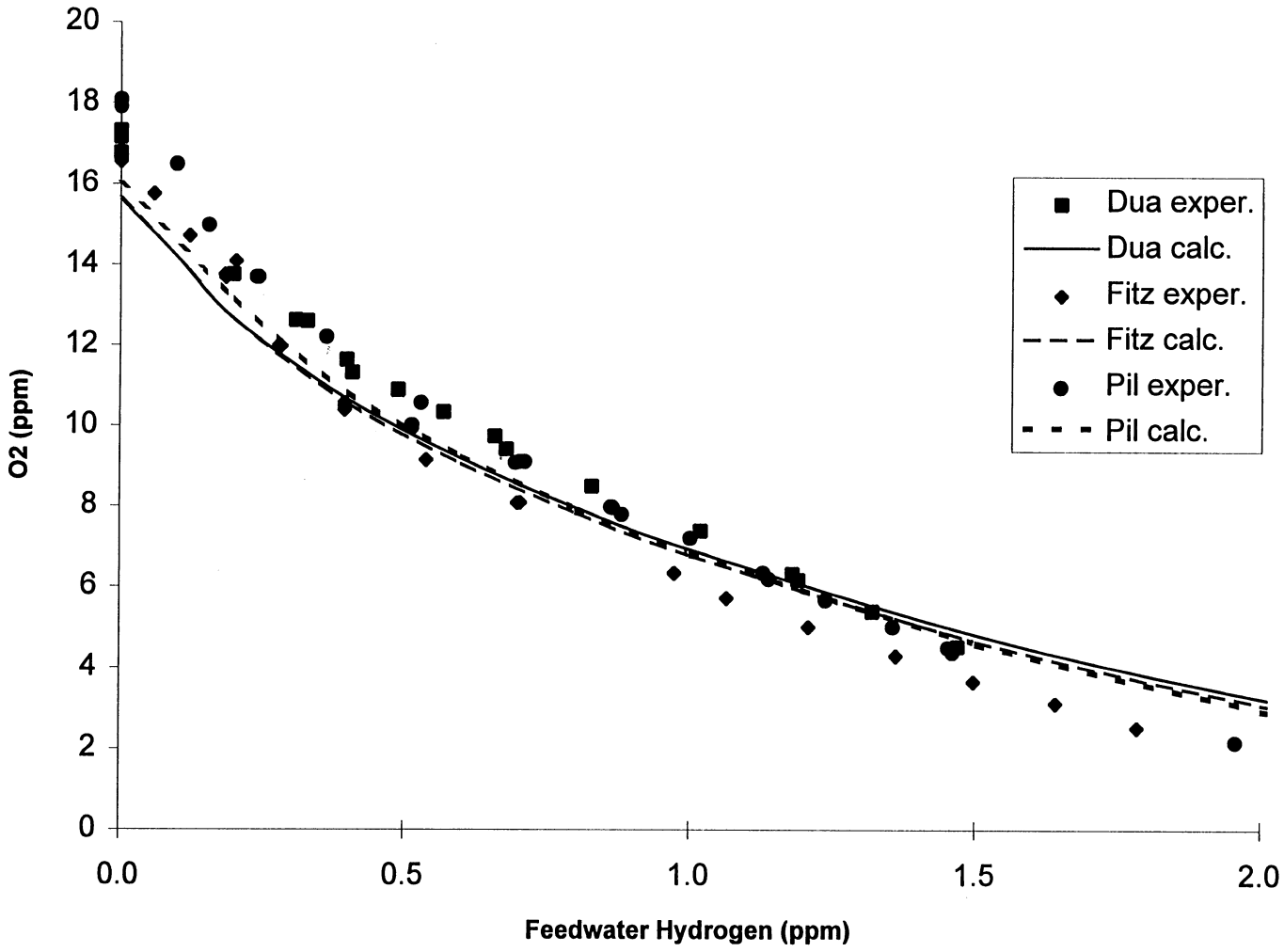

Figure 3-48

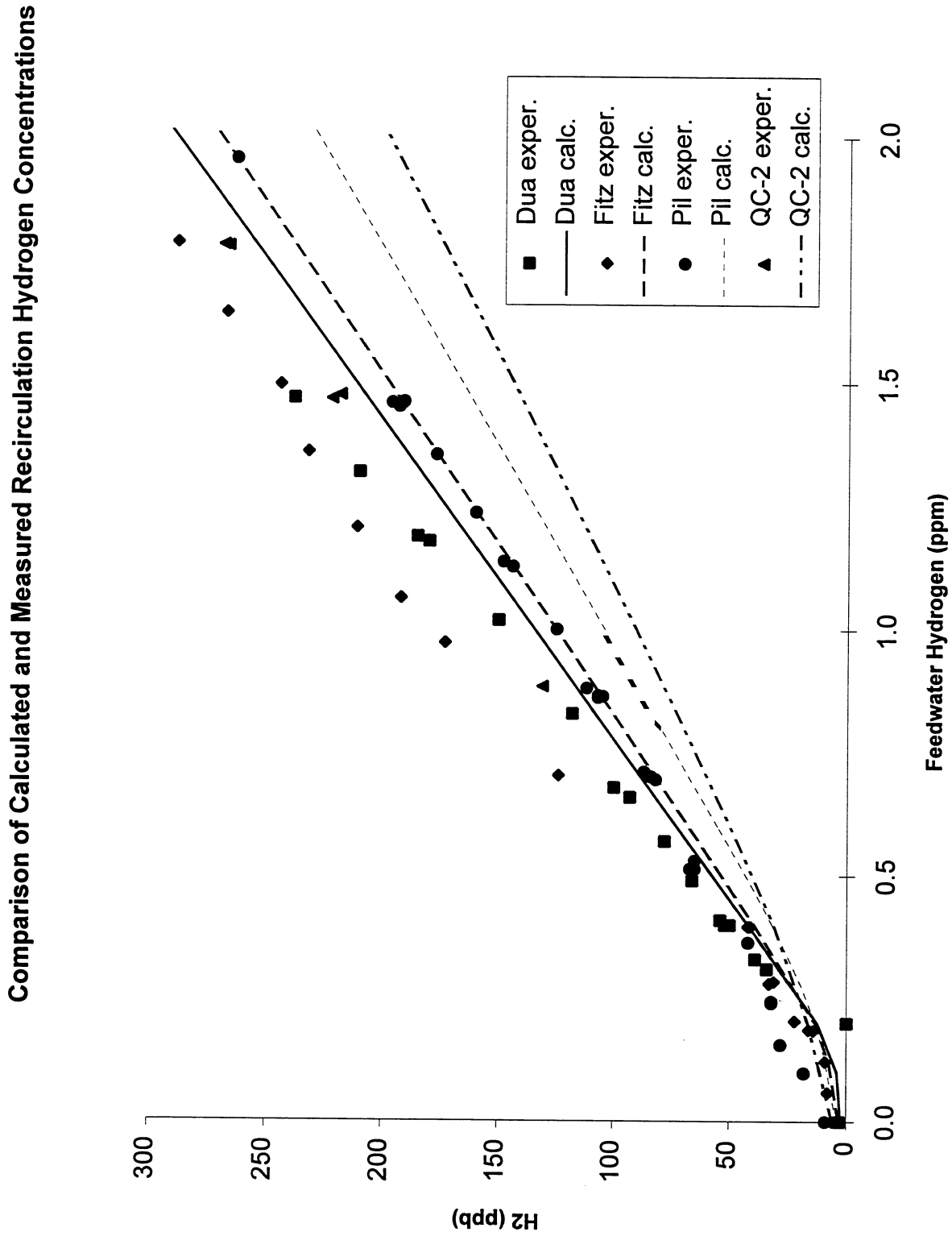
Comparison of Calculated and Measured Recirculation Hydrogen Concentrations
H2 (ppb)
300
250
200
150
100
50
0
0.0
0.5
1.0
1.5
2.0
Feedwater Hydrogen (ppm)
Dua exper.
Dua calc.
Fitz exper.
Fitz calc.
Pil exper.
Pil calc.
QC-2 exper.
QC-2 calc.

Figure 3-49

Comparison of Calculated and Measured Recirculation Oxidant Concentrations

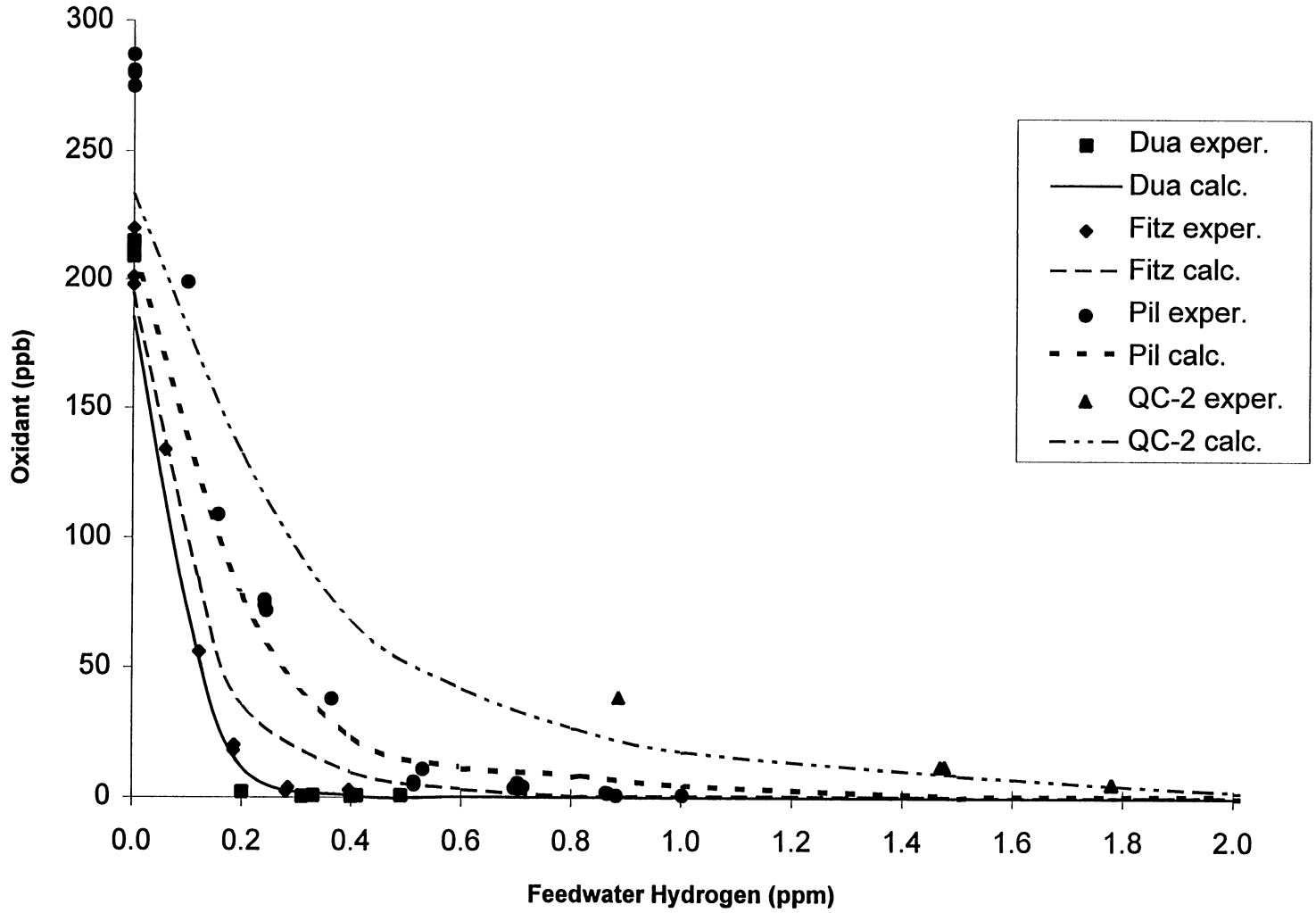

Figure 3-50

SECTION 4

CHEMISTRY IN THE MODIFIED LPRMs

4.1 LPRM Model

The radiolysis model was extended to include the LPRMs modified to encase electrochemical potential (ECP) sensors. The modified LPRMs were modeled for two BWRs, Fitzpatrick and Quad Cities-2, as a series of pipes of various lengths and diameters, based upon detailed mechanical drawings. The inlet concentrations were set equal to the concentrations in the lower plenum at the appropriate elevation. Since the same trends were found for the Fitzpatrick results as for the Quad Cities-2 results, this discussion references Fitzpatrick figures. The corresponding figures for Quad Cities are in Appendix B.

The major differences between the LPRM and the local flow path, whether in the lower plenum or the core bypass, are in the velocity and the surface-to-volume ratios. The primary effect of these variables is to change the rate of the peroxide decomposition surface reaction

$$2\,H_2O_2 \rightarrow 2\,H_2O + O_2.$$

This is because the forward rate constant for this reaction is

$$K_{31} = 4 \cdot f \cdot V \cdot (Sc^{-0.67})/D$$

where V is the velocity, D is the hydraulic diameter, f is the Fanning friction factor, and Sc is the Schmidt number. These last two items are defined as

$$f = (1.58 * \mathrm{Log}(Re) - 3.28)^{-2}$$

with $Re = V \cdot D \cdot \rho / D_{O2}$, where Re is the Reynolds number, and

$$Sc = \mu/(\rho \cdot D_{O2})$$

with μ = viscosity of water, ρ = density of water, and D_{O2} = diffusivity of oxygen in water.

Using this formulation, K_{31} is approximately proportional to V/D. (Note that D = 4/surface-to-volume). Since V/D is approximately 160 in the LPRM, 7 in the lower plenum, and 12 in the core bypass, the peroxide decomposition rate is 10 to 25 times faster in the LPRM than outside of it. This directly results in lower hydrogen peroxide

and higher oxygen in the LPRM. In addition, these differences lead to a lowering of the H_2 concentration in the LPRM because of its reaction with the oxygen.

The ECP in the LPRM also differs from the environment ECP, due both to the concentration differences and velocity differences. The ECP increases with increasing oxygen, hydrogen peroxide, and velocity, and decreases with increasing hydrogen.

4.2 Effect of Flow Rate and Feedwater Hydrogen on LPRM Chemistry and ECP Sensors

Parametric studies were performed to quantify the effect of LPRM velocity and feedwater hydrogen on hydrogen, oxygen and hydrogen peroxide concentrations, and ECP. Figures 4-1 to 4-5 show the effect on hydrogen, with each figure referring to a particular sensor. Below the core plate (sensors 1, 2, and 3), the hydrogen is only affected by flow rate for flow rates below the nominal value (0.5 kg/s) and for hydrogen feedwater concentrations below 0.5 ppm. With a combination of low flow rate and low feedwater hydrogen, the hydrogen can be up to double the concentrations of higher flow rates. At high flow rates, the hydrogen is independent of flow rate. In general, the hydrogen concentration in the LPRM increases with increasing feedwater hydrogen, because of the dominant effect of the feedwater hydrogen input .

The upper core sensors' dependence on flow rate follows the same trend as that of the sensors below the core plate (Figures 4-4 and 4-5). The hydrogen concentration is independent of flow rate for rates above 0.5 kg/s. It is also independent of flow rate for rates below 0.5 kg/s for feedwater hydrogen concentrations of 0.2 ppm or higher. Unlike below the core plate, at low flow and low feedwater hydrogen, the hydrogen decreases as the flow rate decreases. The least expected result for the upper core sensors was that the hydrogen concentrations for 0.0 and 0.1 ppm feedwater hydrogen were generally higher than for 0.2 and 0.5 ppm feedwater hydrogen. We have not yet been able to explain this result.

The effect of flow rate on oxygen at the LPRM sensors is shown in Figures 4-6 to 4-10. As with hydrogen, there is no effect of flow rate below the core plate on oxygen for flow rates greater than 0.5 kg/s, and changes in the slope of the curves can be seen at low flow rates for low feedwater hydrogen. There, the oxygen decreases as the flow rate decreases. The oxygen decreases monotonically with increasing feedwater hydrogen, and essentially vanishes for 0.5 ppm feedwater hydrogen.

For the upper core sensors, at low feedwater hydrogen injections the oxygen increases substantially with increasing flow rate for all cases, with a sixfold increase over the range of flow rates. However, for 0.5 ppm feedwater hydrogen and above, the oxygen concentration is negligible at the lower sensors.

The effect of flow rate on hydrogen peroxide at the LPRM sensors is shown in Figures 4-11 to 4-15. As with hydrogen and oxygen, there is no effect of flow rate below the core

plate on hydrogen peroxide for flow rates greater than 0.5 kg/s, and effects at low flow rates can be seen at low feedwater hydrogen. There, the hydrogen peroxide increases as the flow rate decreases, a trend opposite to the one seen for oxygen. The hydrogen peroxide decreases monotonically with increasing feedwater hydrogen, but, unlike oxygen, its concentration is not negligible even at 1.0 ppm feedwater hydrogen.

At the upper sensors (Figures 4-14 and 4-15), the hydrogen peroxide is weakly dependent on flow rate for 0.0 through 0.2 ppm feedwater hydrogen, and independent of flow rate for higher feedwater hydrogen concentrations. As at the lower sensors, the hydrogen peroxide concentration decreases with increasing feedwater hydrogen, but never vanishes.

The ECP at all sensors increases with increasing flow rate (Figures 4-16 to 4-20), as expected from the ECP experimental data on velocity. There are no exceptions to this result. The slopes of the curves decrease with increasing flow rate, so that the minimum sensitivity to flow rate occurs at high flow rate.

The ECP generally decreases with increasing feedwater hydrogen concentrations, as expected, but there are exceptions below the core plate when both velocity and feedwater hydrogen are low. For example, at Sensor 3, the ECP under normal water chemistry is slightly less than the ECP at 0.2 ppm feedwater hydrogen for flow rates from 0 through 0.1 kg/s (Figure 4-18). This is due to the higher hydrogen concentration under normal water chemistry conditions. In a similar vein, above the core plate, the hydrogen in the LPRM is lower at 0.2 ppm feedwater hydrogen than at 0.0 or 0.1 ppm feedwater hydrogen(Figures 4-4 and 4-5), and so the ECP is higher (Figures 4-19 and 4-20). At 0.5 ppm feedwater hydrogen, we would expect the ECP to be lower than at 0.2 ppm feedwater hydrogen. However, this is not the case at flow rates above 0.5 kg/s. This effect too needs further investigation.

The difference in ECP between curves of constant feedwater hydrogen is fairly insensitive to flow rate. In other words, the ECP curves are quite parallel. This means that any change in ECP we would expect due to a change in feedwater hydrogen is independent of the flow rate through the LPRM.

4.3 Differences in Concentrations and ECP Inside and Outside LPRM

The concentrations and ECPs are generally different inside and outside the LPRM. These relationships are demonstrated at three flow rates (0.01, 0.1, and 1. kg/s) for hydrogen (Figures 4-21 to 4-25), oxygen(Figures 4-26 to 4-30), hydrogen peroxide (Figures 4-31 to 4-35), and ECP (Figures 4-36 to 4-40). The first three sensors are compared with lower plenum calculations at the same elevations (left side of figures), and the last two sensors are compared with core bypass calculations (right side of figures).

The hydrogen concentration in the LPRM under normal water chemistry can be either higher or lower than outside (Figure 4-21). The concentration is always higher under the core plate inside the LPRM than outside, but at high flow rates (1 kg/s), the inside and

outside concentrations are virtually identical. In the upper core, the LPRM concentration is higher at low flow rates and lower at high flow rates than in the core bypass. Again, there is little difference in hydrogen concentration inside versus outside for high flow rates. The relative differences in hydrogen concentrations become small as the feedwater hydrogen increases, and are insignificant for 0.5 ppm feedwater hydrogen (Figure 4-24).

The oxygen concentrations are generally different inside and outside the LPRM. The largest differences occur above the core at high flow rates (i.e. 1 kg/s) for 0 through 0.2 ppm feedwater hydrogen, where the oxygen can be 5 times higher than in the core bypass (Figures 4-26 to 4-28). At high feedwater hydrogen, the differences in oxygen, appear large on the scale used, but in reality are very small, because the oxygen itself is so small (Figure 4-30).

The hydrogen peroxide concentrations inside the LPRM can be either higher or lower than outside. Below the core plate, the LPRM hydrogen peroxide can be close to the outside value at high flow rates (1 kg/s), or 600 ppb higher at low ones (Figure 4-31). These differences fade with increasing feedwater hydrogen. Above the core plate, the low feedwater hydrogen relationship is reversed, so that the LPRM hydrogen peroxide is close to the outside value at low flow rates, but 400 ppb lower at high rates (1.0 kg/s).

Unlike the oxygen, the hydrogen peroxide concentrations do not reach zero at high feedwater hydrogen. The LPRM values below the core plate are fairly close to the outside values at high flow rates. In the upper core, at the higher feedwater hydrogen the absolute concentration differences are large, with the LPRM 20 to 30 ppb below the core bypass (Figures 4-34 and 4-35).

At low feedwater hydrogen, no single LPRM flow rate yields a "best" match with the environment. As an example, at 0.2 ppm hydrogen - for which the concentration differences between LPRM and environment can be significant - below the core plate, the closest match for hydrogen, is 1 kg/s, for oxygen is 0.01 kg/s, and for hydrogen peroxide is 1 kg/s (Figures 4-23, 4-28 and 4-33). In the upper core, the closest match for hydrogen is 1 kg/s, for oxygen is 0.1 kg/s, and for hydrogen peroxide is 1 kg/s. At higher flow rates (1 kg/s) and feedwater hydrogen of 0.5 ppm or more, the differences in the concentrations in the LPRM concentrations are insignificant.

No single feedwater hydrogen concentration yields a thoroughly close match between LPRM and environment. At 0.0 through 0.2 ppm feedwater hydrogen, major discrepancies are found in hydrogen (Figures 4- 21 to 4-23), oxygen (Figures 4-26 to 4-28), and hydrogen peroxide (Figures 4-31 to 4-33). At higher feedwater hydrogen, the hydrogen and oxygen concentrations inside and outside the LPRM are reasonably close, but the hydrogen peroxide concentrations are not, especially in the upper core.

Given the general disparities in concentration, combined with the differences in velocities, we expect the ECP inside and outside the LPRM to differ, and they do (Figures 4-36 to 4-40). However, the ECP of the LPRM is fairly close to that of the core bypass for 0.1 kg/s flow in the upper core (Figures 4-36 to 4-40).

The concentrations of hydrogen, oxygen and hydrogen peroxide and the ECP values depend on the elevation below the core plate. In some instances, the ECP dependence is quite strong, and so the measured values will be sensitive to the actual installed elevation of the sensors. Such a dependence is less important for the upper core sensors, for which a slight misplacement would not alter significantly the measurements.

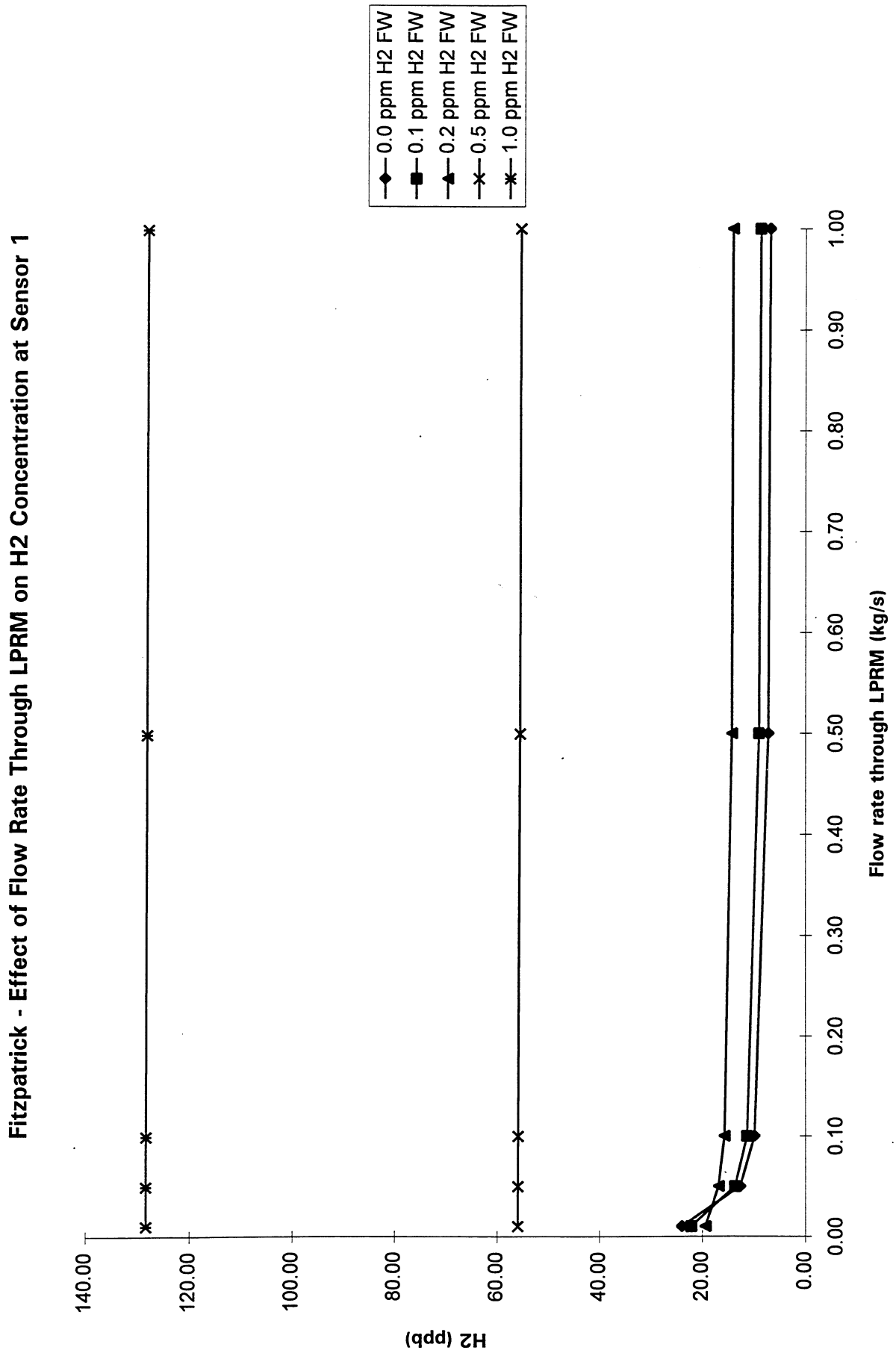
Fitzpatrick - Effect of Flow Rate Through LPRM on H2 Concentration at Sensor 1
0.0 ppm H2 FW
0.1 ppm H2 FW
0.2 ppm H2 FW
0.5 ppm H2 FW
1.0 ppm H2 FW
H2 (ppb)
140.00
120.00
100.00
80.00
60.00
40.00
20.00
0.00
0.00
0.10
0.20
0.30
0.40
0.50
0.60
0.70
0.80
0.90
1.00
Flow rate through LPRM (kg/s)

Figure 4-1

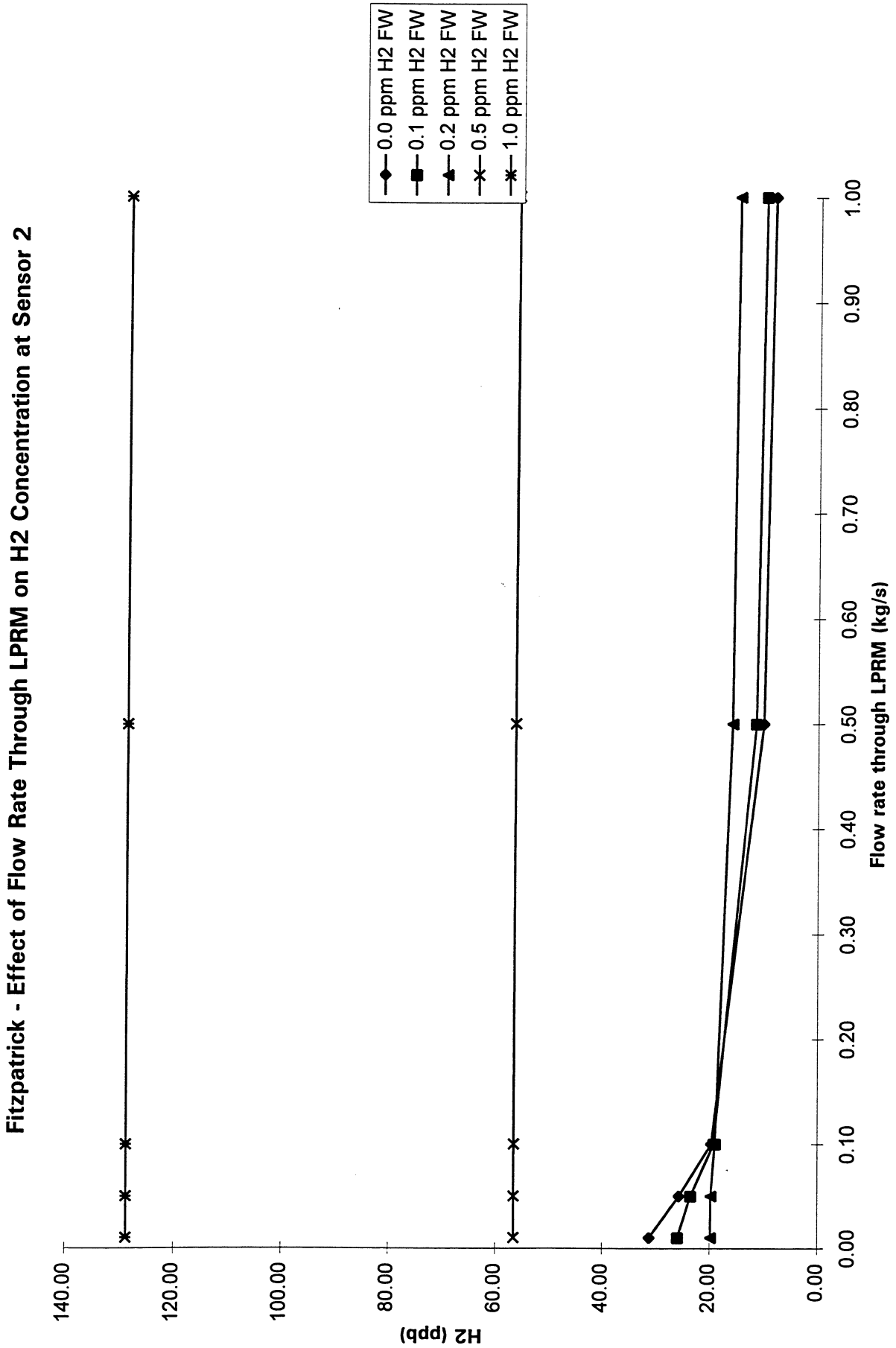
Fitzpatrick - Effect of Flow Rate Through LPRM on H2 Concentration at Sensor 2
0.0 ppm H2 FW
0.1 ppm H2 FW
0.2 ppm H2 FW
0.5 ppm H2 FW
1.0 ppm H2 FW
H2 (ppb)
140.00
120.00
100.00
80.00
60.00
40.00
20.00
0.00
0.00
0.10
0.20
0.30
0.40
0.50
0.60
0.70
0.80
0.90
1.00
Flow rate through LPRM (kg/s)

Figure 4-2

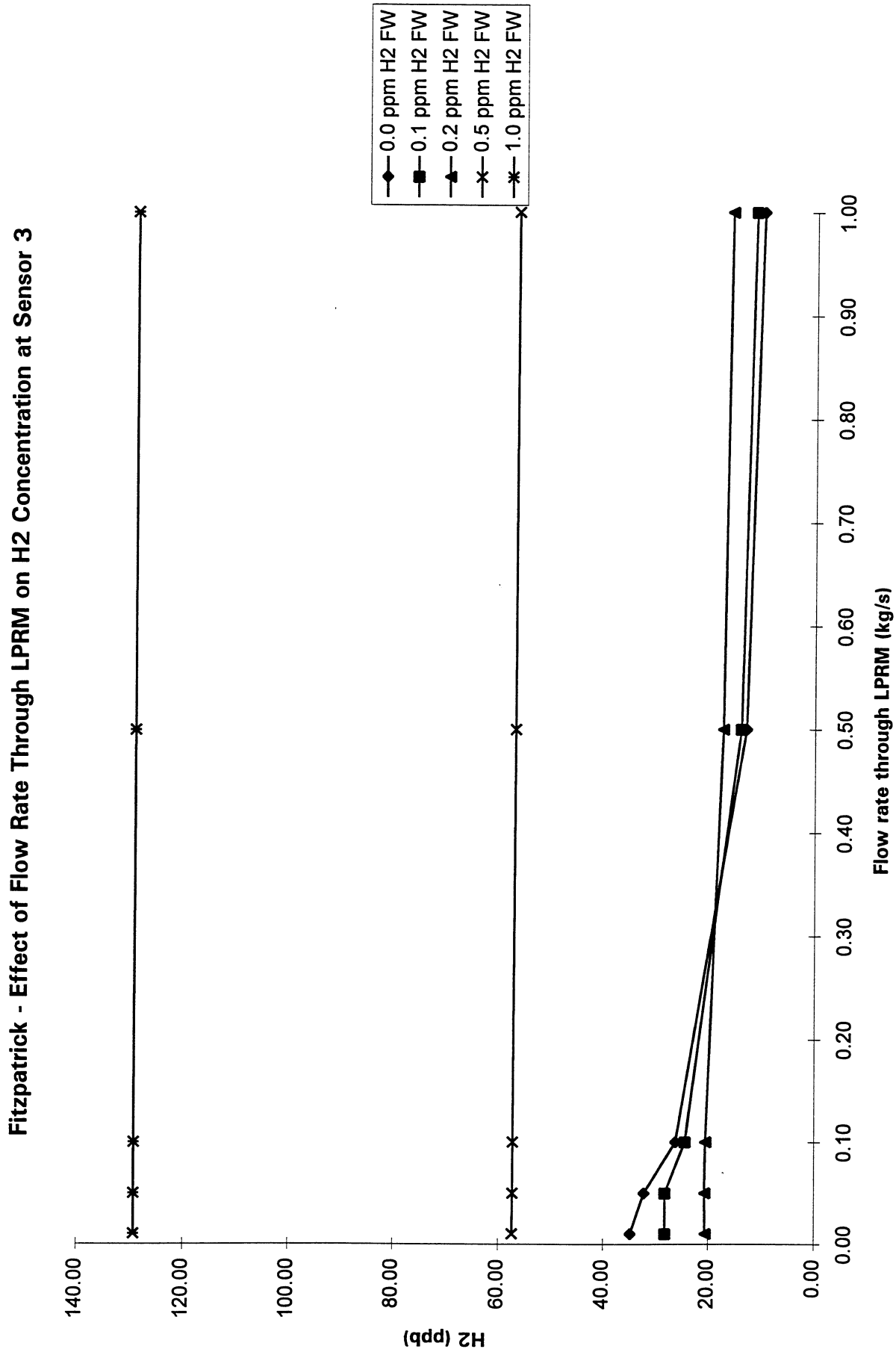
Fitzpatrick - Effect of Flow Rate Through LPRM on H2 Concentration at Sensor 3
0.0 ppm H2 FW
0.1 ppm H2 FW
0.2 ppm H2 FW
0.5 ppm H2 FW
1.0 ppm H2 FW
H2 (ppb)
140.00
120.00
100.00
80.00
60.00
40.00
20.00
0.00
0.00
0.10
0.20
0.30
0.40
0.50
0.60
0.70
0.80
0.90
1.00
Flow rate through LPRM (kg/s)

Figure 4-3

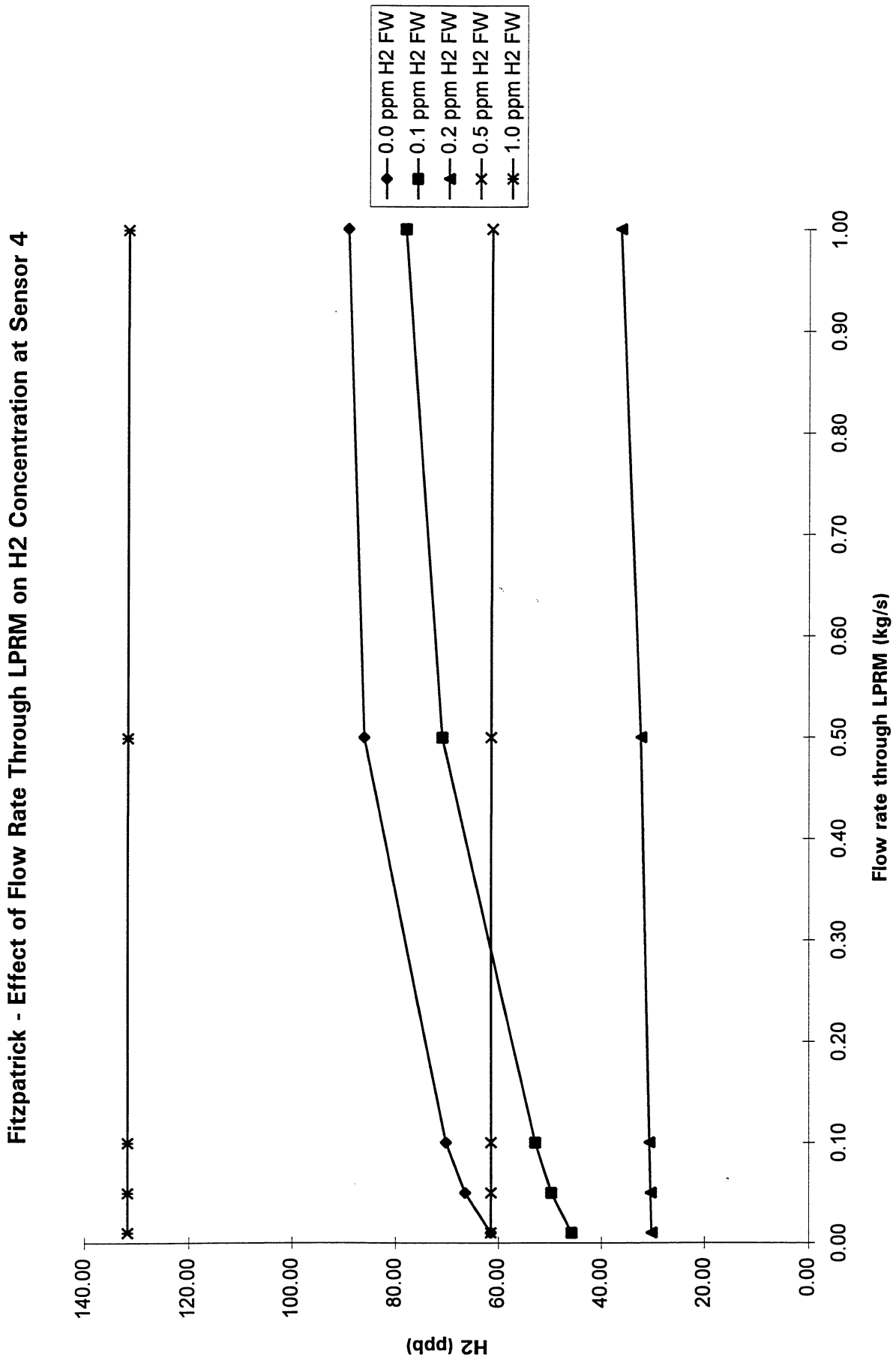
Fitzpatrick - Effect of Flow Rate Through LPRM on H2 Concentration at Sensor 4
0.0 ppm H2 FW
0.1 ppm H2 FW
0.2 ppm H2 FW
0.5 ppm H2 FW
1.0 ppm H2 FW
H2 (ppb)
140.00
120.00
100.00
80.00
60.00
40.00
20.00
0.00
0.00
0.10
0.20
0.30
0.40
0.50
0.60
0.70
0.80
0.90
1.00
Flow rate through LPRM (kg/s)

Figure 4-4

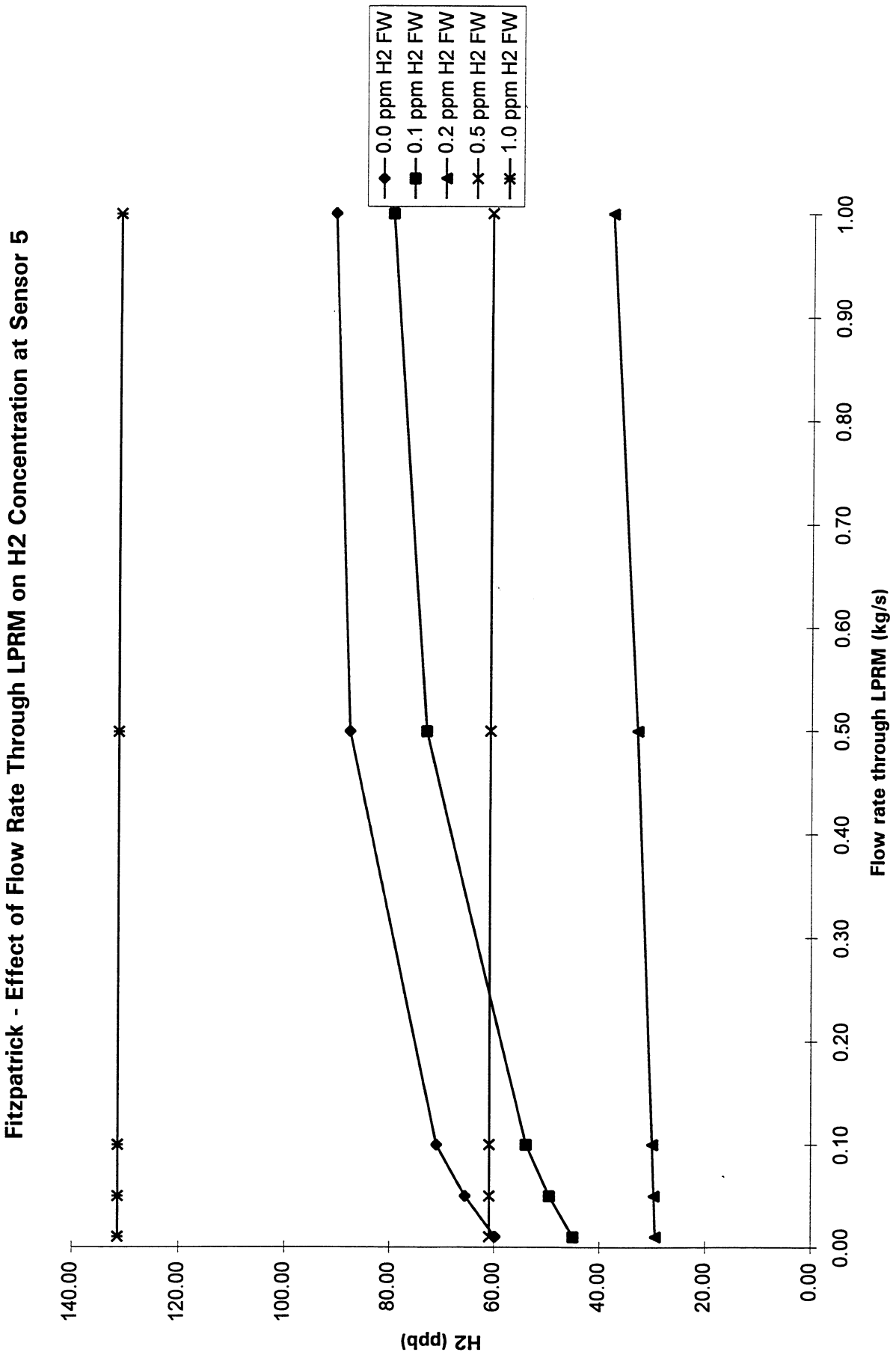
Fitzpatrick - Effect of Flow Rate Through LPRM on H2 Concentration at Sensor 5
0.0 ppm H2 FW
0.1 ppm H2 FW
0.2 ppm H2 FW
0.5 ppm H2 FW
1.0 ppm H2 FW
H2 (ppb)
140.00
120.00
100.00
80.00
60.00
40.00
20.00
0.00
0.00
0.10
0.20
0.30
0.40
0.50
0.60
0.70
0.80
0.90
1.00
Flow rate through LPRM (kg/s)

Figure 4-5

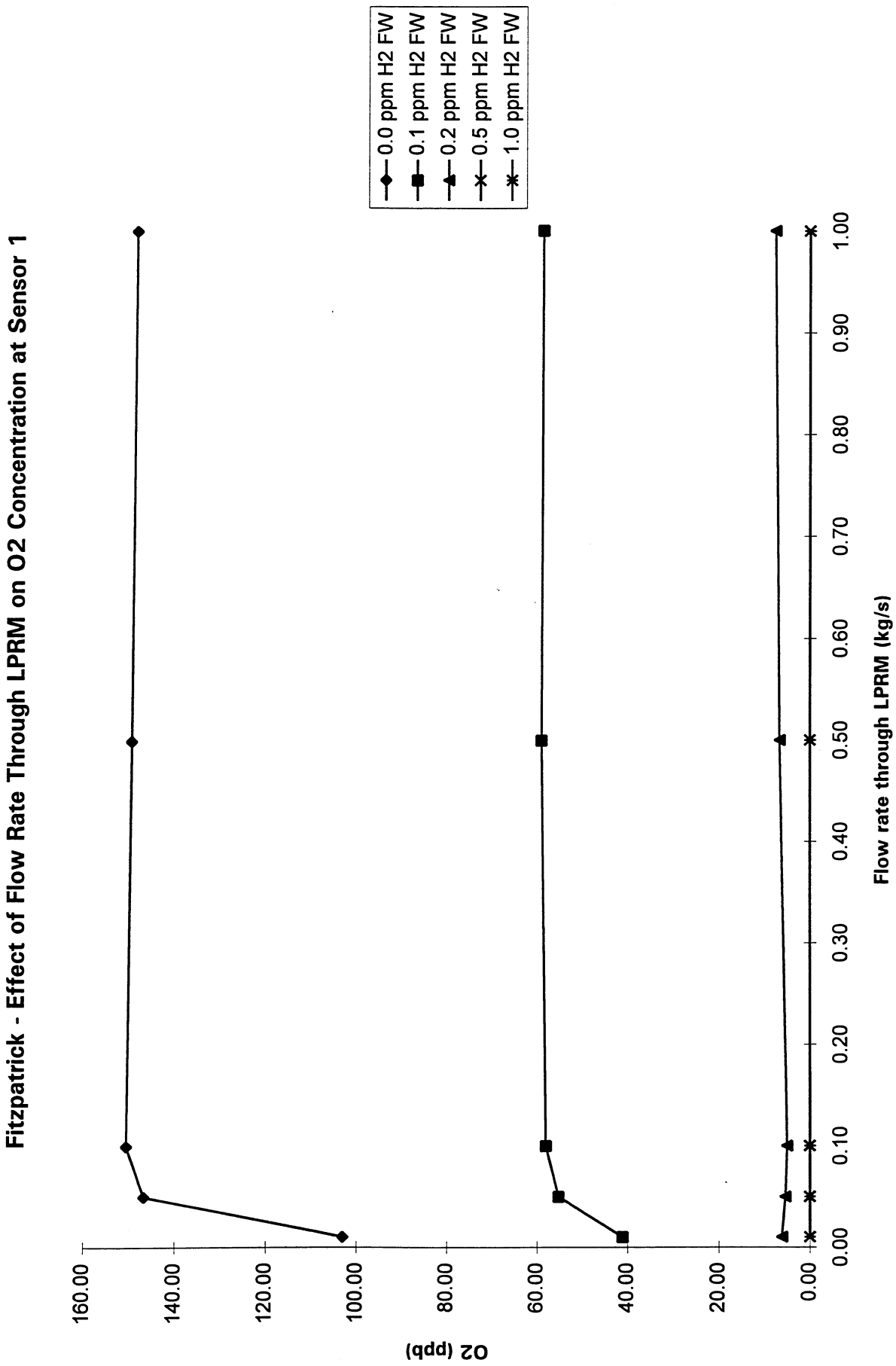
Fitzpatrick - Effect of Flow Rate Through LPRM on O2 Concentration at Sensor 1
0.0 ppm H2 FW
0.1 ppm H2 FW
0.2 ppm H2 FW
0.5 ppm H2 FW
1.0 ppm H2 FW
O2 (ppb)
160.00
140.00
120.00
100.00
80.00
60.00
40.00
20.00
0.00
0.00
0.10
0.20
0.30
0.40
0.50
0.60
0.70
0.80
0.90
1.00
Flow rate through LPRM (kg/s)

Figure 4-6

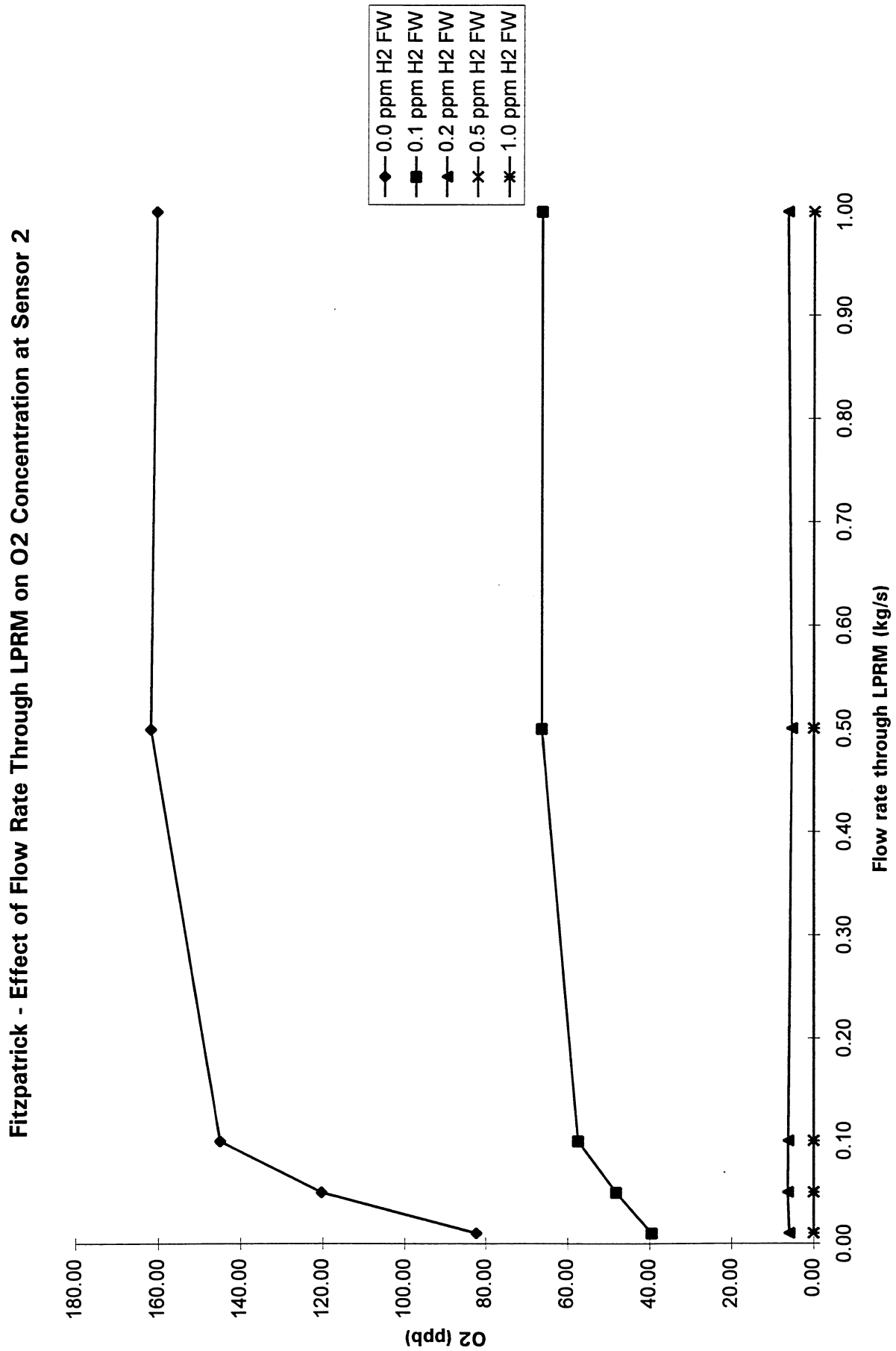
Fitzpatrick - Effect of Flow Rate Through LPRM on O2 Concentration at Sensor 2
0.0 ppm H2 FW
0.1 ppm H2 FW
0.2 ppm H2 FW
0.5 ppm H2 FW
1.0 ppm H2 FW
O2 (ppb)
180.00
160.00
140.00
120.00
100.00
80.00
60.00
40.00
20.00
0.00
0.00
0.10
0.20
0.30
0.40
0.50
0.60
0.70
0.80
0.90
1.00
Flow rate through LPRM (kg/s)

Figure 4-7

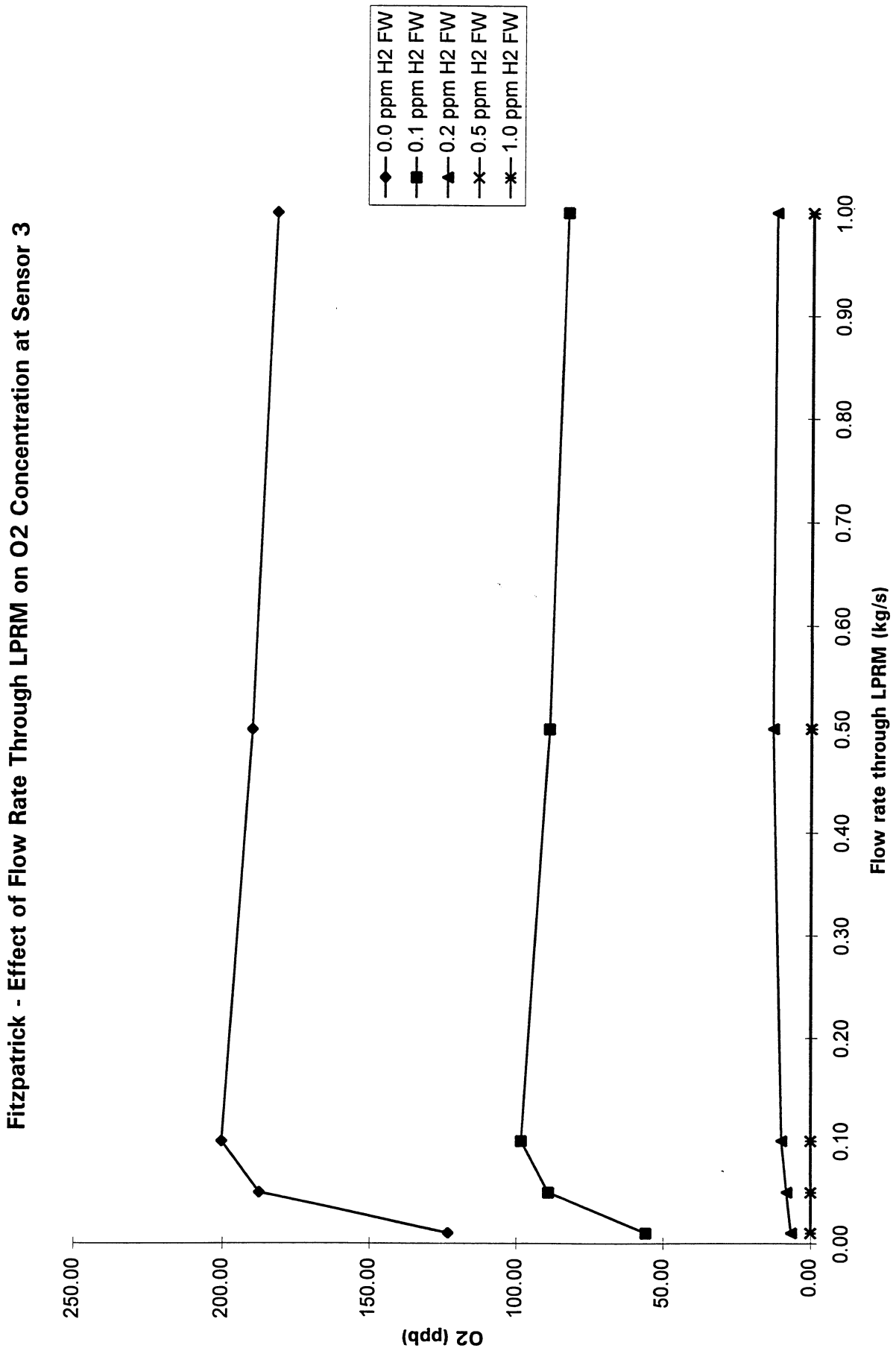
Fitzpatrick - Effect of Flow Rate Through LPRM on O2 Concentration at Sensor 3
0.0 ppm H2 FW
0.1 ppm H2 FW
0.2 ppm H2 FW
0.5 ppm H2 FW
1.0 ppm H2 FW
O2 (ppb)
250.00
200.00
150.00
100.00
50.00
0.00
0.00
0.10
0.20
0.30
0.40
0.50
0.60
0.70
0.80
0.90
1.00
Flow rate through LPRM (kg/s)

Figure 4-8

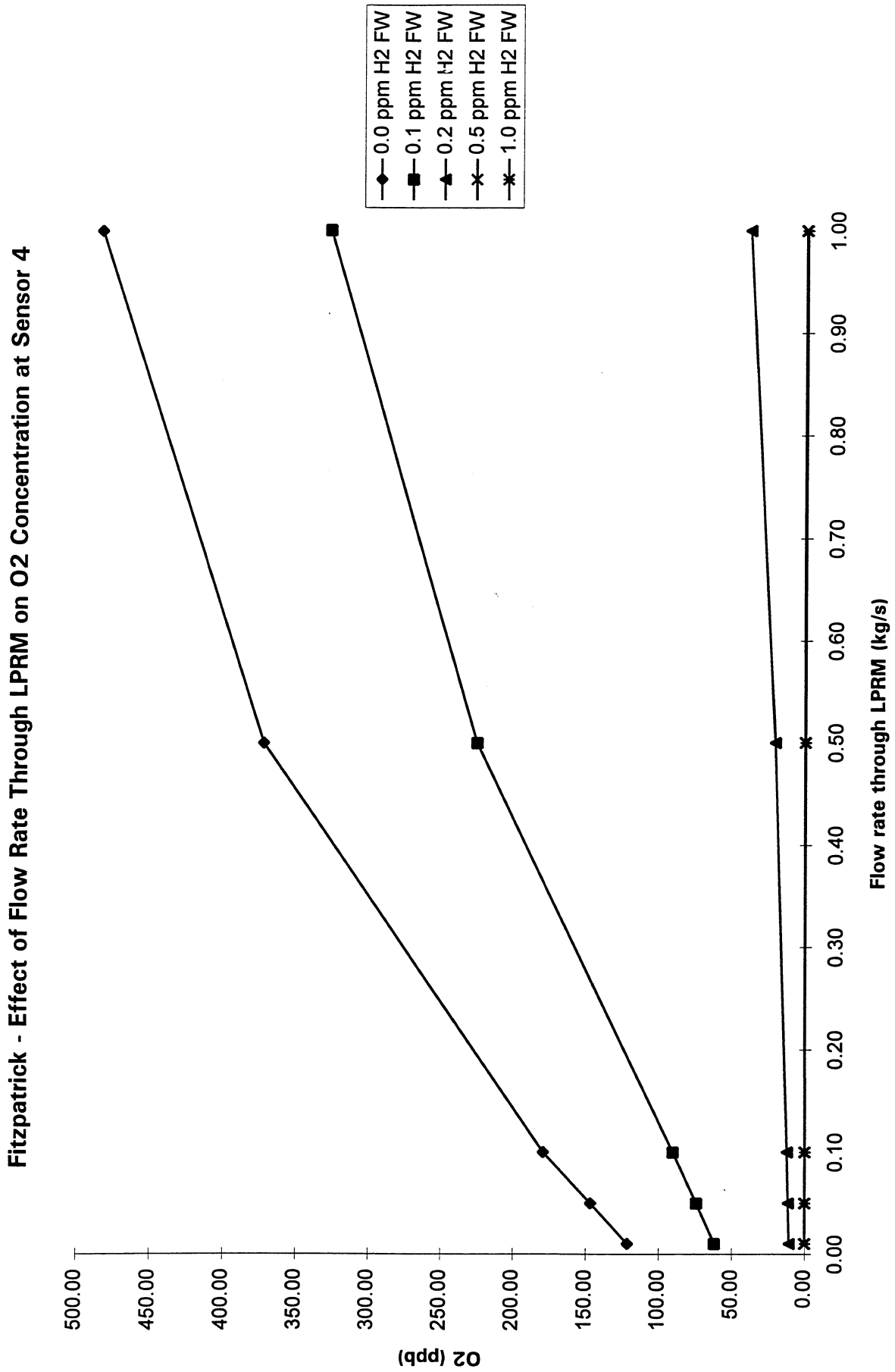
Fitzpatrick - Effect of Flow Rate Through LPRM on O2 Concentration at Sensor 4
0.0 ppm H2 FW
0.1 ppm H2 FW
0.2 ppm H2 FW
0.5 ppm H2 FW
1.0 ppm H2 FW
O2 (ppb)
500.00
450.00
400.00
350.00
300.00
250.00
200.00
150.00
100.00
50.00
0.00
0.00
0.10
0.20
0.30
0.40
0.50
0.60
0.70
0.80
0.90
1.00
Flow rate through LPRM (kg/s)

Figure 4-9

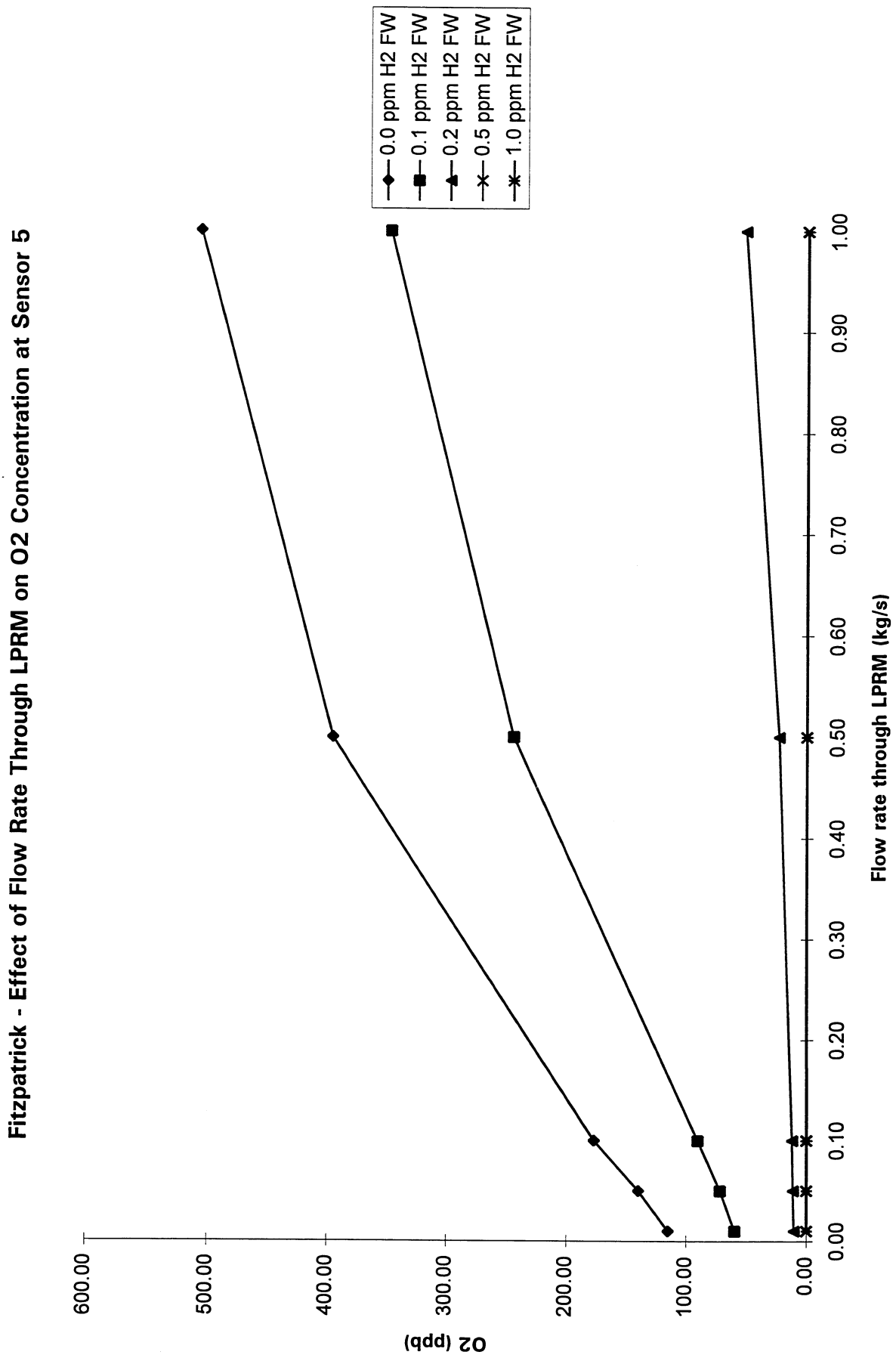
Fitzpatrick - Effect of Flow Rate Through LPRM on O2 Concentration at Sensor 5
0.0 ppm H2 FW
0.1 ppm H2 FW
0.2 ppm H2 FW
0.5 ppm H2 FW
1.0 ppm H2 FW
O2 (ppb)
600.00
500.00
400.00
300.00
200.00
100.00
0.00
0.00
0.10
0.20
0.30
0.40
0.50
0.60
0.70
0.80
0.90
1.00
Flow rate through LPRM (kg/s)

Figure 4-10

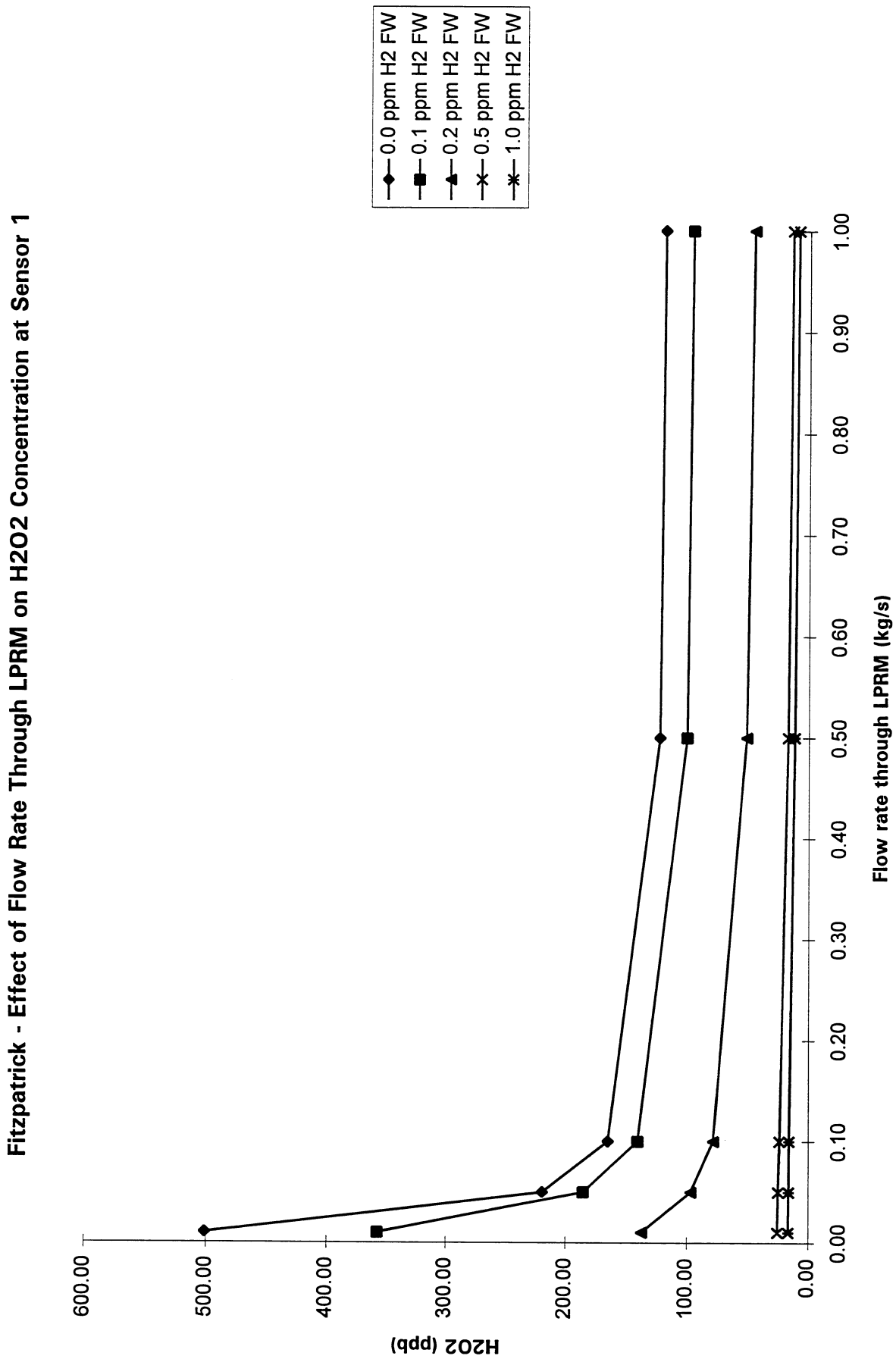
Fitzpatrick - Effect of Flow Rate Through LPRM on H2O2 Concentration at Sensor 1
0.0 ppm H2 FW
0.1 ppm H2 FW
0.2 ppm H2 FW
0.5 ppm H2 FW
1.0 ppm H2 FW
H2O2 (ppb)
600.00
500.00
400.00
300.00
200.00
100.00
0.00
0.00
0.10
0.20
0.30
0.40
0.50
0.60
0.70
0.80
0.90
1.00
Flow rate through LPRM (kg/s)

Figure 4-11

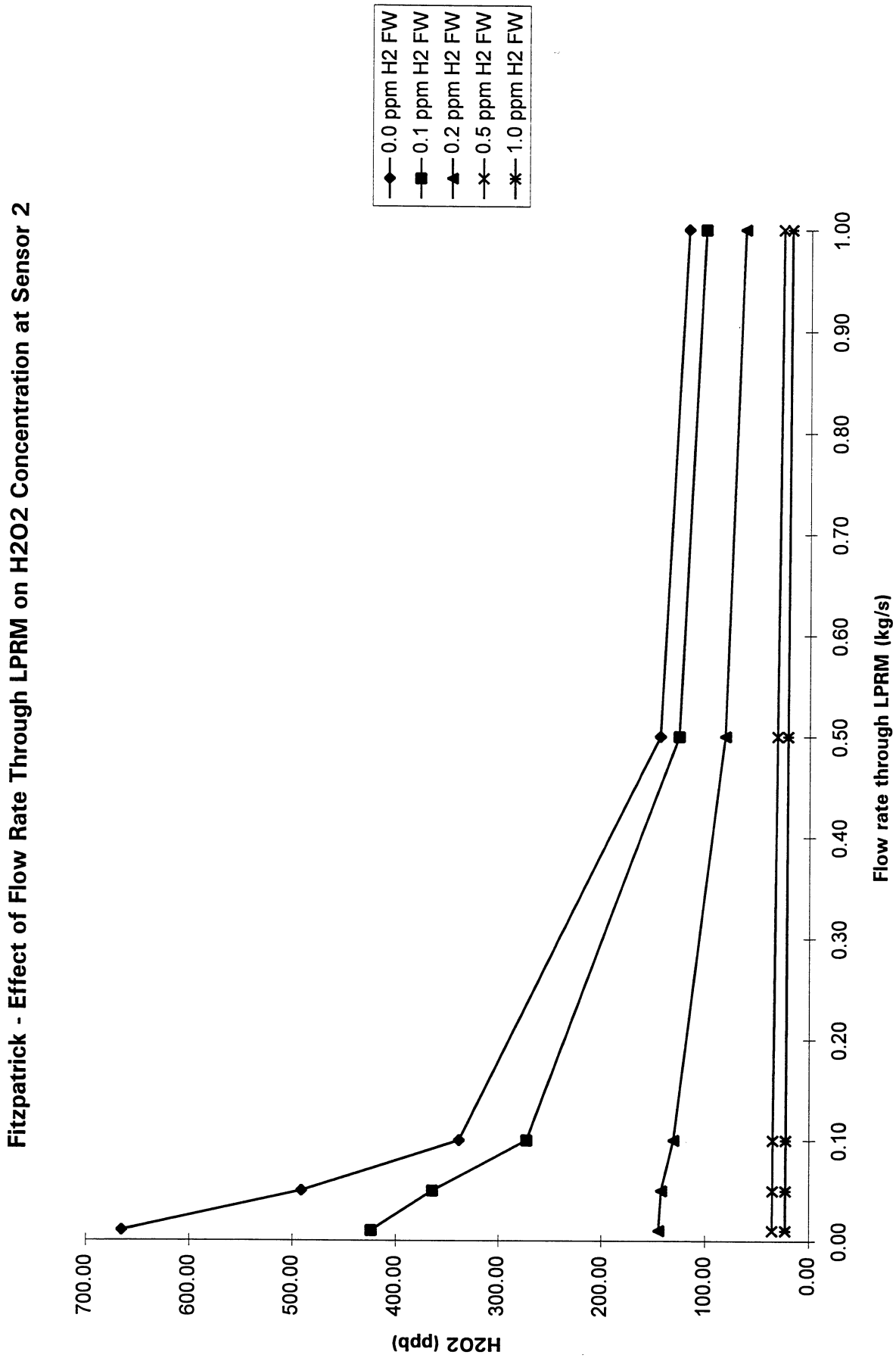
Fitzpatrick - Effect of Flow Rate Through LPRM on H2O2 Concentration at Sensor 2
0.0 ppm H2 FW
0.1 ppm H2 FW
0.2 ppm H2 FW
0.5 ppm H2 FW
1.0 ppm H2 FW
H2O2 (ppb)
700.00
600.00
500.00
400.00
300.00
200.00
100.00
0.00
0.00
0.10
0.20
0.30
0.40
0.50
0.60
0.70
0.80
0.90
1.00
Flow rate through LPRM (kg/s)

Figure 4-12

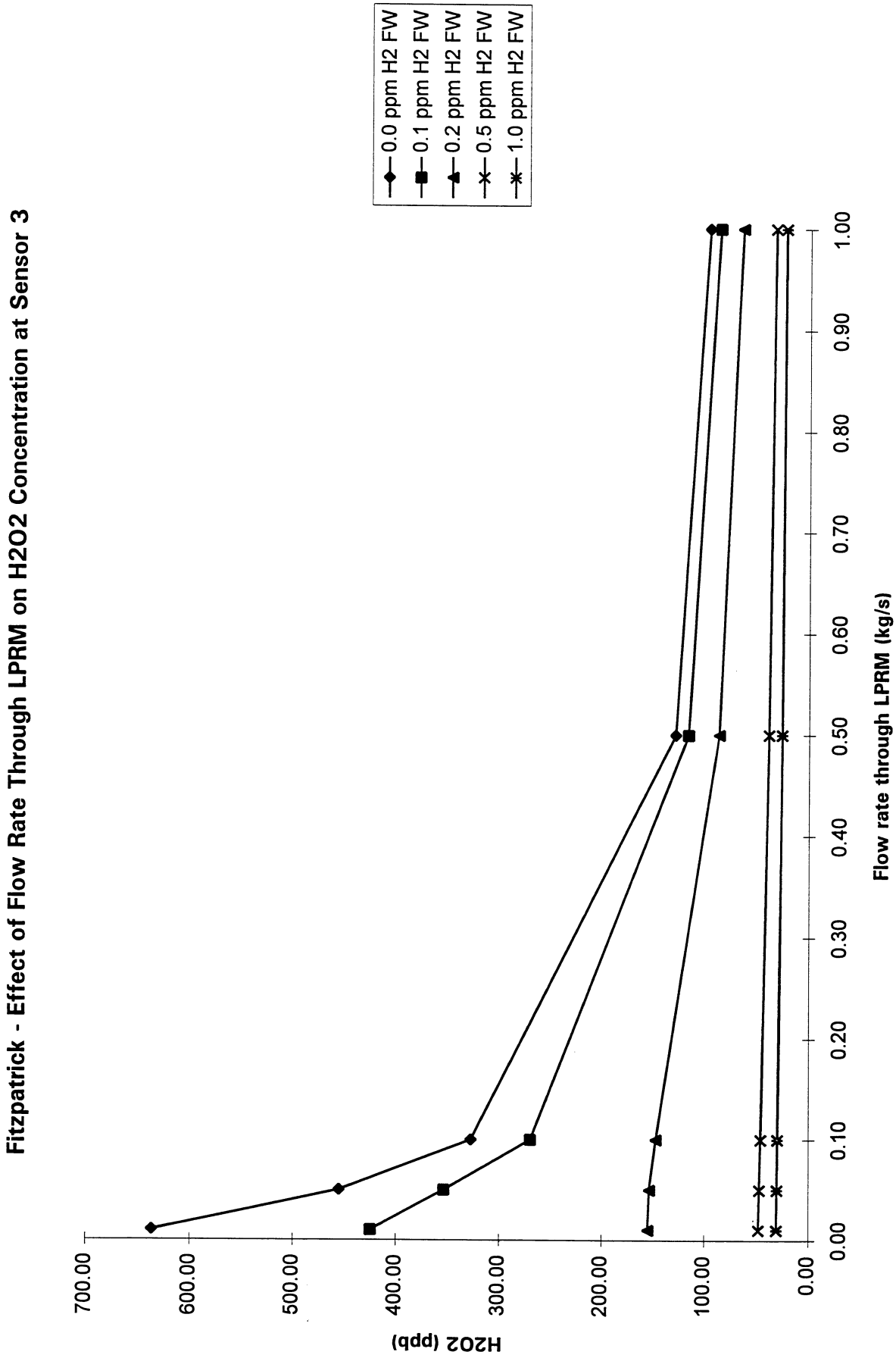
Fitzpatrick - Effect of Flow Rate Through LPRM on H2O2 Concentration at Sensor 3
0.0 ppm H2 FW
0.1 ppm H2 FW
0.2 ppm H2 FW
0.5 ppm H2 FW
1.0 ppm H2 FW
H2O2 (ppb)
700.00
600.00
500.00
400.00
300.00
200.00
100.00
0.00
0.00
0.10
0.20
0.30
0.40
0.50
0.60
0.70
0.80
0.90
1.00
Flow rate through LPRM (kg/s)

Figure 4-13

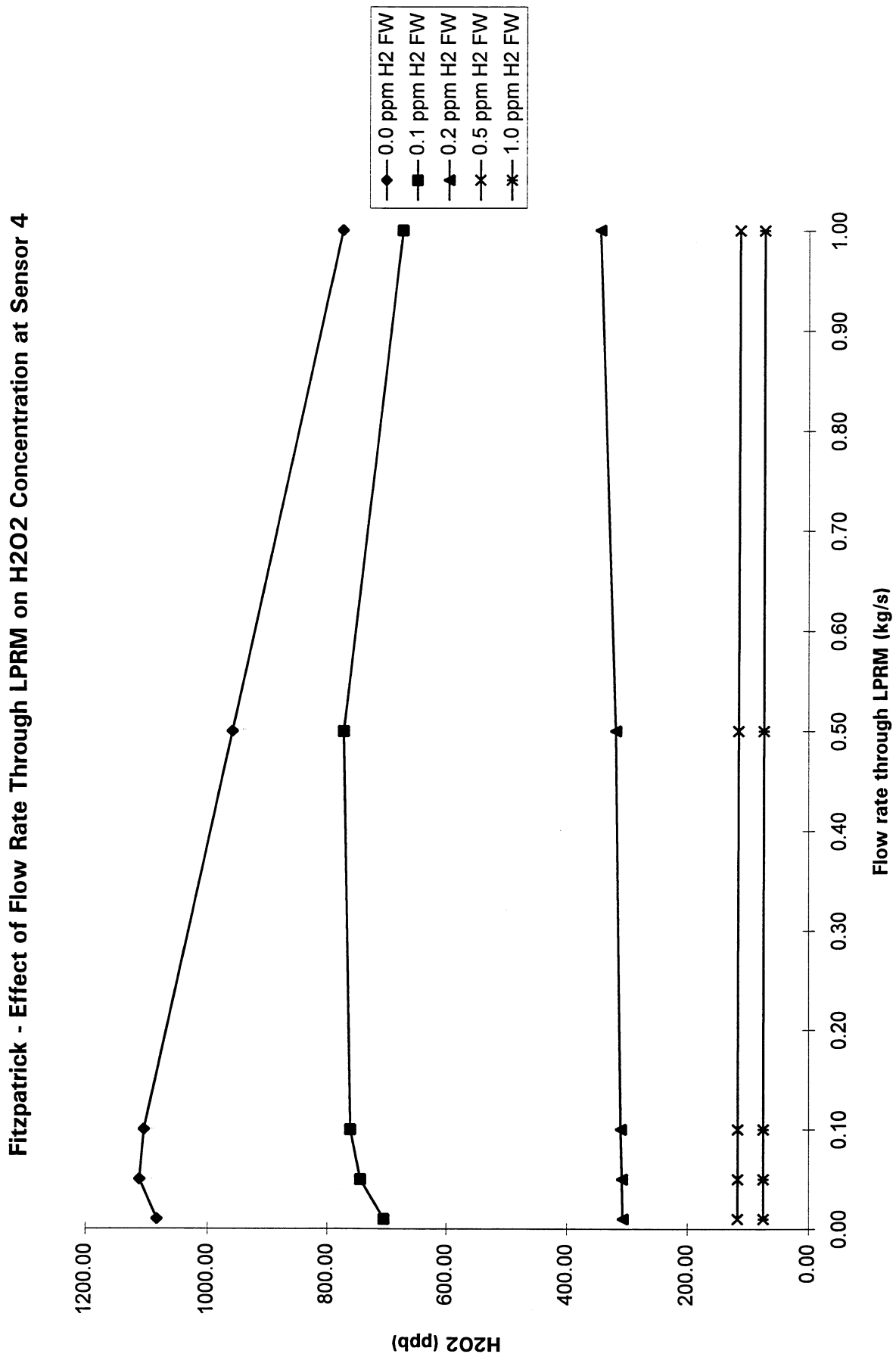
Fitzpatrick - Effect of Flow Rate Through LPRM on H2O2 Concentration at Sensor 4
0.0 ppm H2 FW
0.1 ppm H2 FW
0.2 ppm H2 FW
0.5 ppm H2 FW
1.0 ppm H2 FW
H2O2 (ppb)
1200.00
1000.00
800.00
600.00
400.00
200.00
0.00
0.00
0.10
0.20
0.30
0.40
0.50
0.60
0.70
0.80
0.90
1.00
Flow rate through LPRM (kg/s)

Figure 4-14

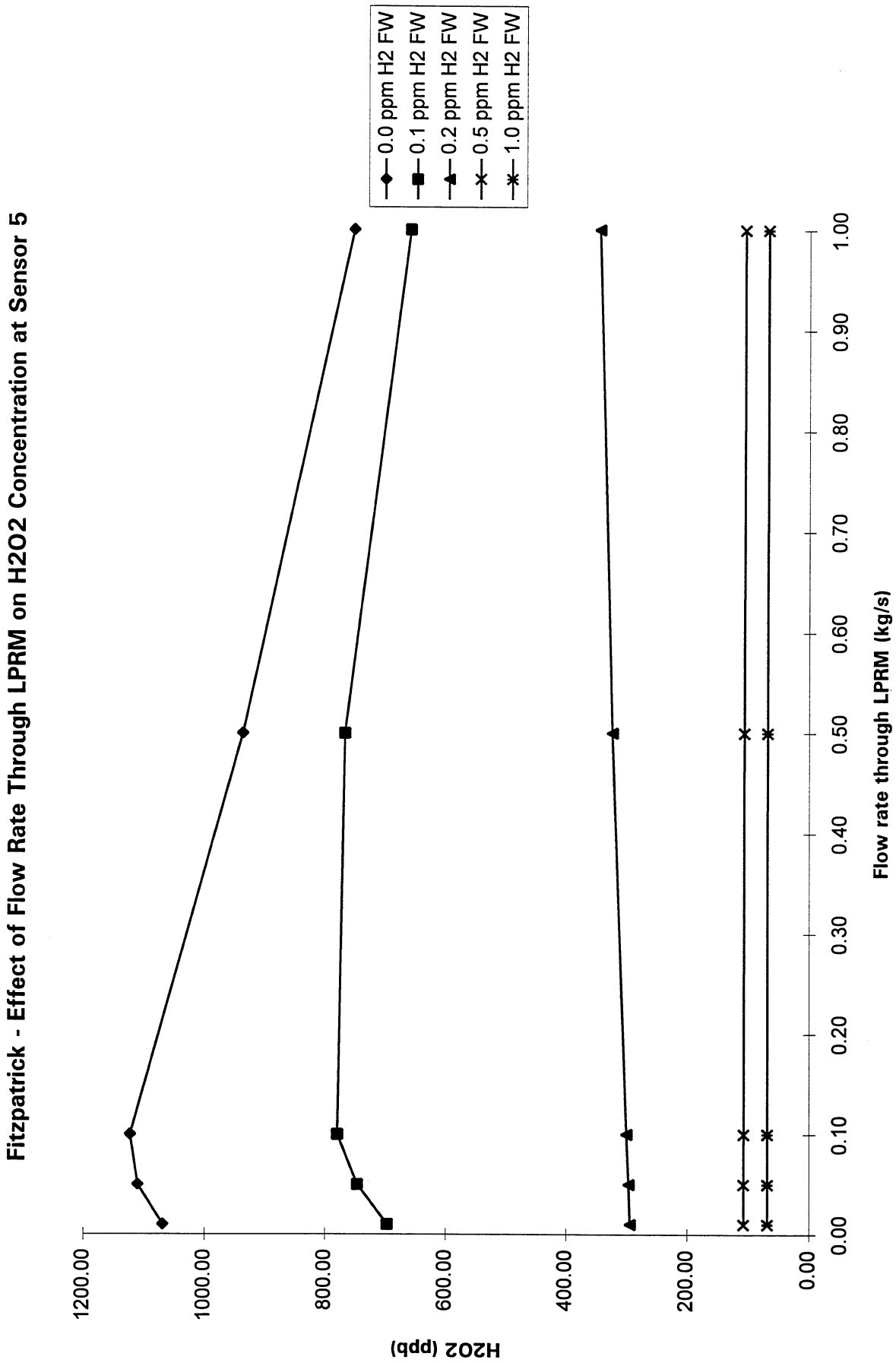
Fitzpatrick - Effect of Flow Rate Through LPRM on H2O2 Concentration at Sensor 5
0.0 ppm H2 FW
0.1 ppm H2 FW
0.2 ppm H2 FW
0.5 ppm H2 FW
1.0 ppm H2 FW
H2O2 (ppb)
1200.00
1000.00
800.00
600.00
400.00
200.00
0.00
0.00
0.10
0.20
0.30
0.40
0.50
0.60
0.70
0.80
0.90
1.00
Flow rate through LPRM (kg/s)

Figure 4-15

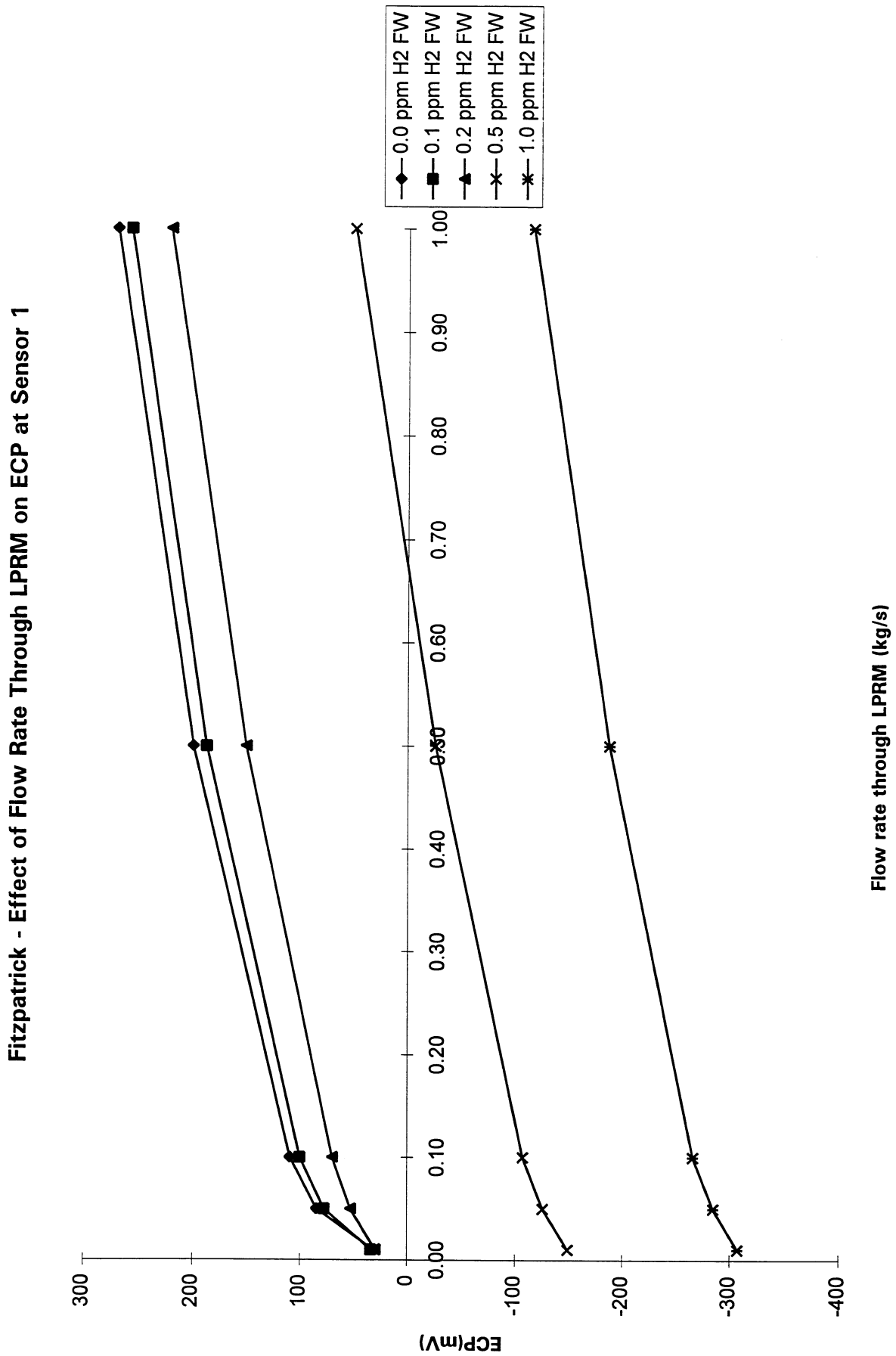
Fitzpatrick - Effect of Flow Rate Through LPRM on ECP at Sensor 1
0.0 ppm H2 FW
0.1 ppm H2 FW
0.2 ppm H2 FW
0.5 ppm H2 FW
1.0 ppm H2 FW
ECP(mV)
300
200
100
0
-100
-200
-300
-400
0.00
0.10
0.20
0.30
0.40
0.50
0.60
0.70
0.80
0.90
1.00
Flow rate through LPRM (kg/s)

Figure 4-16

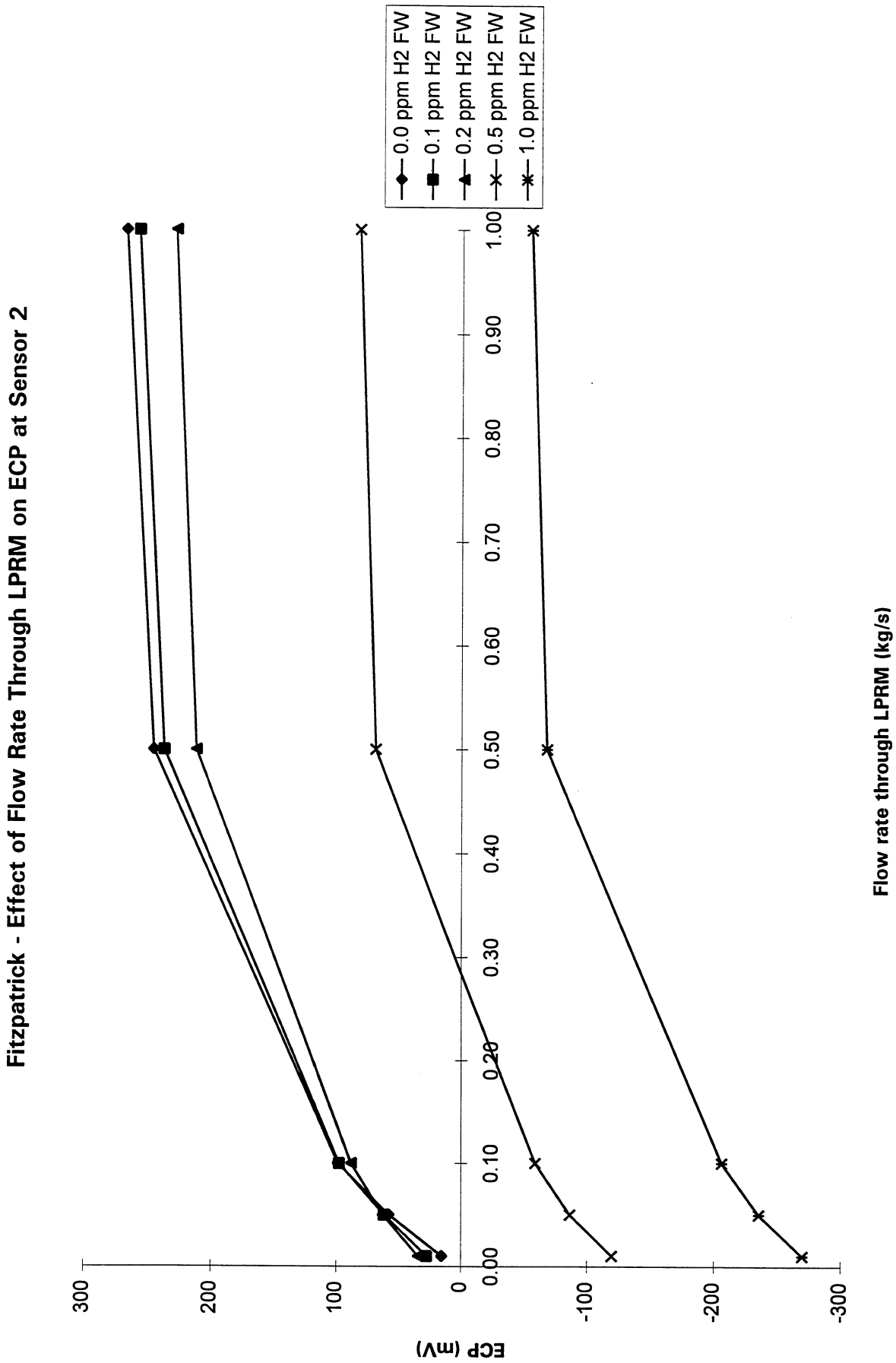
Fitzpatrick - Effect of Flow Rate Through LPRM on ECP at Sensor 2
0.0 ppm H2 FW
0.1 ppm H2 FW
0.2 ppm H2 FW
0.5 ppm H2 FW
1.0 ppm H2 FW
ECP (mV)
300
200
100
0
-100
-200
-300
0.00
0.10
0.20
0.30
0.40
0.50
0.60
0.70
0.80
0.90
1.00
Flow rate through LPRM (kg/s)

Figure 4-17

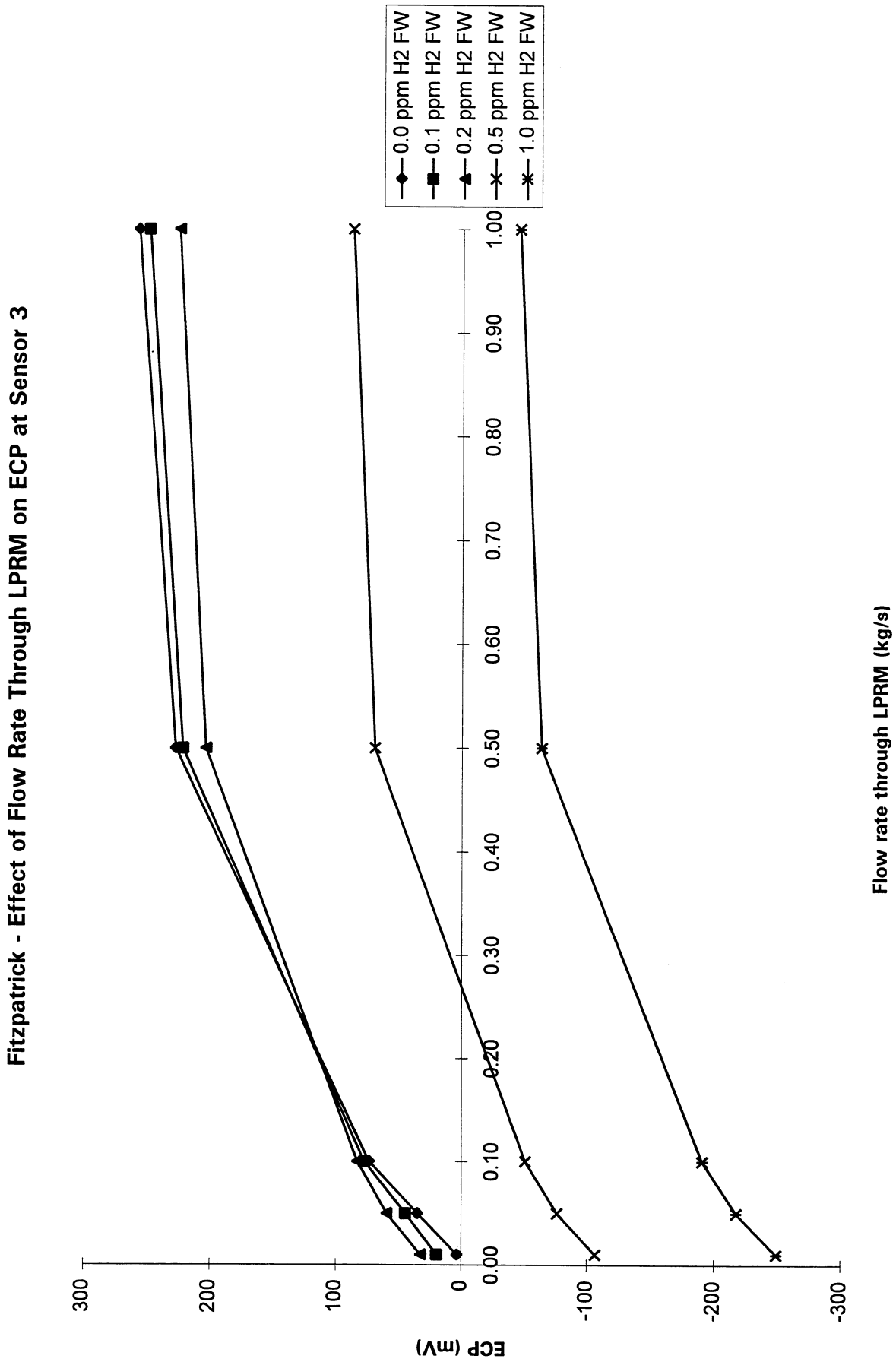
Fitzpatrick - Effect of Flow Rate Through LPRM on ECP at Sensor 3
0.0 ppm H2 FW
0.1 ppm H2 FW
0.2 ppm H2 FW
0.5 ppm H2 FW
1.0 ppm H2 FW
ECP (mV)
300
200
100
0
-100
-200
-300
0.00
0.10
0.20
0.30
0.40
0.50
0.60
0.70
0.80
0.90
1.00
Flow rate through LPRM (kg/s)

Figure 4-18

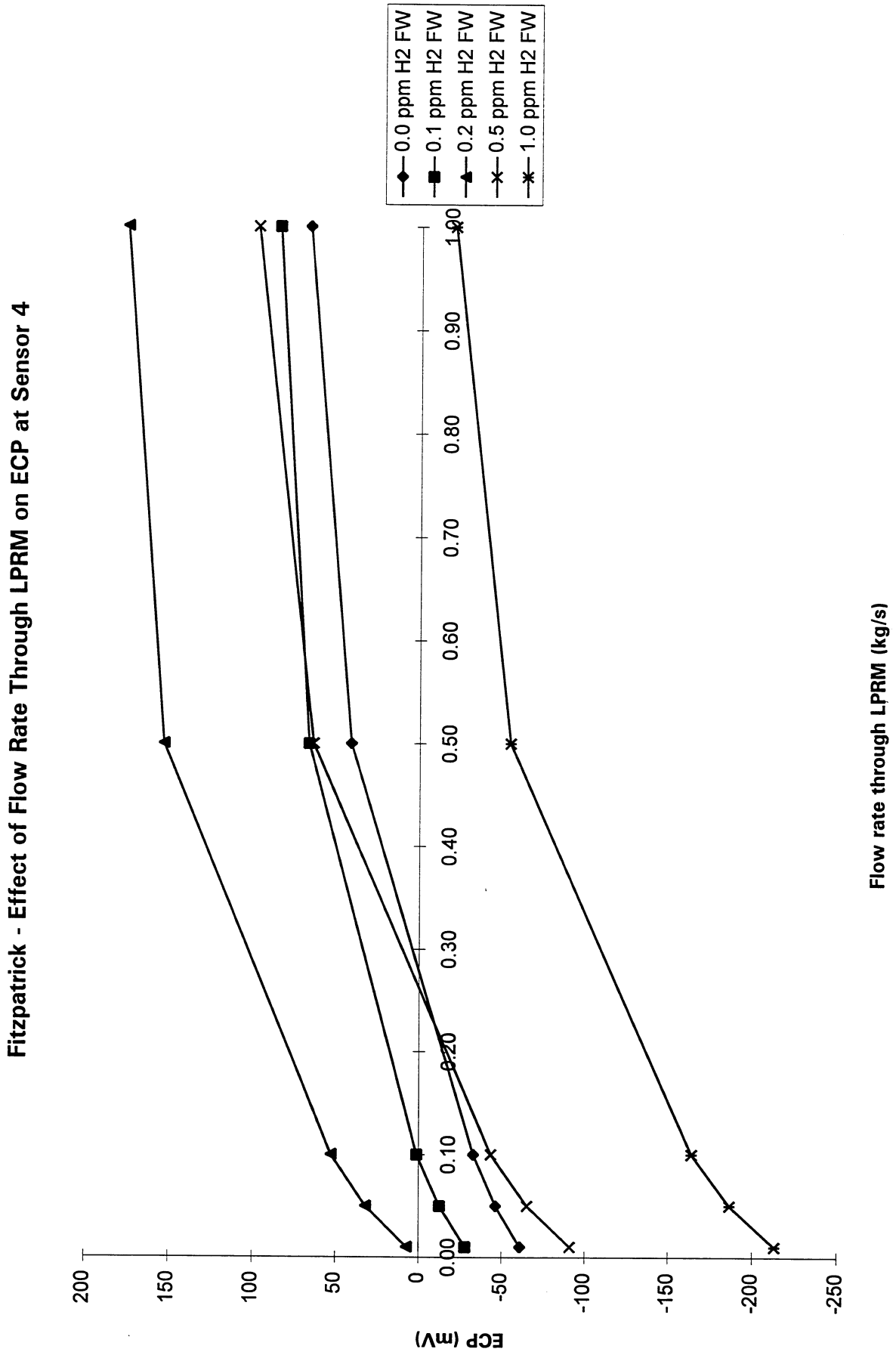
Fitzpatrick - Effect of Flow Rate Through LPRM on ECP at Sensor 4
0.0 ppm H2 FW
0.1 ppm H2 FW
0.2 ppm H2 FW
0.5 ppm H2 FW
1.0 ppm H2 FW
ECP (mV)
200
150
100
50
0
-50
-100
-150
-200
-250
0.00
0.10
0.20
0.30
0.40
0.50
0.60
0.70
0.80
0.90
1.00
Flow rate through LPRM (kg/s)

Figure 4-19

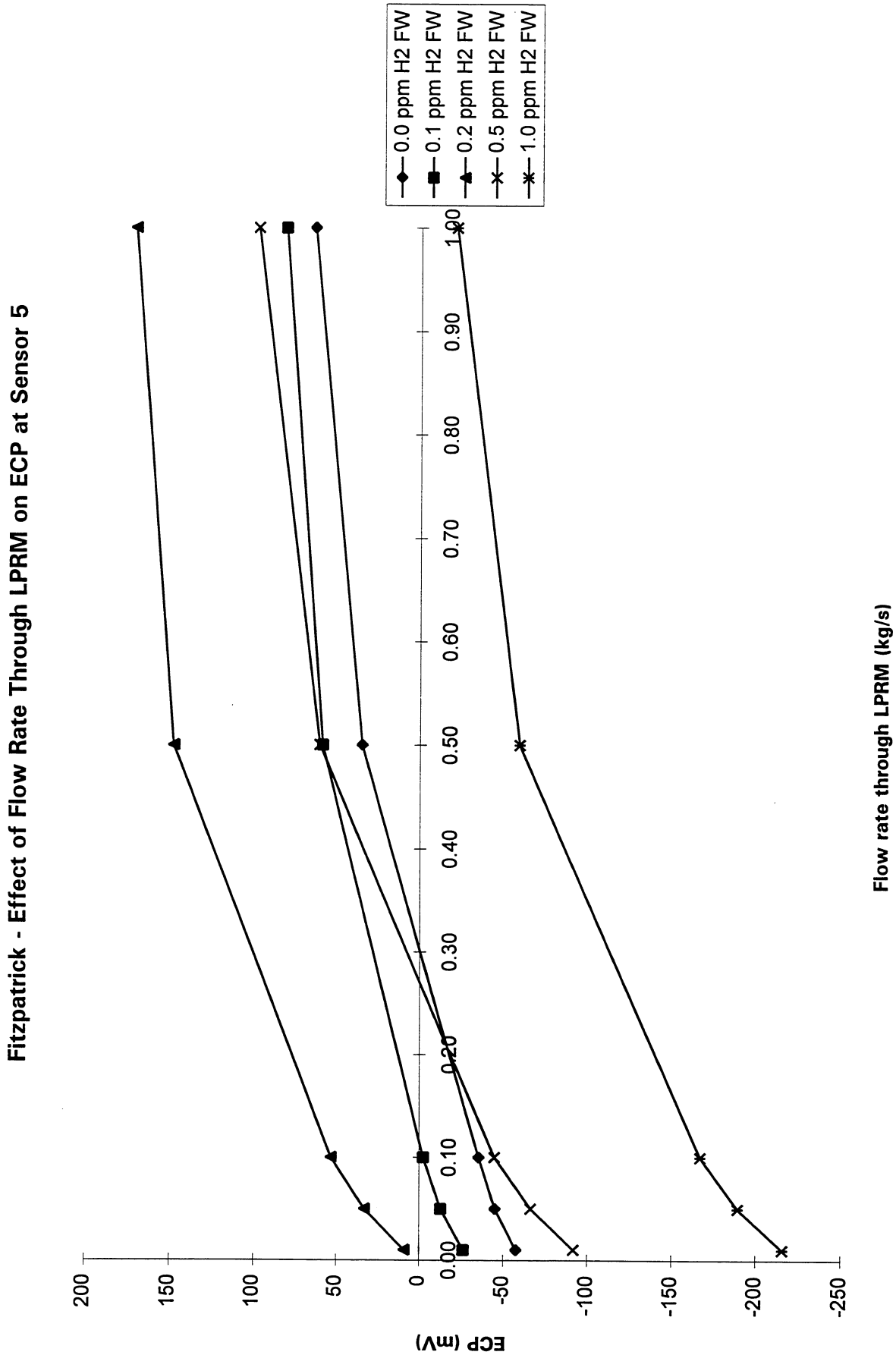
Fitzpatrick - Effect of Flow Rate Through LPRM on ECP at Sensor 5
0.0 ppm H2 FW
0.1 ppm H2 FW
0.2 ppm H2 FW
0.5 ppm H2 FW
1.0 ppm H2 FW
ECP (mV)
200
150
100
50
0
-50
-100
-150
-200
-250
0.00
0.10
0.20
0.30
0.40
0.50
0.60
0.70
0.80
0.90
1.00
Flow rate through LPRM (kg/s)

Figure 4-20

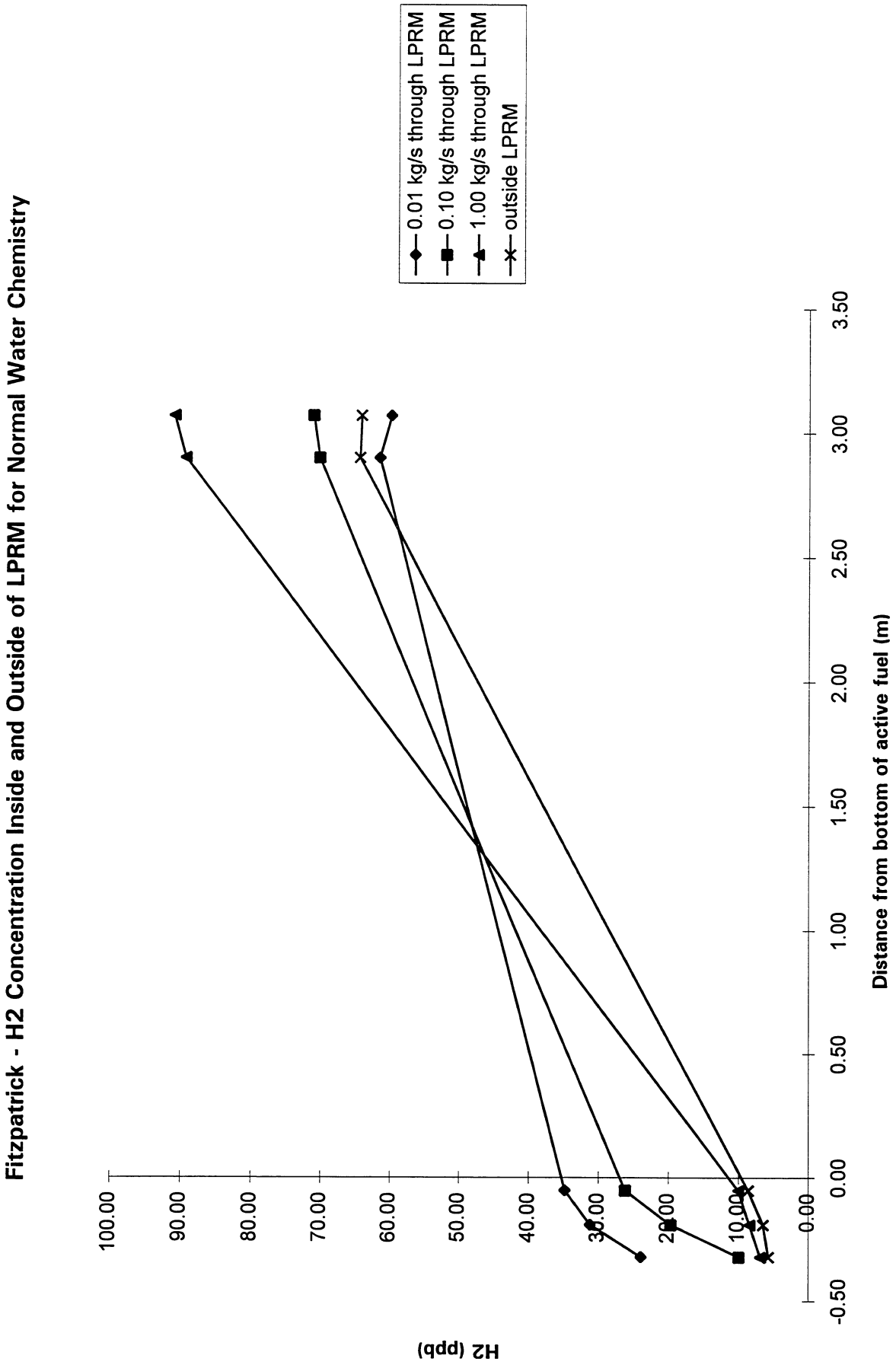
Fitzpatrick - H2 Concentration Inside and Outside of LPRM for Normal Water Chemistry
0.01 kg/s through LPRM
0.10 kg/s through LPRM
1.00 kg/s through LPRM
outside LPRM
H2 (ppb)
100.00
90.00
80.00
70.00
60.00
50.00
40.00
30.00
20.00
10.00
0.00
-0.50
0.00
0.50
1.00
1.50
2.00
2.50
3.00
3.50
Distance from bottom of active fuel (m)

Figure 4-21

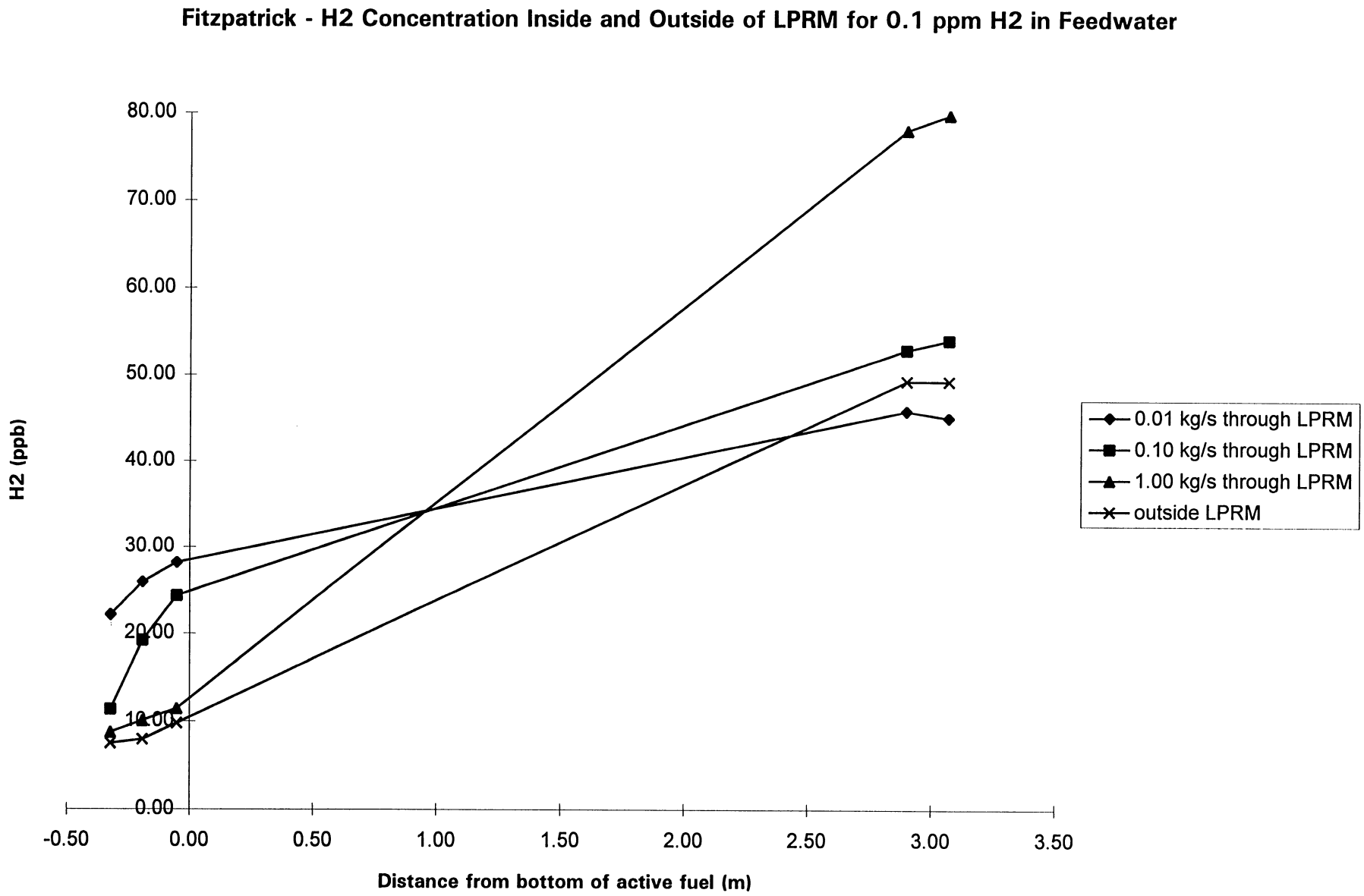
Fitzpatrick - H2 Concentration Inside and Outside of LPRM for 0.1 ppm H2 in Feedwater
H2 (ppb)
80.00
70.00
60.00
50.00
40.00
30.00
20.00
10.00
0.00
-0.50
0.00
0.50
1.00
1.50
2.00
2.50
3.00
3.50
Distance from bottom of active fuel (m)
0.01 kg/s through LPRM
0.10 kg/s through LPRM
1.00 kg/s through LPRM
outside LPRM

Figure 4-22

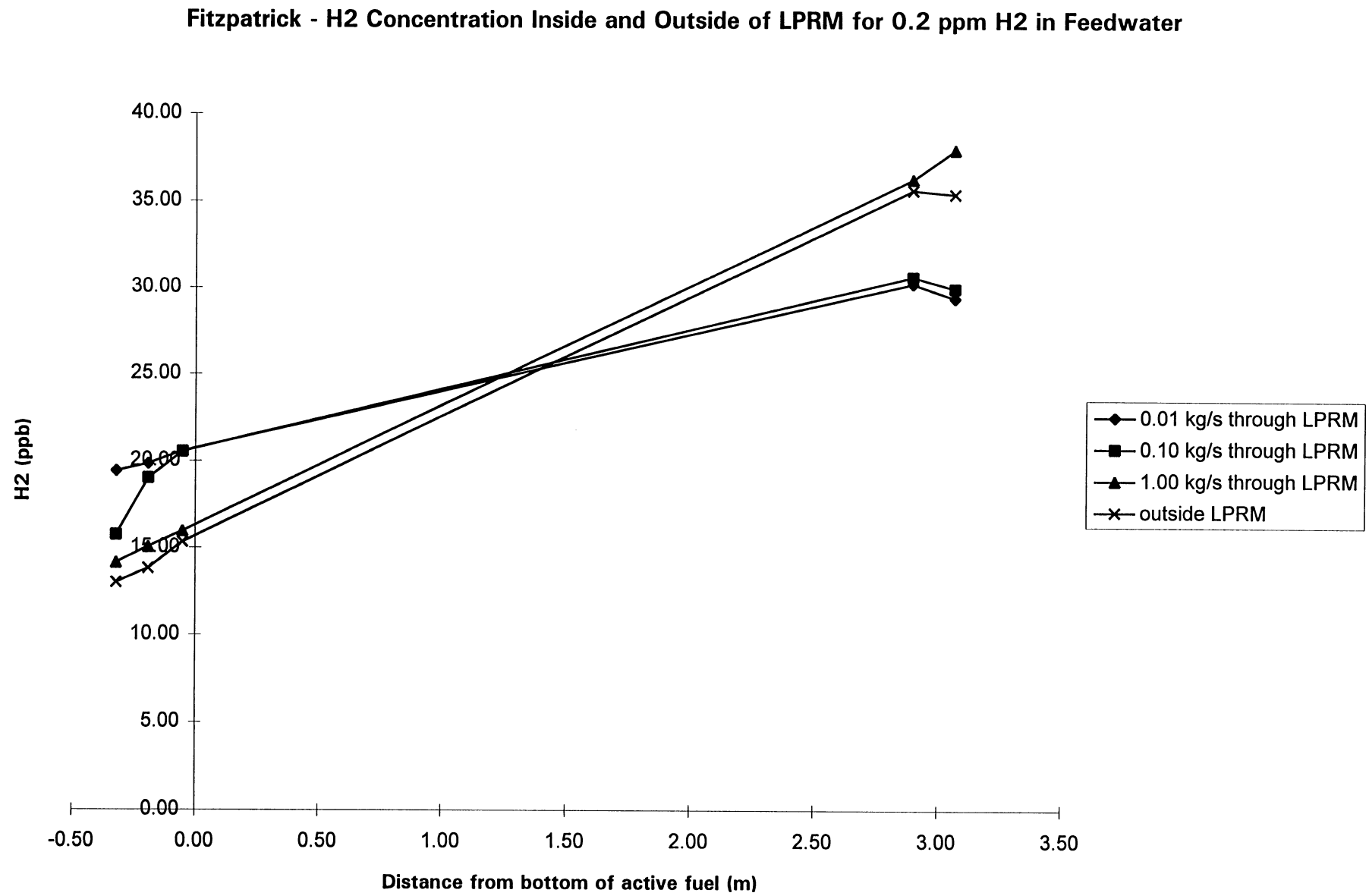
Fitzpatrick - H2 Concentration Inside and Outside of LPRM for 0.2 ppm H2 in Feedwater
H2 (ppb)
40.00
35.00
30.00
25.00
20.00
15.00
10.00
5.00
0.00
-0.50
0.00
0.50
1.00
1.50
2.00
2.50
3.00
3.50
Distance from bottom of active fuel (m)
0.01 kg/s through LPRM
0.10 kg/s through LPRM
1.00 kg/s through LPRM
outside LPRM

Figure 4-23

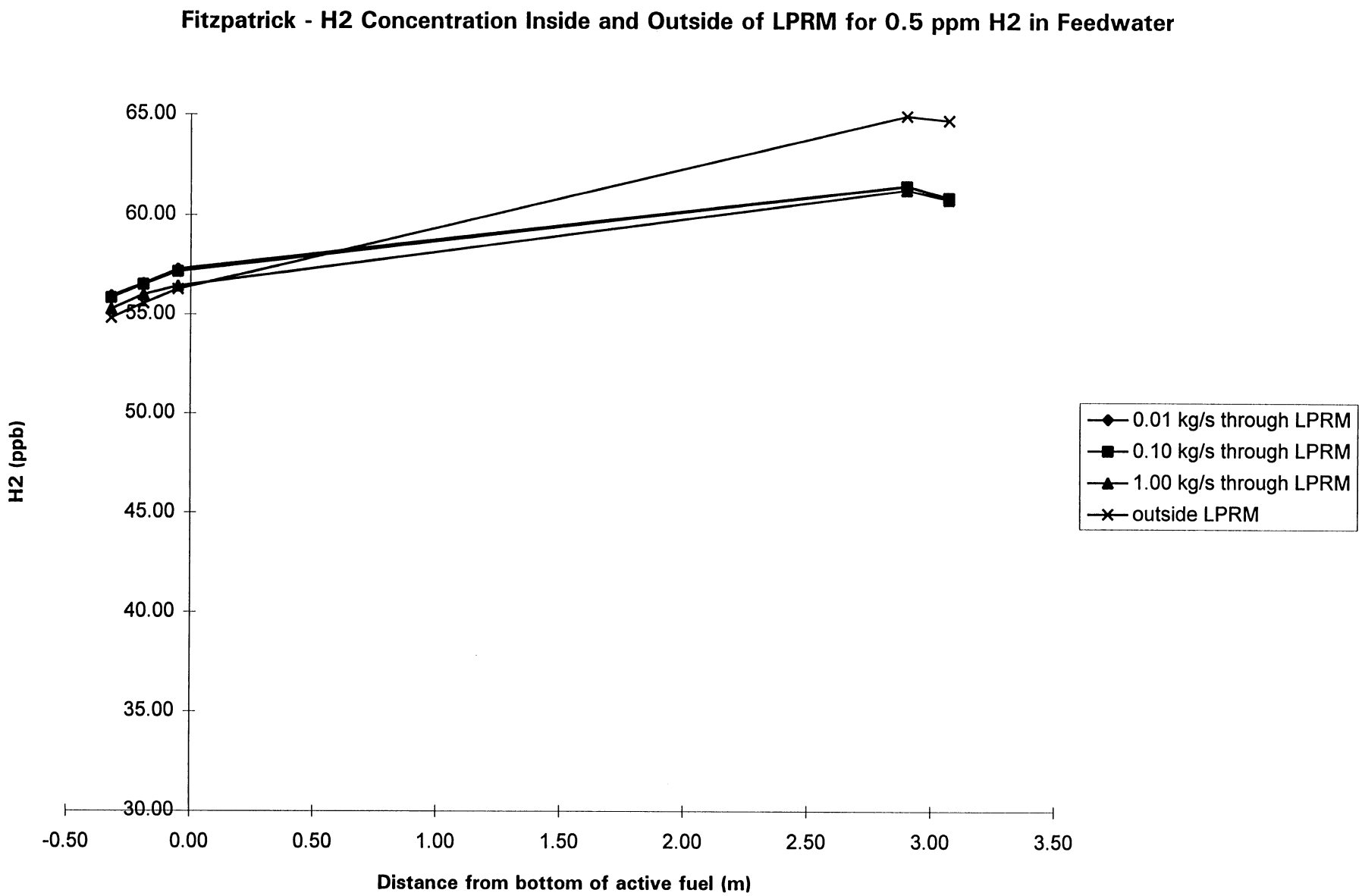
Fitzpatrick - H2 Concentration Inside and Outside of LPRM for 0.5 ppm H2 in Feedwater
65.00
60.00
55.00
50.00
45.00
40.00
35.00
30.00
H2 (ppb)
-0.50
0.00
0.50
1.00
1.50
2.00
2.50
3.00
3.50
Distance from bottom of active fuel (m)
0.01 kg/s through LPRM
0.10 kg/s through LPRM
1.00 kg/s through LPRM
outside LPRM

Figure 4-24

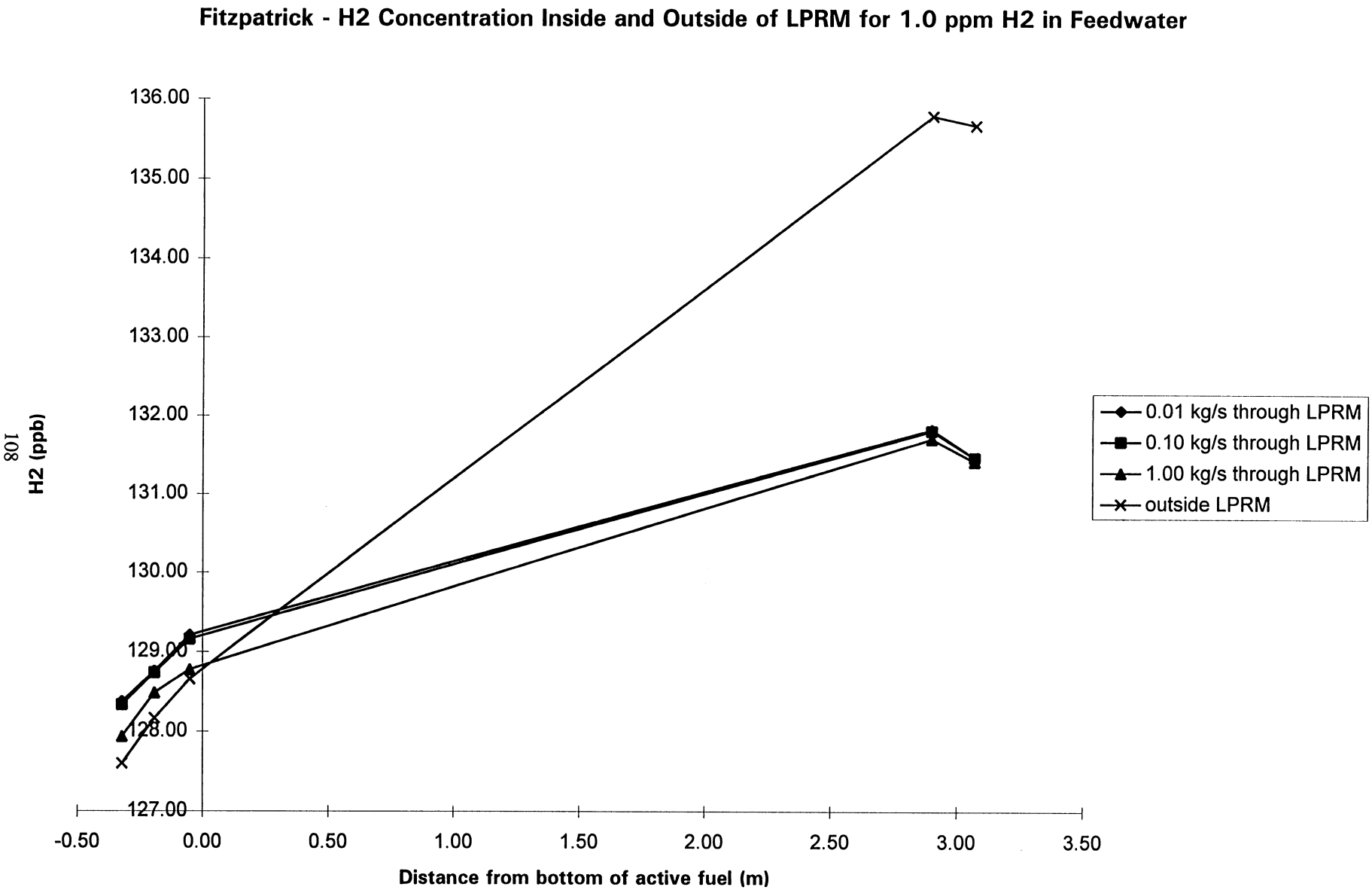
Fitzpatrick - H2 Concentration Inside and Outside of LPRM for 1.0 ppm H2 in Feedwater
H2 (ppb)
136.00
135.00
134.00
133.00
132.00
131.00
130.00
129.00
128.00
127.00
-0.50
0.00
0.50
1.00
1.50
2.00
2.50
3.00
3.50
Distance from bottom of active fuel (m)
0.01 kg/s through LPRM
0.10 kg/s through LPRM
1.00 kg/s through LPRM
outside LPRM

Figure 4-25

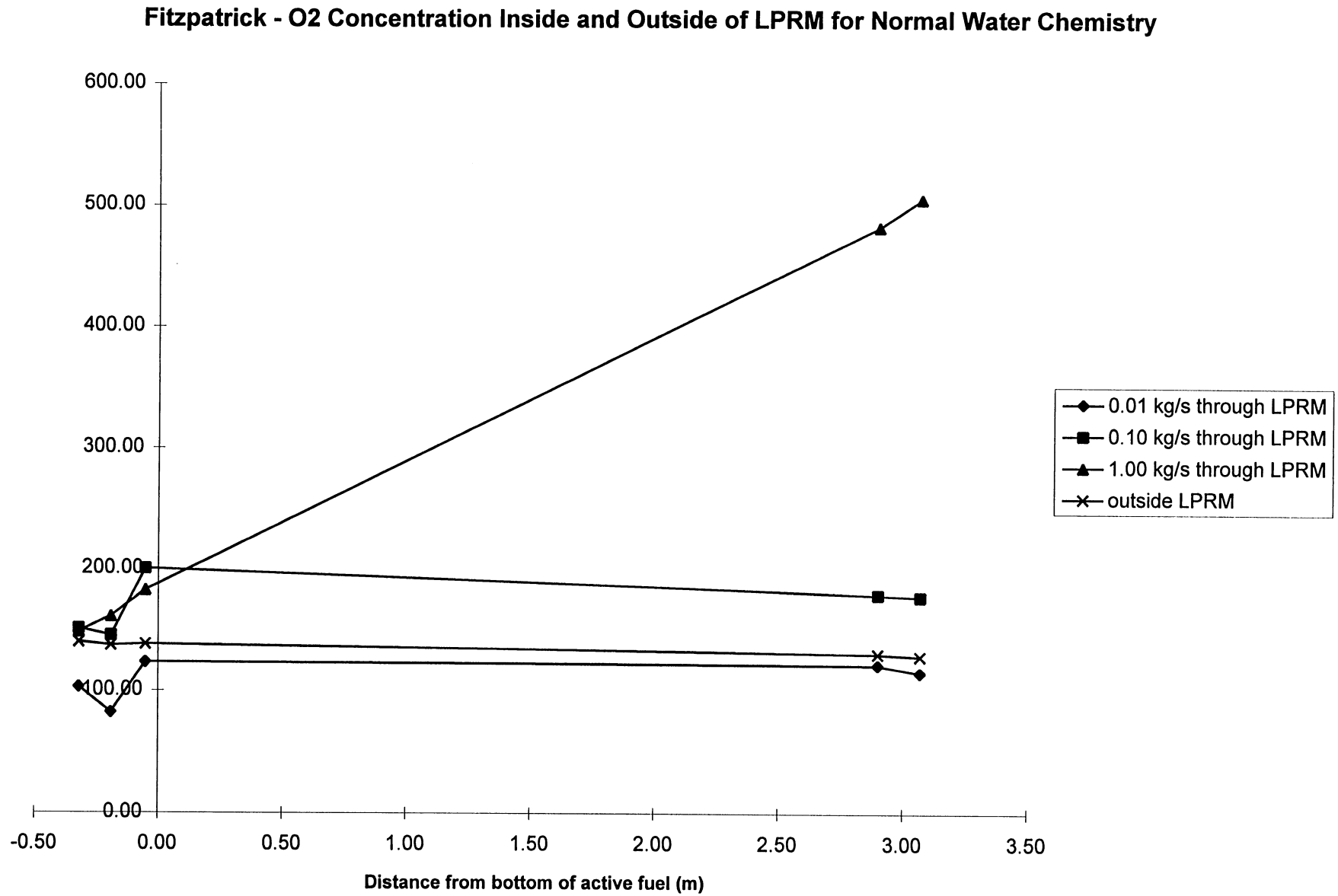
Fitzpatrick - O2 Concentration Inside and Outside of LPRM for Normal Water Chemistry
O2 (ppb)
600.00
500.00
400.00
300.00
200.00
100.00
0.00
-0.50
0.00
0.50
1.00
1.50
2.00
2.50
3.00
3.50
Distance from bottom of active fuel (m)
0.01 kg/s through LPRM
0.10 kg/s through LPRM
1.00 kg/s through LPRM
outside LPRM

Figure 4-26

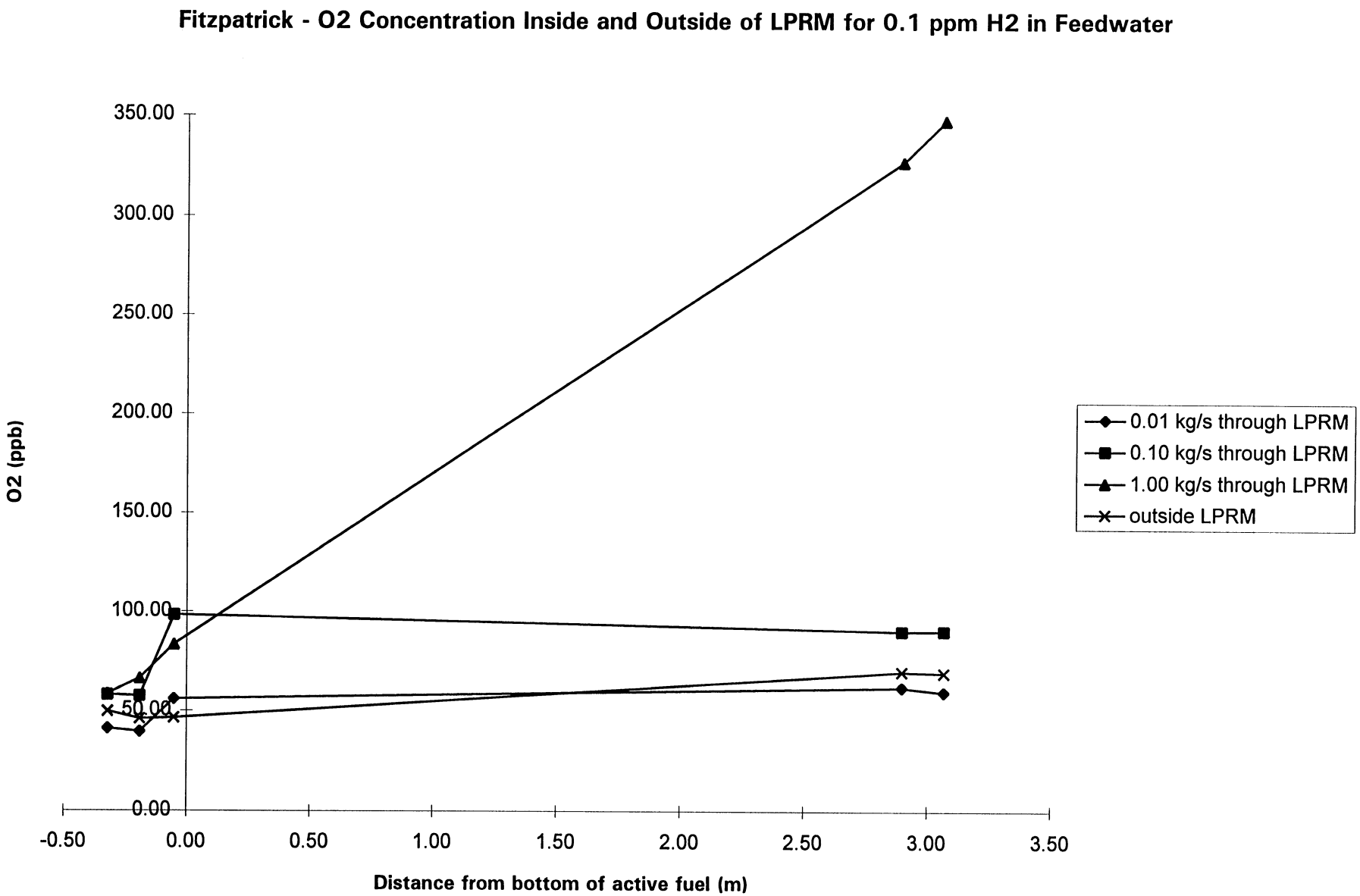
Fitzpatrick - O2 Concentration Inside and Outside of LPRM for 0.1 ppm H2 in Feedwater
O2 (ppb)
350.00
300.00
250.00
200.00
150.00
100.00
50.00
0.00
-0.50
0.00
0.50
1.00
1.50
2.00
2.50
3.00
3.50
Distance from bottom of active fuel (m)
0.01 kg/s through LPRM
0.10 kg/s through LPRM
1.00 kg/s through LPRM
outside LPRM

Figure 4-27

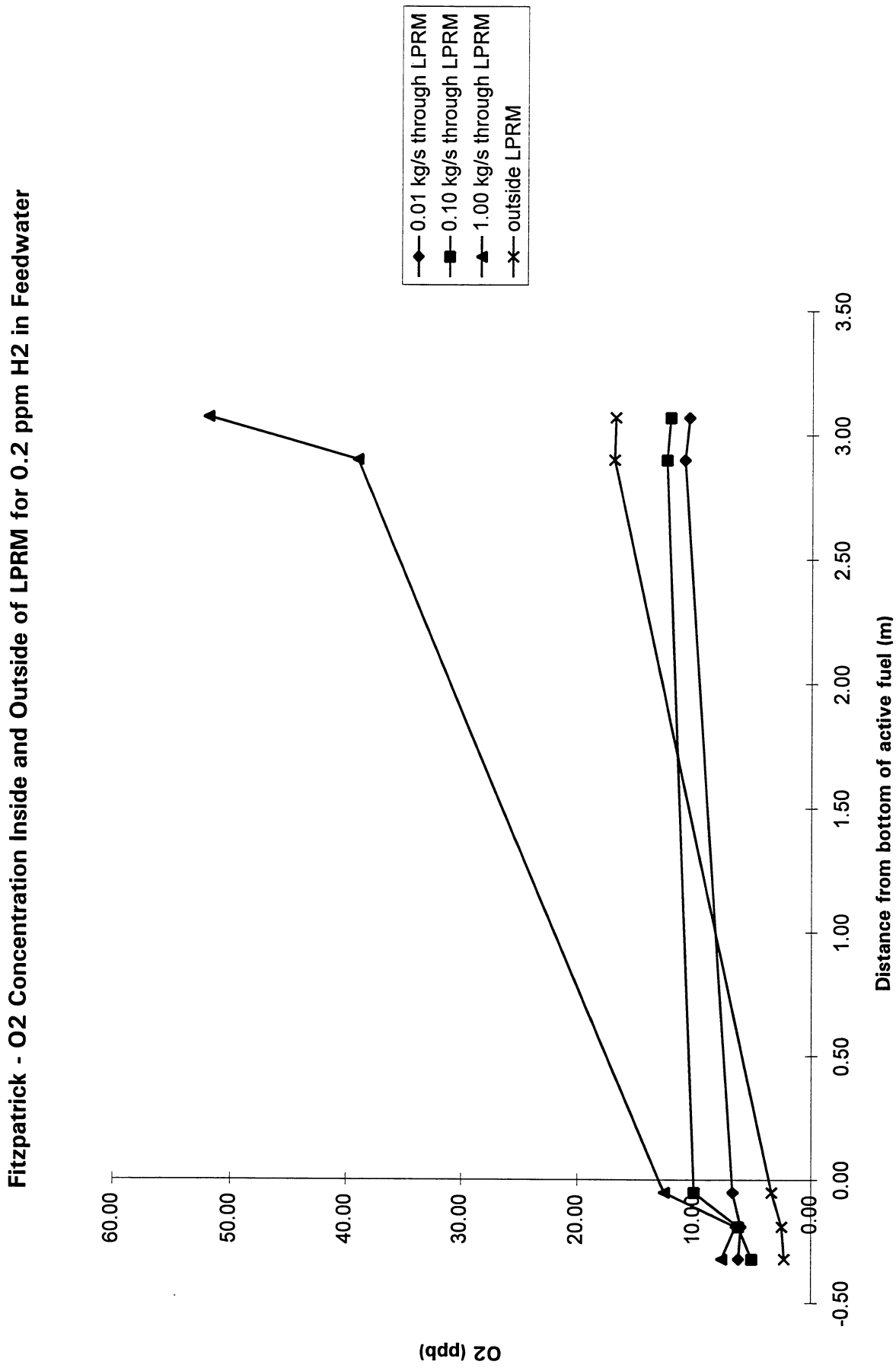
Fitzpatrick - O2 Concentration Inside and Outside of LPRM for 0.2 ppm H2 in Feedwater
0.01 kg/s through LPRM
0.10 kg/s through LPRM
1.00 kg/s through LPRM
outside LPRM
O2 (ppb)
60.00
50.00
40.00
30.00
20.00
10.00
0.00
-0.50
0.00
0.50
1.00
1.50
2.00
2.50
3.00
3.50
Distance from bottom of active fuel (m)

Figure 4-28

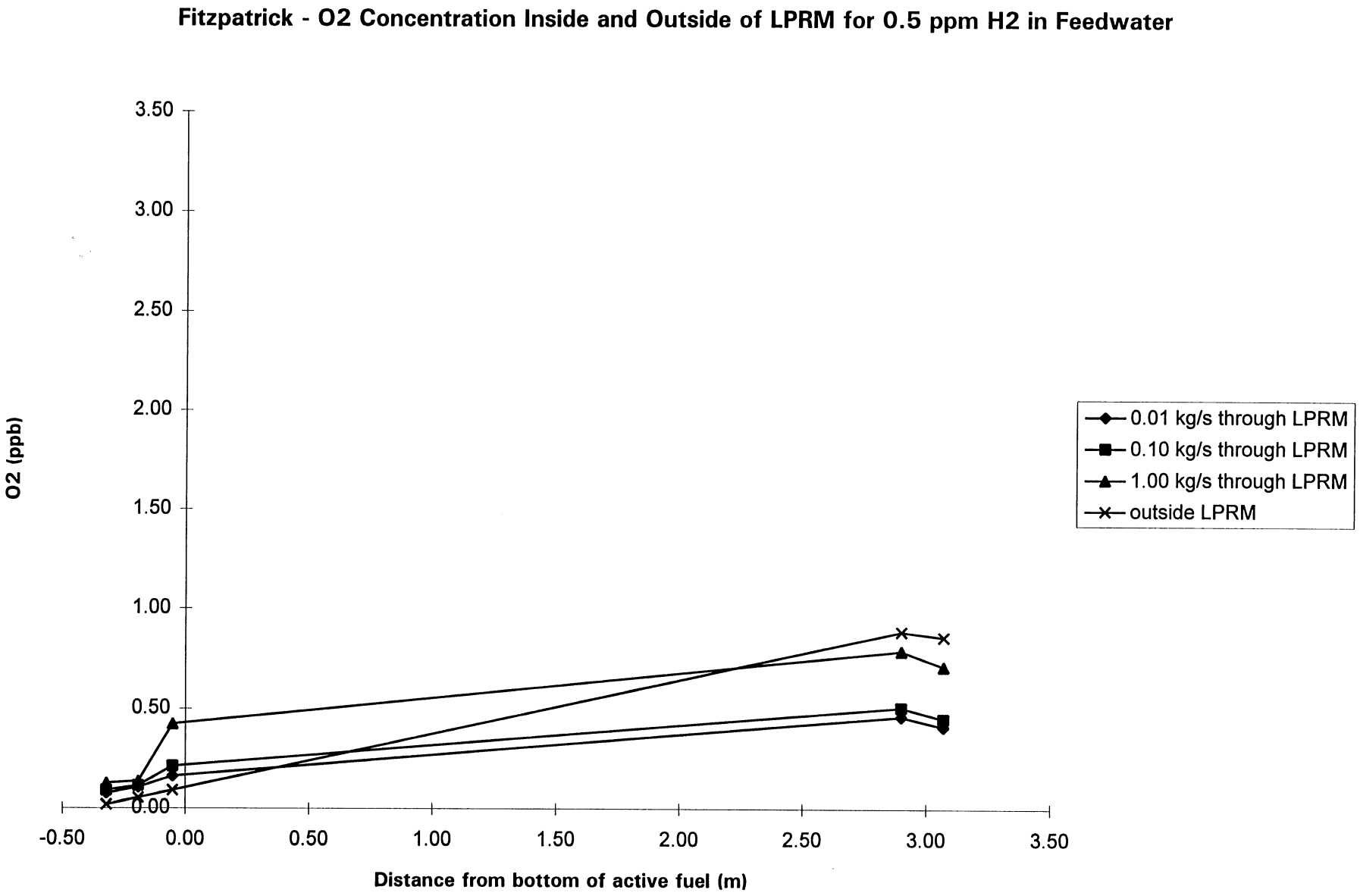
Fitzpatrick - O2 Concentration Inside and Outside of LPRM for 0.5 ppm H2 in Feedwater
O2 (ppb)
3.50
3.00
2.50
2.00
1.50
1.00
0.50
0.00
-0.50
0.00
0.50
1.00
1.50
2.00
2.50
3.00
3.50
Distance from bottom of active fuel (m)
0.01 kg/s through LPRM
0.10 kg/s through LPRM
1.00 kg/s through LPRM
outside LPRM

Figure 4-29

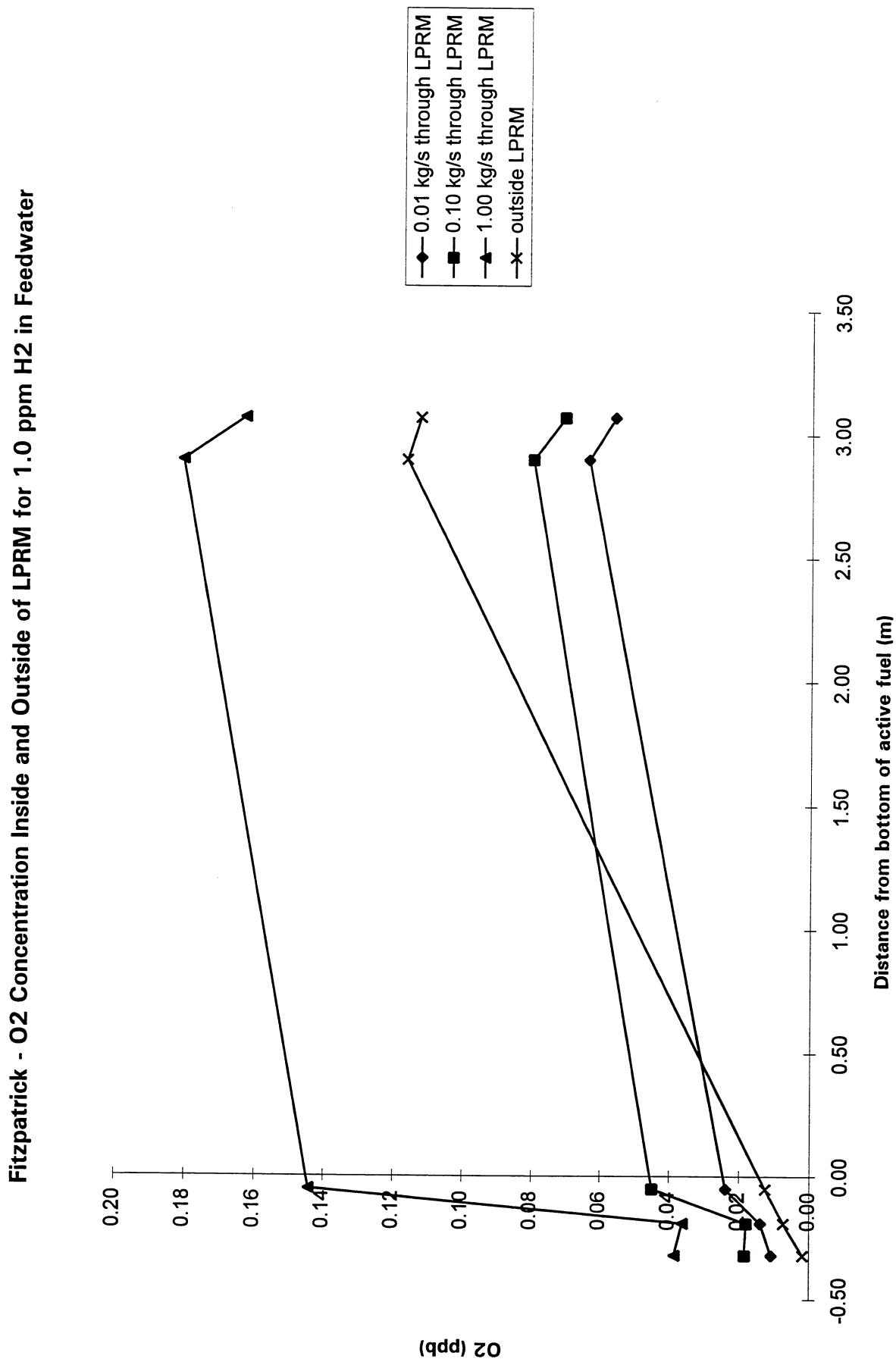
Fitzpatrick - O2 Concentration Inside and Outside of LPRM for 1.0 ppm H2 in Feedwater
0.01 kg/s through LPRM
0.10 kg/s through LPRM
1.00 kg/s through LPRM
outside LPRM
O2 (ppb)
0.20
0.18
0.16
0.14
0.12
0.10
0.08
0.06
0.04
0.02
0.00
-0.50
0.00
0.50
1.00
1.50
2.00
2.50
3.00
3.50
Distance from bottom of active fuel (m)

Figure 4-30

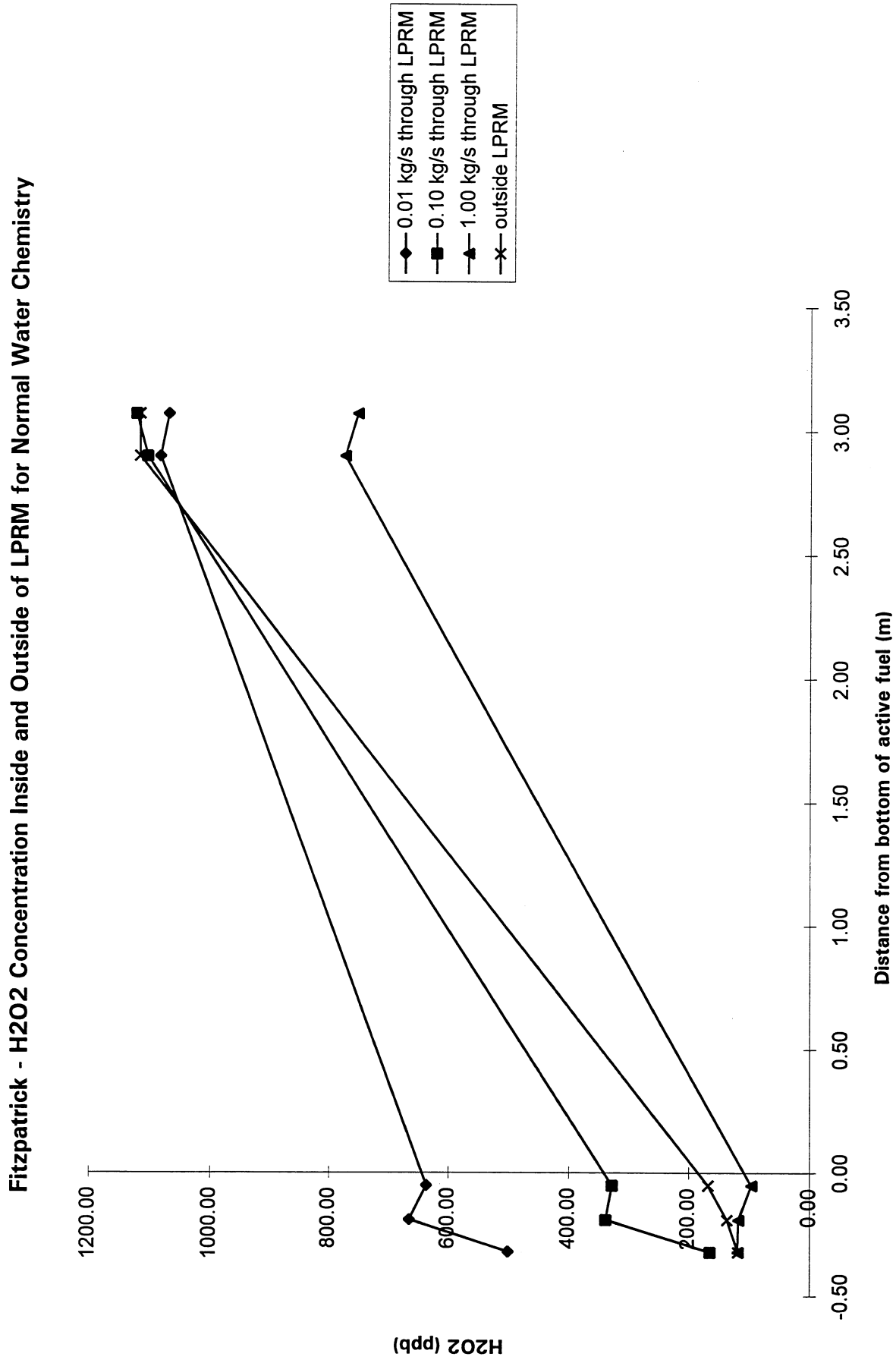
Fitzpatrick - H2O2 Concentration Inside and Outside of LPRM for Normal Water Chemistry
0.01 kg/s through LPRM
0.10 kg/s through LPRM
1.00 kg/s through LPRM
outside LPRM
H2O2 (ppb)
1200.00
1000.00
800.00
600.00
400.00
200.00
0.00
-0.50
0.00
0.50
1.00
1.50
2.00
2.50
3.00
3.50
Distance from bottom of active fuel (m)

Figure 4-31

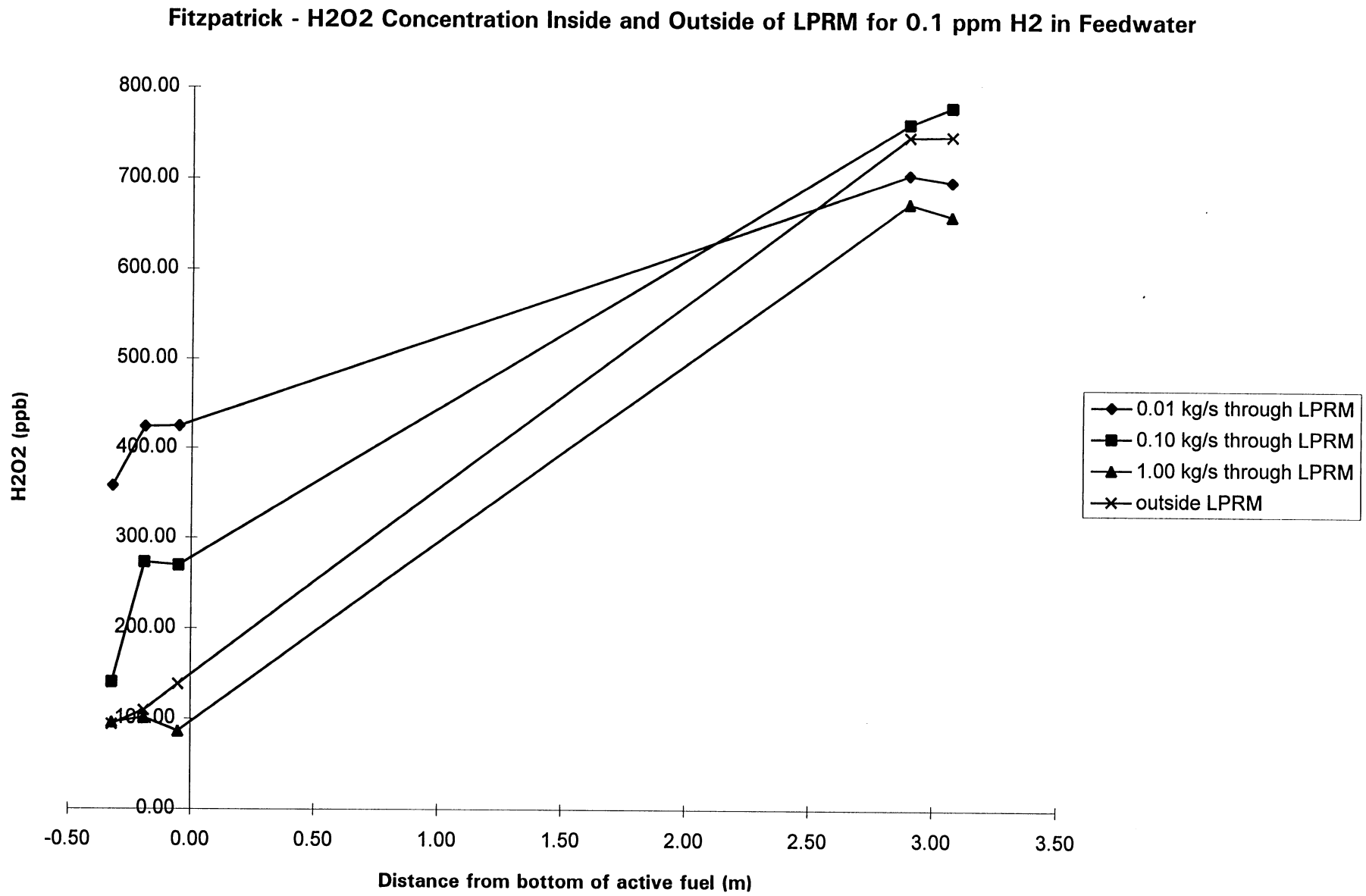

Figure 4-32

EPRI Licensed Material

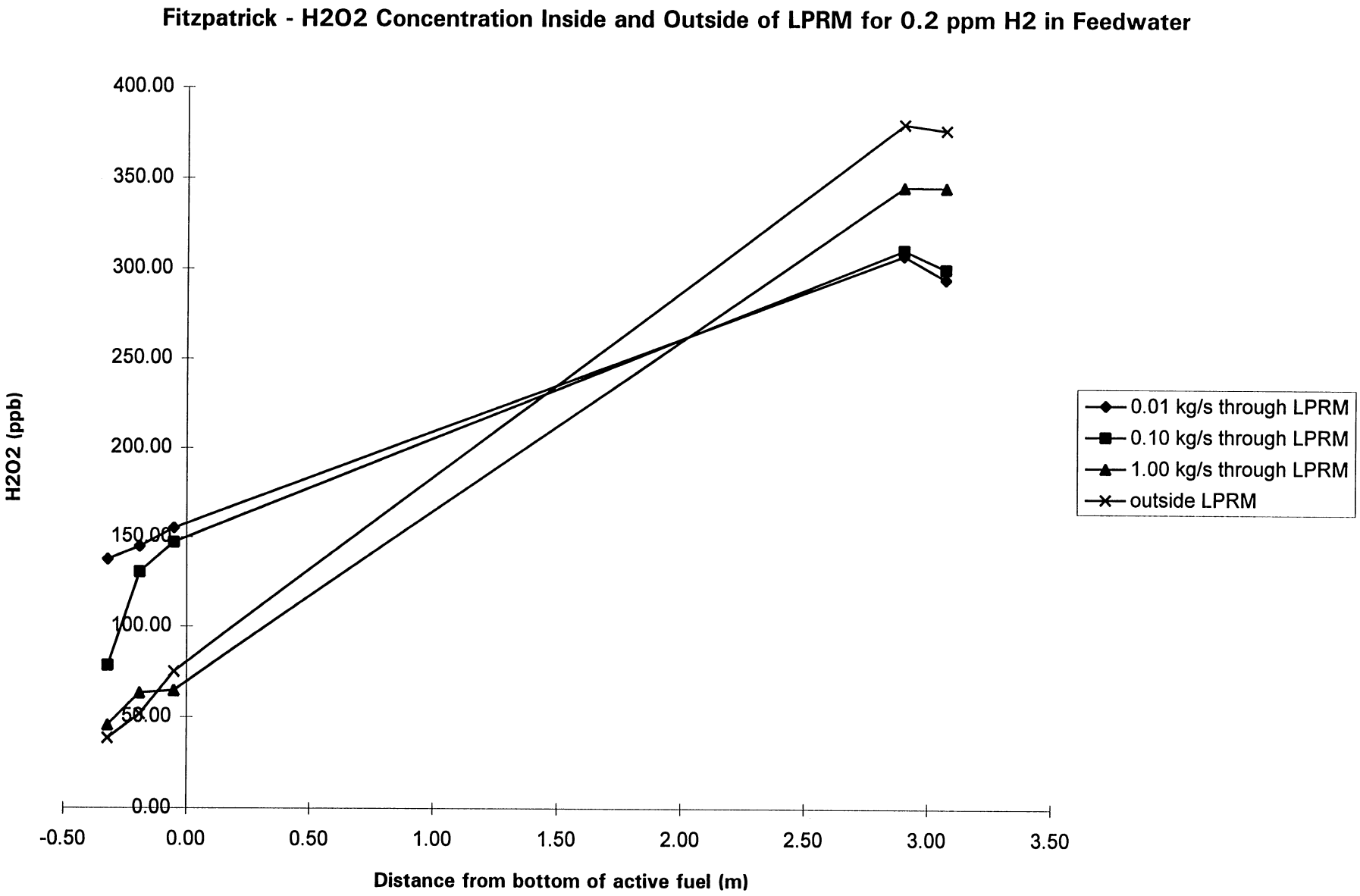
Fitzpatrick - H2O2 Concentration Inside and Outside of LPRM for 0.2 ppm H2 in Feedwater
H2O2 (ppb)
400.00
350.00
300.00
250.00
200.00
150.00
100.00
50.00
0.00
-0.50
0.00
0.50
1.00
1.50
2.00
2.50
3.00
3.50
Distance from bottom of active fuel (m)
0.01 kg/s through LPRM
0.10 kg/s through LPRM
1.00 kg/s through LPRM
outside LPRM

Figure 4-33

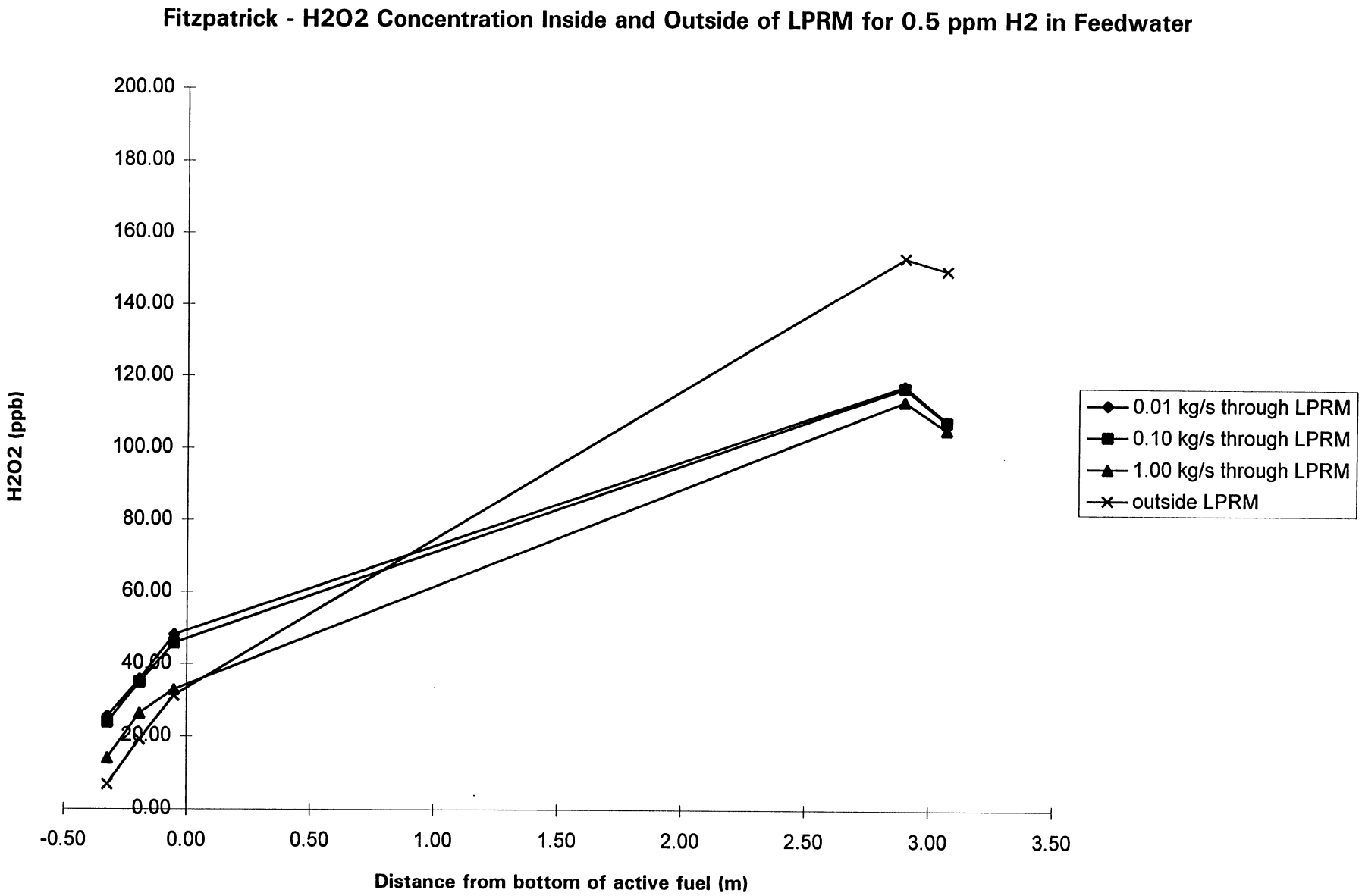
Fitzpatrick - H2O2 Concentration Inside and Outside of LPRM for 0.5 ppm H2 in Feedwater
H2O2 (ppb)
200.00
180.00
160.00
140.00
120.00
100.00
80.00
60.00
40.00
20.00
0.00
-0.50
0.00
0.50
1.00
1.50
2.00
2.50
3.00
3.50
Distance from bottom of active fuel (m)
0.01 kg/s through LPRM
0.10 kg/s through LPRM
1.00 kg/s through LPRM
outside LPRM

Figure 4-34

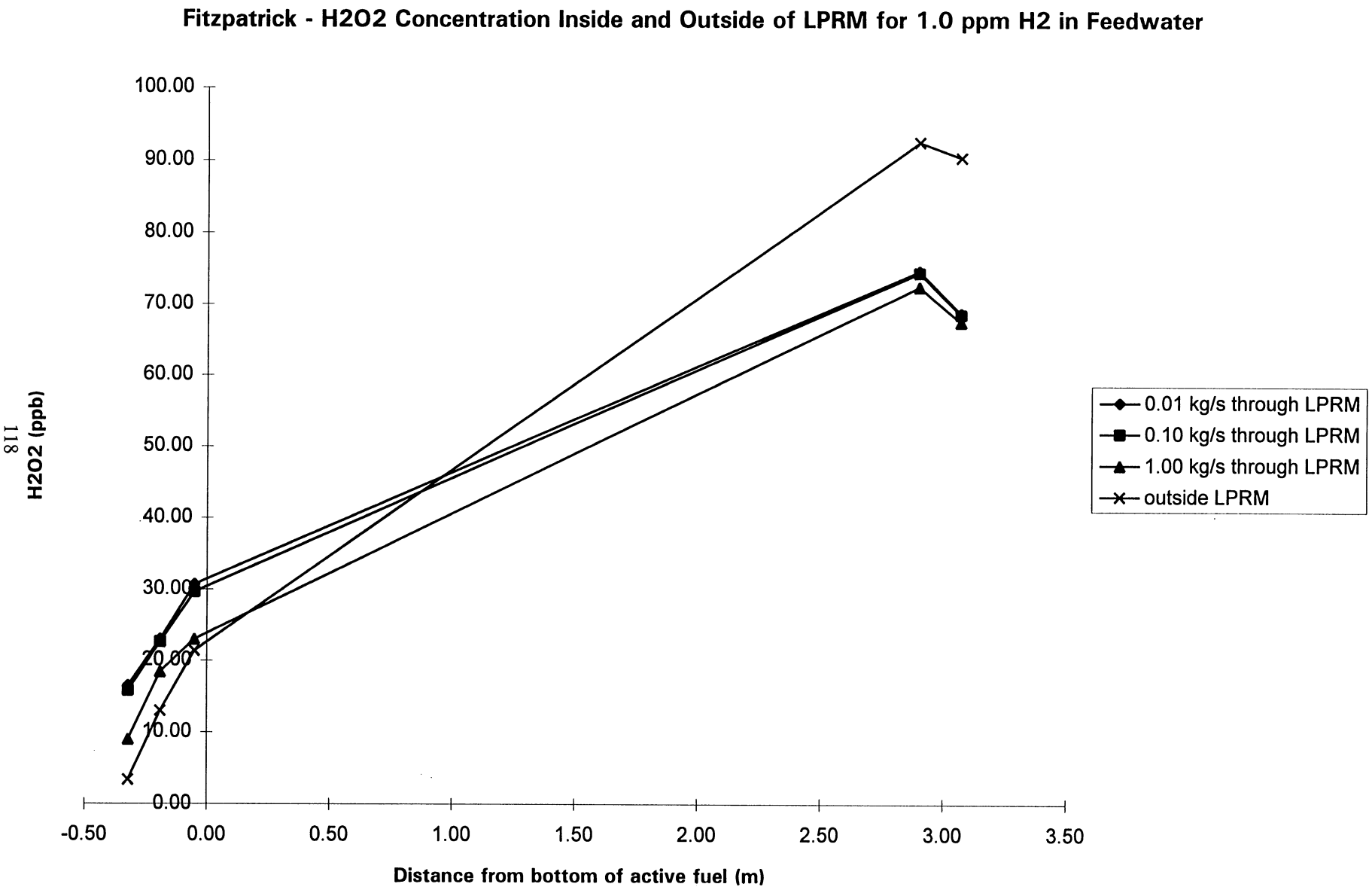

Figure 4-35

EPRI Licensed Material

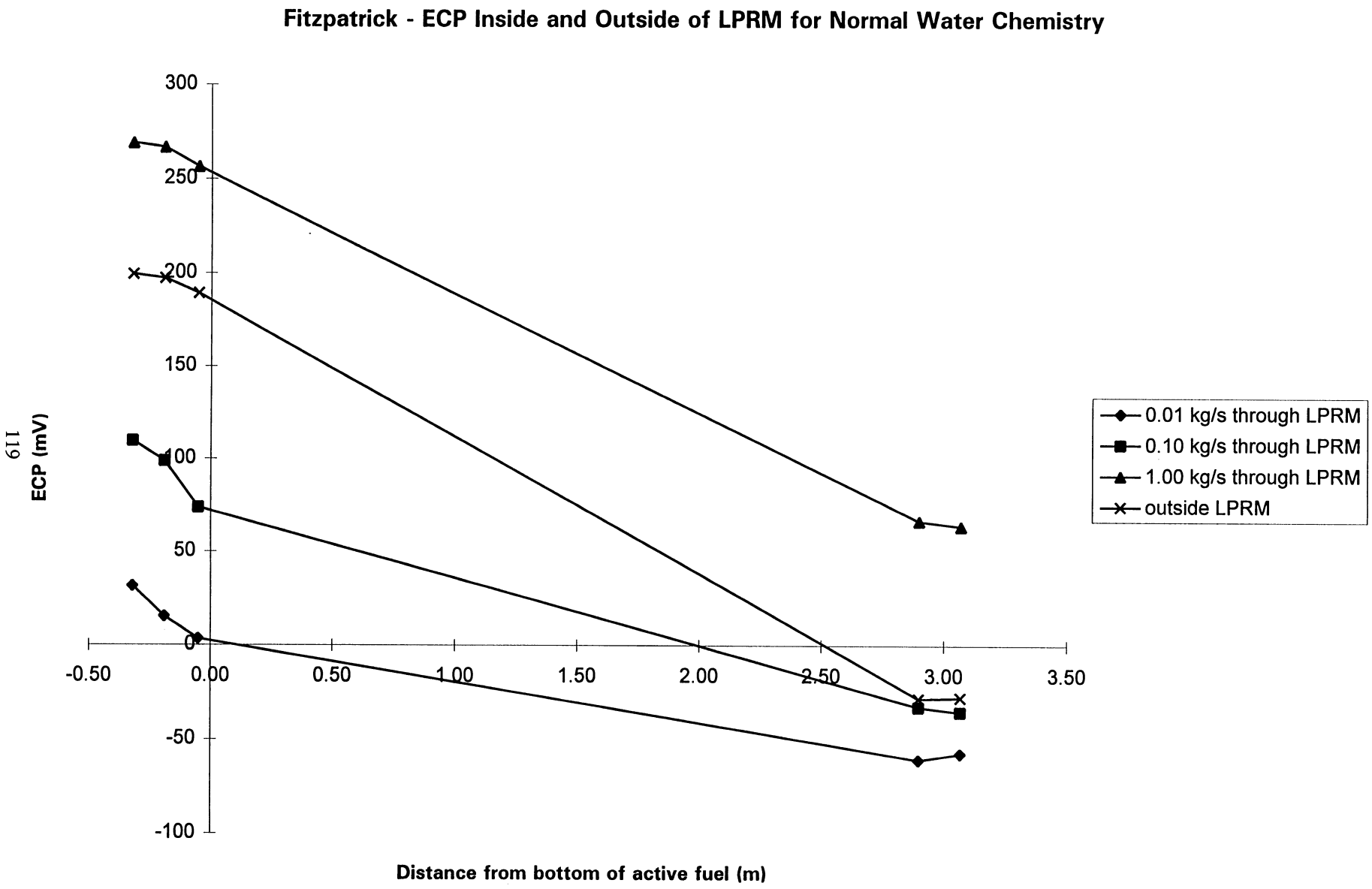
Fitzpatrick - ECP Inside and Outside of LPRM for Normal Water Chemistry
ECP (mV)
300
250
200
150
100
50
0
-50
-100
-0.50
0.00
0.50
1.00
1.50
2.00
2.50
3.00
3.50
Distance from bottom of active fuel (m)
0.01 kg/s through LPRM
0.10 kg/s through LPRM
1.00 kg/s through LPRM
outside LPRM

Figure 4-36

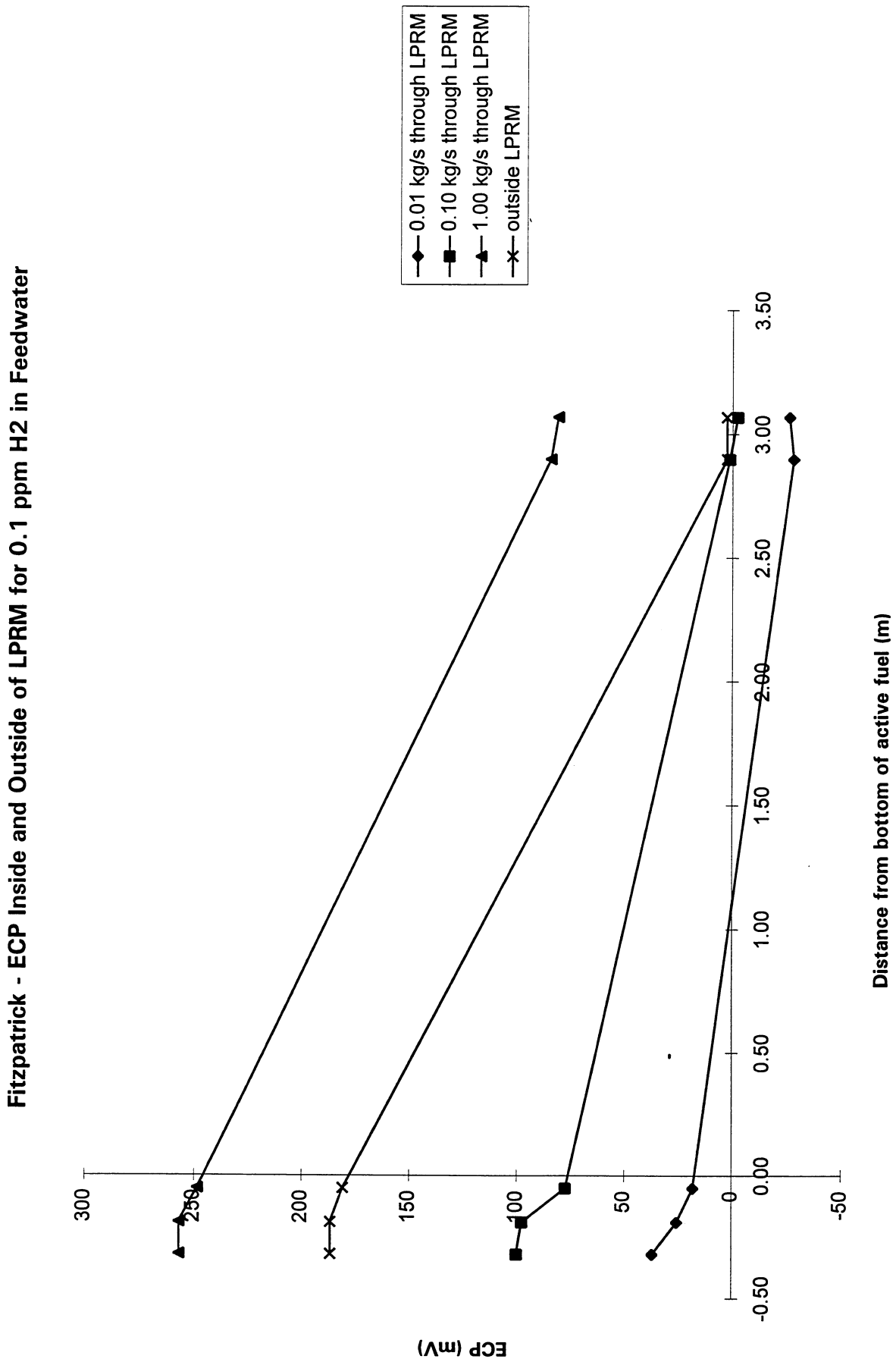
Fitzpatrick - ECP Inside and Outside of LPRM for 0.1 ppm H2 in Feedwater
0.01 kg/s through LPRM
0.10 kg/s through LPRM
1.00 kg/s through LPRM
outside LPRM
ECP (mV)
300
250
200
150
100
50
0
-50
-0.50
0.00
0.50
1.00
1.50
2.00
2.50
3.00
3.50
Distance from bottom of active fuel (m)

Figure 4-37

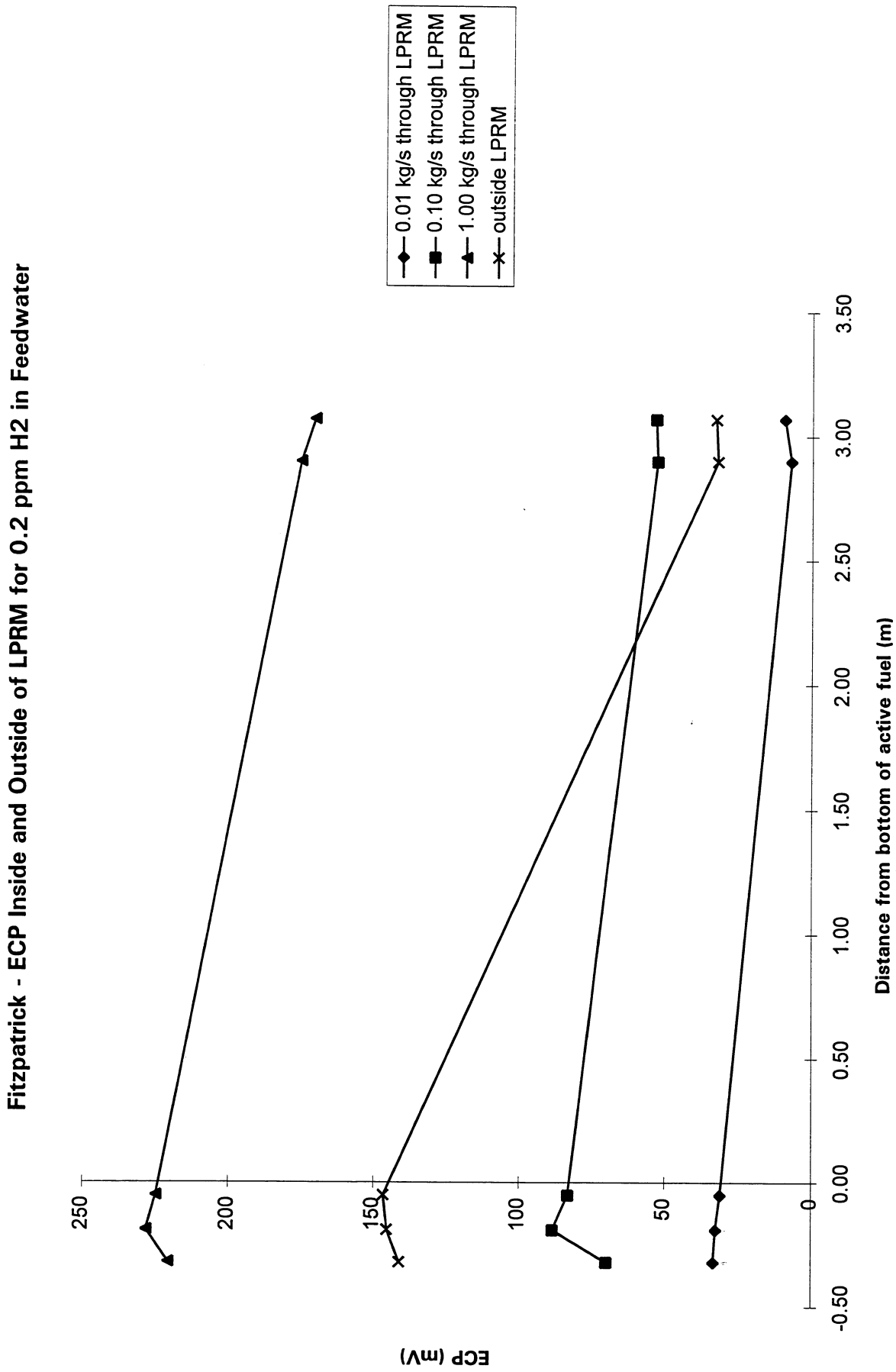
Fitzpatrick - ECP Inside and Outside of LPRM for 0.2 ppm H2 in Feedwater
0.01 kg/s through LPRM
0.10 kg/s through LPRM
1.00 kg/s through LPRM
outside LPRM
ECP (mV)
250
200
150
100
50
0
-0.50
0.00
0.50
1.00
1.50
2.00
2.50
3.00
3.50
Distance from bottom of active fuel (m)

Figure 4-38

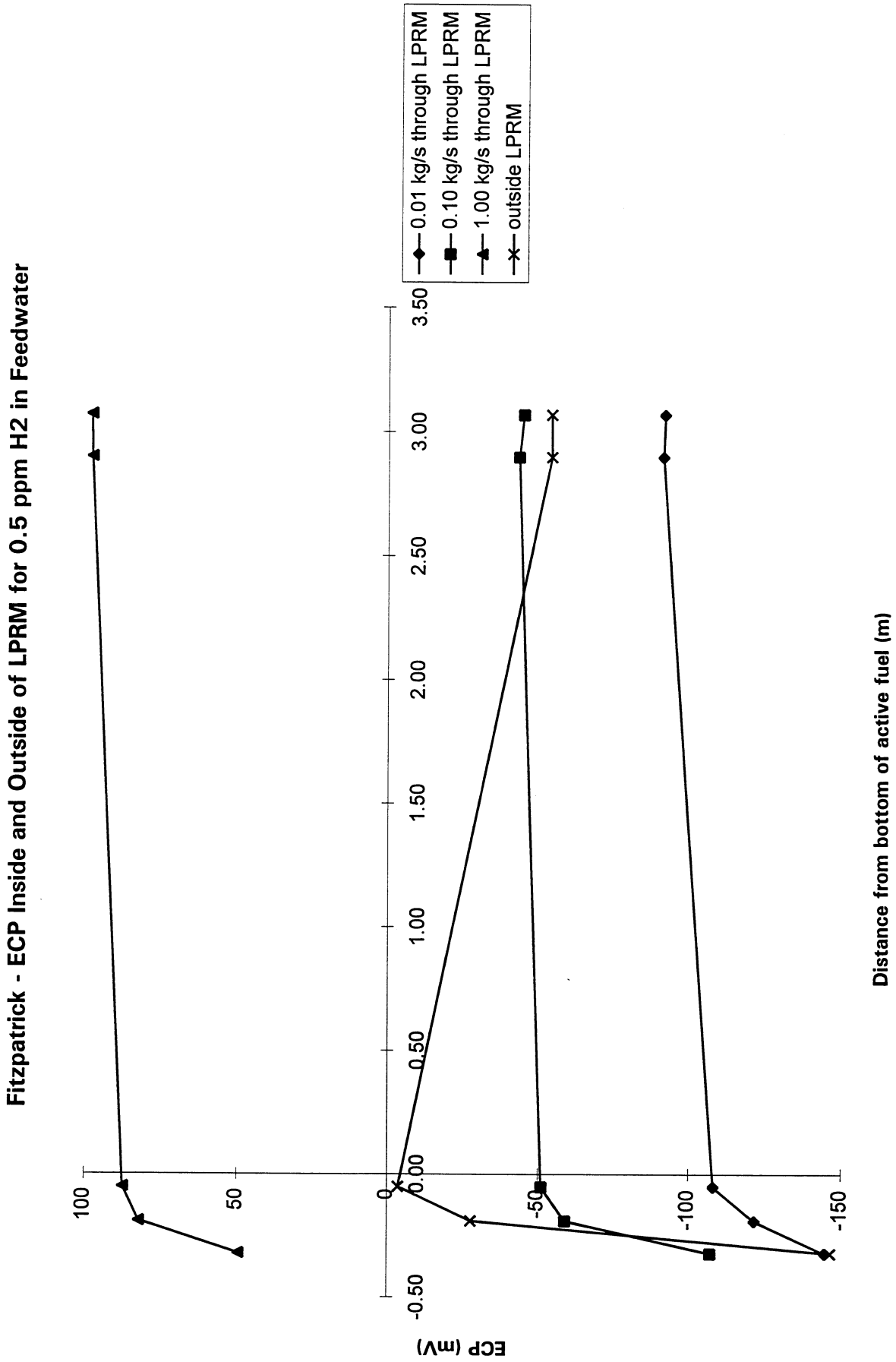
Fitzpatrick - ECP Inside and Outside of LPRM for 0.5 ppm H2 in Feedwater
0.01 kg/s through LPRM
0.10 kg/s through LPRM
1.00 kg/s through LPRM
outside LPRM
ECP (mV)
100
50
0
-50
-100
-150
-0.50
0.00
0.50
1.00
1.50
2.00
2.50
3.00
3.50
Distance from bottom of active fuel (m)

Figure 4-39

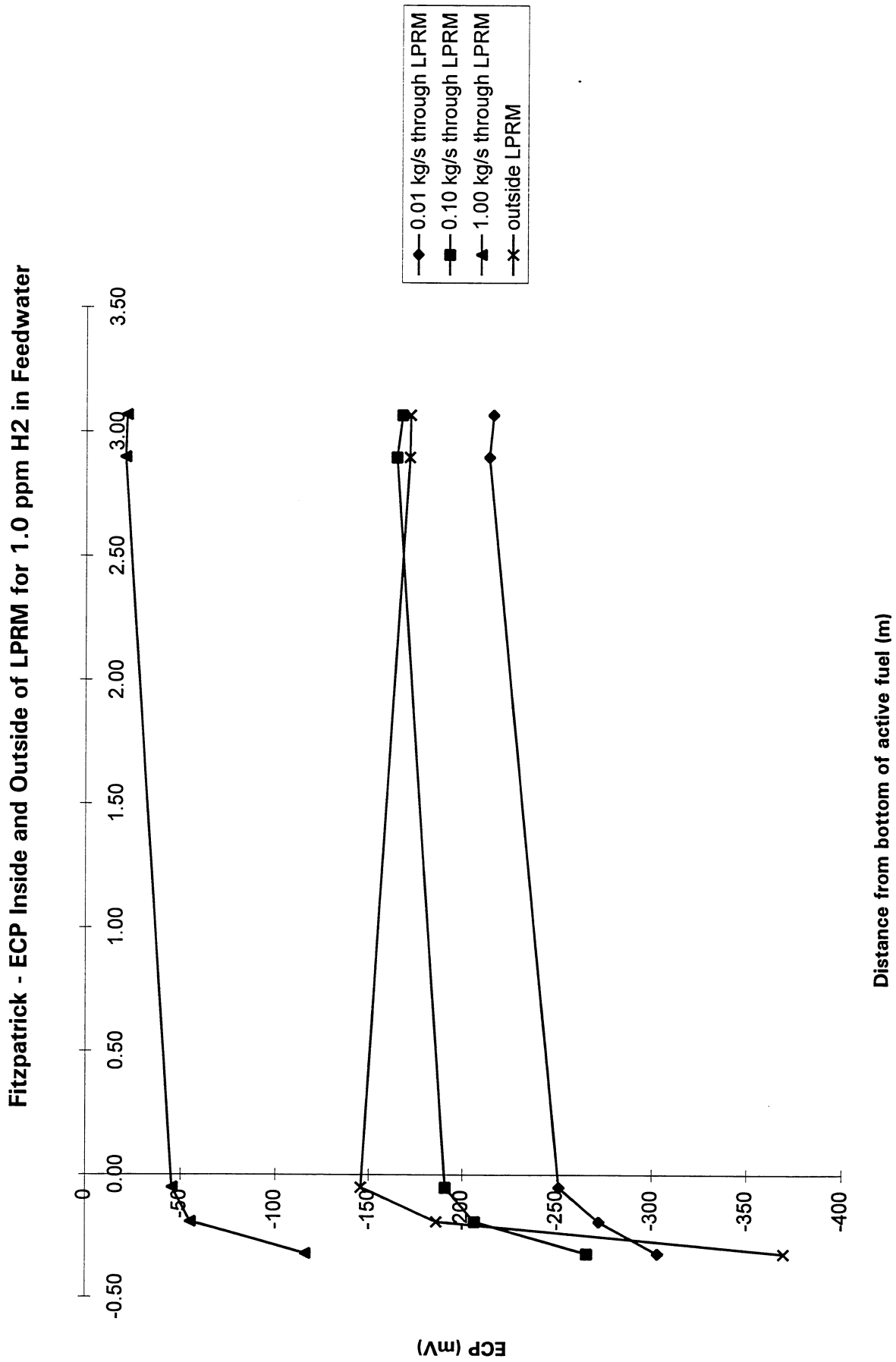
Fitzpatrick - ECP Inside and Outside of LPRM for 1.0 ppm H2 in Feedwater
0.01 kg/s through LPRM
0.10 kg/s through LPRM
1.00 kg/s through LPRM
outside LPRM
ECP (mV)
Distance from bottom of active fuel (m)
0
-50
-100
-150
-200
-250
-300
-350
-400
-0.50
0.00
0.50
1.00
1.50
2.00
2.50
3.00
3.50

Figure 4-40

SECTION 5

CALCULATION OF ECP VALUES

5.1 Development of ECP Models

It has been demonstrated that with increasing hydrogen in the feedwater the electrochemical potential (ECP) decreases. As the ECP on Type 304SS decreases to less than -0.230 V (SHE) (standard hydrogen electrode), cracks from SCC do not initiate and propagation rates of existing cracks become extremely low.

It is believed that the major ECP-determining species in BWRs are oxygen and hydrogen peroxide. The GE/Harwell radiation model has shown that the different components in the BWR circuit require significantly different concentrations of hydrogen in the feedwater system to achieve a given concentration of oxygen and hydrogen peroxide. Since the water chemistry determines the ECP, it is clear that the hydrogen injection requirements necessary to achieve the SCC protection potential, -0.230 V (SHE), vary around the BWR circuit. For this reason, it is important to be able to either measure directly or calculate with the help of a model the ECP in each region where SCC mitigation is essential.

Since, to date, direct ECP measurements have been performed with *in situ* electrodes only in the recirculation lines and the bottom drain line or with in-core probes (modified LPRMs), an estimate of the ECP values in all the other relevant regions can only be obtained through model calculations.

Recent work has shown that ECP values of T-316SS can be obtained in the laboratory as a function of water chemistry, pre-conditioning of the metal surface, and flow rate, using a rotating cylinder electrode in an autoclave.[33] The experimental ECP data thus obtained have shown that the ECP behavior of T-316SS electrode is controlled by hydrodynamic water flow conditions, or by the mass transfer rate of reactants, particularly at a low oxygen or hydrogen peroxide level, as well as by the oxidant concentration.

The experimental data were utilized to develop two separate models: ECP as a function of oxygen concentration and ECP as a function of hydrogen peroxide concentration. A hyperbolic tangent (tanh) model form with a slope term was chosen to model ECP versus each oxidant:

$$\mathrm{ECP} = C_1 \tanh\left[\frac{\log(oxidant) - C_2}{C_3}\right] + C_4 \log(oxidant) + C_5$$

where *oxidant* is either oxygen or hydrogen peroxide. Other independent variables, such as hydrogen concentration (i.e., $[H_2]$) and the angular velocity of the rotating cylinder electrode, which is related to the flow rate, where included in the C_n parameters.

5.2 Calculated ECP Values

The calculations were further elaborated to obtain the ECP values resulting from the presence of both oxygen and hydrogen peroxide. Initially the ECPs were calculated assuming only the presence of oxygen or of hydrogen peroxide, using the corresponding equations. Then it was determined which ECP had the greater value. For example, if the ECP due to hydrogen peroxide was greater than that due to oxygen, the concentration of oxygen equivalent to that of hydrogen peroxide (i.e., the concentration of oxygen that would have generated the same ECP as the hydrogen peroxide), was calculated. This equivalent oxygen concentration was added to the oxygen concentration obtained with the radiolysis model, and the final ECP value was calculated with the ECP equation for oxygen only. Alternatively, if the ECP due to only oxygen was greater than that due to the hydrogen peroxide, with a similar methodology the final ECP could be calculated with the equation for hydrogen peroxide. The difficulty of obtaining equivalent concentrations of *oxidant* by solving the hyperbolic tangent equation was overcome by using a numerical method (the "secant" method) in conjunction with a computer program.

This approach will be replaced when a single equation combining hydrogen, oxygen and hydrogen peroxide concentrations, as well as velocity, becomes available.

ECP values were obtained for each of the ten model regions and each of the ten BWRs considered in this study. The charts of Figures 5-1 to 5-10 provide a generic example of the ECP variations in each model region. According to these results, in the channel region the ECP is always above the SCC mitigation value. In the core bypass protection is obtained only above 1.5 ppm of feedwater hydrogen. In the outer bypass, SCC mitigation appears to be available at approximately 0.7 ppm feedwater hydrogen. No protection is available in the upper plenum, steam separator and mixing plenum regions. In the downcomer, at approximately 40% of the region length SCC mitigation becomes available around 0.8 ppm feedwater hydrogen. SCC mitigation of the recirculation lines can be achieved at approximately 0.7 ppm feedwater hydrogen. Higher concentrations of feedwater hydrogen are required in the jet pumps. Finally, in the lower plenum SCC mitigation can be achieved at approximately 1.0 ppm feedwater hydrogen, except in the last portion of the region, in the proximity of the core plate.

ALL VALUES ATTACHED TO CURVES INDICATE PPM OF FW H2

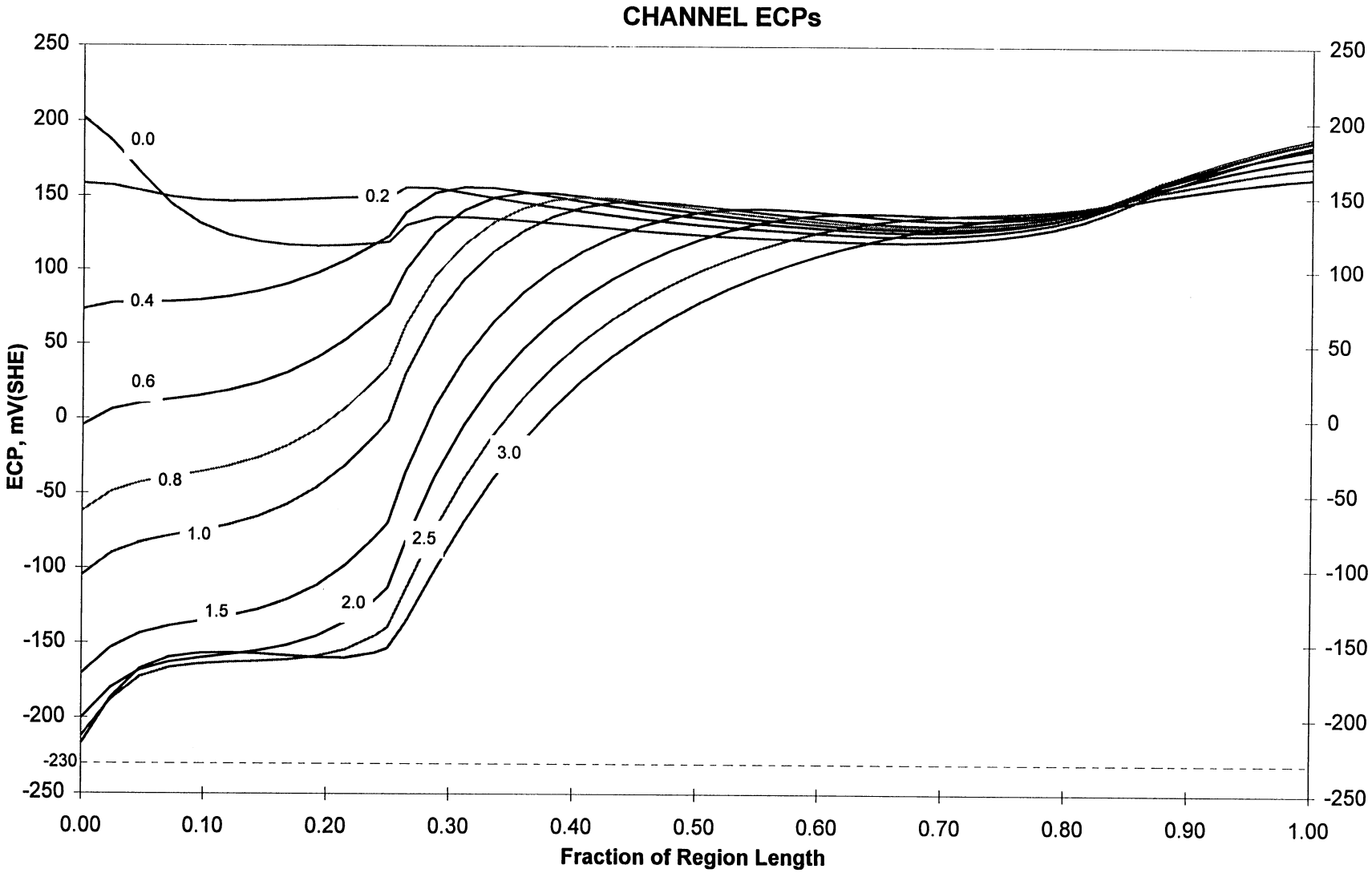

Figure 5-1

BWRJP438 (VERSION 4.38.5)DATED 12/20/94

FITICECP.xlc

EPRI Licensed Material

ALL VALUES ATTACHED TO CURVES INDICATE PPM OF FW H2

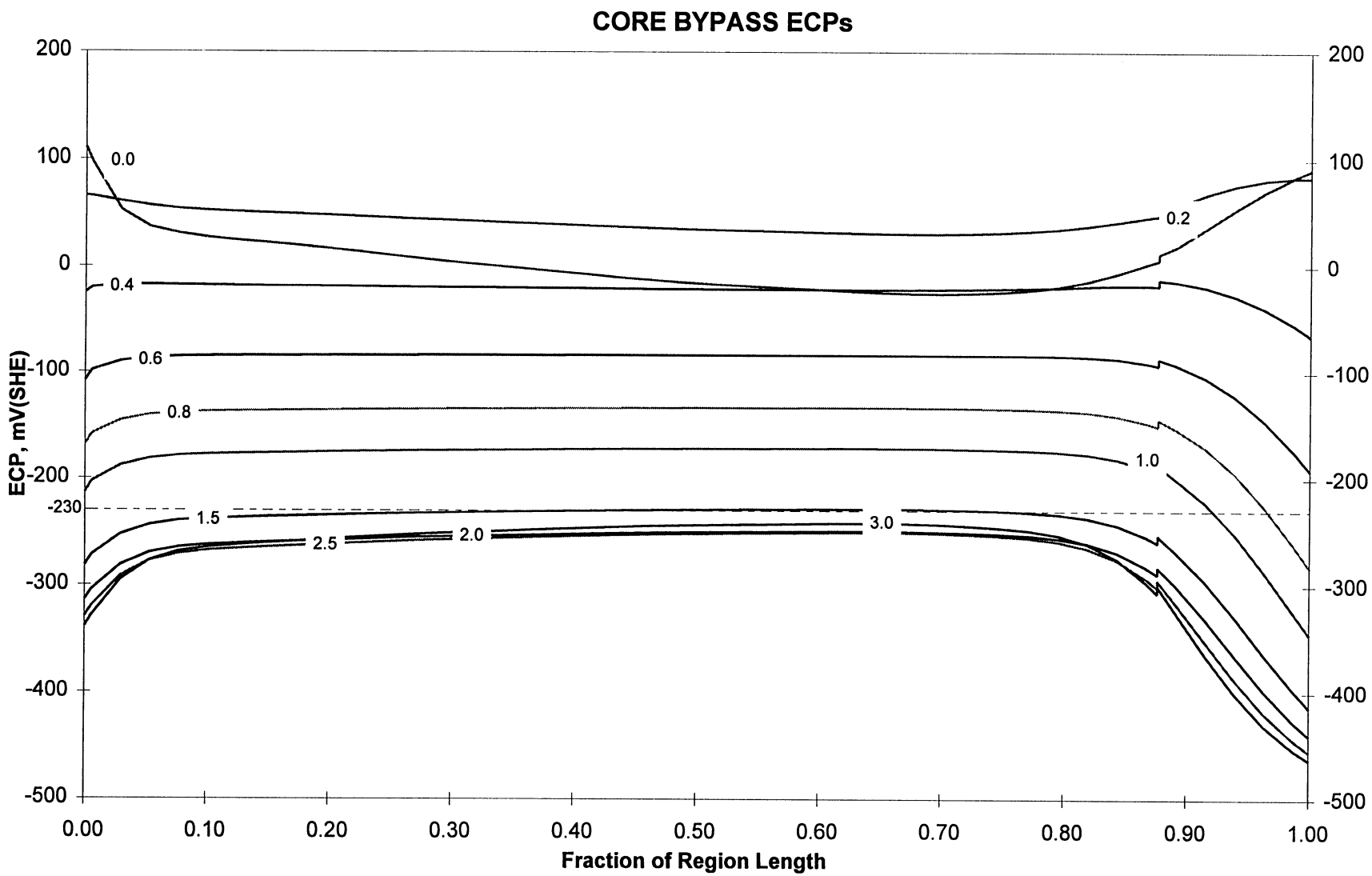

Figure 5-2

BWRJP438 (VERSION 4.38.5)DATED 12/20/94

FITCBECP.xlc

EPRI Licensed Material

ALL VALUES ATTACHED TO CURVES INDICATE PPM OF FW H2

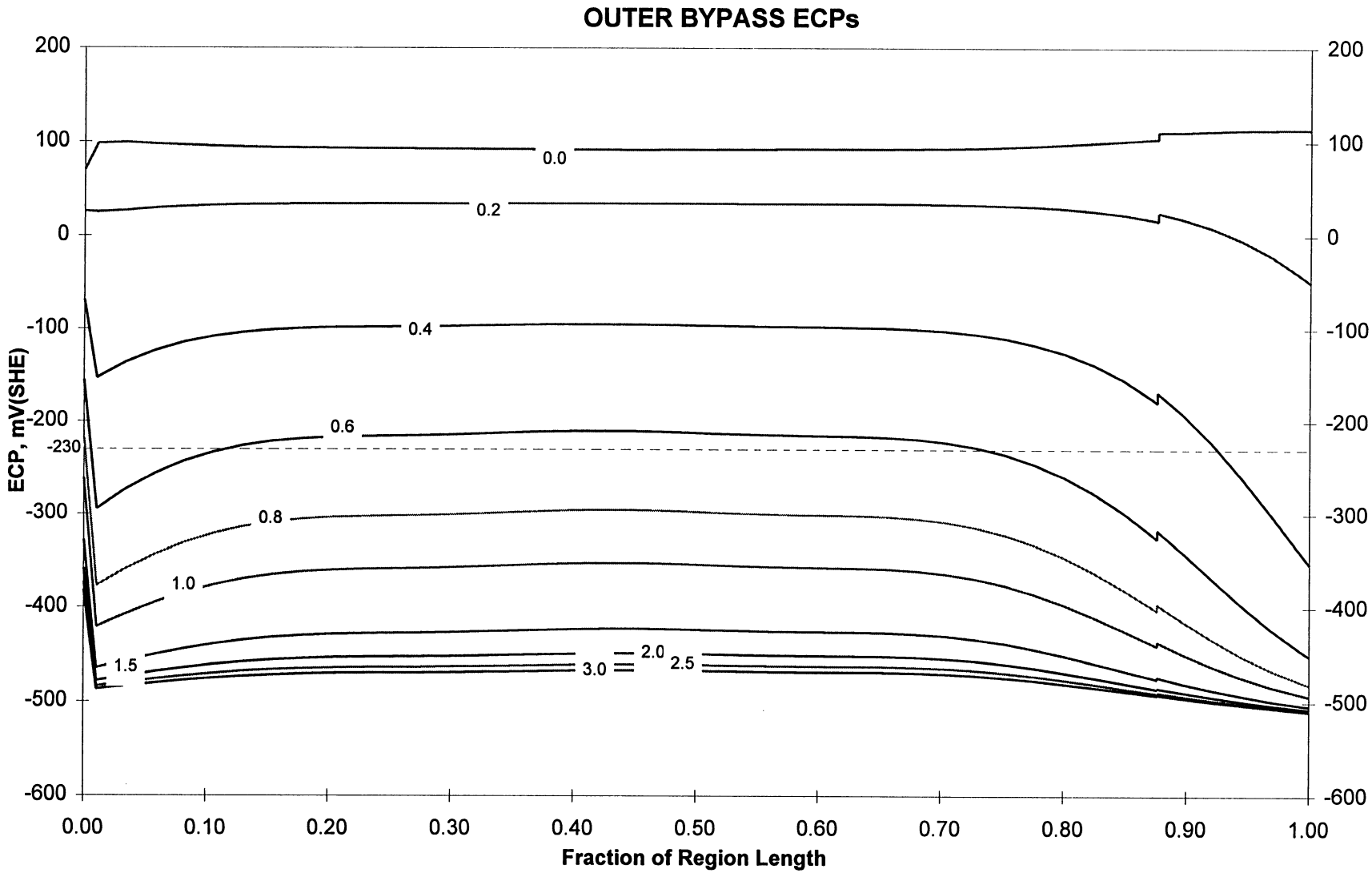

Figure 5-3

BWRJP438 (VERSION 4.38.5)DATED 12/20/94

FITOBECP.xlc

EPRI Licensed Material

ALL VALUES ATTACHED TO CURVES INDICATE PPM OF FW H2

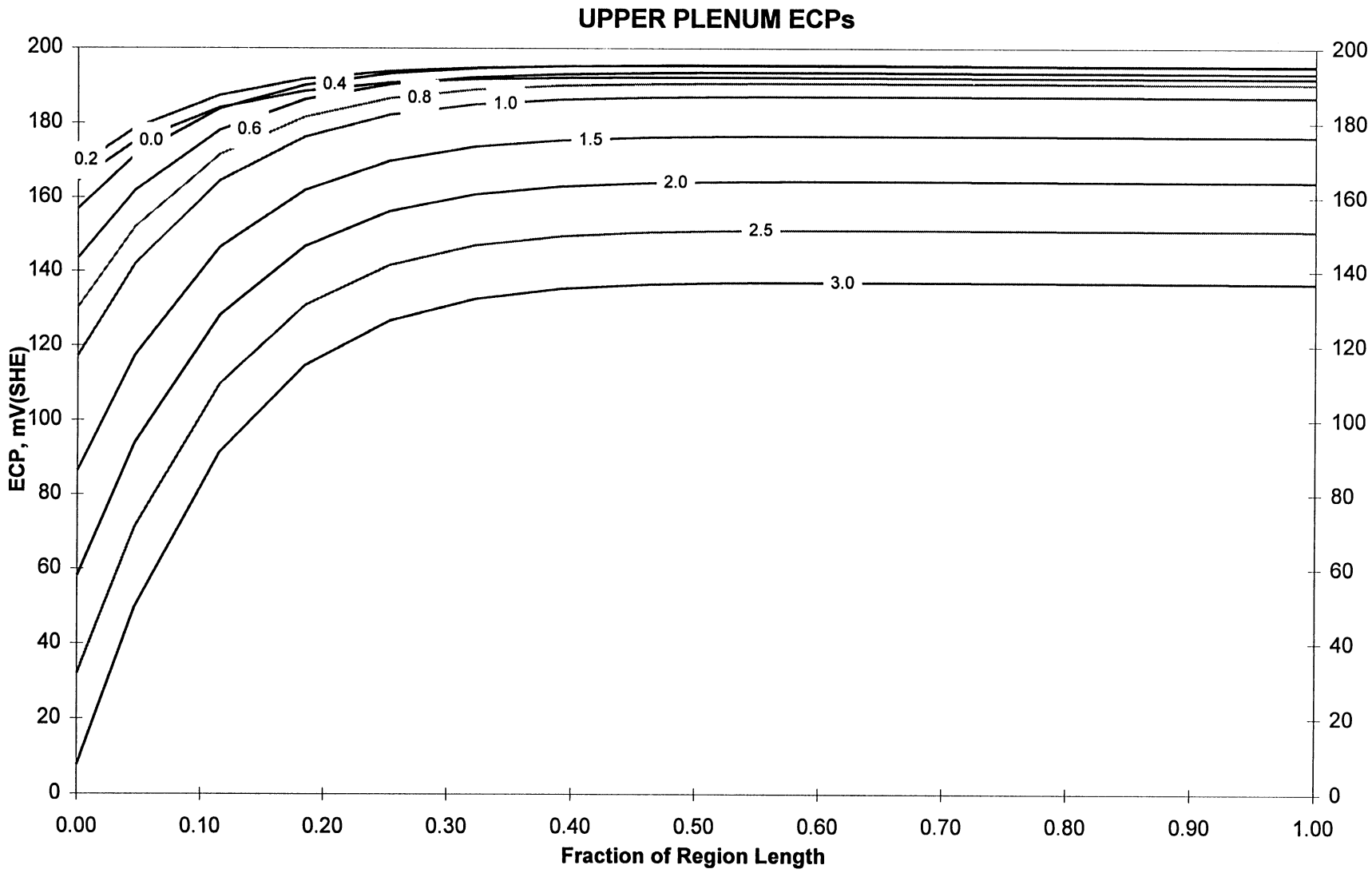

Figure 5-4

BWRJP438 (VERSION 4.38.5)DATED 12/20/94

FITUPECP.xlc

EPRI Licensed Material

ALL VALUES ATTACHED TO CURVES INDICATE PPM OF FW H2

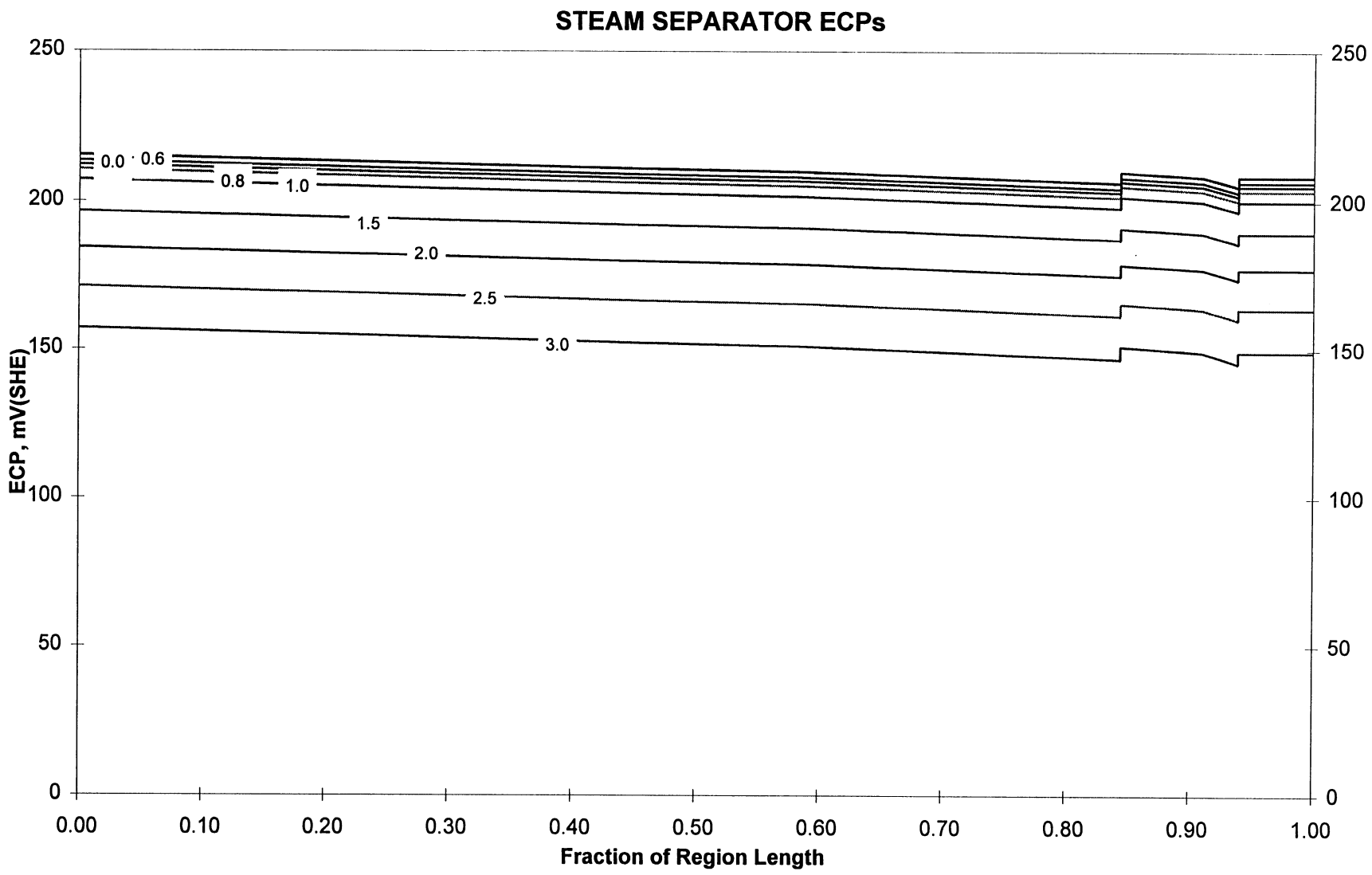

Figure 5-5

BWRJP438 (VERSION 4.38.5)DATED 12/20/94

FITSSECP.xlc

EPRI Licensed Material

ALL VALUES ATTACHED TO CURVES INDICATE PPM OF FW H2

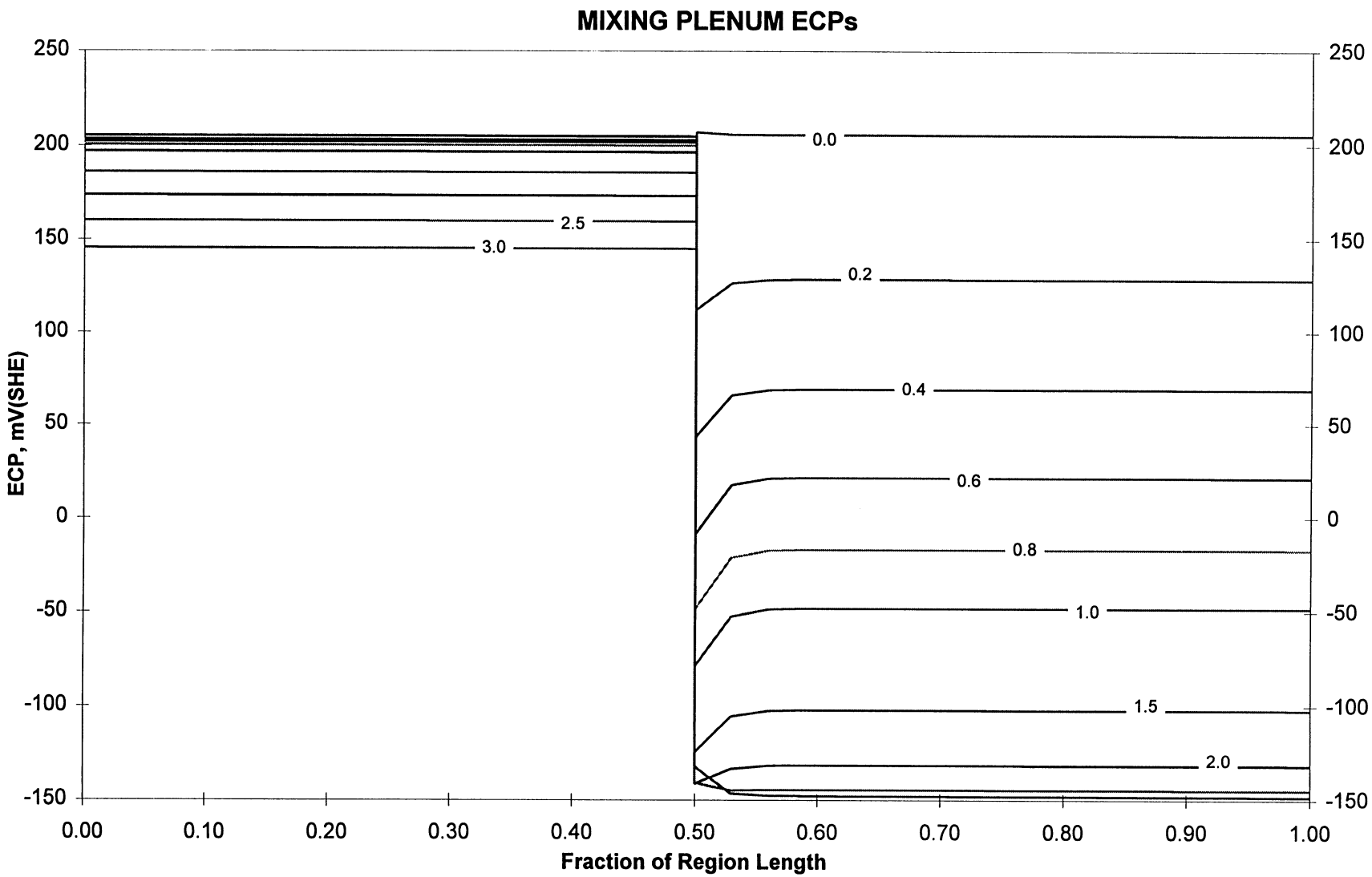

Figure 5-6

BWRJP438 (VERSION 4.38.5)DATED 12/20/94

FITMPECP.xlc

EPRI Licensed Material

GE Radiolysis Model

ALL VALUES ATTACHED TO CURVES INDICATE PPM OF FW H2

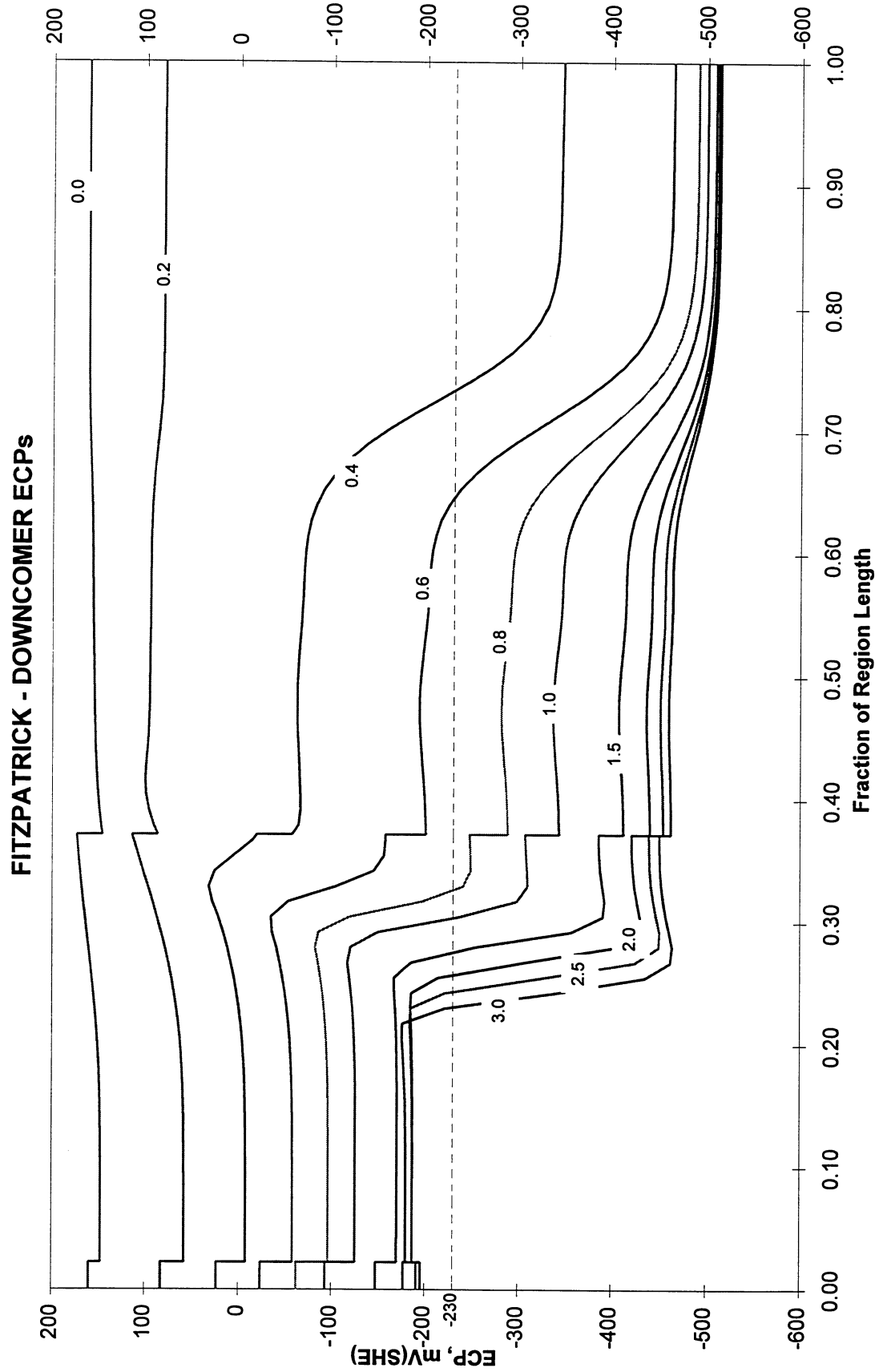

BWRJP438 (VERSION 4.38.5)DATED 12/20/94

FITDCECP.xlc

Figure 5-7

ALL VALUES ATTACHED TO CURVES INDICATE PPM OF FW H2

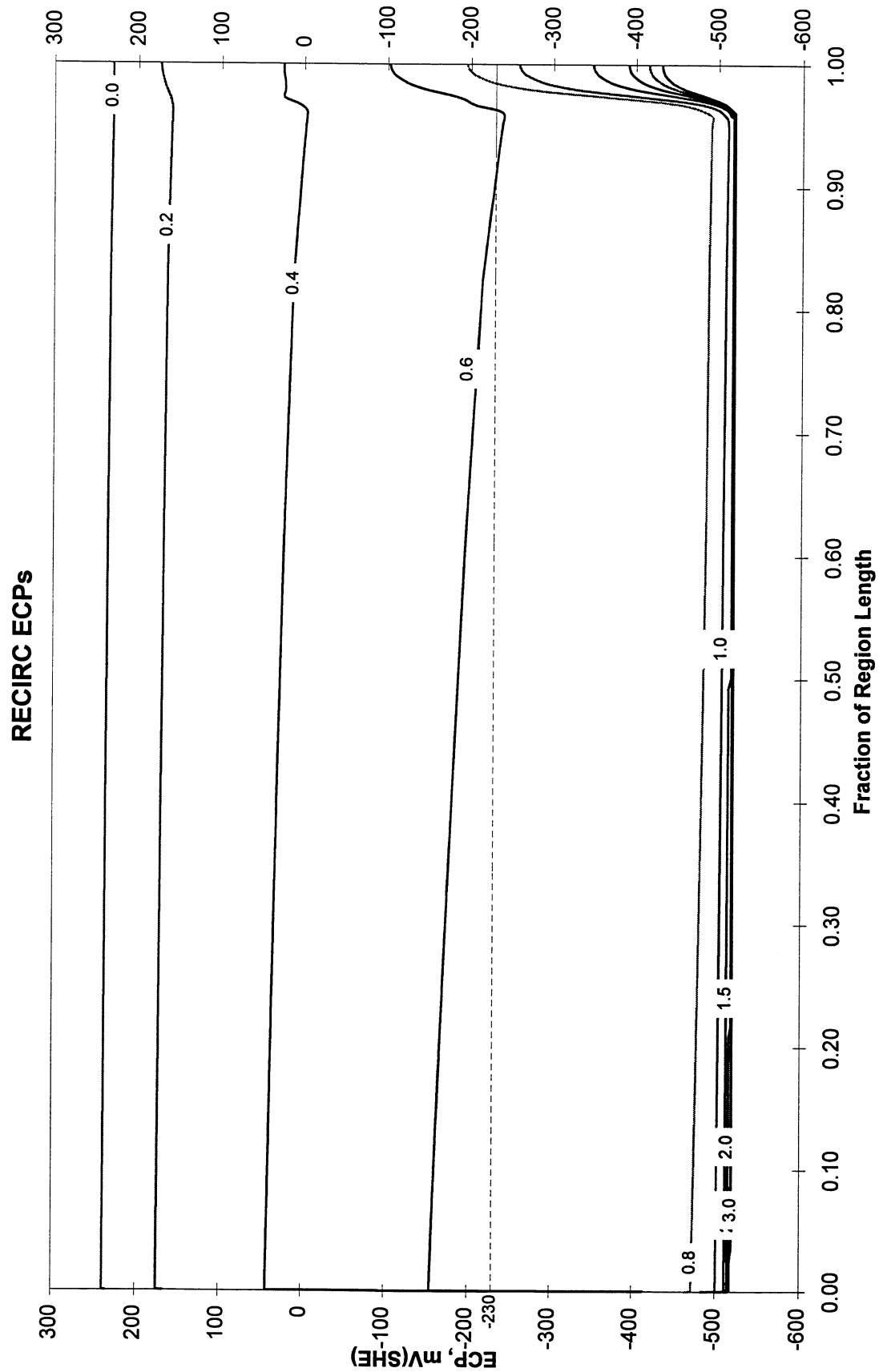

GE Radiolysis Model

BWRJP438 (VERSION 4.38.5)DATED 12/20/94

FITREECP.xlc

Figure 5-8

ALL VALUES ATTACHED TO CURVES INDICATE PPM OF FW H2

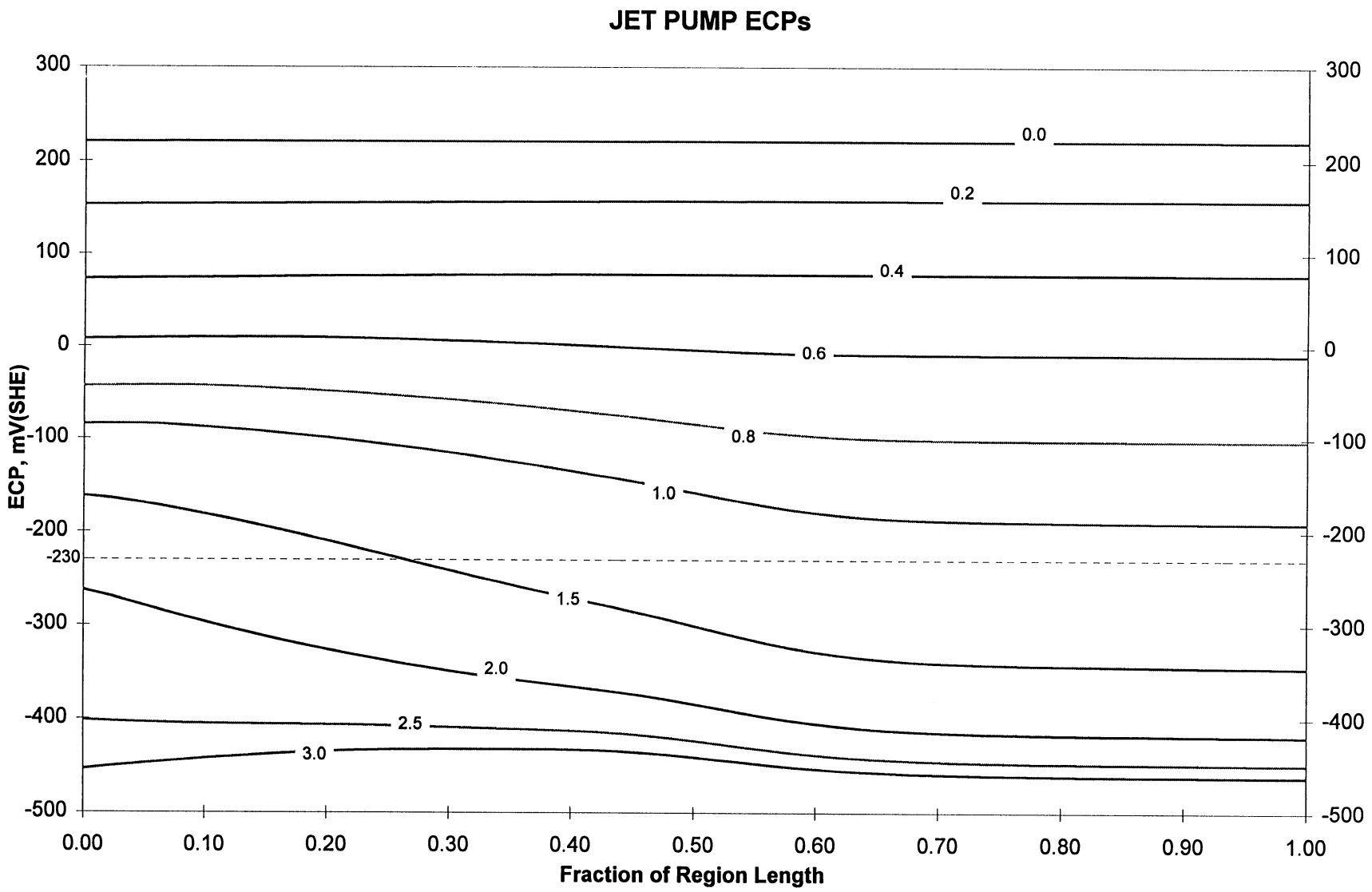

Figure 5-9

BWRJP438 (VERSION 4.38.5)DATED 12/20/94

FITJPECP.xlc

EPRI Licensed Material

ALL VALUES ATTACHED TO CURVES INDICATE PPM OF FW H2

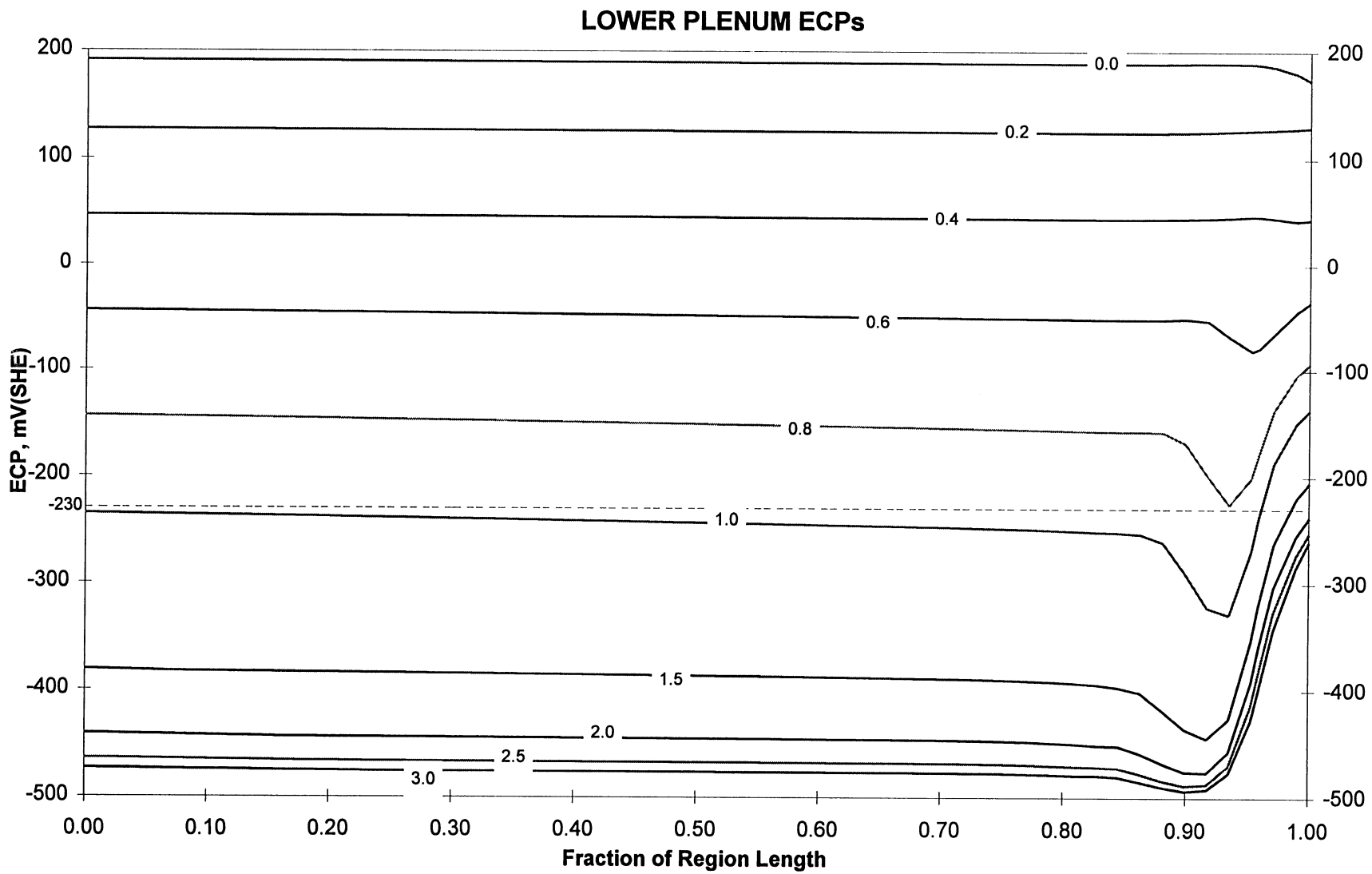

Figure 5-10

EPRI Licensed Material

SECTION 6

CONCLUSIONS

6.1 Conclusions

This study, a continuation and expansion of previous work, has provided additional insight into the chemistry of the primary BWR system and its interdependence with failure mechanisms of component materials. Improvements and additions to the radiolysis model have enabled a more reliable calculation of hydrogen, oxygen and hydrogen peroxide concentrations in ten different regions of ten BWRs. In particular, the addition of a steam separator section has provided a more accurate estimate of the concentrations in the mixing plenum and the downcomer. The behavior of hydrogen peroxide in the downcomer, not observed in previous versions of the model, may indicate that protection of the lower section of the downcomer is attained at relatively low feedwater hydrogen concentrations (i.e., <1 ppm). A comparison with measurements effected at four BWRs has shown, in general, satisfactory agreement between experimental and calculated results for the hydrogen and oxidant concentrations in the recirculation lines and the condensed steam. In general, the effect of hydrogen addition is dependent on the BWR region and the location within each region. Suppression of oxygen can be achieved more easily than that of hydrogen peroxide.

6.1.1 Modified LPRMs

The radiolysis model was extended to include LPRMs modified to contain the ECP sensors. The results for two BWRs show that the concentrations of hydrogen, oxygen, hydrogen peroxide and the corresponding ECP values are generally different inside and outside the LPRM. Variation in these differences are dependent upon the flow rate. Thus the measured ECPs do not necessarily correspond to the ECPs at the same elevation outside the LPRM.

Because of the dependence of the ECP on flow rate, the ability to predict ECPs with the current version of the model was somewhat limited. Consequently, benchmarking of ECP values calculated with the radiolysis model by comparison with the measured ECP values is not feasible at present. The development of a suitable correlation between measured and calculated ECPs is part of future work.

It was also observed that at the top of the core the ECP is not sensitive to sensor position. In other words, a slight misplacement of the sensors is not significant. On the other hand, the sensors are very sensitive to their position below the core plate, especially at high feedwater hydrogen injection rates.

No major difference in the response of the two types of modified LPRMs was determined as due to their differences in design.

6.1.2 ECP Calculations

On the basis of oxidant concentrations and other parameters, ECP values were calculated for the ten model regions of each of the ten BWRs object of this study. The corresponding charts included in this report provide an estimate of the degree of SCC mitigation, in each region of the ten BWRs, afforded by the use of HWC. Regions that appear more easily protected (i.e., at FW H_2 $\leq$1 ppm) are the outer bypass, the recirculation lines, the lower portion of the downcomer, and most of the lower plenum. Higher concentrations of feedwater hydrogen are required to protect the jet pumps and the core bypass. The application of only HWC appears to provide no SCC mitigation to the channel, upper plenum, steam separator, and mixing plenum regions. In this case, the concurrent application of other technologies presently under development, for example, NMT (noble metal technology), would probably provide the required mitigation.

SECTION 7

FUTURE WORK

7.1 Projected Developments

Improvements to the radiolysis model have been identified that will allow more accurate predictions of conditions leading to SCC. In particular, determining more accurately the concentration of oxidizing species and the corresponding ECP values at specific locations in the BWR primary system (for example, shroud welds), is part of the scope of future work. The following items are planned for further development :

7.2 ECP Correlation Upgrade

As additional data become available, the correlation between ECP, water composition and velocity will be upgraded.

7.3 Effect of Copper Impurities

The impact of the presence of copper on water radiolysis and on the effectiveness of hydrogen injection is well known. Refinements of the model will provide a better fit of model calculations to experimental data.

7.4 Radiation Fields

The present version of the model utilizes a generic neutron and gamma dose rate profile for every BWR. A new version will incorporate radiation profiles specific to each BWR.

7.5 Liquid/Gas Transport

In the new version of the code, transport of oxygen and hydrogen between liquid and gas phase will be based on a more detailed consideration of the details of the mass transfer in the channel, upper plenum and steam separator regions. Improvements planned include two-phase flow, liquid film thickness, interfacial area, and slip ratio.

7.6 Velocity Mapping

The possibility of incorporating detailed velocity maps in the model will be investigated. This work will be done for the outer bypass, the downcomer and the lower plenum, the three regions of greatest potential impact with respect to SCC.

7.7 Sensitivity Studies

An effort will be made to quantify the effect on the model results of variations in selected input parameters. The aim of this work is to identify the input parameters that influence significantly the output of the code, and those that are less important.

7.8 Two Dimensional Modeling

The present version of the model takes into account only longitudinal transport of chemical species. A new version would involve modifications to the code to allow radial transport as well as longitudinal transport. The first approach to 2D modeling will be a "shell" model, in which regions of the reactor circuit, for example the downcomer, will be divided into a finite number of cylindrical shells. Chemical species will be transported continuously across the shell walls and in the direction of the flow. Mixing will be determined by cross-flow velocity and diffusion. Flow along these shells would take place at the same velocity. Such a shell model could be applied to particular regions or to the whole reactor circuit, and would take into account the difference between surface chemistry and bulk chemistry, and also the effect of this different surface chemistry on the bulk chemistry. The shell model would be developed initially for the downcomer, and then applied to the other regions of the reactor.

A more elaborate version of a 2D model, aiming at the determination of localized concentrations, may be the object of further development. In this version, transport would be modeled along and across all the regions in the reactor circuit. This model would determine the effect of longitudinal velocity on the whole reactor chemistry. This effort, however, would involve a considerable re-write of the current code, first to define the grid representing the reactor, and then to determine the transport coefficients between adjacent grid points. Again, this effort could be initially restricted to the downcomer and subsequently extended to other regions of the circuit.

SECTION 8

REFERENCES

1. B. M. Gordon, et. al., "Mitigation of Stress Corrosion Cracking Through Suppression of Radiolytic Oxygen", paper presented at the International Symposium on Environmental Degradation of Materials in Nuclear Power Systems - Water Reactor, Myrtle Beach, S. C., August, 1983, published in NACE preceedings, Houston, 1984.

2. E. L. Burley, "Alternate Water Chemistry Program -- Quarterly Report 1, From Program Start to September 31, 1977." General Electric Company Document NEDC-23856, August, 1978.

3. E. L. Burley, "Oxygen Suppression in Boiling Water Reactors -- Quarterly Report 2, January 1 to March 31, 1978." C00/2985-2, (NEDC-23856-1), October, 1978.

4. E. L. Burley, "Oxygen Suppression in Boiling Water Reactors -- Quarterly Report 3, April 1 to June 30, 1978." General Electric Company Document NEDC-23856-2, December, 1978.

5 E. L. Burley, "Oxygen Suppression in Boiling Water Reactors -- Quarterly Report 4, April 1 to July 1 to September 30, 1978." DOE/ET/34203-38, (NEDC-23856-3, March, 1979.

6. E. L. Burley, "Oxygen Suppression in Boiling Water Reactors -- Phase 1 Final Report, July 1, 1981." DOE/ET/34203-44, (NEDC-23856-4), July, 1981.

7. E. L. Burley, "Oxygen Suppression in Boiling Water Reactors -- Phase 2, Annual Report 1981 December 2, 1980 to December 31, 1981." DOE/ET/34203-46, (NEDC-23856-6), July, 1982.

8. E. L. Burley, "Oxygen Suppression in Boiling Water Reactors -- Phase 2 Final Report." DOE/ET/34203-47, (NEDC-23856-7), October, 1982.

9. L. L. Sundberg, et. al., "Operation of Hydrogen Water Chemistry For 18-Month Cycle at Dresden-2", EPRI NP-4470, March, 1986.

10. C. P. Ruiz, et. al., "Dresden Unit 2 Hydrogen Water Chemistry - Chemical Surveillance, Oxide Film Characterization, and Recontamination During Cycle 10", EPRI NP-6278-SD, March 1989.

11. B. M. Gordon, et. al., "Hydrogen Water Chemistry for BWRs - Materials Behavior Interim Report", April 1982 - (July 1986 - NEDE-31142, EPRI RP 1930-1, August, 1986.

12. G. C. Martin, et. al., 'Hydrogen Water Chemistry Fuel Materials Surveillance, Fuel Rod Crud Deposit Examinations - First Inspection NEDC-31164, November, 1985.

13. B. Cheng, et. al., "Hydrogen Water Chemistry Fuel Materials Surveillance Dresden-2 EOC 9 - Site Examination Final Report, NEDC 31163, November 1985.

14. B. Cheng, et. al., "Hydrogen Water Chemistry Fuel Materials Surveillance, Post Irradiation Examination of Fuel Compnents After One Cycle of Hydrogen Water Chemistry in Dresden-2, NEDC-31324, July, 1986.

15. B. Chang and R. N. Ikemoto, "Dresden-2 EOC10-Site Examination Final Report" Hydrogen Water Chemistry Fuel Materials Surveillance, NEDC-31474 Class II, August, 1987.

16. C. R. Judd, et. al., "Dresden-2 Fuel Rod Crud Deposit Examinations - Second Inspection", Hydrogen Water Chemistry Fuel Material Surveillance, NEDC-31475 July, 1987.

17. C. P. Ruiz, et. al., "Modeling Hydrogen Water Chemistry for BWR Applications", EPRI-NP-6386, June, 1989; C.P. Ruiz, R.N. Robinson, C.C. Lin, W.G. Burns, J. Henshaw, and R. Pathania, Water Chemistry of Nuclear Reactor Systems, Vol.2, 141, BNES, 1992.

18. C. P. Ruiz, C. C. Lin and T. L. Wong, "Control of N-16 in BWR Main Steam Lines Under Hydrogen Water Chemistry Concentrations", EPRI NP-6424-SD, July 1989.

19. R. A. Head, M. E. Indig, "Measure of In Core and Recirculation System Response to HWC at NMP-1", EPRI-NP-7200-M, March 1991.

20. K. Ishigure, et. al., "Hydrogen Injection in BWR and Related Radiation Chemistry" Radiat. Phys. Chem. 29, No. 3, pp. 195-199, 1987.

21. E. Ibe, et. al., "Radiolytic Environments in Boiling Water Reactor Cores", J. Nucl. Sci. Tech., 24, 220 (1987).

22. N. Ichikawa, et. al., "Effect of Dissolved Oxygen on Corrosion Behavior of Stainless Steel in Gamma Ray Irradiation Environment", Third Int. Sym. Environmental Degradation of Material in Nuclear Power Systems - Water Reactors, (1986).

23. E. Ibe, et. al., "Theoretical Model Analysis for Effects of Hydrogen Injection on Radiolysis of Coolant Water in BWR", J. Nucl. Sci. Tech. 23, 11 (1986) .

24. K. Ramp, "Plant HWC Status Update", Memo to Ed Kiss, March 24, 1993.

25. A. R. Curtes and W. P. Sweetham, "FACSIMILE Release H User's Manual", AERE-R11771, 1985.

26. P. B. Whalley, "HTFS-UM7 - HAA Users Manual - Harwell Annular Flow Program", AERE-R7994, April, 1985.

27. C. P. Ruiz, et. al., "Model Calculations of Water Radiolysis and Electrochemical Potentials in BWR Primary Coolant-II", Water Chemistry 6, Vol. 2, BNES, London, Oct. 1992.

28. A. J. Elliott, et. al., "Estimation of Rate Contracts for Near-Diffusion-Controlled Reactors in Water at Elevated Temperatures", J. Chem. Soc. Faraday Temp., 86, 499 (1190).

29. G. V. Buxton, "Assessment of the Radiation Chemistry of Water at Elevated Temperatures", Water Chemistry of Nuclear Reactor Systems 5, Vol. 1, p. 123, BNES, London (1989).

30. C. C. Lin, et. al., Decomposition of Hydrogen Peroxide in Aqueous Solutions at Elevated Temperature", Int. J. Chem. Kinetics, 23, 971 (1991).

31. E.L. Strickland, "Operating Plant Parameters", NEDE 21398, 1984

32. C.C. Lin, "Prediction of Electrochemical Potentials in BWR Primary Systems - Volume 1: Evaluation of Water Chemistry and ECP Measurements Under Hydrogen Water Chemistry", Appendix A, EPRI TR-102766, August 1993.

33. C.C. Lin, Y.J. Kim and L.W. Niedrach, "Prediction of Electrochemical Potentials in BWR Primary Systems - Volume 2: Development of Stainless Steel ECP Models", EPRI report in publication.

APPENDIX A

MODEL RESULTS FOR TEN BWRS REPRESENTED AS CHARTS DEPICTING ECP, H_2, 0_2, AND H_20_2 CONCENTRATIONS AS A FUNCTION OF FEEDWATER H_2 ADDITION AND VESSEL REGION LENGTH FRACTION (CHARTS GENERATED BY EPRI BASED ON GE'S SUPPLIED DATA FILES CONTAINING RADIOLYSIS/ECP MODEL CALCULATION RESULTS)

EPRI Licensed Material

Figure A-1: In-Channel Region ECPs at 0.5 Length Fraction

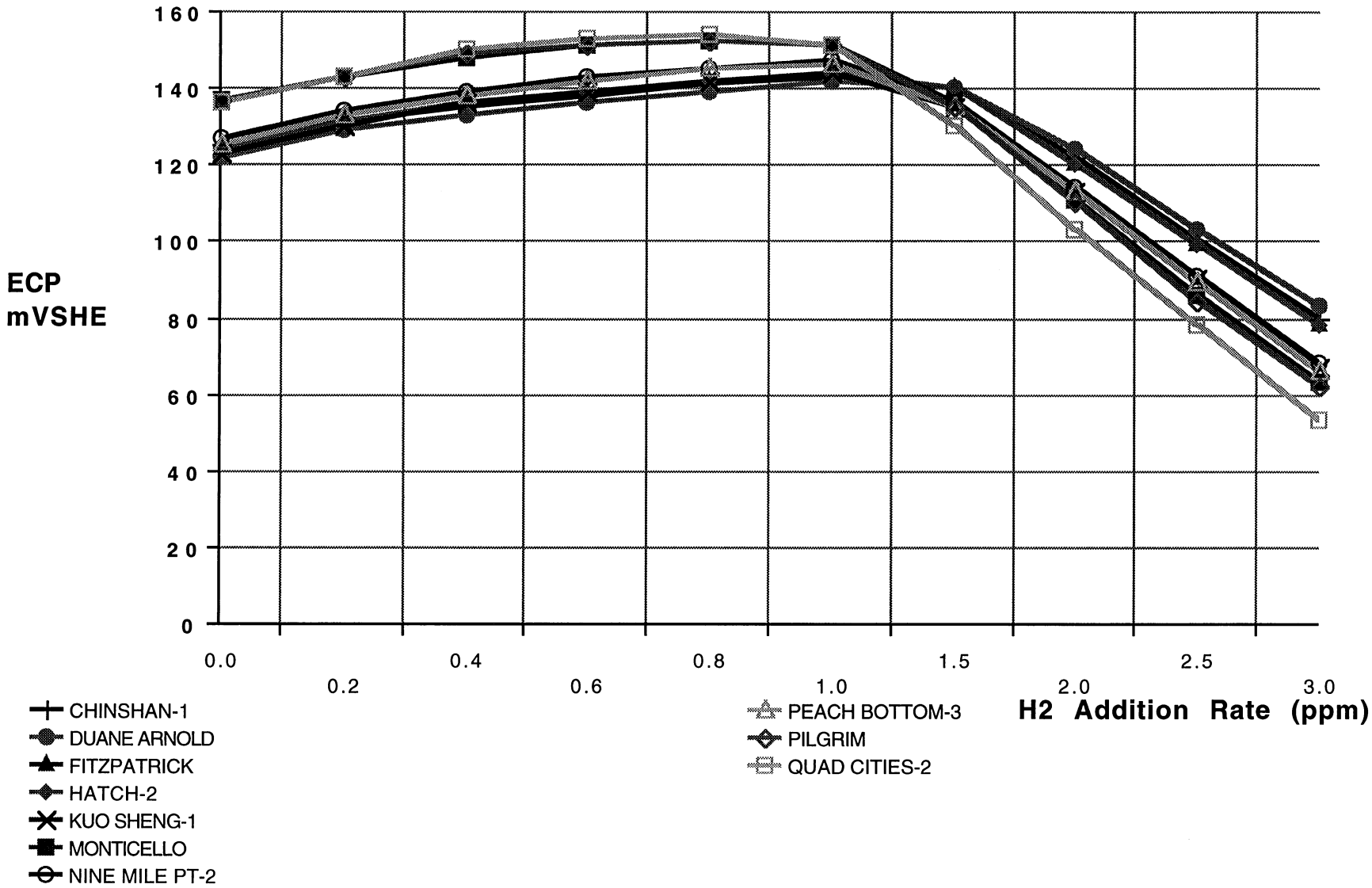

EPRI Licensed Material

Figure A-2: Core Bypass Region ECPs at 0.5 Length Fraction

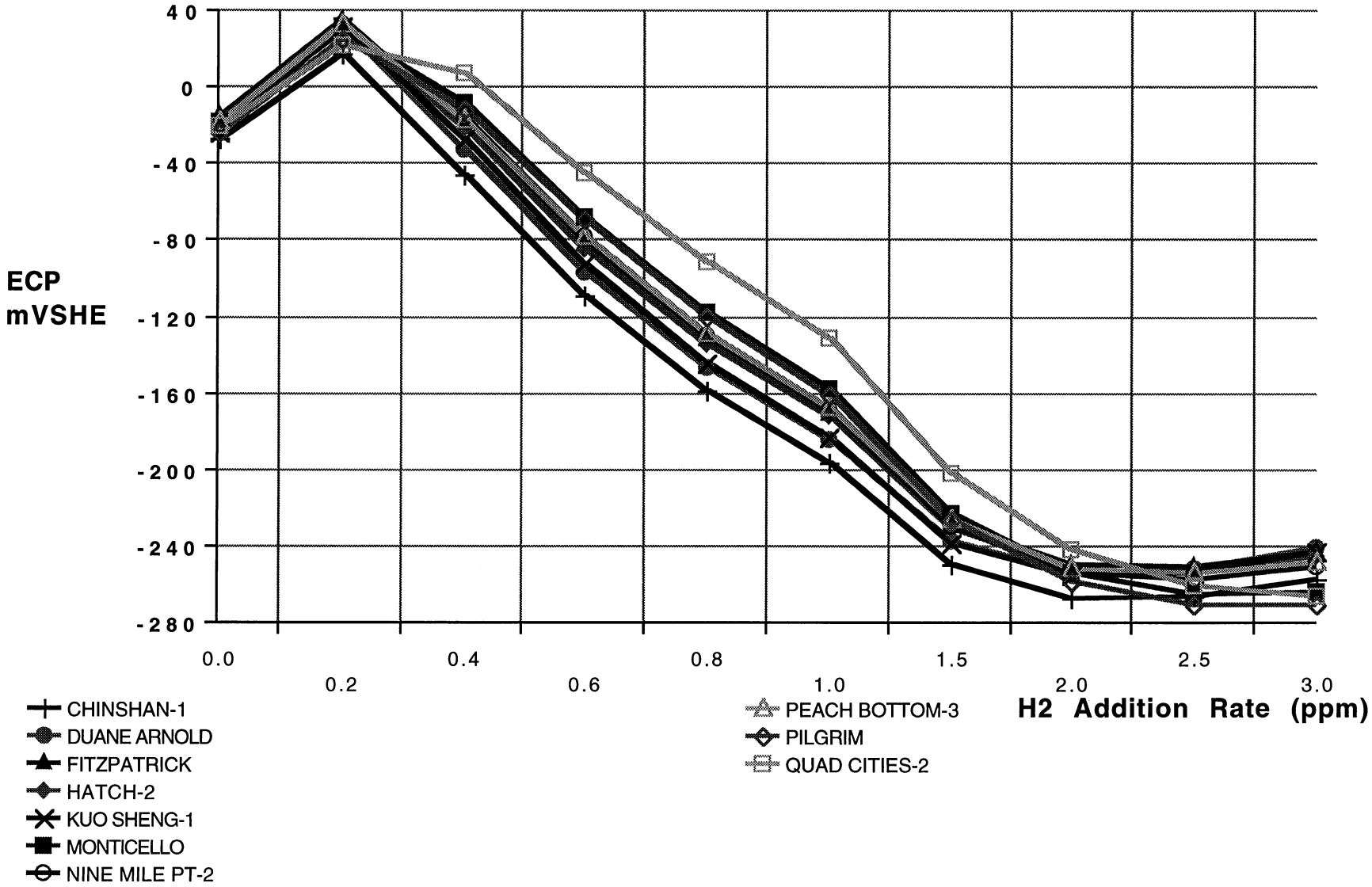

EPRI Licensed Material

Figure A-3: Outer Bypass Region ECPs at 0.5 Length Fraction

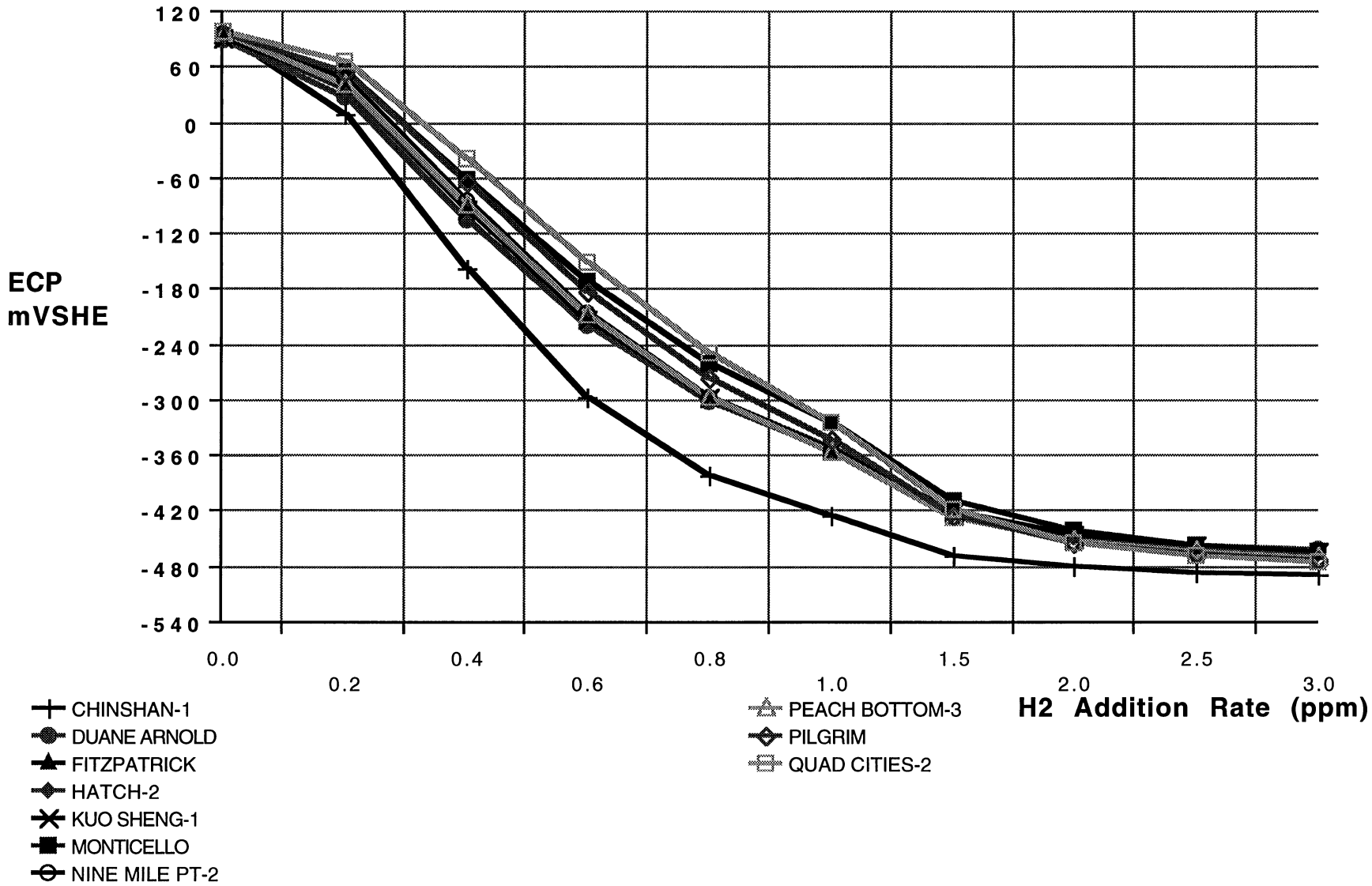

EPRI Licensed Material

Figure A-4: Upper Plenum Region ECPs at 0.5 Length Fraction

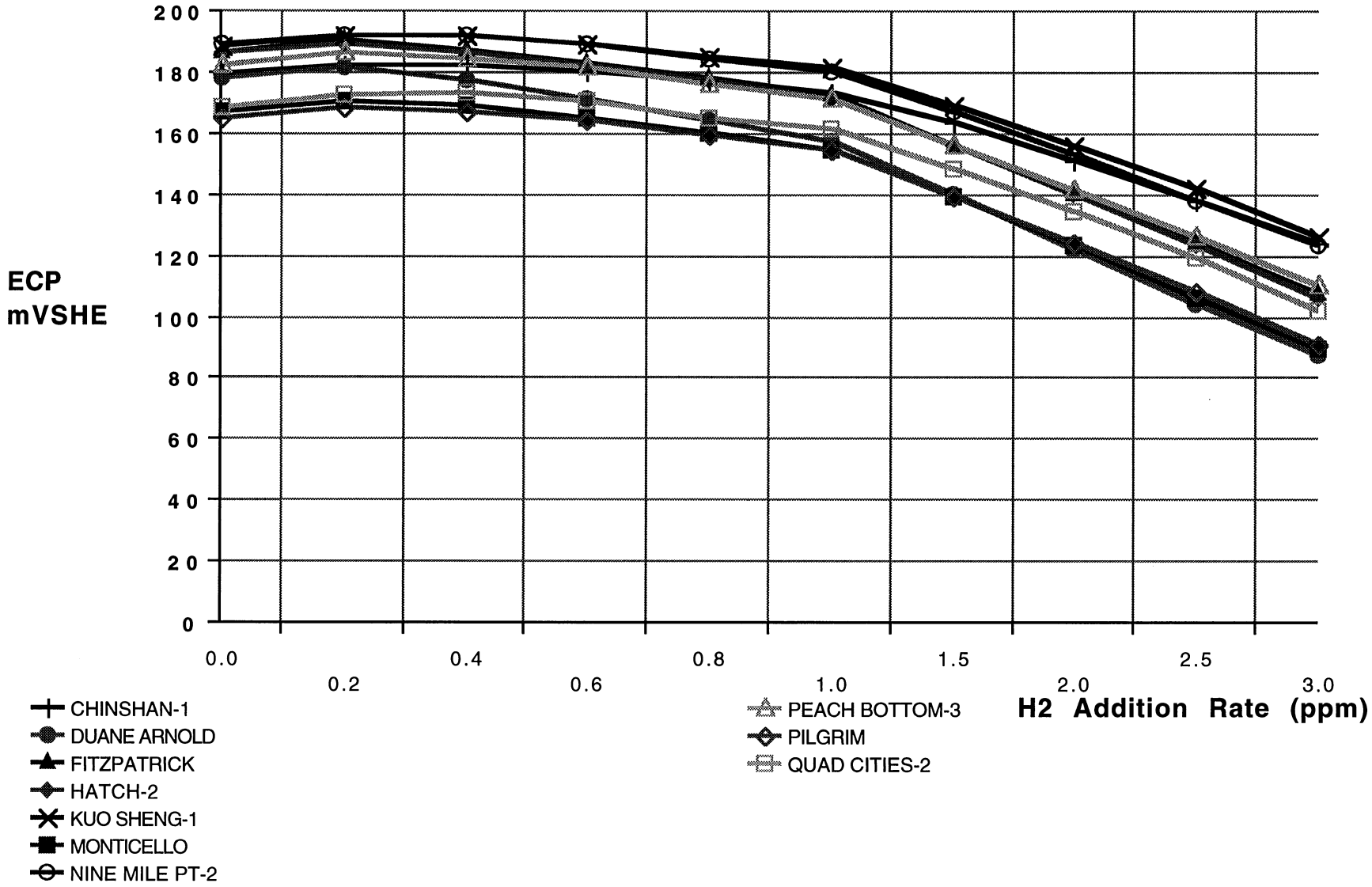

EPRI Licensed Material

Figure A-5: Steam Separator Region ECPs at 0.5 Length Fraction

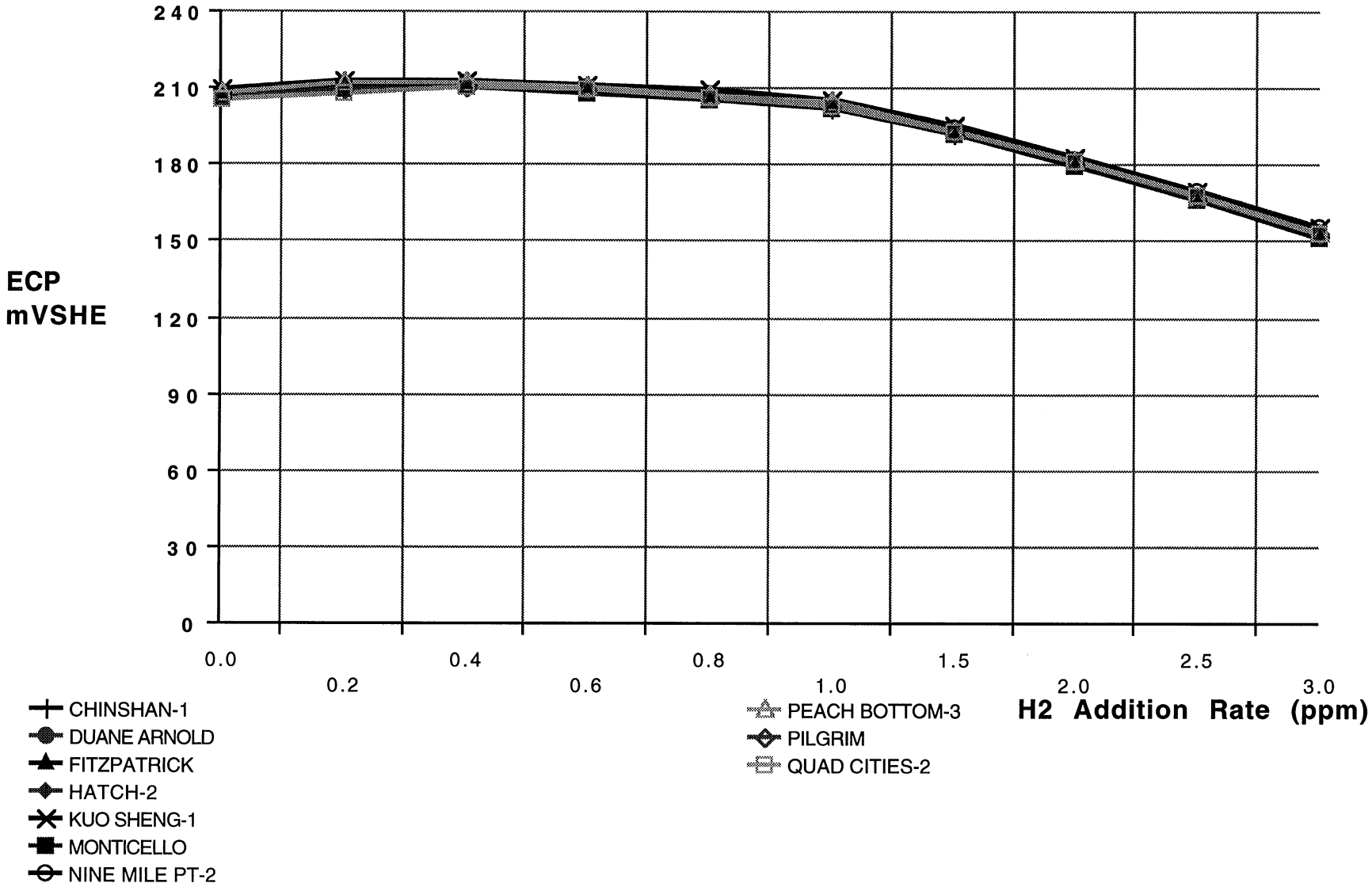

EPRI Licensed Material

Figure A-6: Mixing Plenum Region ECPs at 0.5 Length Fraction

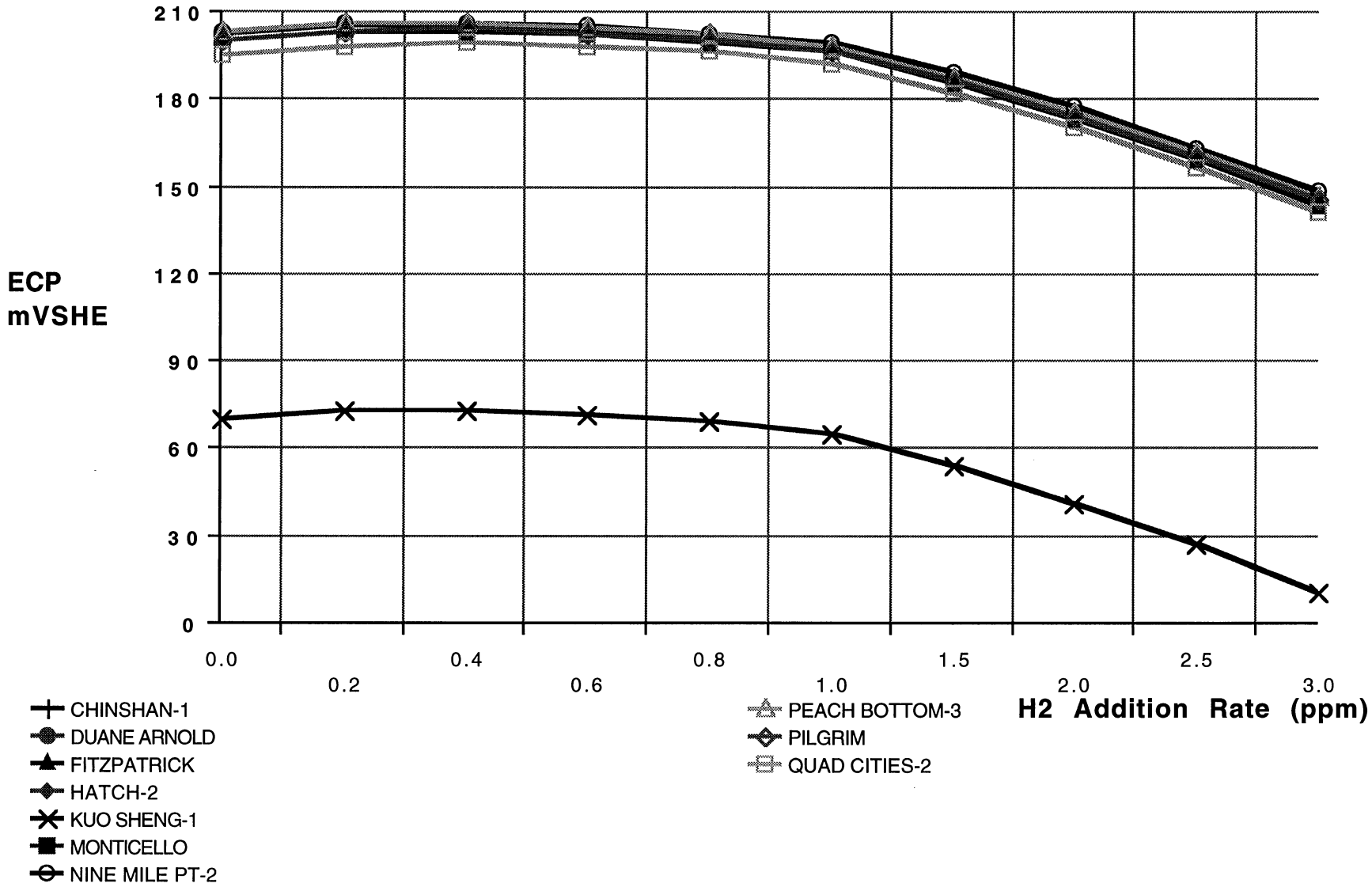

EPRI Licensed Material

Figure A-7: Downcomer Region ECPs at 0.5 Length Fraction

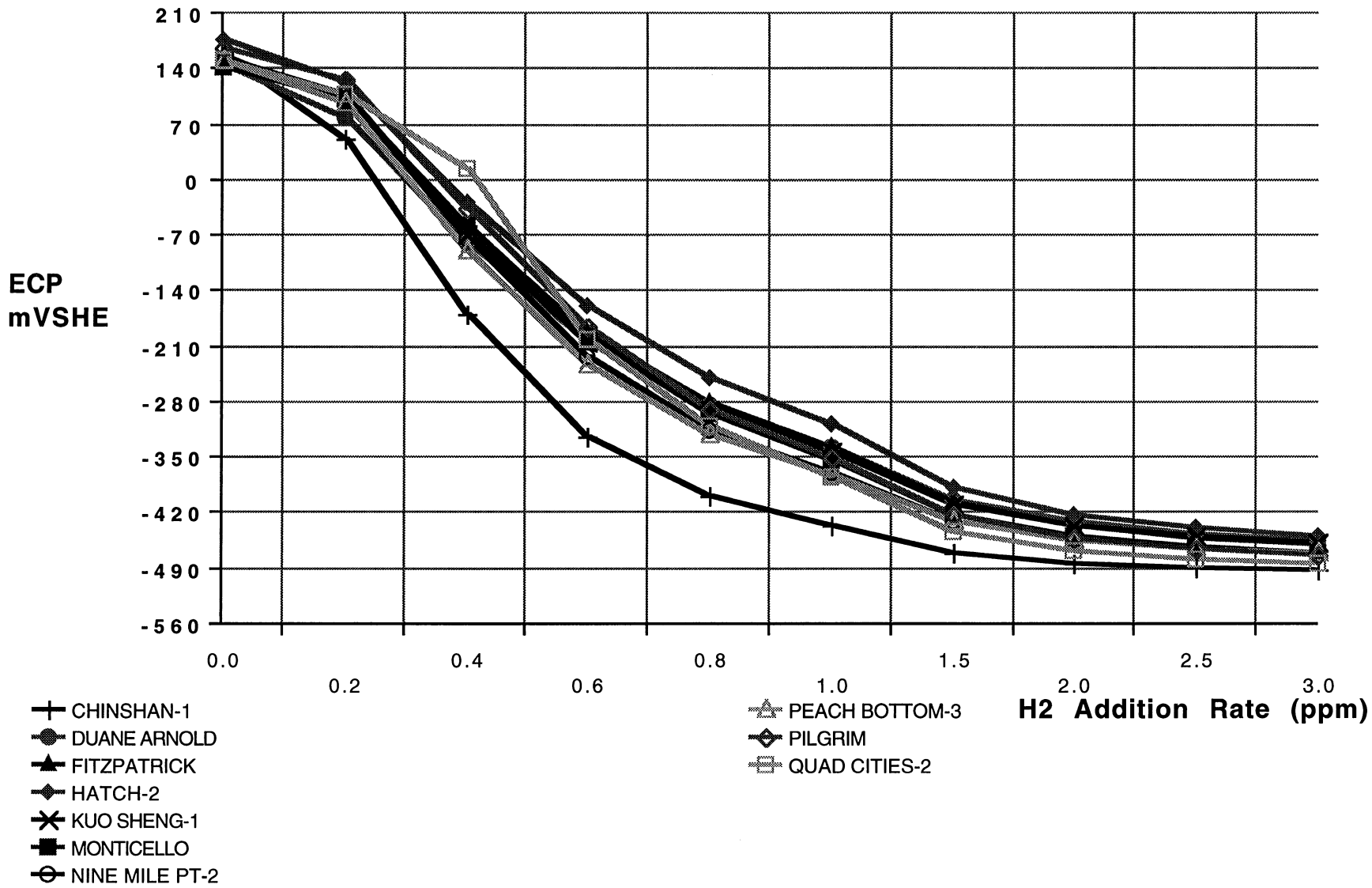

EPRI Licensed Material

Figure A-8: Recirculation Region ECPs at 0.5 Length Fraction

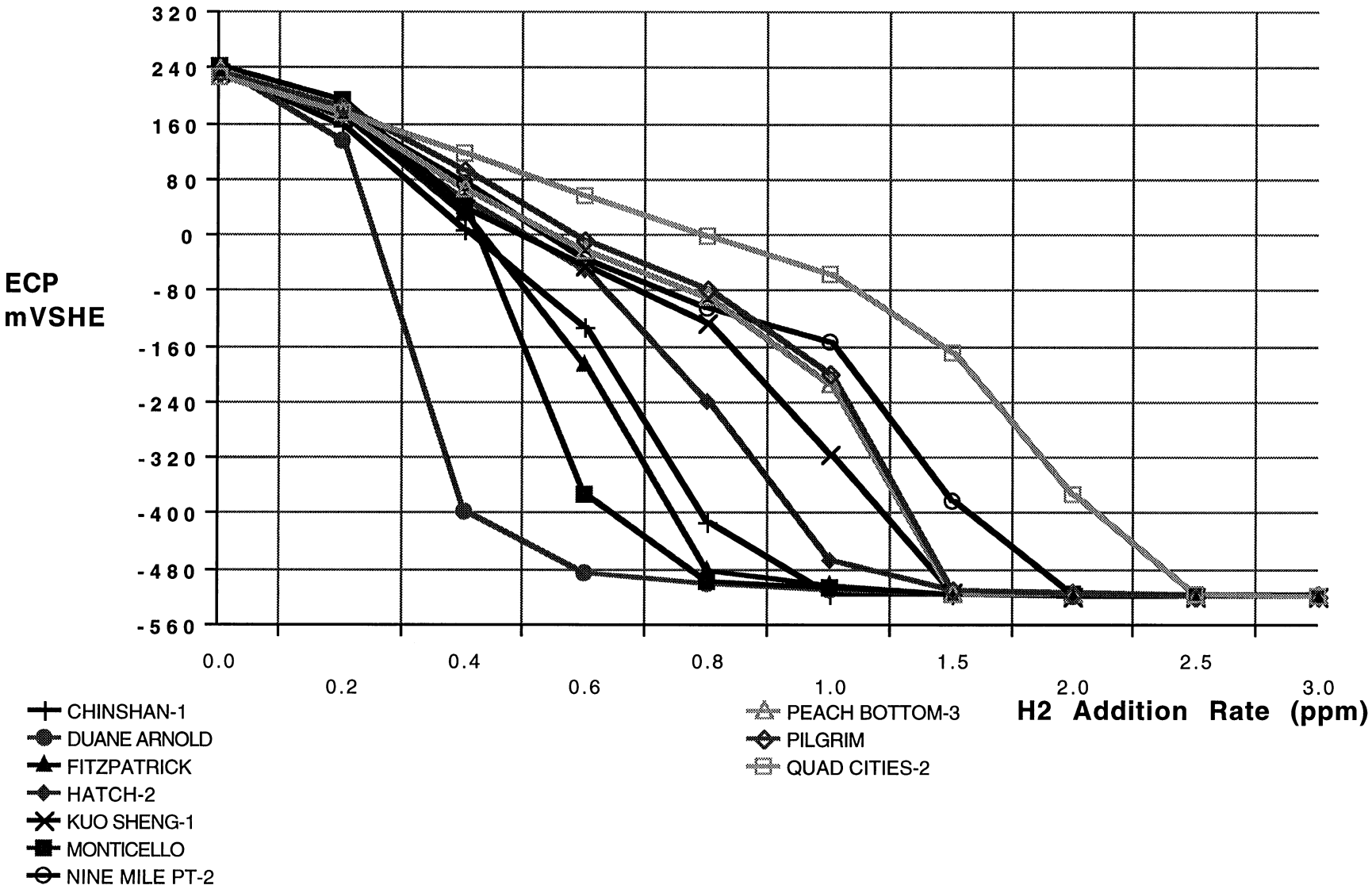

EPRI Licensed Material

Figure A-9: Jet Pump Region ECPs at 0.5 Length Fraction

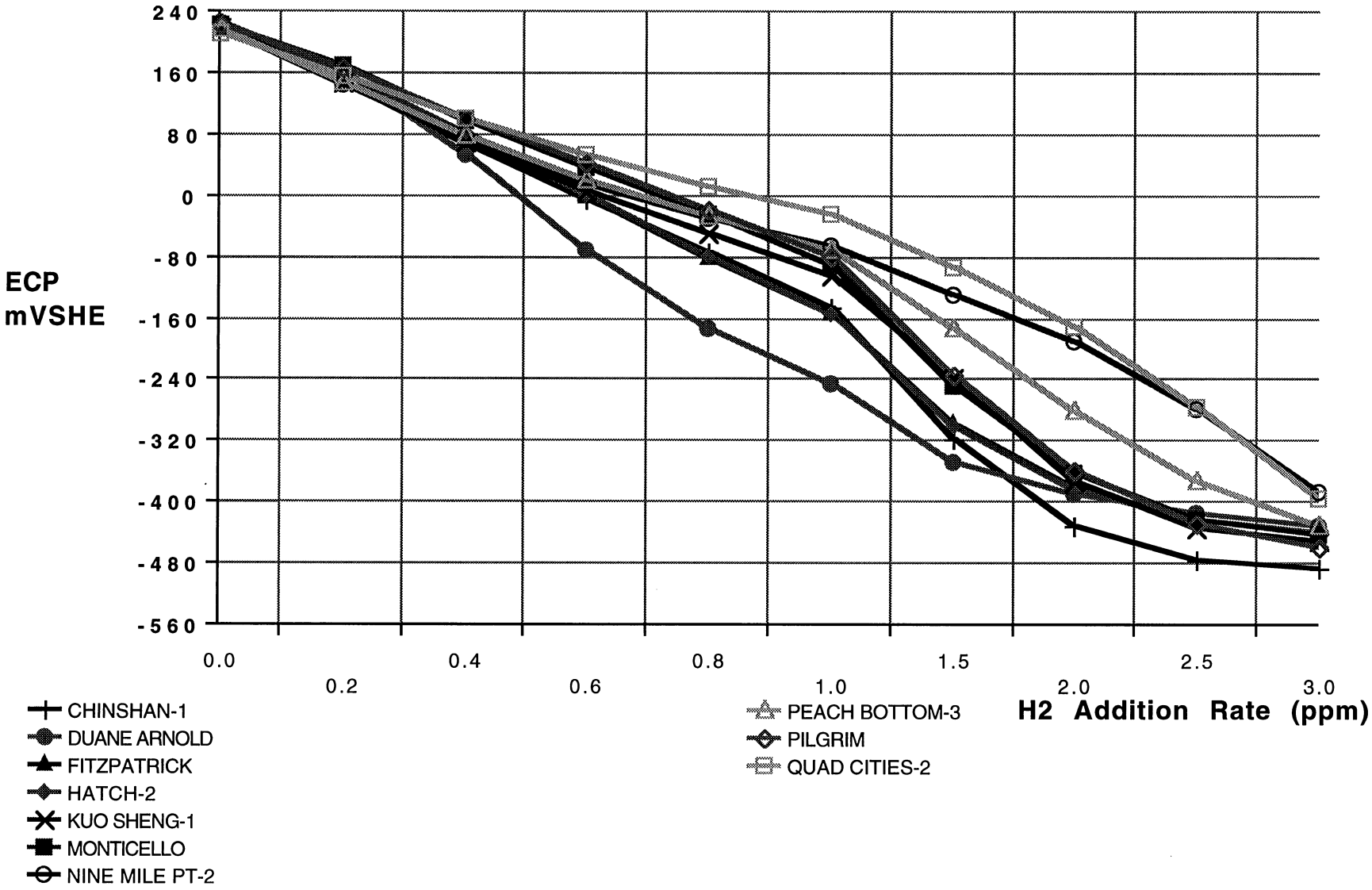

EPRI Licensed Material

Figure A-10: Lower Plenum Region ECPs at 0.5 Length Fraction

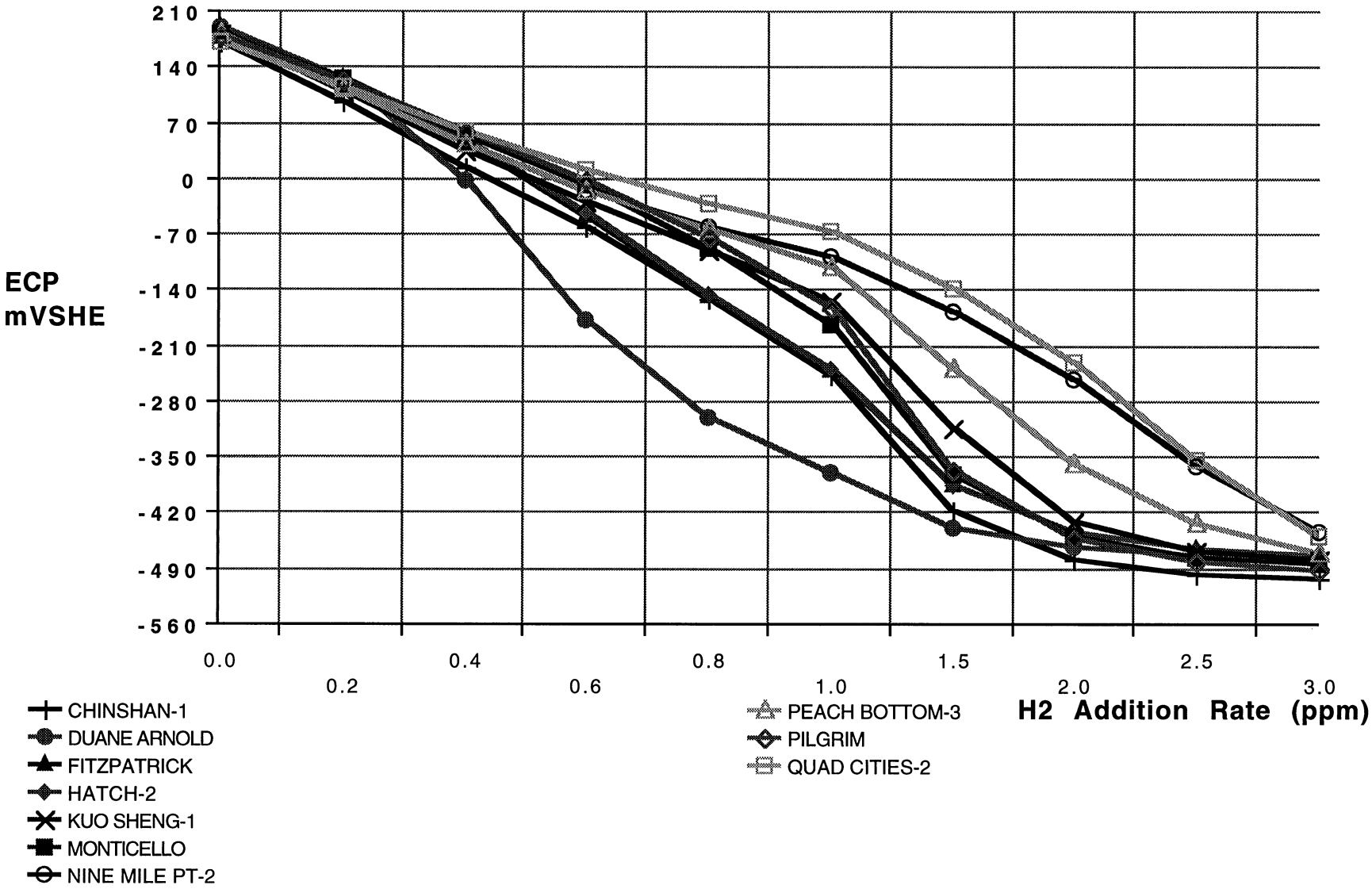

EPRI Licensed Material

Figure A-11: In-Channel Region ECPs with 0 ppm Feedwater H2 Addition

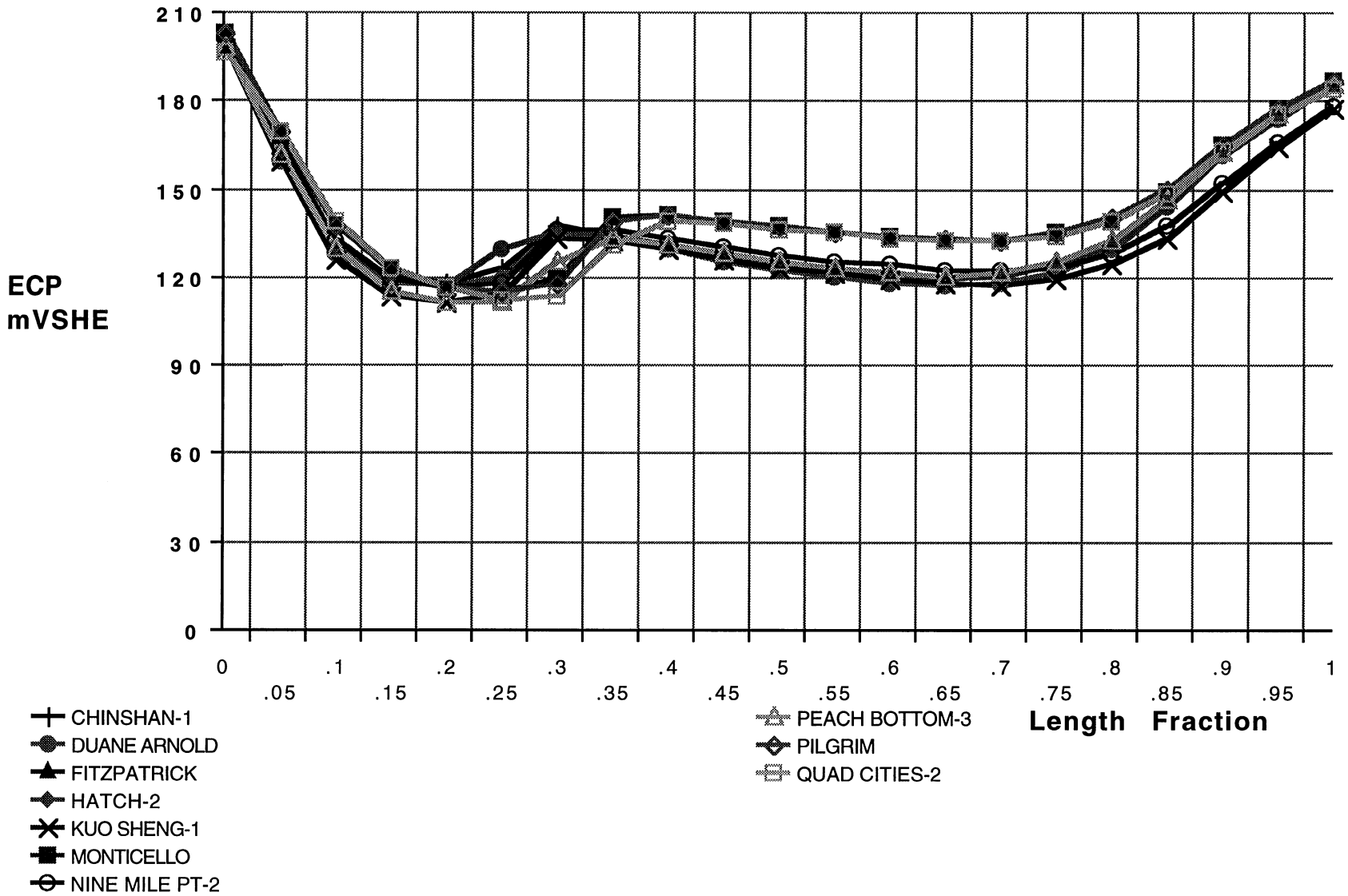

EPRI Licensed Material

Figure A-12: In-Channel Region ECPs with 0.6 ppm Feedwater H2 Addition

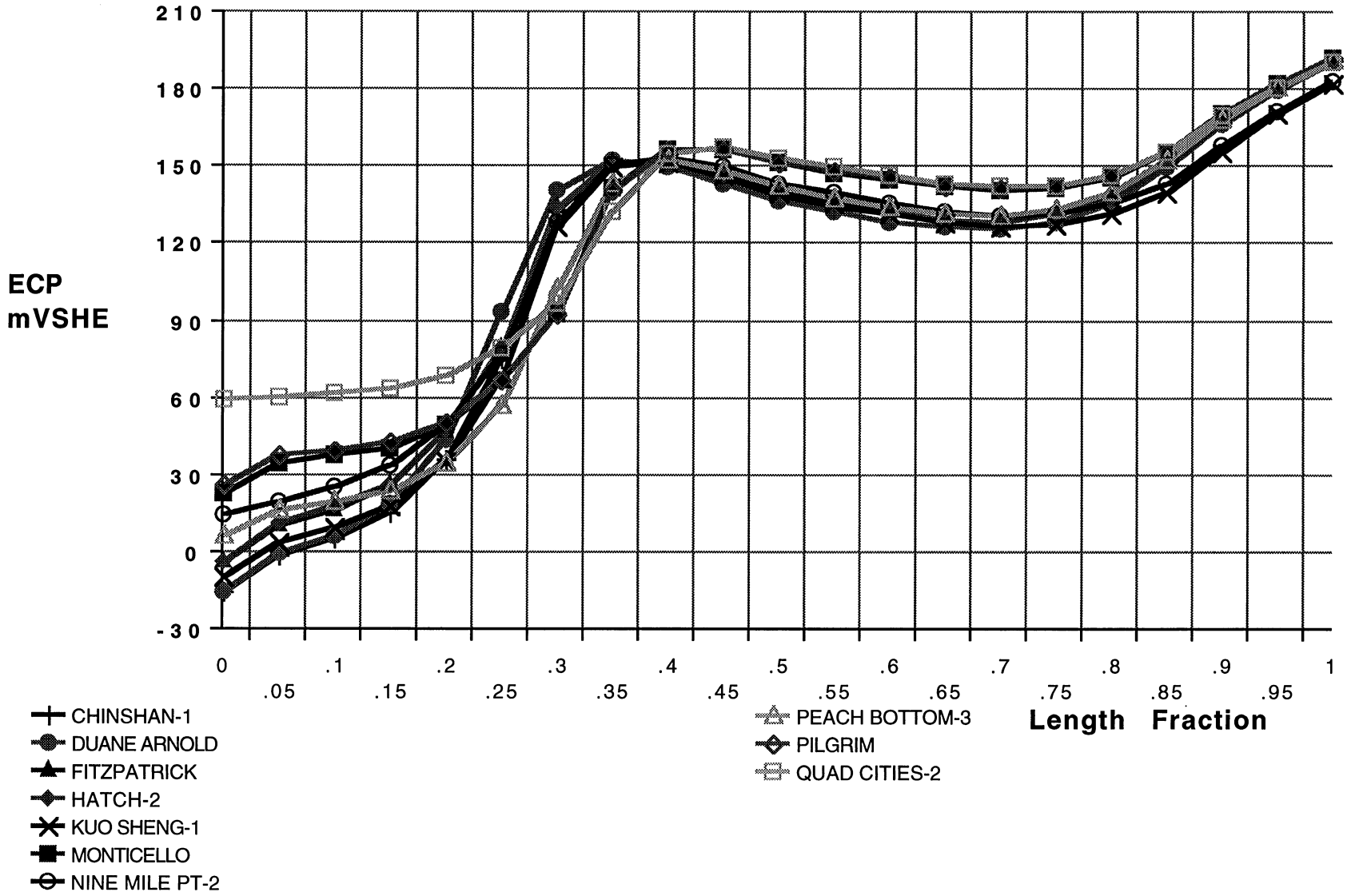

EPRI Licensed Material

Figure A-13: In-Channel Region ECPs with 1.5 ppm Feedwater H2 Addition

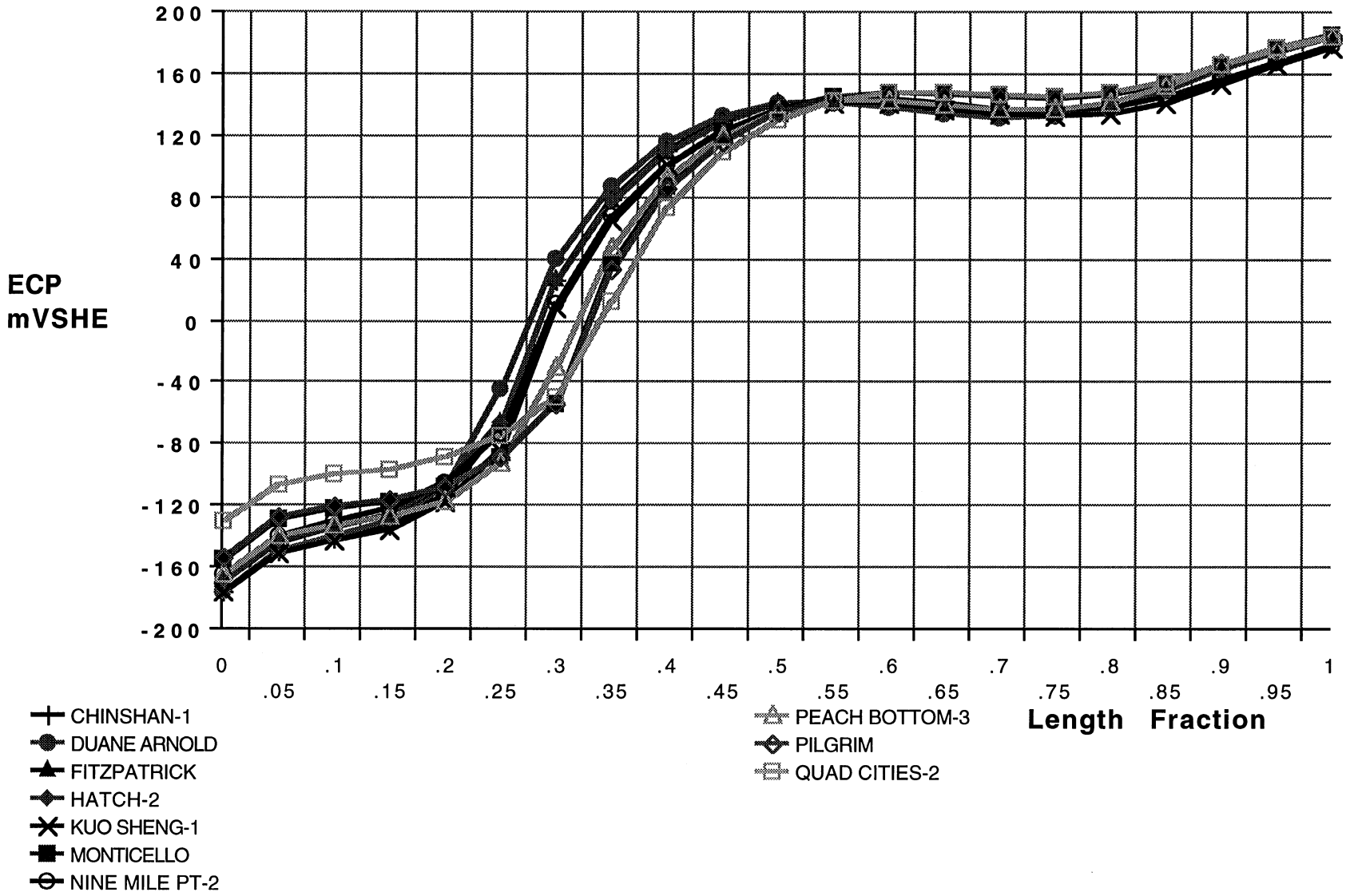

EPRI Licensed Material

Figure A-14: In-Channel Region ECPs with 3.0 ppm Feedwater H2 Addition

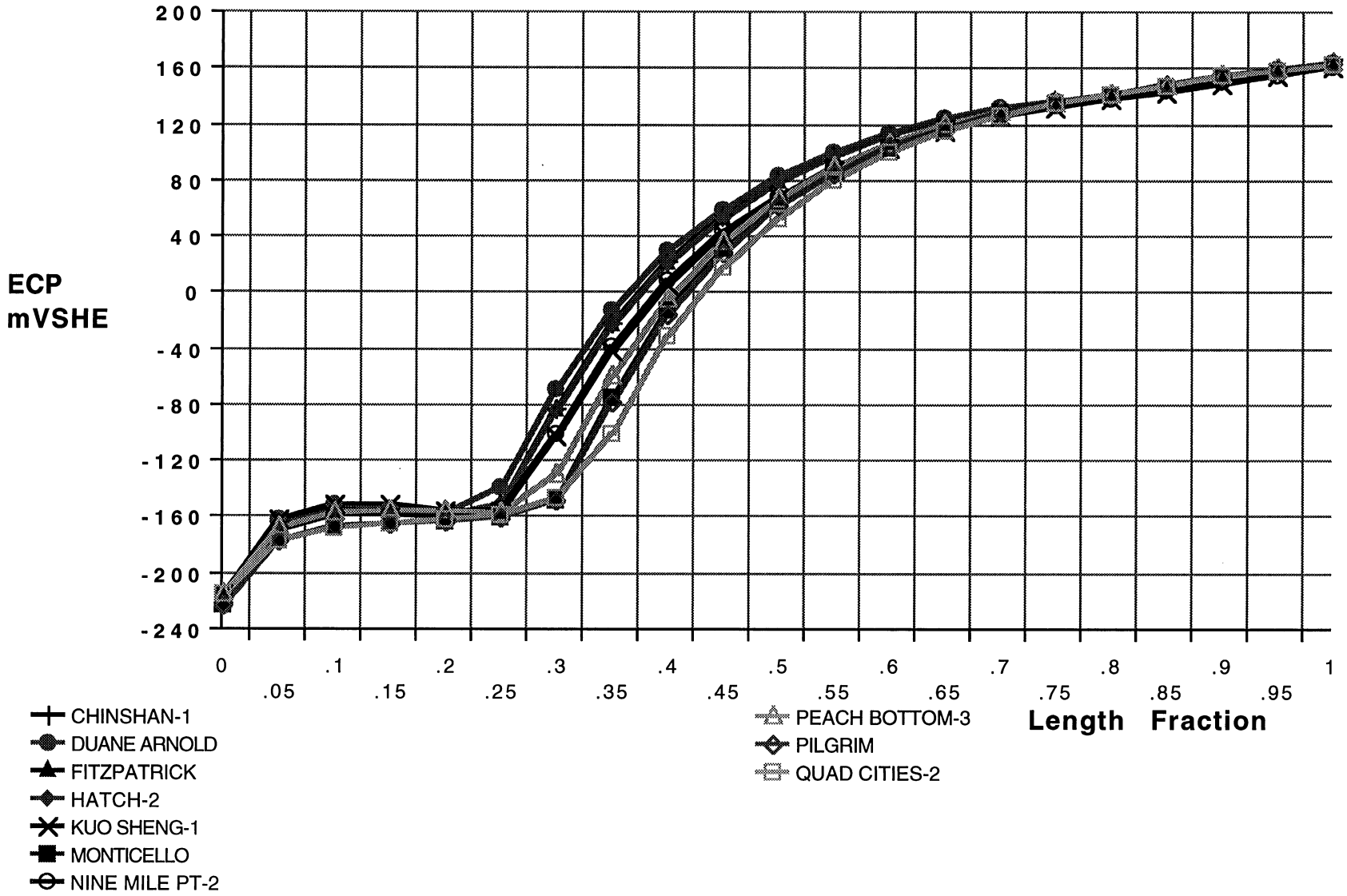

EPRI Licensed Material

Figure A-15: In-Channel Hydrogen Levels with 0 ppm Feedwater H2 Addition

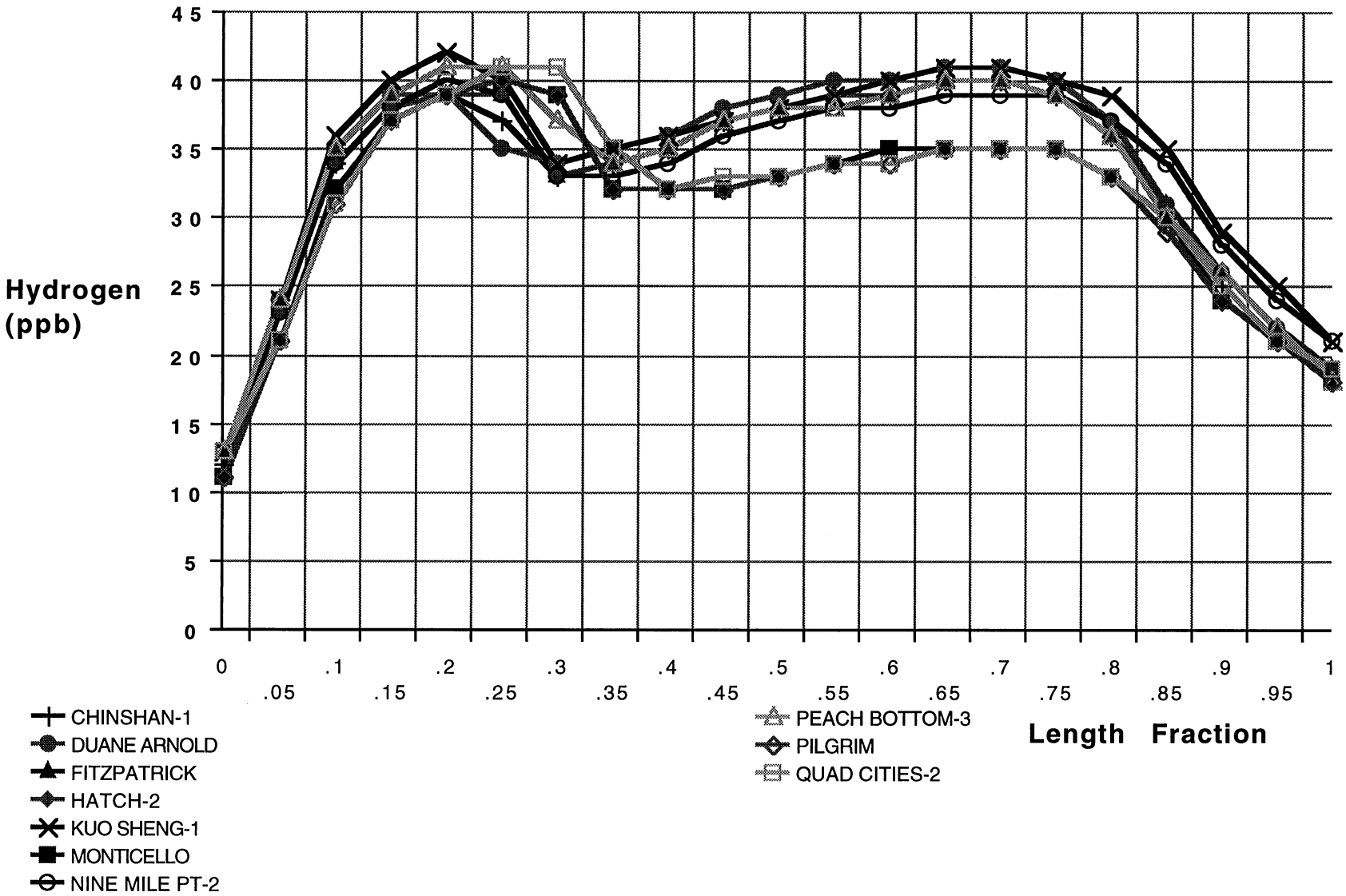

EPRI Licensed Material

Figure A-16: In-Channel Hydrogen Levels with 0.6 ppm Feedwater H2 Addition

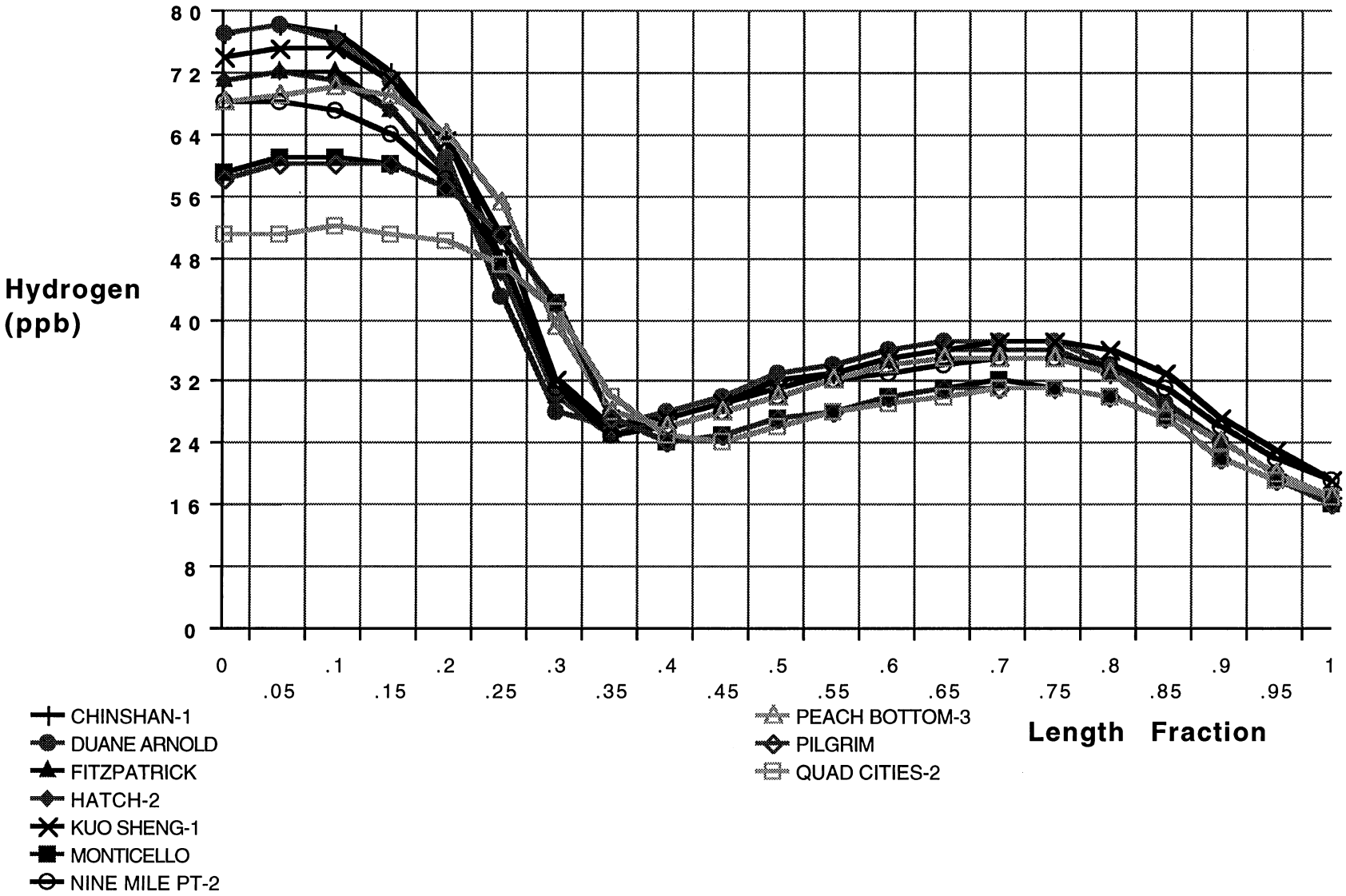

EPRI Licensed Material

Figure A-17: In-Channel Hydrogen Levels with 1.5 ppm Feedwater H2 Addition

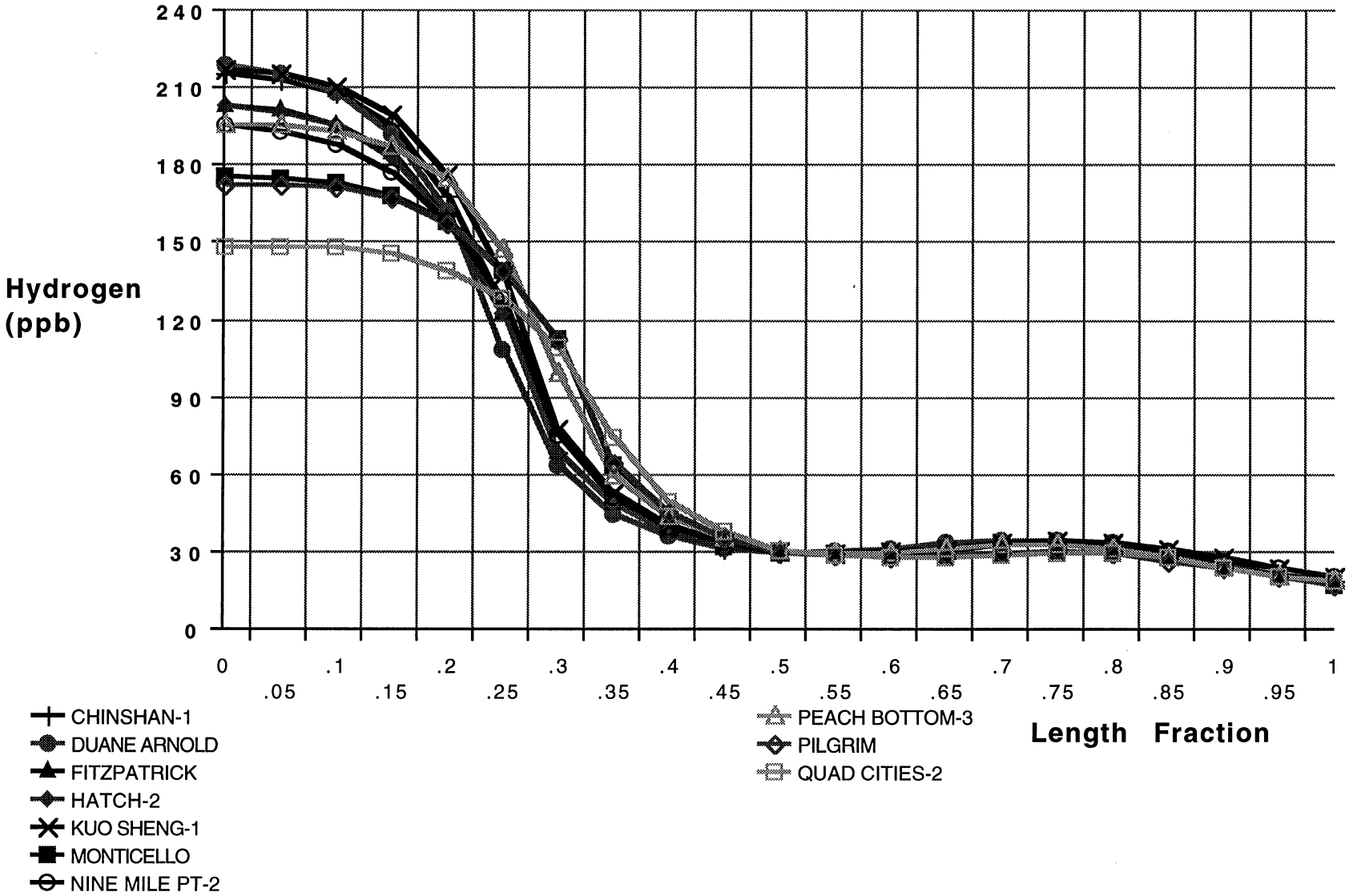

EPRI Licensed Material

Figure A-18: In-Channel Hydrogen Levels with 3.0 ppm Feedwater H2 Addition

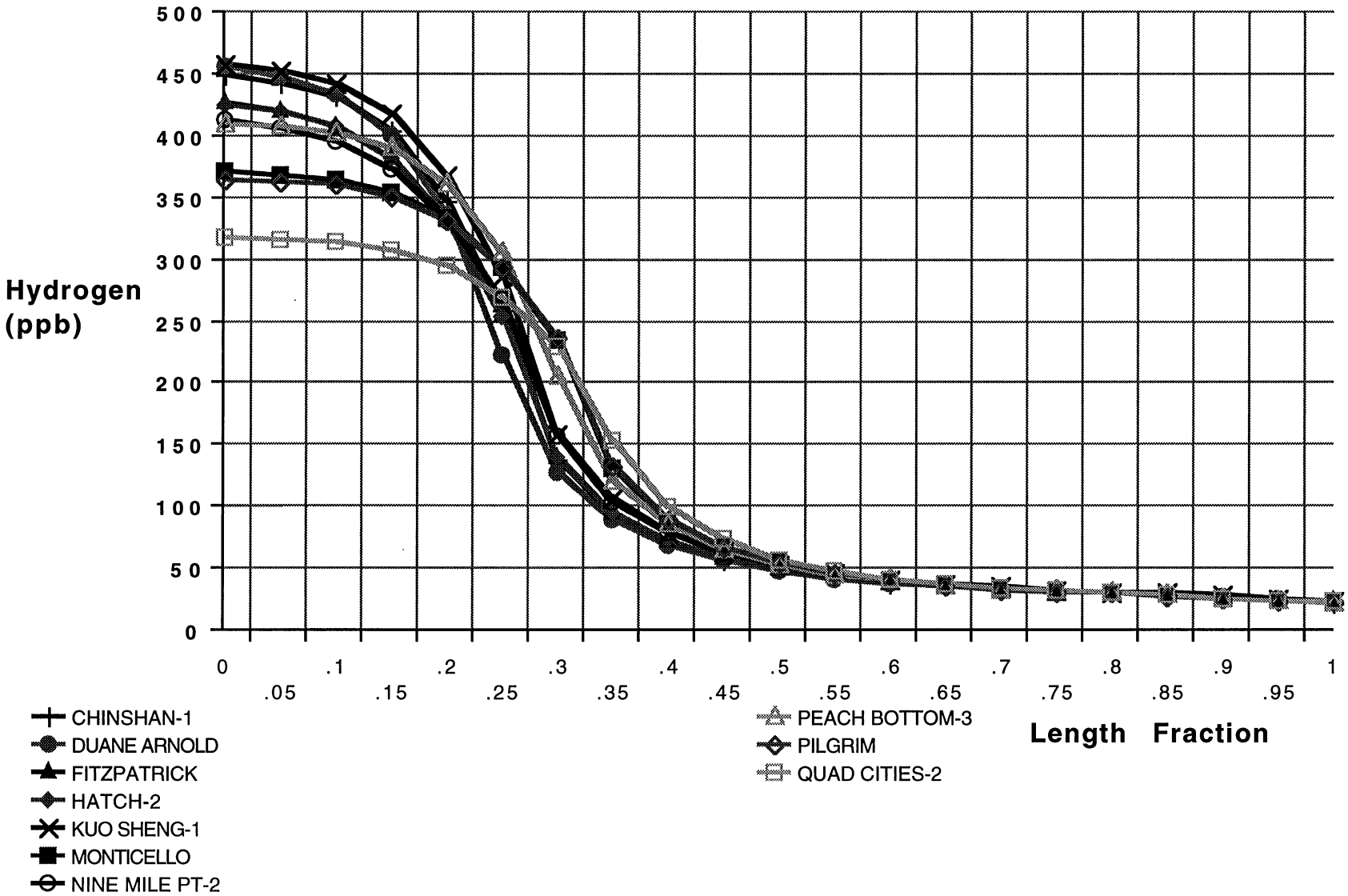

EPRI Licensed Material

Figure A-19: In-Channel Oxygen Levels with 0 ppm Feedwater H2 Addition

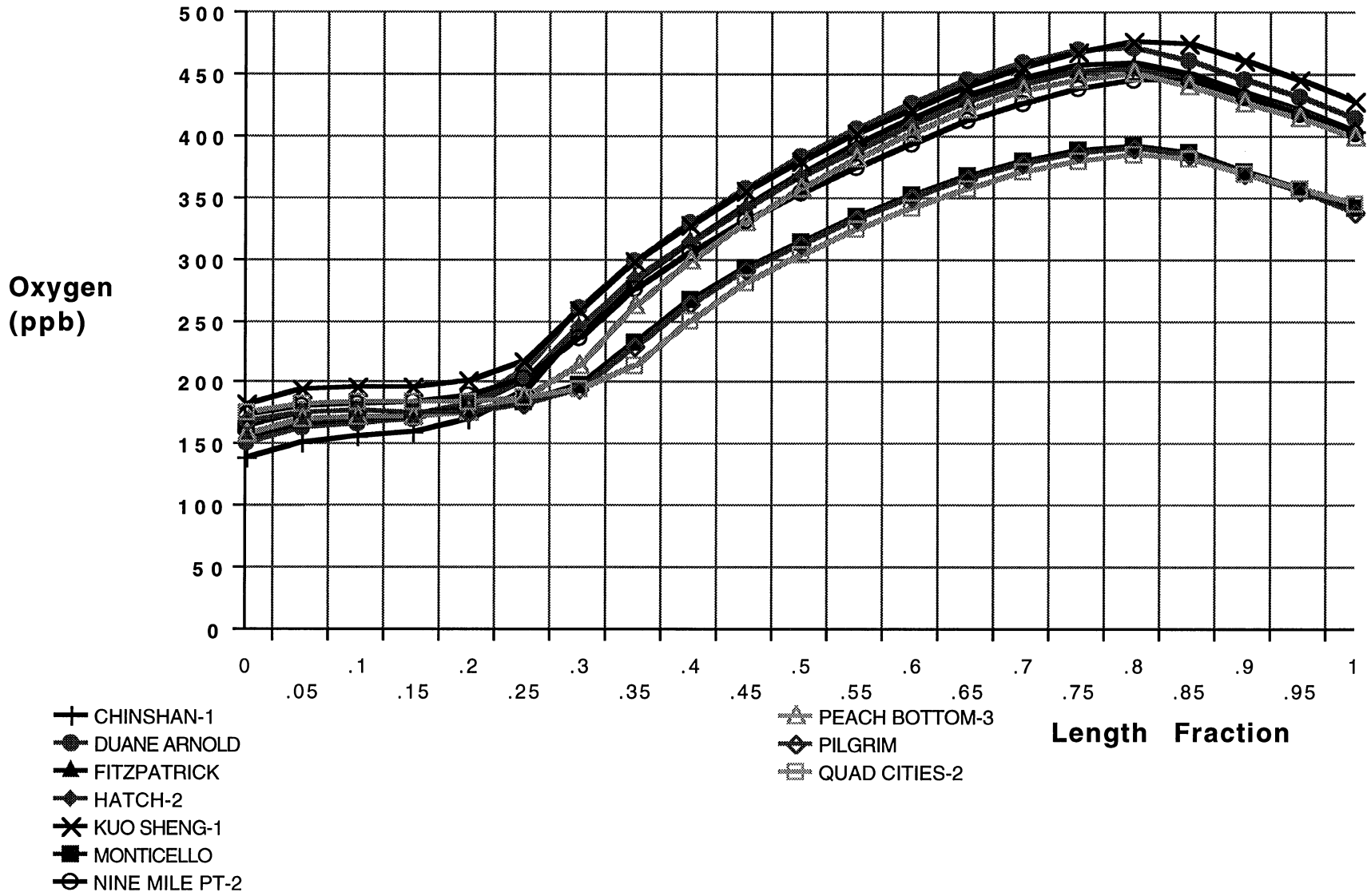

EPRI Licensed Material

Figure A-20: In-Channel Oxygen Levels with 0.6 ppm Feedwater H2 Addition

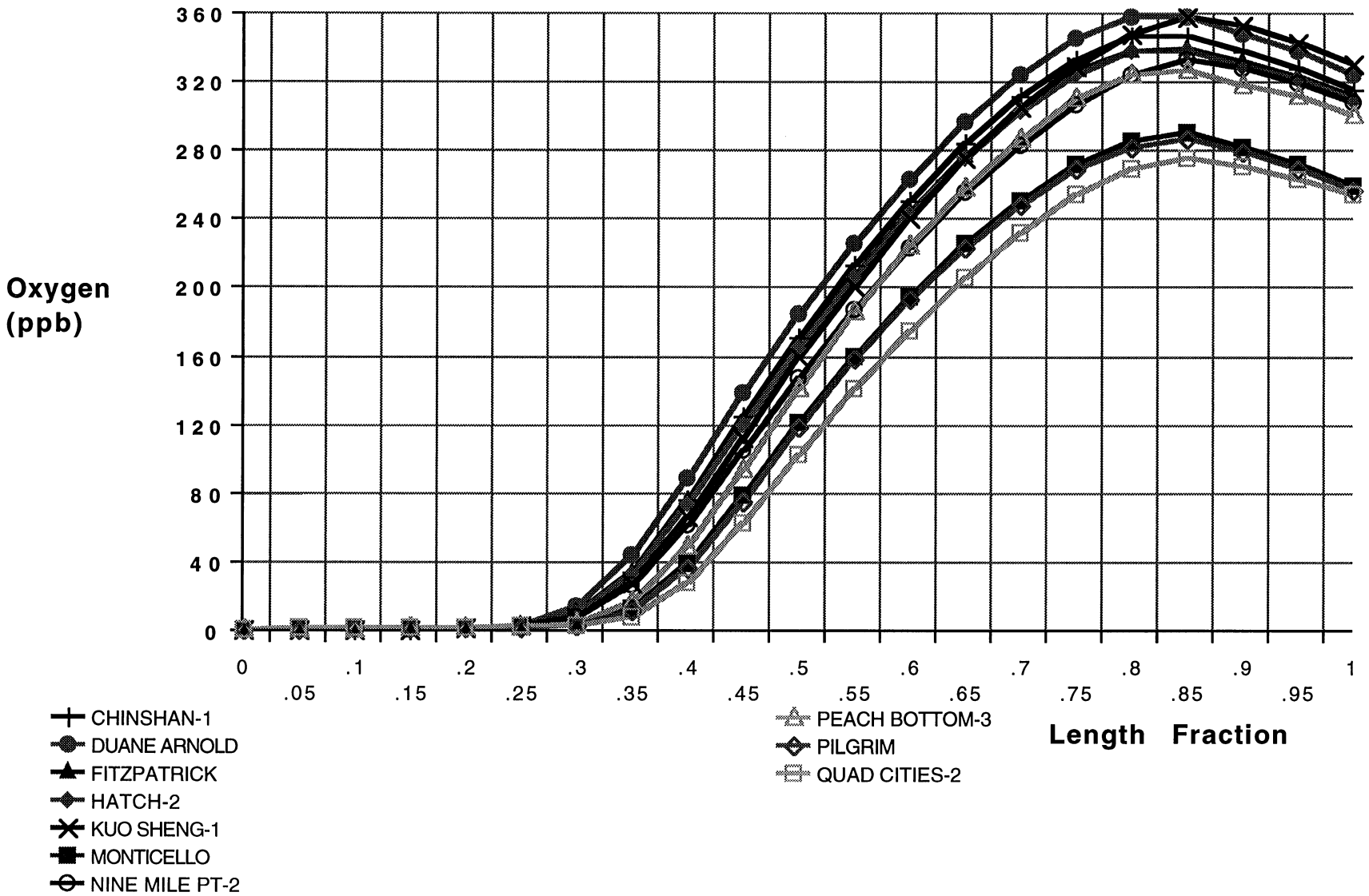

EPRI Licensed Material

Figure A-21: In-Channel Oxygen Levels with 1.5 ppm Feedwater H2 Addition

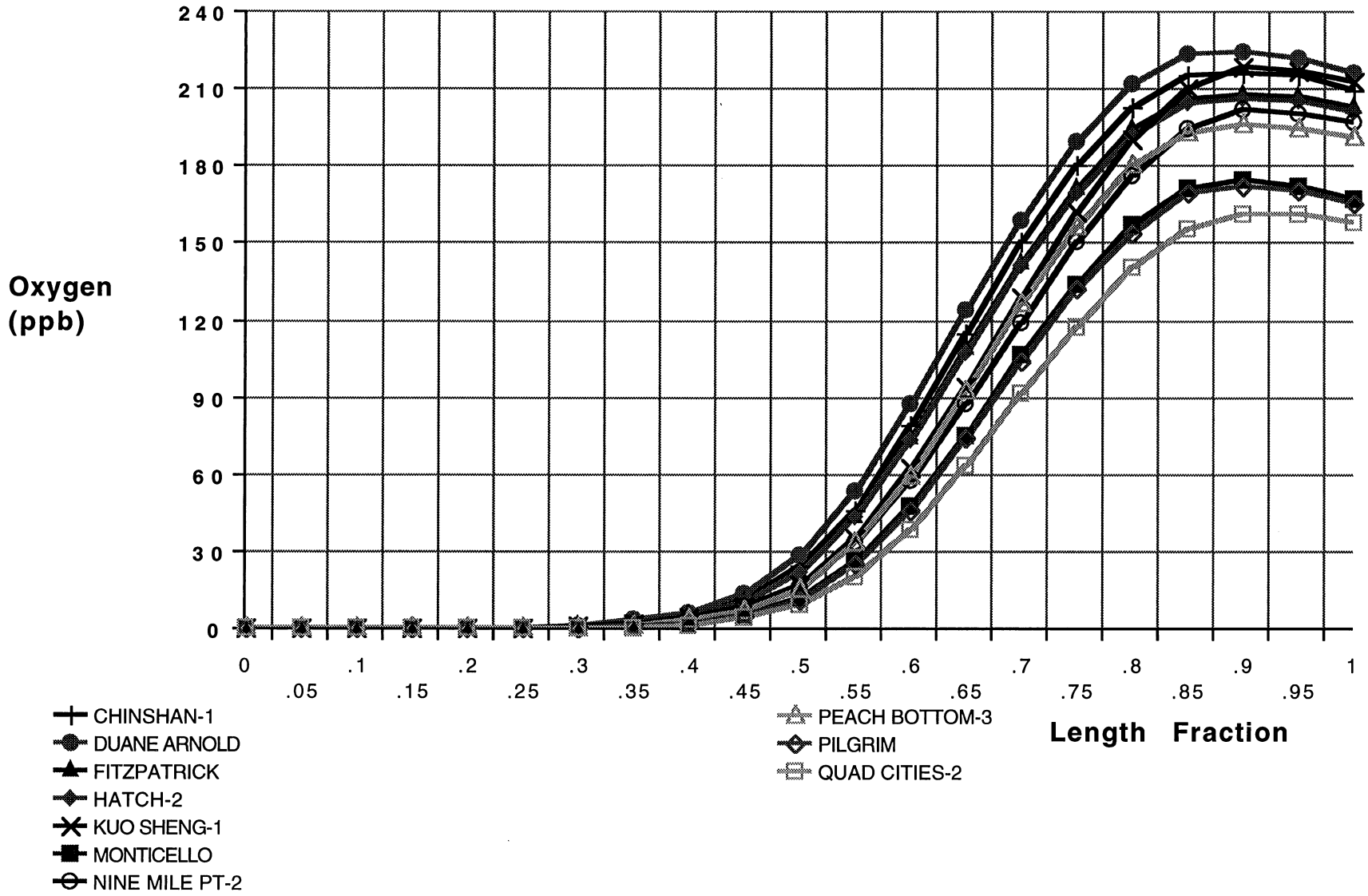

EPRI Licensed Material

Figure A-22: In-Channel Oxygen Levels with 3.0 ppm Feedwater H2 Addition

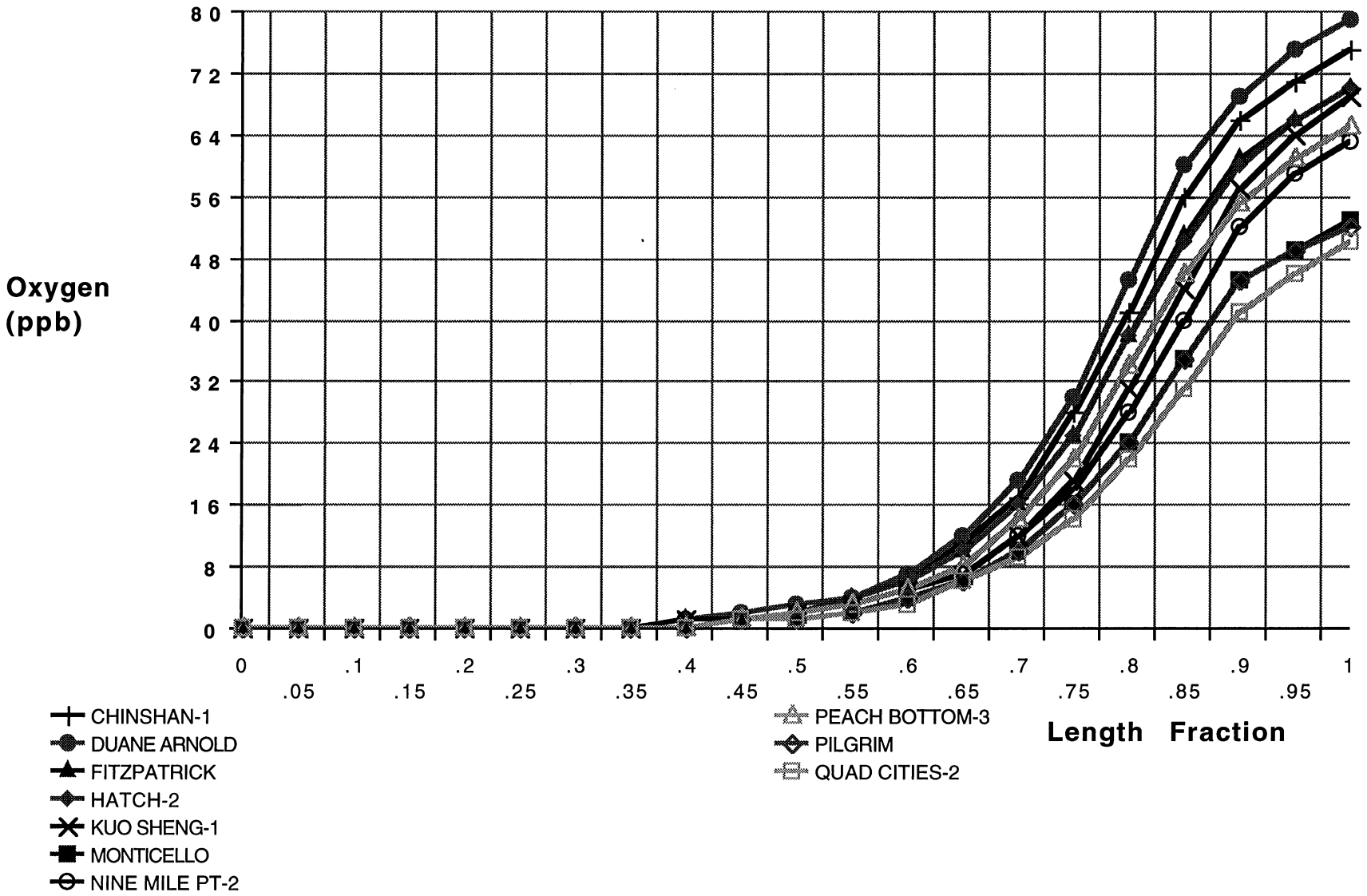

EPRI Licensed Material

Figure A-23: In-Channel Peroxide Levels with 0 ppm Feedwater H2 Addition

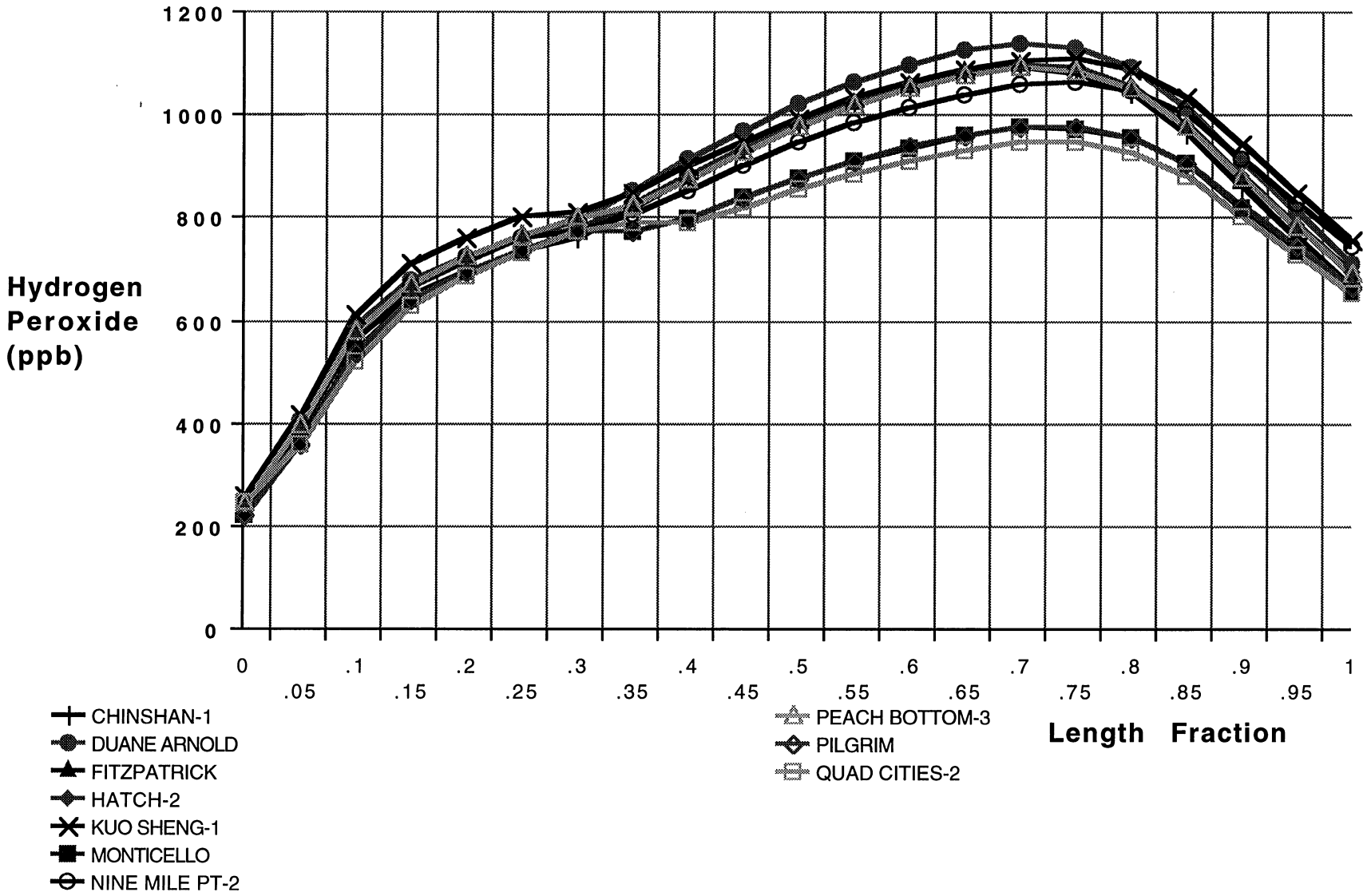

EPRI Licensed Material

Figure A-24: In-Channel Peroxide Levels with 0.6 ppm Feedwater H2 Addition

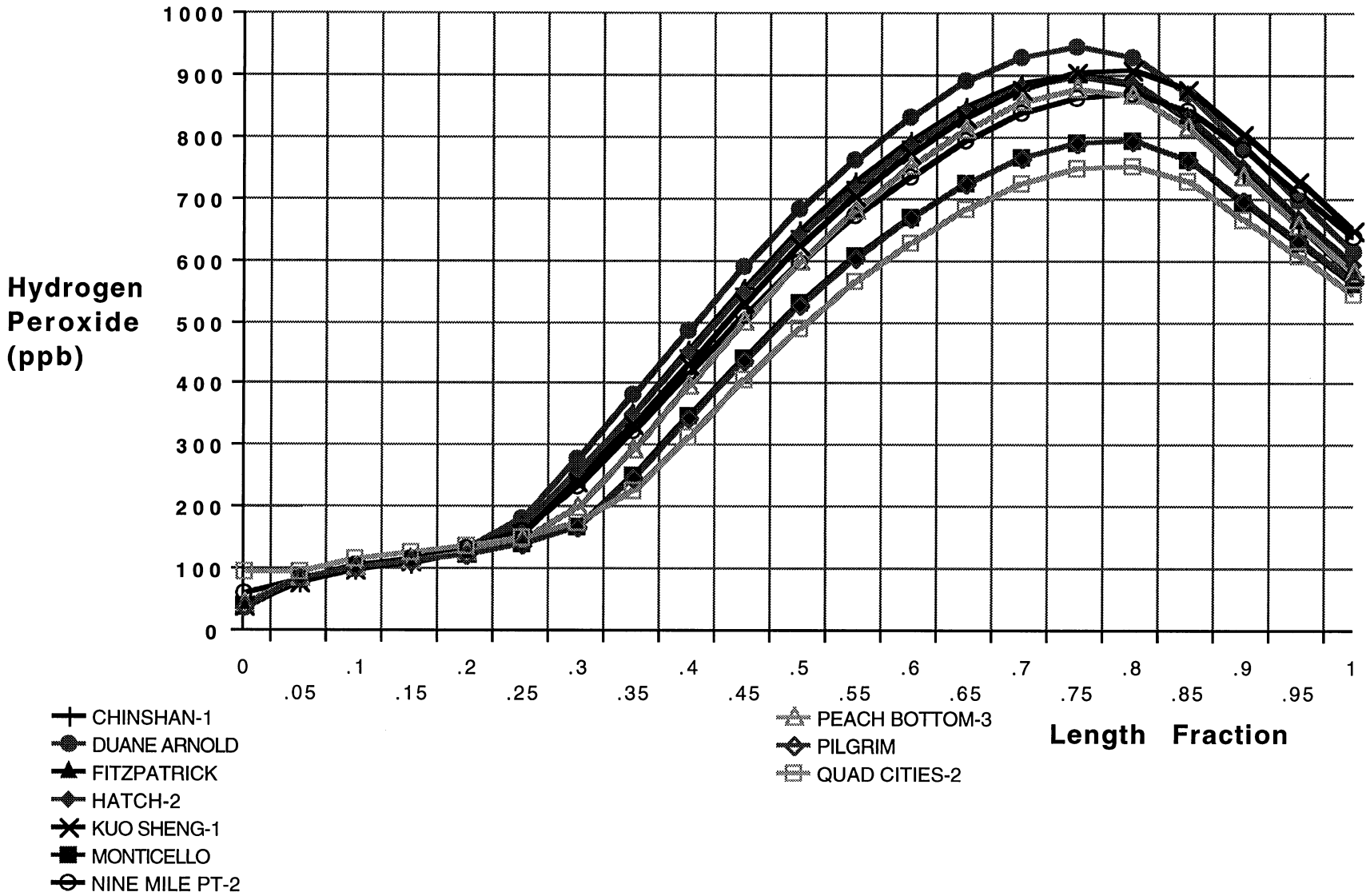

EPRI Licensed Material

Figure A-25: In-Channel Peroxide Levels with 1.5 ppm Feedwater H2 Addition

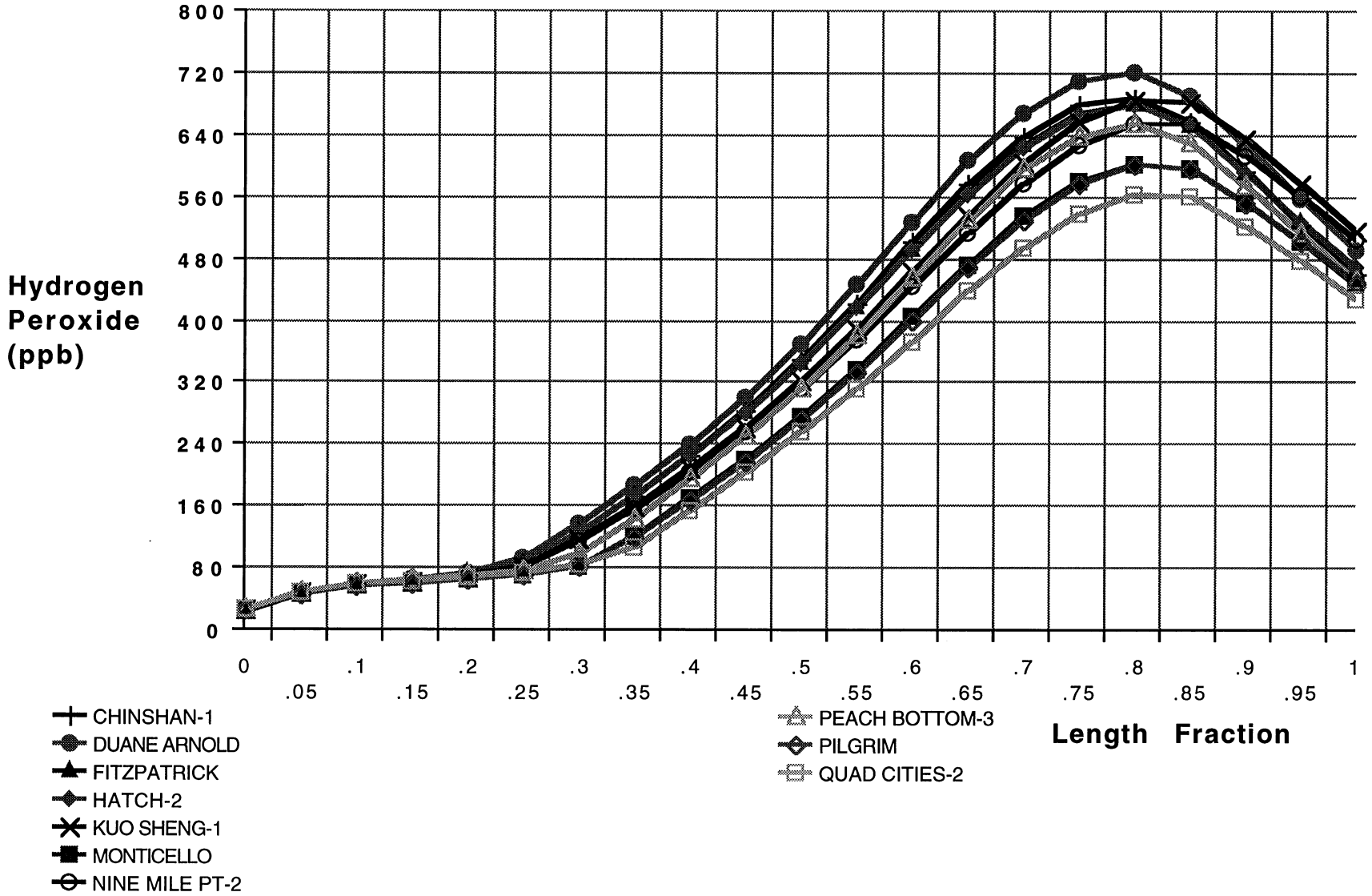

EPRI Licensed Material

Figure A-26: In-Channel Peroxide Levels with 3.0 ppm Feedwater H2 Addition

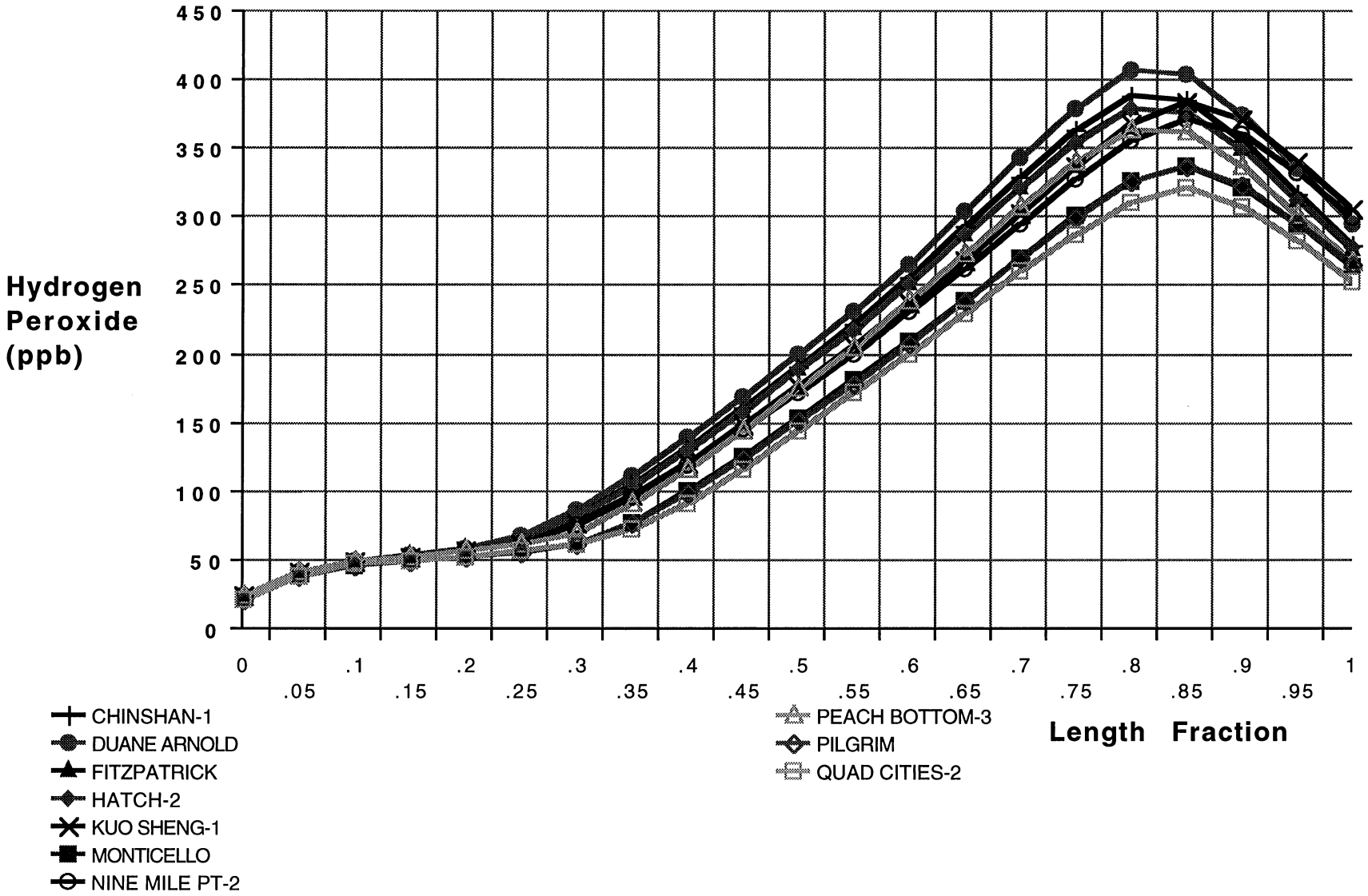

EPRI Licensed Material

Figure A-27: Core Bypass Region ECPs with 0 ppm Feedwater H2 Addition

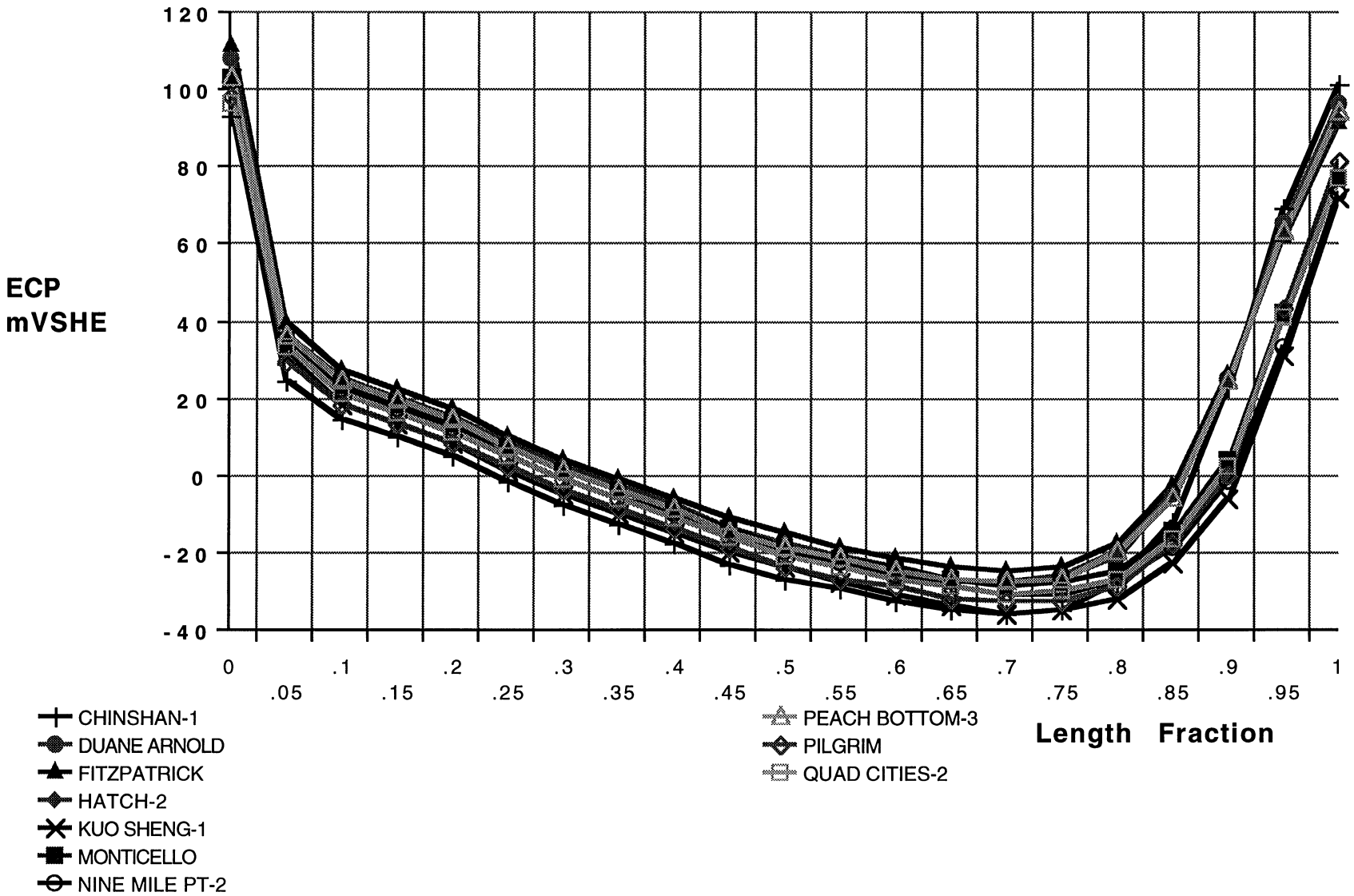

EPRI Licensed Material

Figure A-28: Core Bypass Region ECPs with 0.6 ppm Feedwater H2 Addition

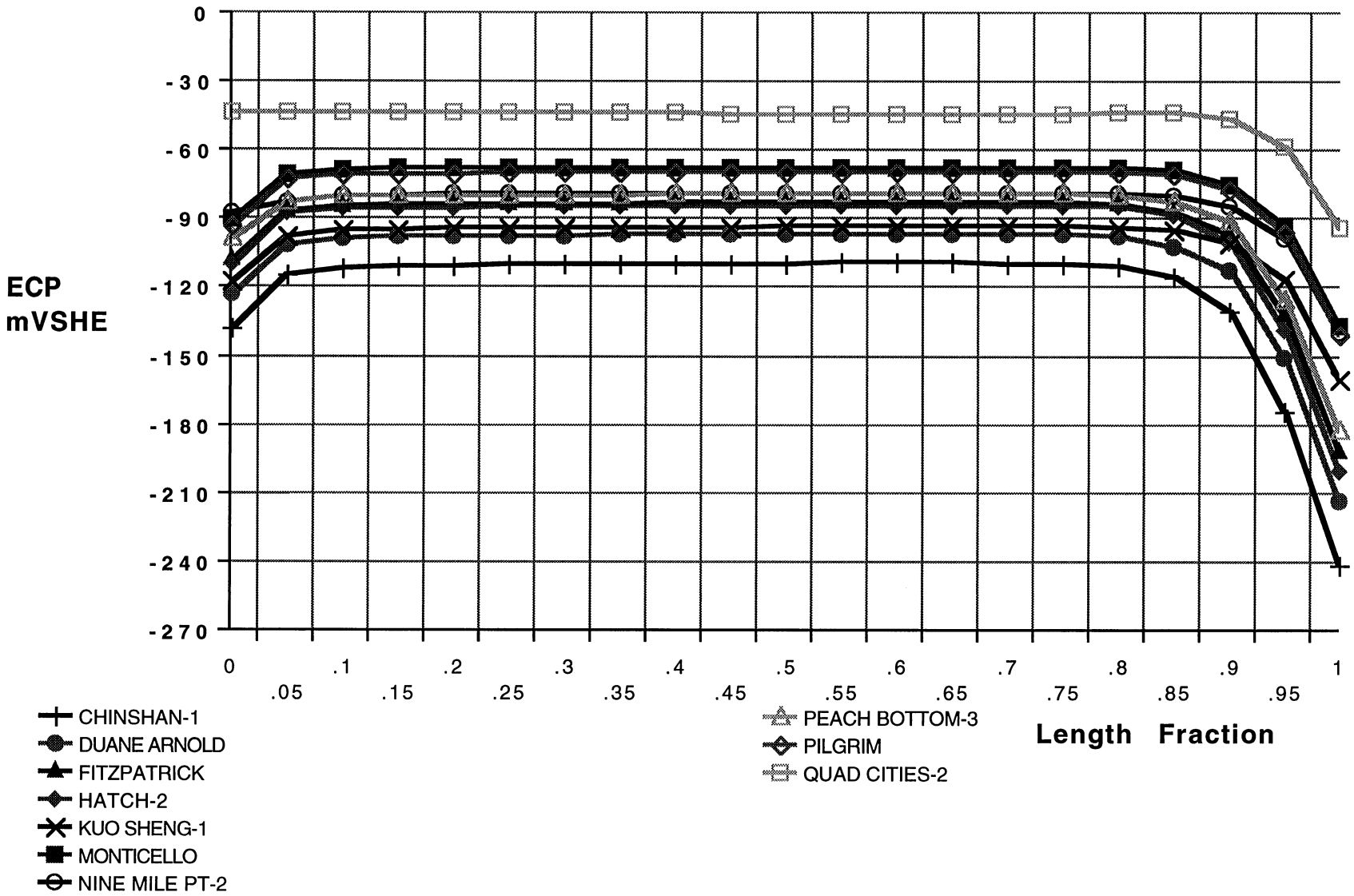

EPRI Licensed Material

Figure A-29: Core Bypass Region ECPs with 1.5 ppm Feedwater H2 Addition

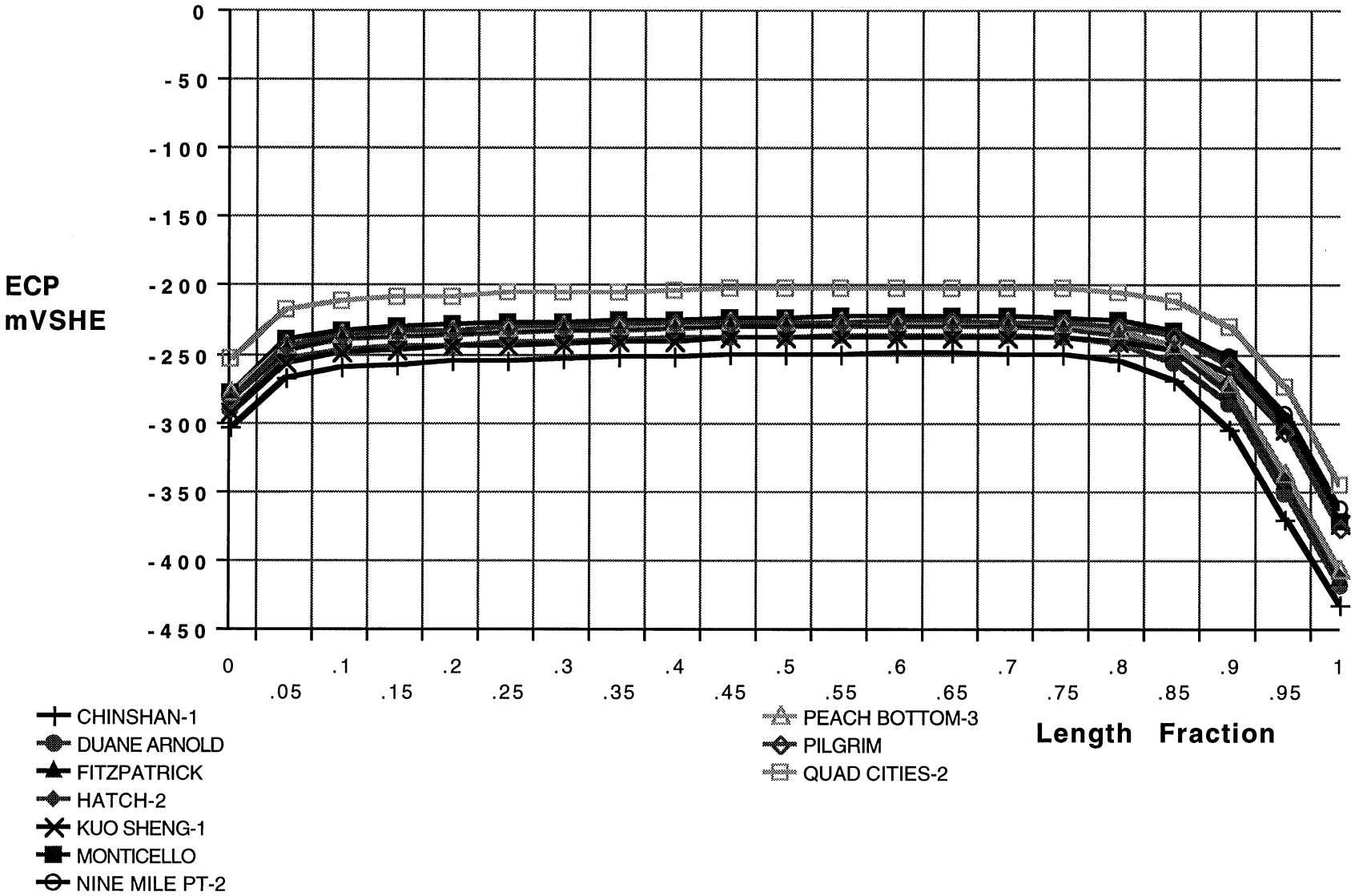

EPRI Licensed Material

Figure A-30: Core Bypass Region ECPs with 3.0 ppm Feedwater H2 Addition

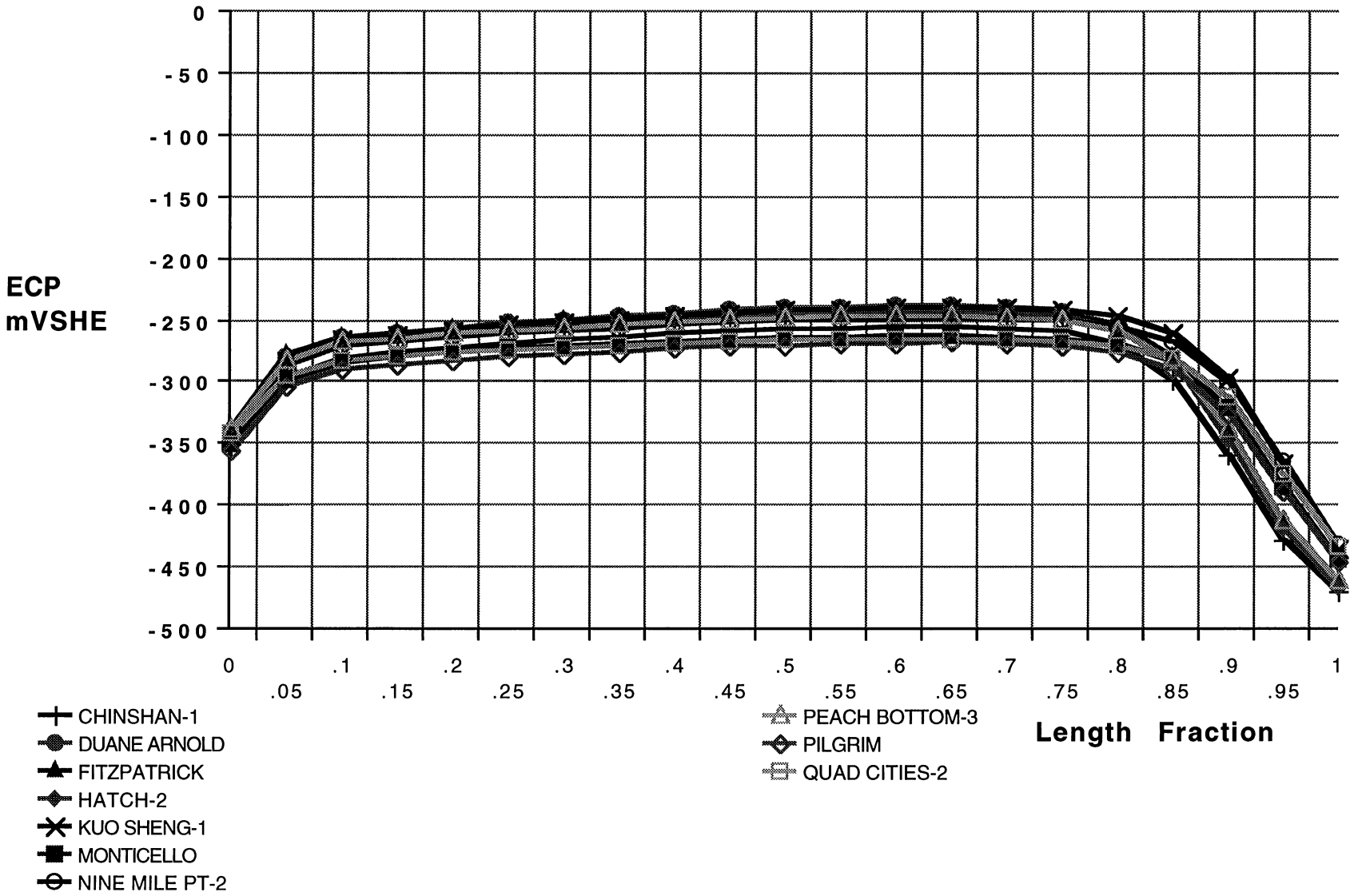

EPRI Licensed Material

Figure A-31: Core Bypass Hydrogen Levels with 0 ppm Feedwater H2 Addition

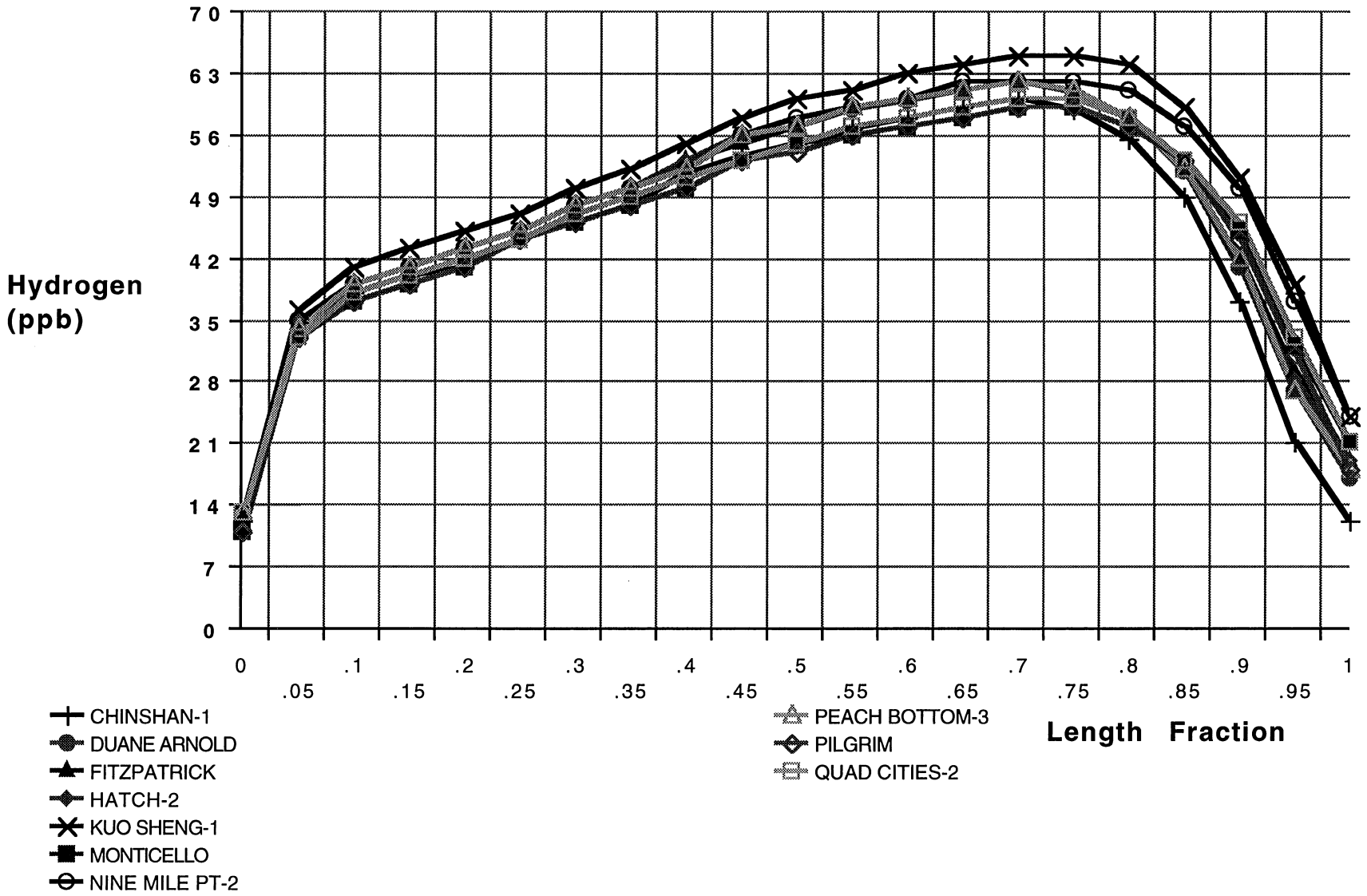

EPRI Licensed Material

Figure A-32: Core Bypass Hydrogen Levels with 0.6 ppm Feedwater H2 Addition

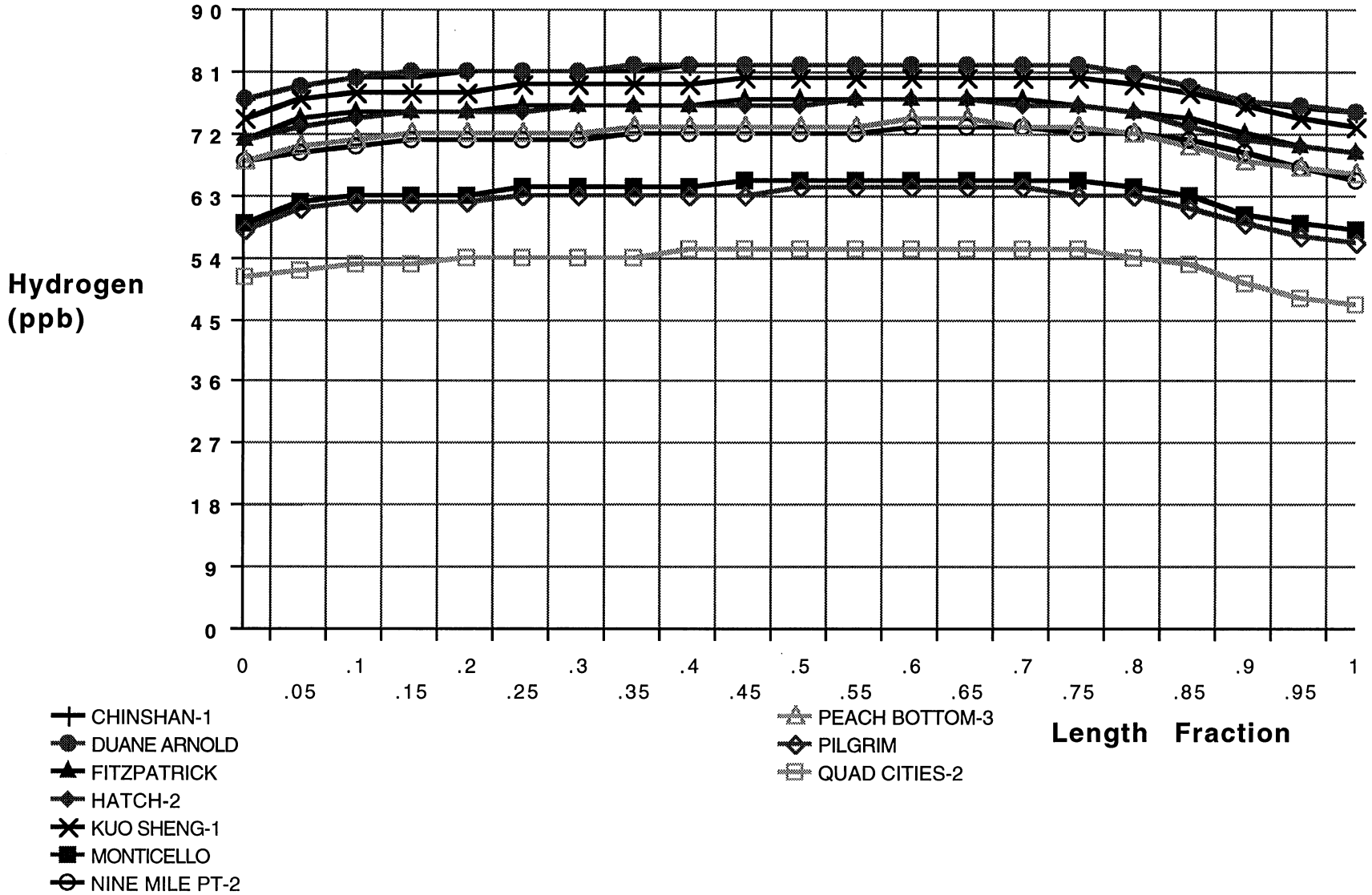

EPRI Licensed Material

Figure A-33: Core Bypass Hydrogen Levels with 1.5 ppm Feedwater H2 Addition

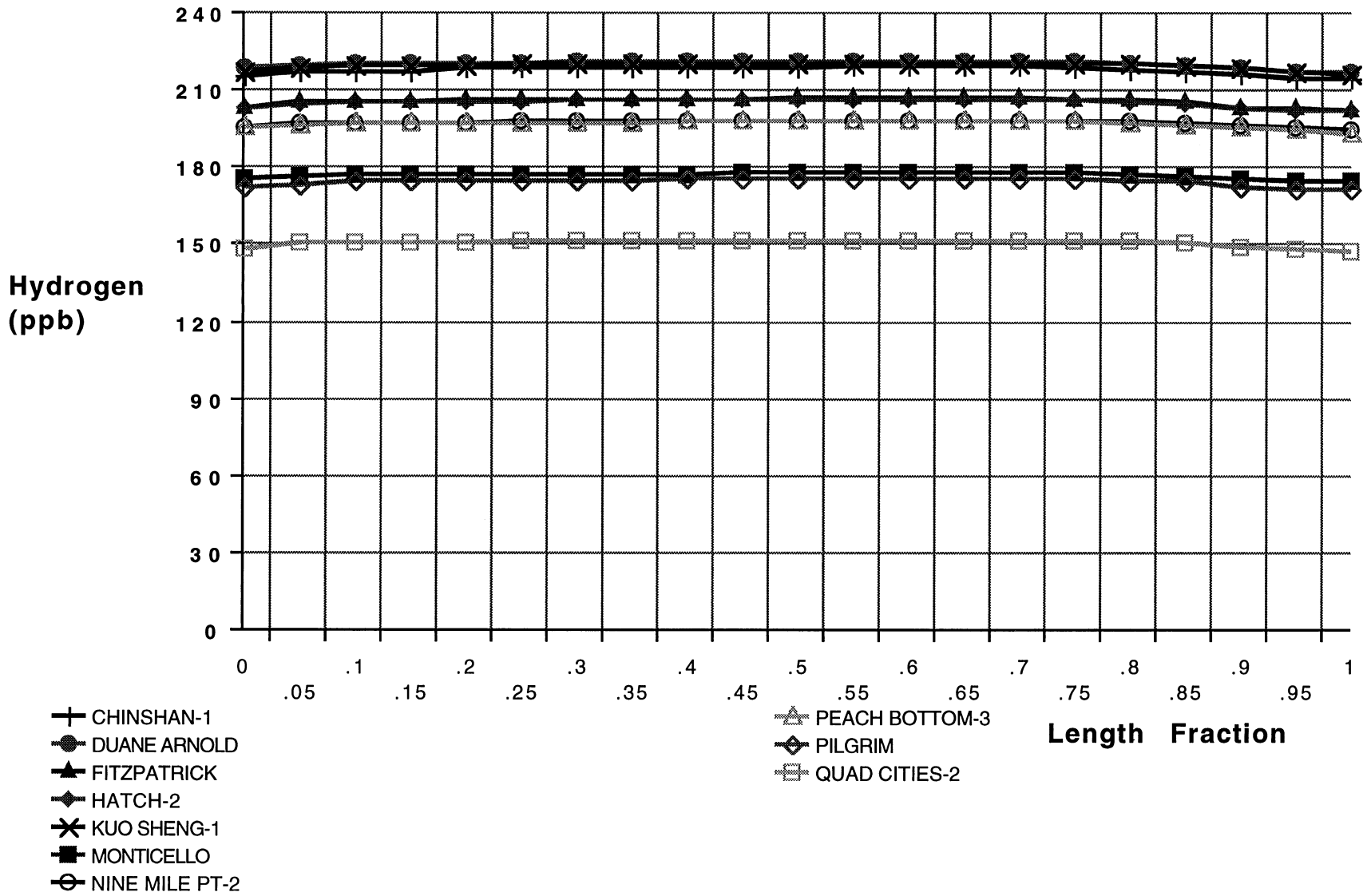

EPRI Licensed Material

Figure A-34: Core Bypass Hydrogen Levels with 3.0 ppm Feedwater H2 Addition

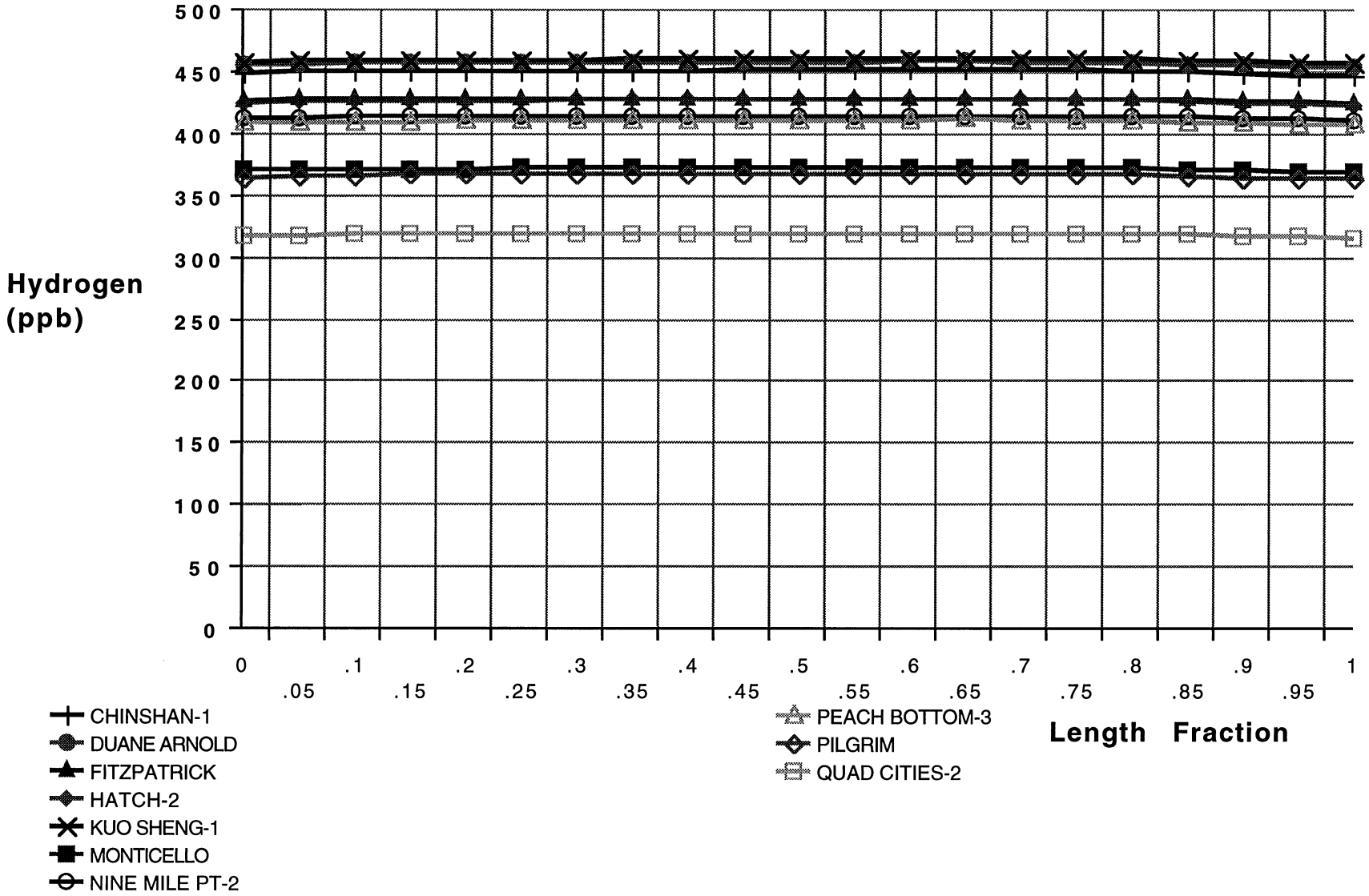

EPRI Licensed Material

Figure A-35: Core Bypass Oxygen Levels with 0 ppm Feedwater H2 Addition

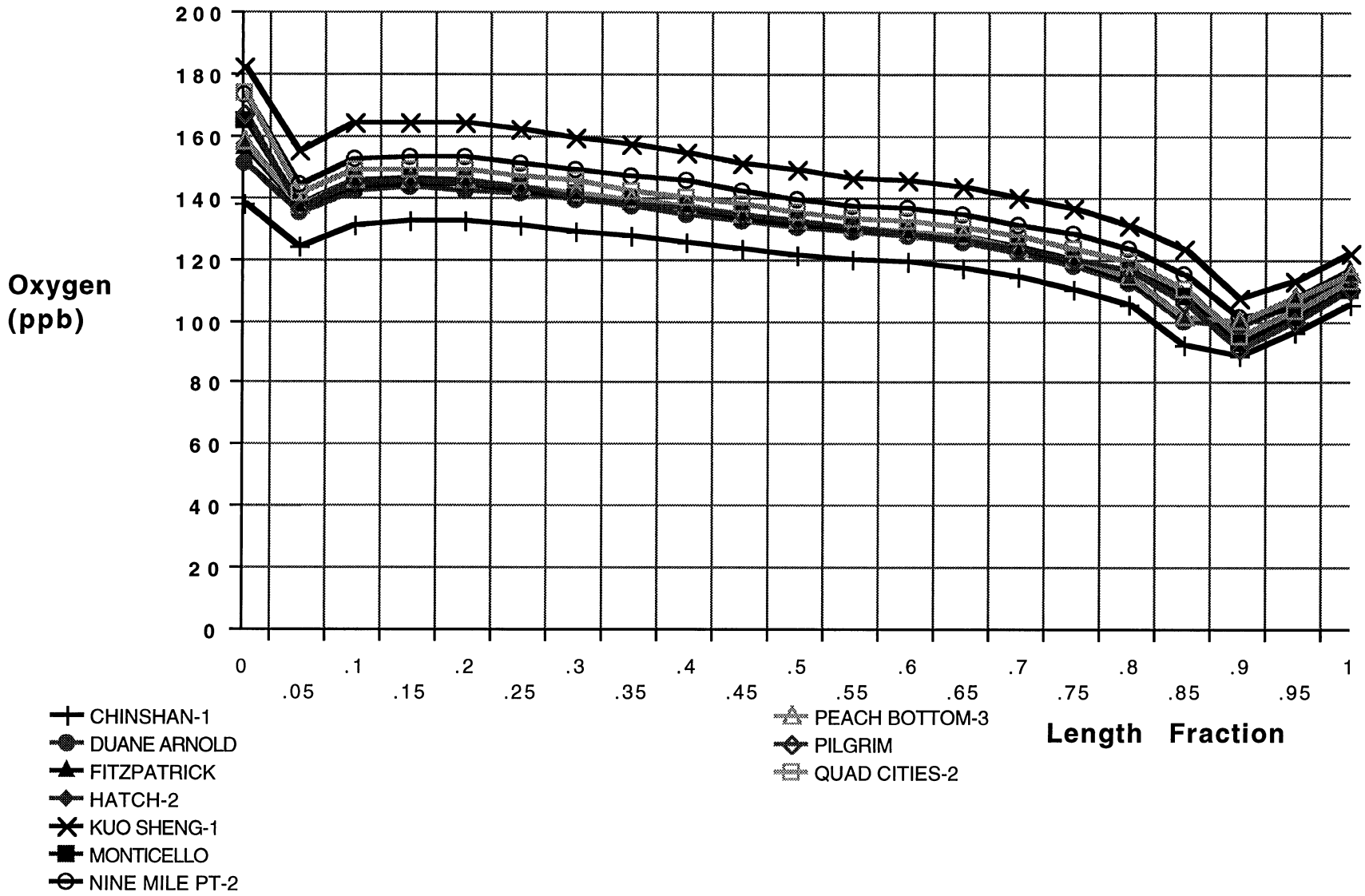

EPRI Licensed Material

Figure A-36: Core Bypass Oxygen Levels with 0.6 ppm Feedwater H2 Addition

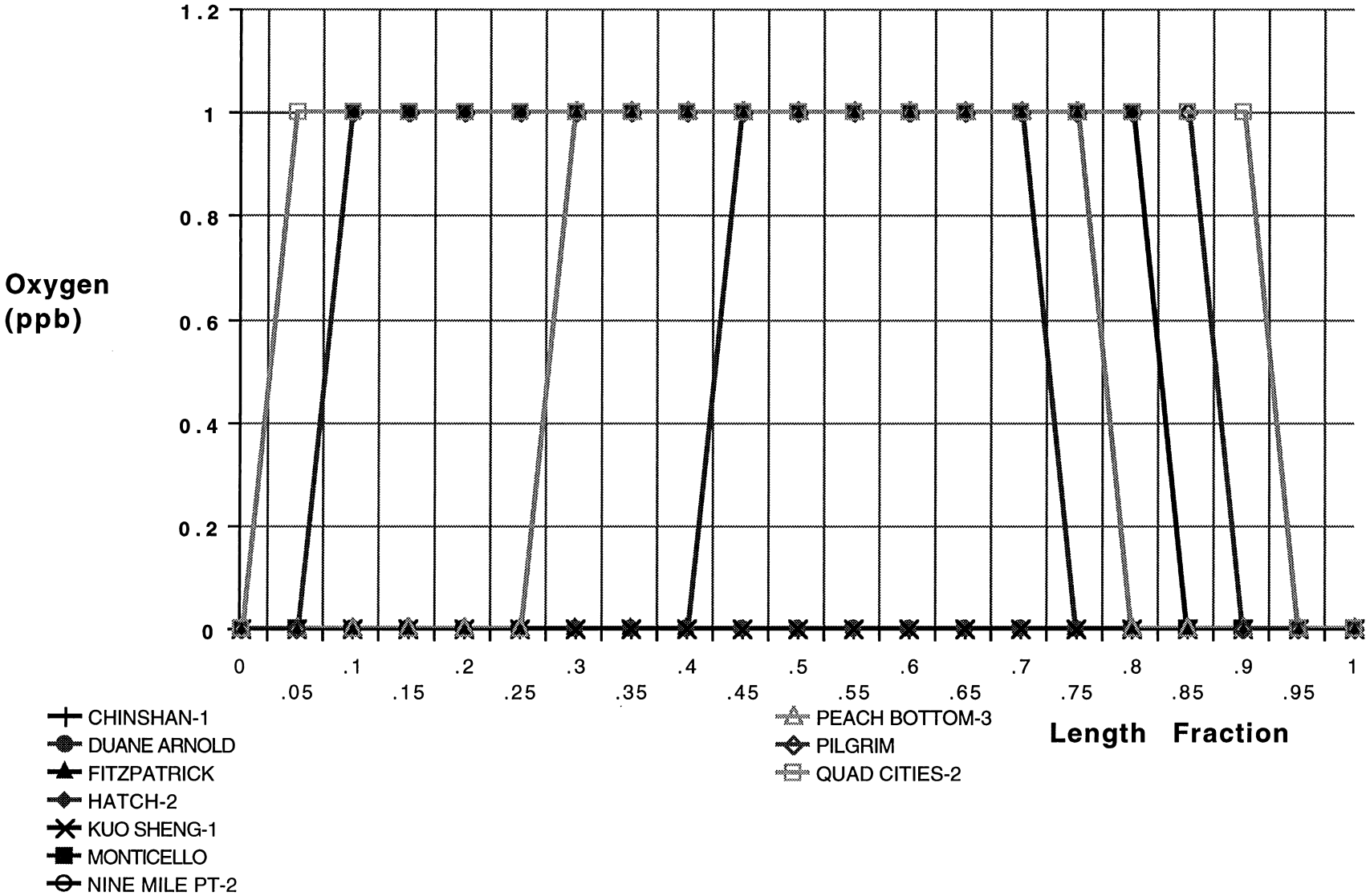

EPRI Licensed Material

Figure A-37: Core Bypass Peroxide Levels with 0 ppm Feedwater H2 Addition

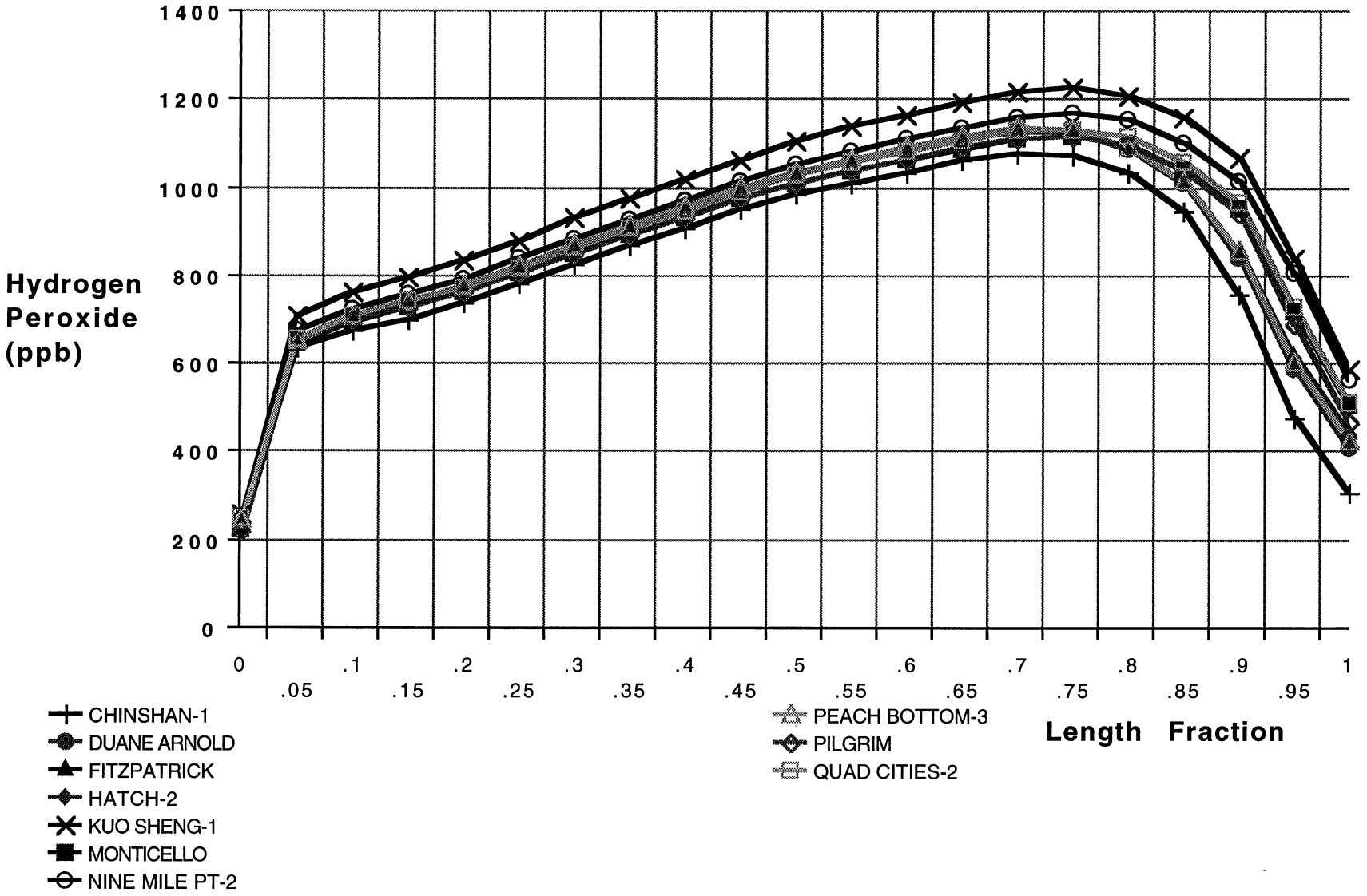

EPRI Licensed Material

Figure A-38: Core Bypass Peroxide Levels with 0.6 ppm Feedwater H2 Addition

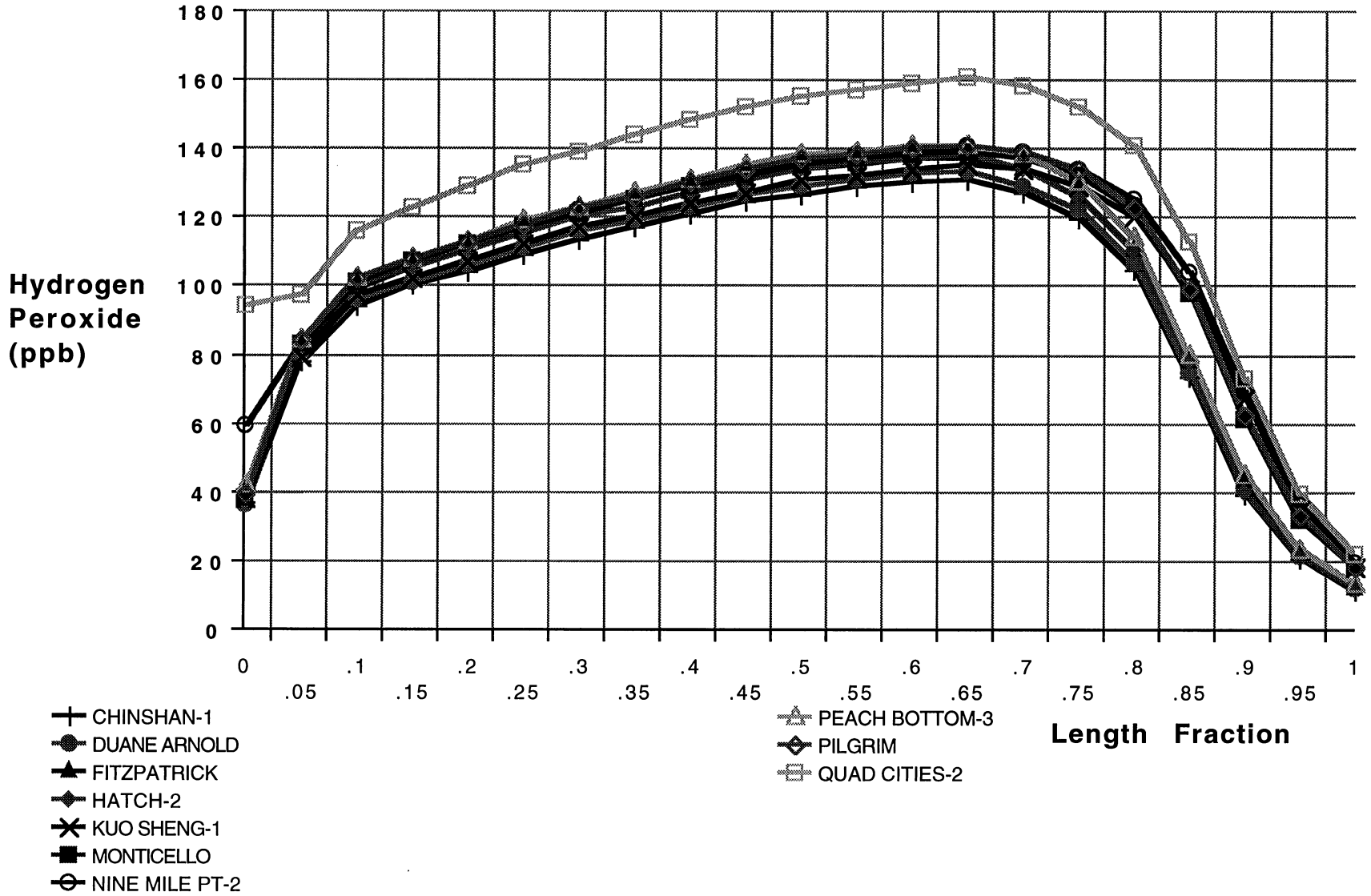

EPRI Licensed Material

Figure A-39: Core Bypass Peroxide Levels with 1.5 ppm Feedwater H2 Addition

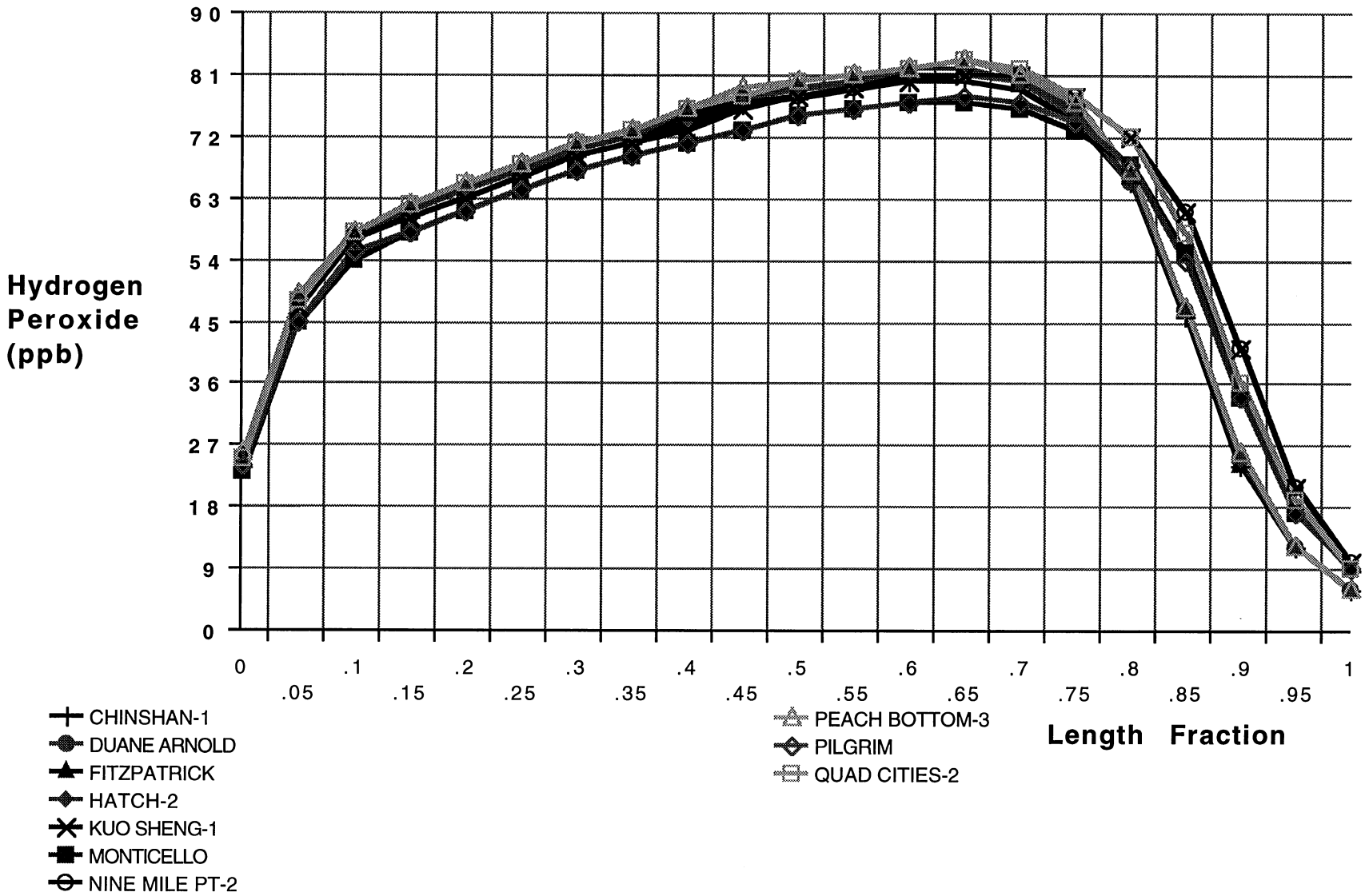

EPRI Licensed Material

Figure A-40: Core Bypass Peroxide Levels with 3.0 ppm Feedwater H2 Addition

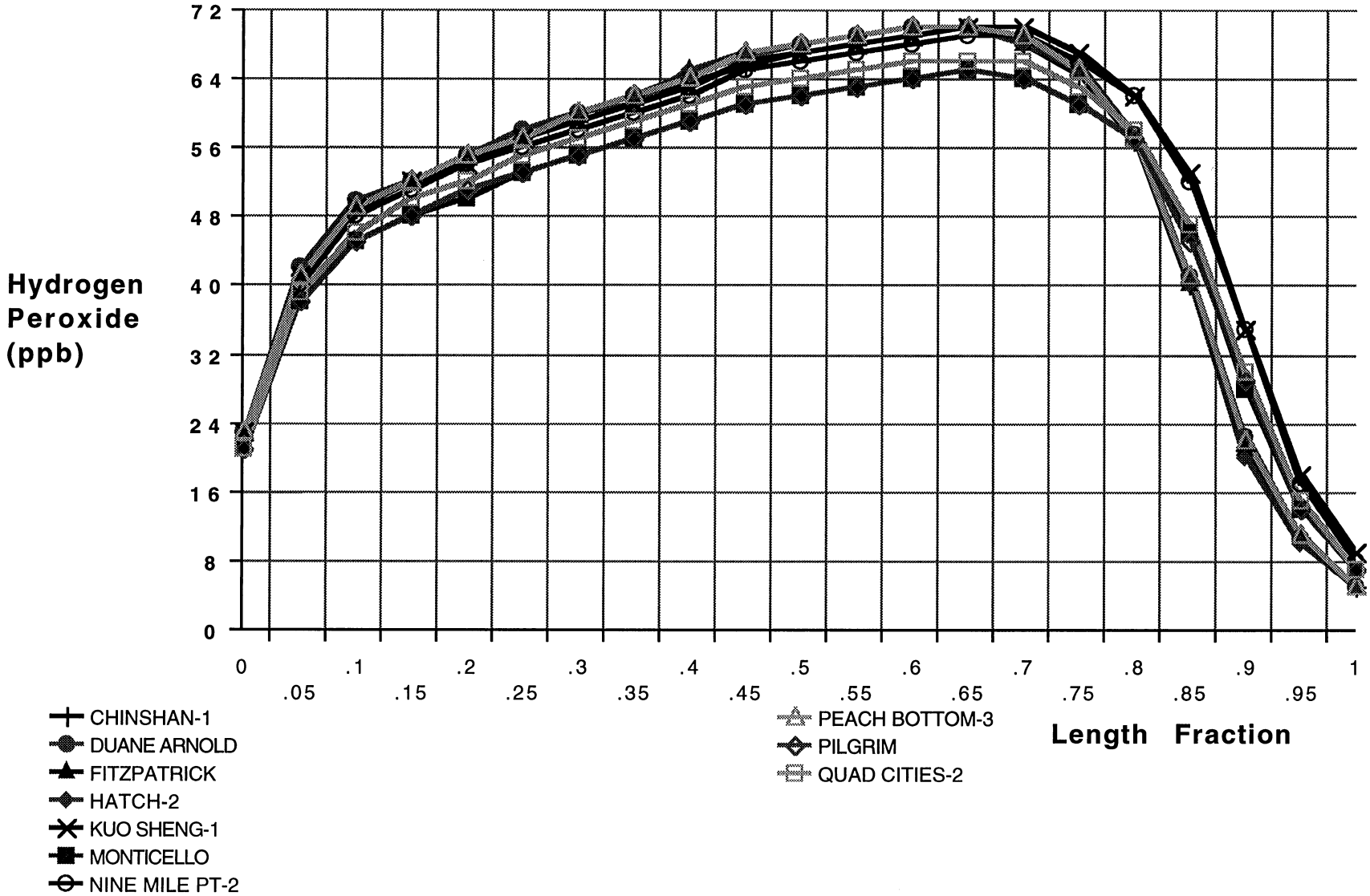

EPRI Licensed Material

Figure A-41: Outer Bypass Region ECPs with 0 ppm Feedwater H2 Addition

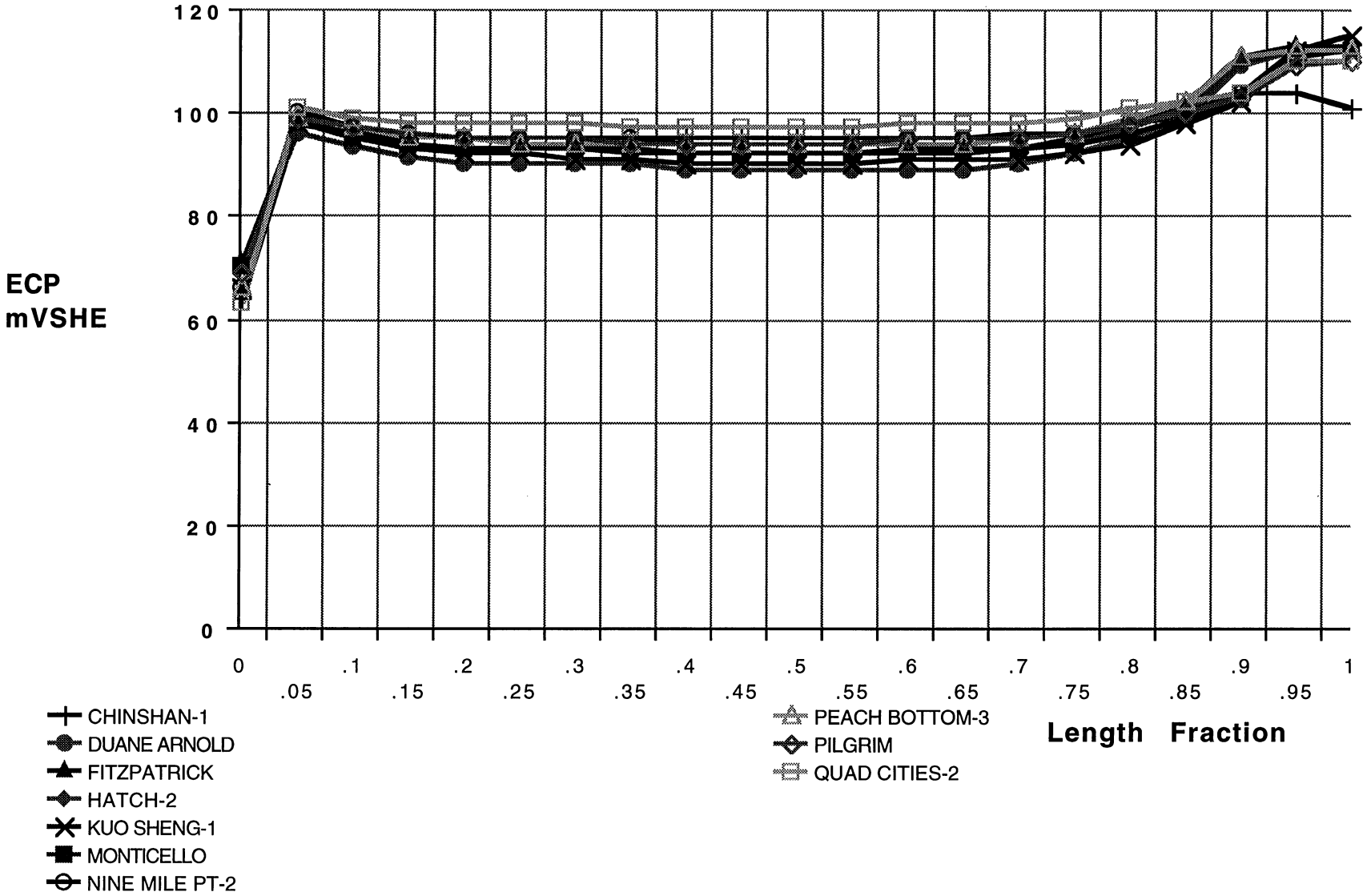

EPRI Licensed Material

Figure A-42: Outer Bypass Region ECPs with 0.6 ppm Feedwater H2 Addition

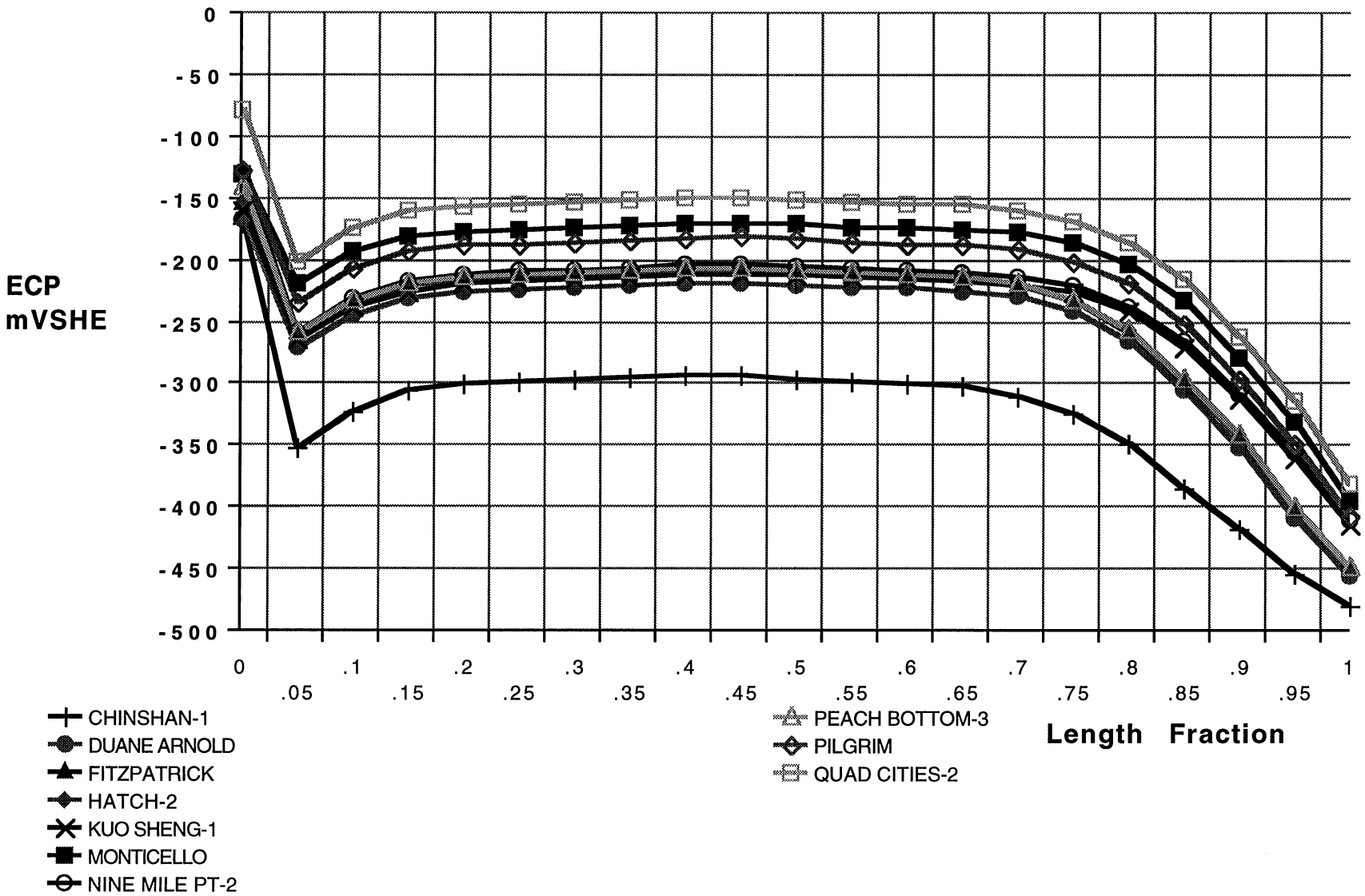

EPRI Licensed Material

Figure A-43: Outer Bypass Region ECPs with 1.5 ppm Feedwater H2 Addition

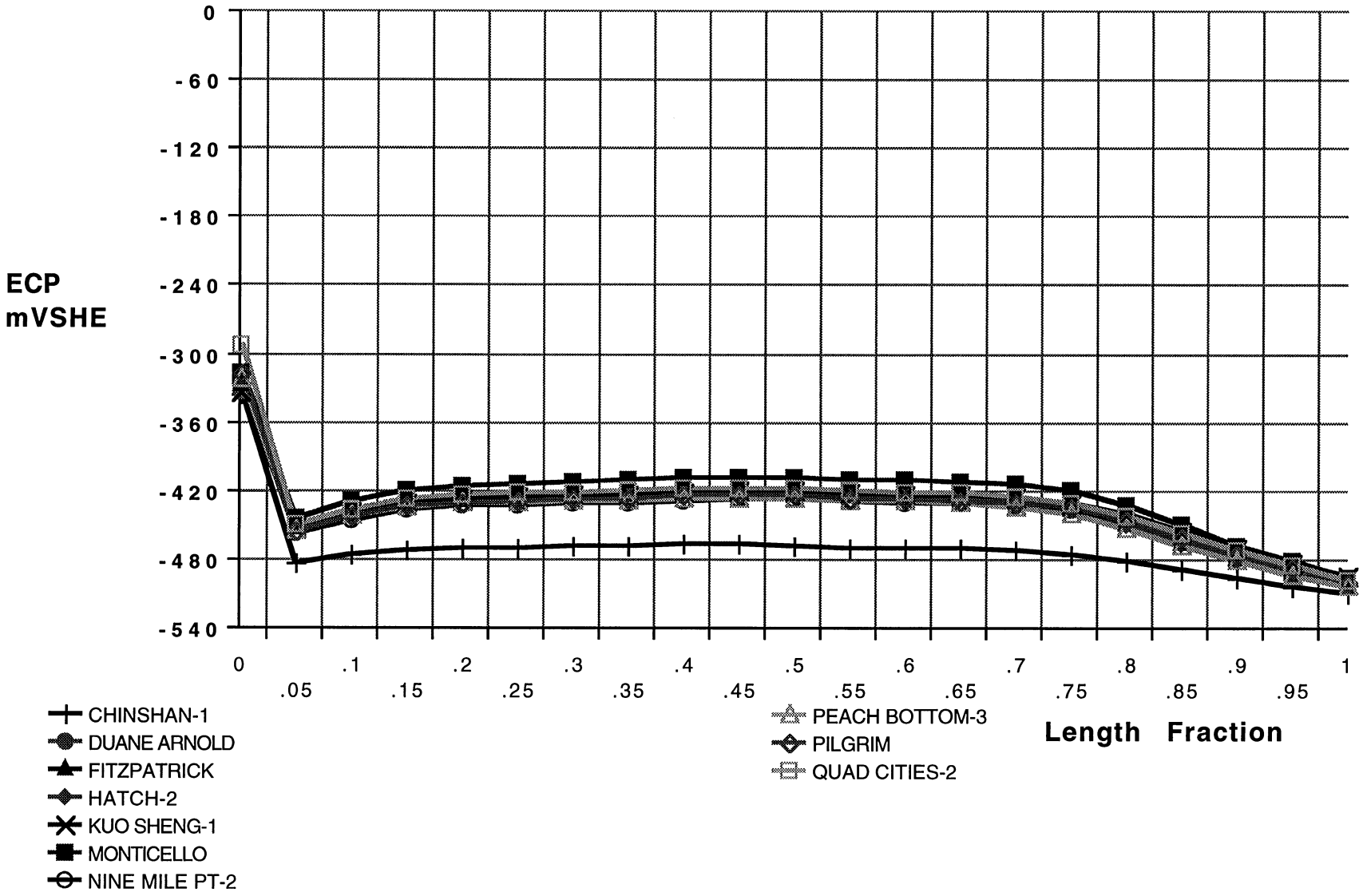

EPRI Licensed Material

Figure A-44: Outer Bypass Region ECPs with 3.0 ppm Feedwater H2 Addition

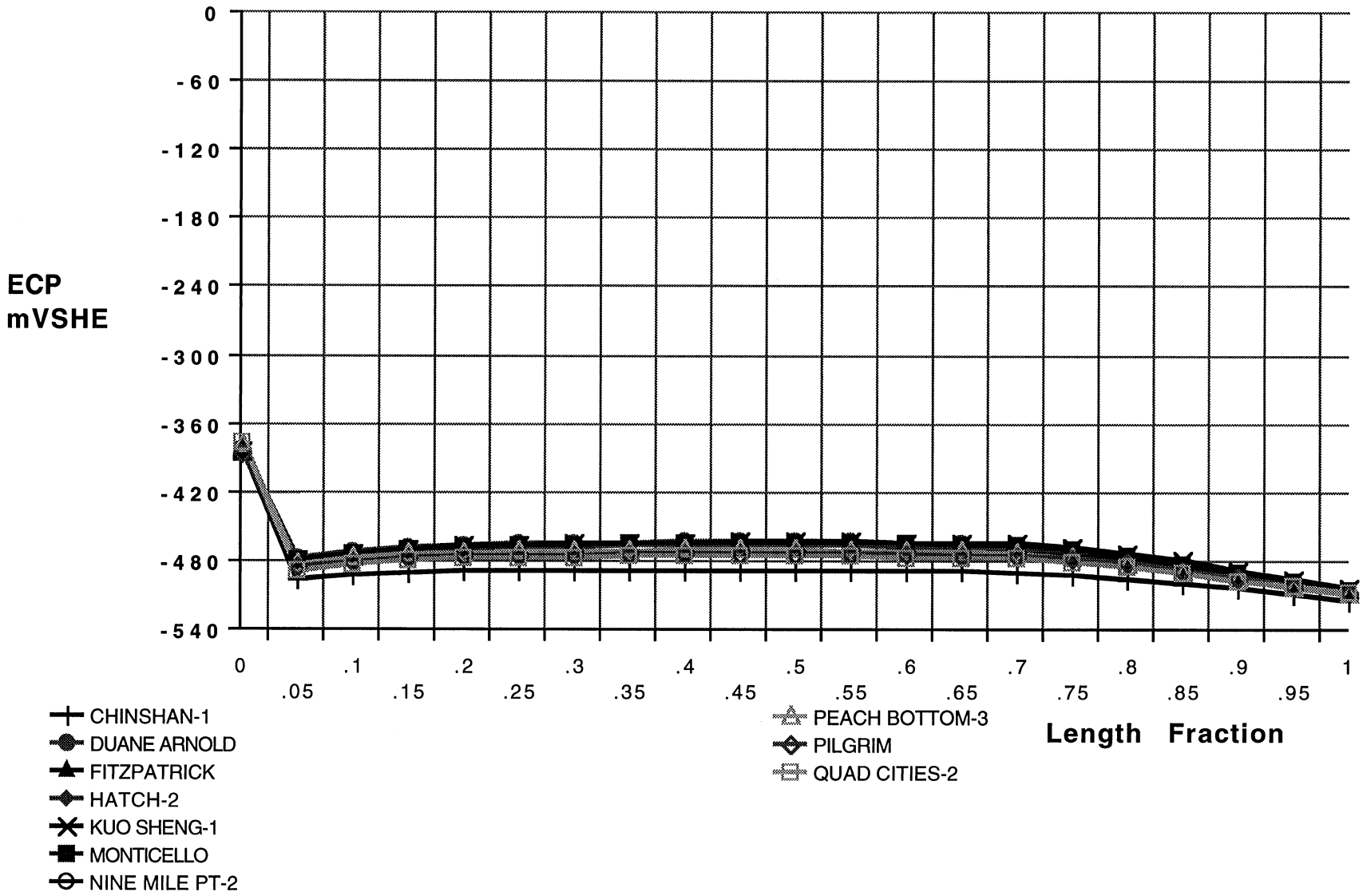

EPRI Licensed Material

Figure A-45: Outer Bypass Hydrogen Levels with 0 ppm Feedwater H2 Addition

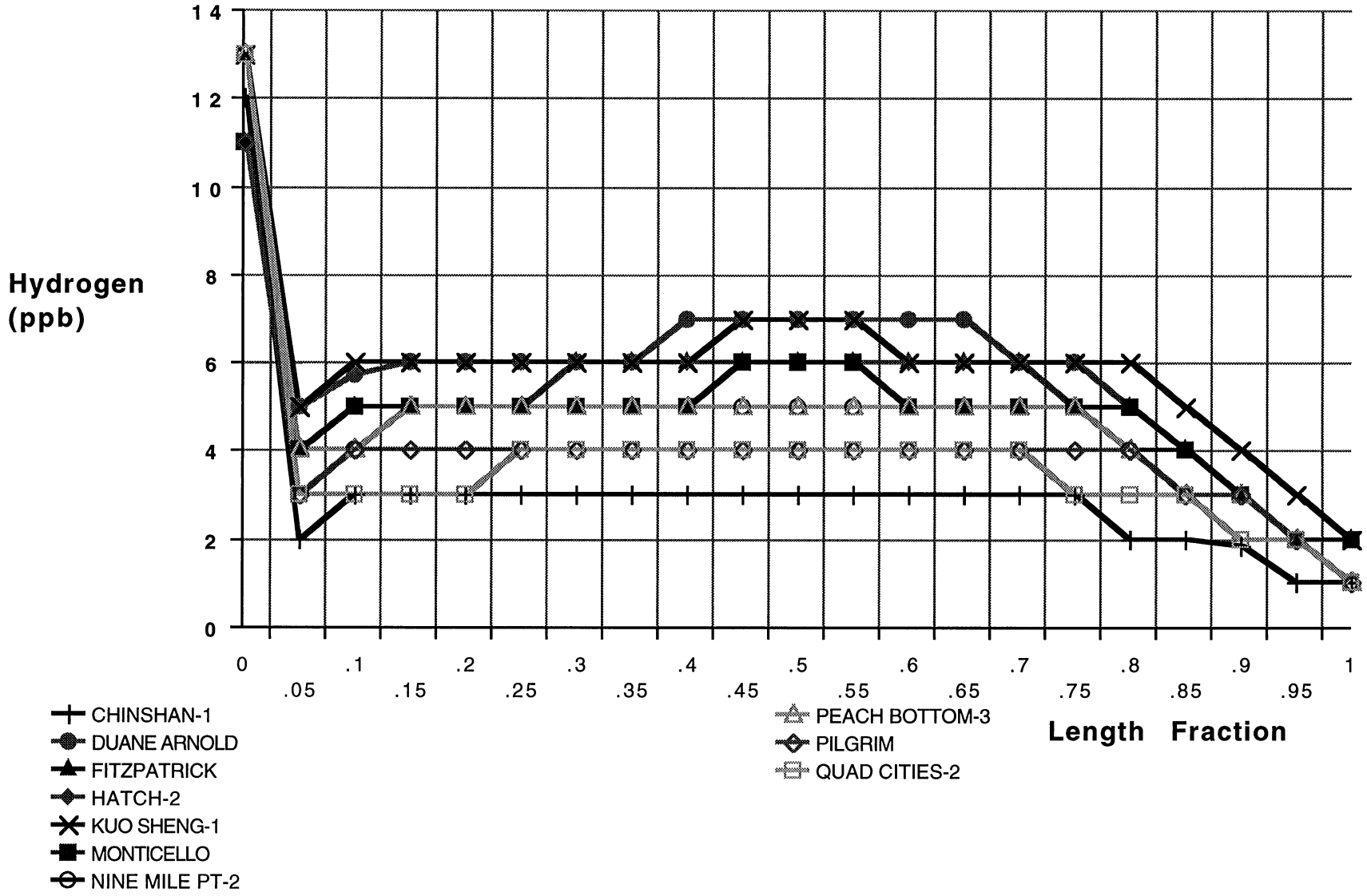

EPRI Licensed Material

Figure A-46: Outer Bypass Hydrogen Levels with 0.6 ppm Feedwater H2 Addition

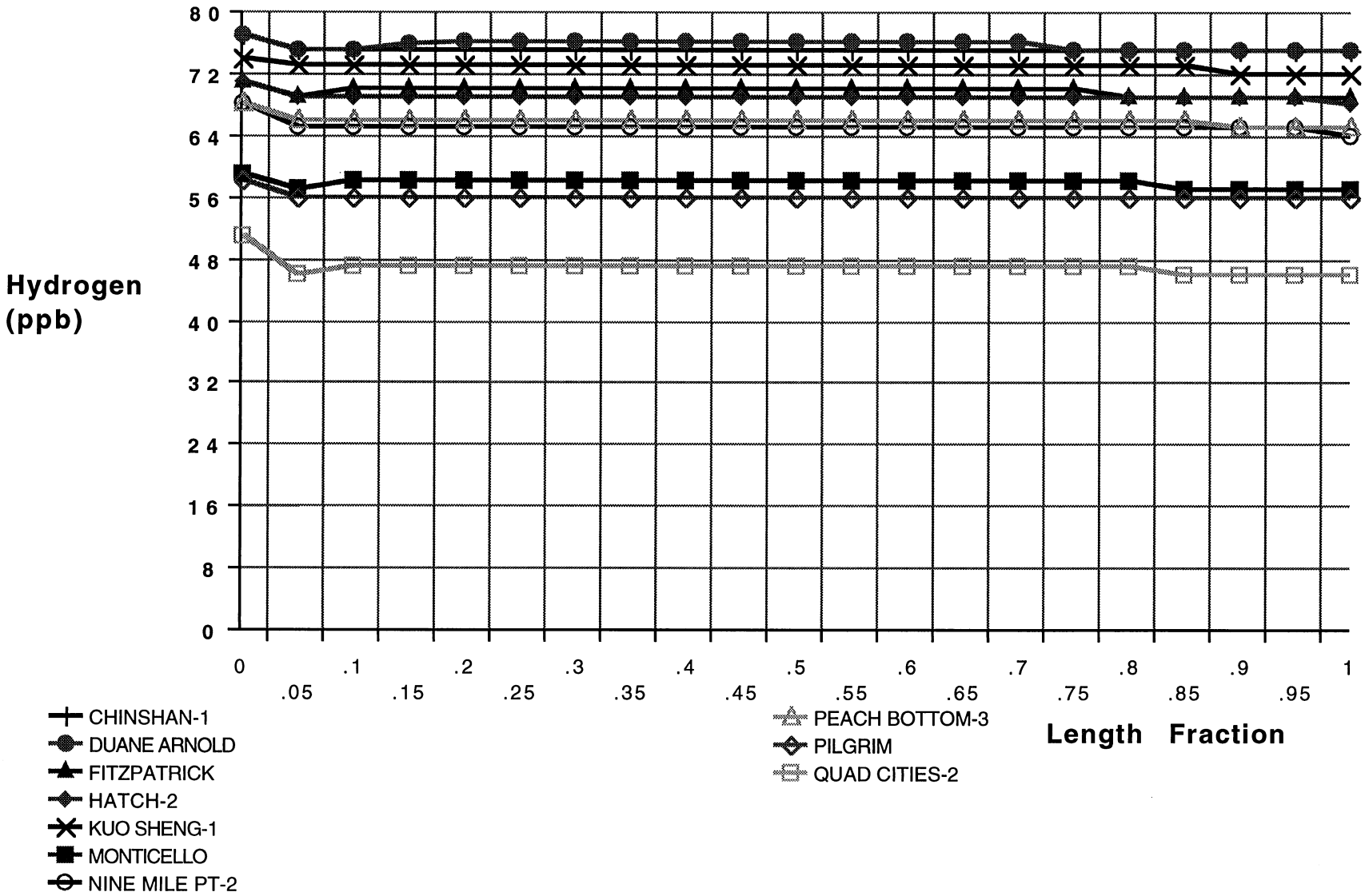

EPRI Licensed Material

Figure A-47: Outer Bypass Hydrogen Levels with 1.5 ppm Feedwater H2 Addition

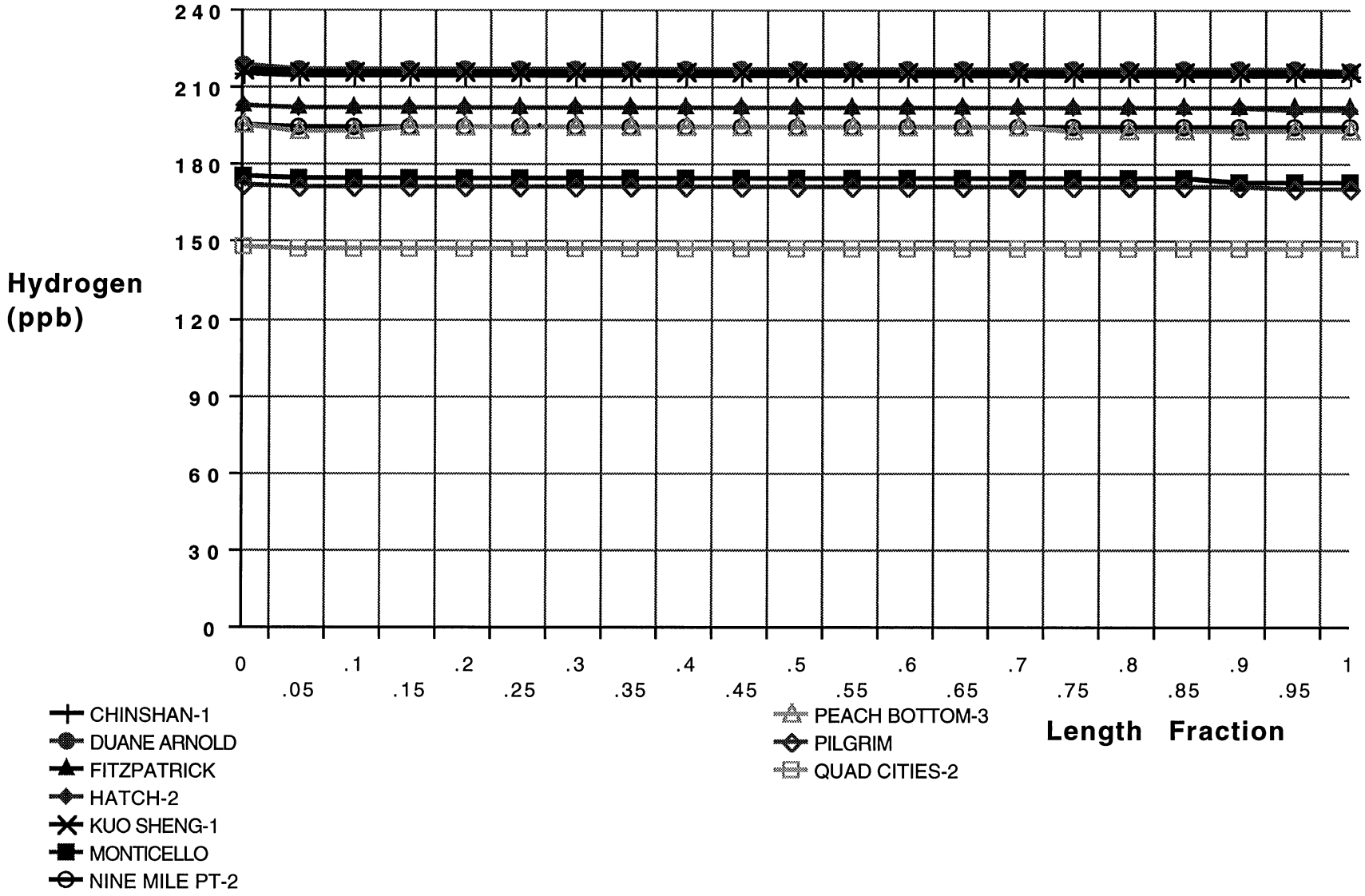

EPRI Licensed Material

Figure A-48: Outer Bypass Hydrogen Levels with 3.0 ppm Feedwater H2 Addition

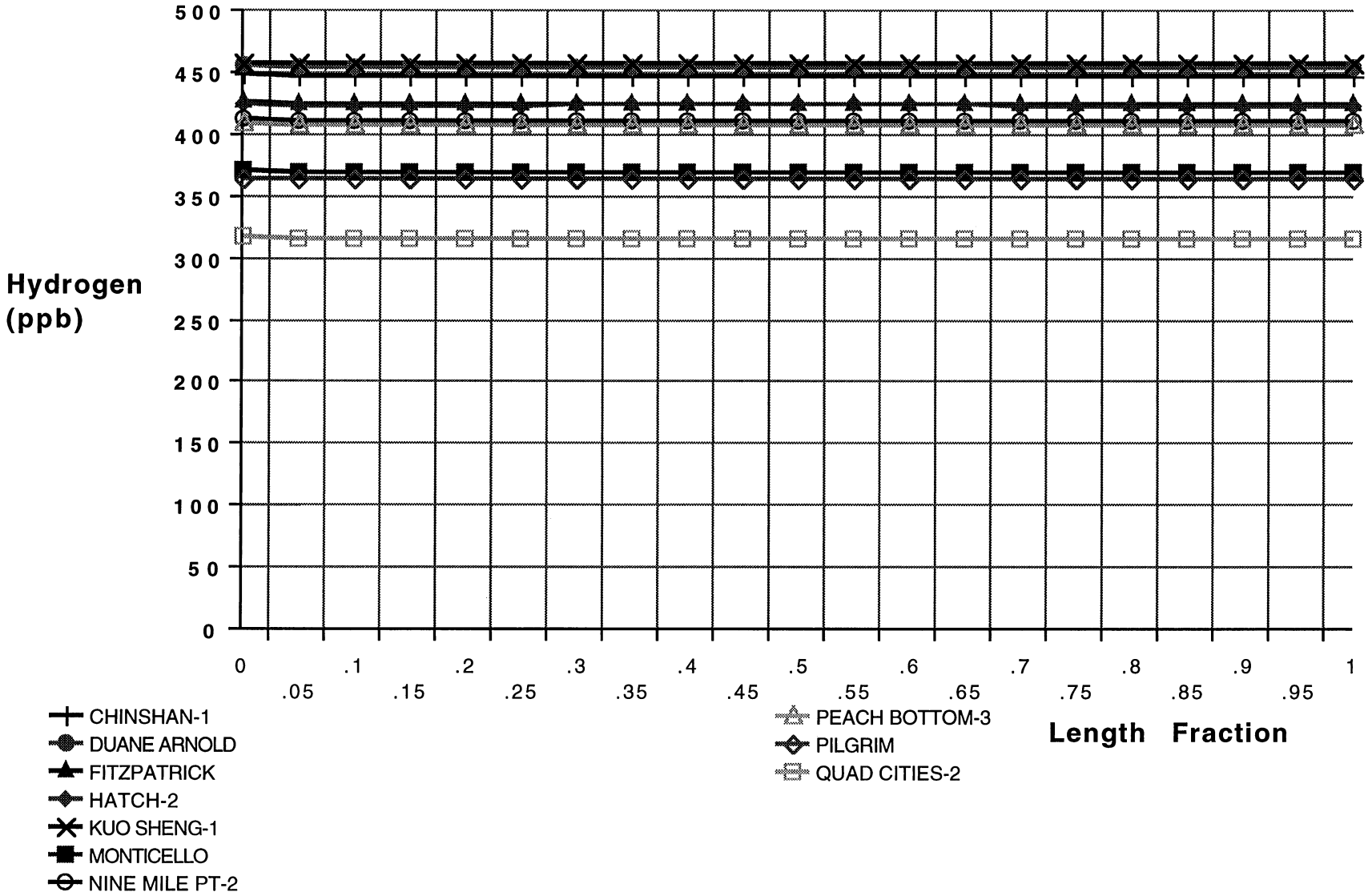

EPRI Licensed Material

Figure A-49: Outer Bypass Oxygen Levels with 0 ppm Feedwater H2 Addition

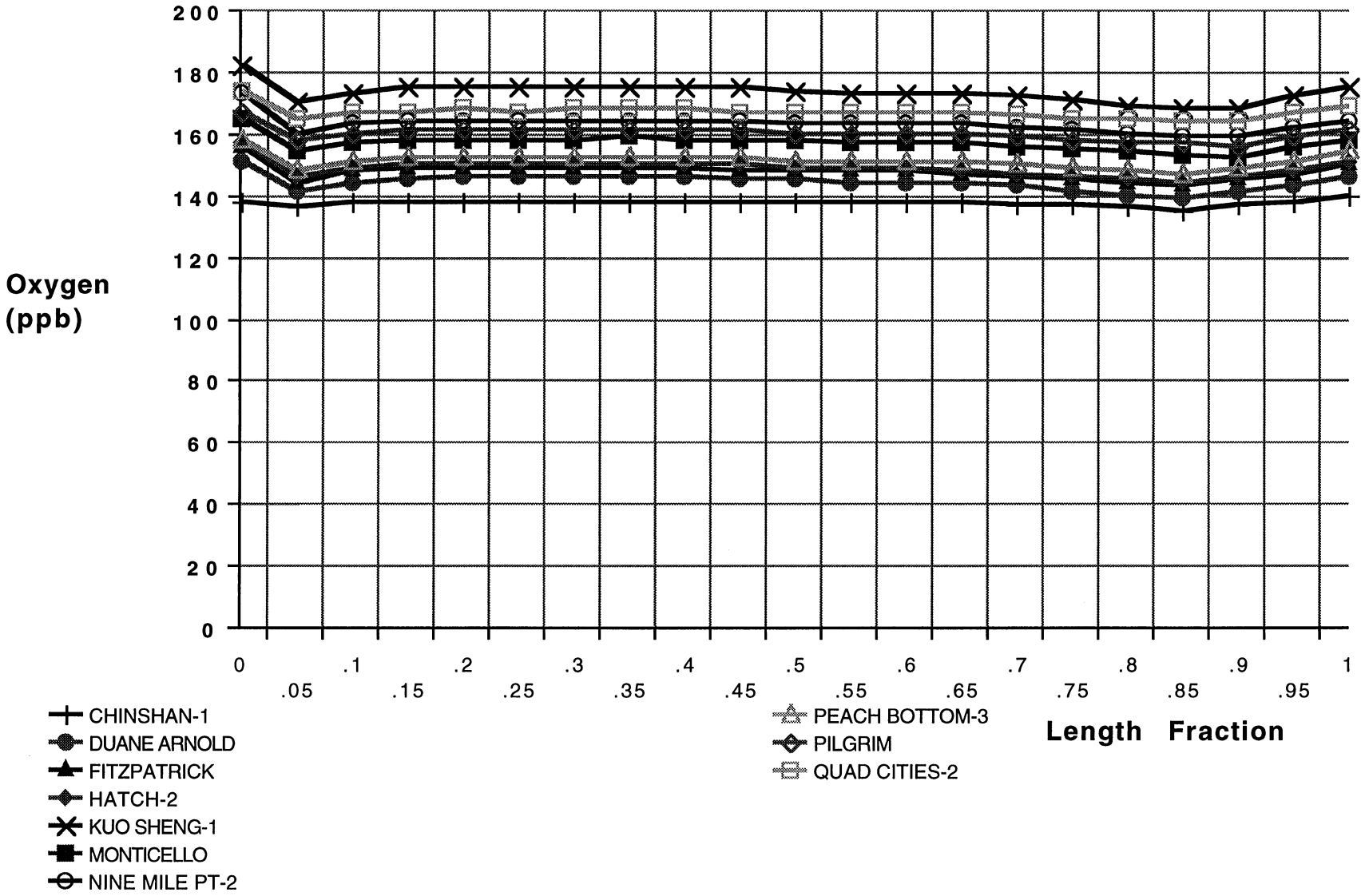

EPRI Licensed Material

Figure A-50: Outer Bypass Oxygen Levels with 0.4 ppm Feedwater H2 Addition

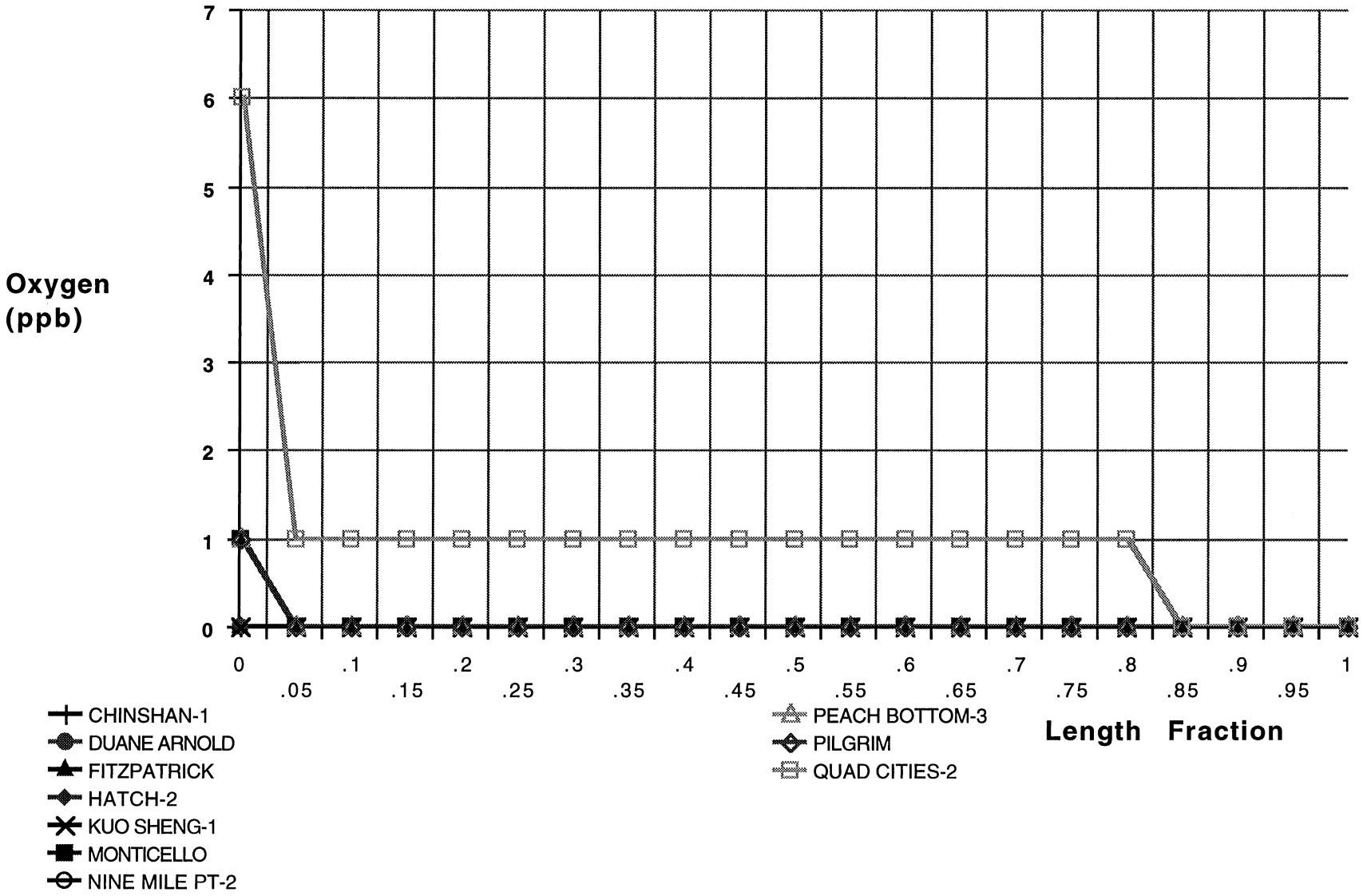

EPRI Licensed Material

Figure A-51: Outer Bypass Peroxide Levels with 0 ppm Feedwater H2 Addition

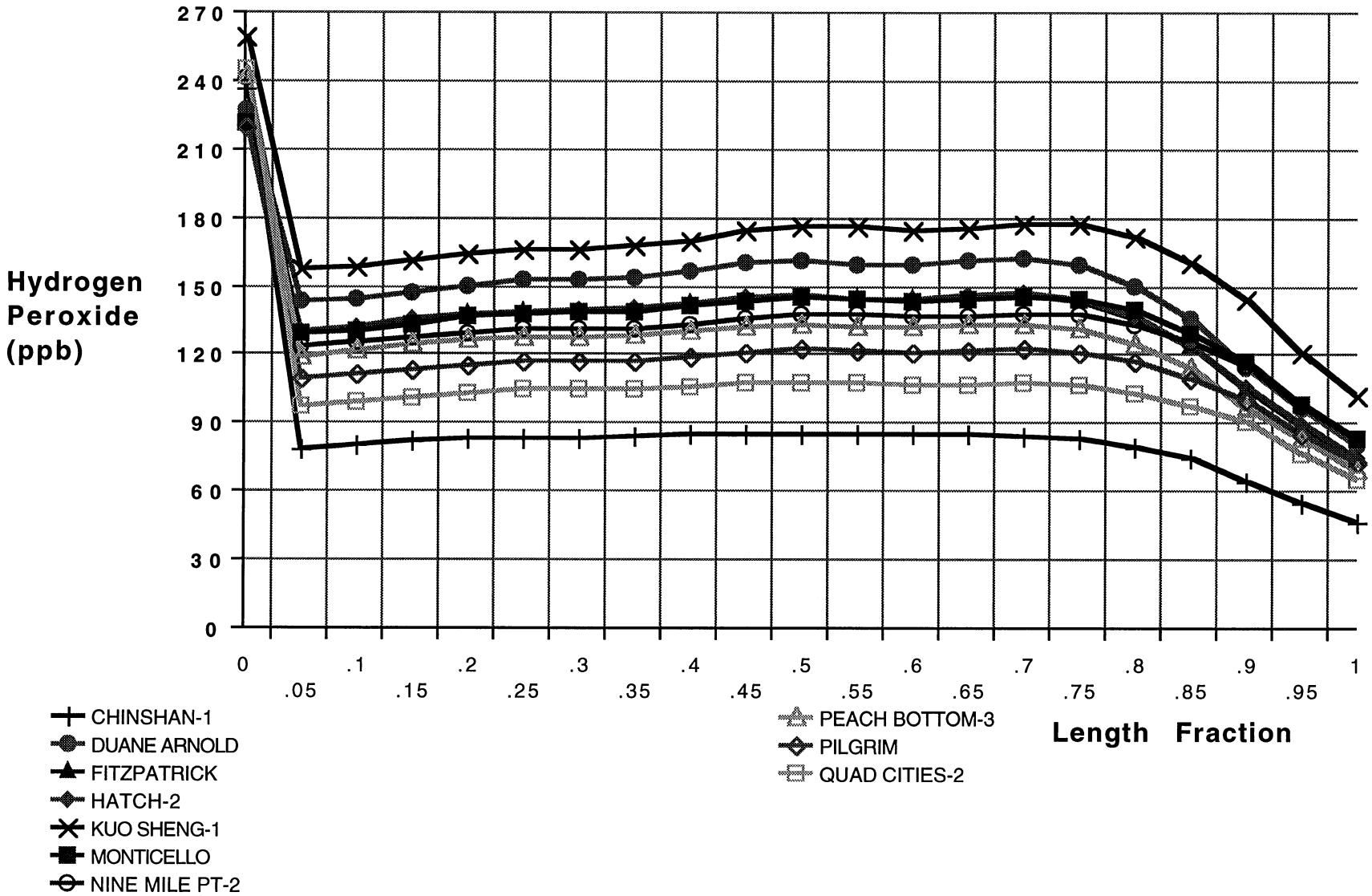

EPRI Licensed Material

Figure A-52: Outer Bypass Peroxide Levels with 0.6 ppm Feedwater H2 Addition

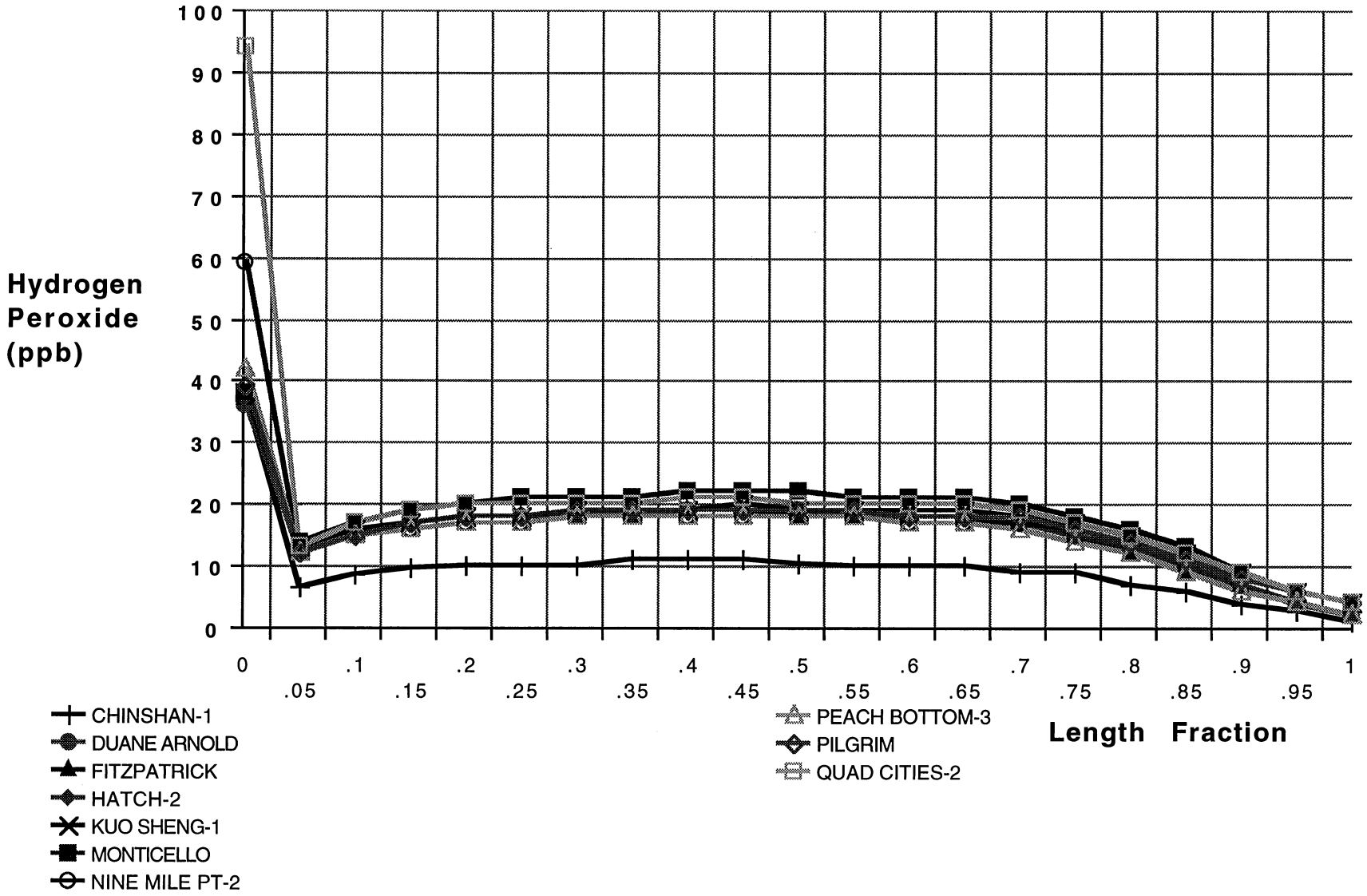

EPRI Licensed Material

Figure A-53: Outer Bypass Peroxide Levels with 1.5 ppm Feedwater H2 Addition

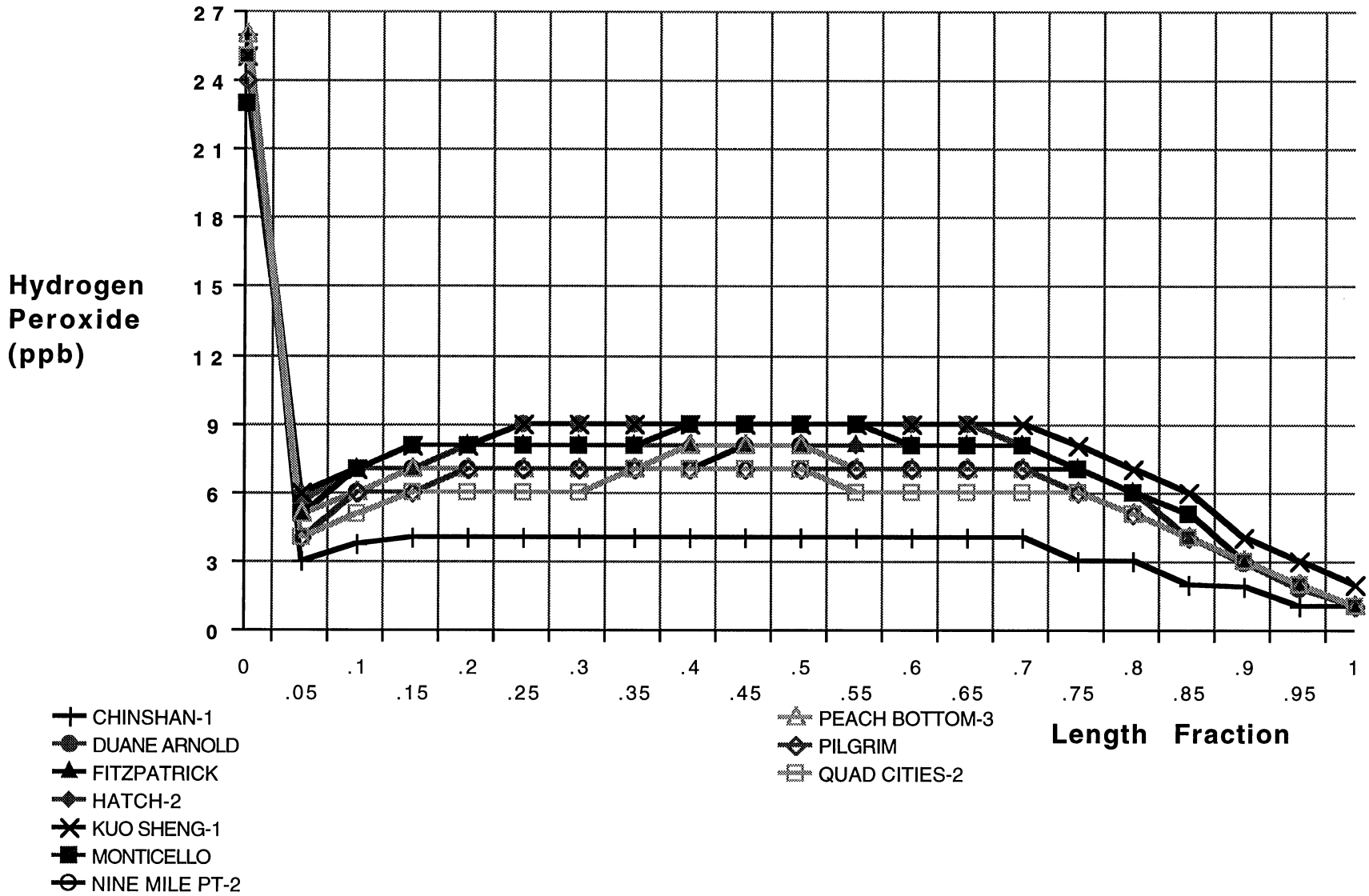

EPRI Licensed Material

Figure A-54: Outer Bypass Peroxide Levels with 3.0 ppm Feedwater H2 Addition

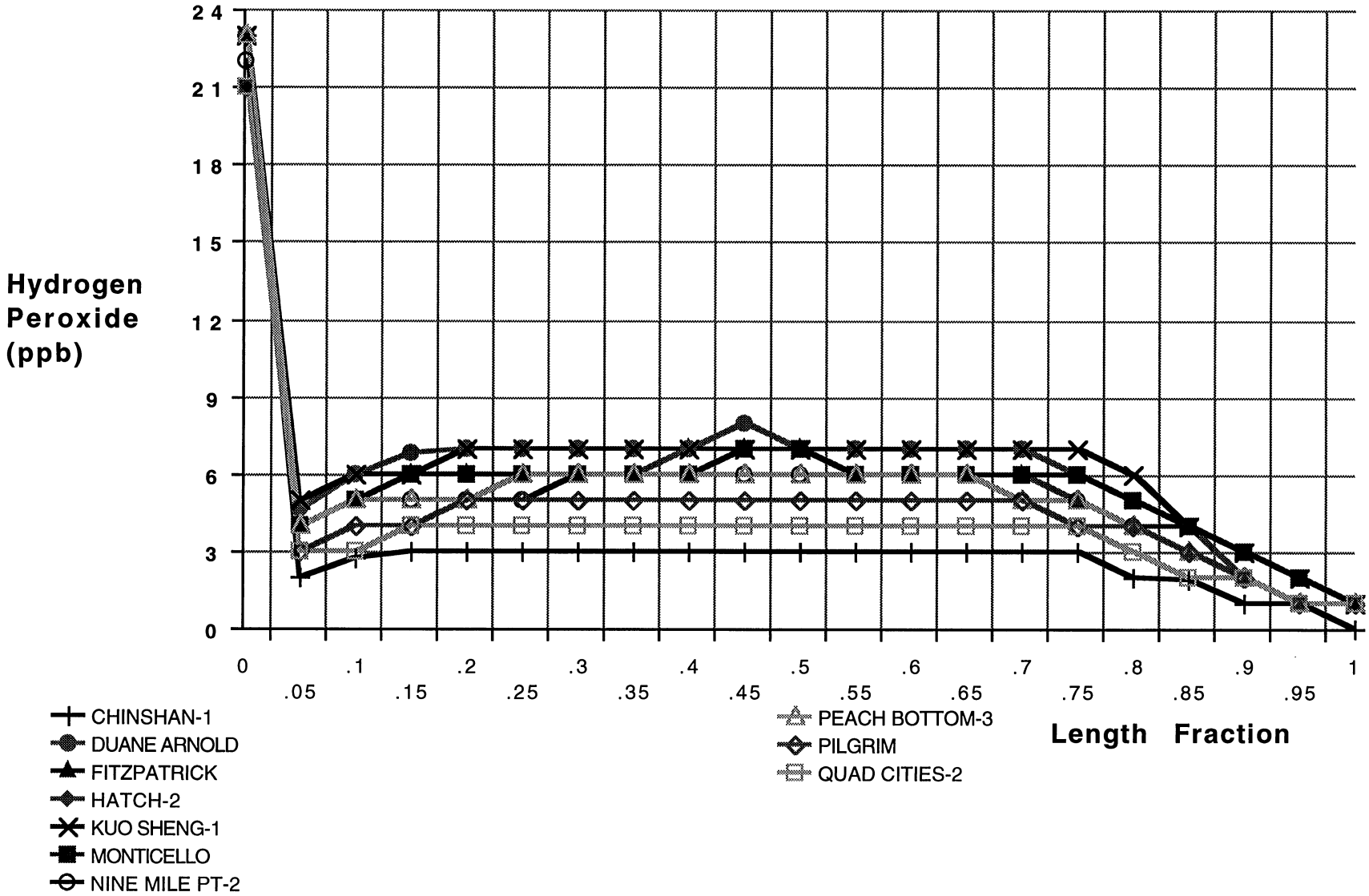

EPRI Licensed Material

Figure A-55: Upper Plenum Region ECPs with 0 ppm Feedwater H2 Addition

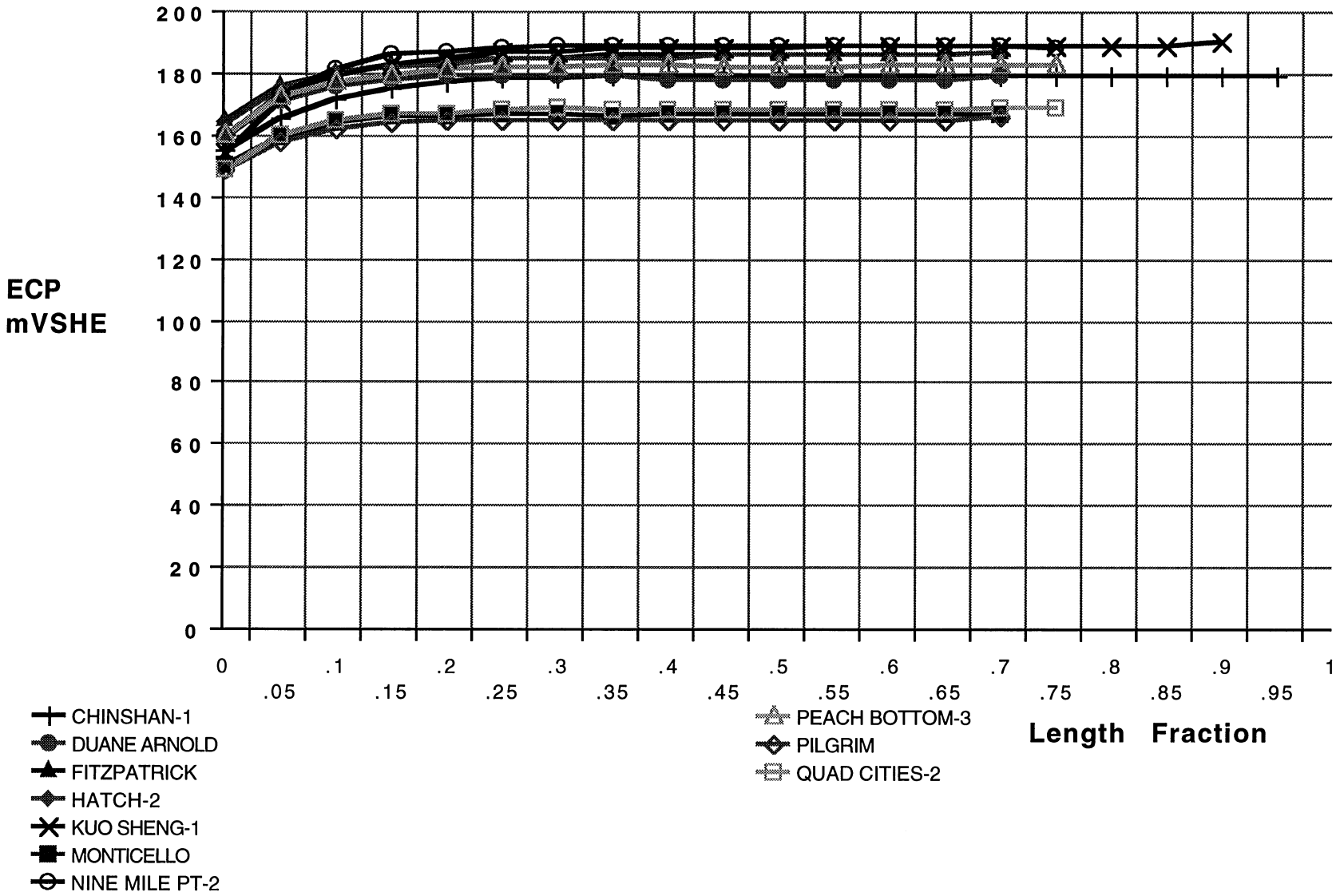

EPRI Licensed Material

Figure A-56: Upper Plenum Region ECPs with 0.6 ppm Feedwater H2 Addition

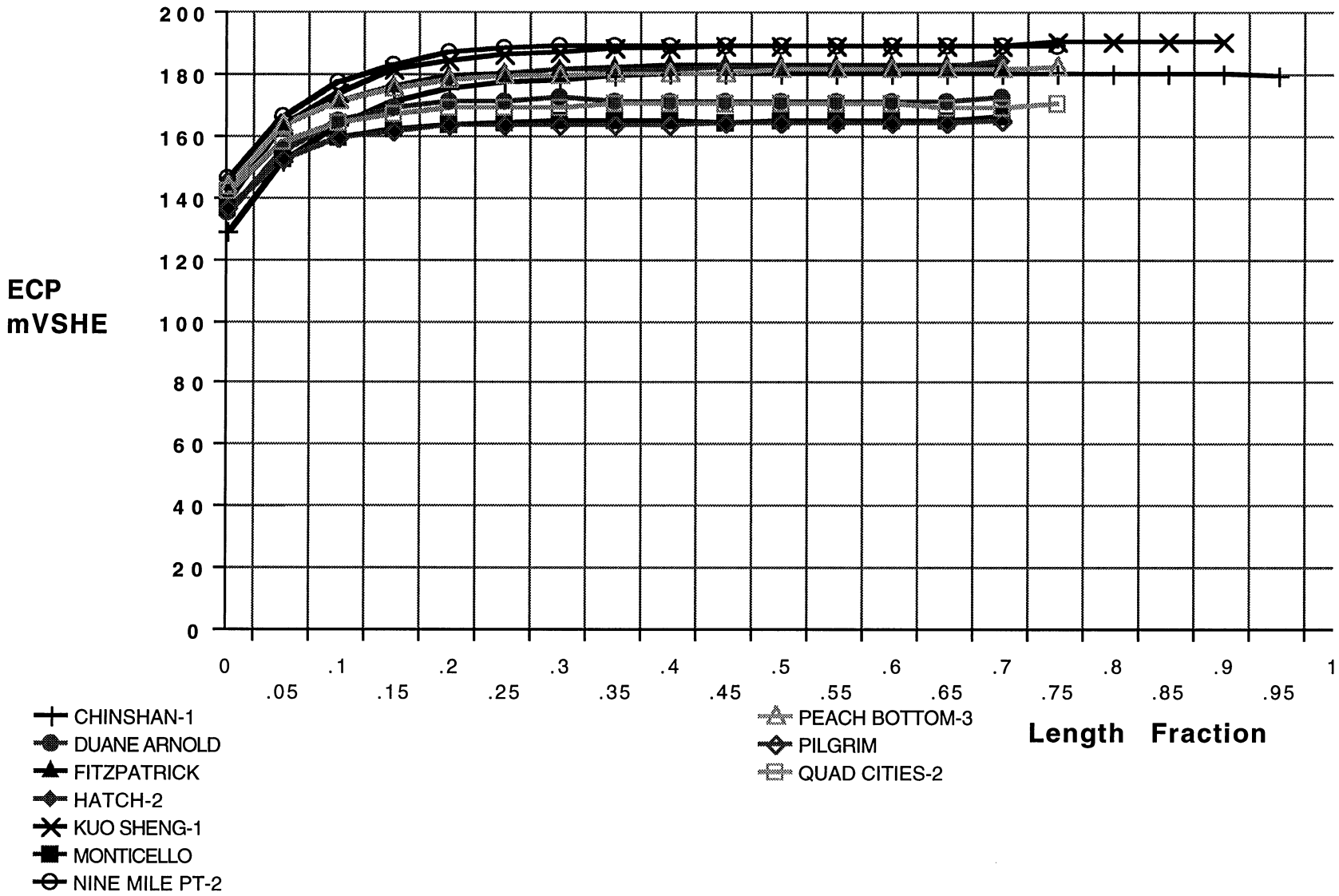

EPRI Licensed Material

Figure A-57: Upper Plenum Region ECPs with 1.5 ppm Feedwater H2 Addition

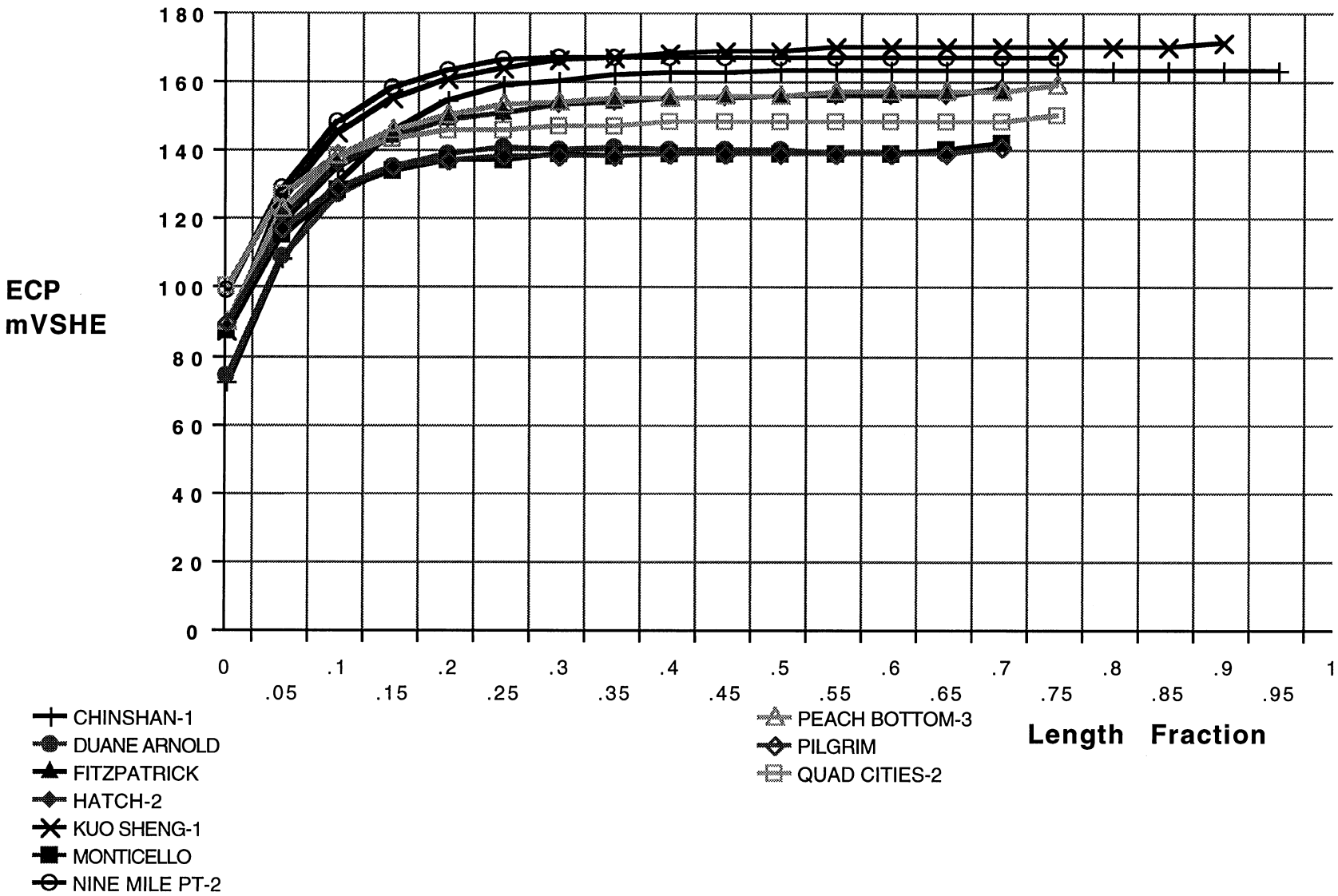

EPRI Licensed Material

Figure A-58: Upper Plenum Region ECPs with 3.0 ppm Feedwater H2 Addition

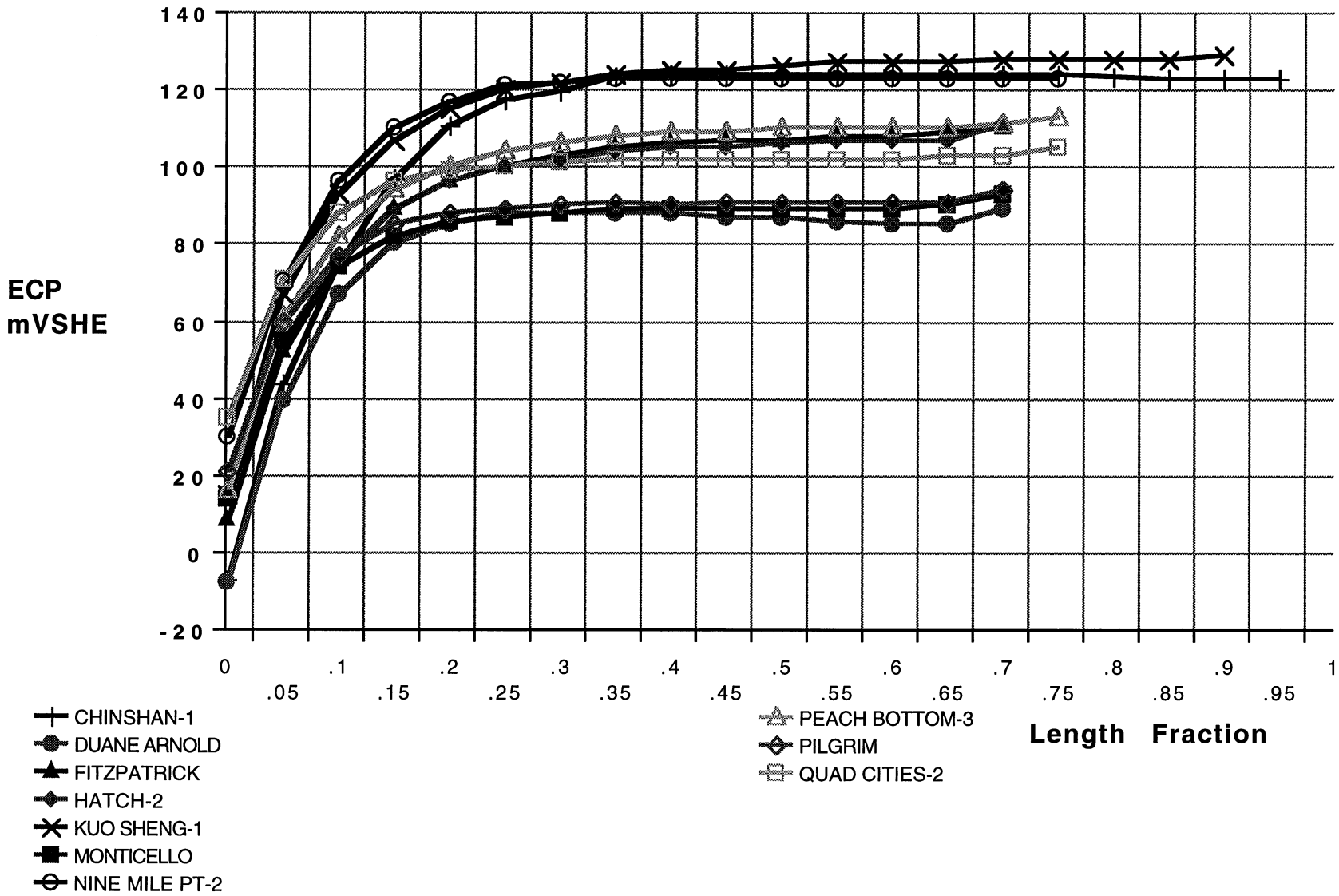

EPRI Licensed Material

Figure A-59: Upper Plenum Hydrogen Levels with 0 ppm Feedwater H2 Addition

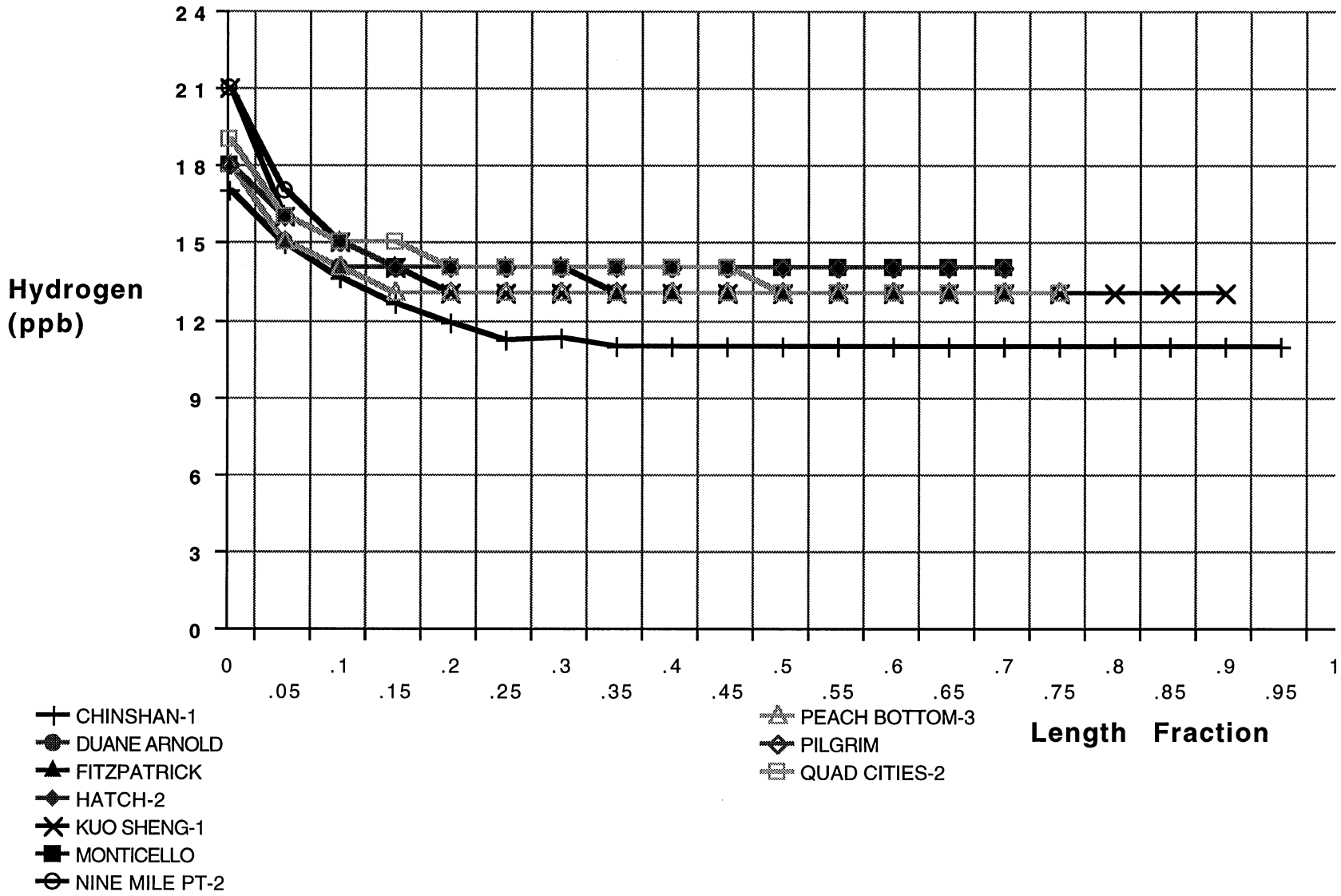

EPRI Licensed Material

Figure A-60: Upper Plenum Hydrogen Levels with 0.6 ppm Feedwater H2 Addition

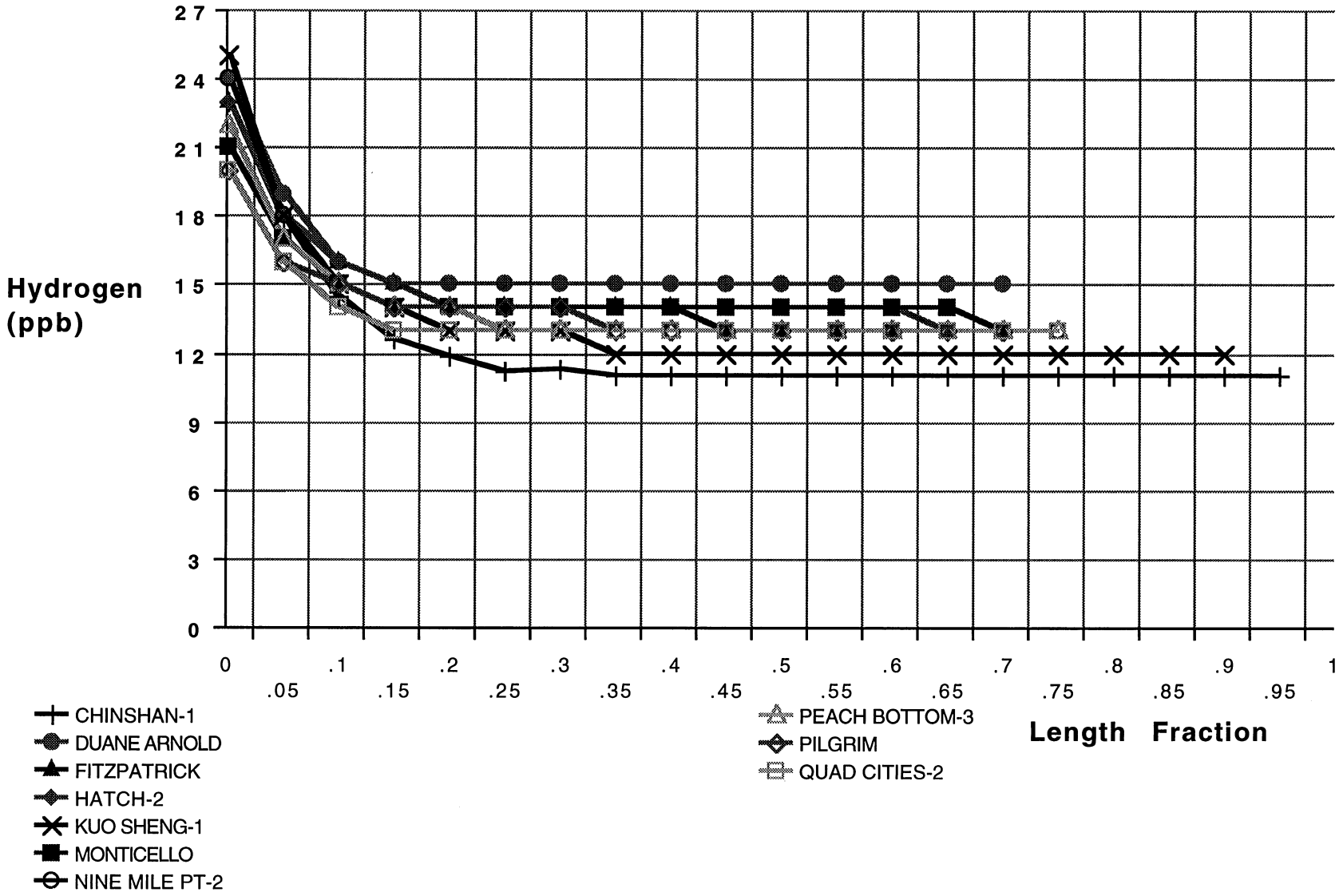

EPRI Licensed Material

Figure A-61: Upper Plenum Hydrogen Levels with 1.5 ppm Feedwater H2 Addition

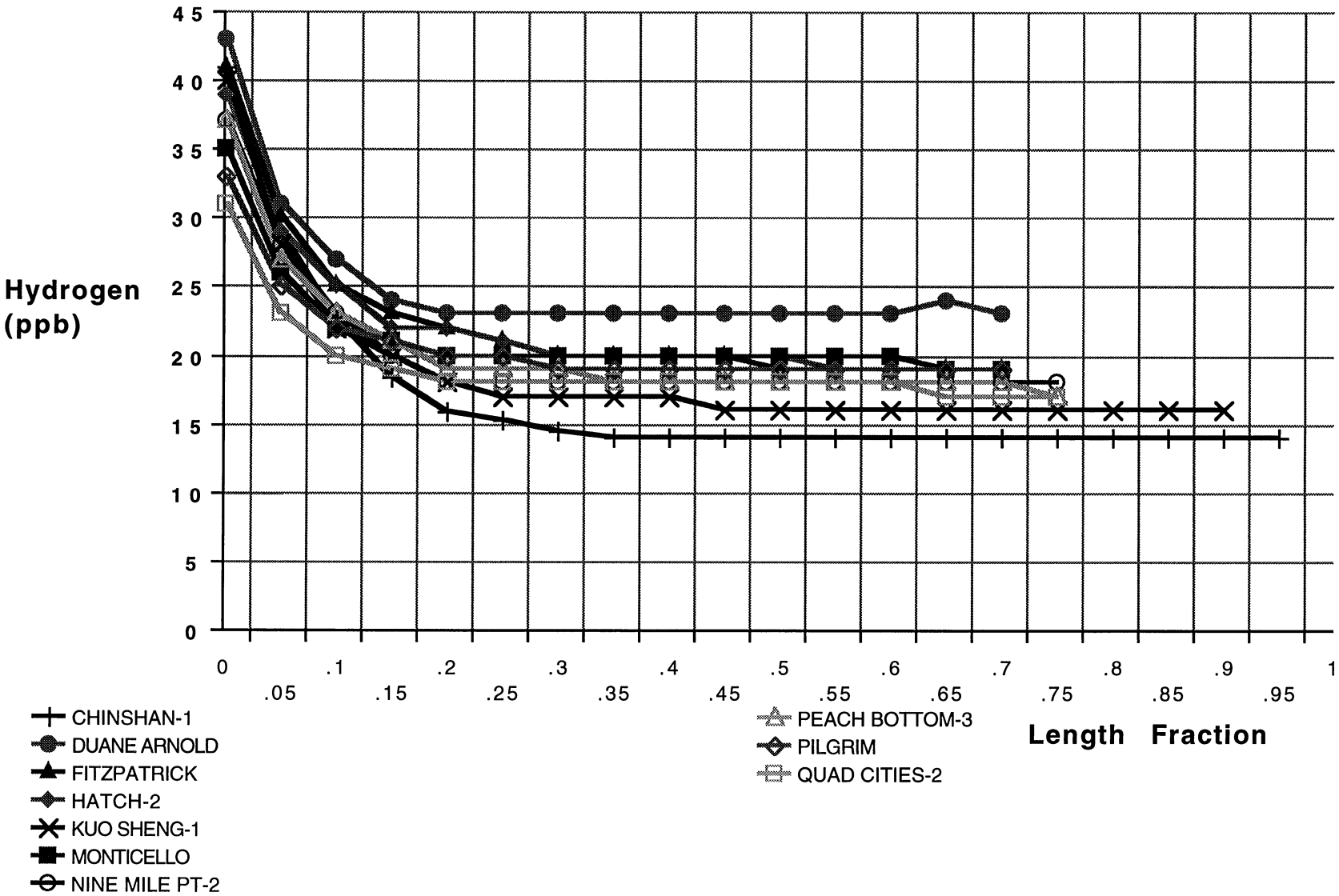

EPRI Licensed Material

Figure A-62: Upper Plenum Hydrogen Levels with 3.0 ppm Feedwater H2 Addition

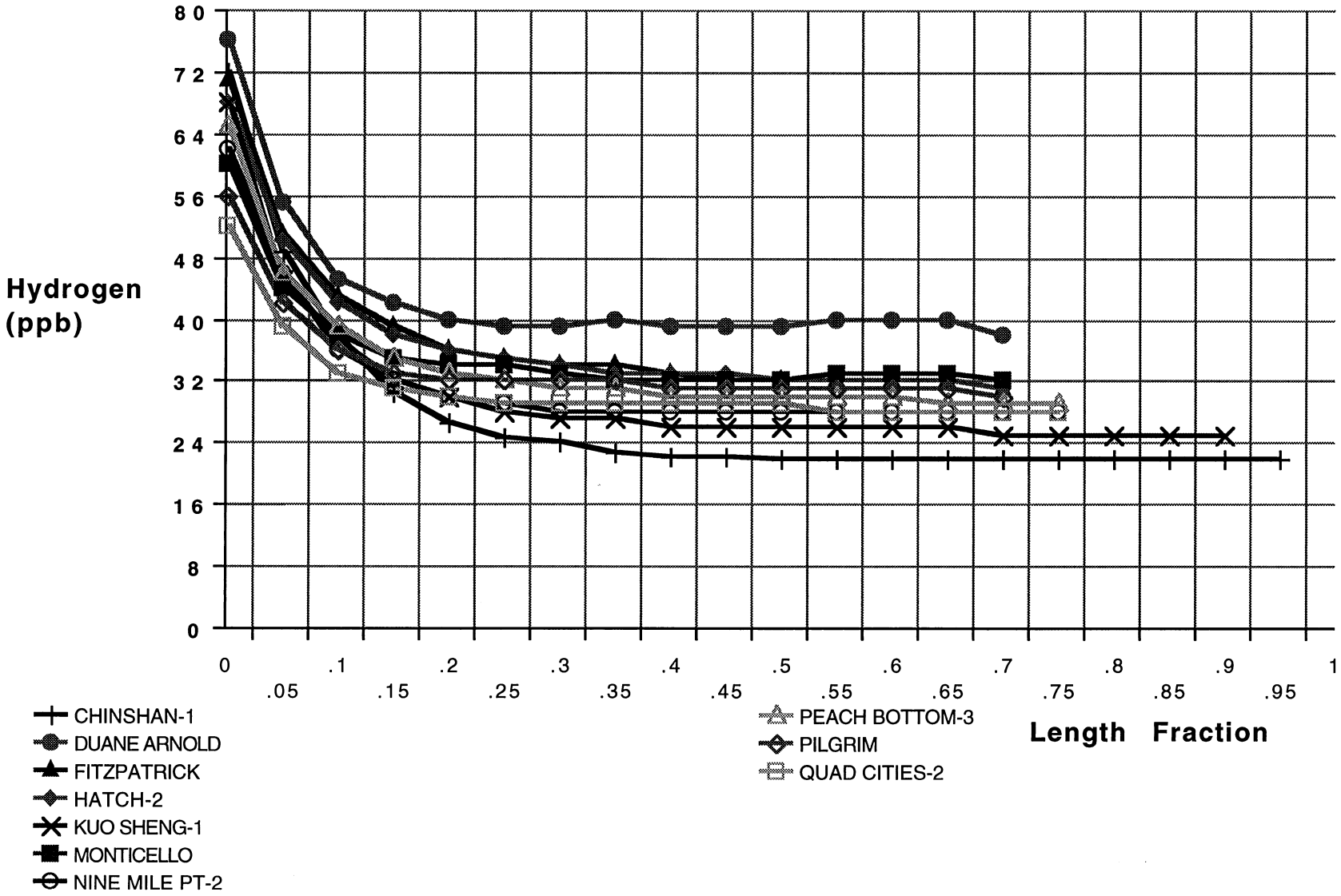

EPRI Licensed Material

Figure A-63: Upper Plenum Oxygen Levels with 0 ppm Feedwater H2 Addition

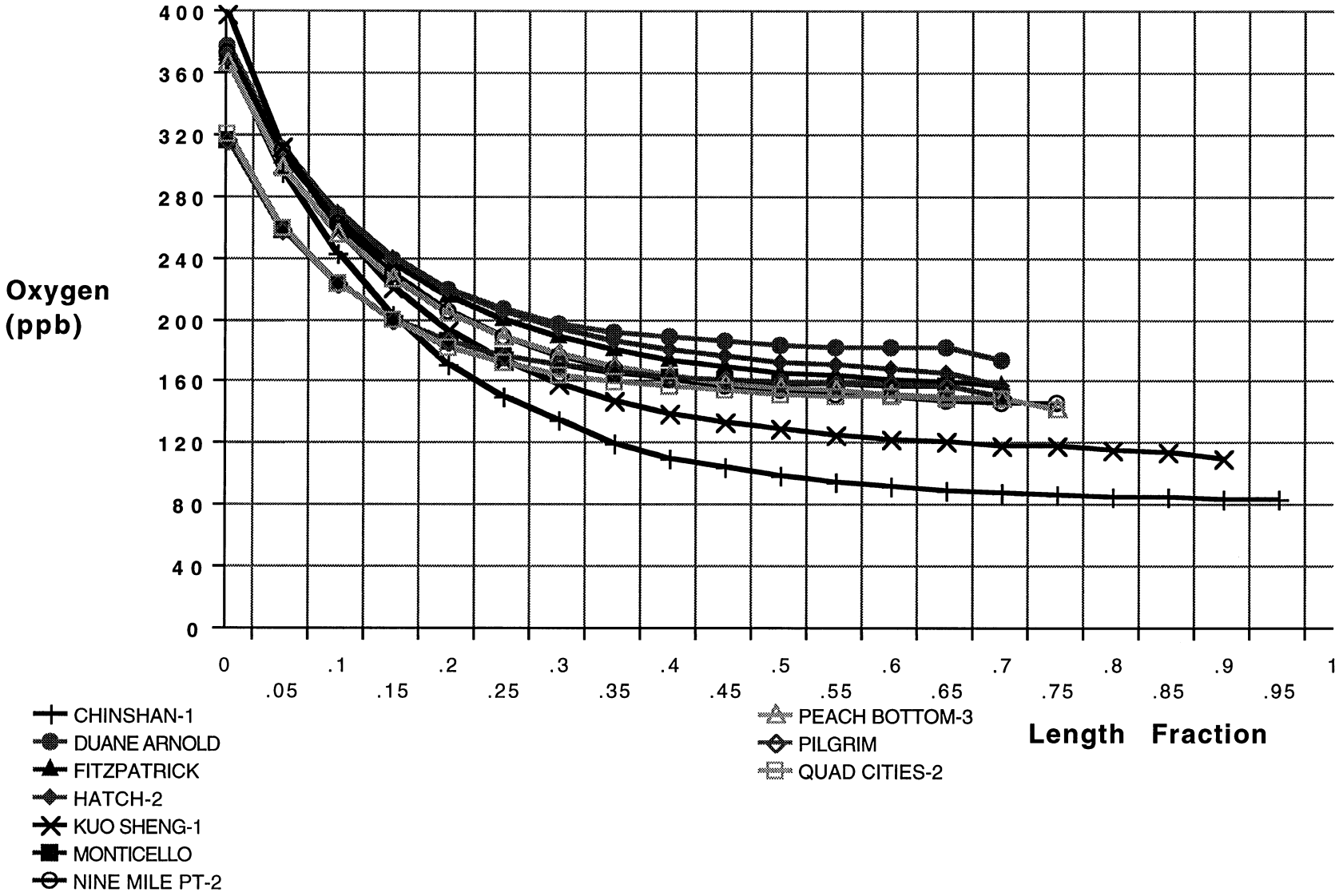

EPRI Licensed Material

Figure A-64: Upper Plenum Oxygen Levels with 0.6 ppm Feedwater H2 Addition

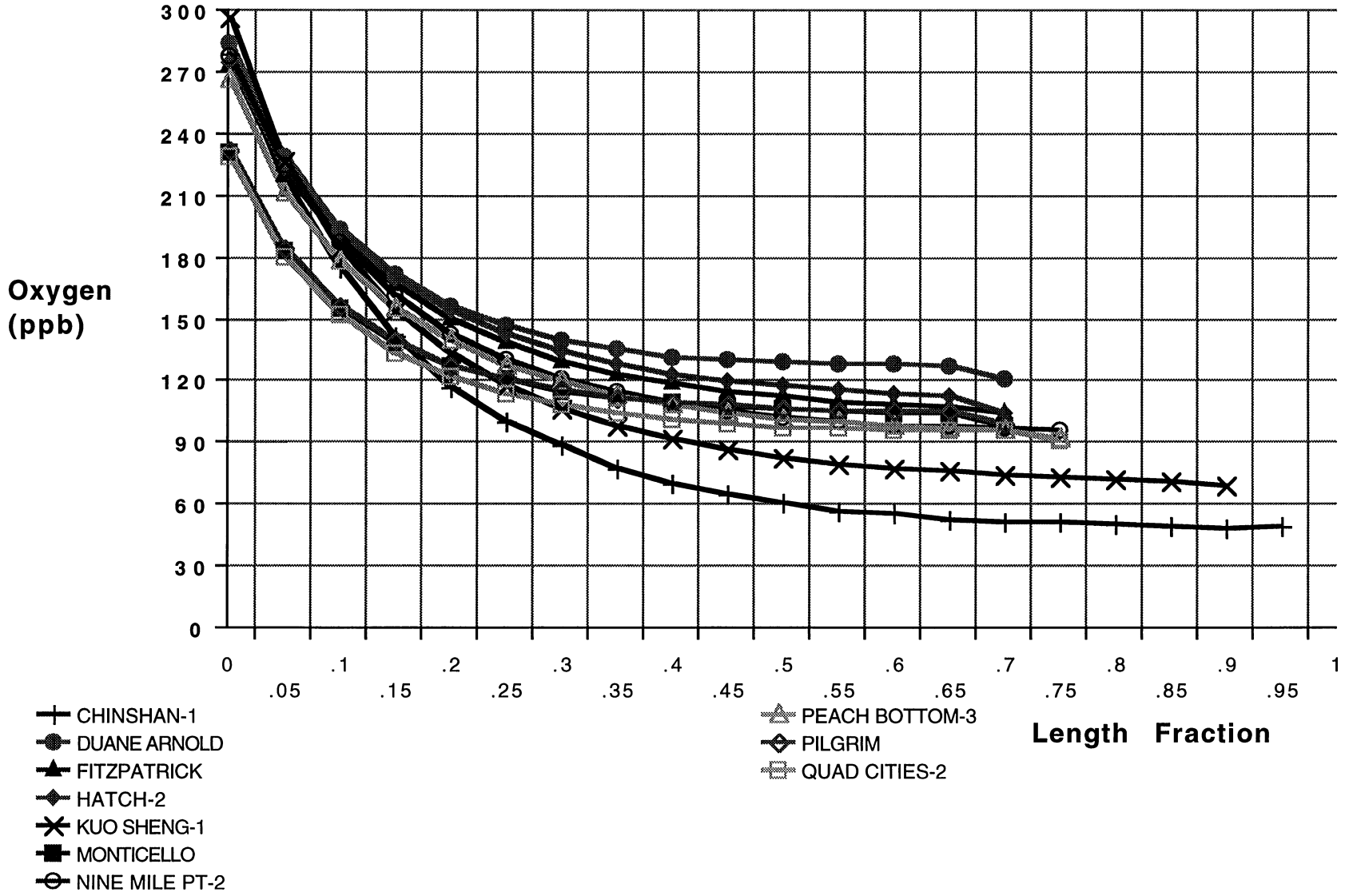

EPRI Licensed Material

Figure A-65: Upper Plenum Oxygen Levels with 1.5 ppm Feedwater H2 Addition

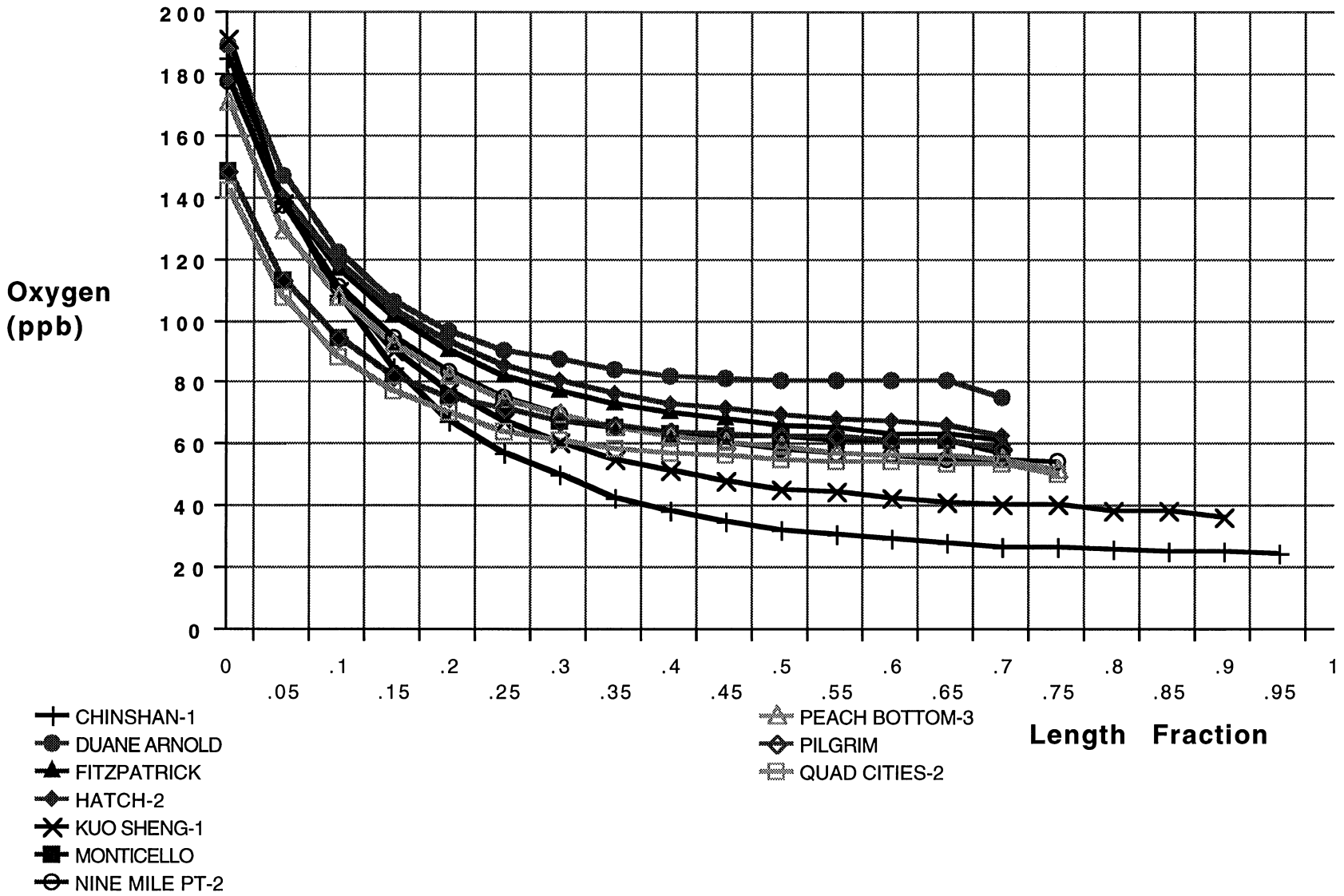

EPRI Licensed Material

Figure A-66: Upper Plenum Oxygen Levels with 3.0 ppm Feedwater H2 Addition

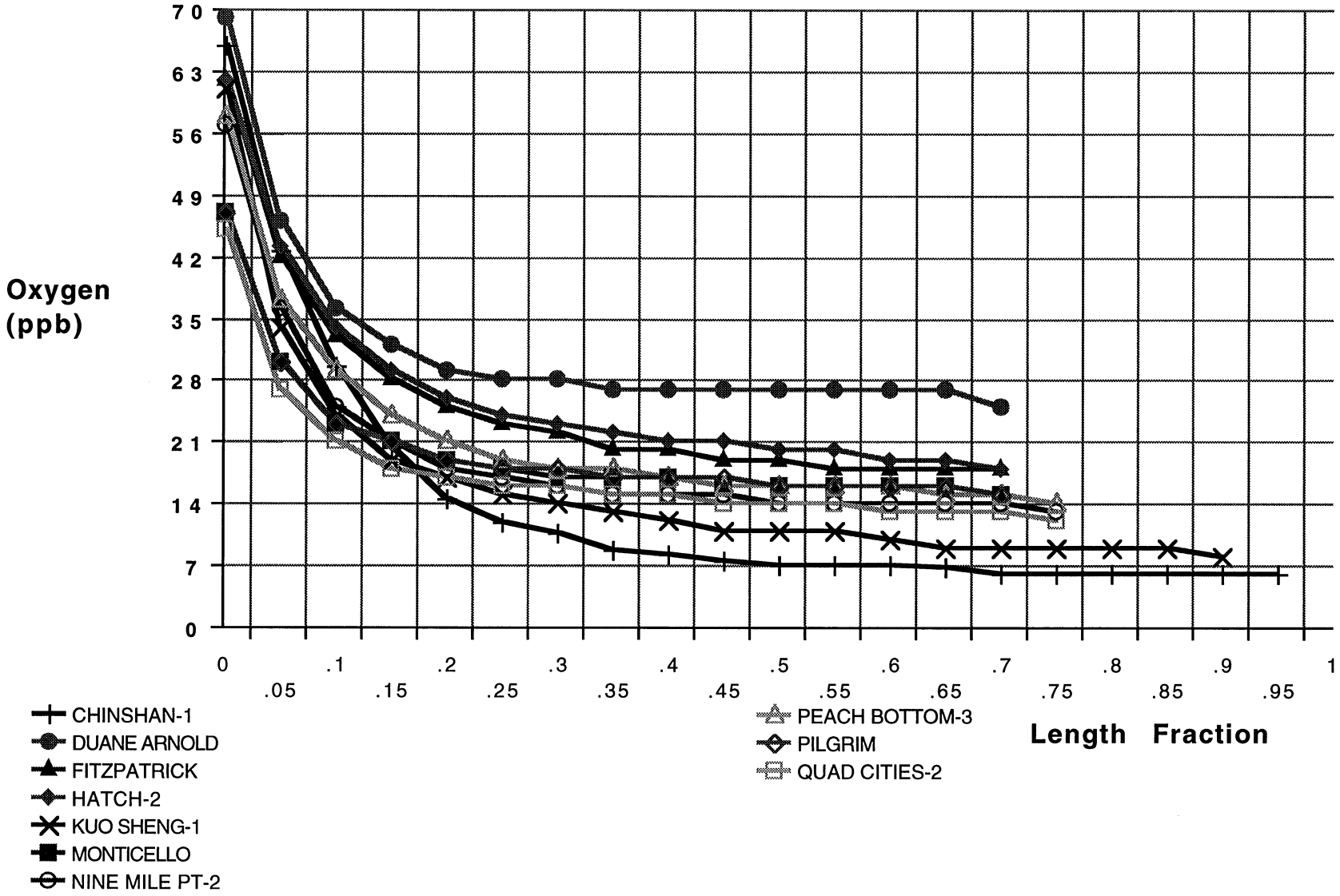

EPRI Licensed Material

Figure A-67: Upper Plenum Peroxide Levels with 0 ppm Feedwater H2 Addition

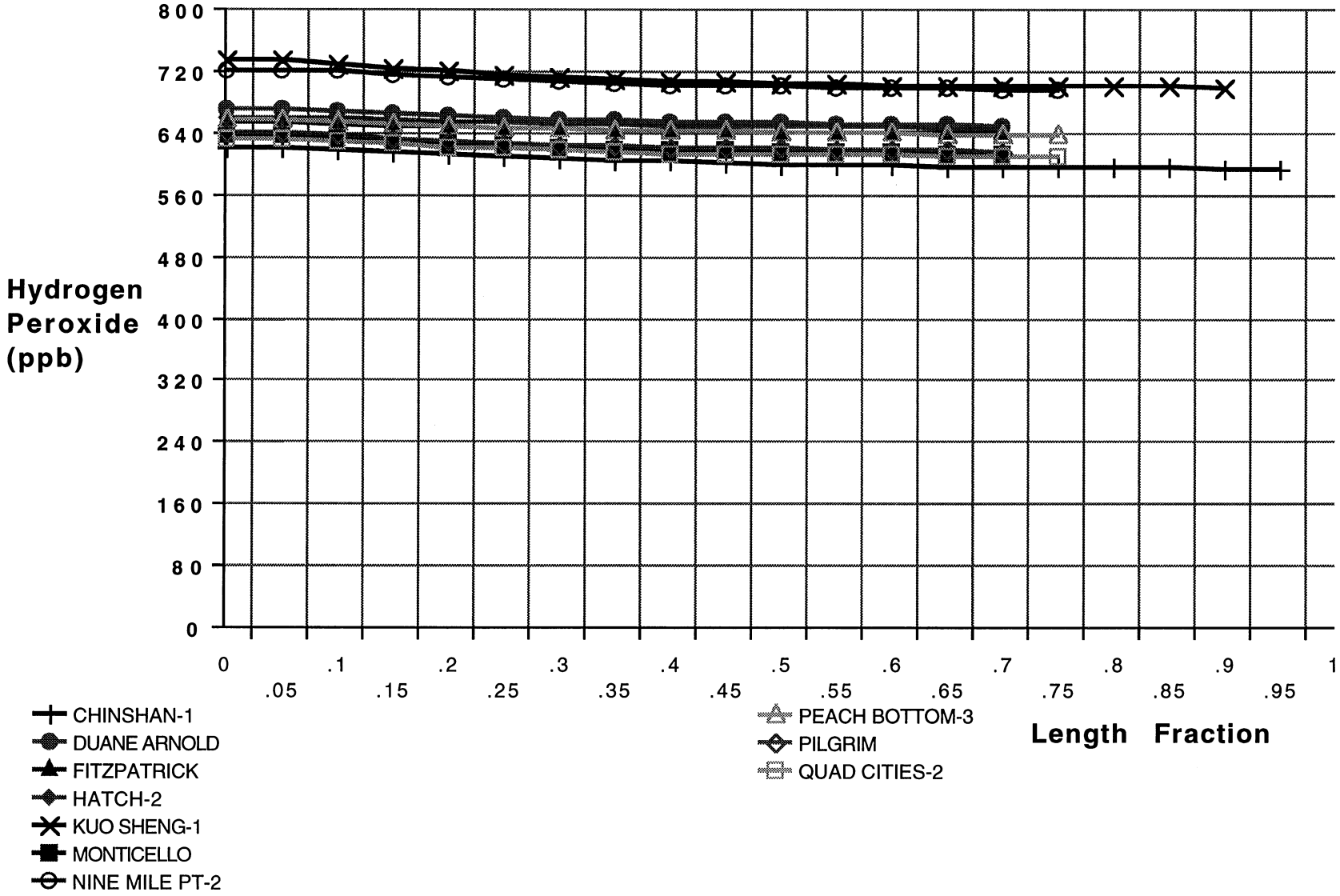

EPRI Licensed Material

Figure A-68: Upper Plenum Peroxide Levels with 0.6 ppm Feedwater H2 Addition

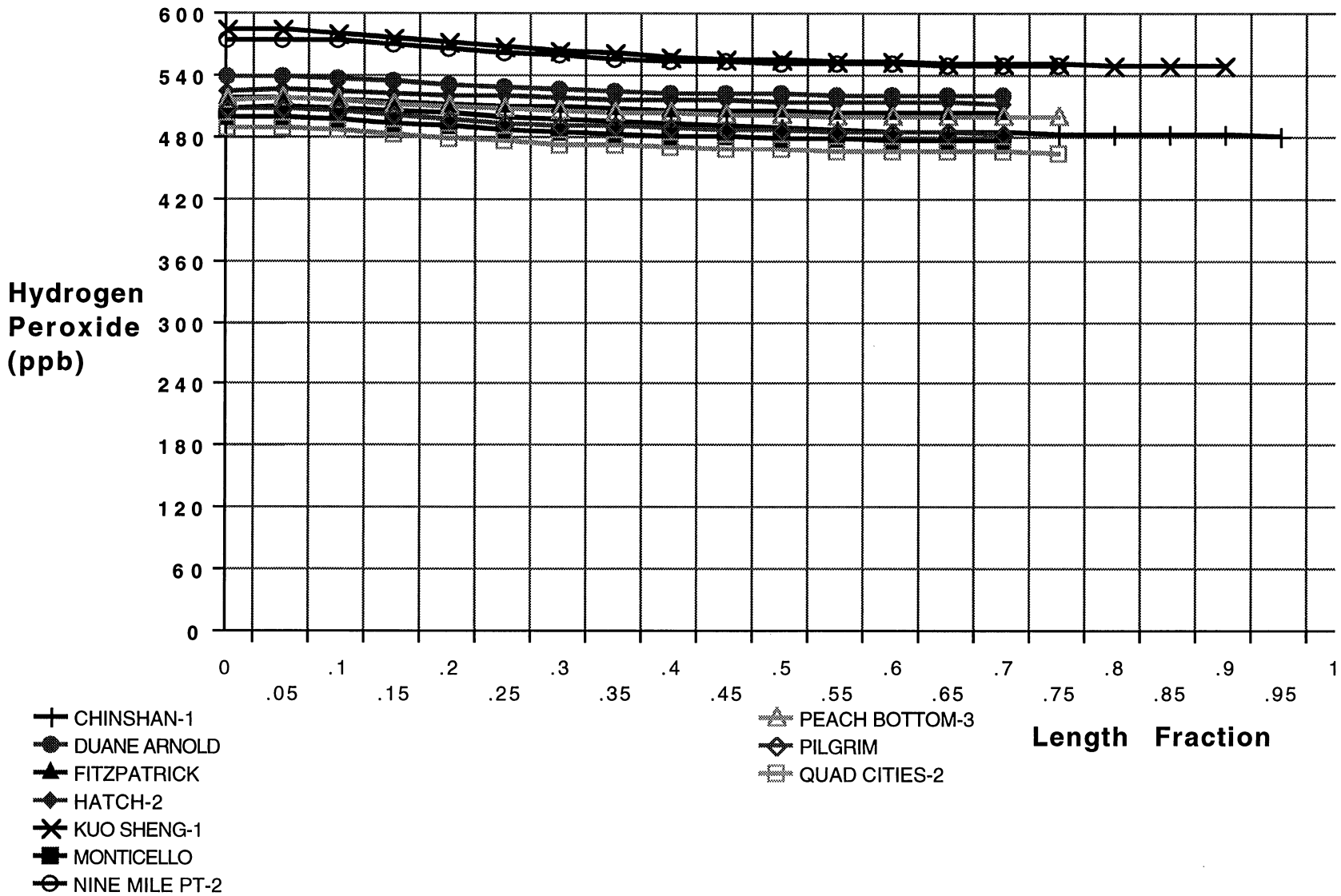

EPRI Licensed Material

Figure A-69: Upper Plenum Peroxide Levels with 1.5 ppm Feedwater H2 Addition

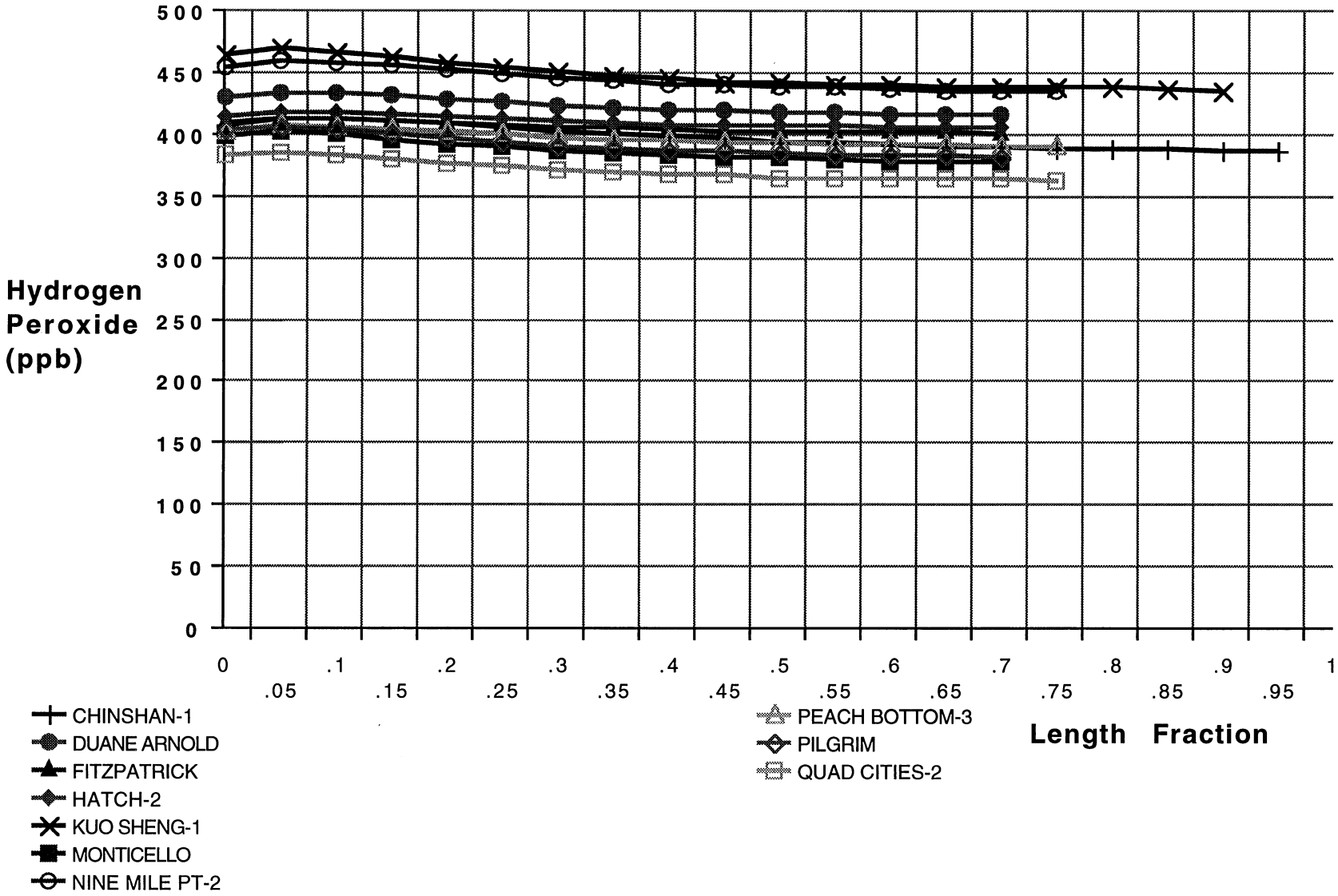

EPRI Licensed Material

Figure A-70: Upper Plenum Peroxide Levels with 3.0 ppm Feedwater H2 Addition

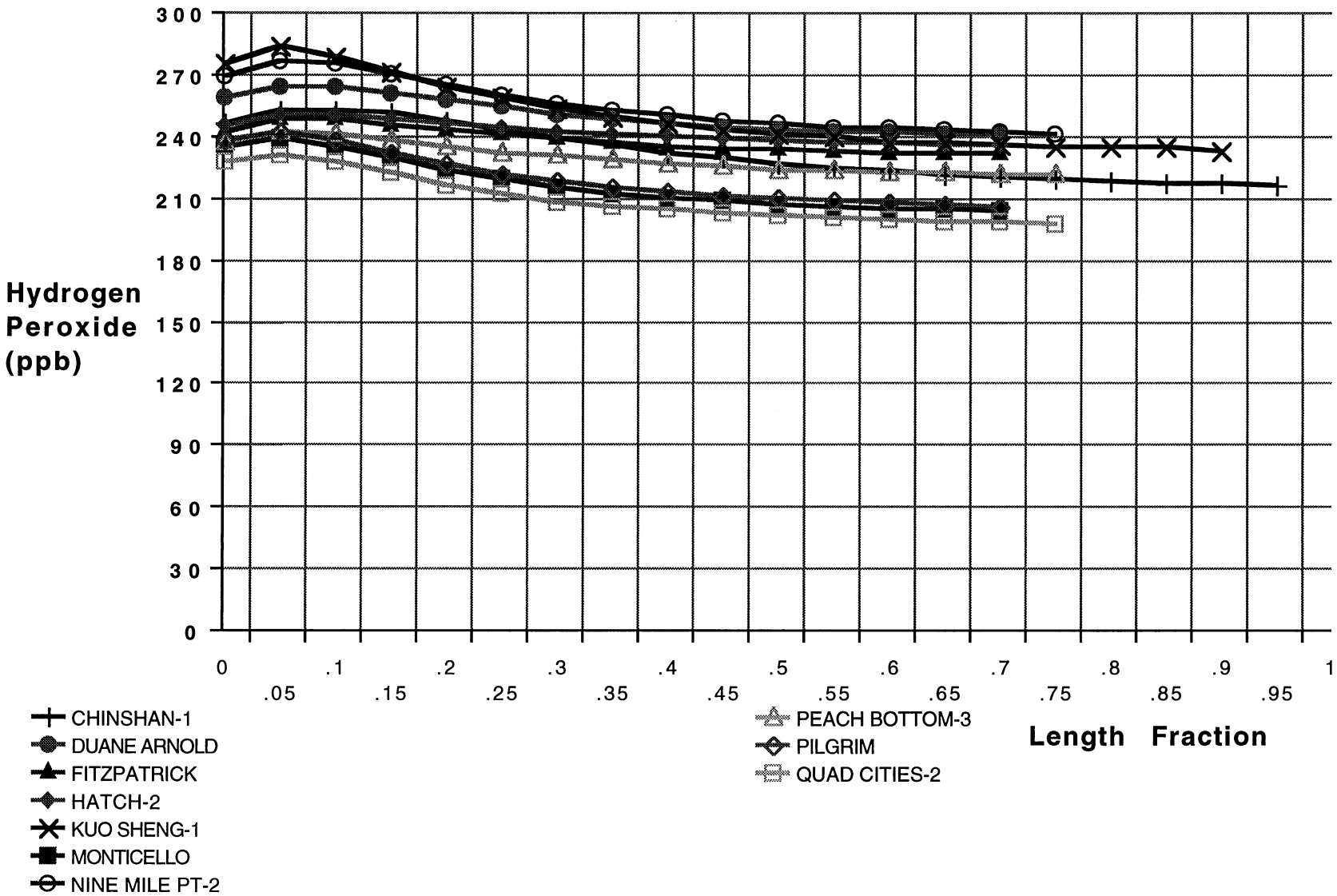

EPRI Licensed Material

Figure A-71: Steam Separator Region ECPs with 0 ppm Feedwater H2 Addition

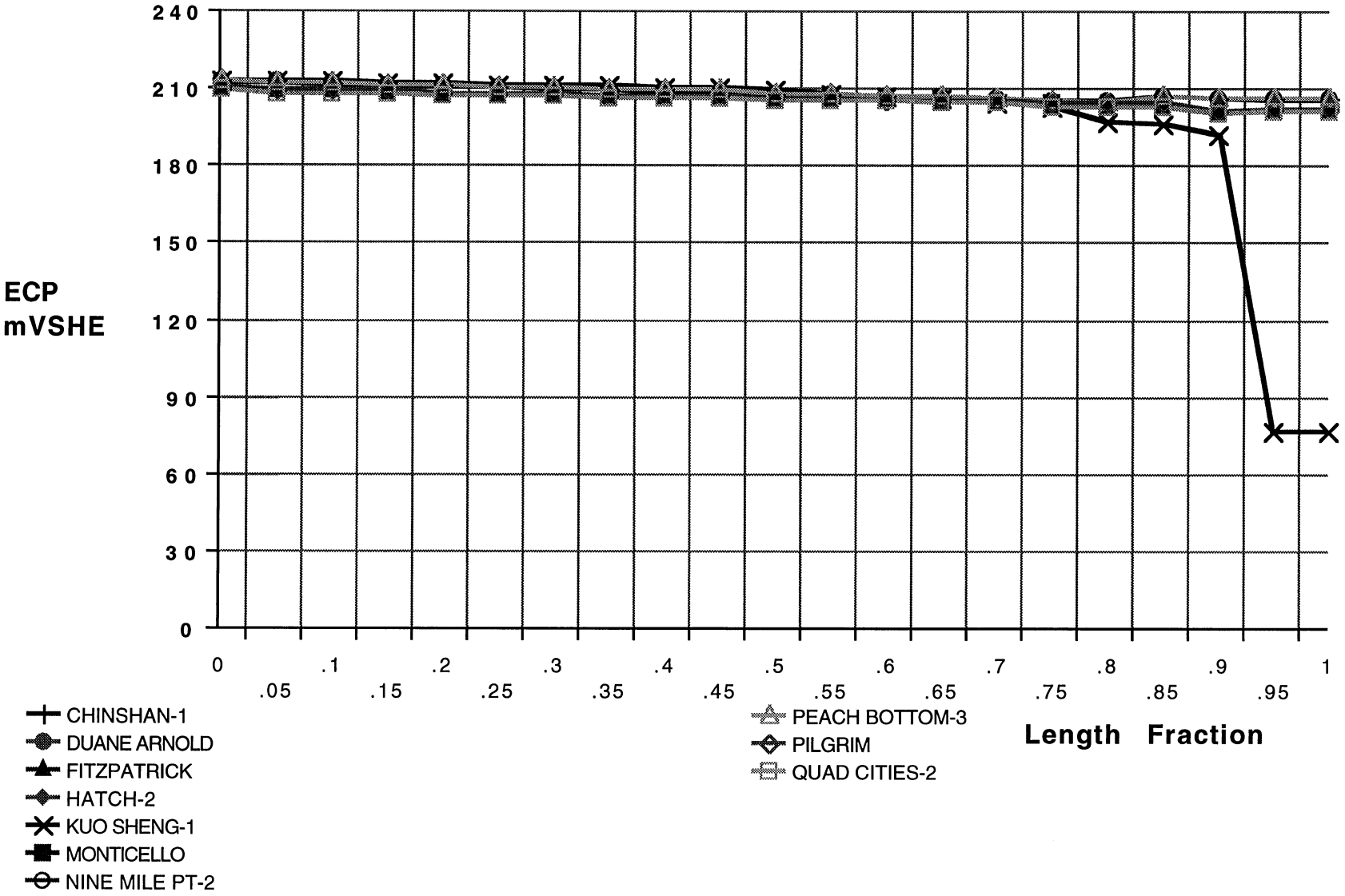

EPRI Licensed Material

Figure A-72: Steam Separator Region ECPs with 0.6 ppm Feedwater H2 Addition

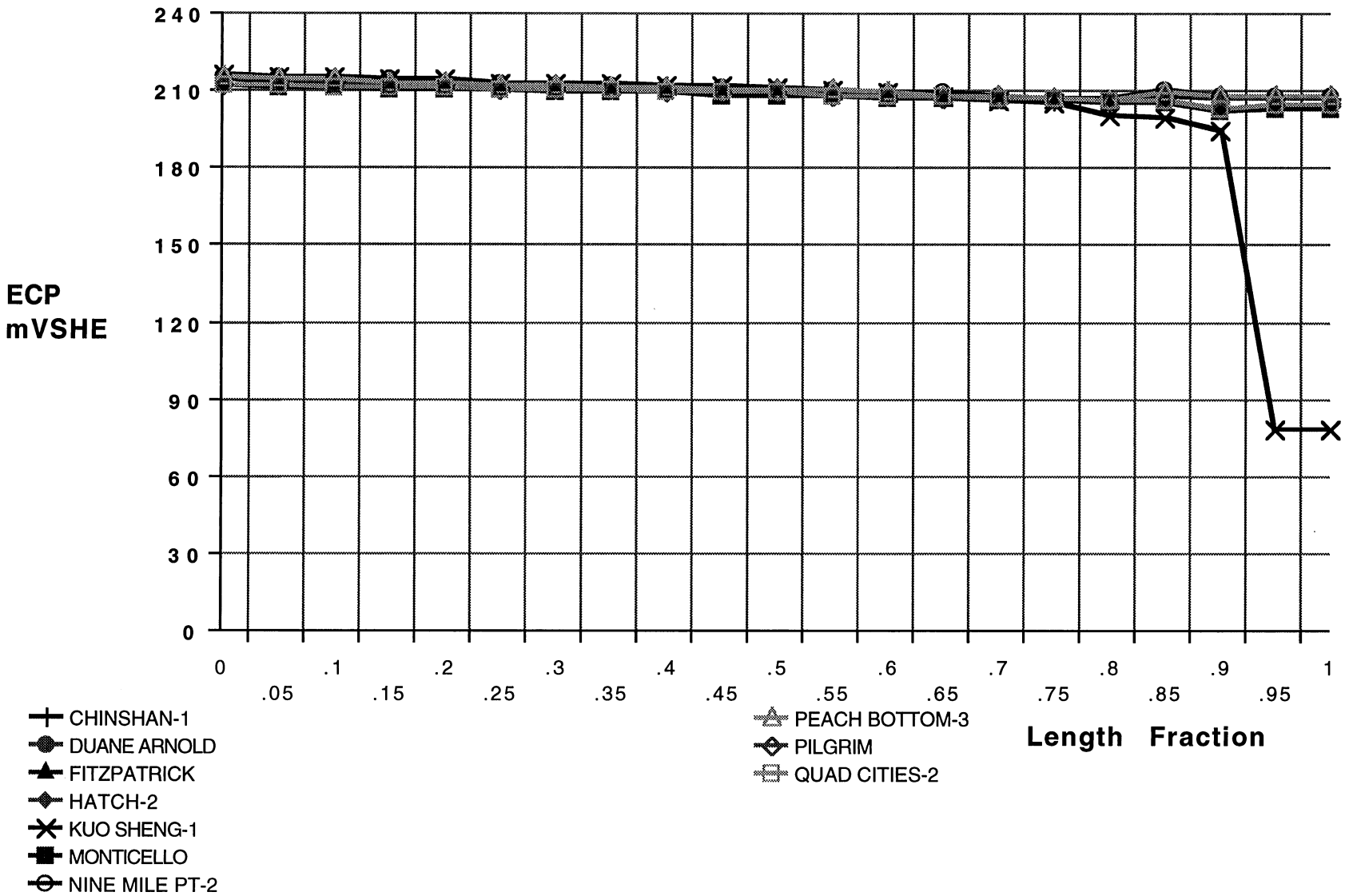

EPRI Licensed Material

Figure A-73: Steam Separator Region ECPs with 1.5 ppm Feedwater H2 Addition

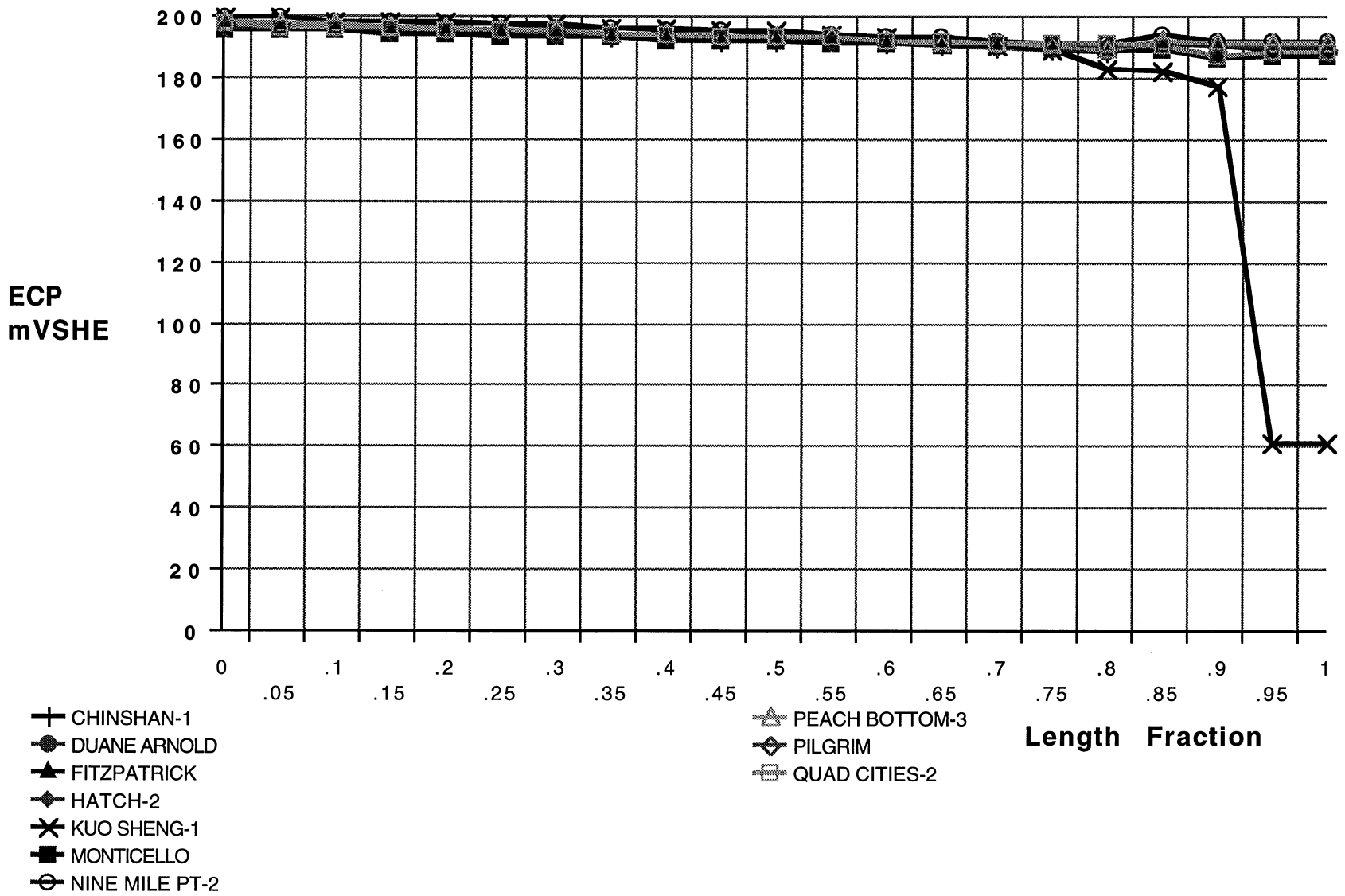

EPRI Licensed Material

Figure A-74: Steam Separator Region ECPs with 3.0 ppm Feedwater H2 Addition

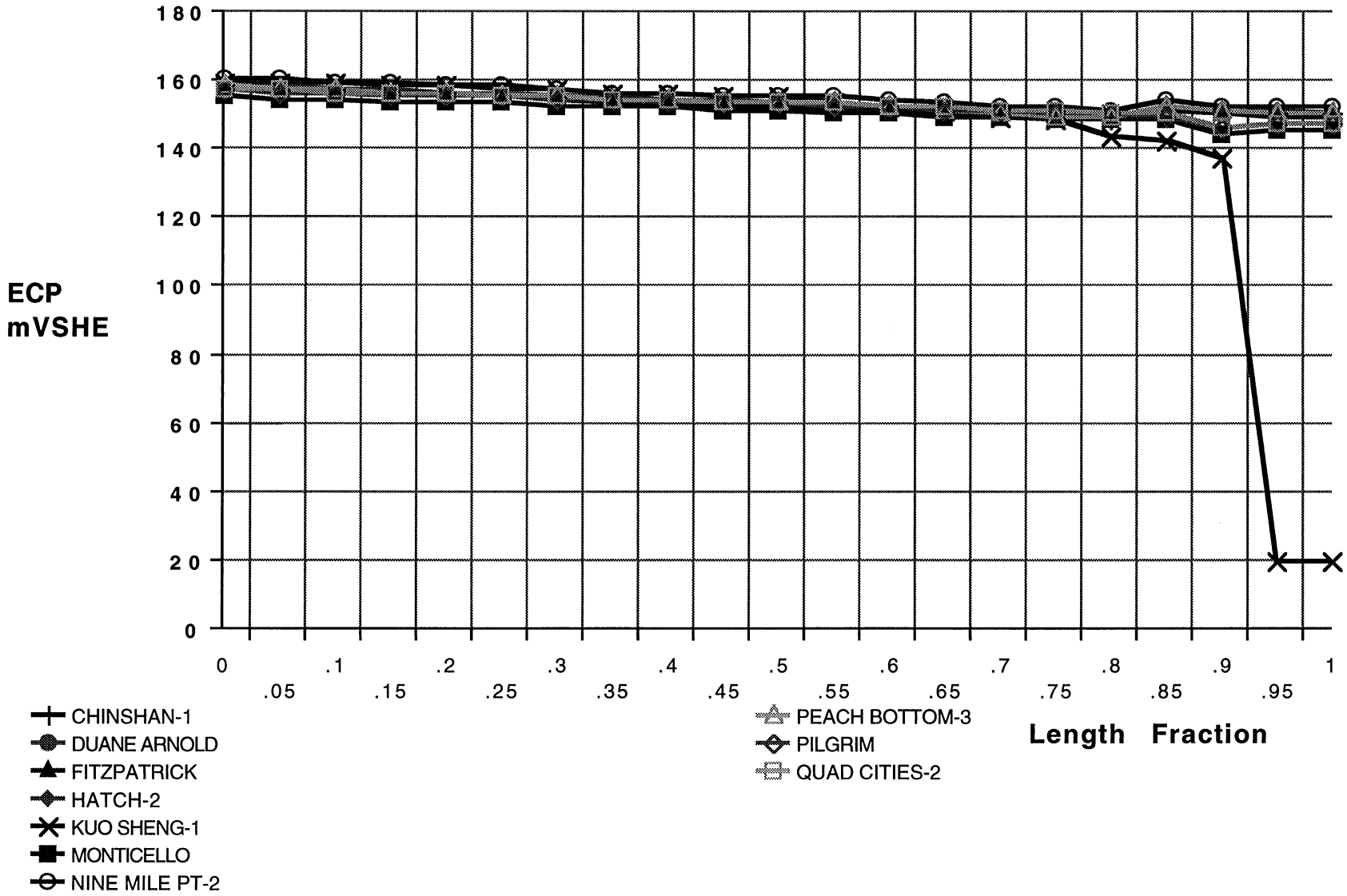

EPRI Licensed Material

Figure A-75: Steam Separator Hydrogen Levels with 0 ppm Feedwater H2 Addition

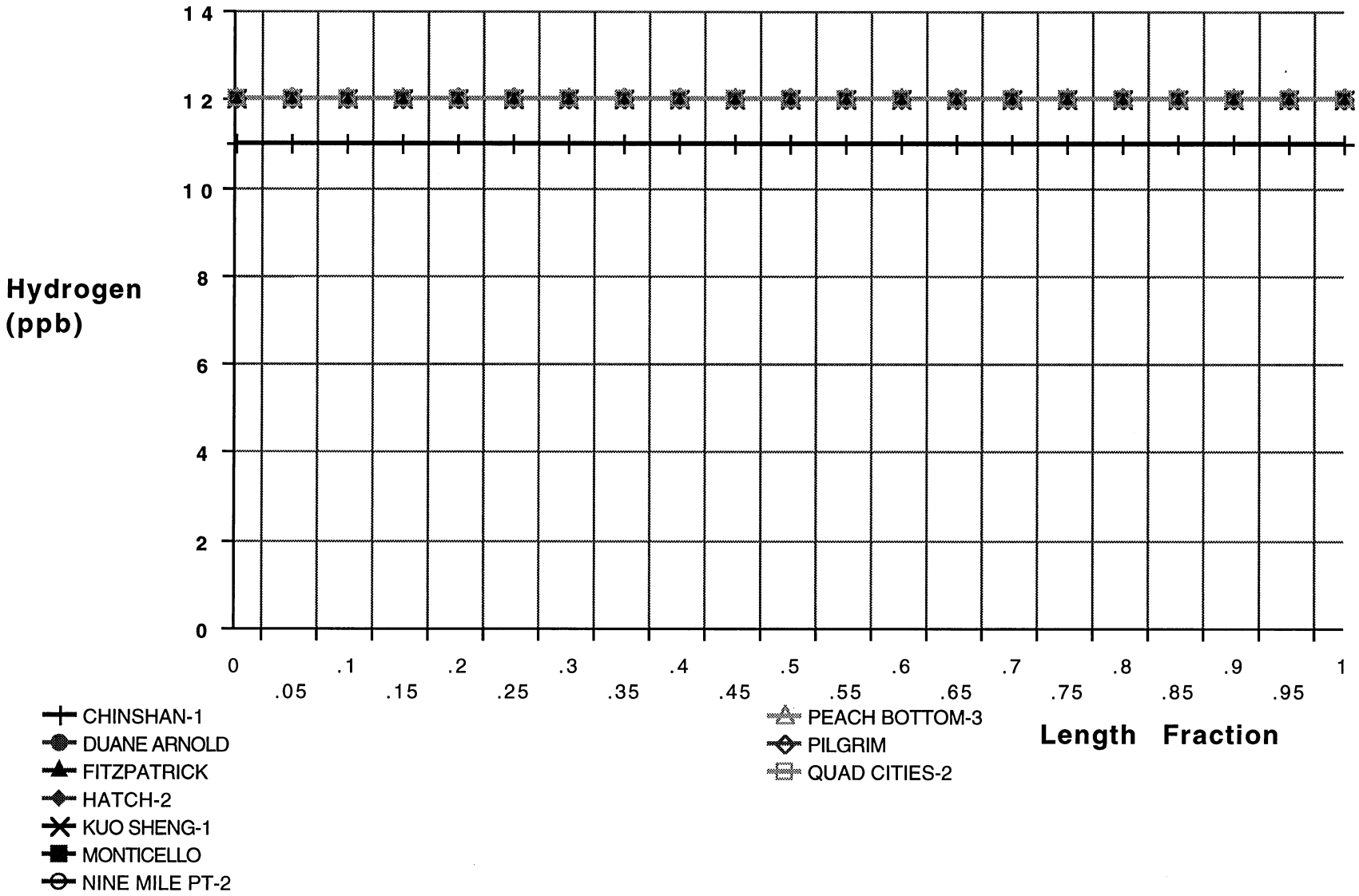

EPRI Licensed Material

Figure A-76: Steam Separator Hydrogen Levels with 0.6 ppm Feedwater H2 Addition

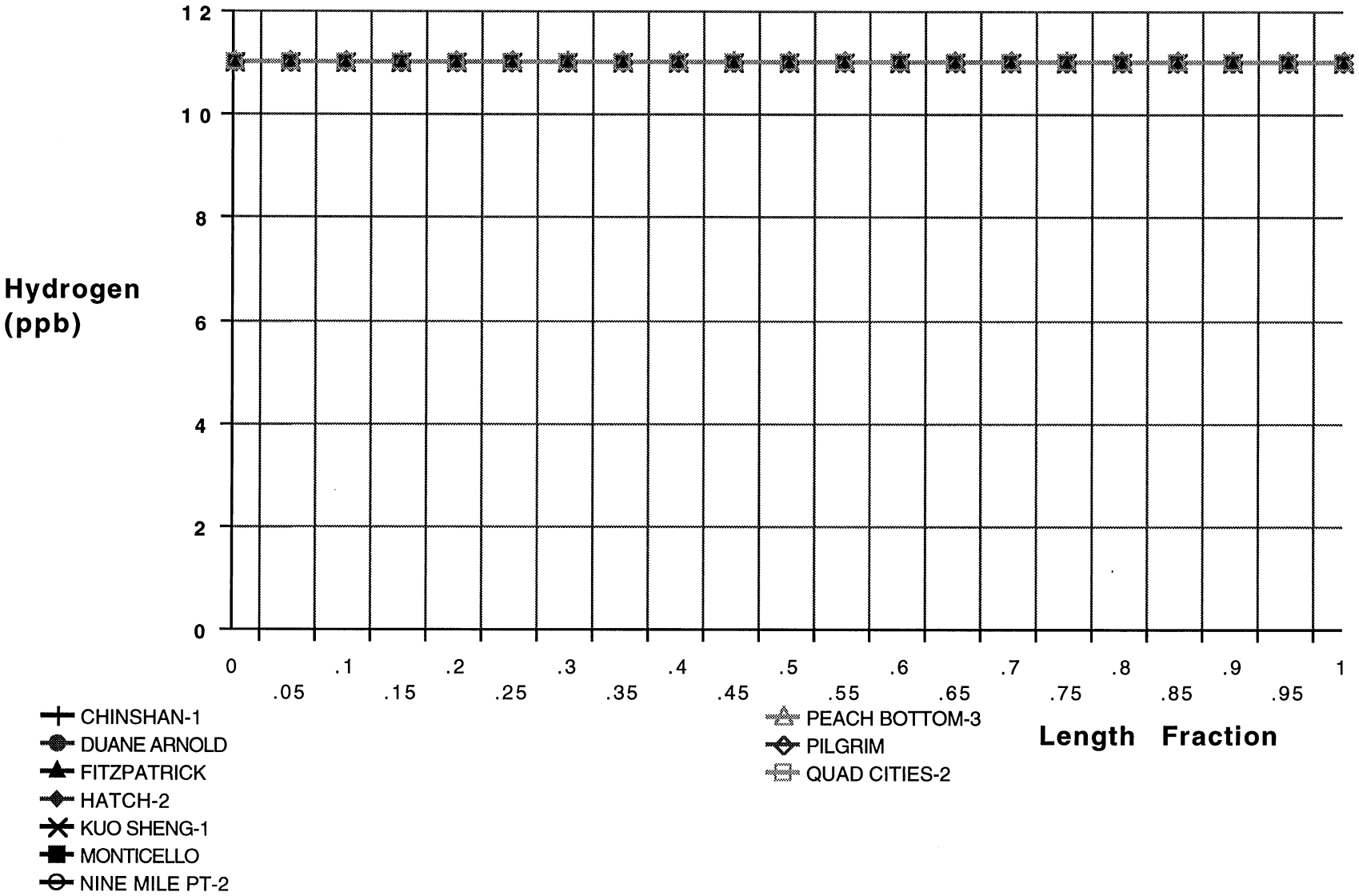

EPRI Licensed Material

Figure A-77: Steam Separator Hydrogen Levels with 1.5 ppm Feedwater H2 Addition

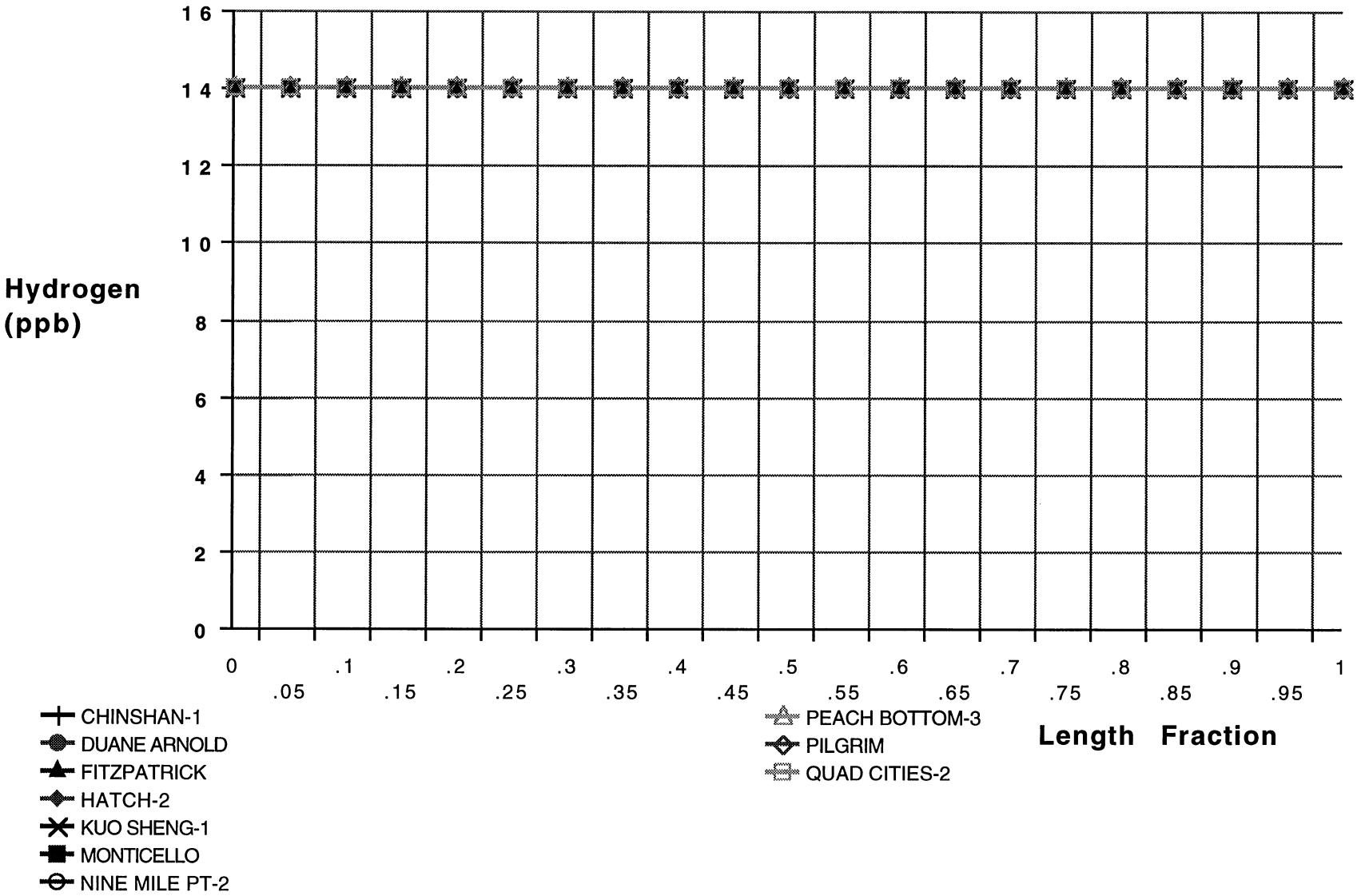

EPRI Licensed Material

Figure A-78: Steam Separator Hydrogen Levels with 3.0 ppm Feedwater H2 Addition

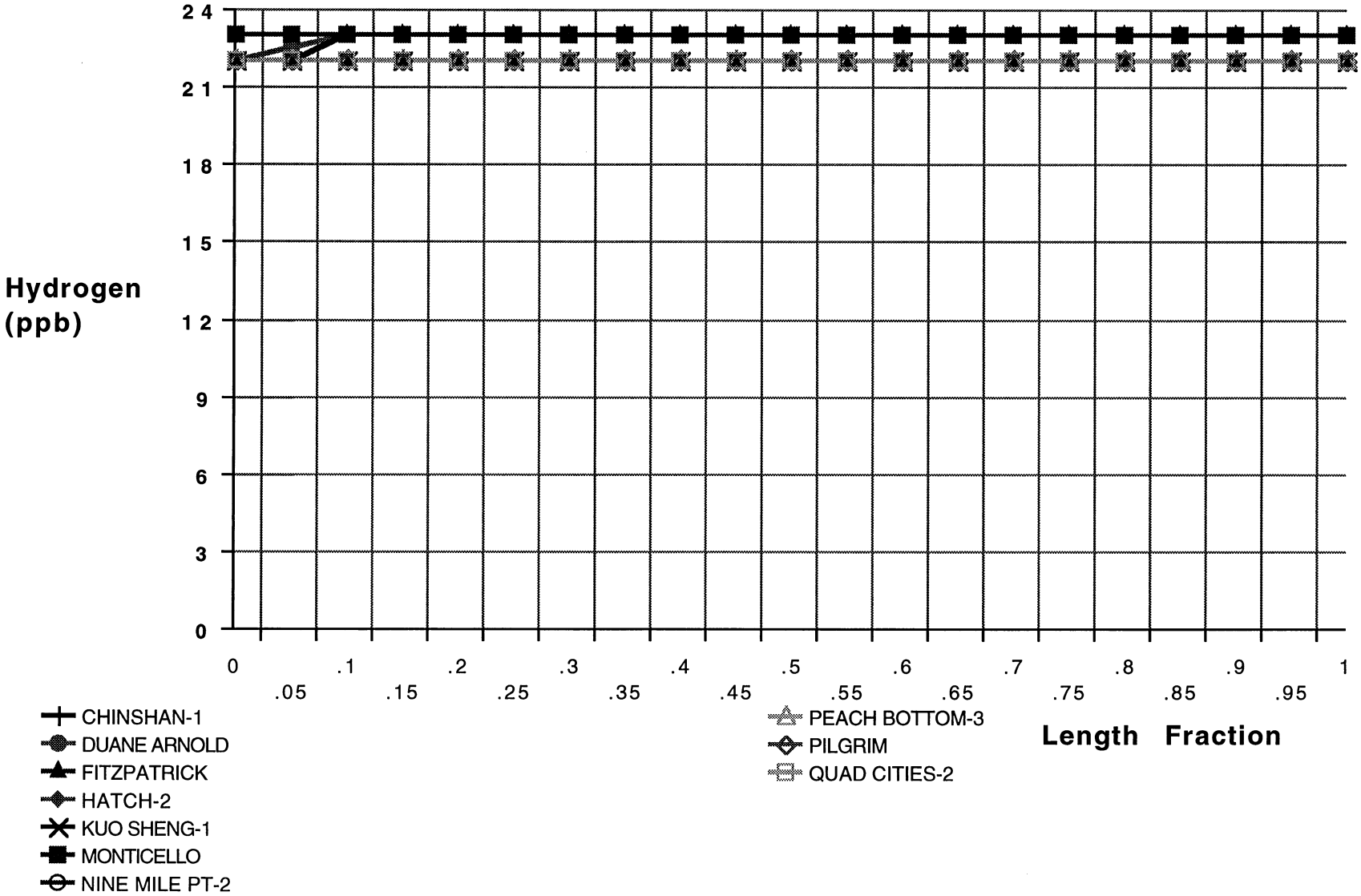

EPRI Licensed Material

Figure A-79: Steam Separator Oxygen Levels with 0 ppm Feedwater H2 Addition

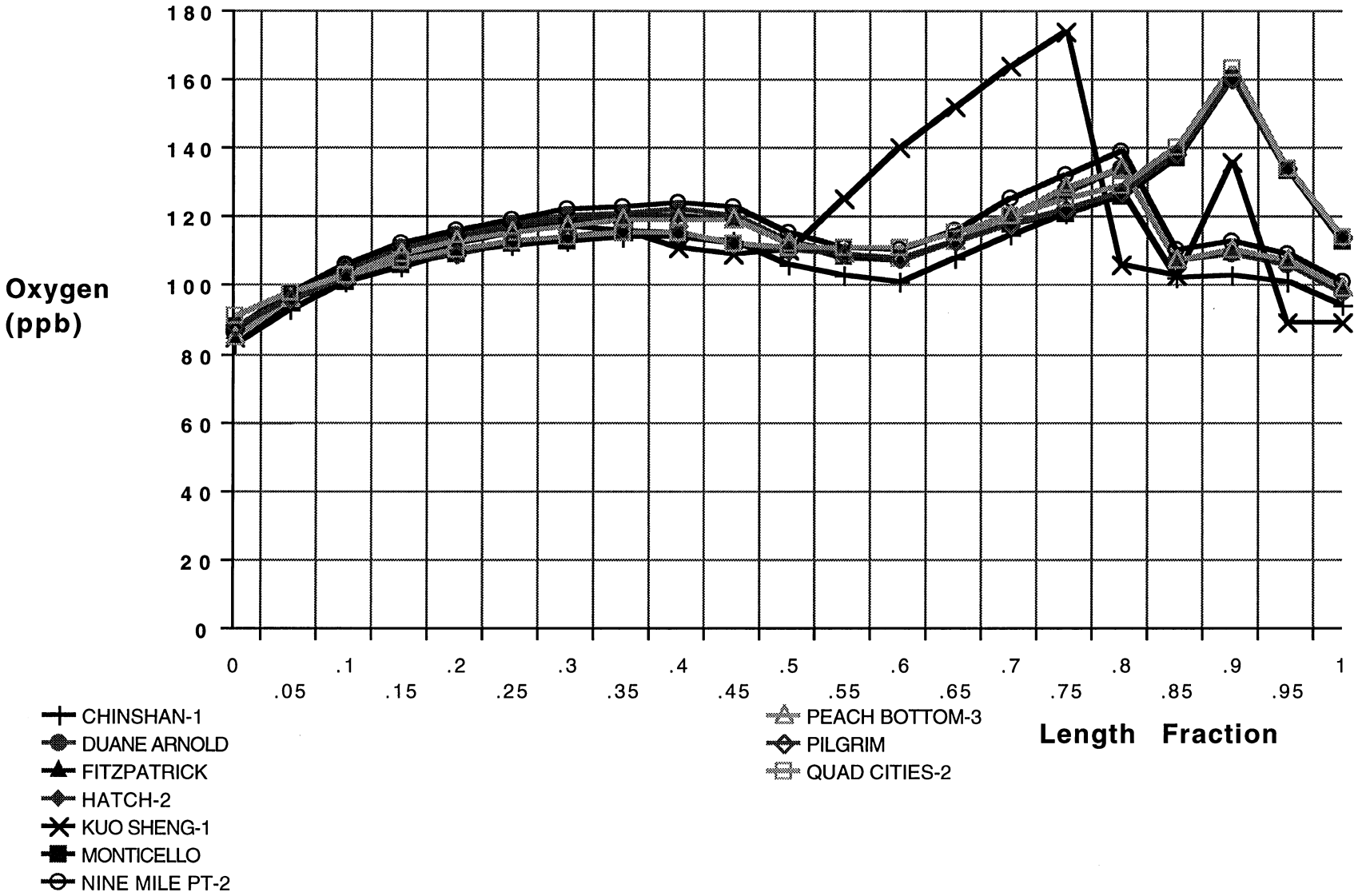

EPRI Licensed Material

Figure A-80: Steam Separator Oxygen Levels with 0.6 ppm Feedwater H2 Addition

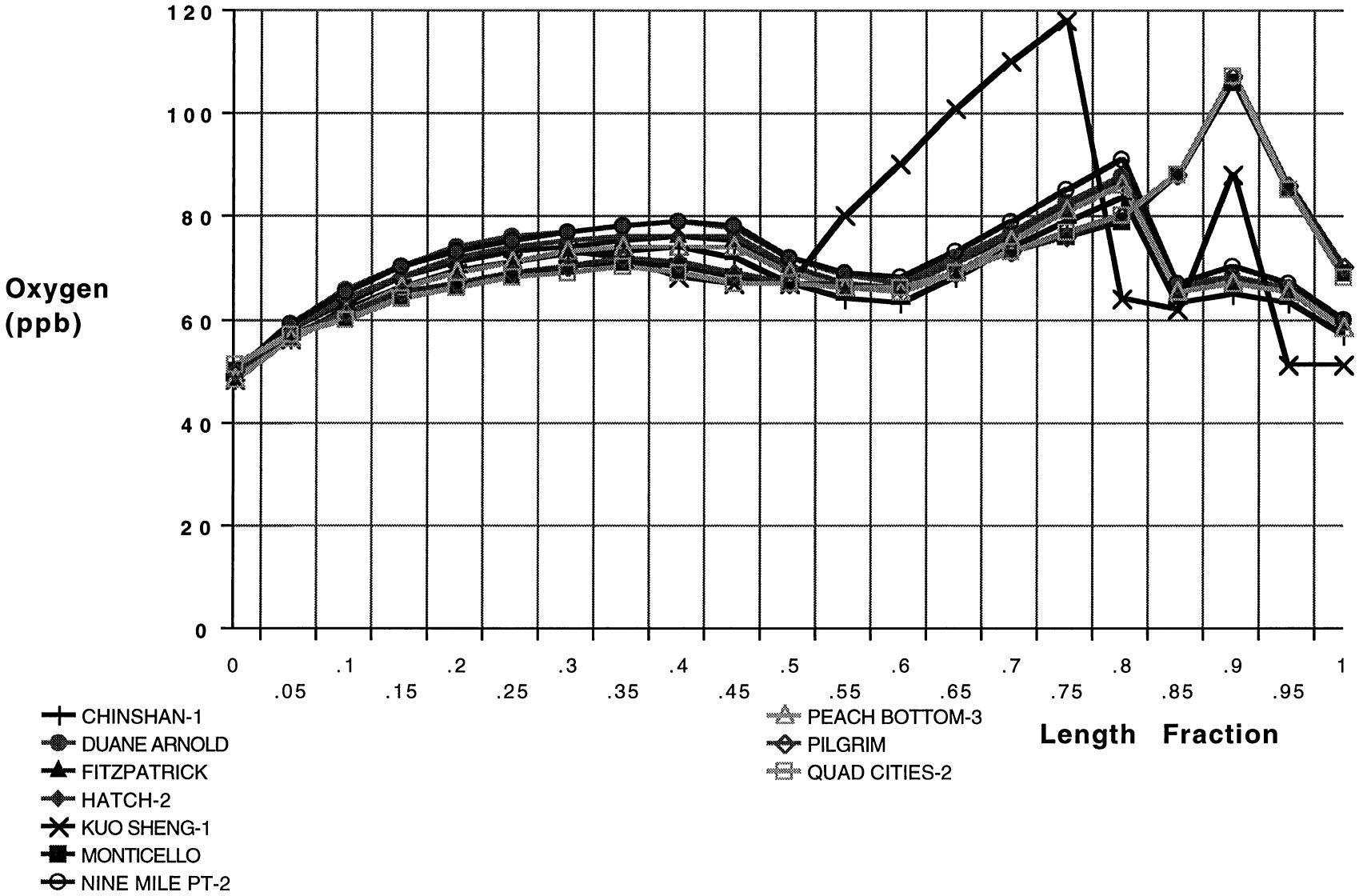

EPRI Licensed Material

Figure A-81: Steam Separator Oxygen Levels with 1.5 ppm Feedwater H2 Addition

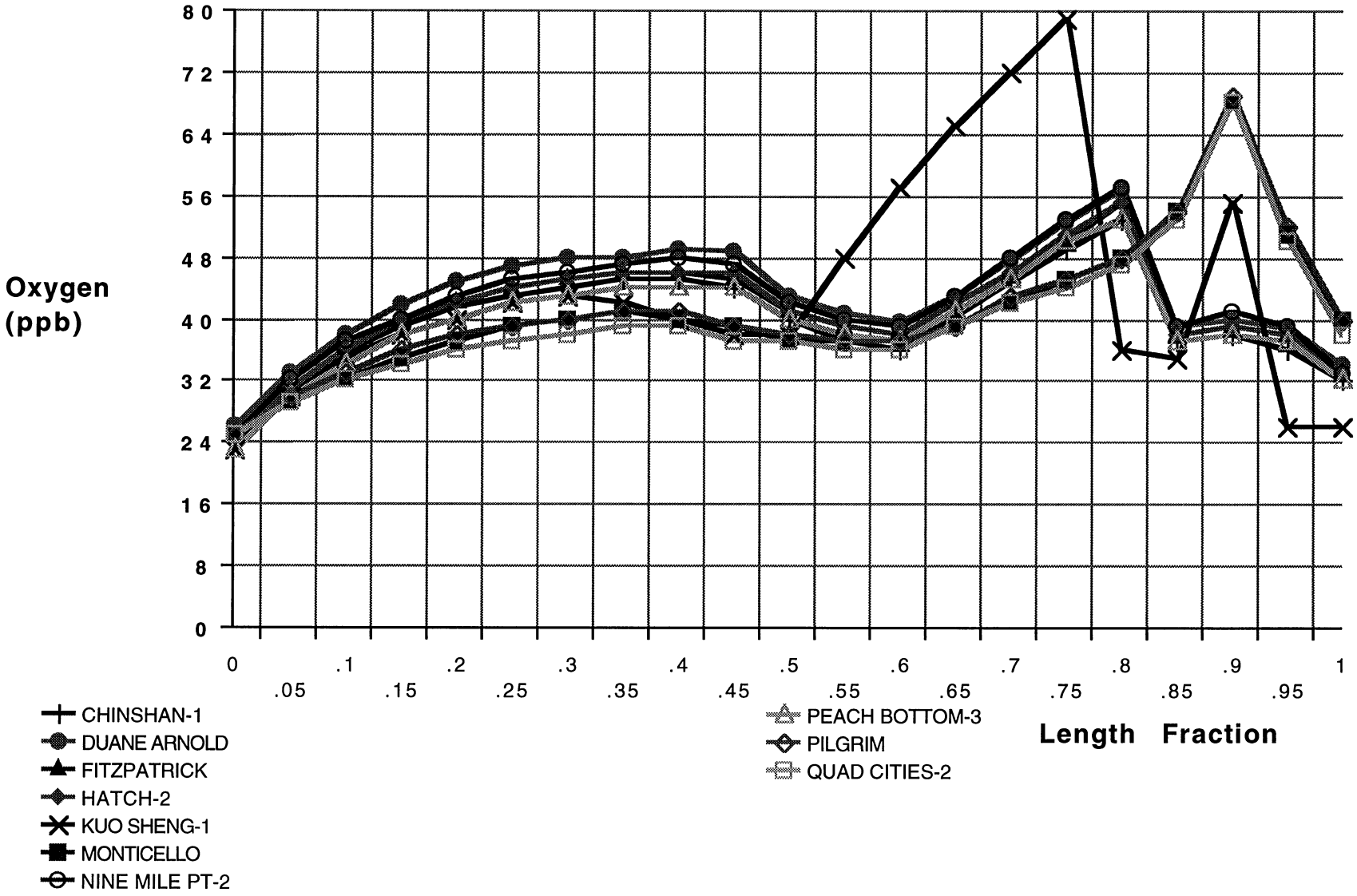

EPRI Licensed Material

Figure A-82: Steam Separator Oxygen Levels with 3.0 ppm Feedwater H2 Addition

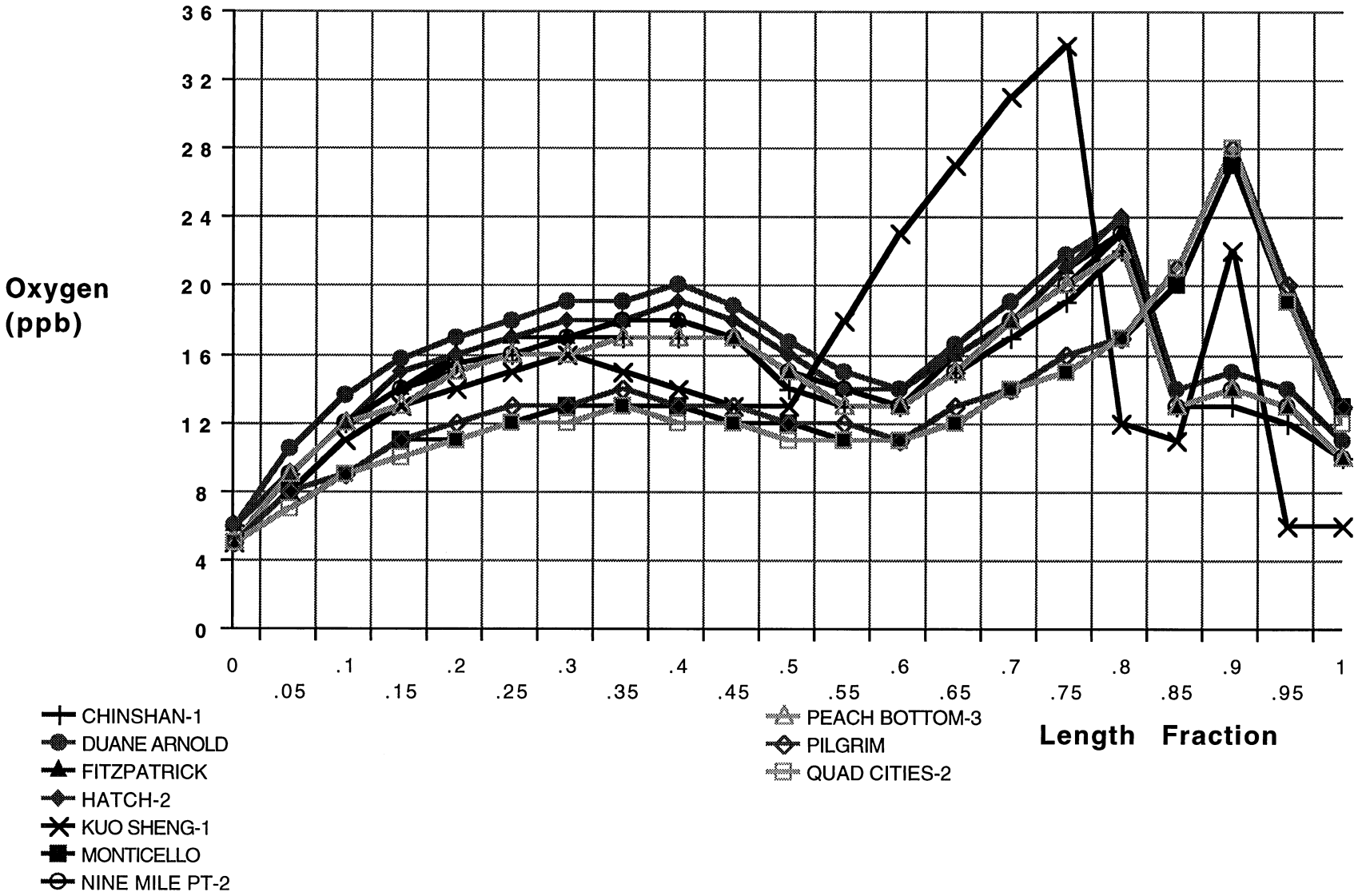

EPRI Licensed Material

Figure A-83: Steam Separator Peroxide Levels with 0 ppm Feedwater H2 Addition

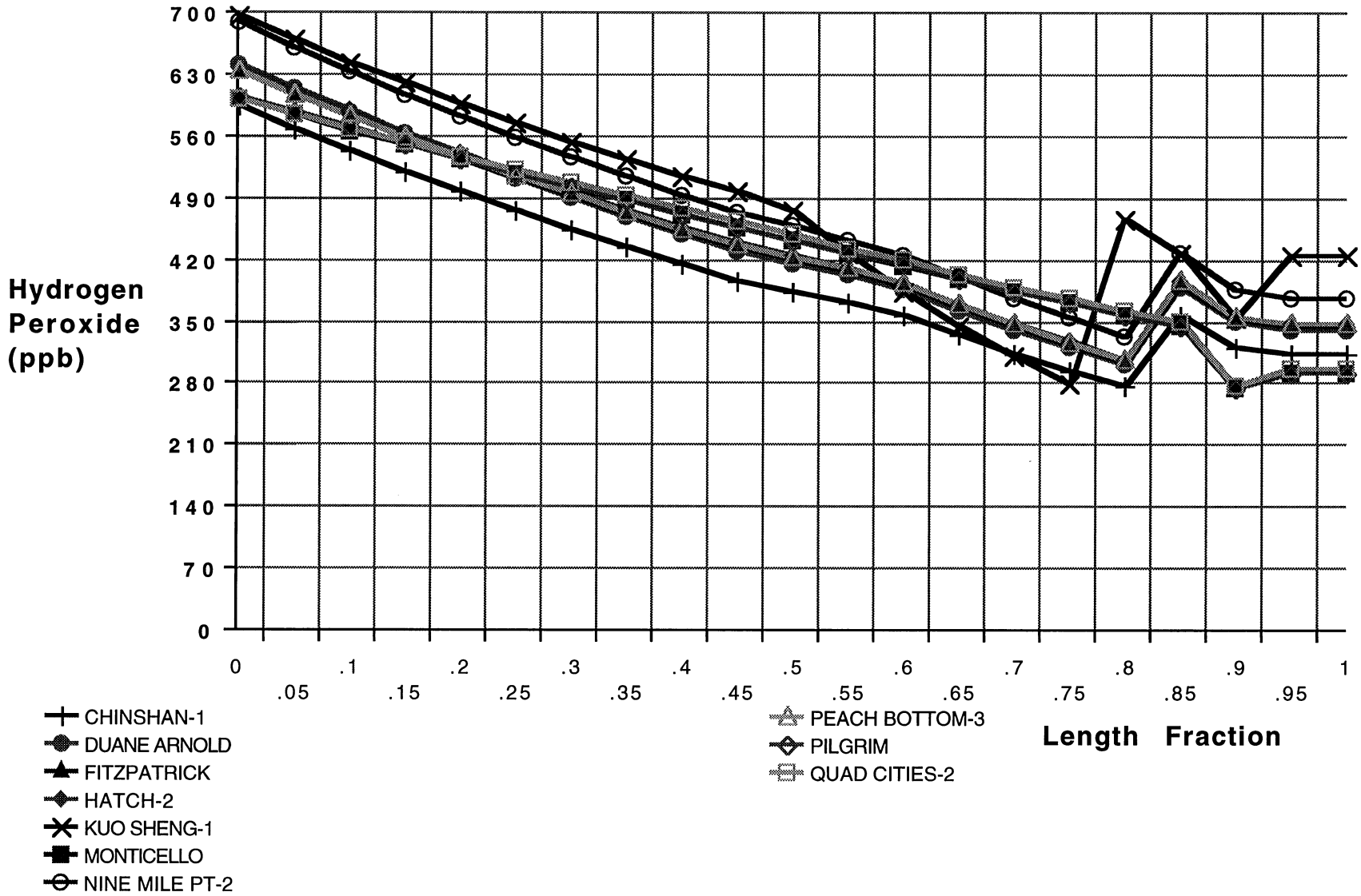

EPRI Licensed Material

Figure A-84: Steam Separator Peroxide Levels with 0.6 ppm Feedwater H2 Addition

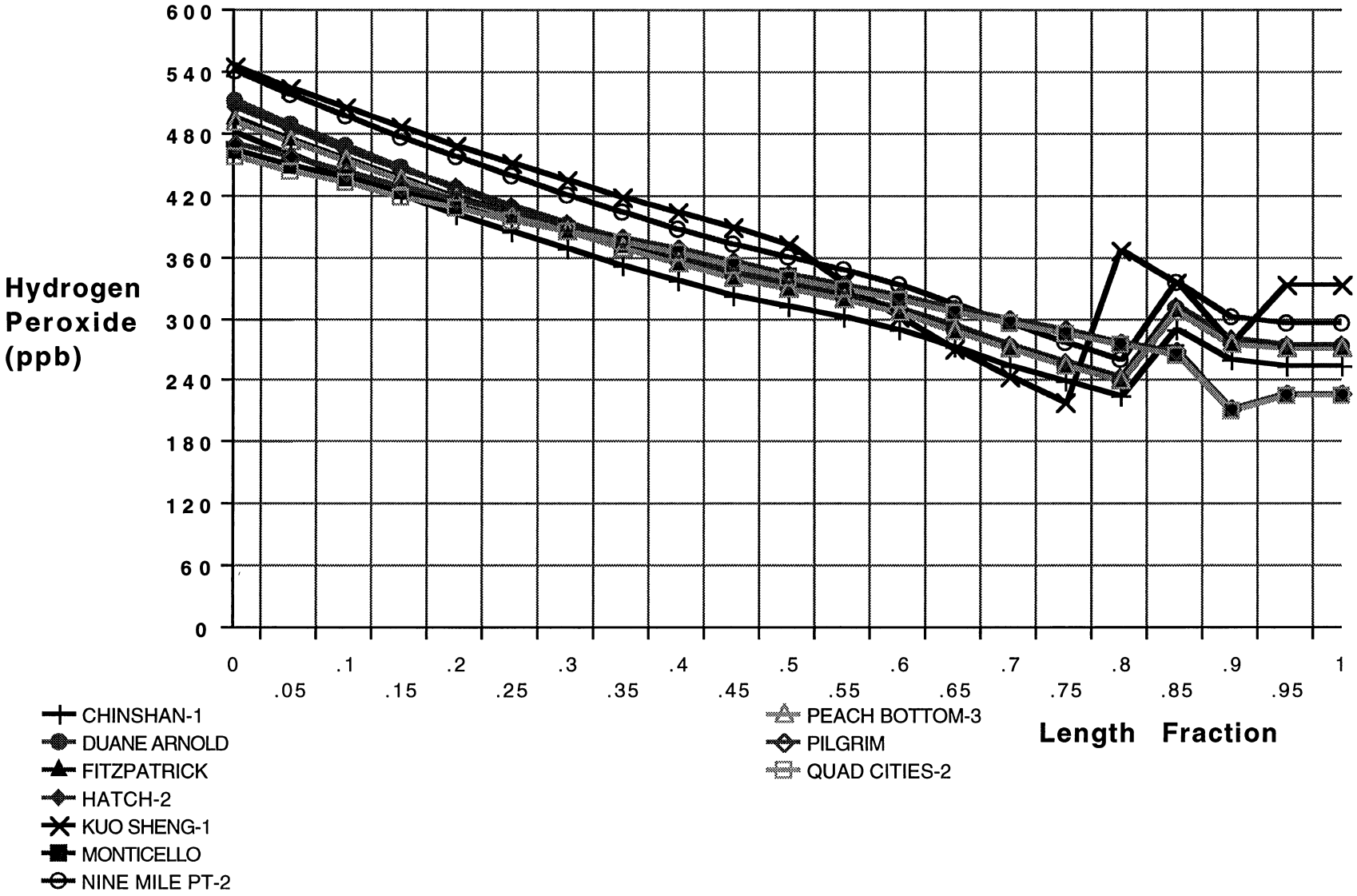

EPRI Licensed Material

Figure A-85: Steam Separator Peroxide Levels with 1.5 ppm Feedwater H2 Addition

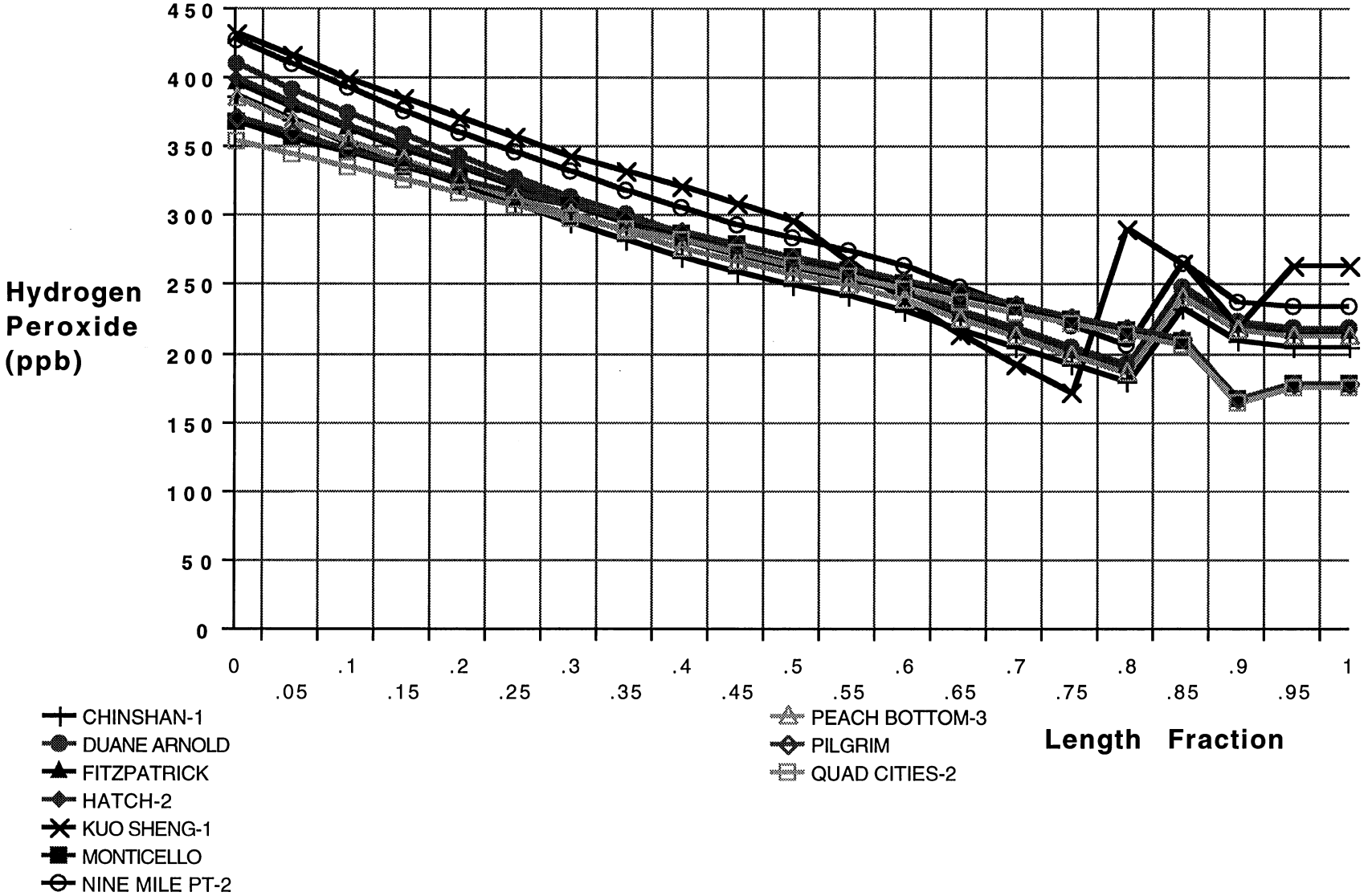

EPRI Licensed Material

Figure A-86: Steam Separator Peroxide Levels with 3.0 ppm Feedwater H2 Addition

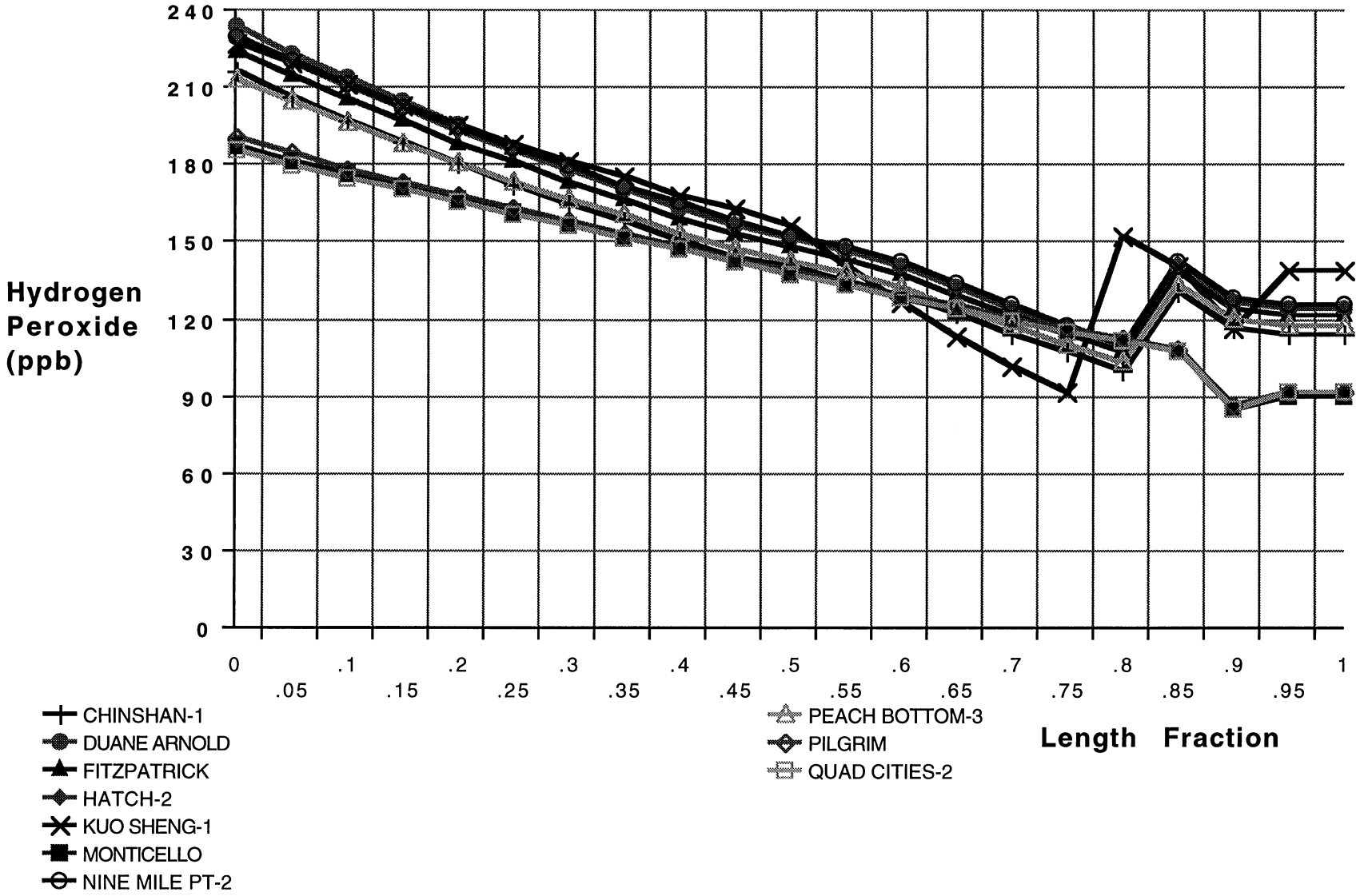

EPRI Licensed Material

Figure A-87: Mixing Plenum Region ECPs with 0 ppm Feedwater H2 Addition

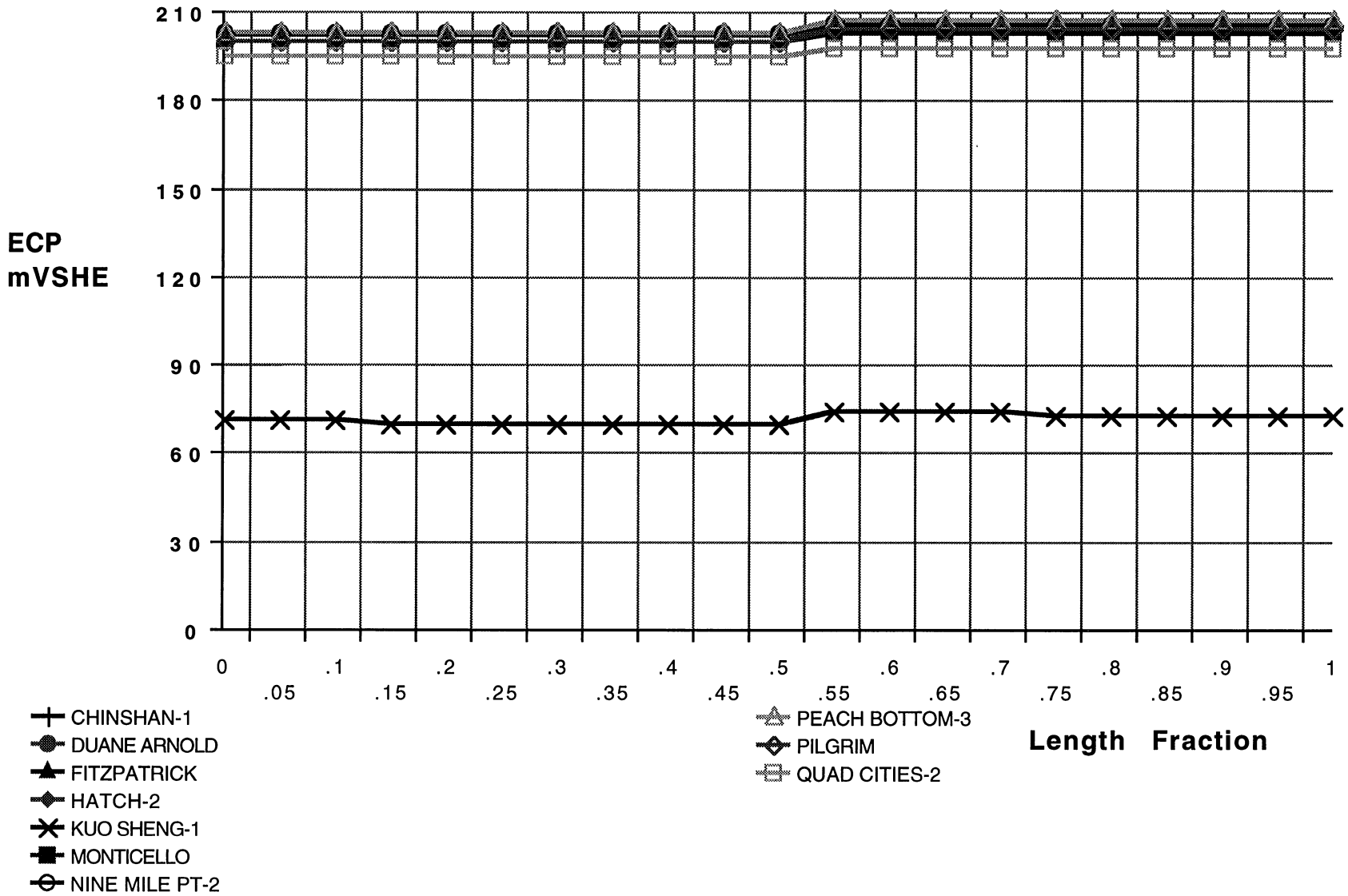

EPRI Licensed Material

Figure A-88: Mixing Plenum Region ECPs with 0.6 ppm Feedwater H2 Addition

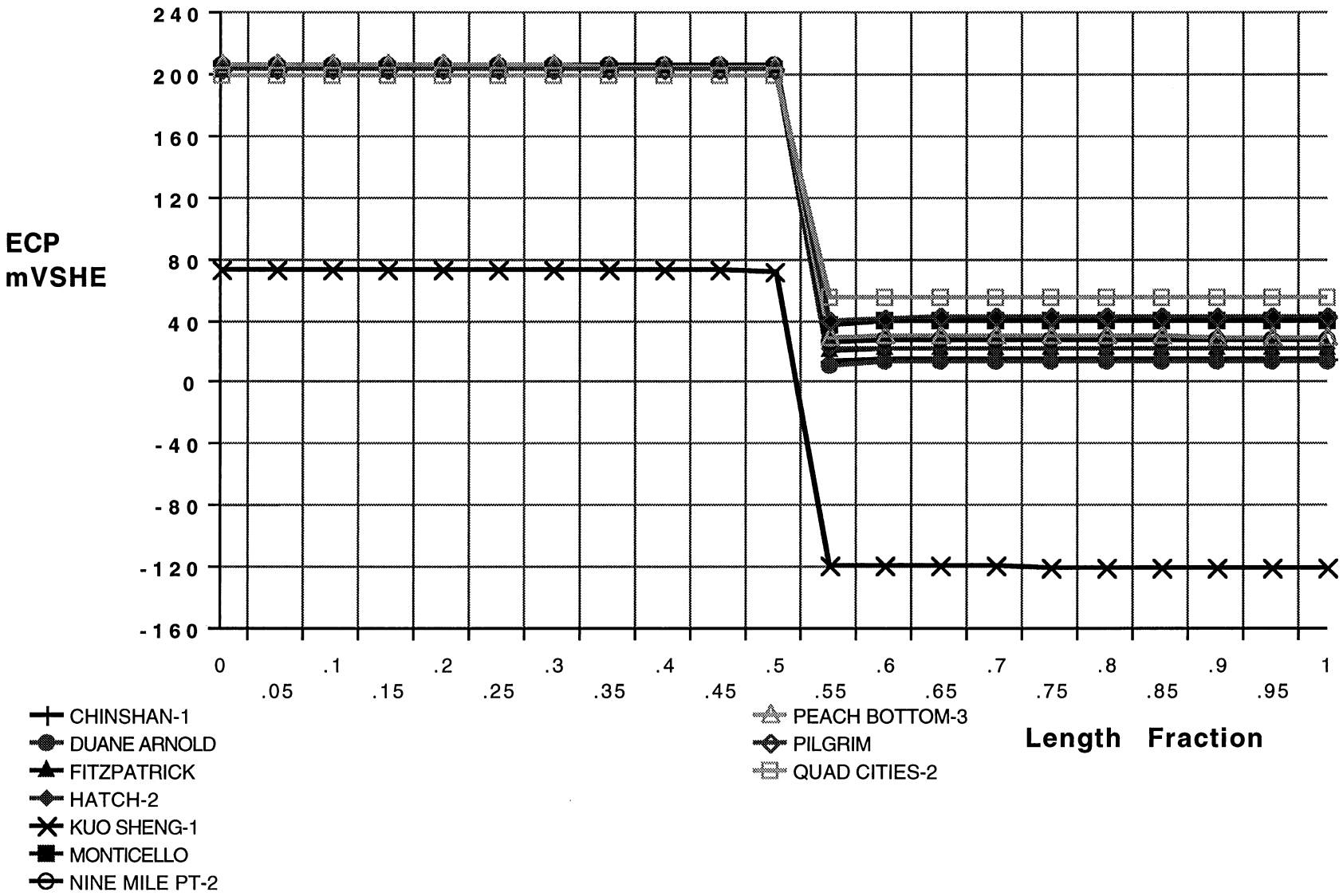

EPRI Licensed Material

Figure A-89: Mixing Plenum Region ECPs with 1.5 ppm Feedwater H2 Addition

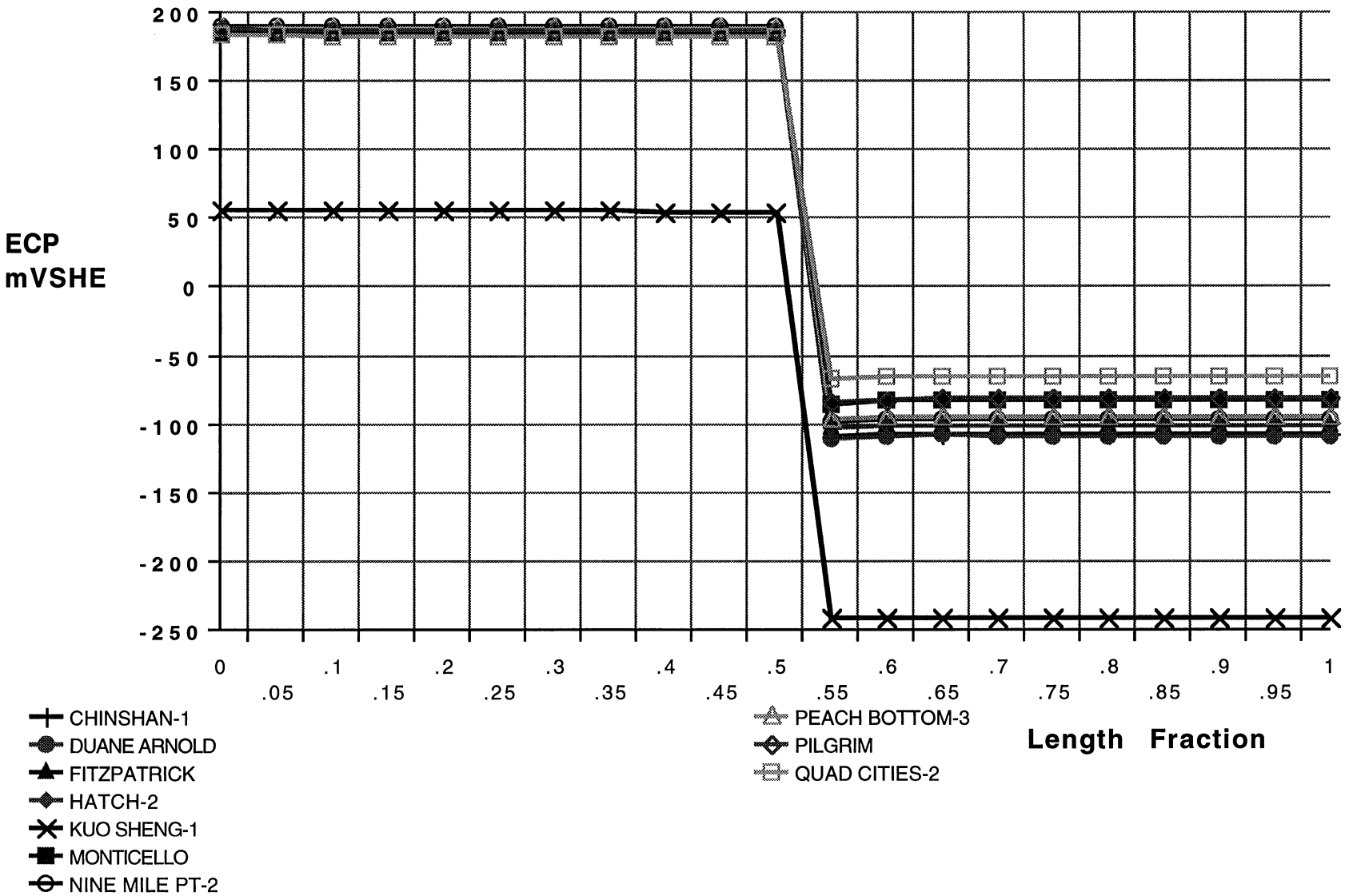

EPRI Licensed Material

Figure A-90: Mixing Plenum Region ECPs with 3.0 ppm Feedwater H2 Addition

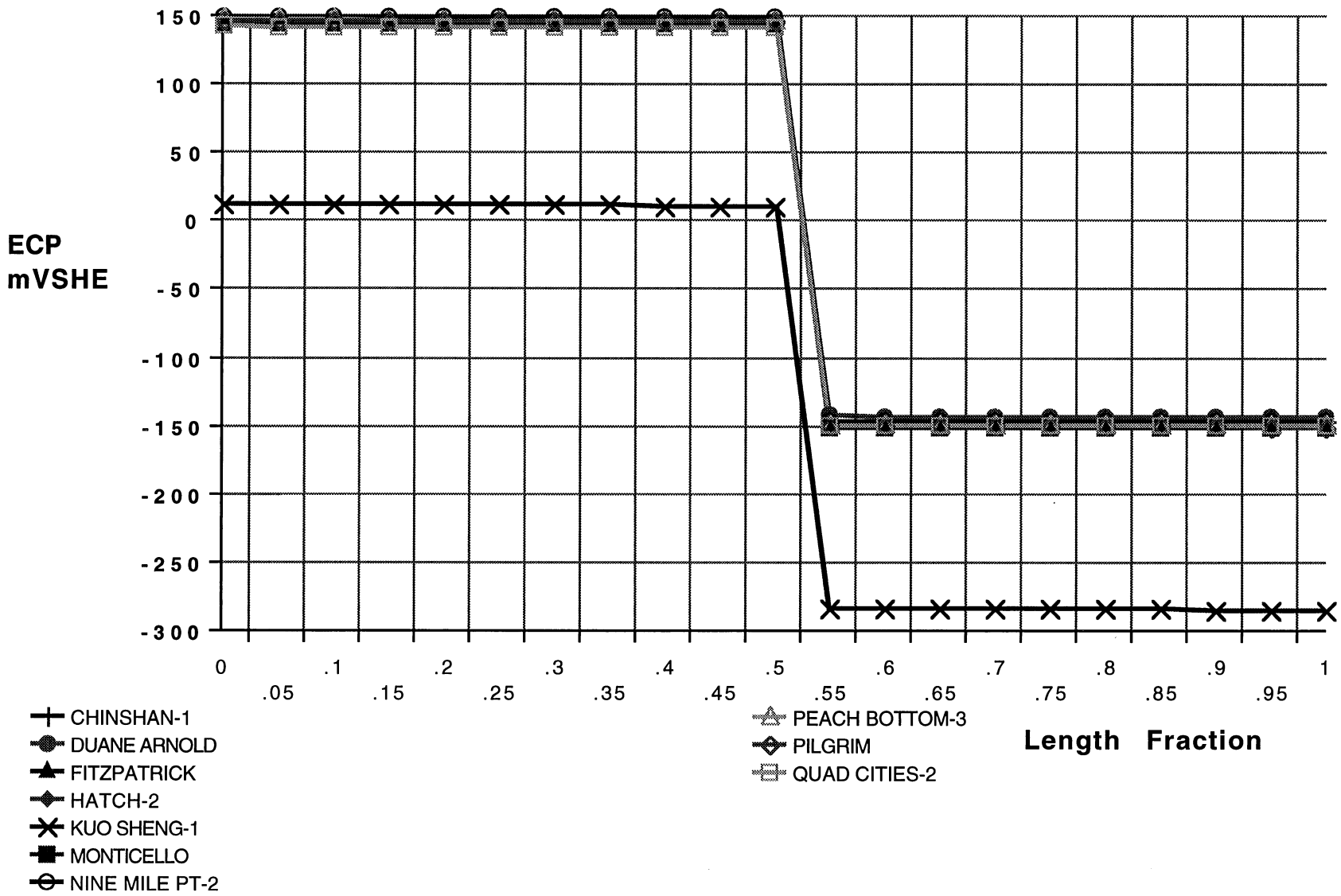

EPRI Licensed Material

Figure A-91: Mixing Plenum Hydrogen Levels with 0 ppm Feedwater H2 Addition

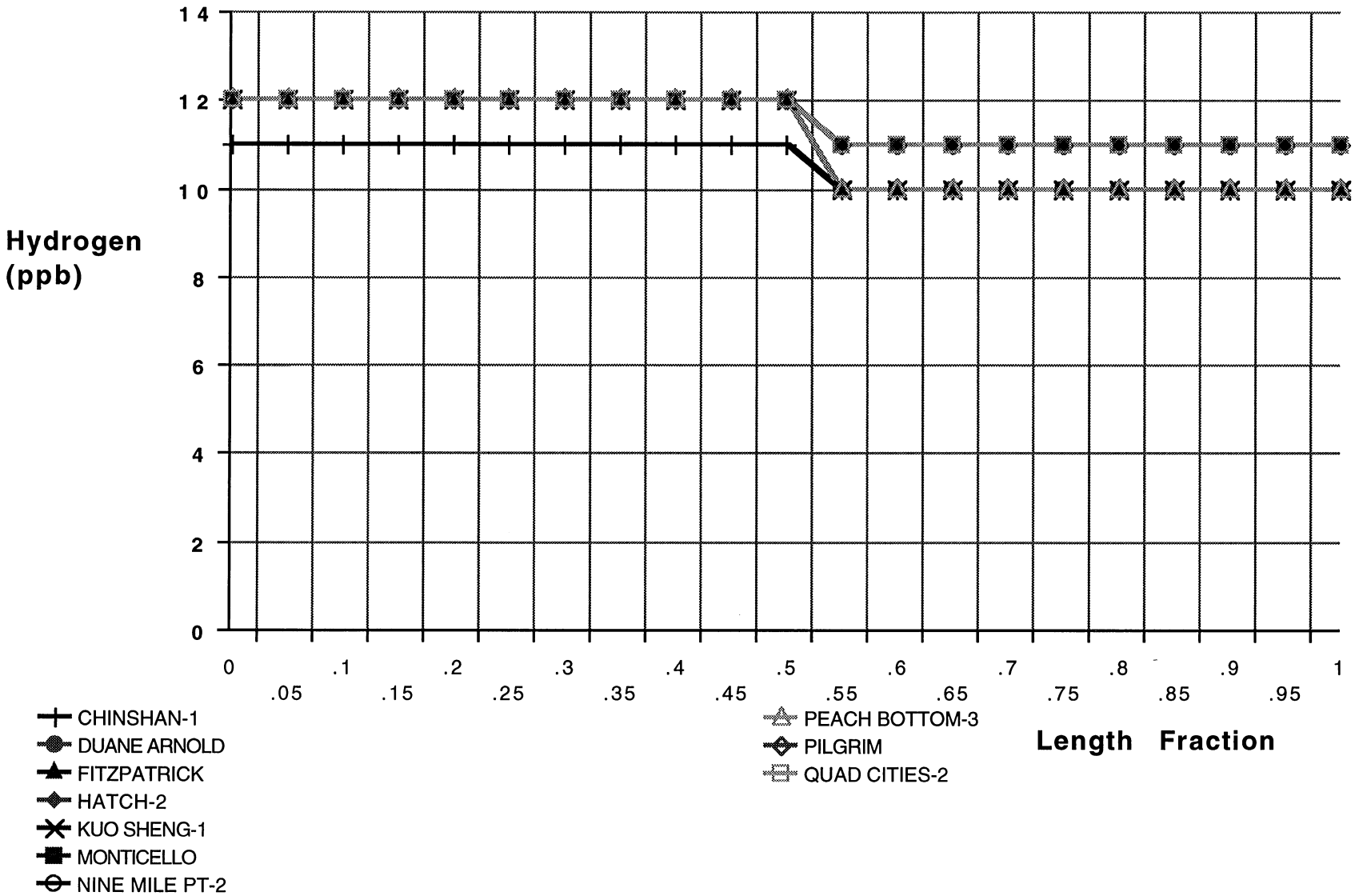

EPRI Licensed Material

Figure A-92: Mixing Plenum Hydrogen Levels with 0.6 ppm Feedwater H2 Addition

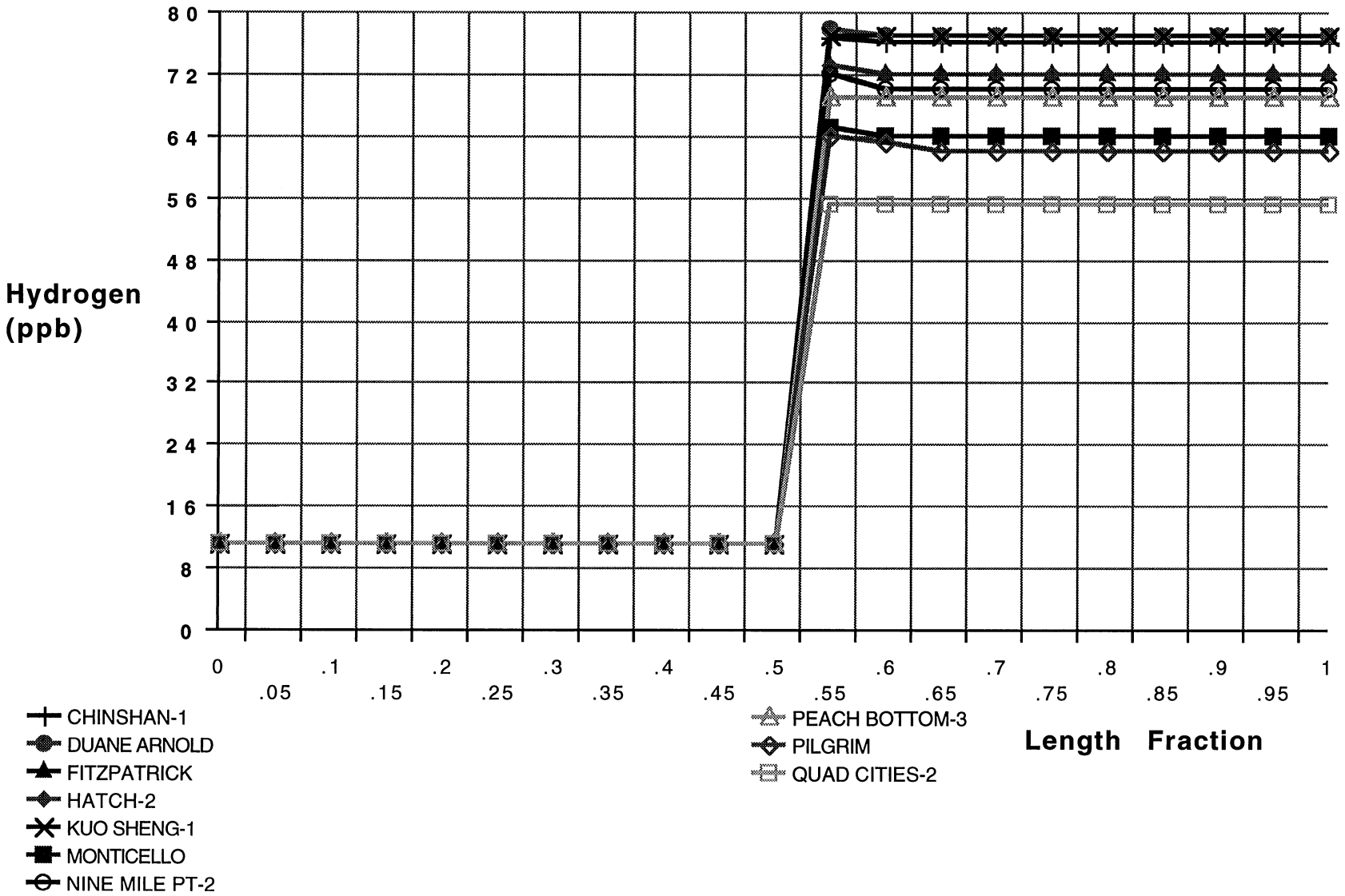

EPRI Licensed Material

Figure A-93: Mixing Plenum Hydrogen Levels with 1.5 ppm Feedwater H2 Addition

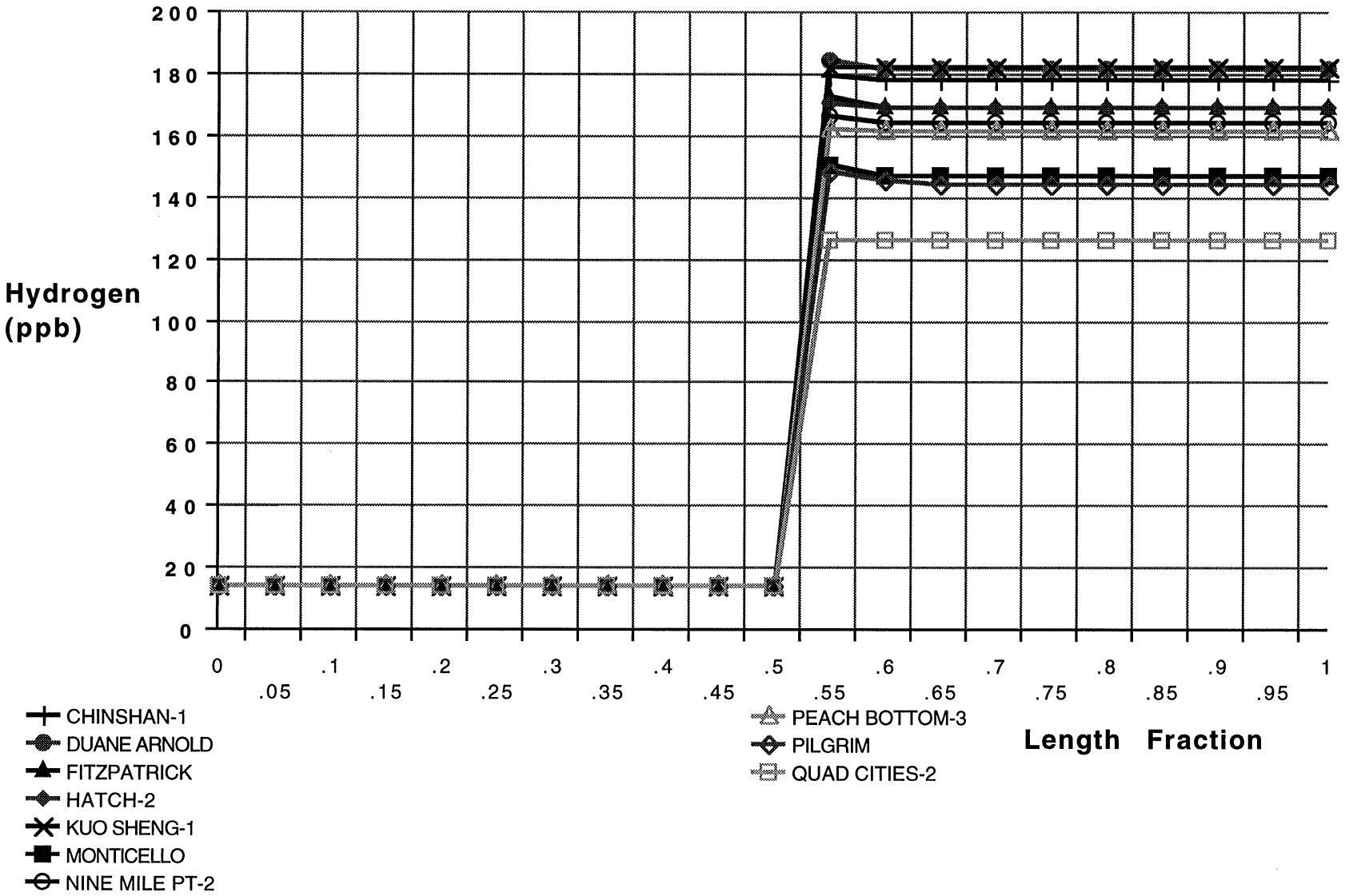

EPRI Licensed Material

Figure A-94: Mixing Plenum Hydrogen Levels with 3.0 ppm Feedwater H2 Addition

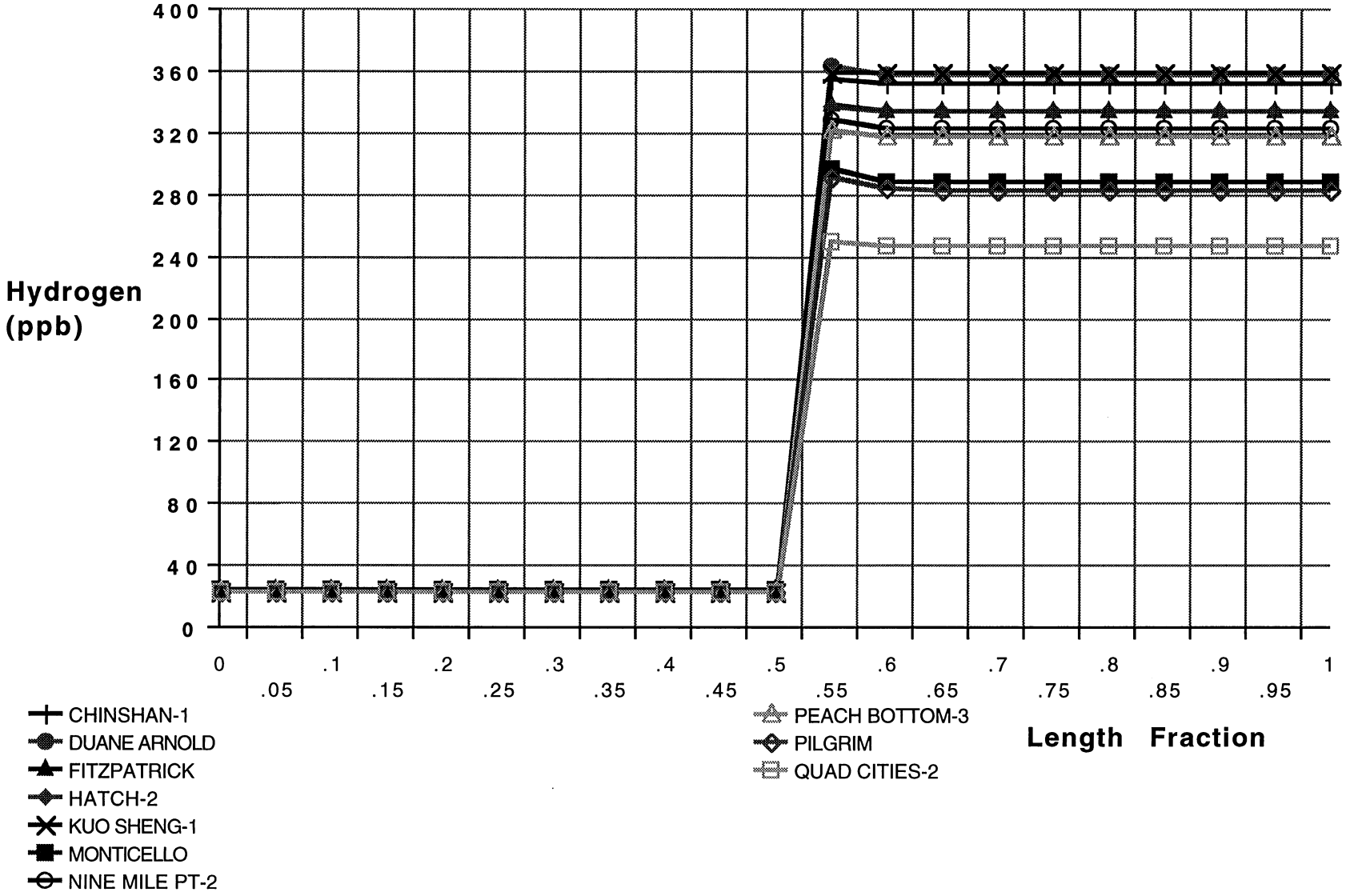

EPRI Licensed Material

Figure A-95: Mixing Plenum Oxygen Levels with 0 ppm Feedwater H2 Addition

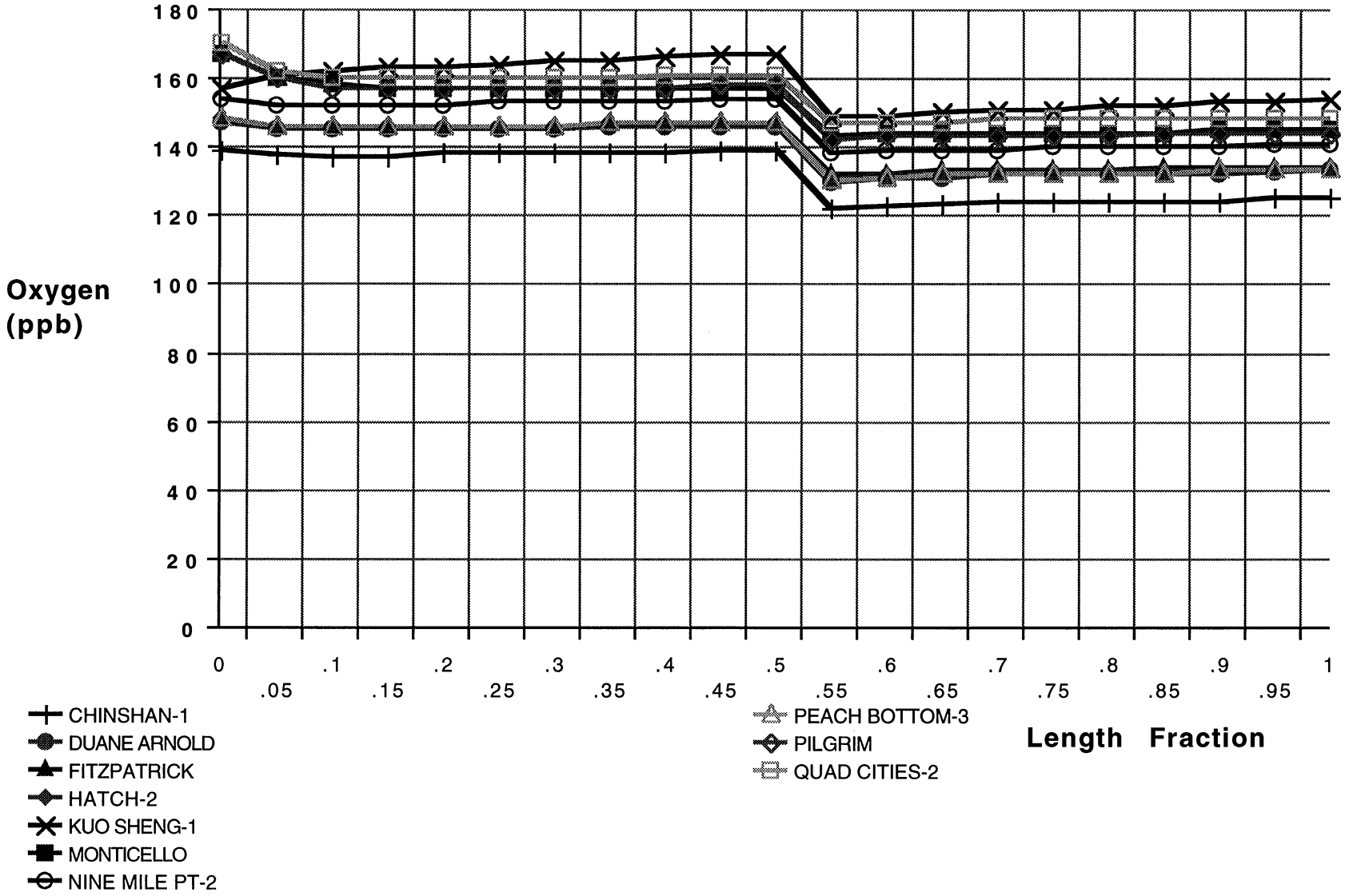

EPRI Licensed Material

Figure A-96: Mixing Plenum Oxygen Levels with 0.6 ppm Feedwater H2 Addition

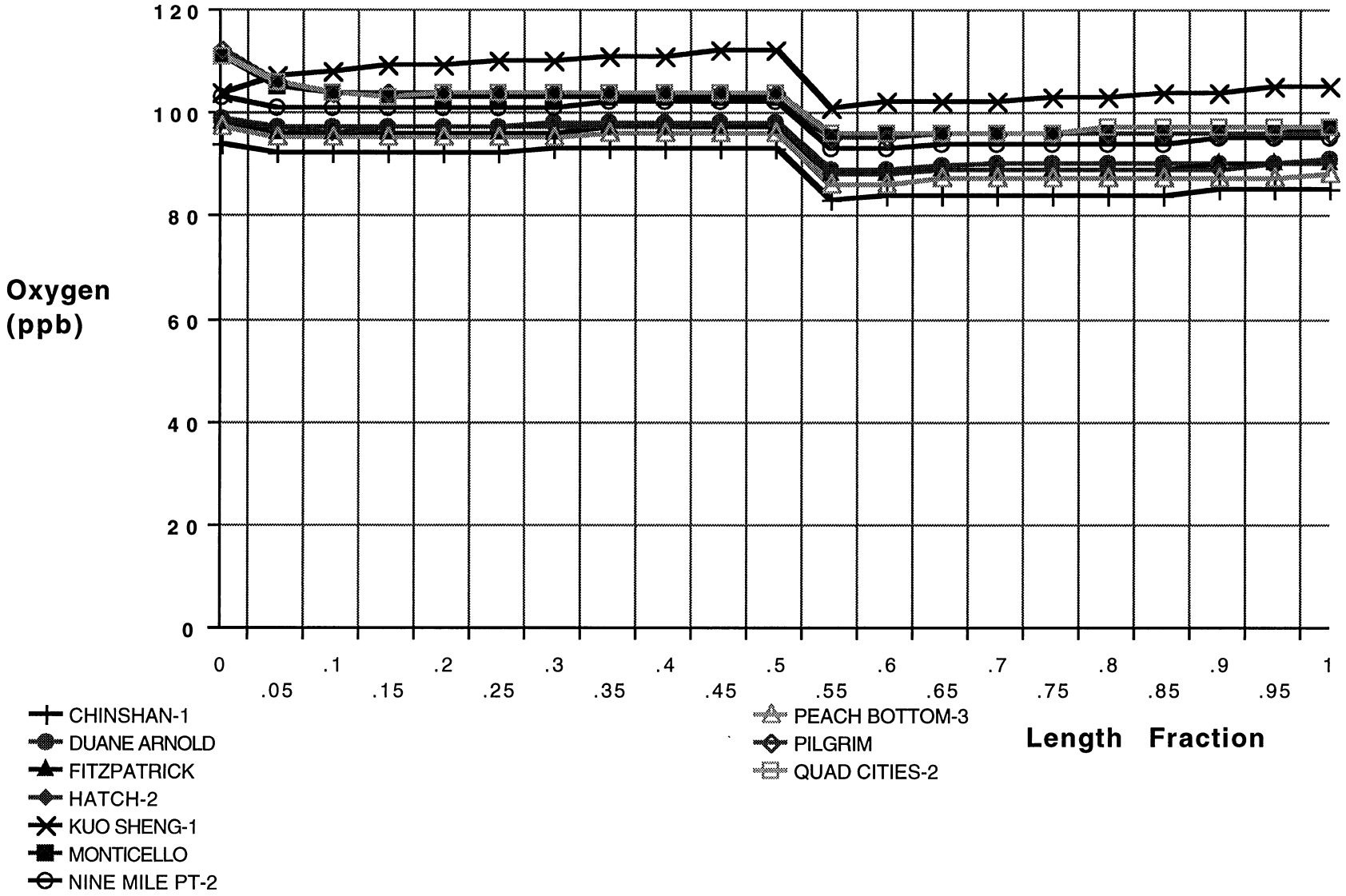

EPRI Licensed Material

Figure A-97: Mixing Plenum Oxygen Levels with 1.5 ppm Feedwater H2 Addition

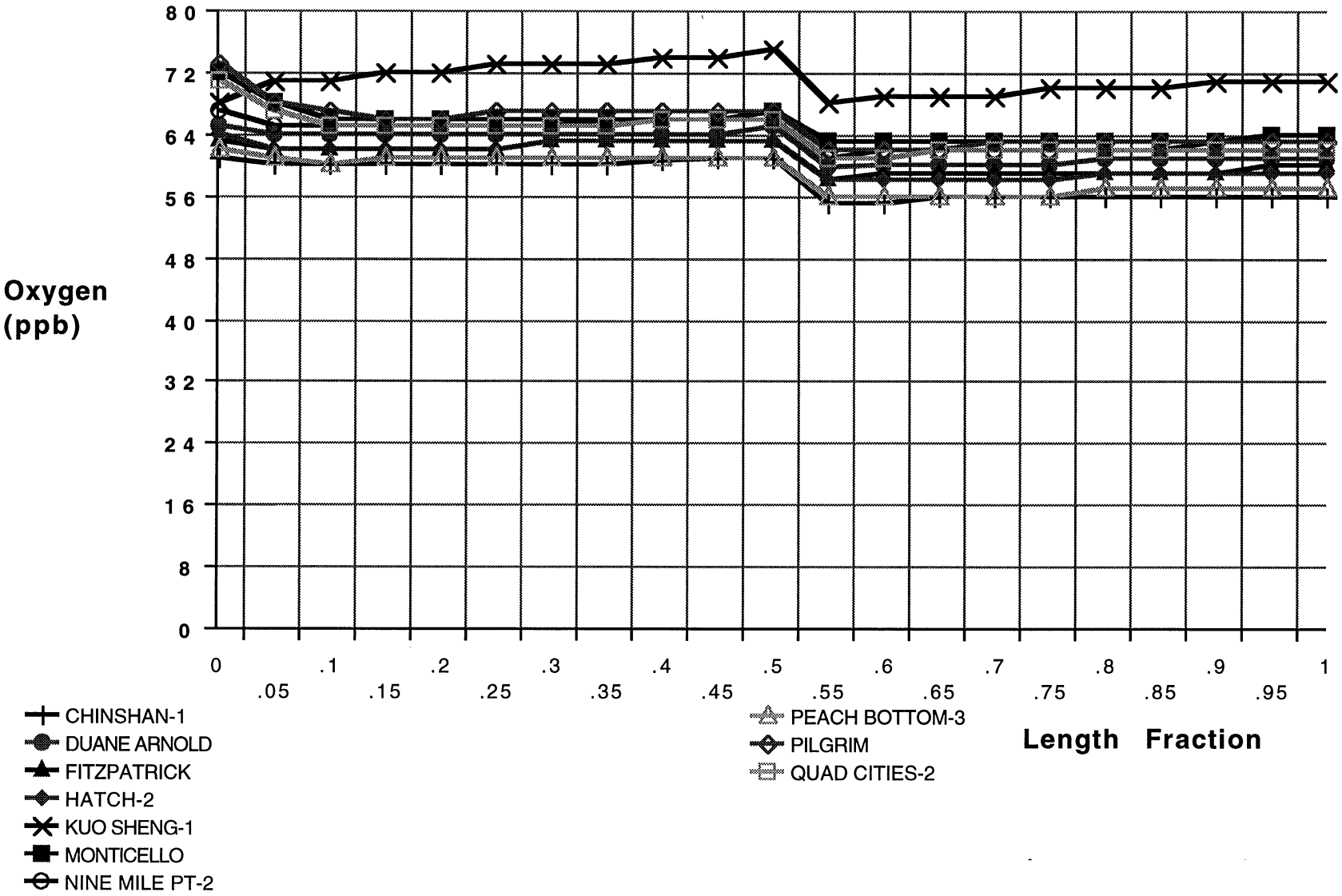

EPRI Licensed Material

Figure A-98: Mixing Plenum Oxygen Levels with 3.0 ppm Feedwater H2 Addition

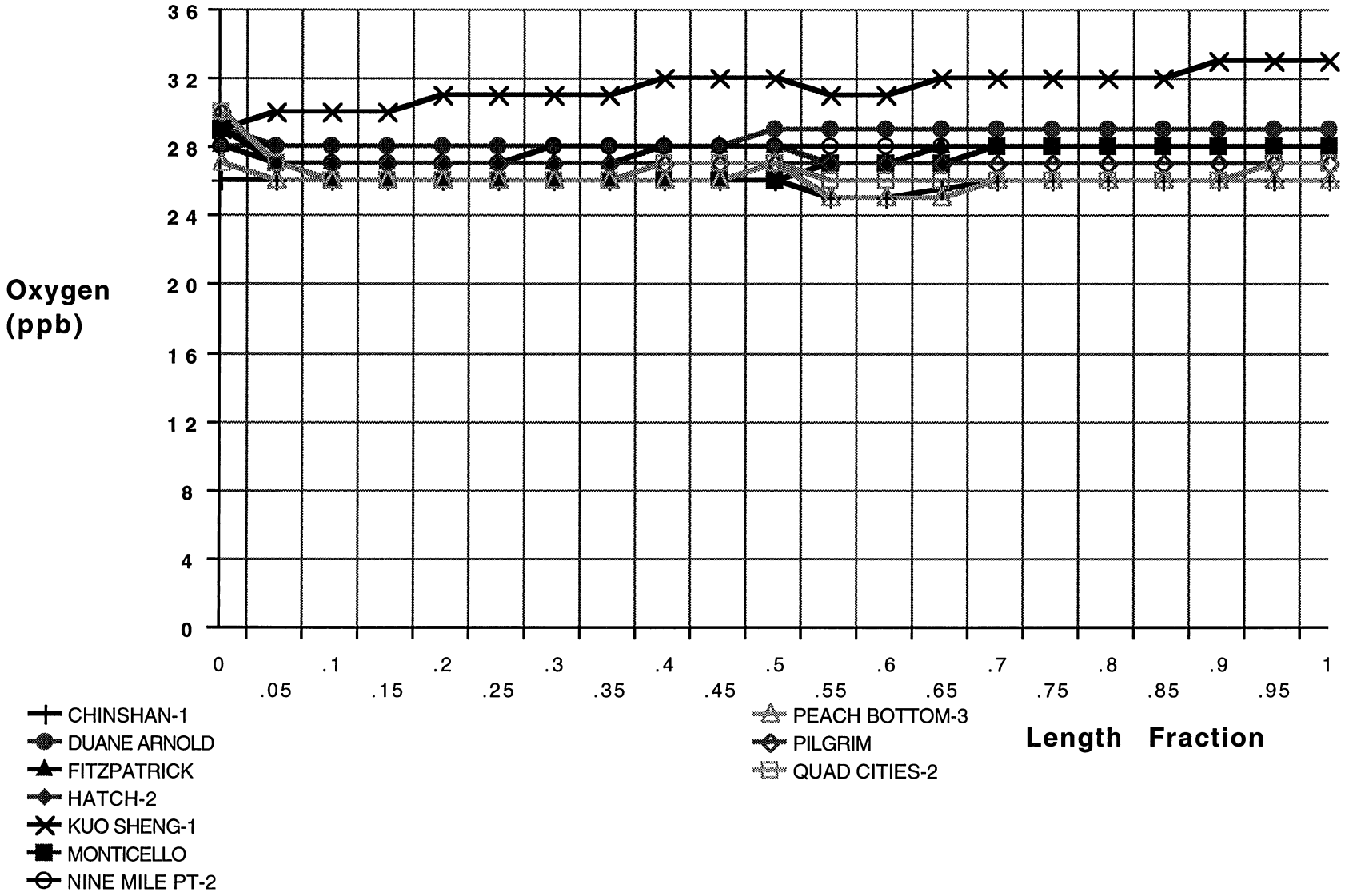

EPRI Licensed Material

Figure A-99: Mixing Plenum Peroxide Levels with 0 ppm Feedwater H2 Addition

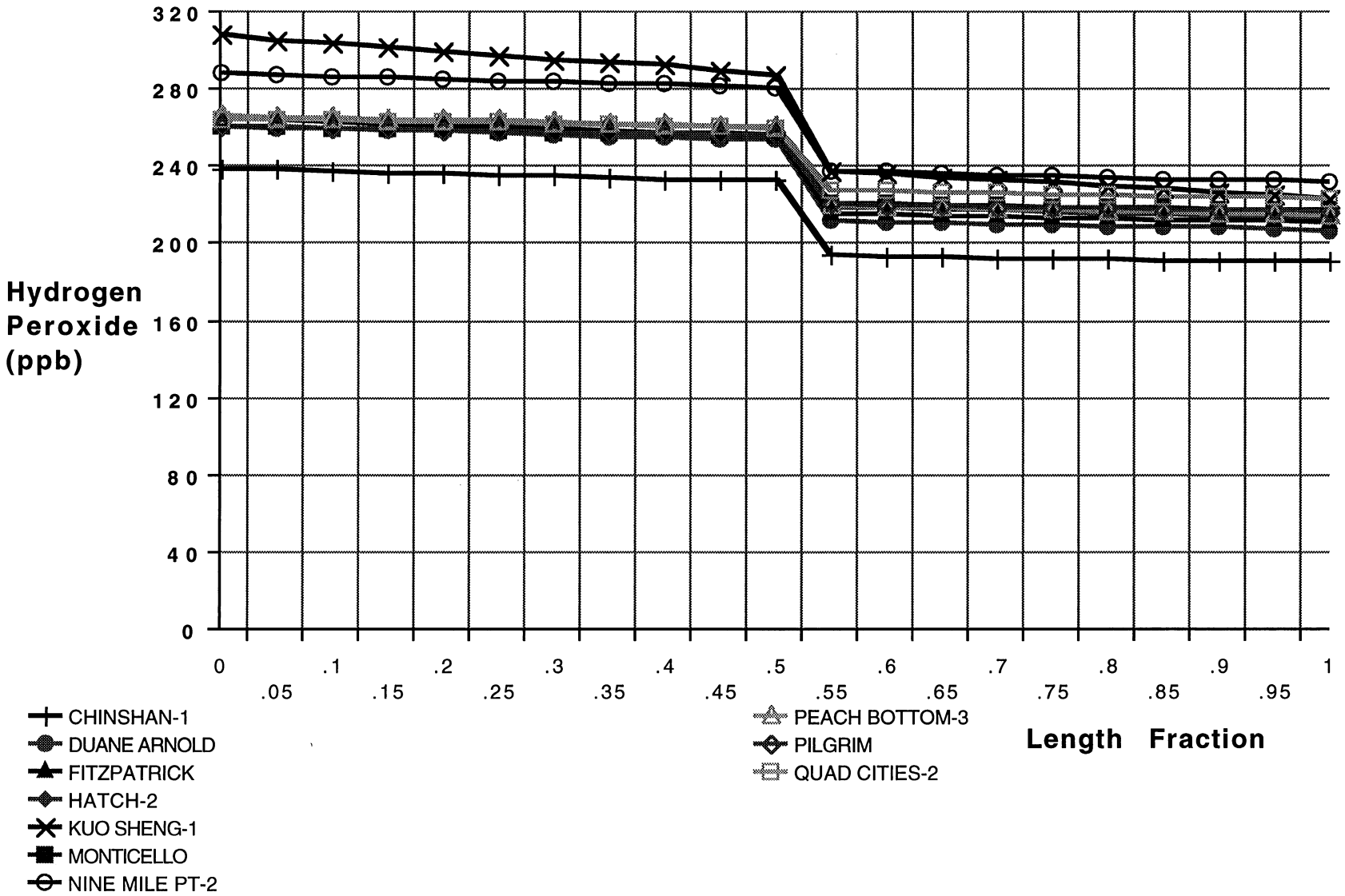

EPRI Licensed Material

Figure A-100: Mixing Plenum Peroxide Levels with 0.6 ppm Feedwater H2 Addition

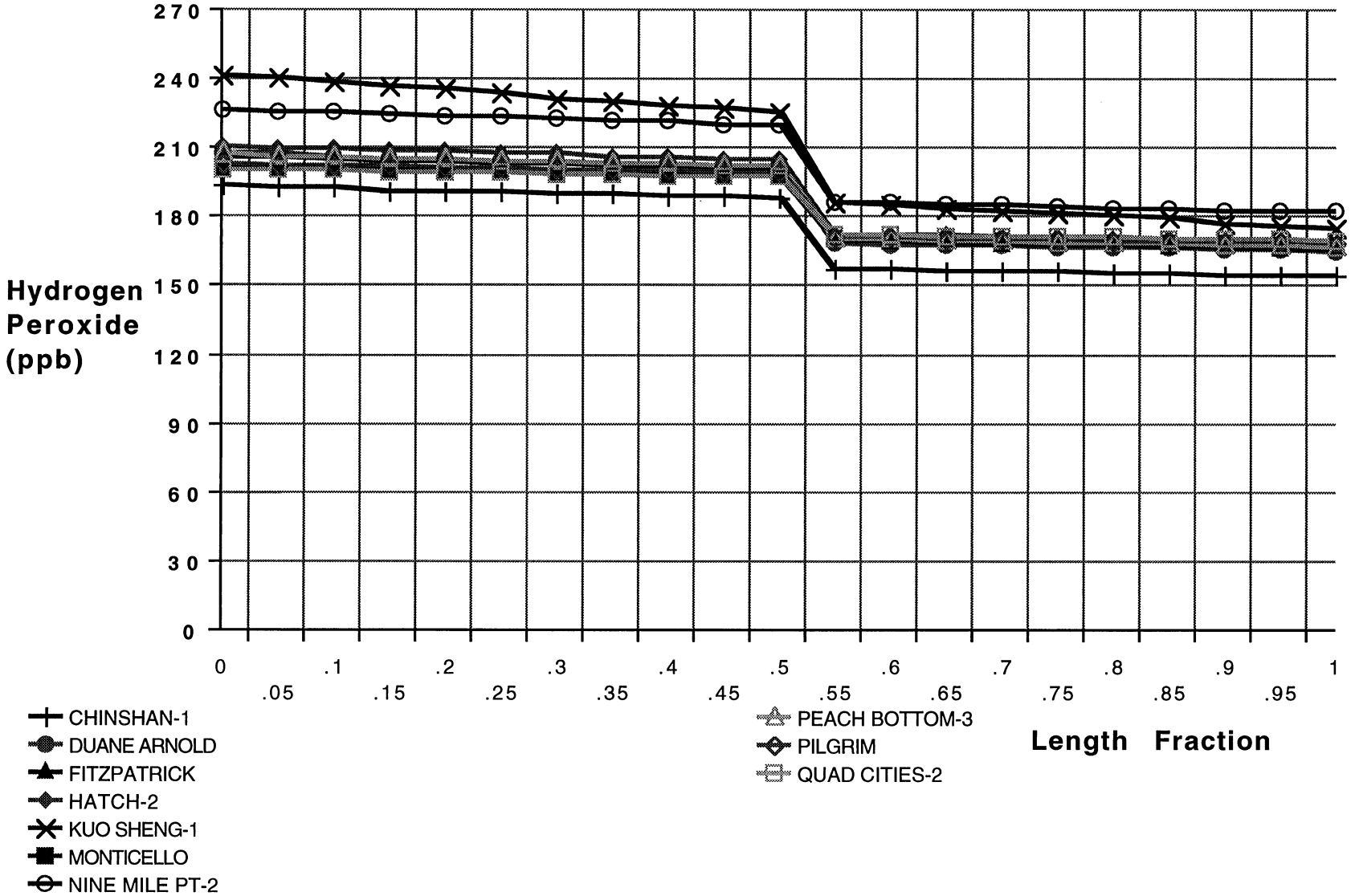

EPRI Licensed Material

Figure A-101: Mixing Plenum Peroxide Levels with 1.5 ppm Feedwater H2 Addition

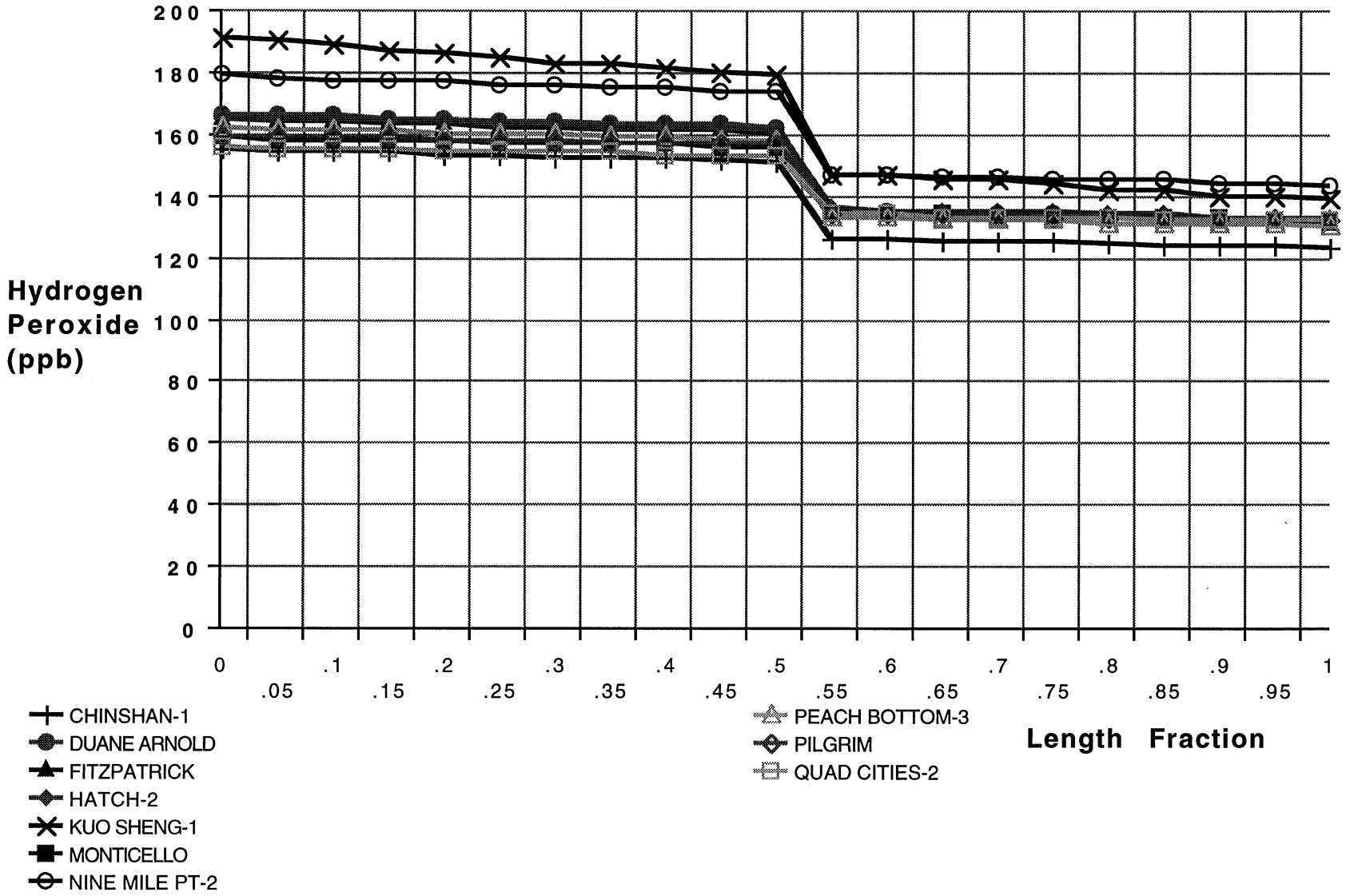

EPRI Licensed Material

Figure A-102: Mixing Plenum Peroxide Levels with 3.0 ppm Feedwater H2 Addition

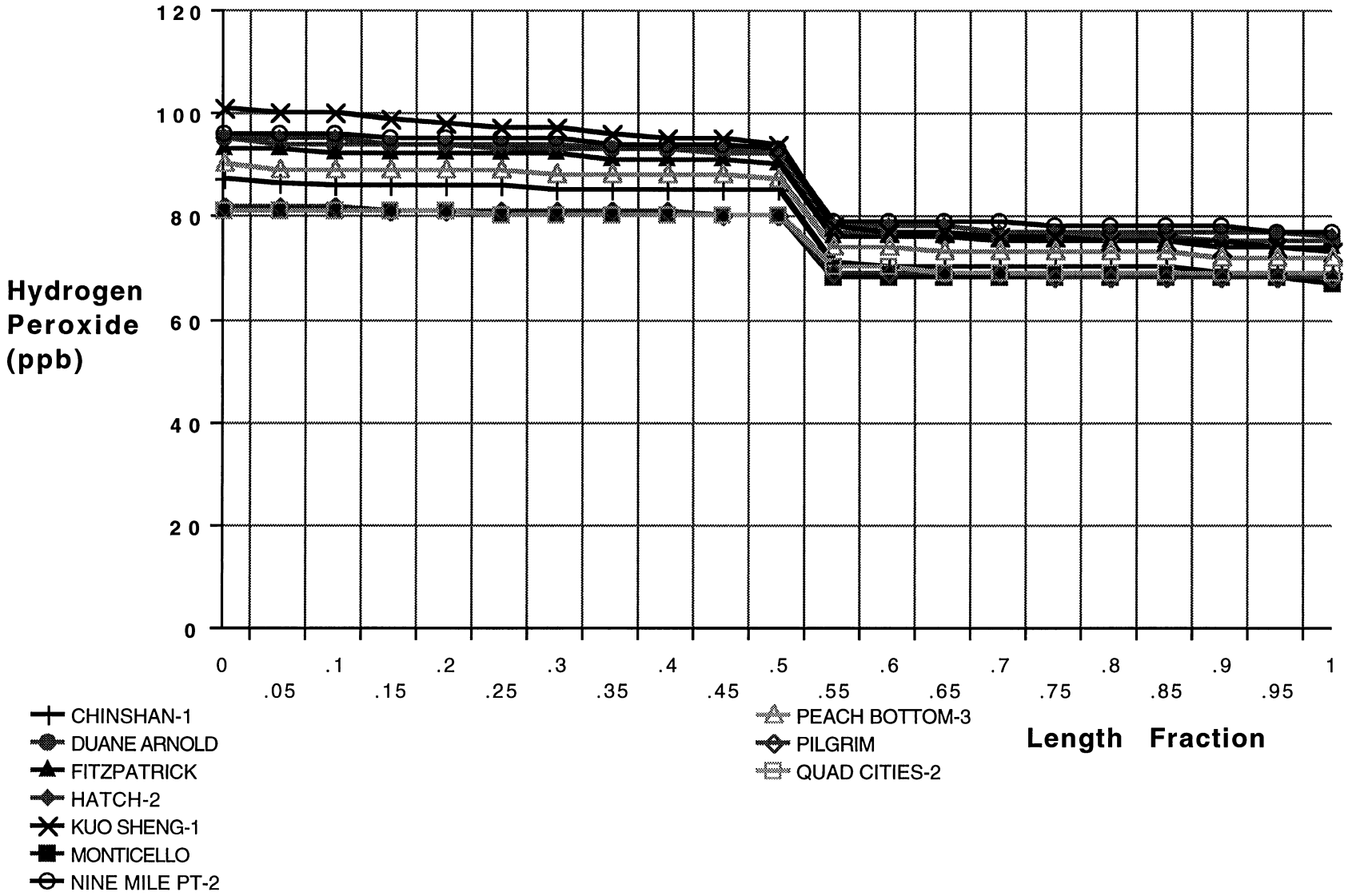

EPRI Licensed Material

Figure A-103: Downcomer Region ECPs with 0 ppm Feedwater H2 Addition

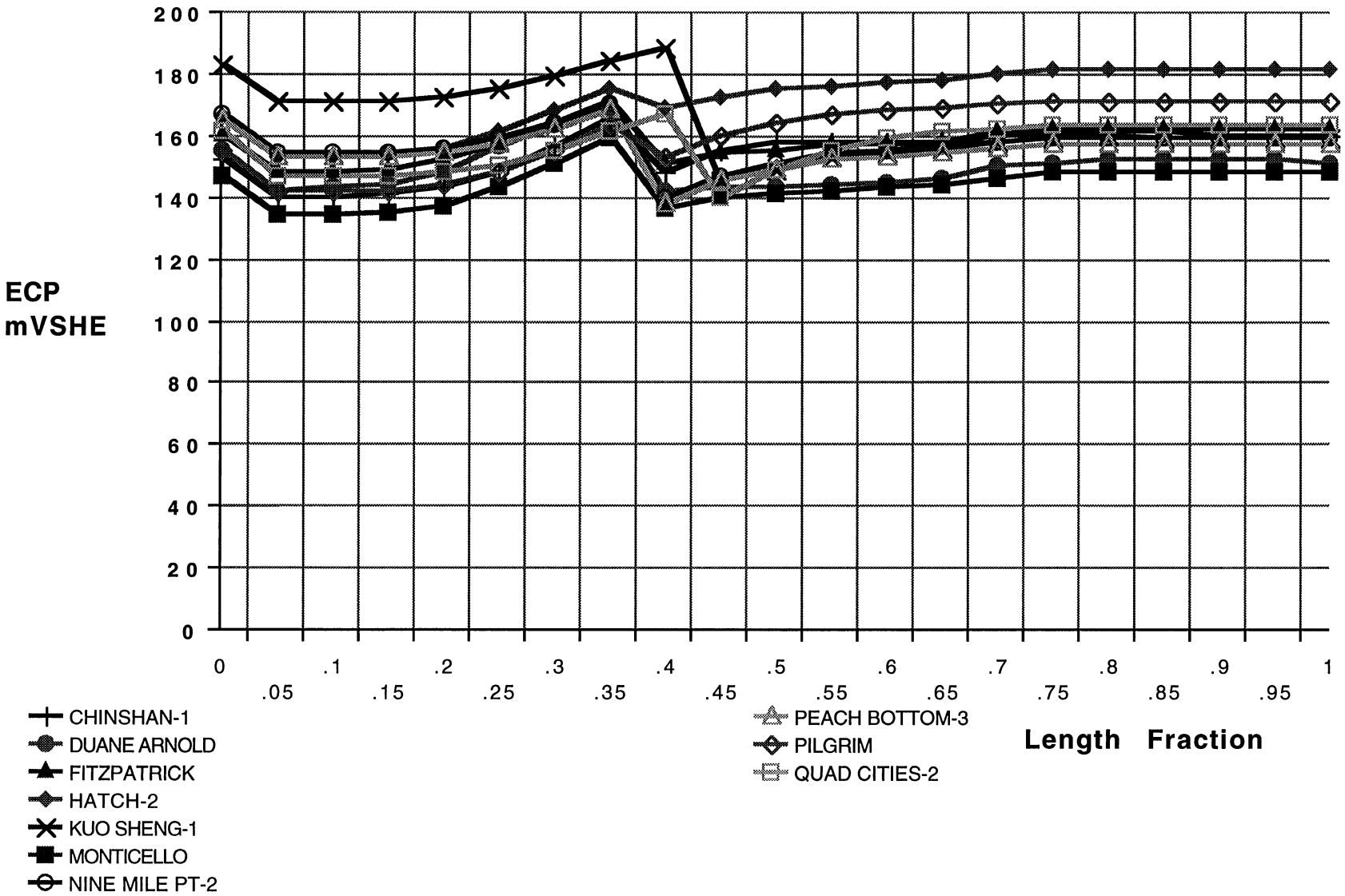

EPRI Licensed Material

Figure A-104: Downcomer Region ECPs with 0.6 ppm Feedwater H2 Addition

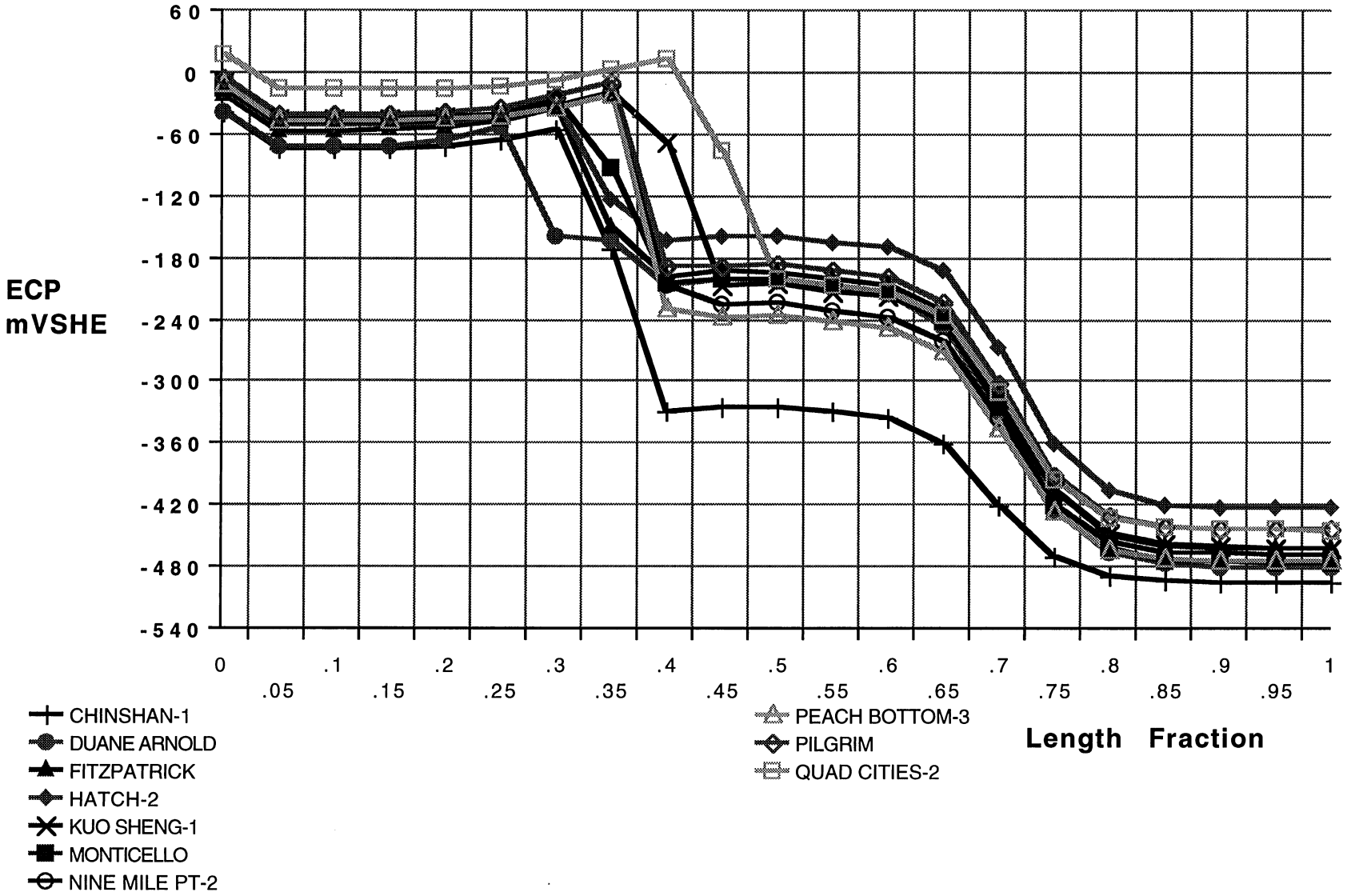

EPRI Licensed Material

Figure A-105: Downcomer Region ECPs with 1.5 ppm Feedwater H2 Addition

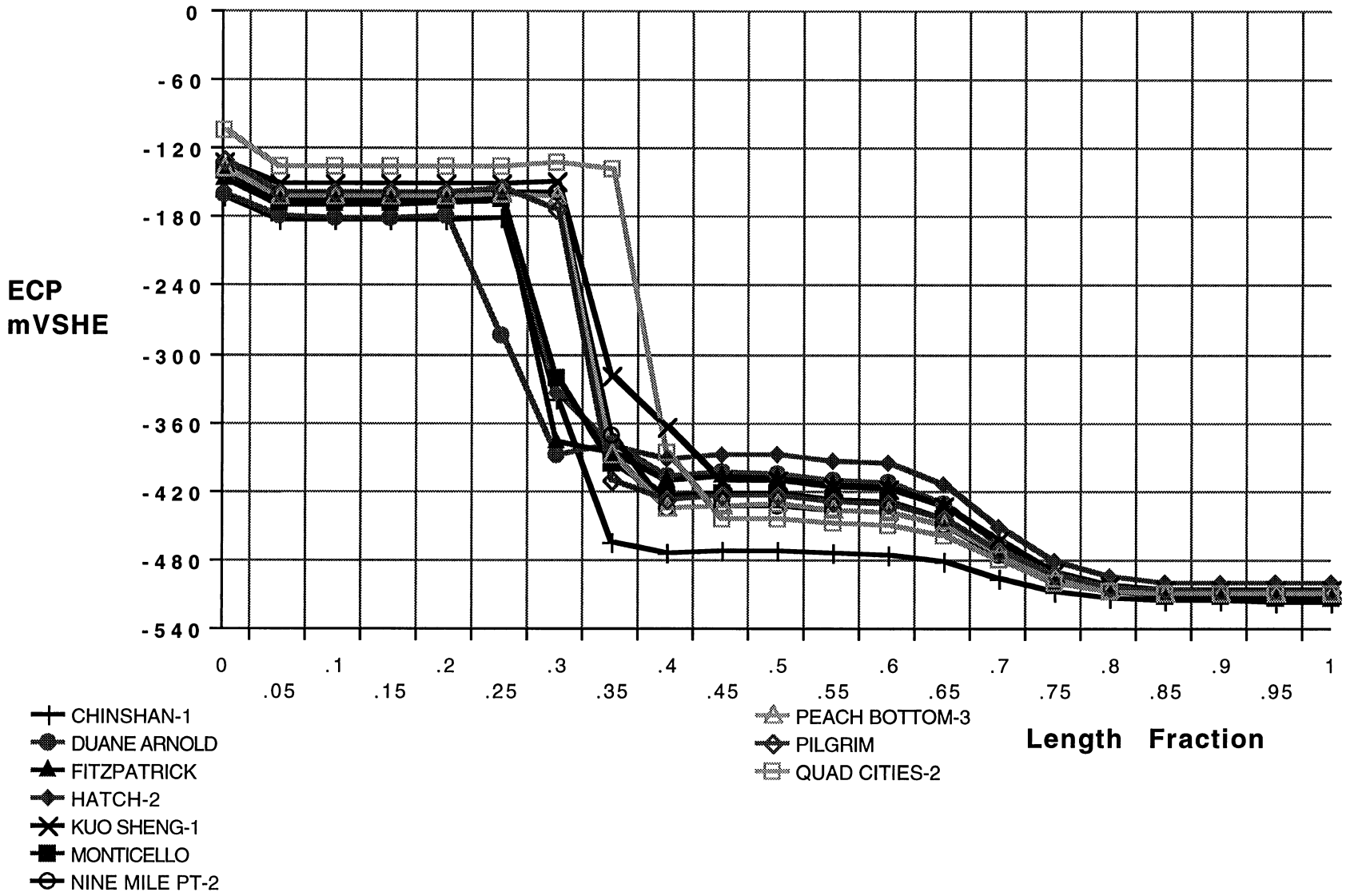

EPRI Licensed Material

Figure A-106: Downcomer Region ECPs with 3.0 ppm Feedwater H2 Addition

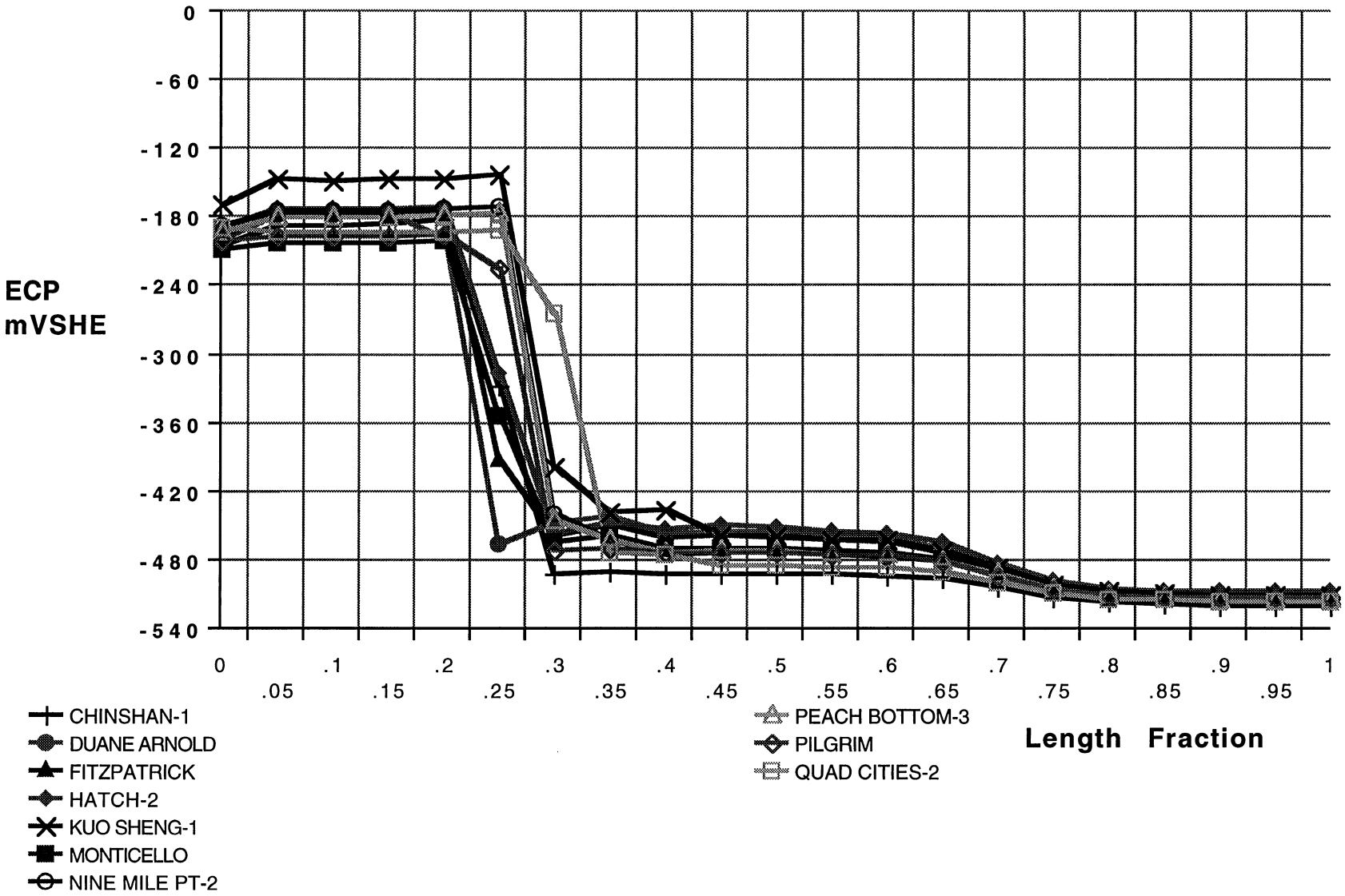

EPRI Licensed Material

Figure A-107: Downcomer Hydrogen Levels with 0 ppm Feedwater H2 Addition

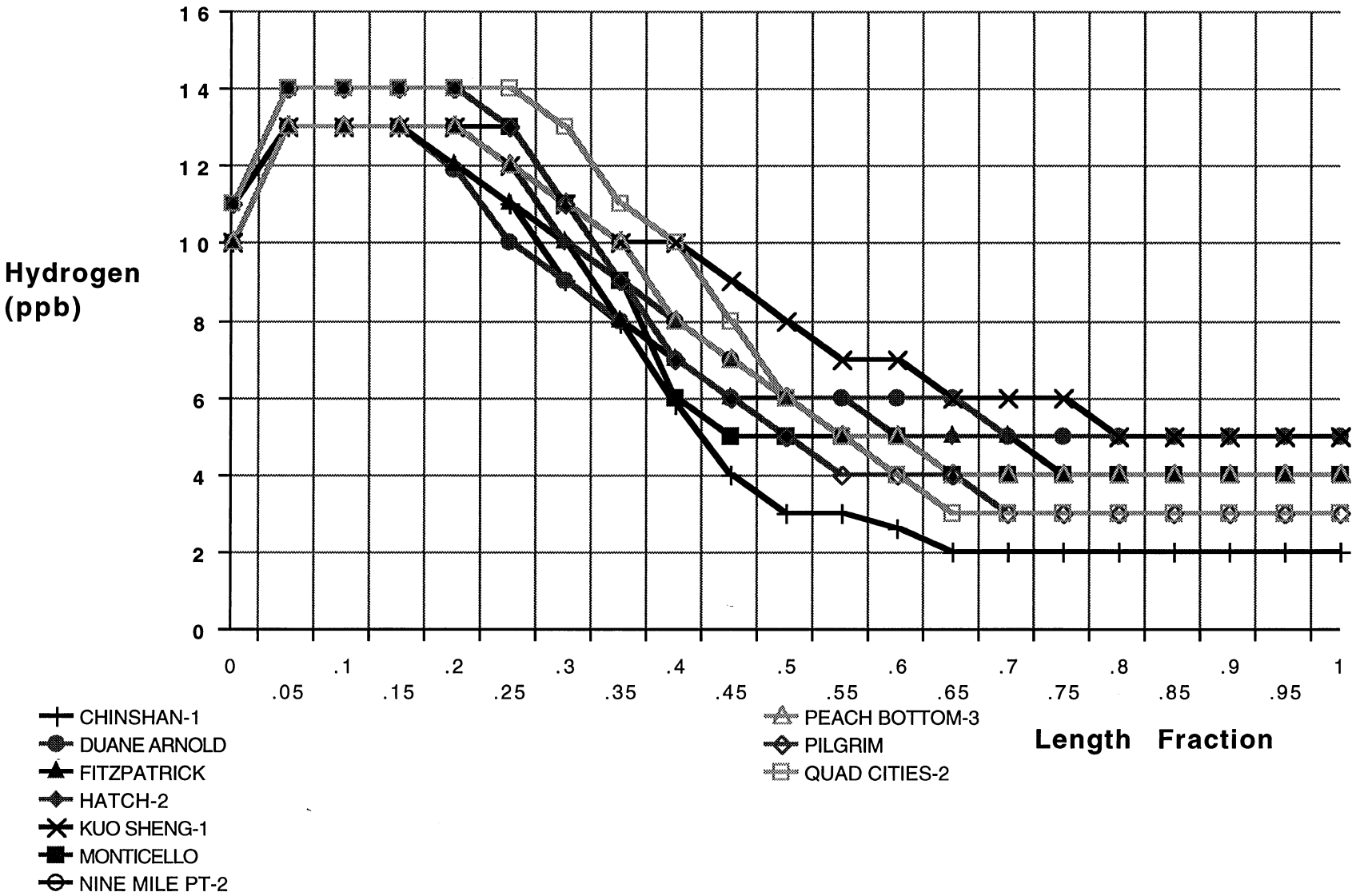

EPRI Licensed Material

Figure A-108: Downcomer Hydrogen Levels with 0.6 ppm Feedwater H2 Addition

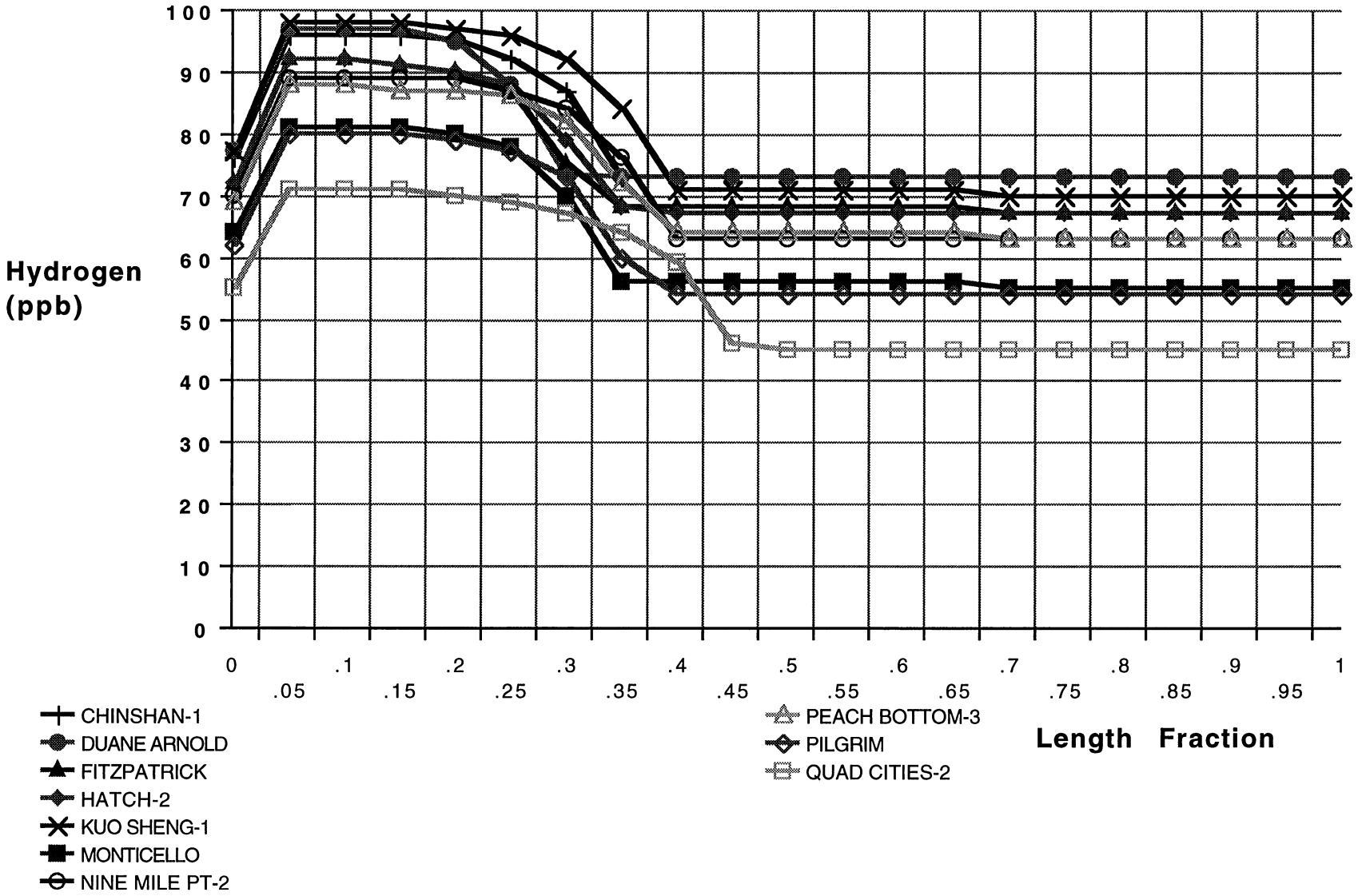

EPRI Licensed Material

Figure A-109: Downcomer Hydrogen Levels with 1.5 ppm Feedwater H2 Addition

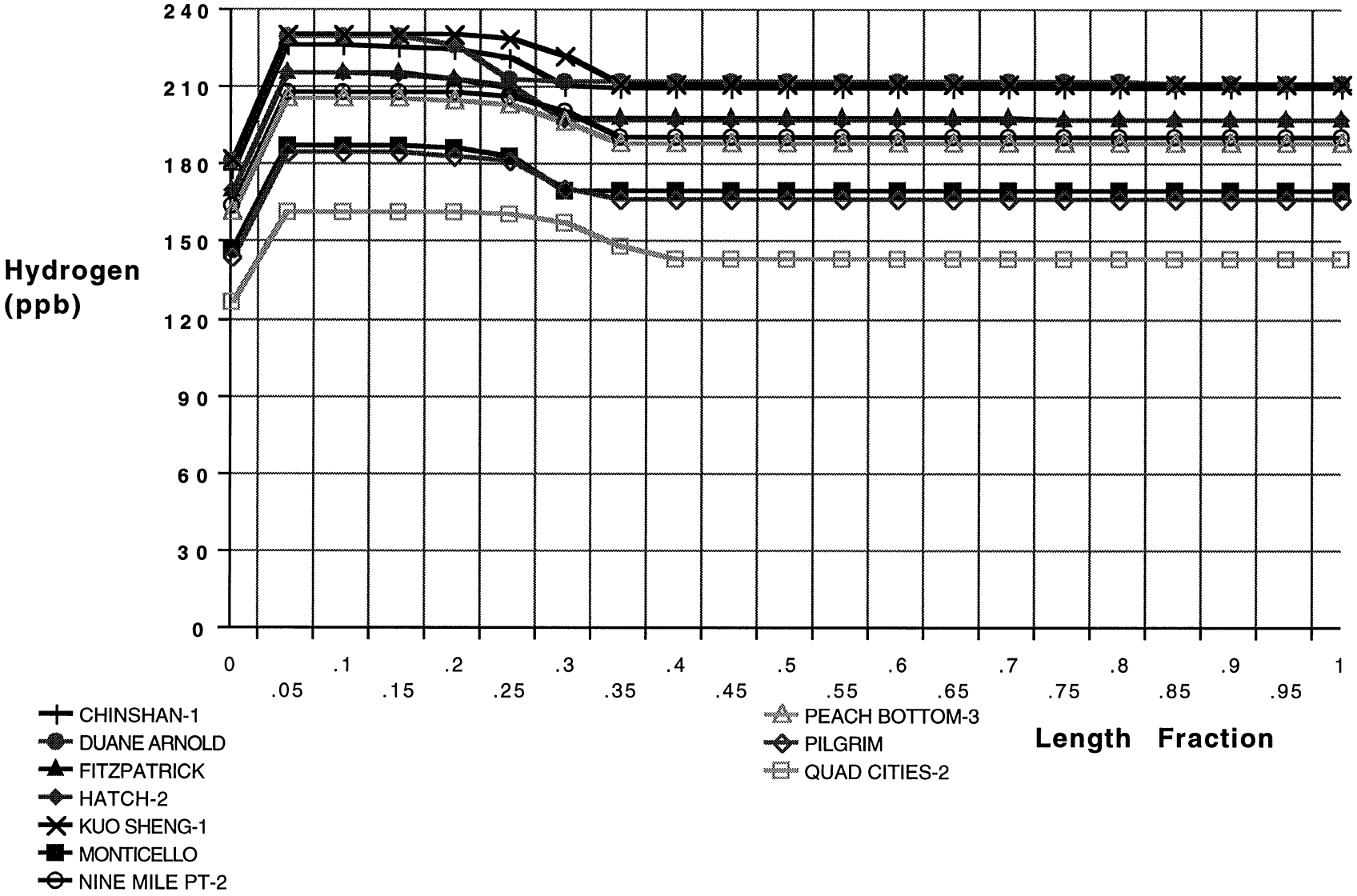

EPRI Licensed Material

Figure A-110: Downcomer Hydrogen Levels with 3.0 ppm Feedwater H2 Addition

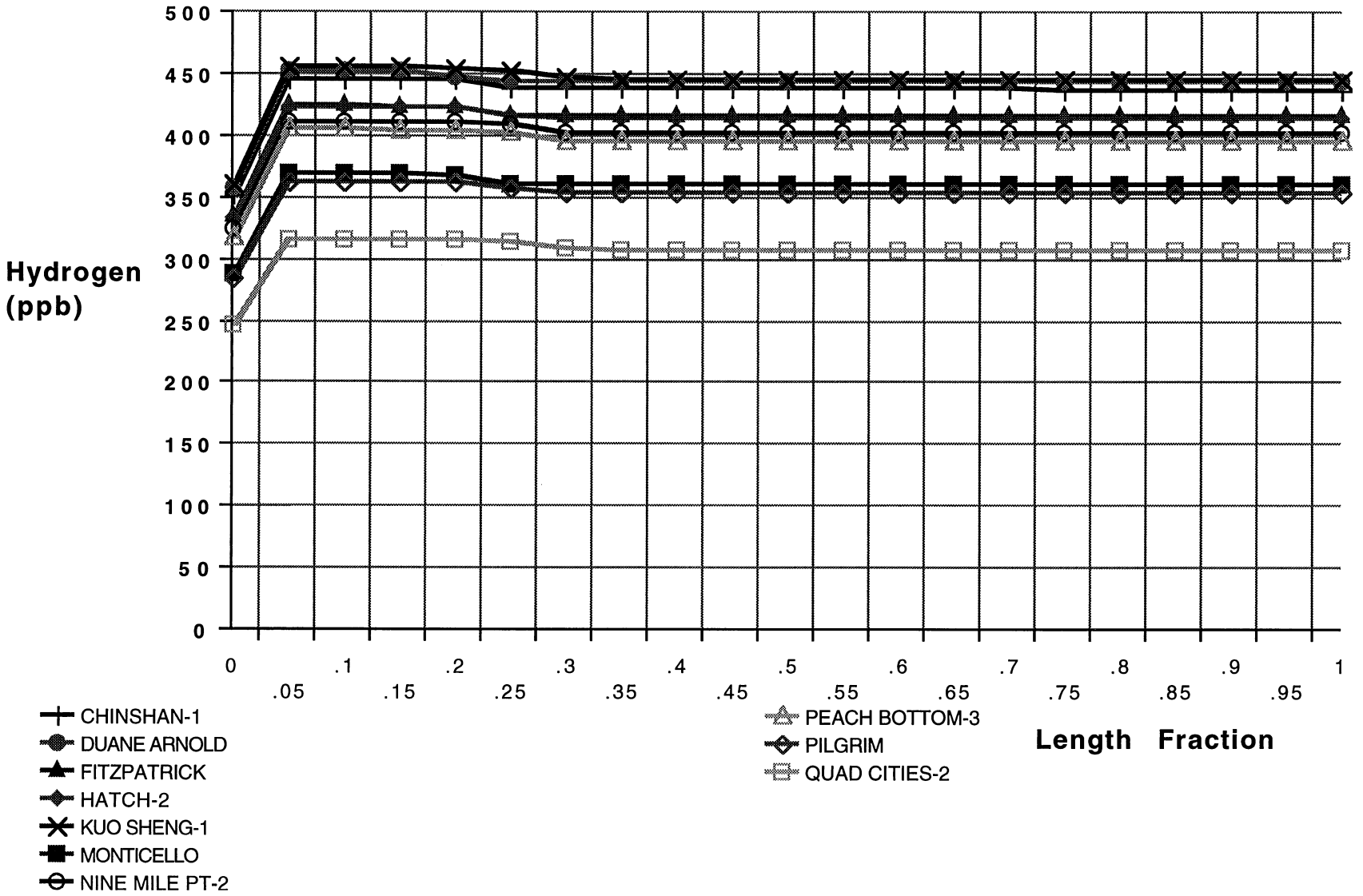

EPRI Licensed Material

Figure A-111: Downcomer Oxygen Levels with 0 ppm Feedwater H2 Addition

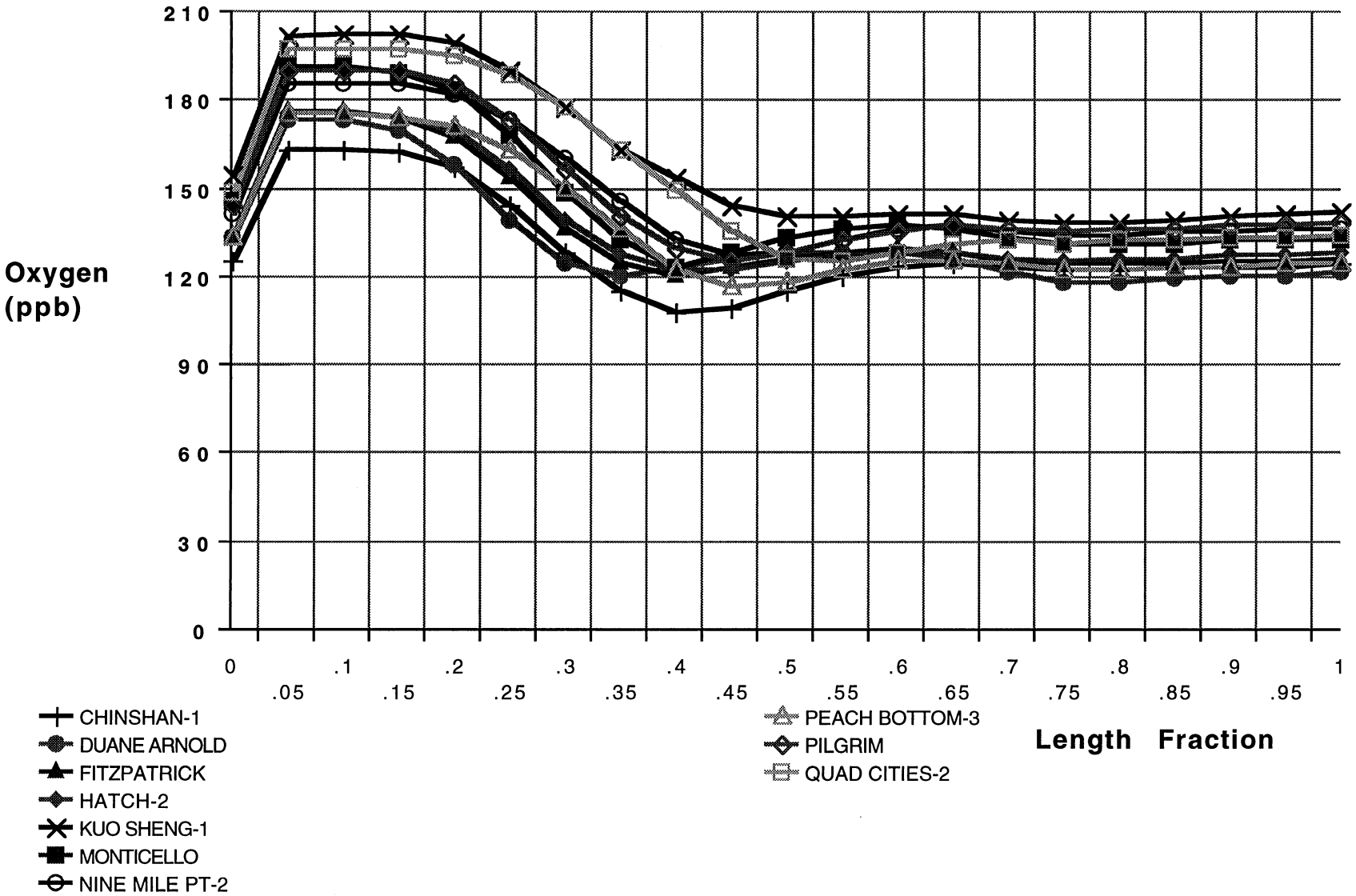

EPRI Licensed Material

Figure A-112: Downcomer Oxygen Levels with 0.6 ppm Feedwater H2 Addition

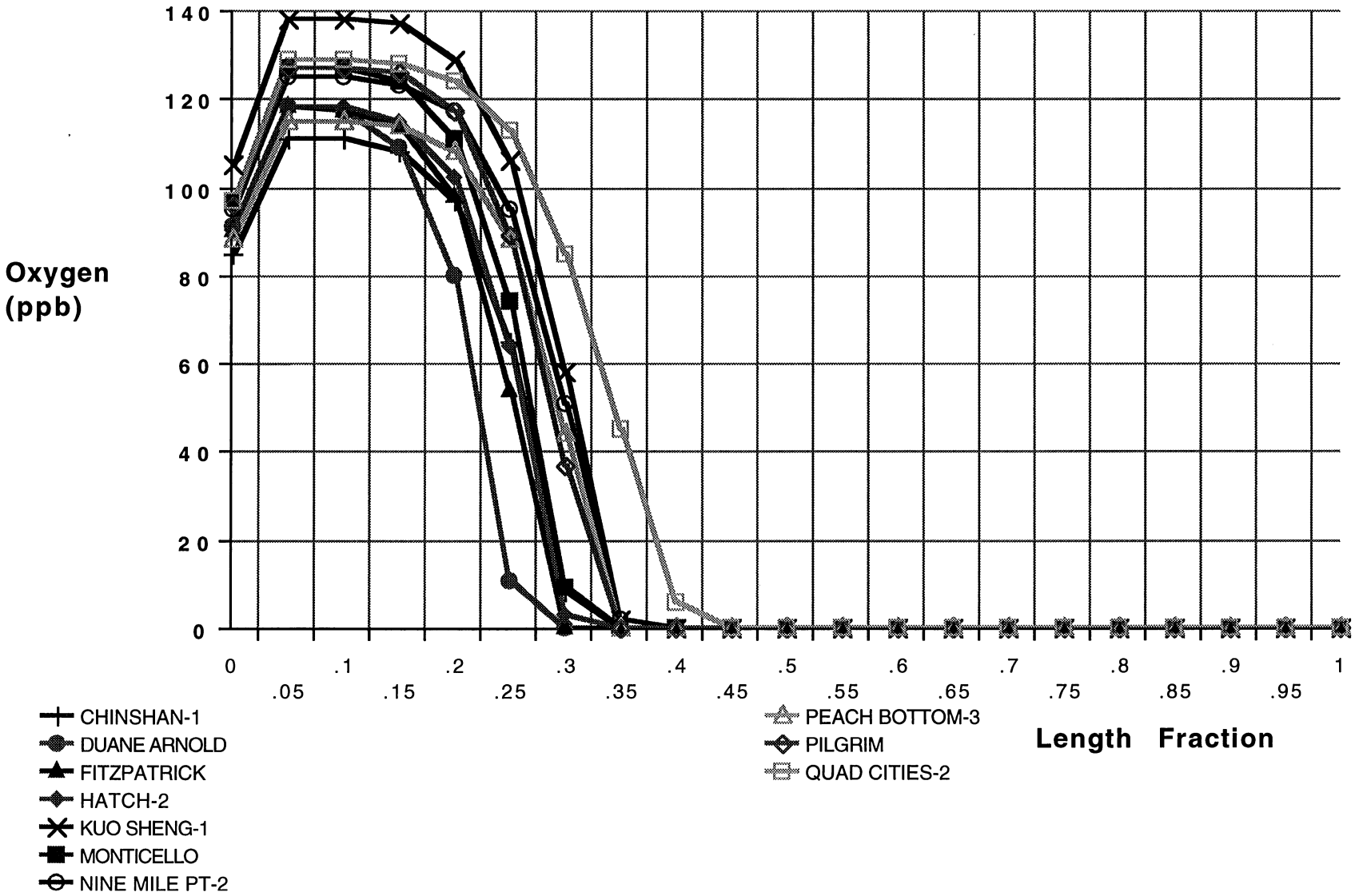

EPRI Licensed Material

Figure A-113: Downcomer Oxygen Levels with 1.5 ppm Feedwater H2 Addition

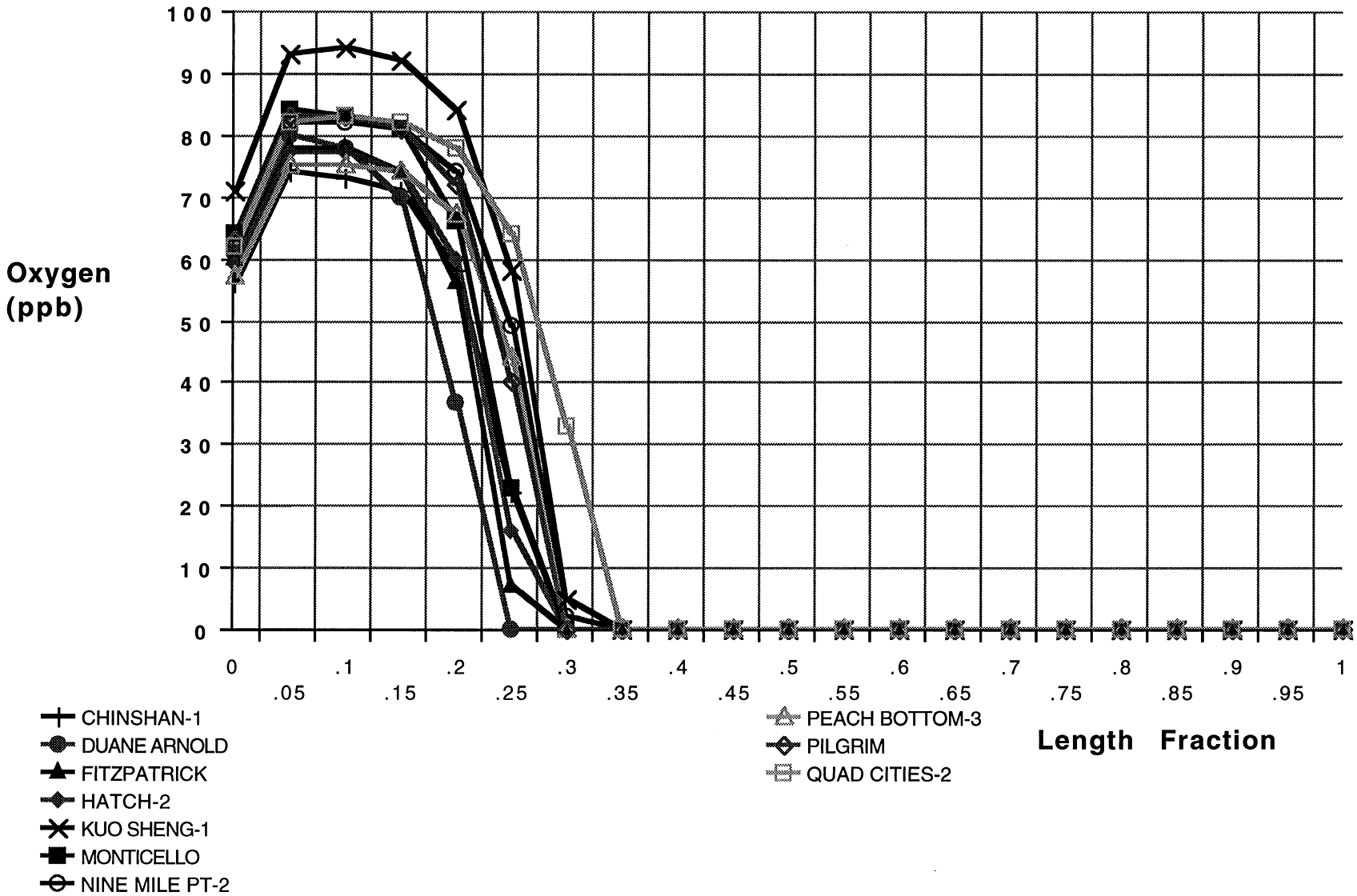

EPRI Licensed Material

Figure A-114: Downcomer Oxygen Levels with 3.0 ppm Feedwater H2 Addition

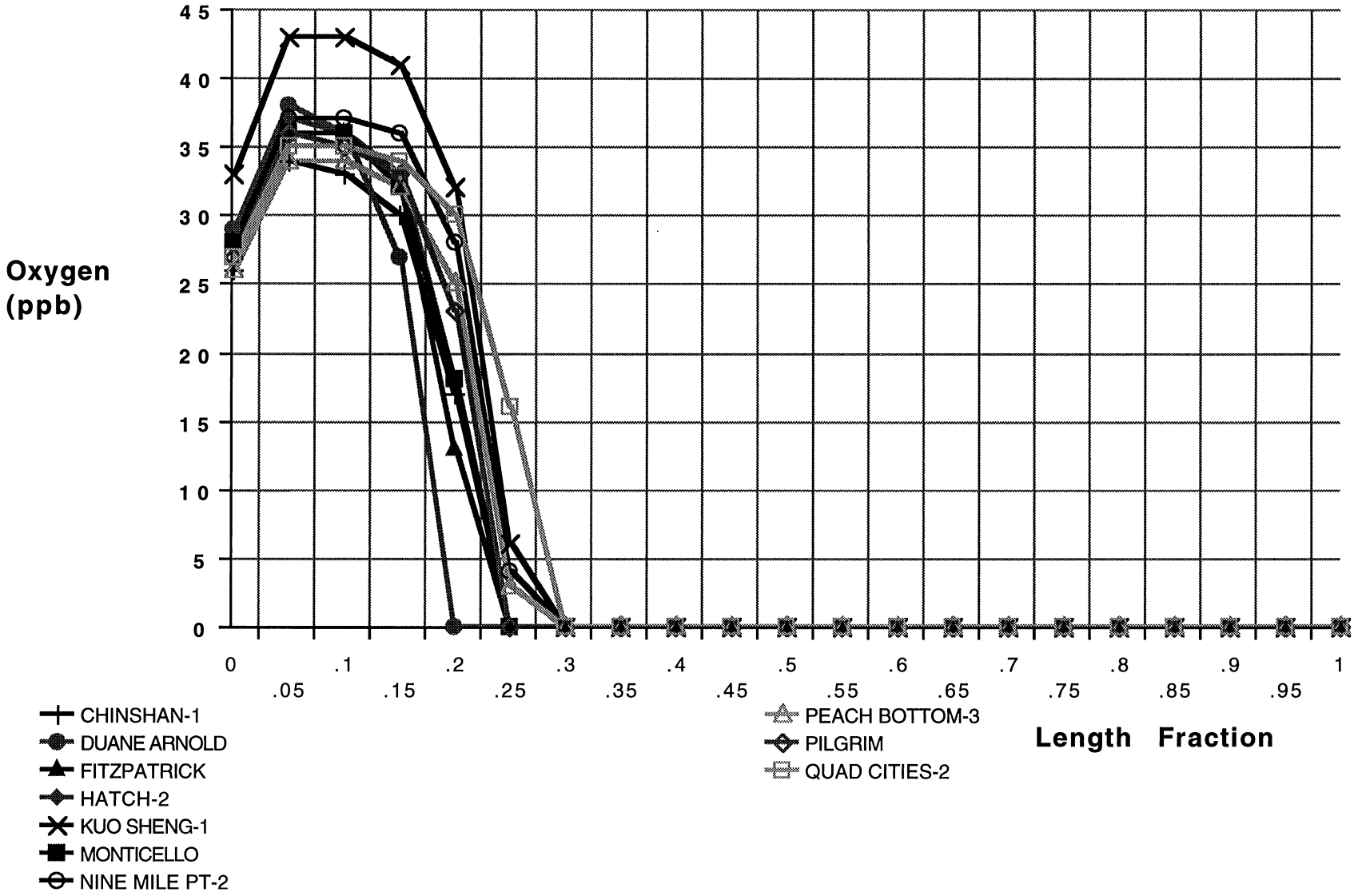

EPRI Licensed Material

Figure A-115: Downcomer Peroxide Levels with 0 ppm Feedwater H2 Addition

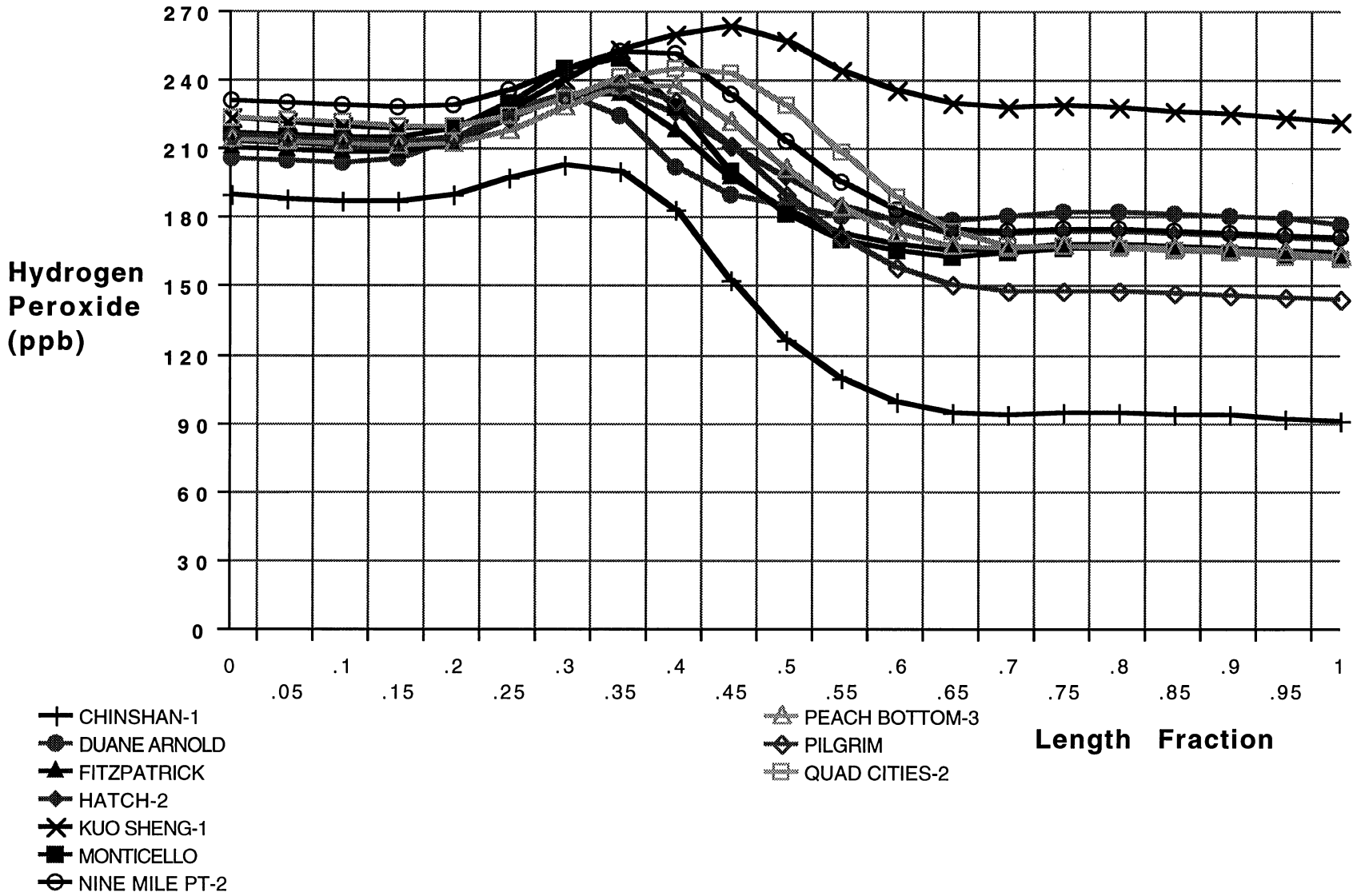

EPRI Licensed Material

Figure A-116: Downcomer Peroxide Levels with 0.6 ppm Feedwater H2 Addition

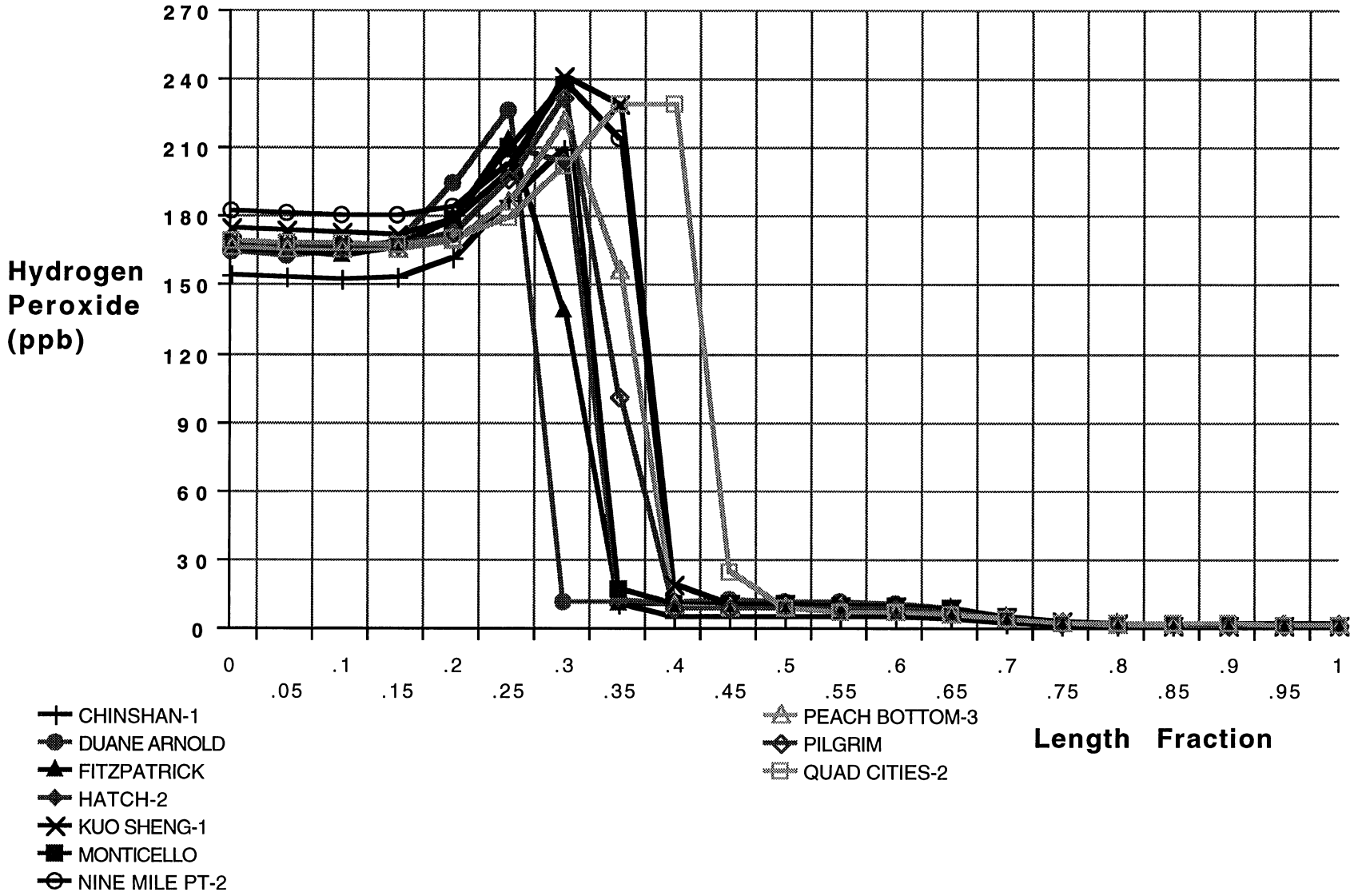

EPRI Licensed Material

Figure A-117: Downcomer Peroxide Levels with 1.5 ppm Feedwater H2 Addition

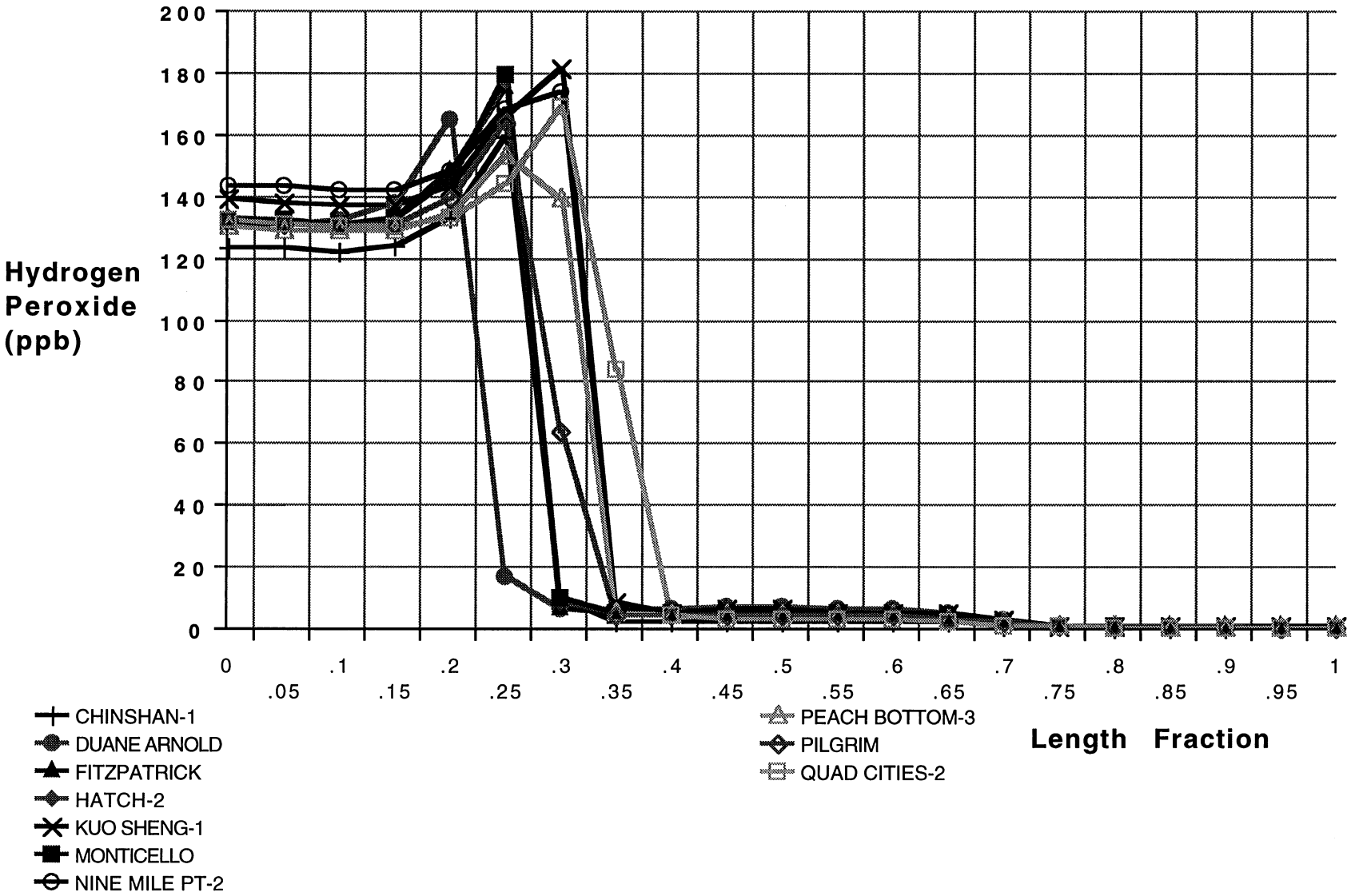

EPRI Licensed Material

Figure A-118: Downcomer Peroxide Levels with 3.0 ppm Feedwater H2 Addition

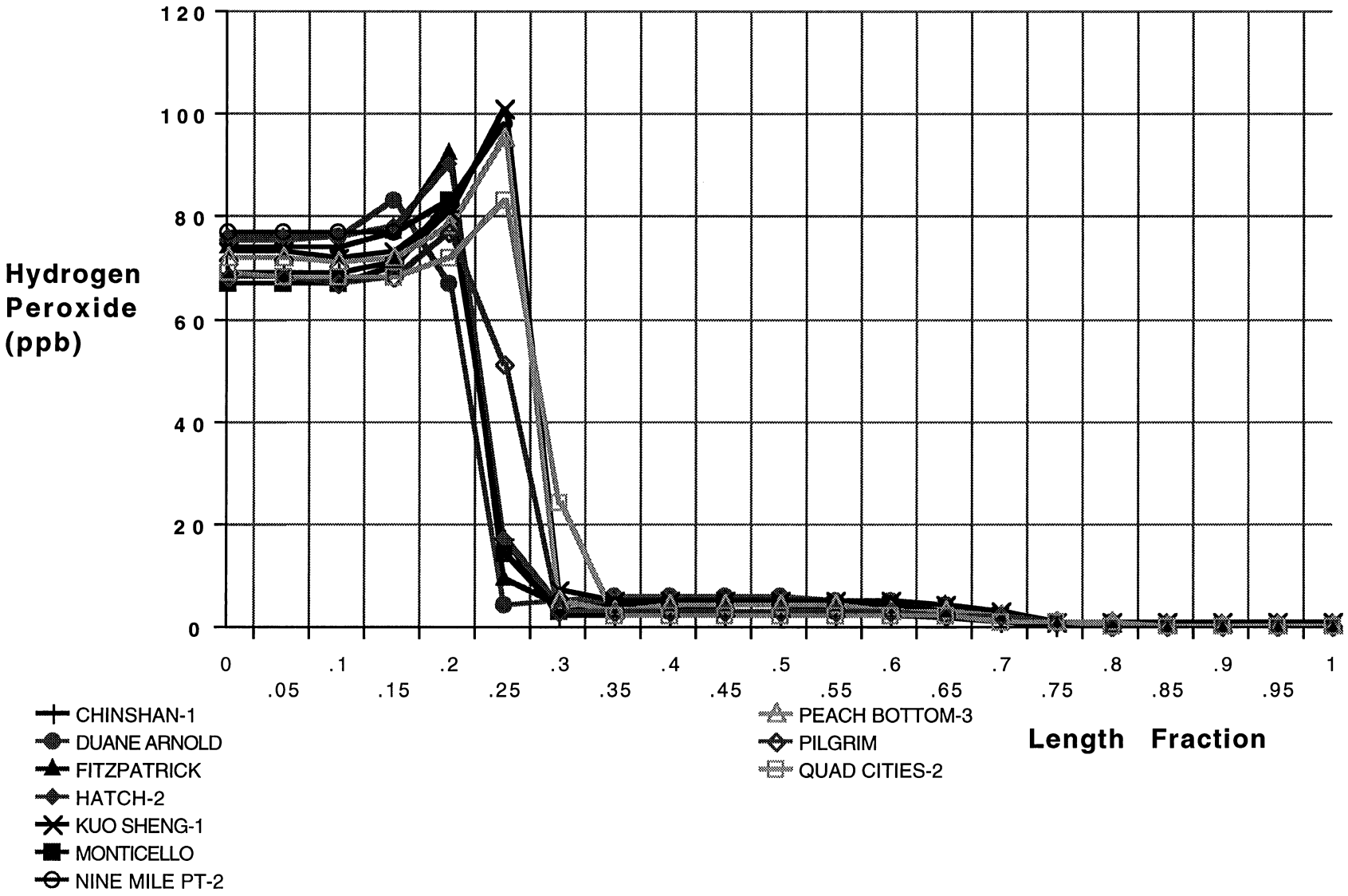

EPRI Licensed Material

Figure A-119: Recirculation System ECPs with 0 ppm Feedwater H2 Addition

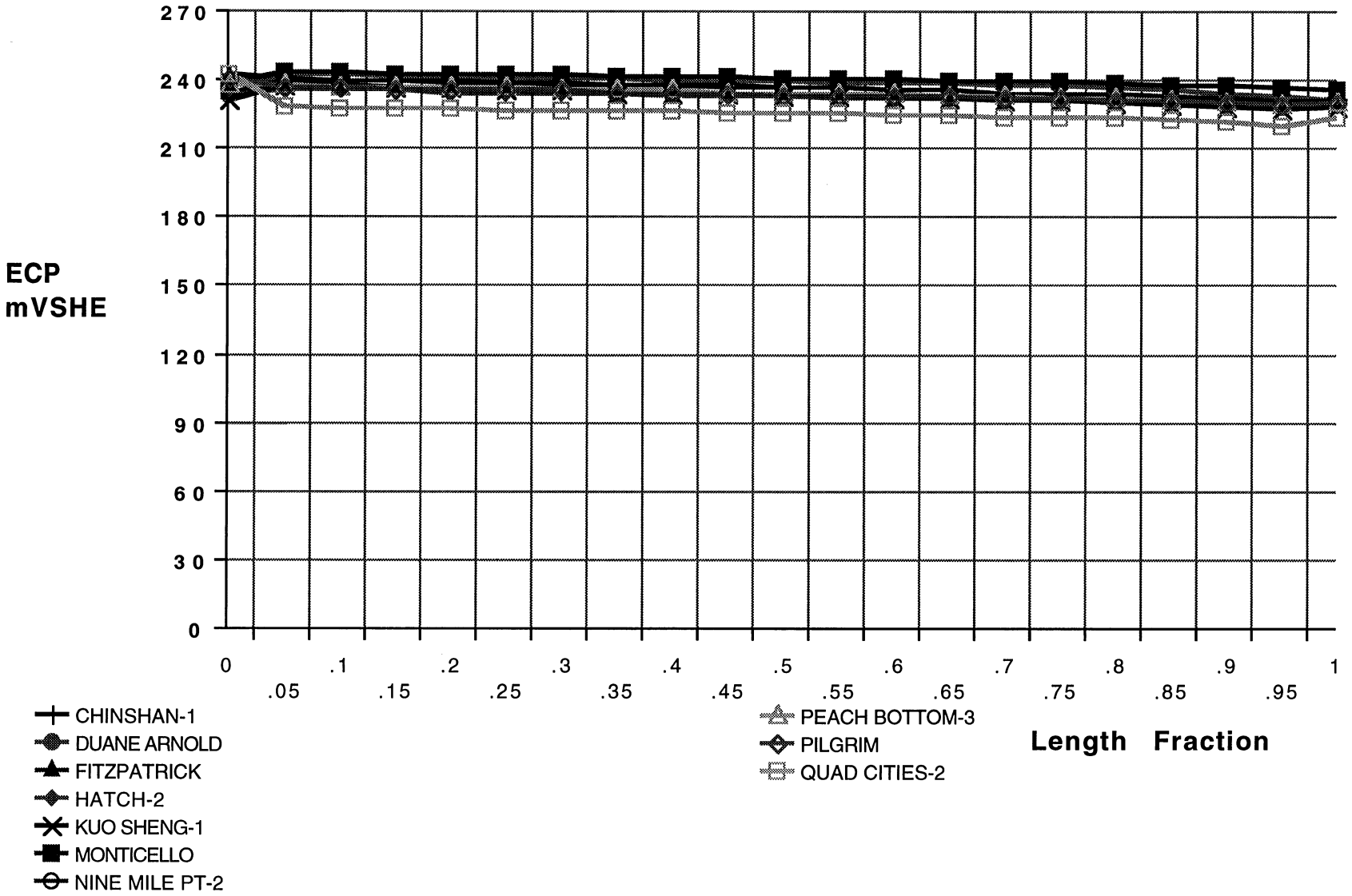

EPRI Licensed Material

Figure A-120: Recirculation System ECPs with 0.6 ppm Feedwater H2 Addition

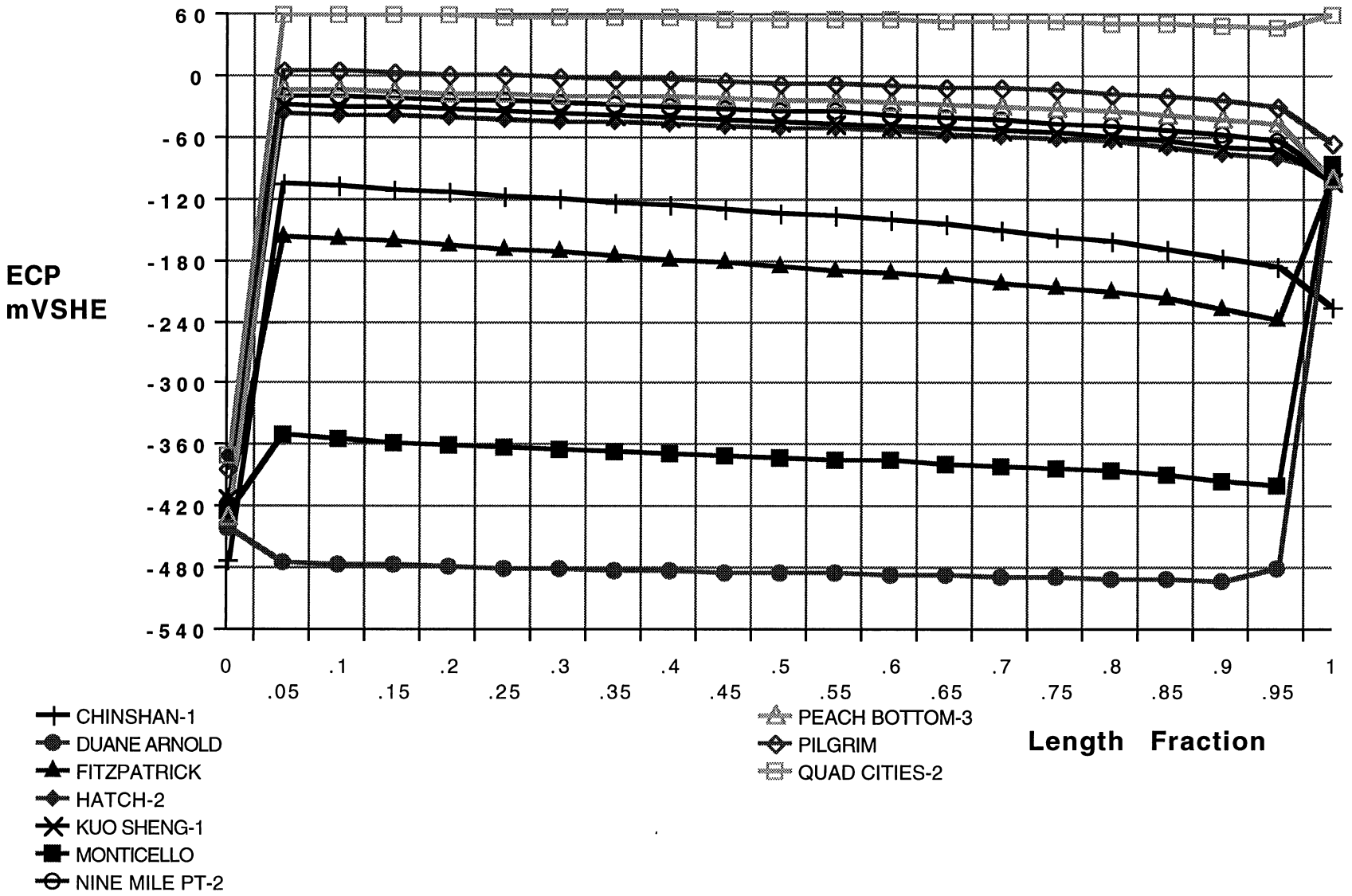

EPRI Licensed Material

Figure A-121: Recirculation System ECPs with 1.5 ppm Feedwater H2 Addition

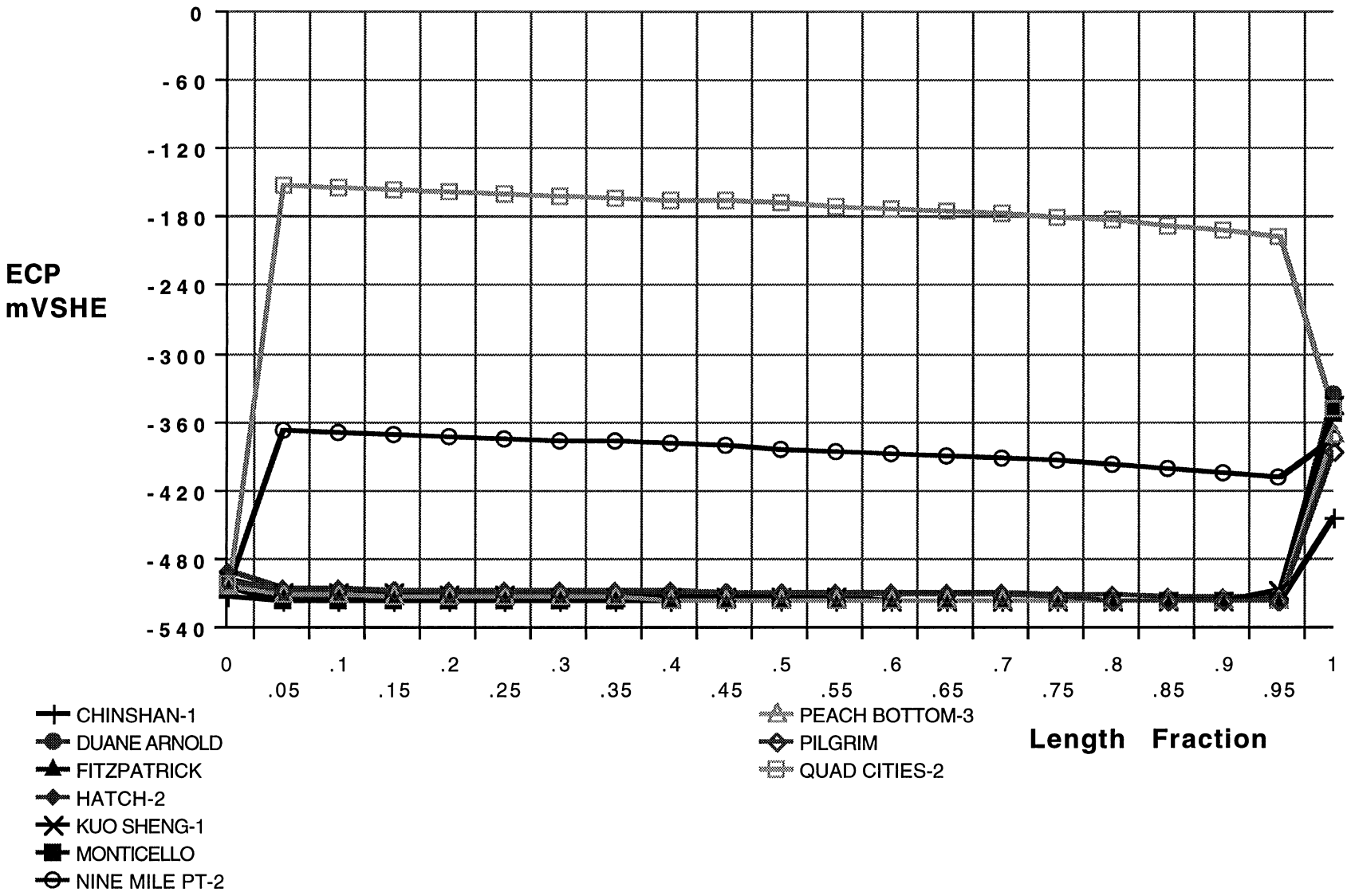

EPRI Licensed Material

Figure A-122: Recirculation System ECPs with 3.0 ppm Feedwater H2 Addition

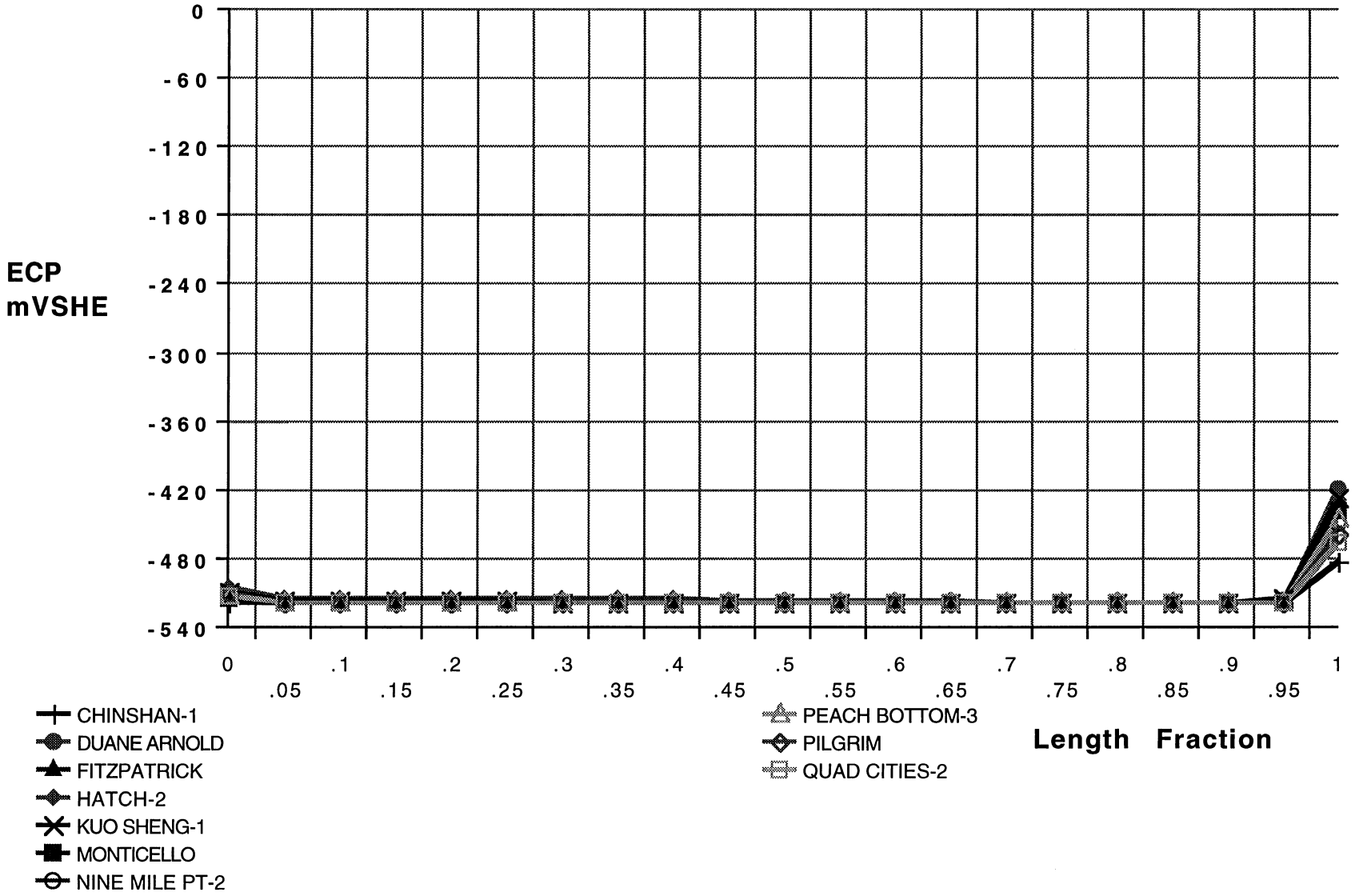

EPRI Licensed Material

Figure A-123: Recirculation Hydrogen Levels with 0 ppm Feedwater H2 Addition

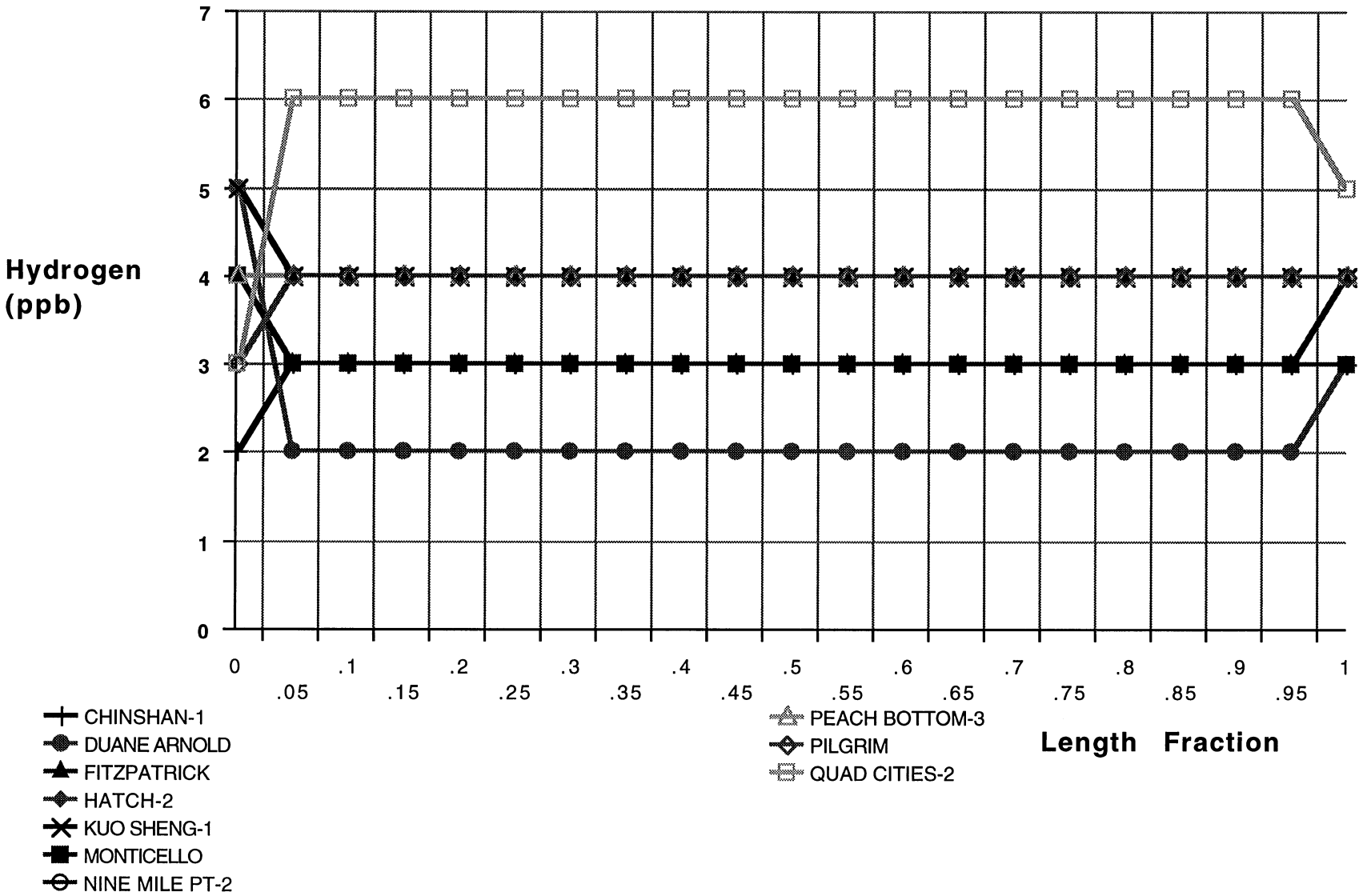

EPRI Licensed Material

Figure A-124: Recirculation Hydrogen Levels with 0.6 ppm Feedwater H2 Addition

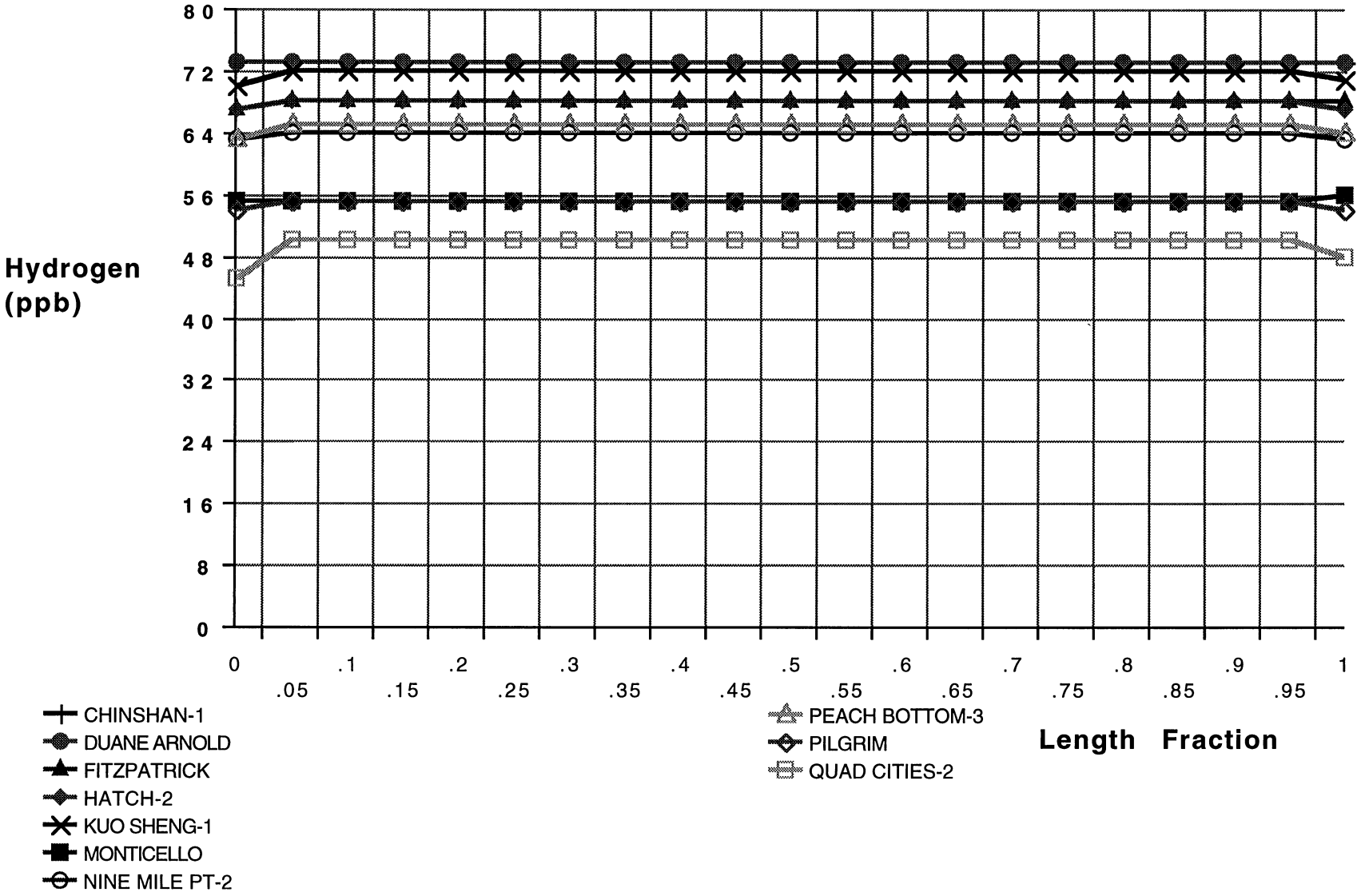

EPRI Licensed Material

Figure A-125: Recirculation Hydrogen Levels with 1.5 ppm Feedwater H2 Addition

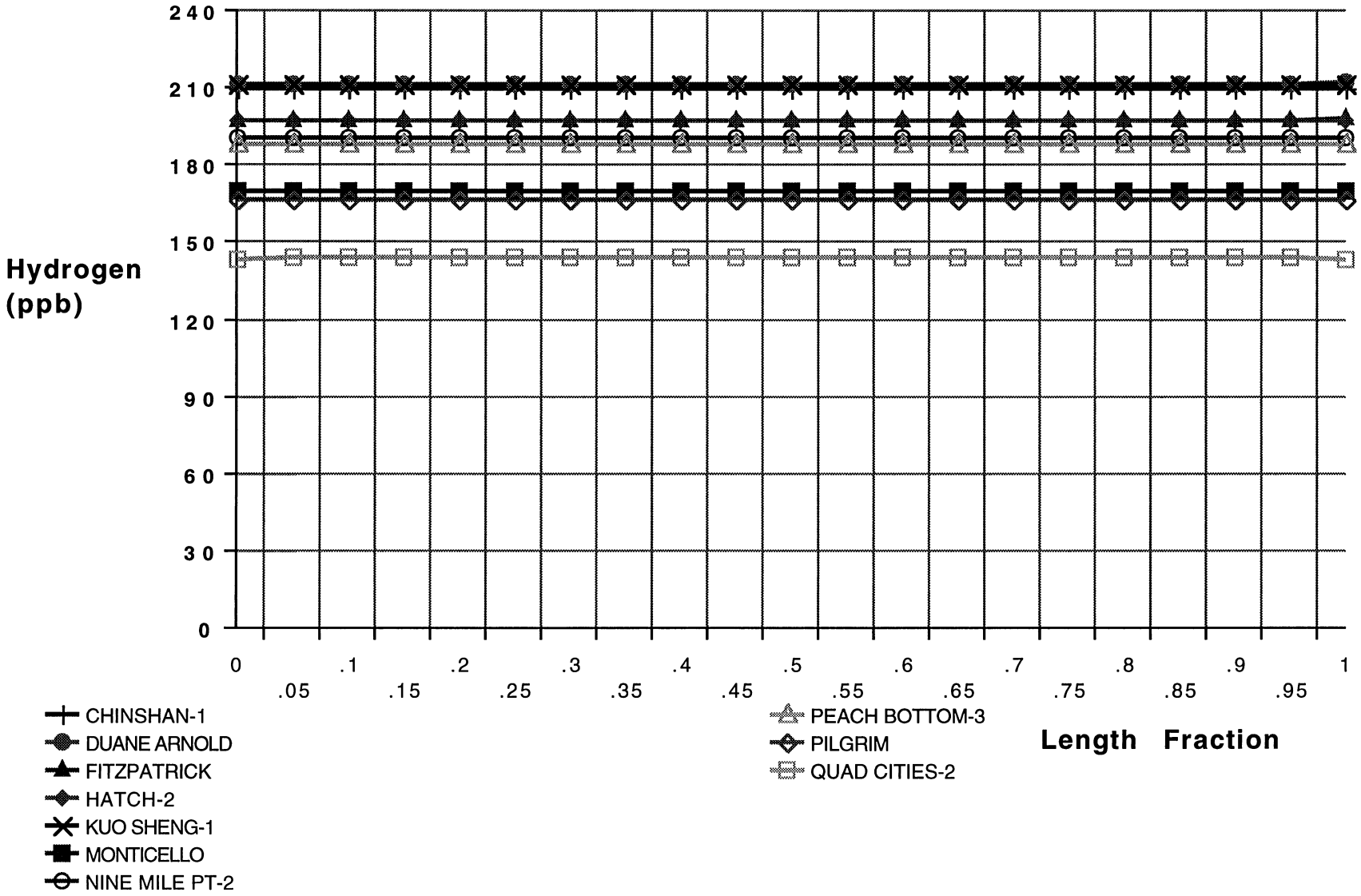

EPRI Licensed Material

Figure A-126: Recirculation Hydrogen Levels with 3.0 ppm Feedwater H2 Addition

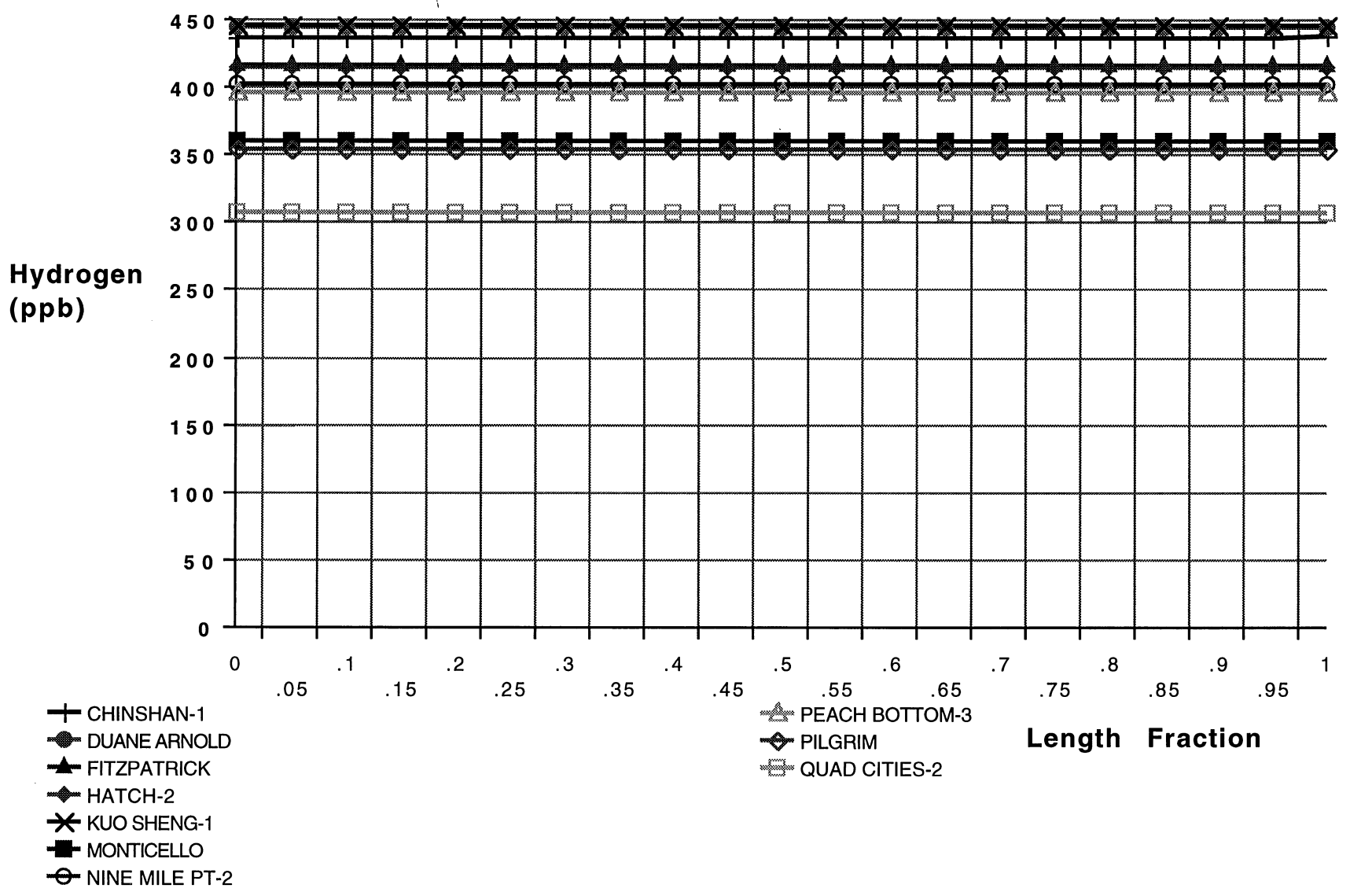

EPRI Licensed Material

Figure A-127: Recirculation Oxygen Levels with 0 ppm Feedwater H2 Addition

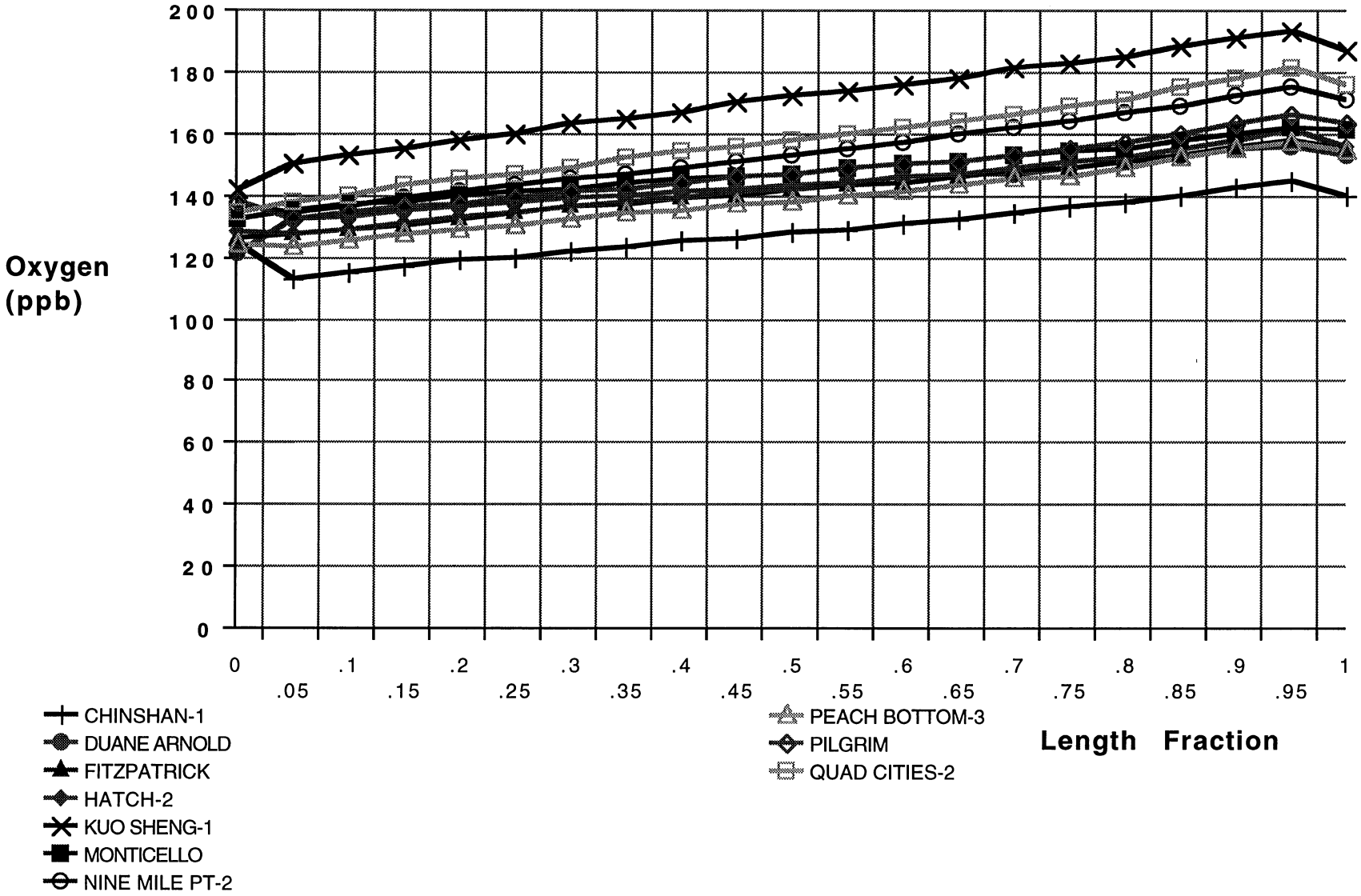

EPRI Licensed Material

Figure A-128: Recirculation Oxygen Levels with 0.6 ppm Feedwater H2 Addition

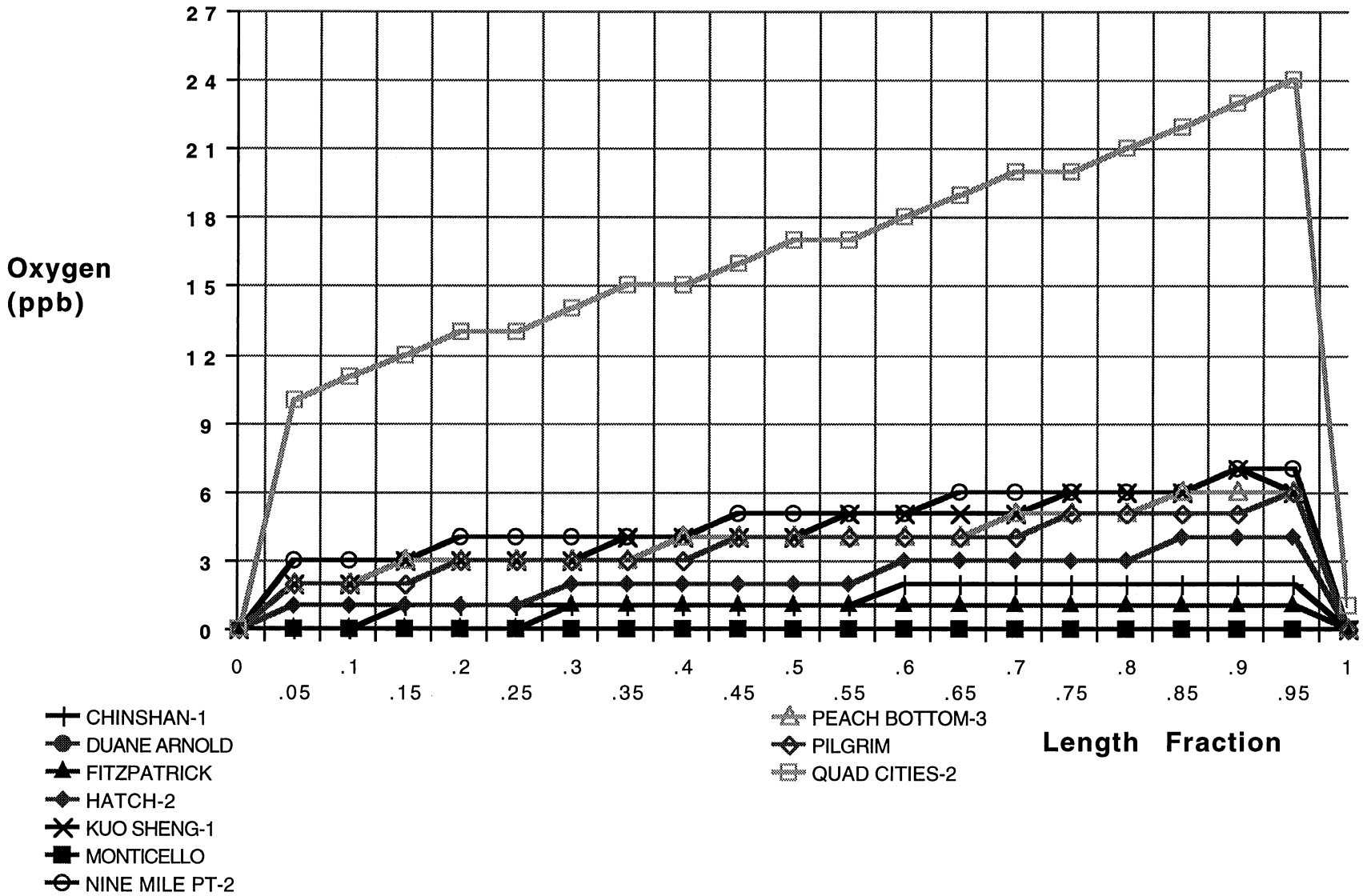

EPRI Licensed Material

Figure A-129: Recirculation Oxygen Levels with 1.5 ppm Feedwater H2 Addition

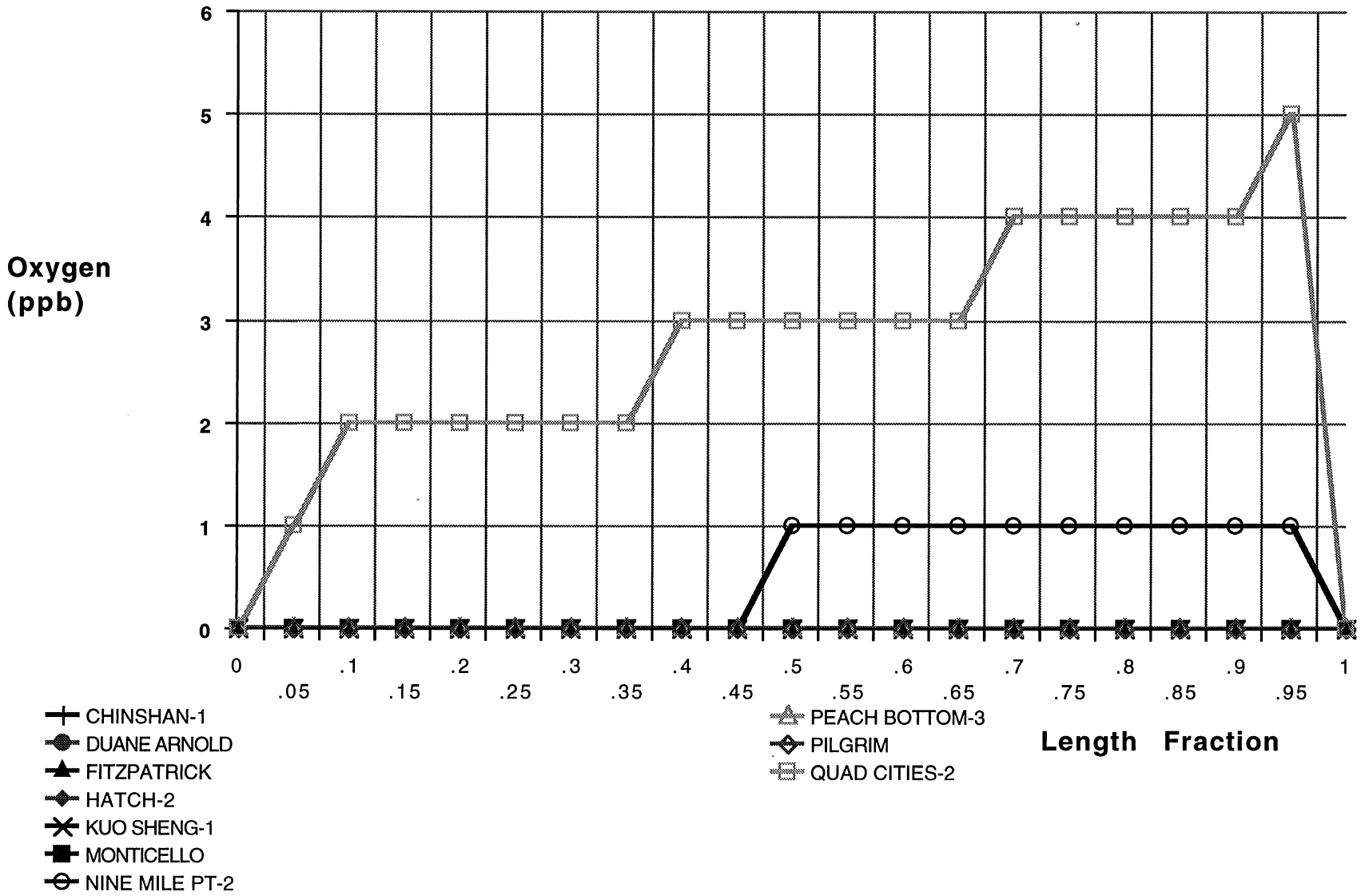

EPRI Licensed Material

Figure A-130: Recirculation Peroxide Levels with 0 ppm Feedwater H2 Addition

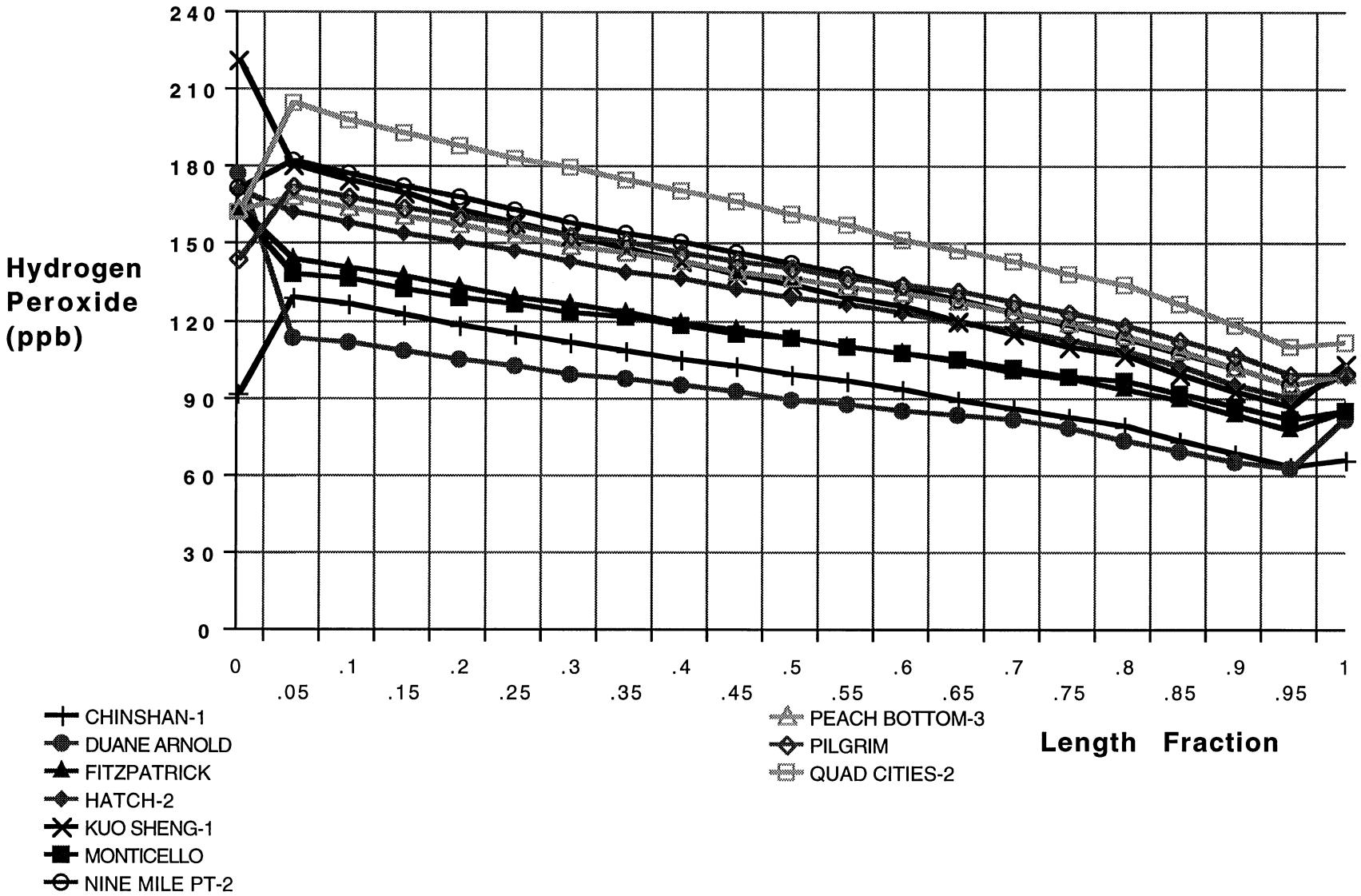

EPRI Licensed Material

Figure A-131: Recirculation Peroxide Levels with 0.6 ppm Feedwater H2 Addition

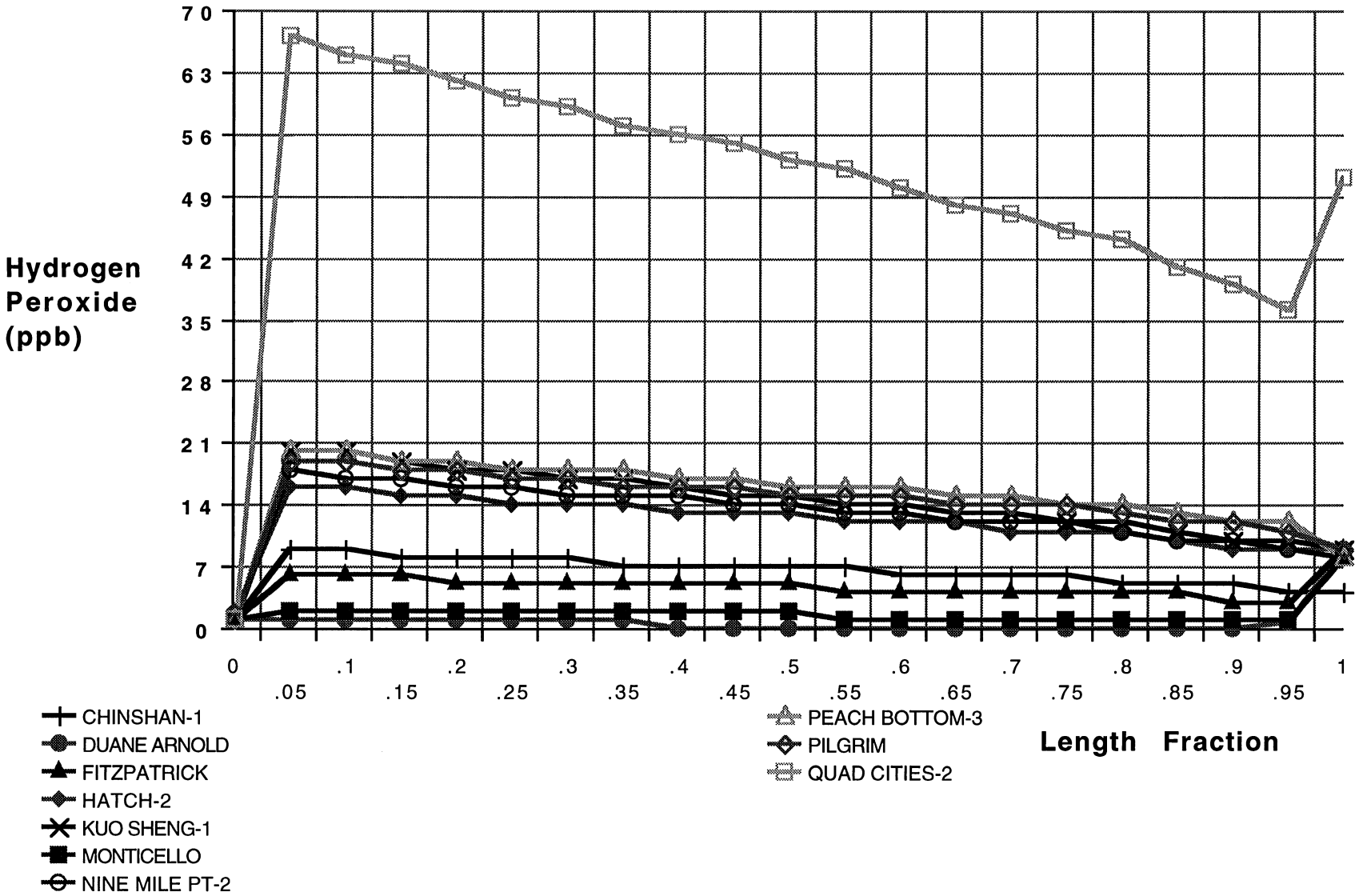

EPRI Licensed Material

Figure A-132: Recirculation Peroxide Levels with 1.5 ppm Feedwater H2 Addition

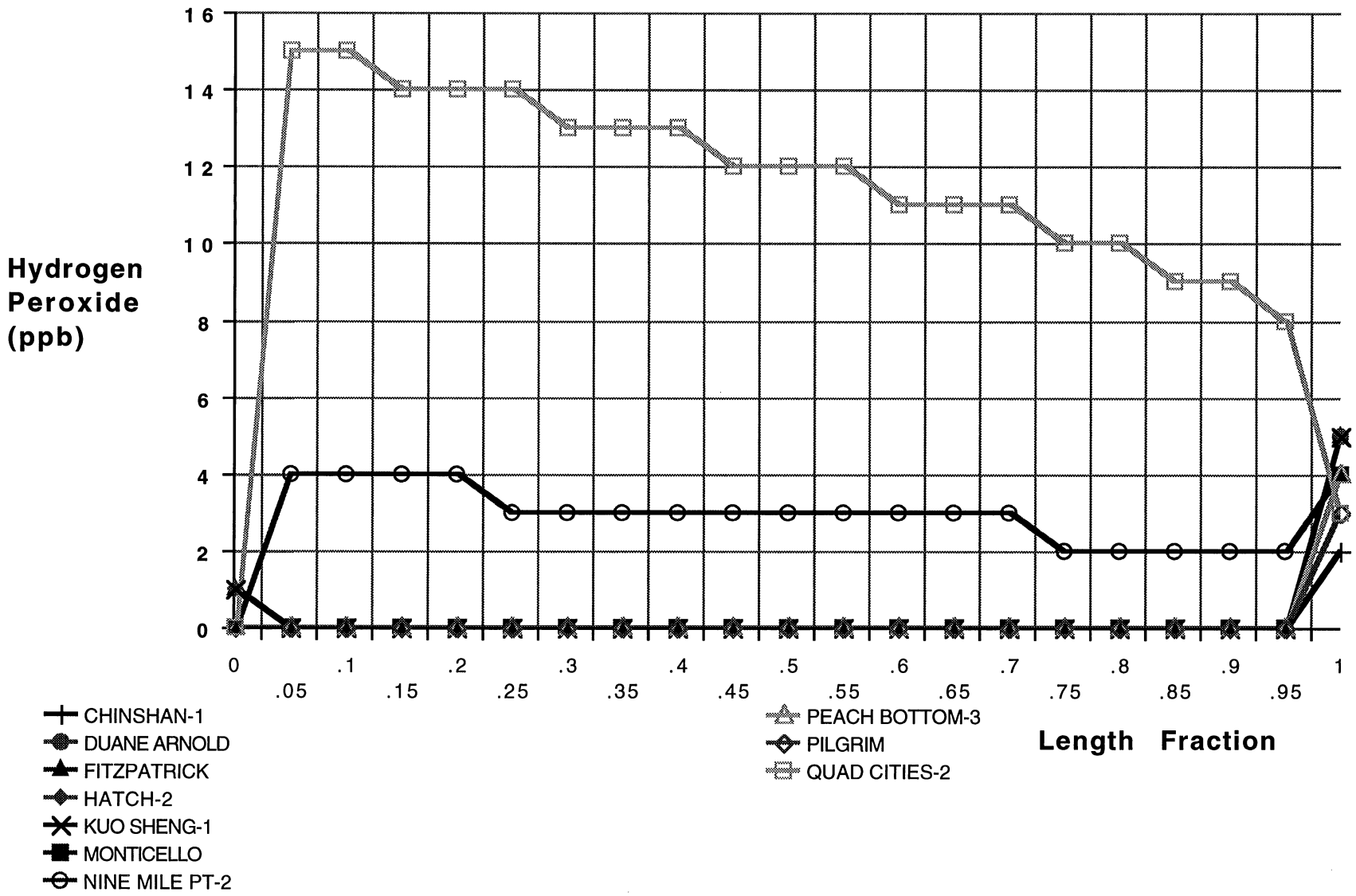

EPRI Licensed Material

Figure A-133: Recirculation Peroxide Levels with 3.0 ppm Feedwater H2 Addition

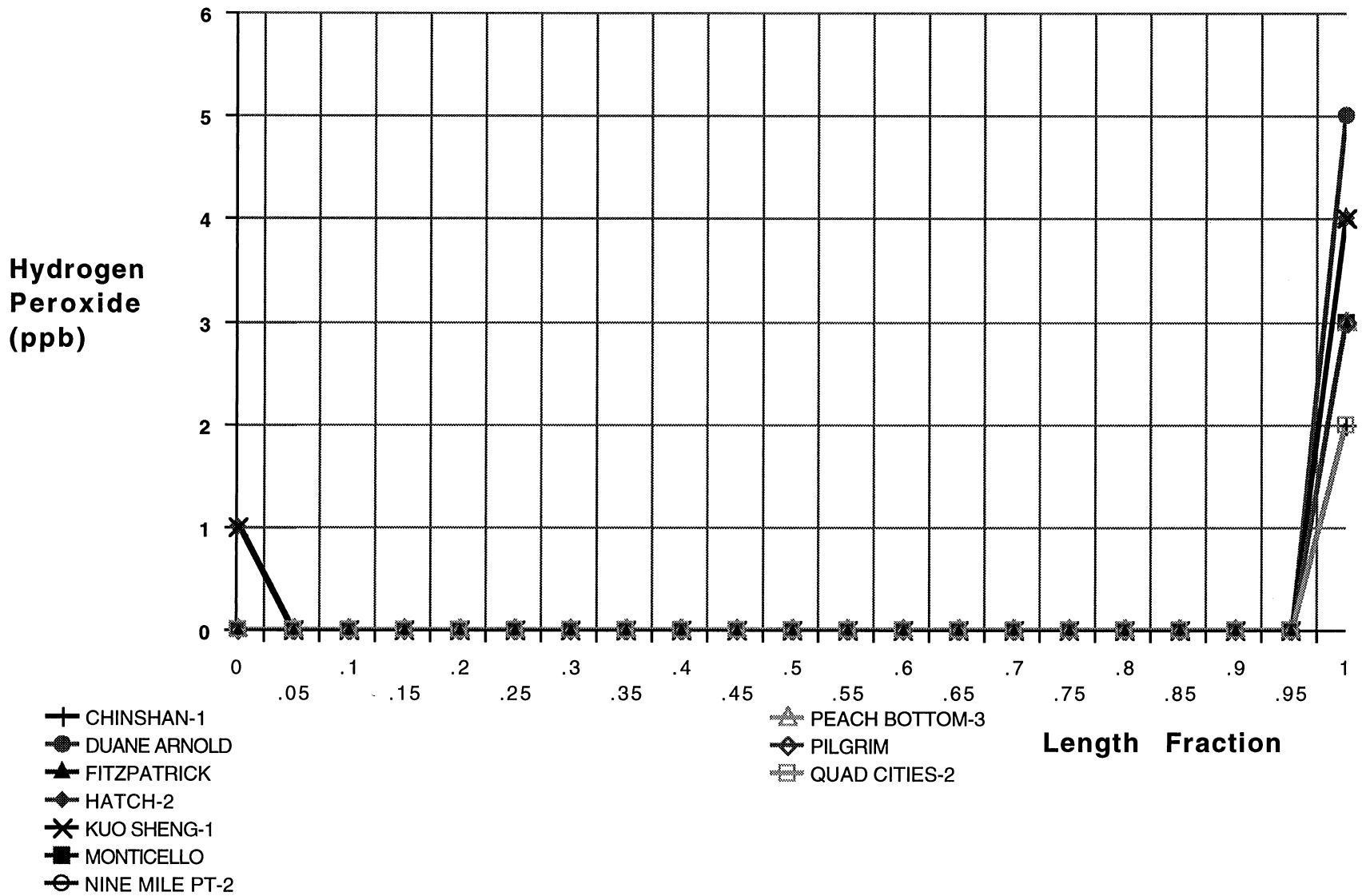

EPRI Licensed Material

Figure A-134: Jet Pump Region ECPs with 0 ppm Feedwater H2 Addition

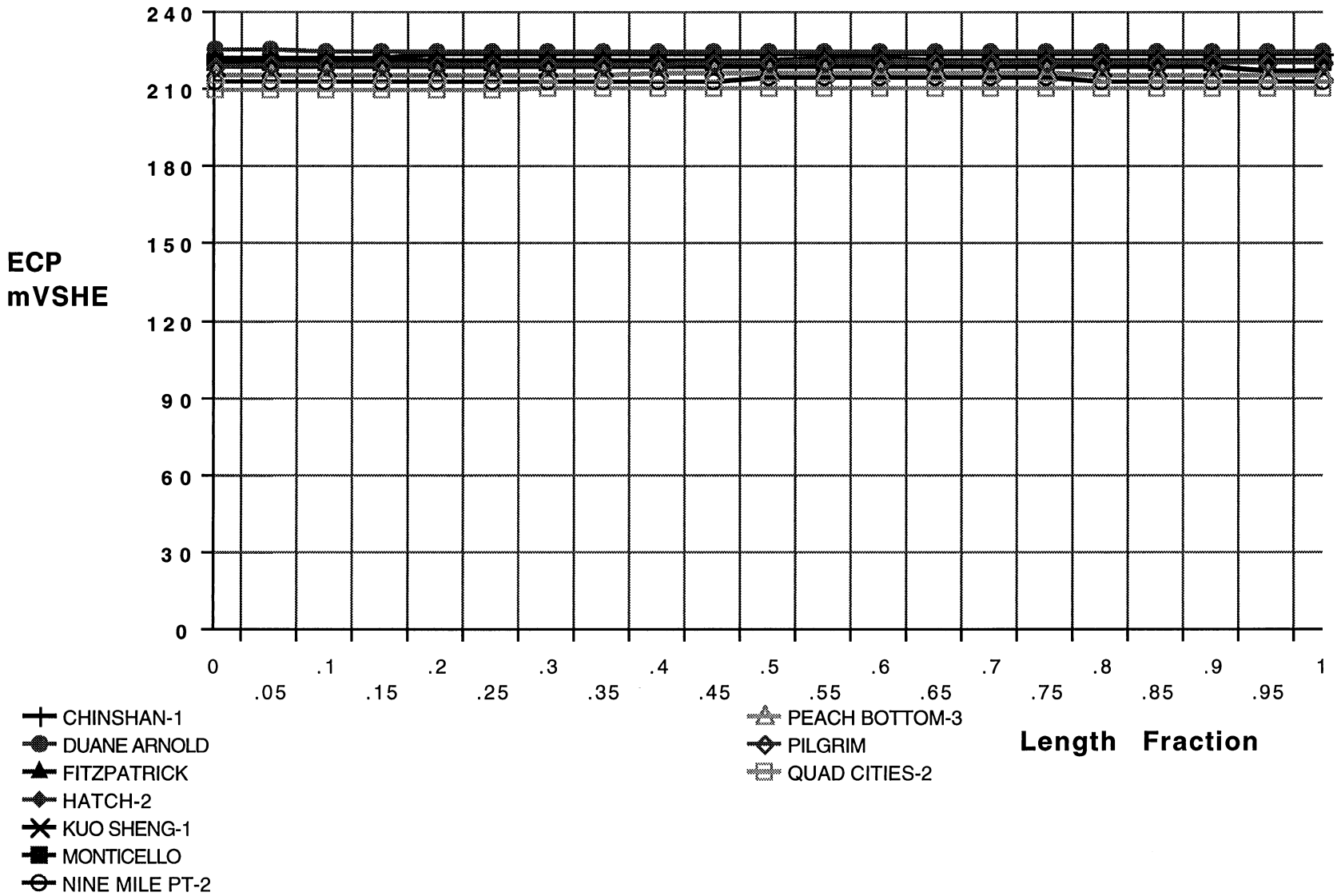

EPRI Licensed Material

Figure A-135: Jet Pump Region ECPs with 0.6 ppm Feedwater H2 Addition

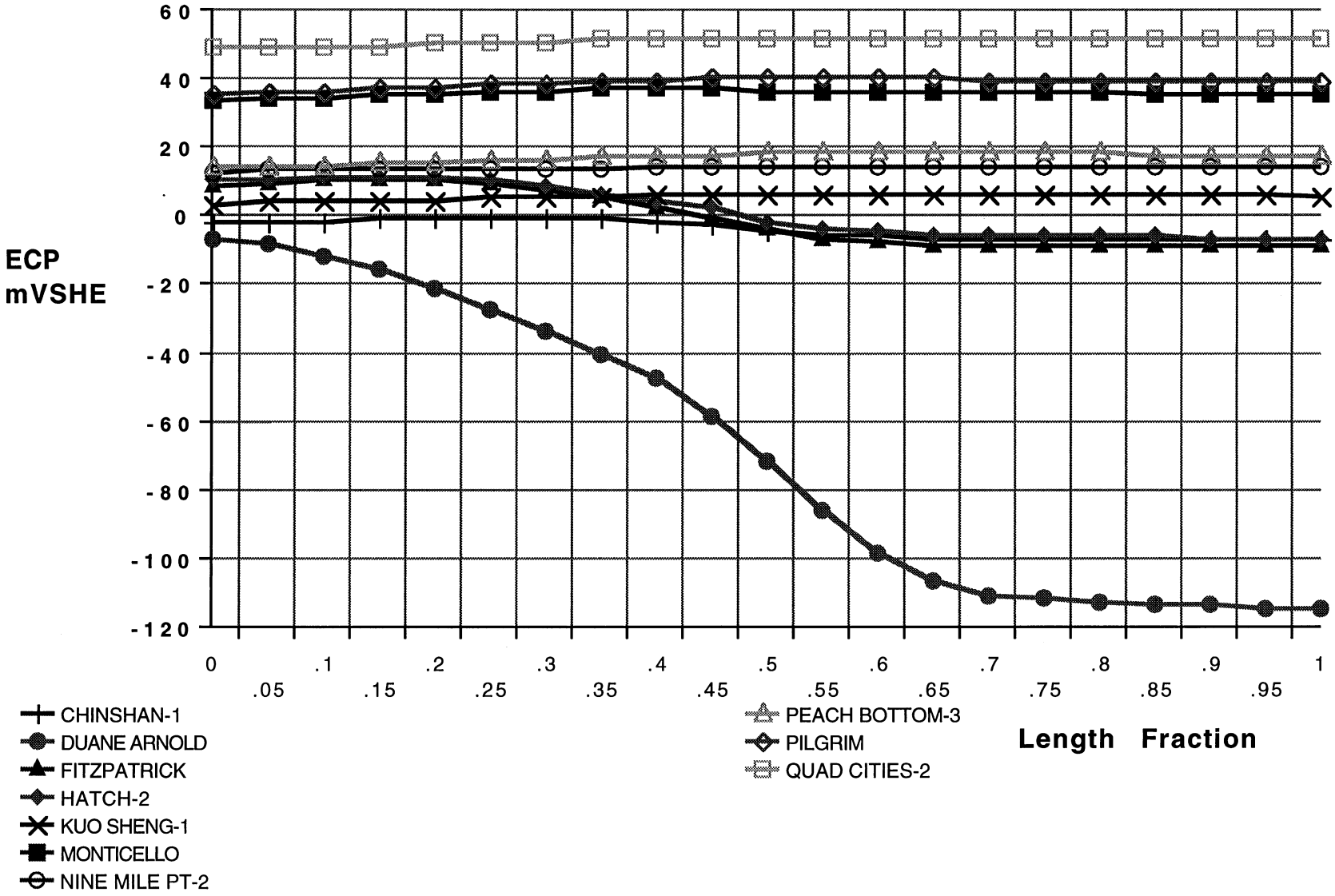

EPRI Licensed Material

Figure A-136: Jet Pump Region ECPs with 1.5 ppm Feedwater H2 Addition

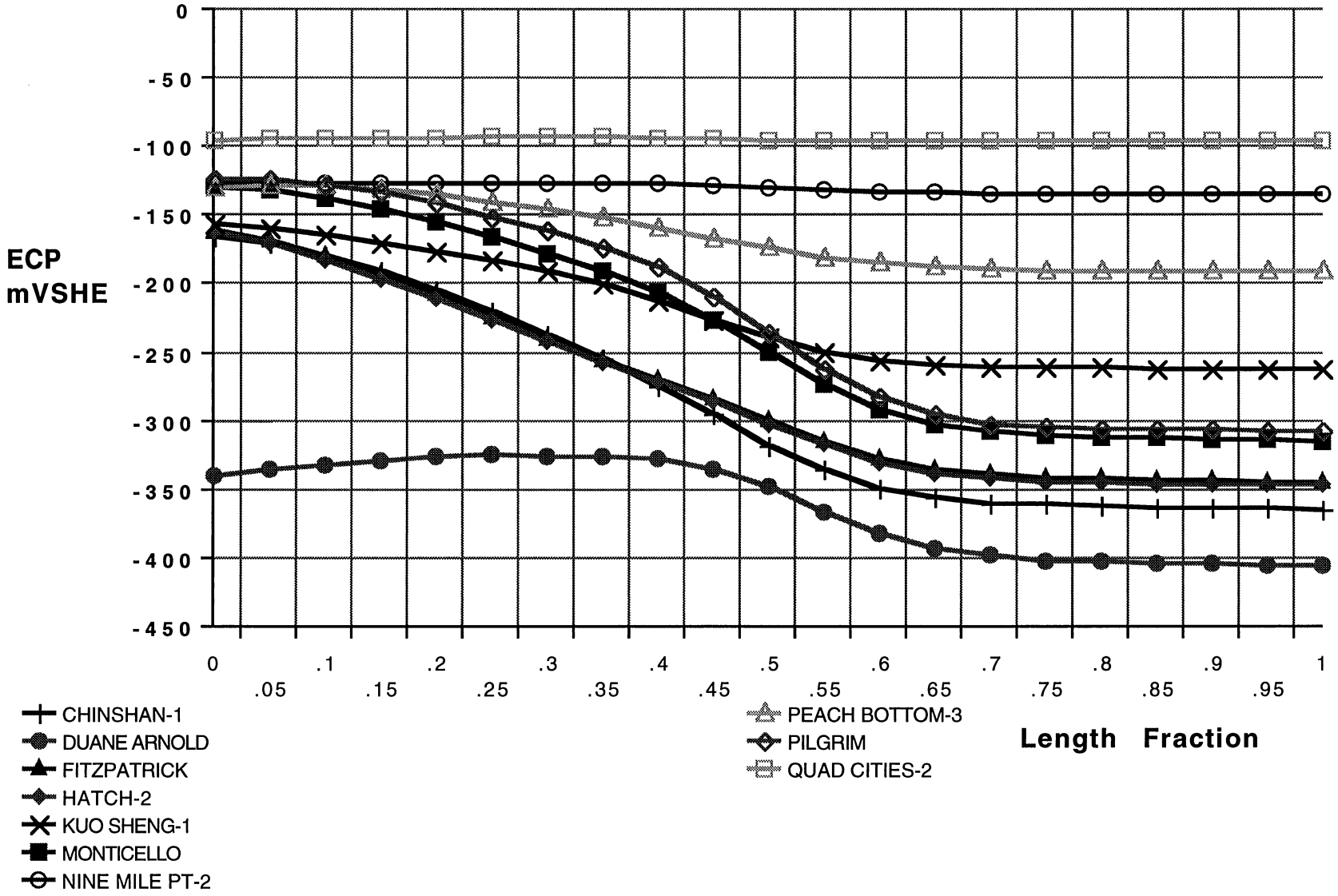

EPRI Licensed Material

Figure A-137: Jet Pump Region ECPs with 3.0 ppm Feedwater H2 Addition

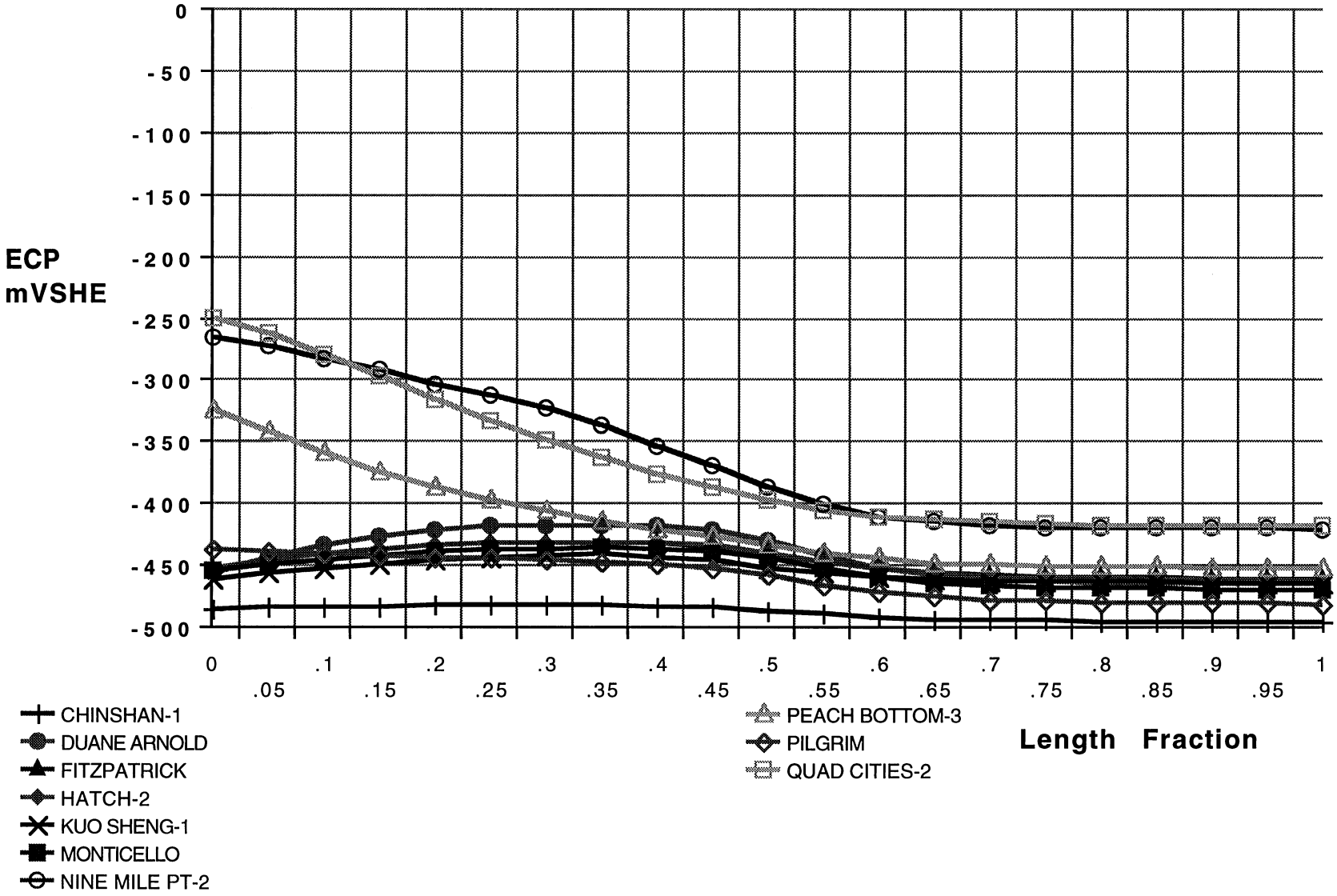

EPRI Licensed Material

Figure A-138: Jet Pump Hydrogen Levels with 0 ppm Feedwater H2 Addition

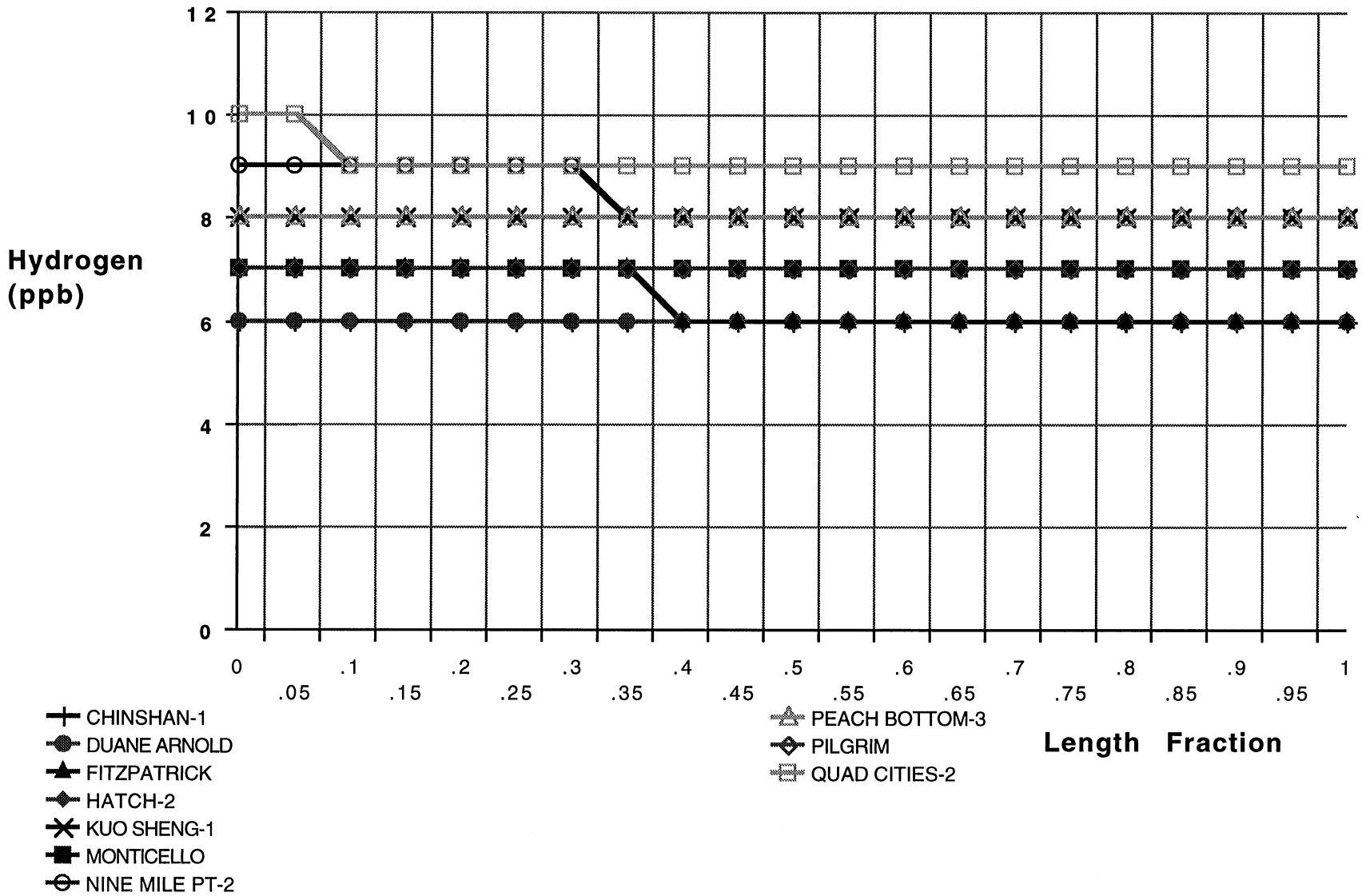

EPRI Licensed Material

Figure A-139: Jet Pump Hydrogen Levels with 0.6 ppm Feedwater H2 Addition

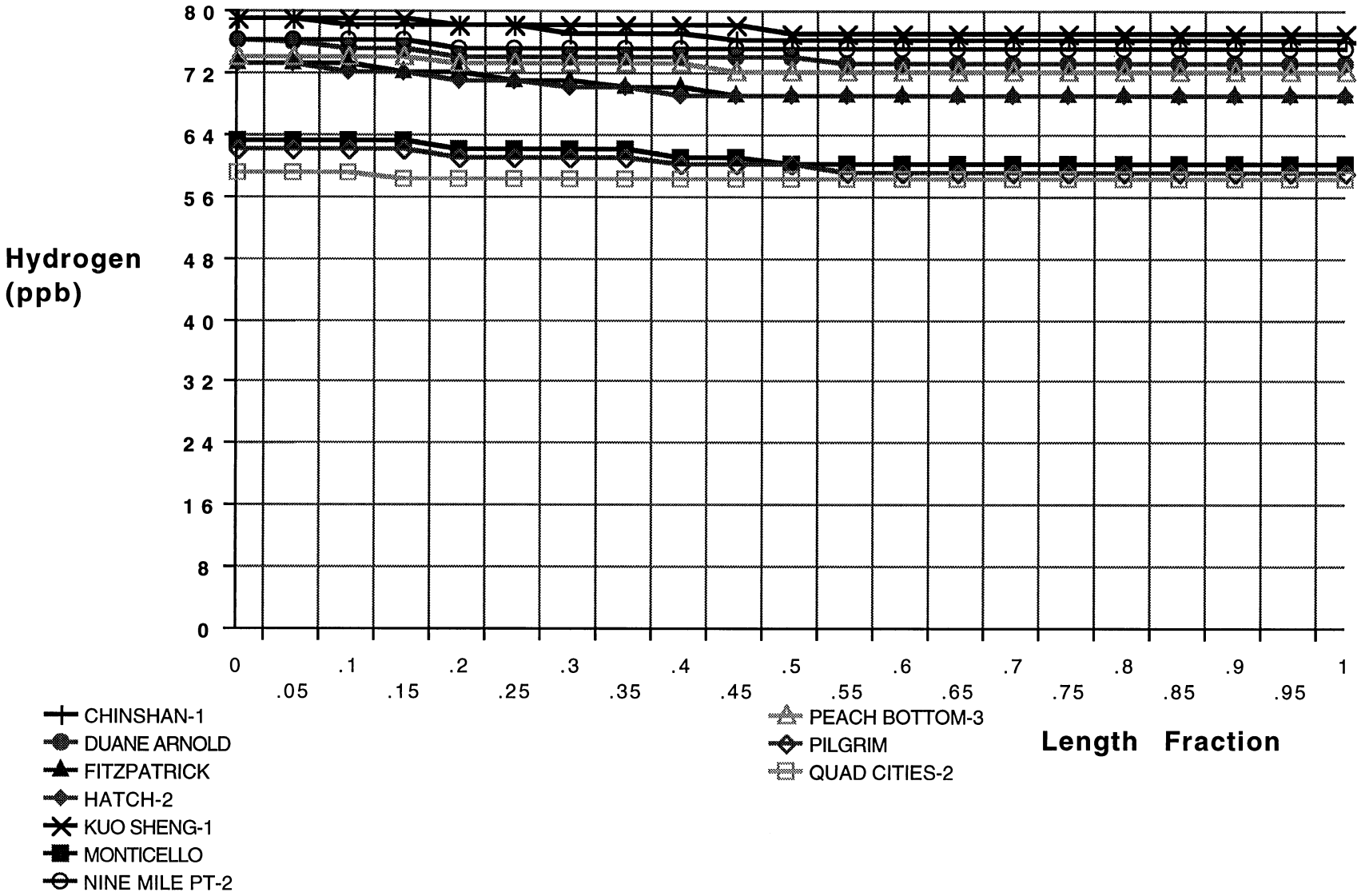

EPRI Licensed Material

Figure A-140: Jet Pump Hydrogen Levels with 1.5 ppm Feedwater H2 Addition

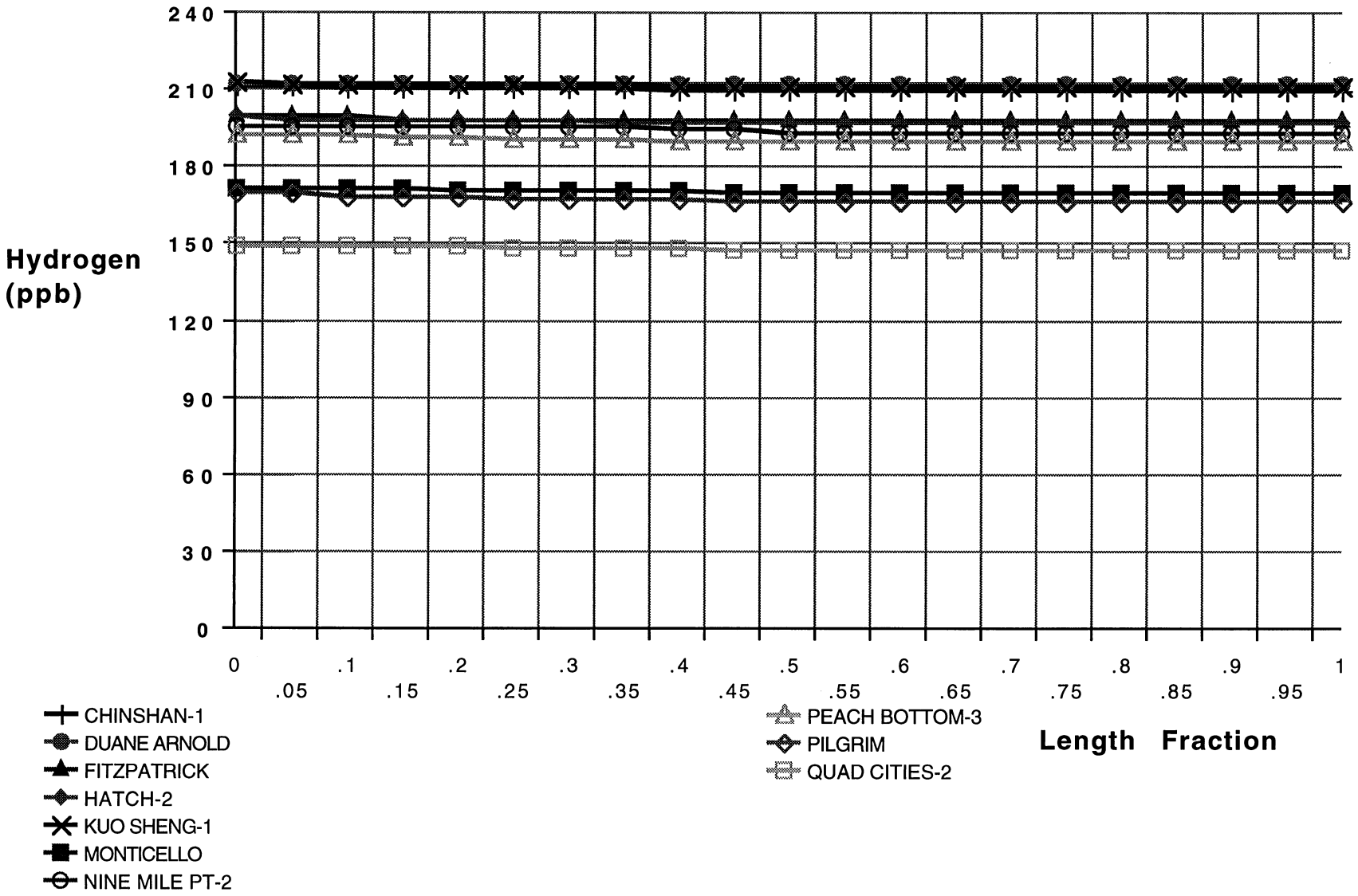

EPRI Licensed Material

Figure A-141: Jet Pump Hydrogen Levels with 3.0 ppm Feedwater H2 Addition

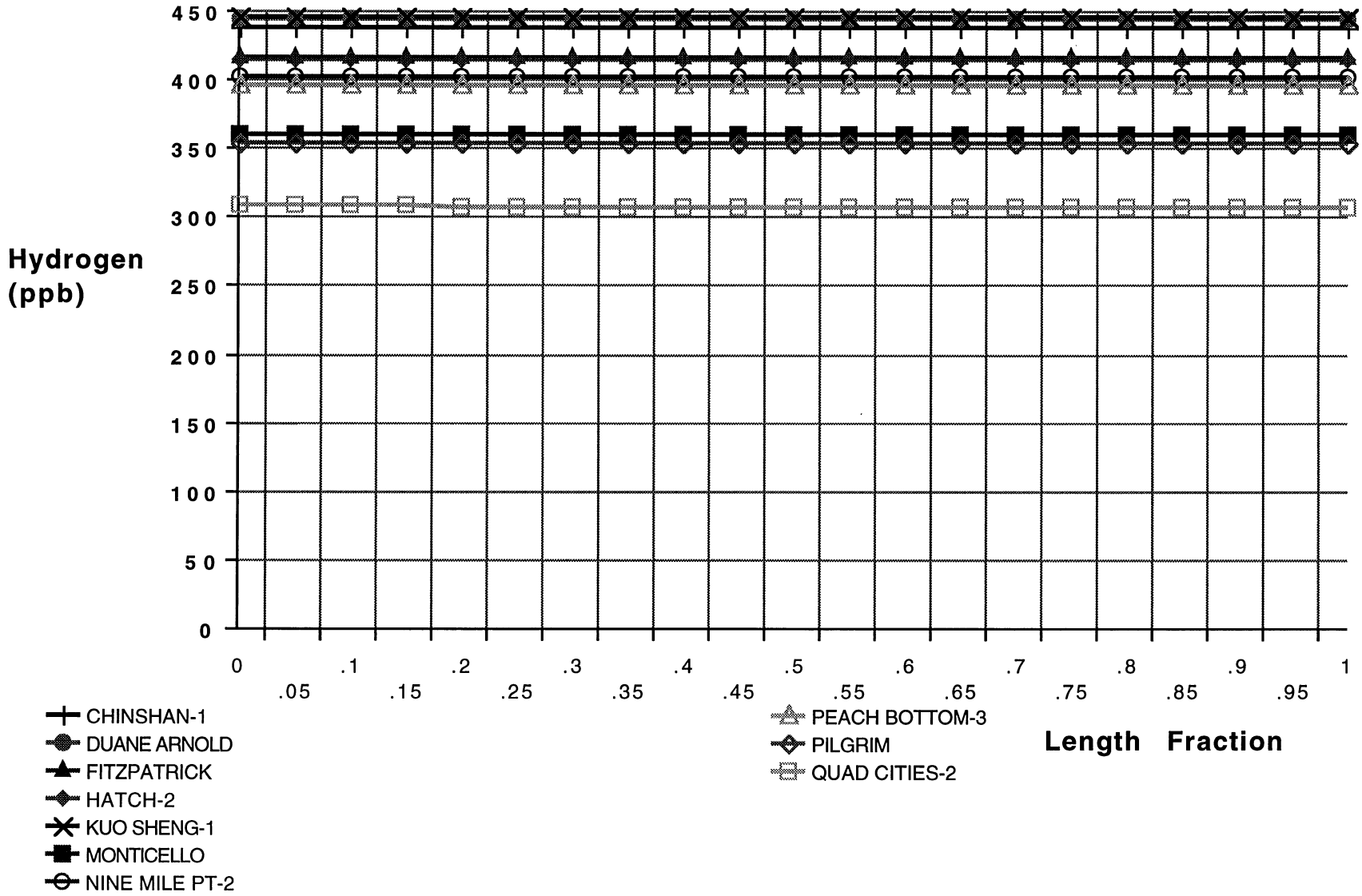

EPRI Licensed Material

Figure A-142: Jet Pump Oxygen Levels with 0 ppm Feedwater H2 Addition

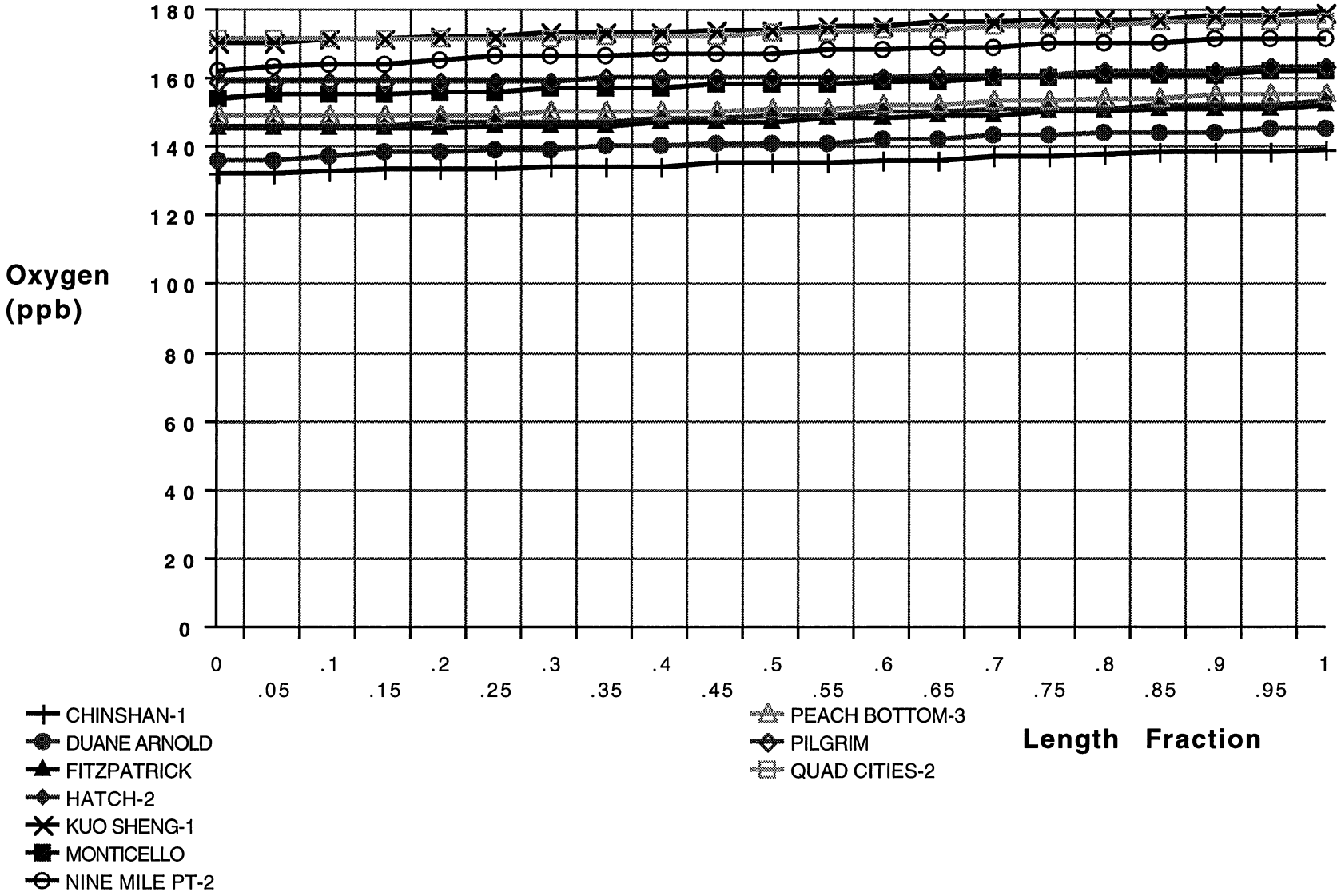

EPRI Licensed Material

Figure A-143: Jet Pump Oxygen Levels with 0.6 ppm Feedwater H2 Addition

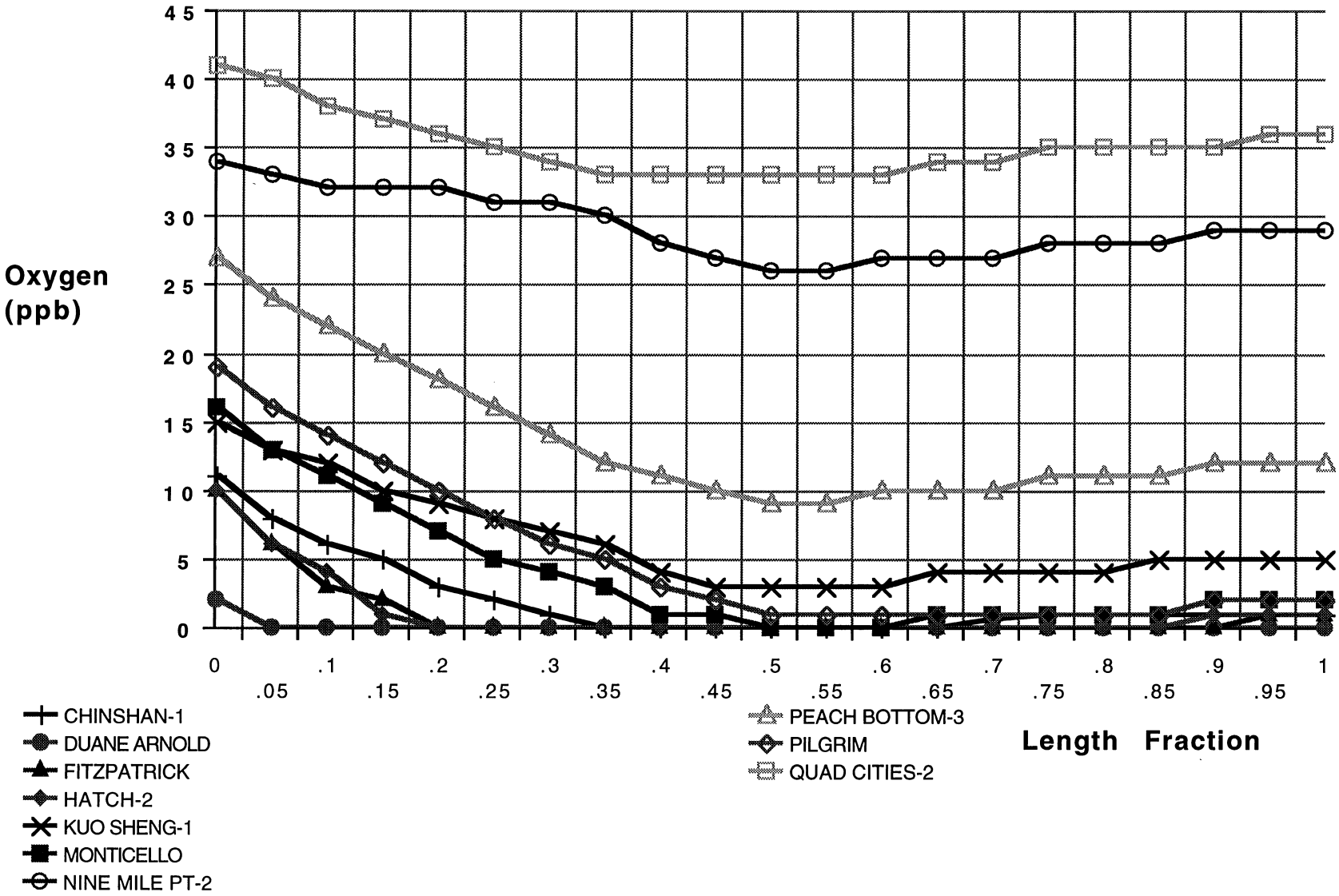

EPRI Licensed Material

Figure A-144: Jet Pump Oxygen Levels with 1.5 ppm Feedwater H2 Addition

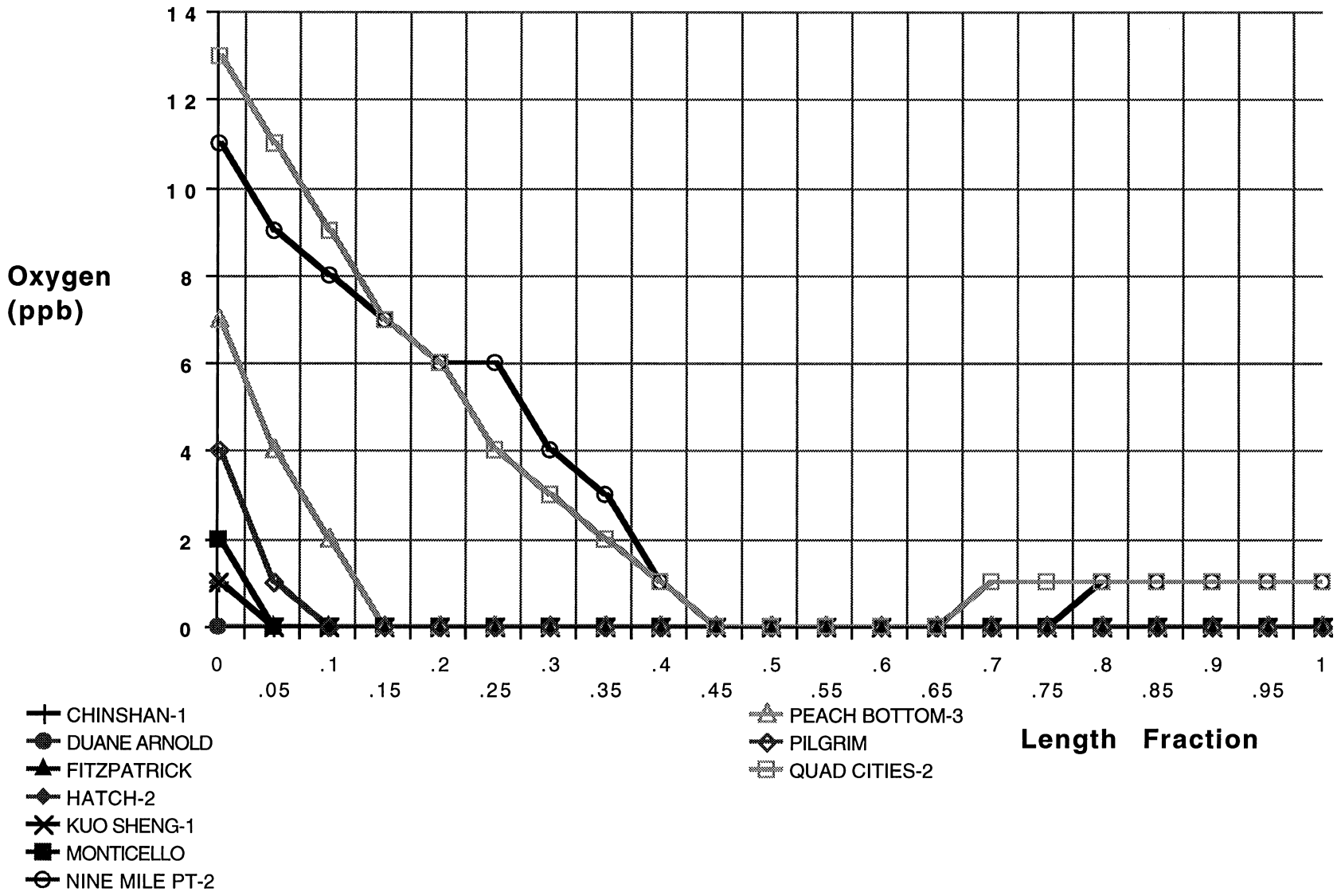

EPRI Licensed Material

Figure A-145: Jet Pump Peroxide Levels with 0 ppm Feedwater H2 Addition

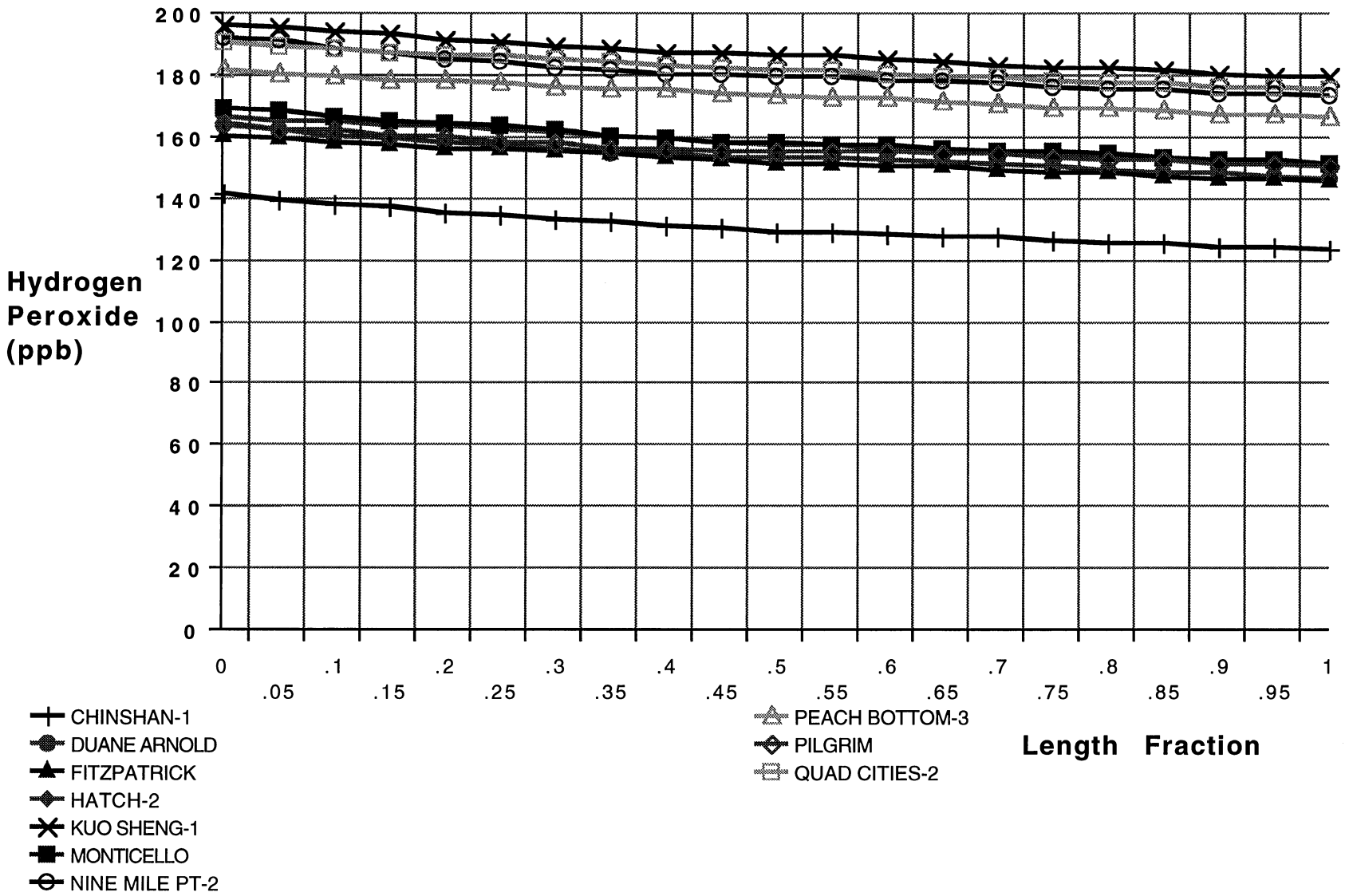

EPRI Licensed Material

Figure A-146: Jet Pump Peroxide Levels with 0.6 ppm Feedwater H2 Addition

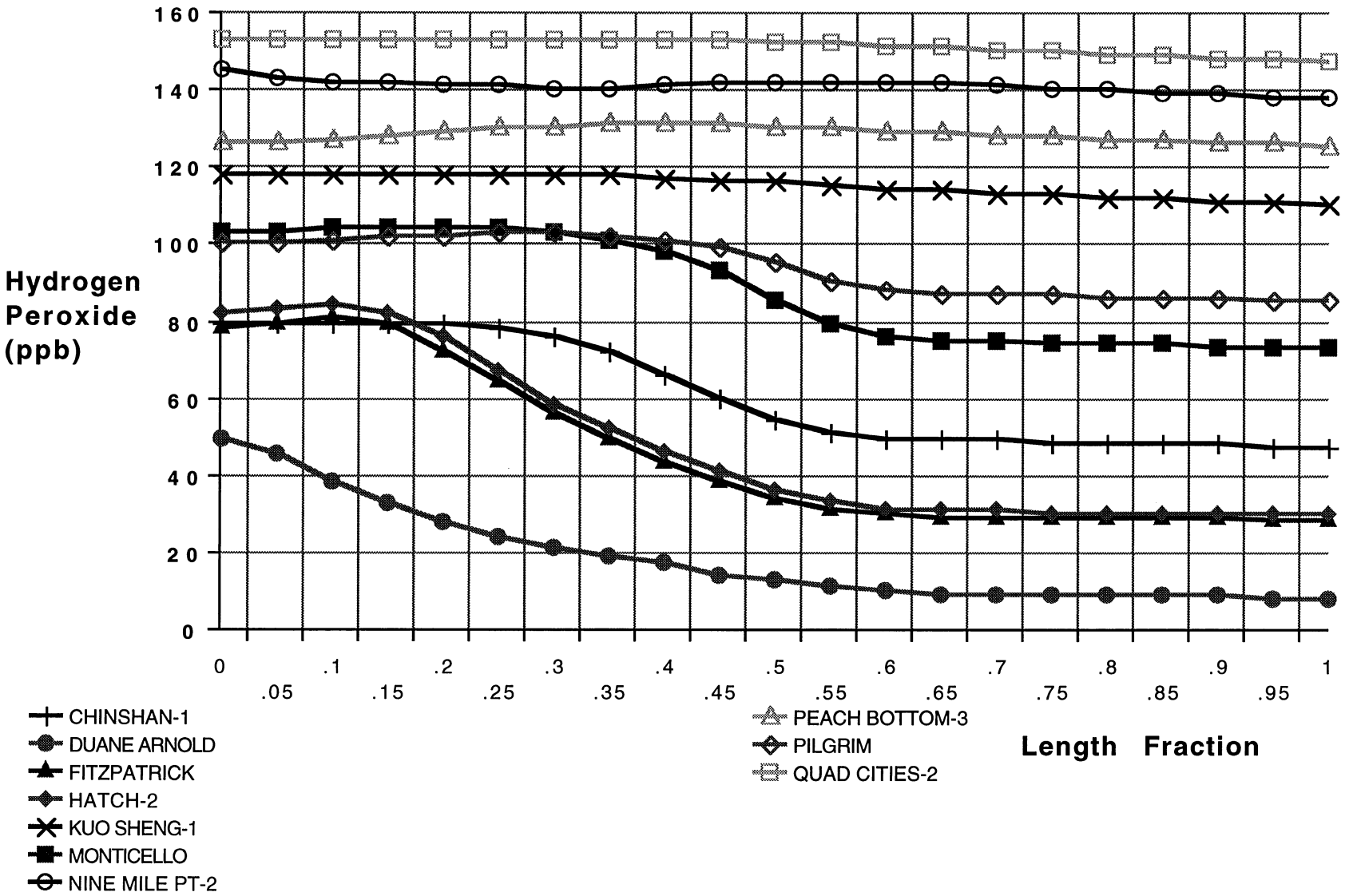

EPRI Licensed Material

Figure A-147: Jet Pump Peroxide Levels with 1.5 ppm Feedwater H2 Addition

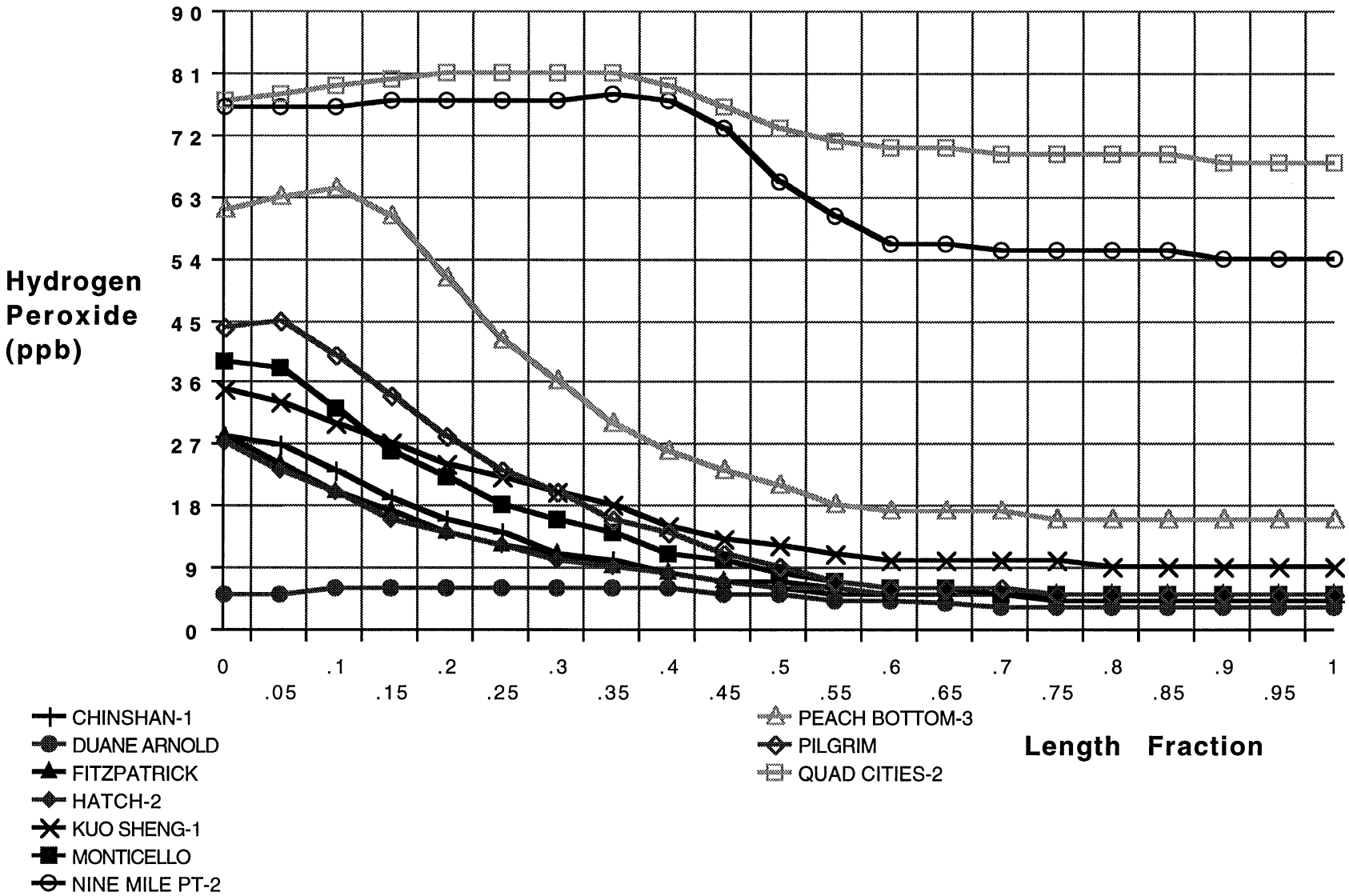

EPRI Licensed Material

Figure A-148: Jet Pump Peroxide Levels with 3.0 ppm Feedwater H2 Addition

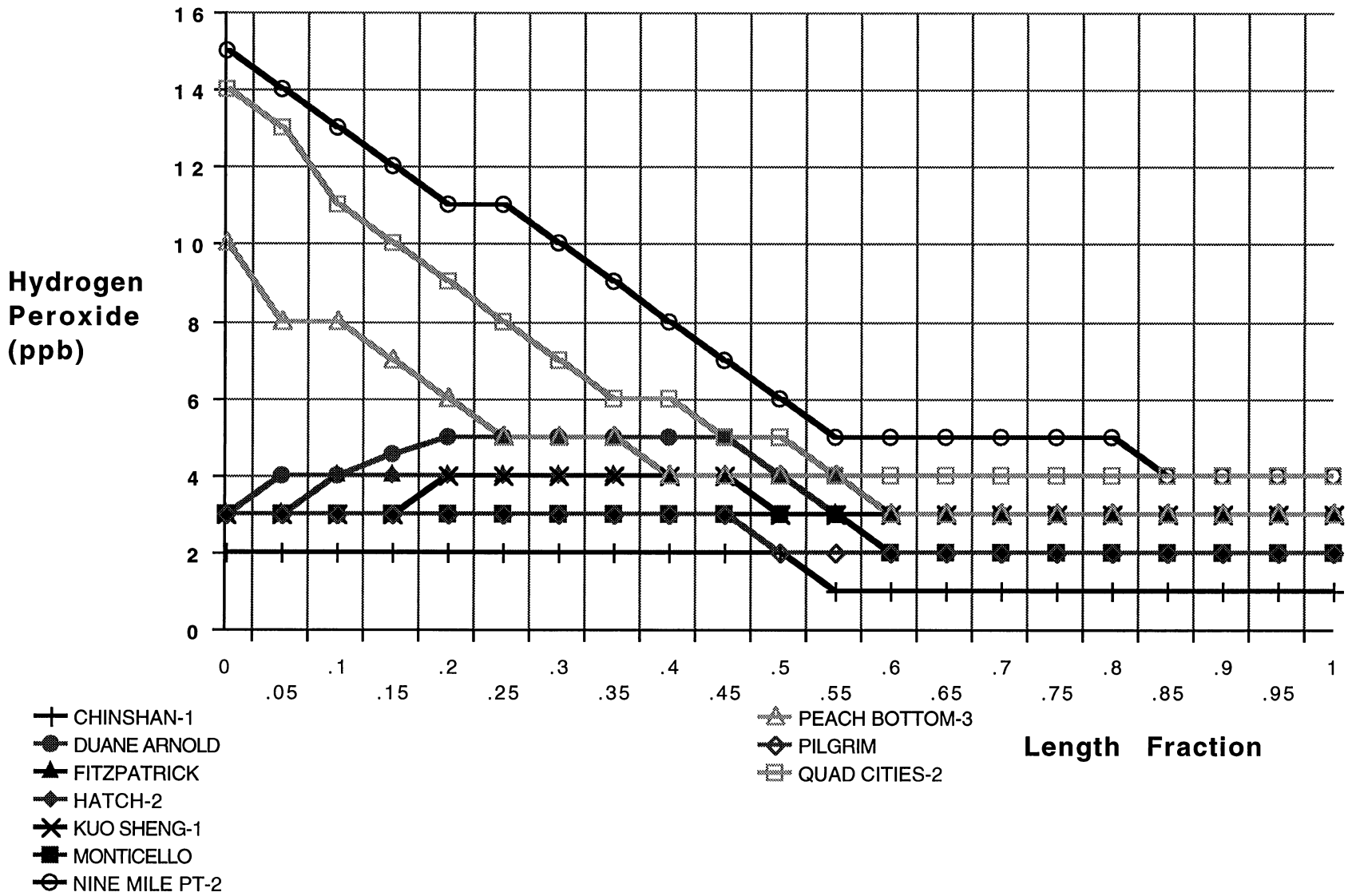

EPRI Licensed Material

Figure A-149: Lower Plenum Region ECPs with 0 ppm Feedwater H2 Addition

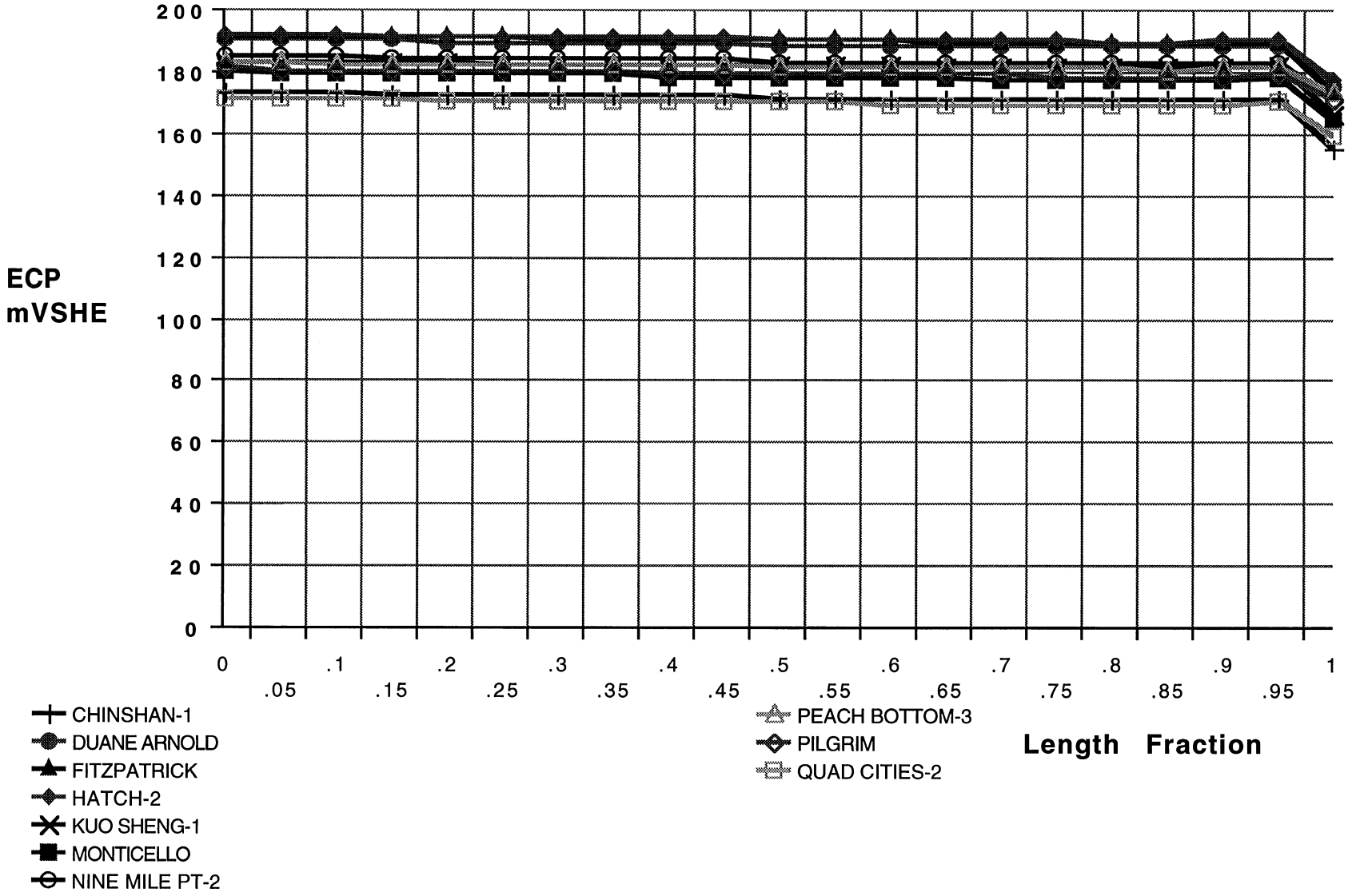

EPRI Licensed Material

Figure A-150: Lower Plenum Region ECPs with 0.6 ppm Feedwater H2 Addition

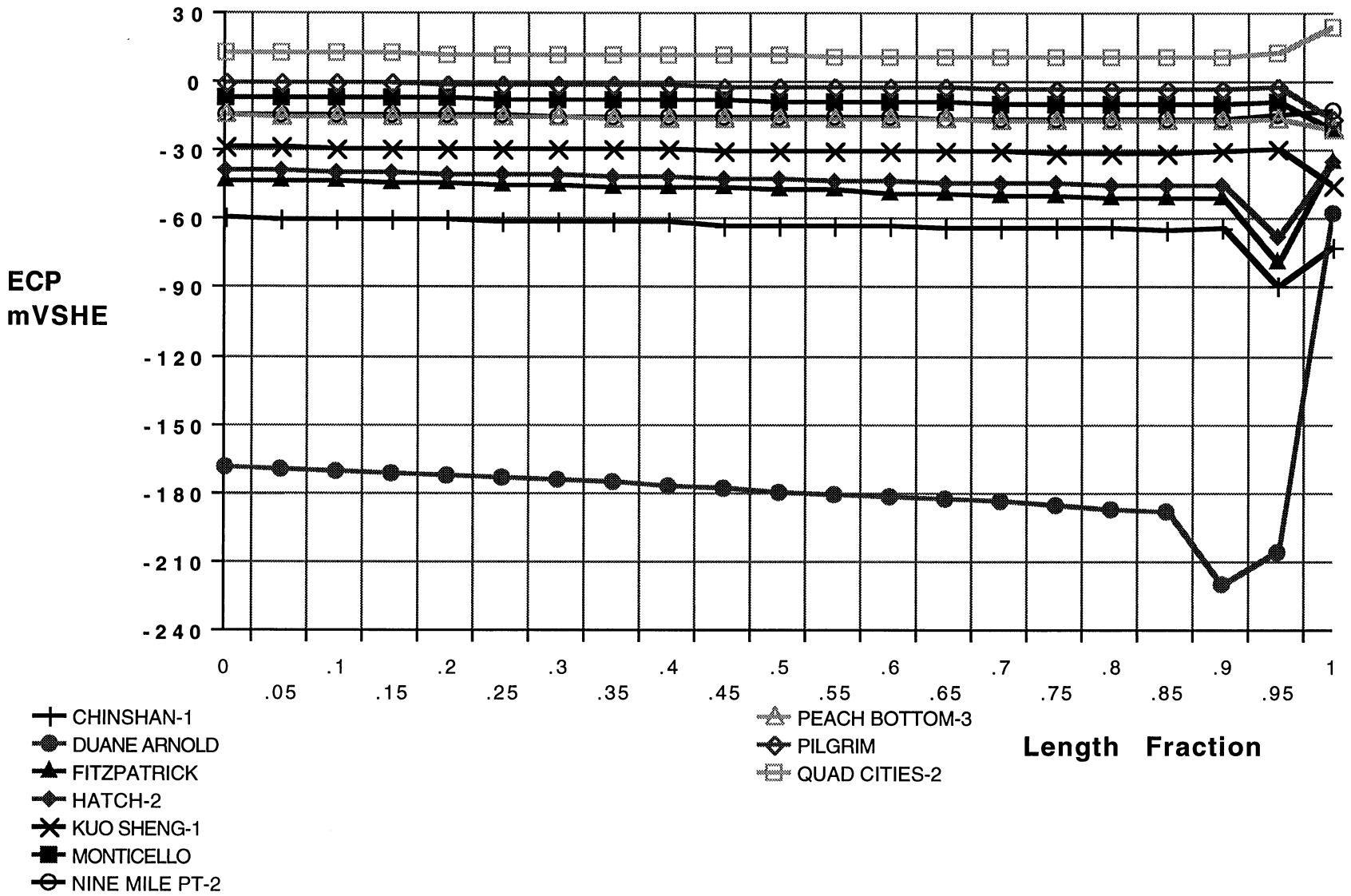

EPRI Licensed Material

Figure A-151: Lower Plenum Region ECPs with 1.5 ppm Feedwater H2 Addition

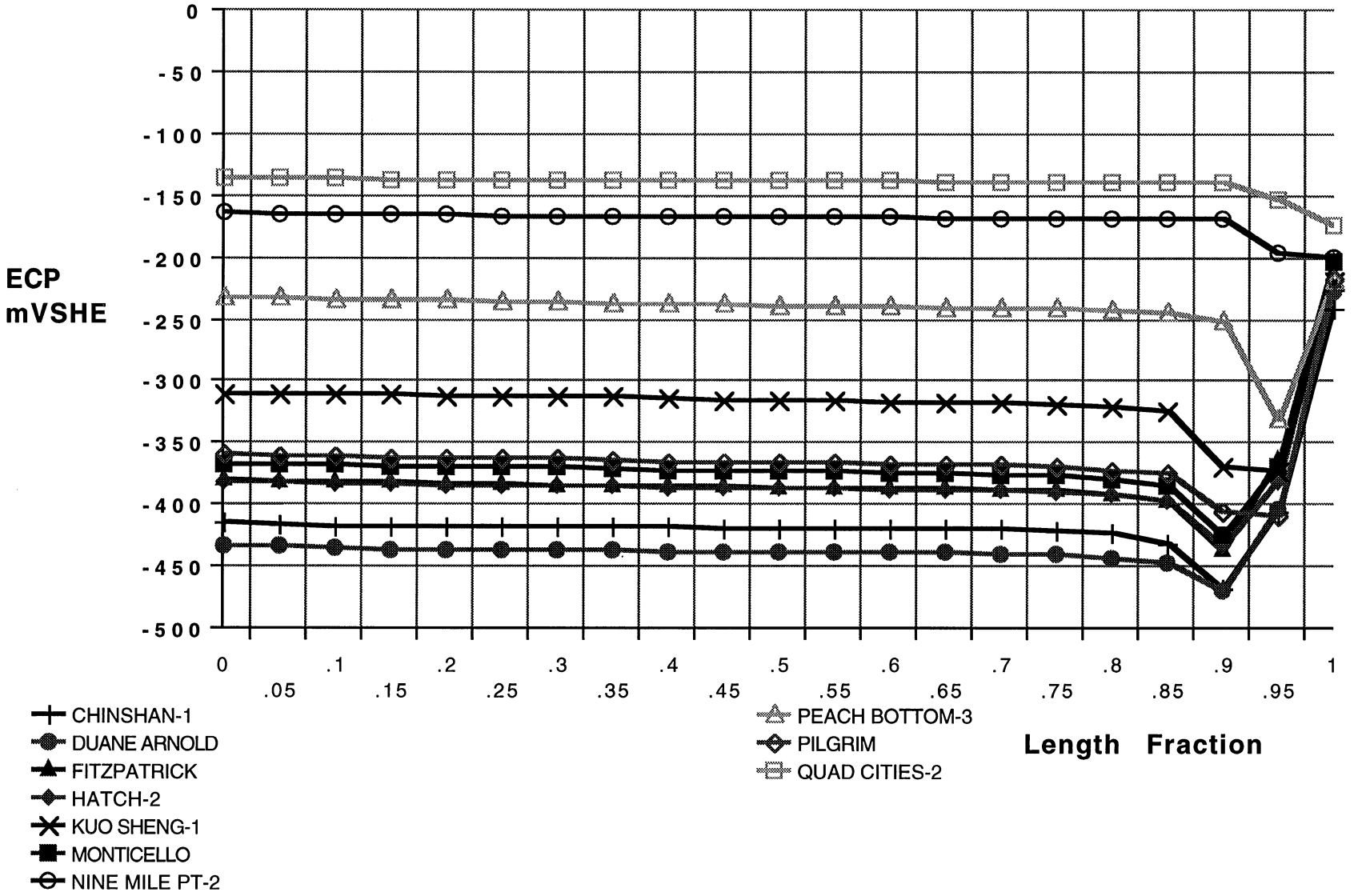

EPRI Licensed Material

Figure A-152: Lower Plenum Region ECPs with 3.0 ppm Feedwater H2 Addition

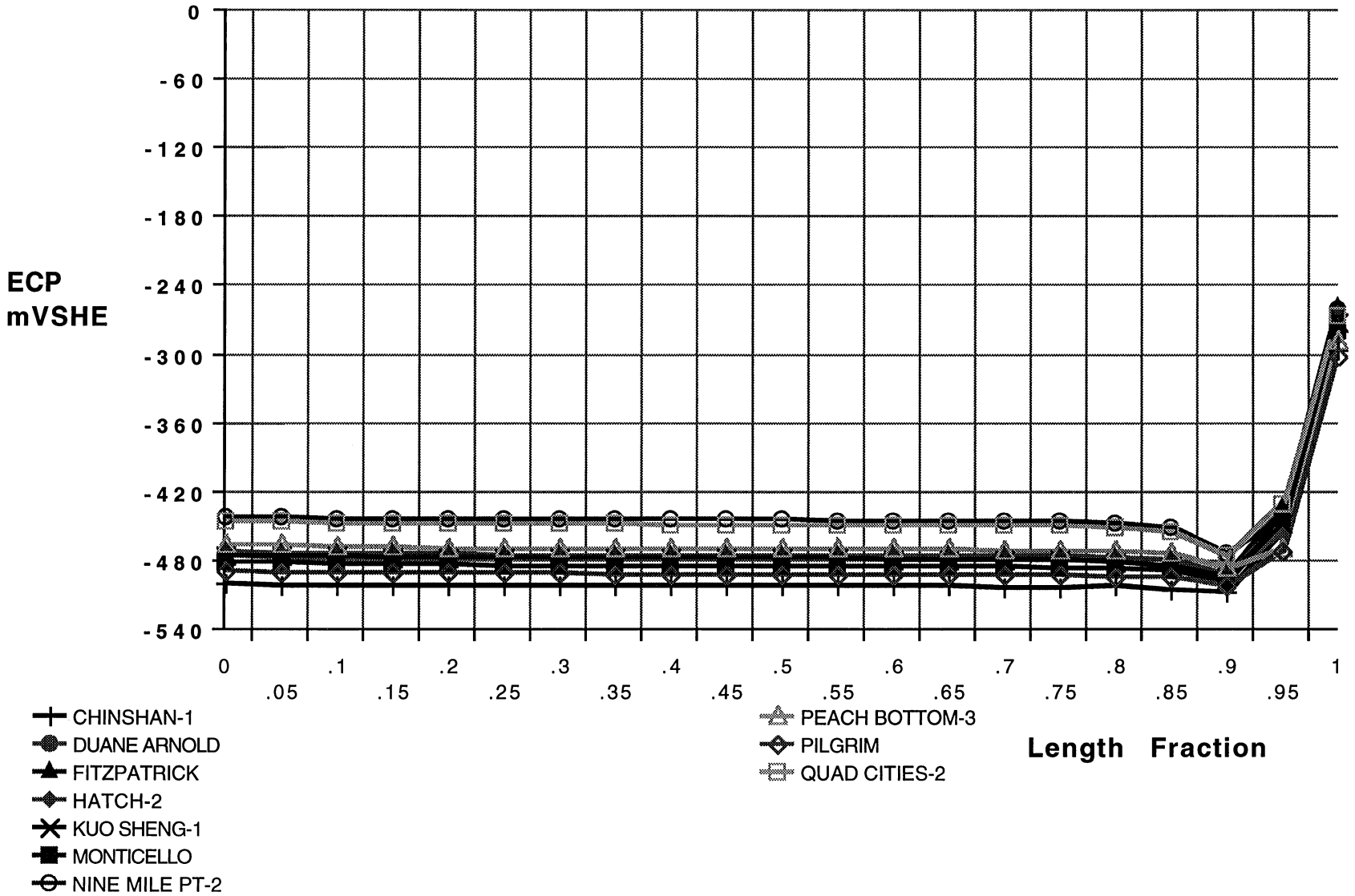

EPRI Licensed Material

Figure A-153: Lower Plenum Hydrogen Levels with 0 ppm Feedwater H2 Addition

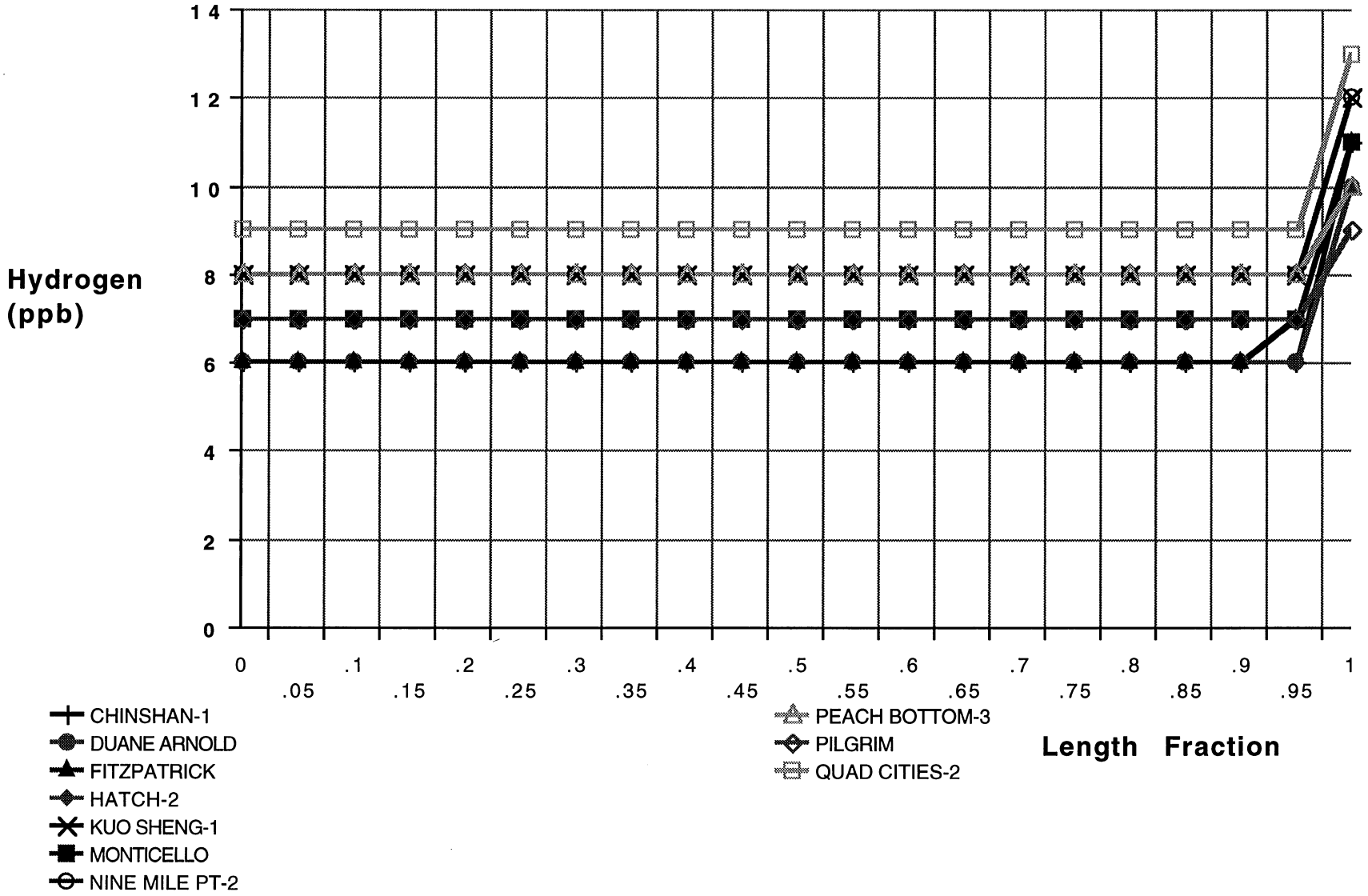

EPRI Licensed Material

Figure A-154: Lower Plenum Hydrogen Levels with 0.6 ppm Feedwater H2 Addition

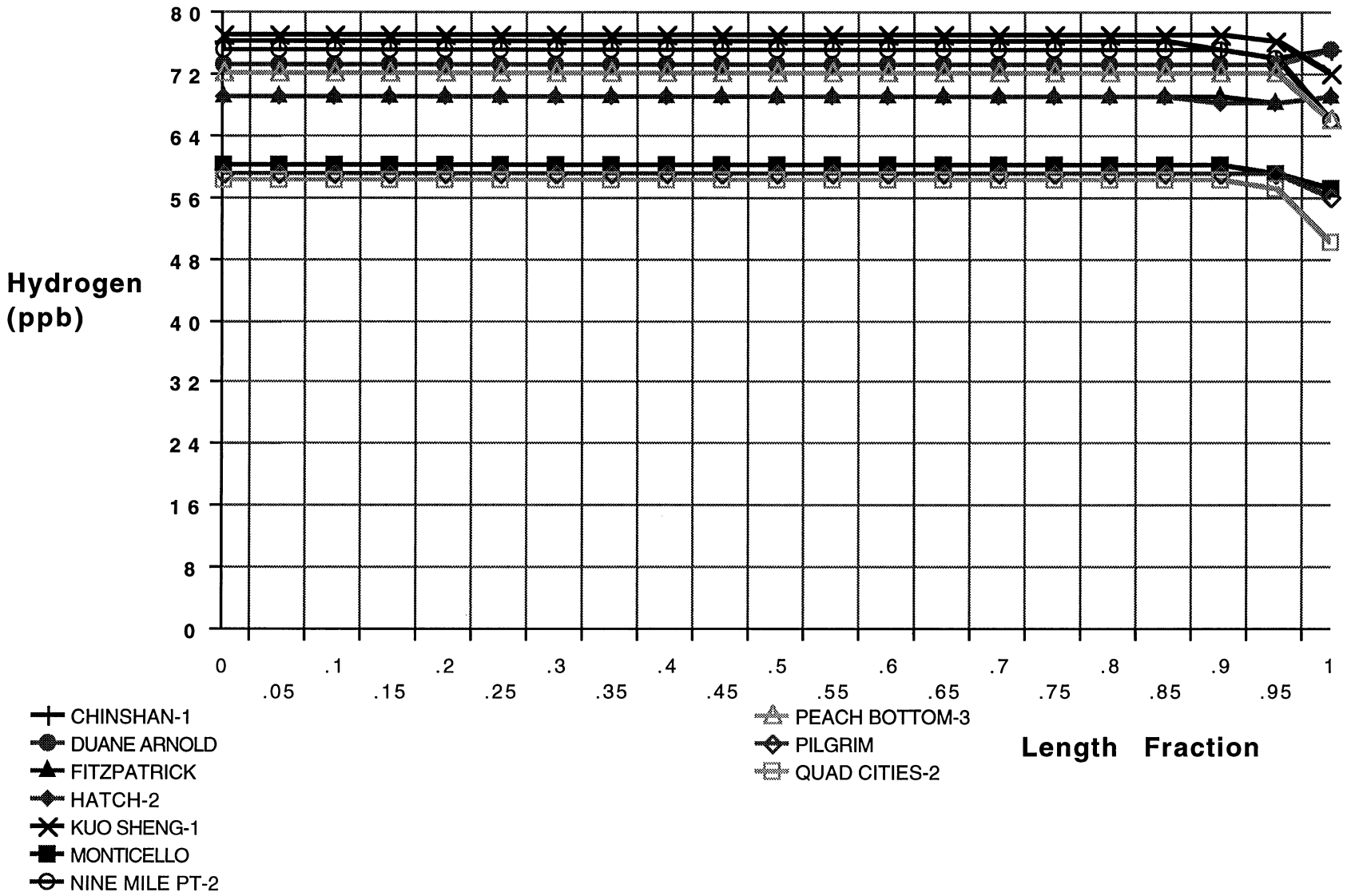

EPRI Licensed Material

Figure A-155: Lower Plenum Hydrogen Levels with 1.5 ppm Feedwater H2 Addition

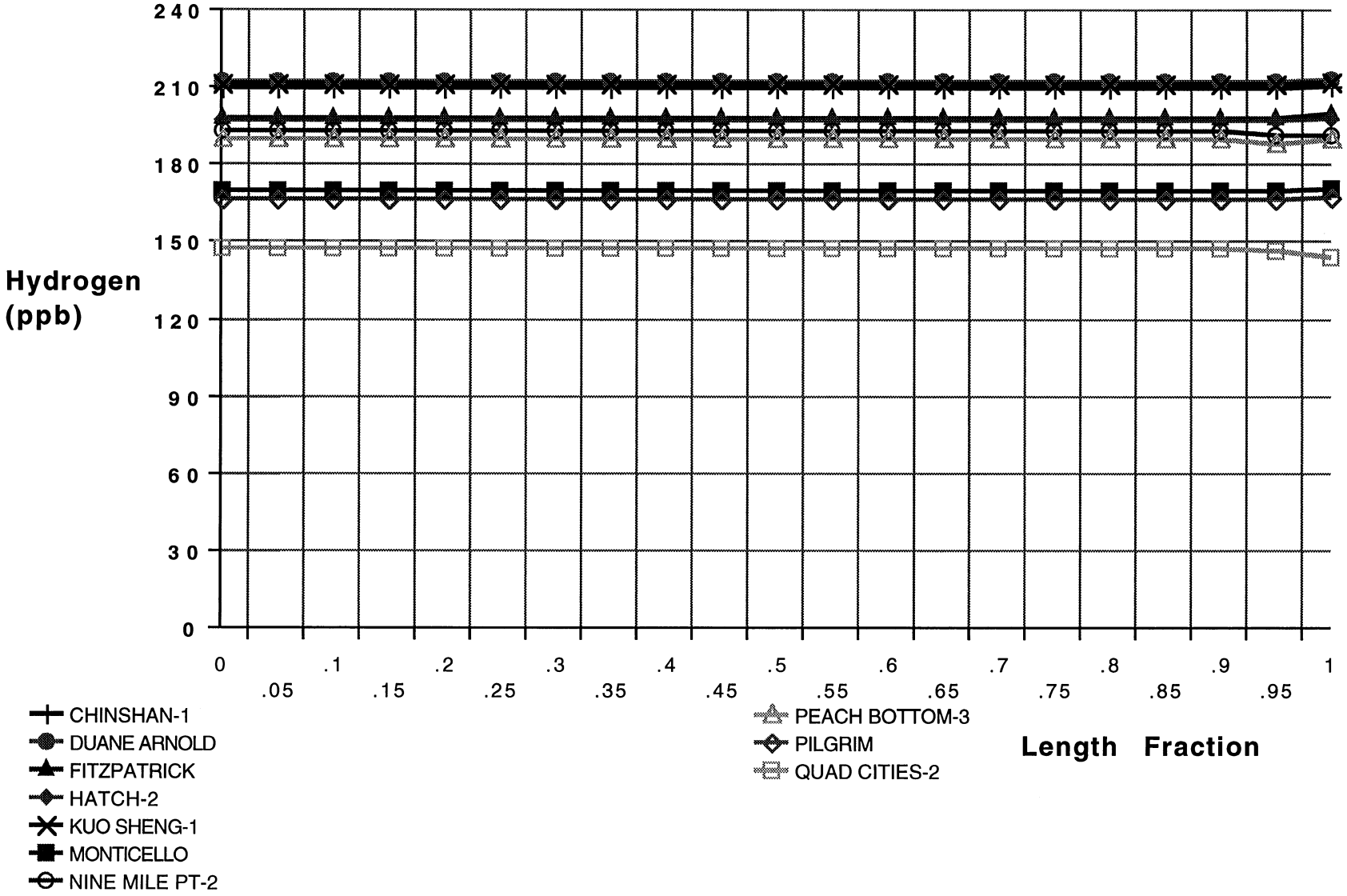

EPRI Licensed Material

Figure A-156: Lower Plenum Hydrogen Levels with 3.0 ppm Feedwater H2 Addition

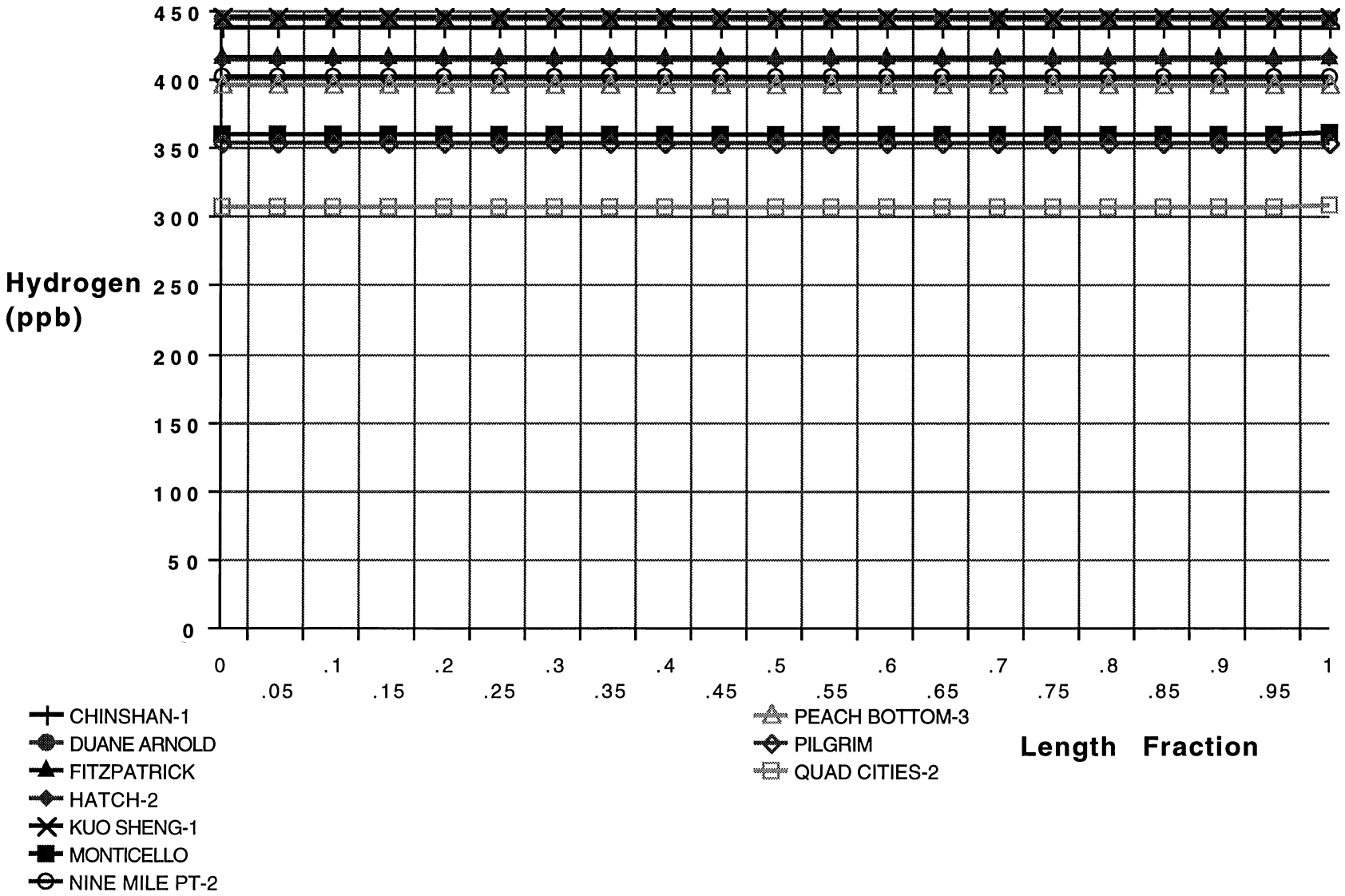

EPRI Licensed Material

Figure A-157: Lower Plenum Oxygen Levels with 0 ppm Feedwater H2 Addition

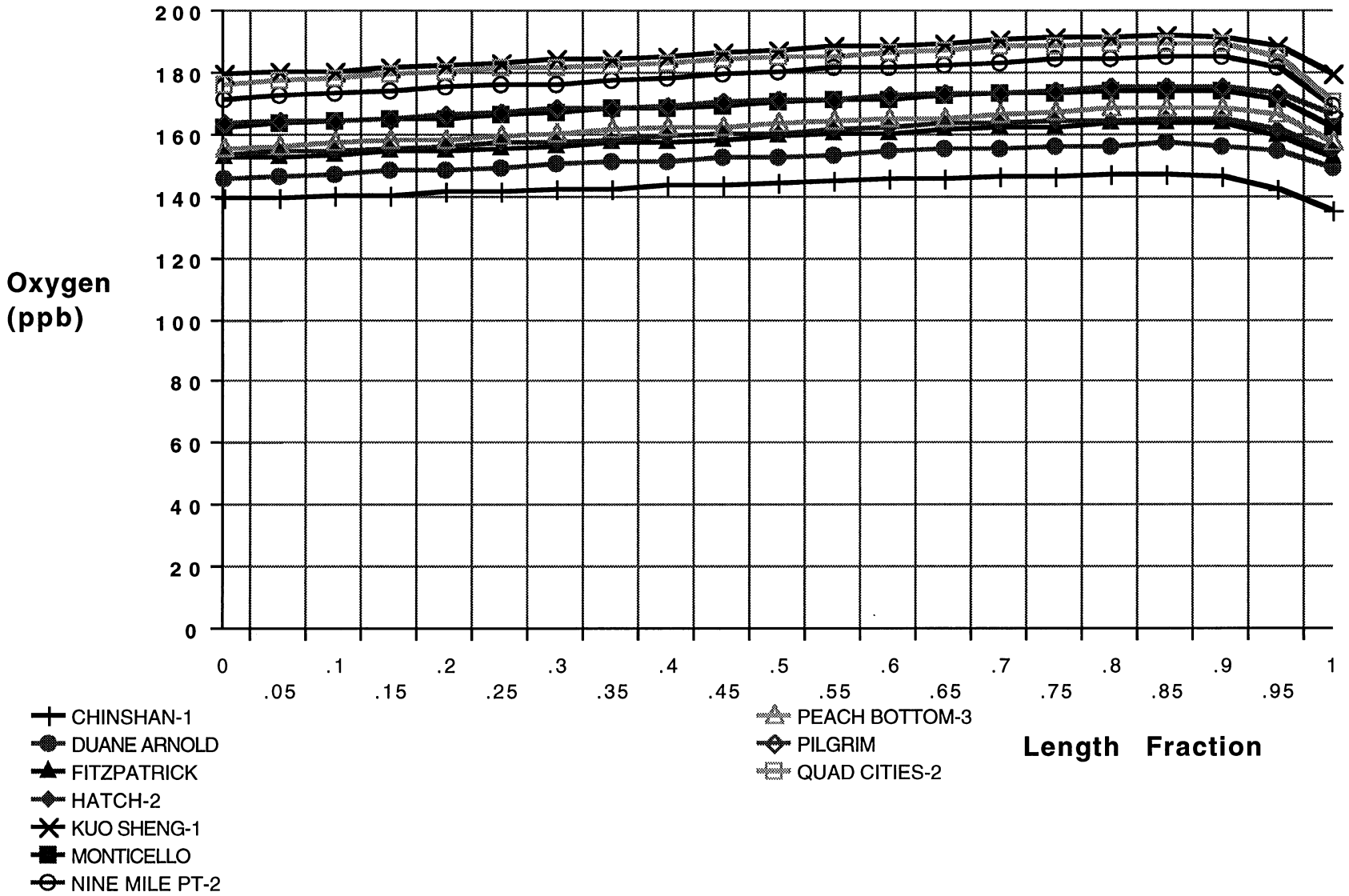

EPRI Licensed Material

Figure A-158: Lower Plenum Oxygen Levels with 0.6 ppm Feedwater H2 Addition

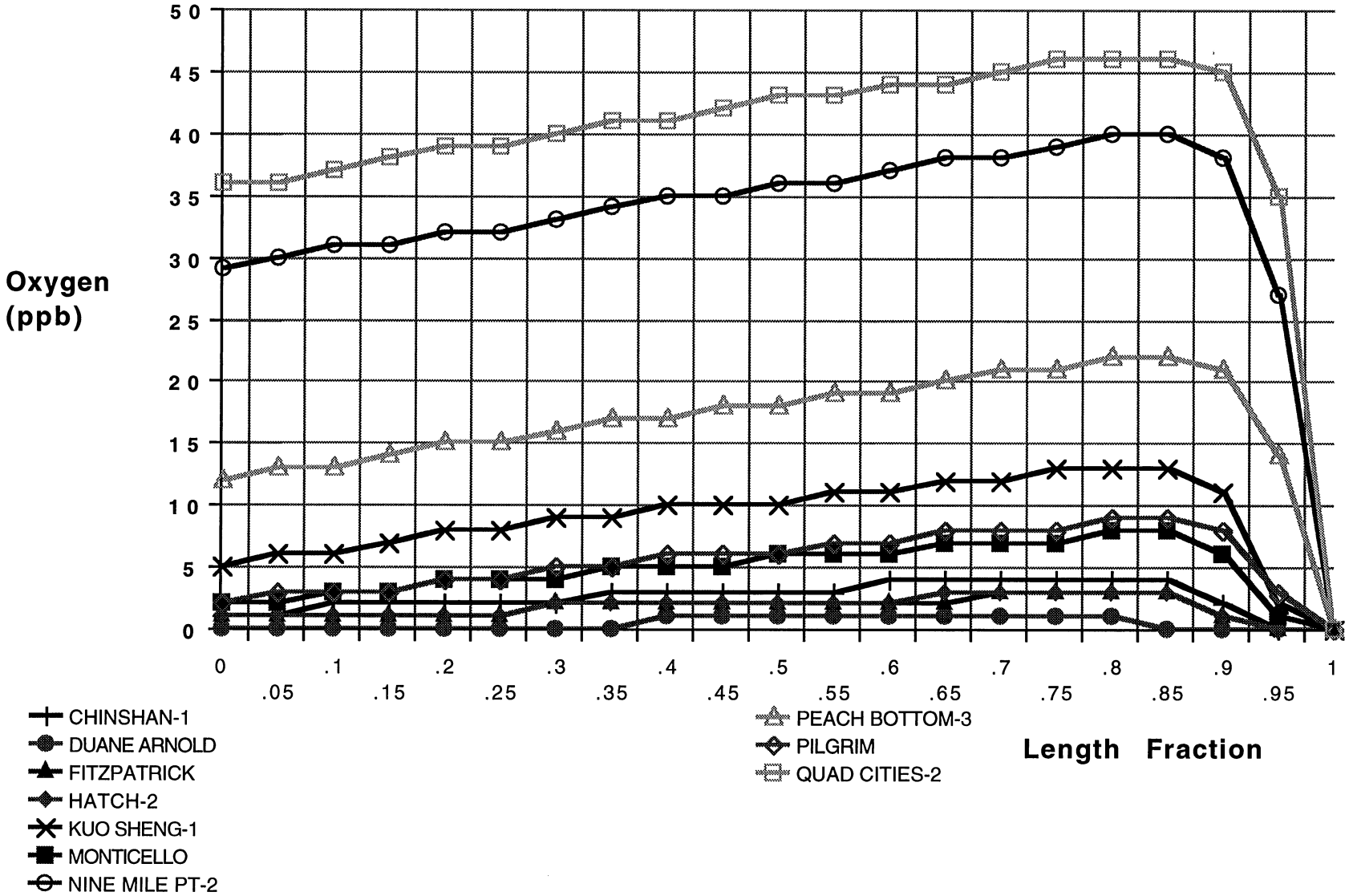

EPRI Licensed Material

Figure A-159: Lower Plenum Oxygen Levels with 1.5 ppm Feedwater H2 Addition

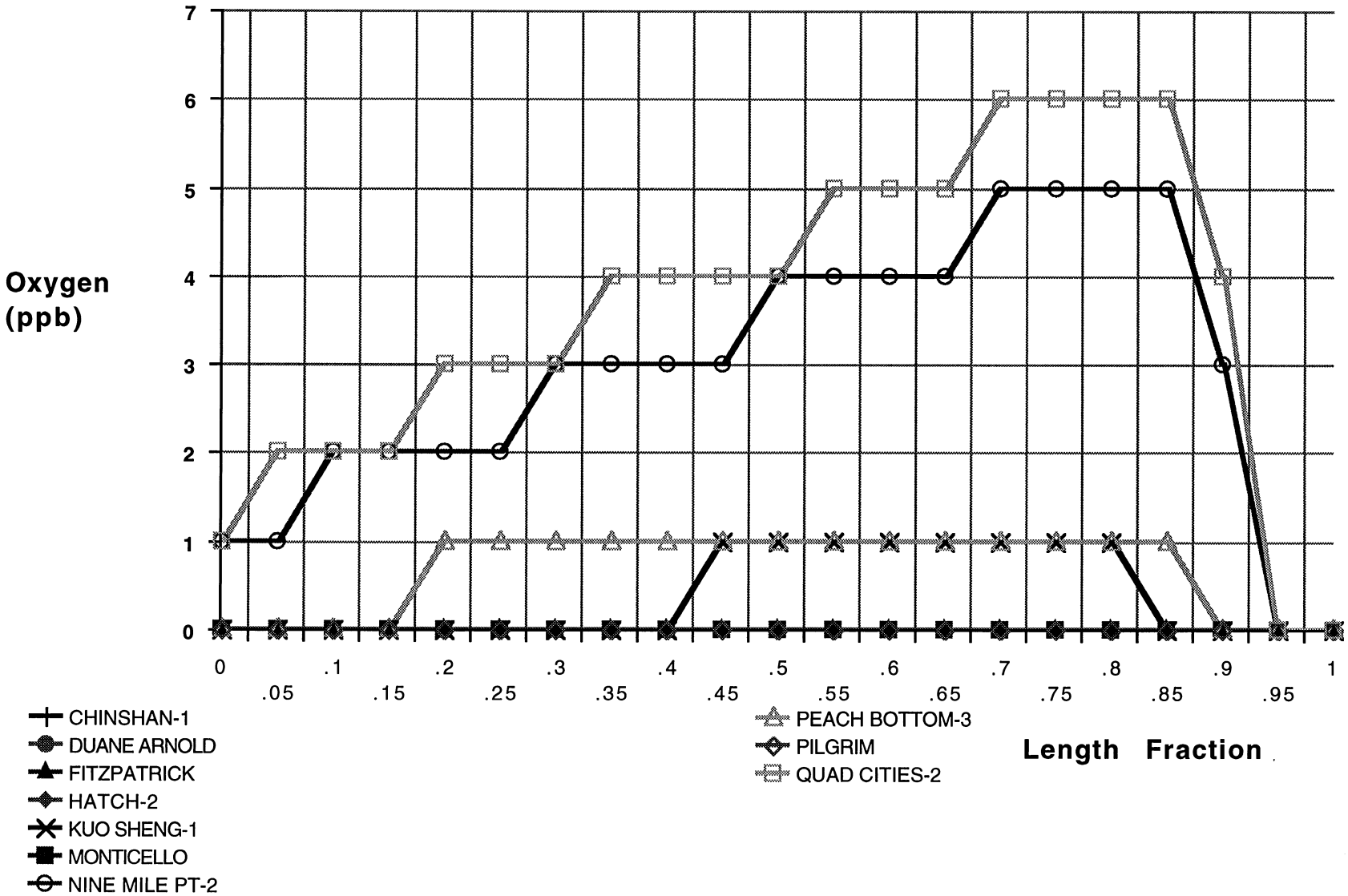

EPRI Licensed Material

Figure A-160: Lower Plenum Peroxide Levels with 0 ppm Feedwater H2 Addition

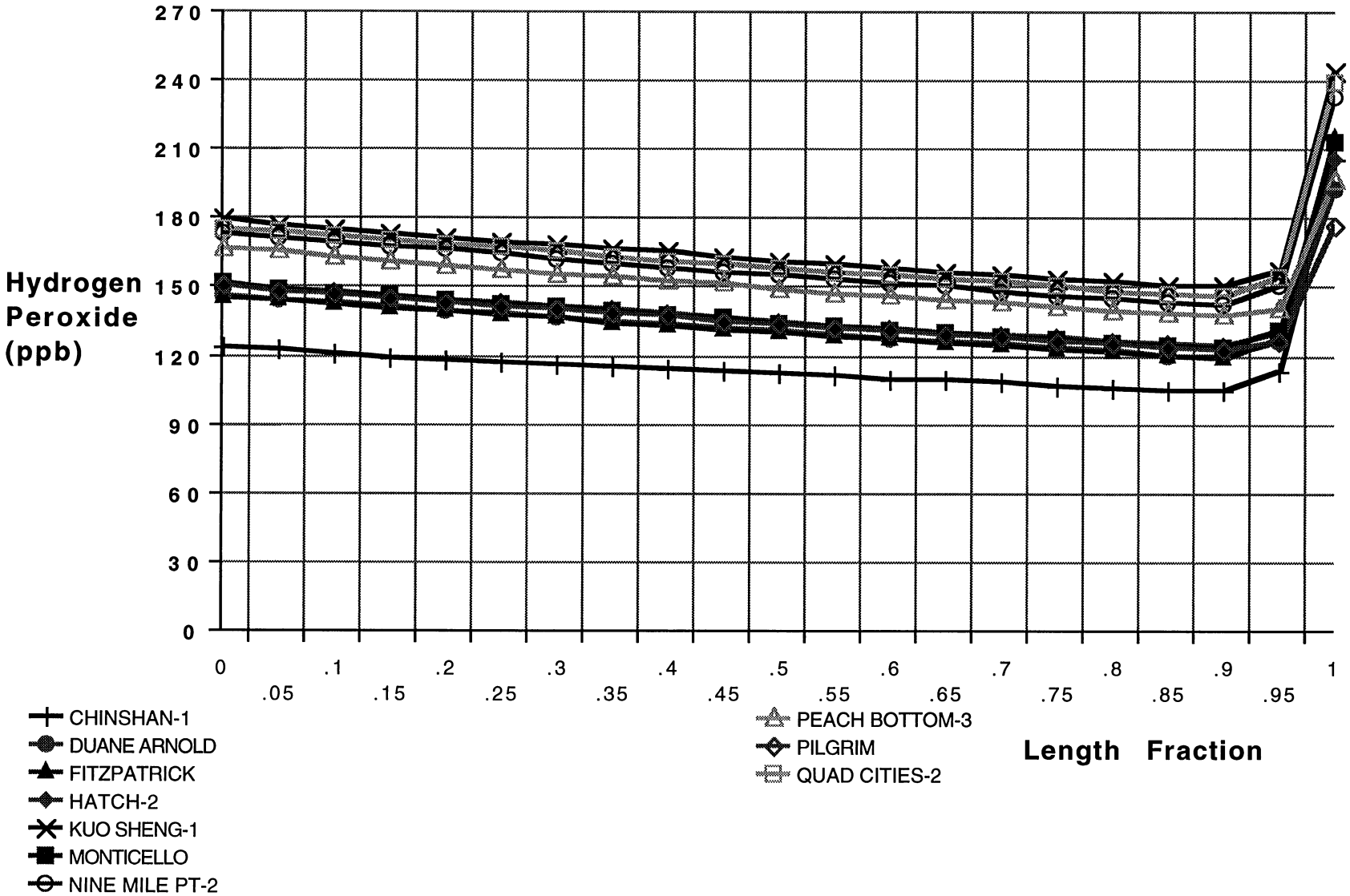

EPRI Licensed Material

Figure A-161: Lower Plenum Peroxide Levels with 0.6 ppm Feedwater H2 Addition

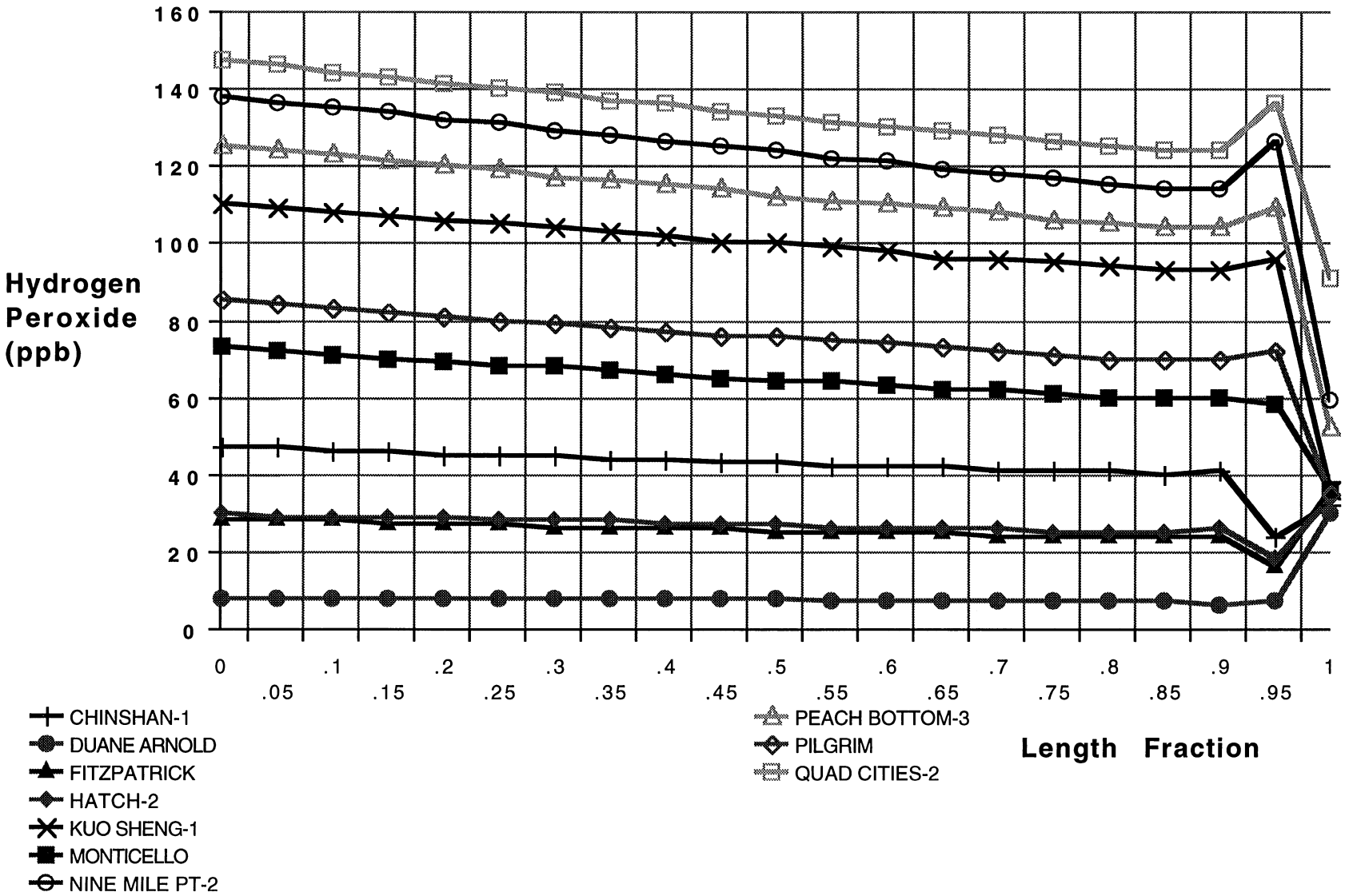

EPRI Licensed Material

Figure A-162: Lower Plenum Peroxide Levels with 1.5 ppm Feedwater H2 Addition

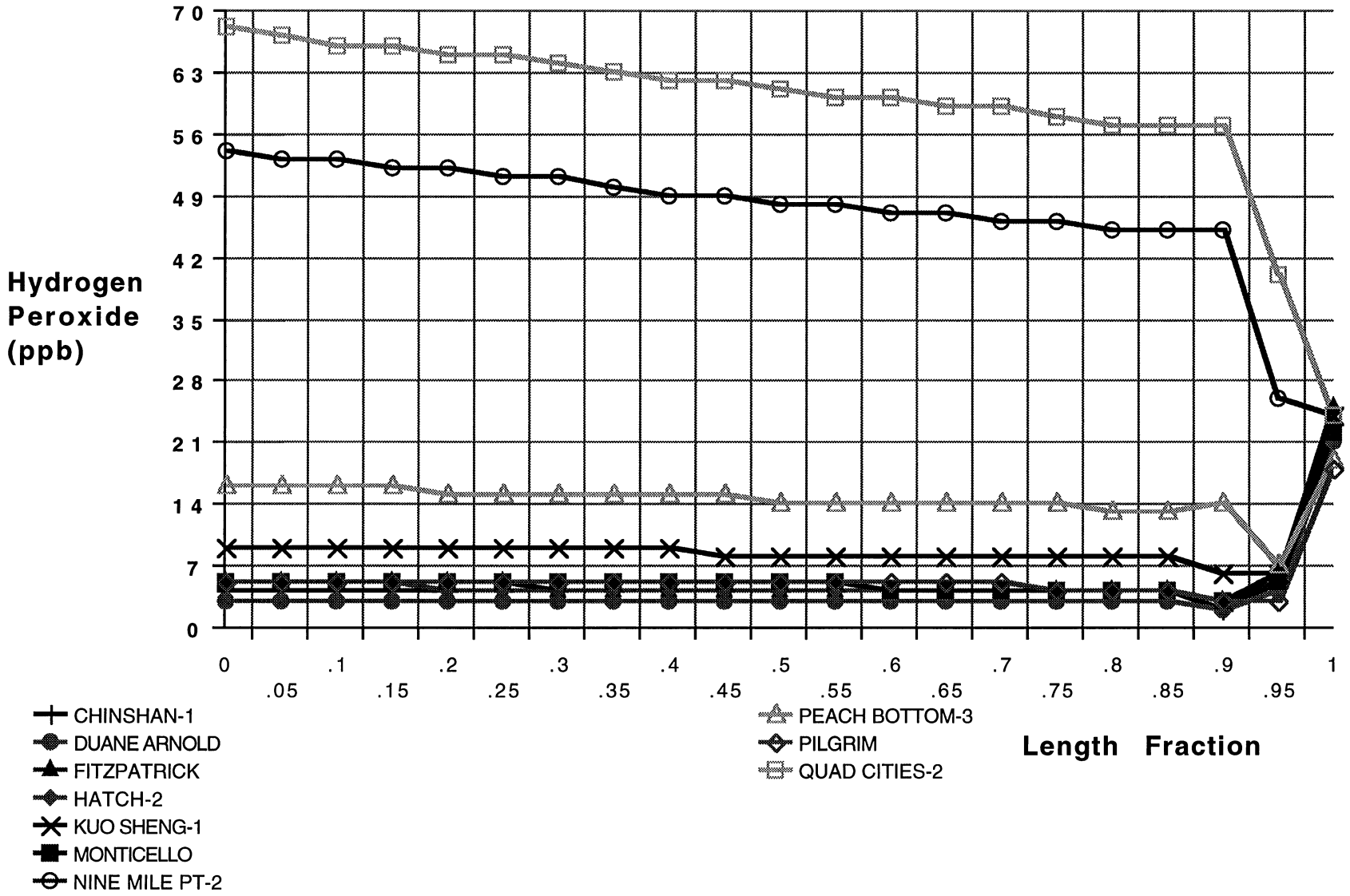

EPRI Licensed Material

Figure A-163: Lower Plenum Peroxide Levels with 3.0 ppm Feedwater H2 Addition

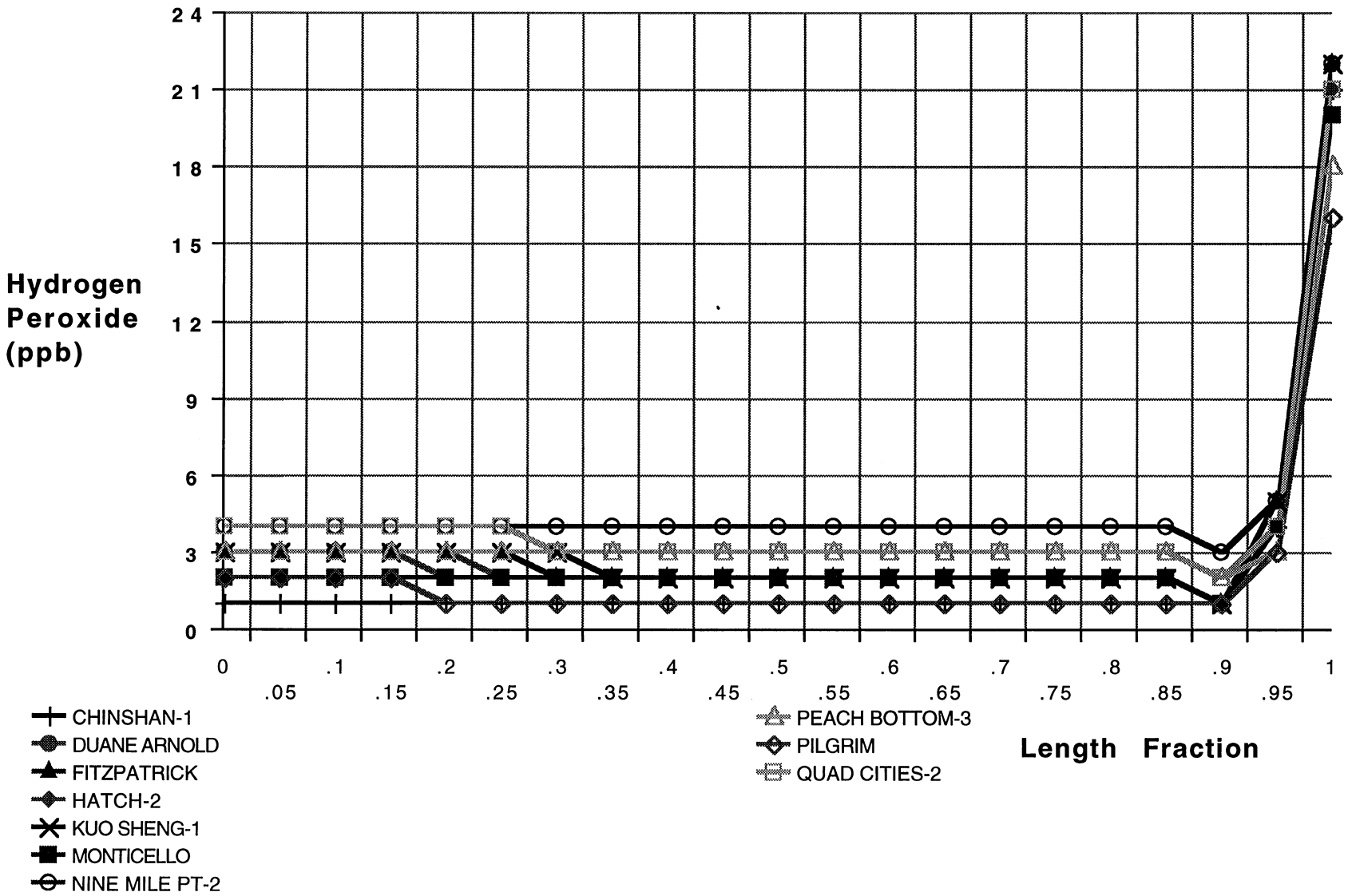

EPRI Licensed Material

EPRI Licensed Material

EPRI Licensed Material

APPENDIX B

CHARTS OF QUAD CITIES-2 MODIFIED LPRM MODEL RESULTS

EPRI Licensed Material

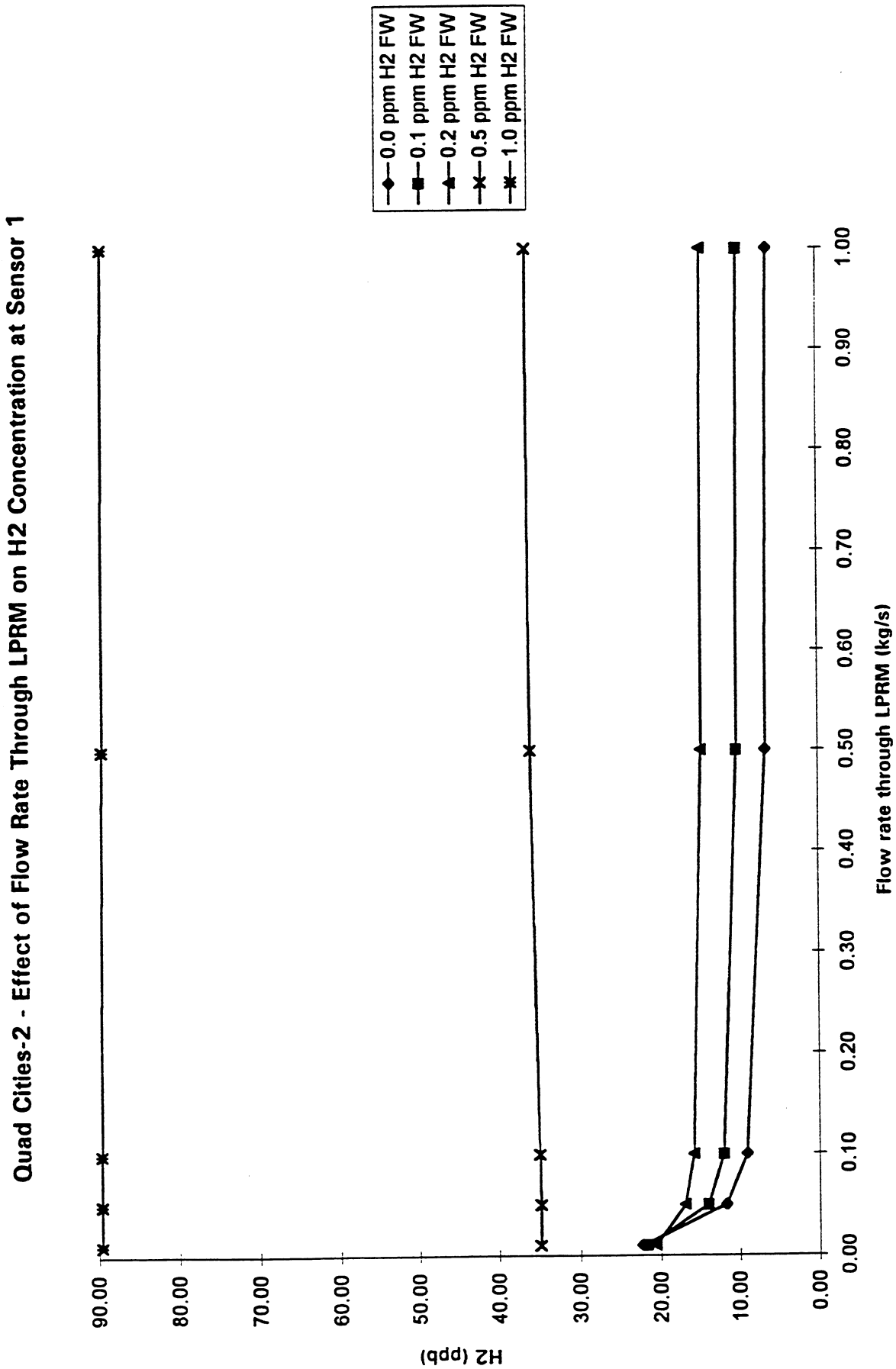
Quad Cities-2 - Effect of Flow Rate Through LPRM on H2 Concentration at Sensor 1
0.0 ppm H2 FW
0.1 ppm H2 FW
0.2 ppm H2 FW
0.5 ppm H2 FW
1.0 ppm H2 FW
H2 (ppb)
90.00
80.00
70.00
60.00
50.00
40.00
30.00
20.00
10.00
0.00
0.00
0.10
0.20
0.30
0.40
0.50
0.60
0.70
0.80
0.90
1.00
Flow rate through LPRM (kg/s)

Figure B-1

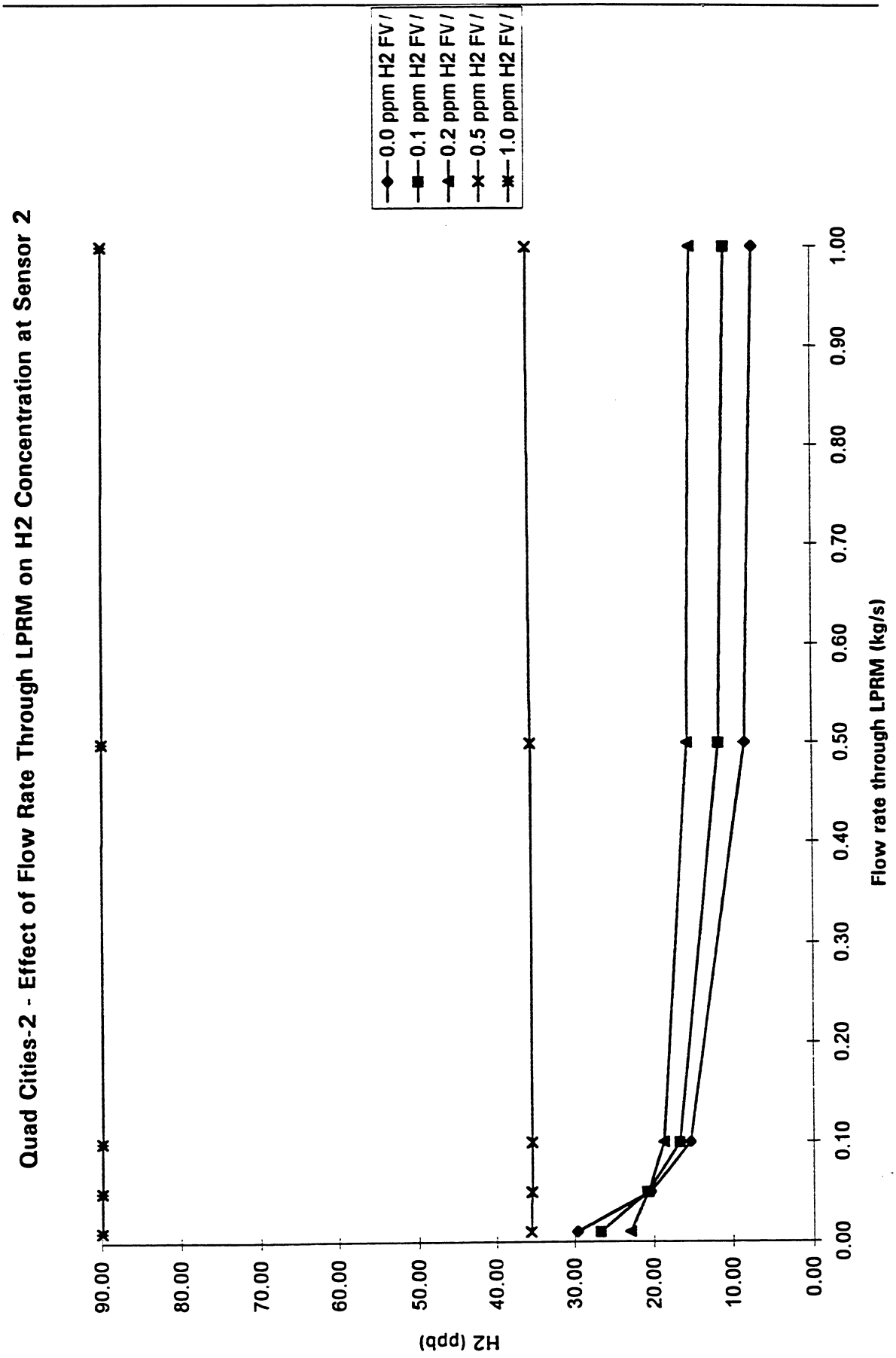
Quad Cities-2 - Effect of Flow Rate Through LPRM on H2 Concentration at Sensor 2
0.0 ppm H2 FV /
0.1 ppm H2 FV /
0.2 ppm H2 FV /
0.5 ppm H2 FV /
1.0 ppm H2 FV /
H2 (ppb)
90.00
80.00
70.00
60.00
50.00
40.00
30.00
20.00
10.00
0.00
0.00
0.10
0.20
0.30
0.40
0.50
0.60
0.70
0.80
0.90
1.00
Flow rate through LPRM (kg/s)

Figure B-2

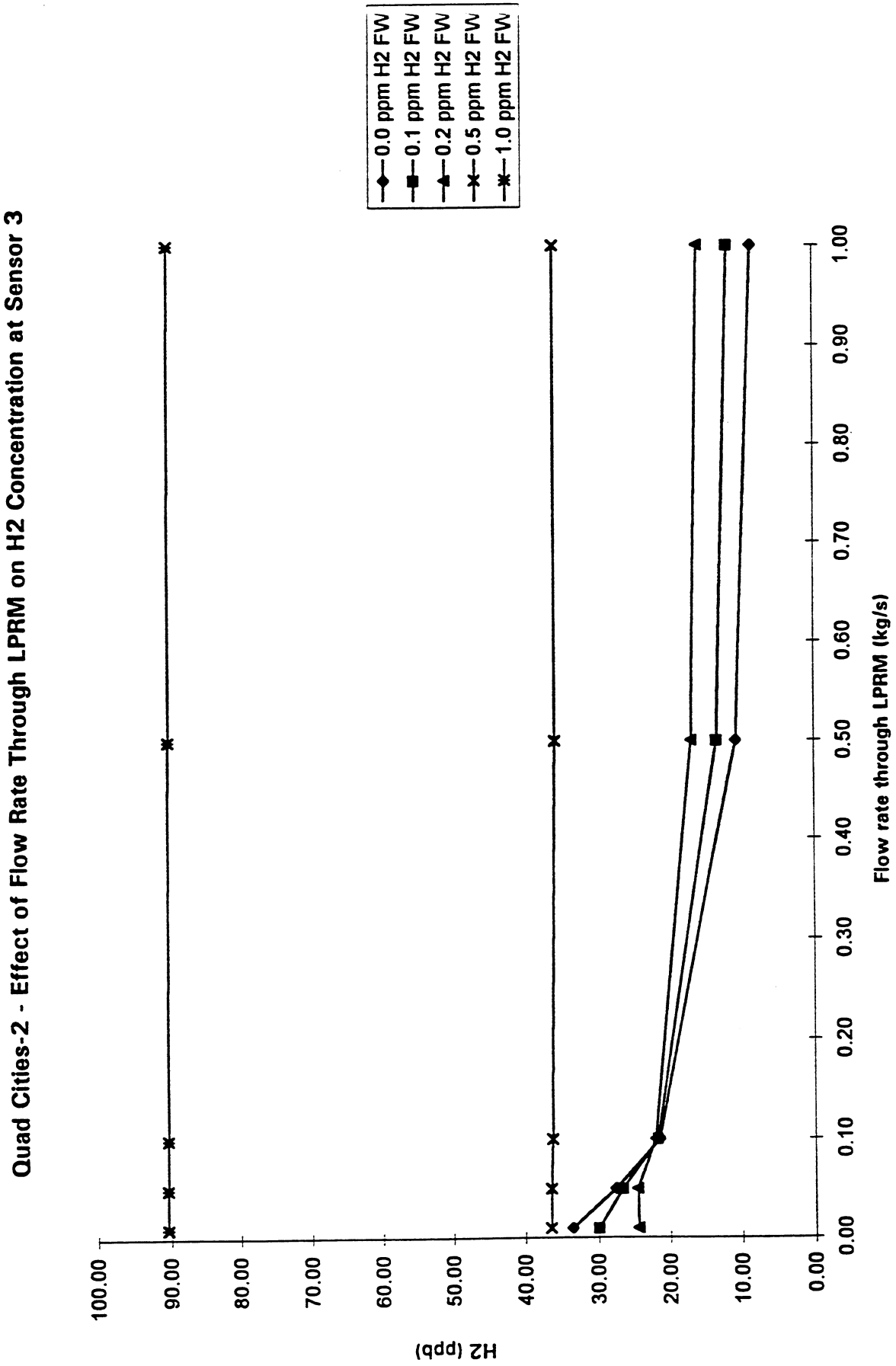
Quad Cities-2 - Effect of Flow Rate Through LPRM on H2 Concentration at Sensor 3
0.0 ppm H2 FW
0.1 ppm H2 FW
0.2 ppm H2 FW
0.5 ppm H2 FW
1.0 ppm H2 FW
H2 (ppb)
100.00
90.00
80.00
70.00
60.00
50.00
40.00
30.00
20.00
10.00
0.00
0.00
0.10
0.20
0.30
0.40
0.50
0.60
0.70
0.80
0.90
1.00
Flow rate through LPRM (kg/s)

Figure B-3

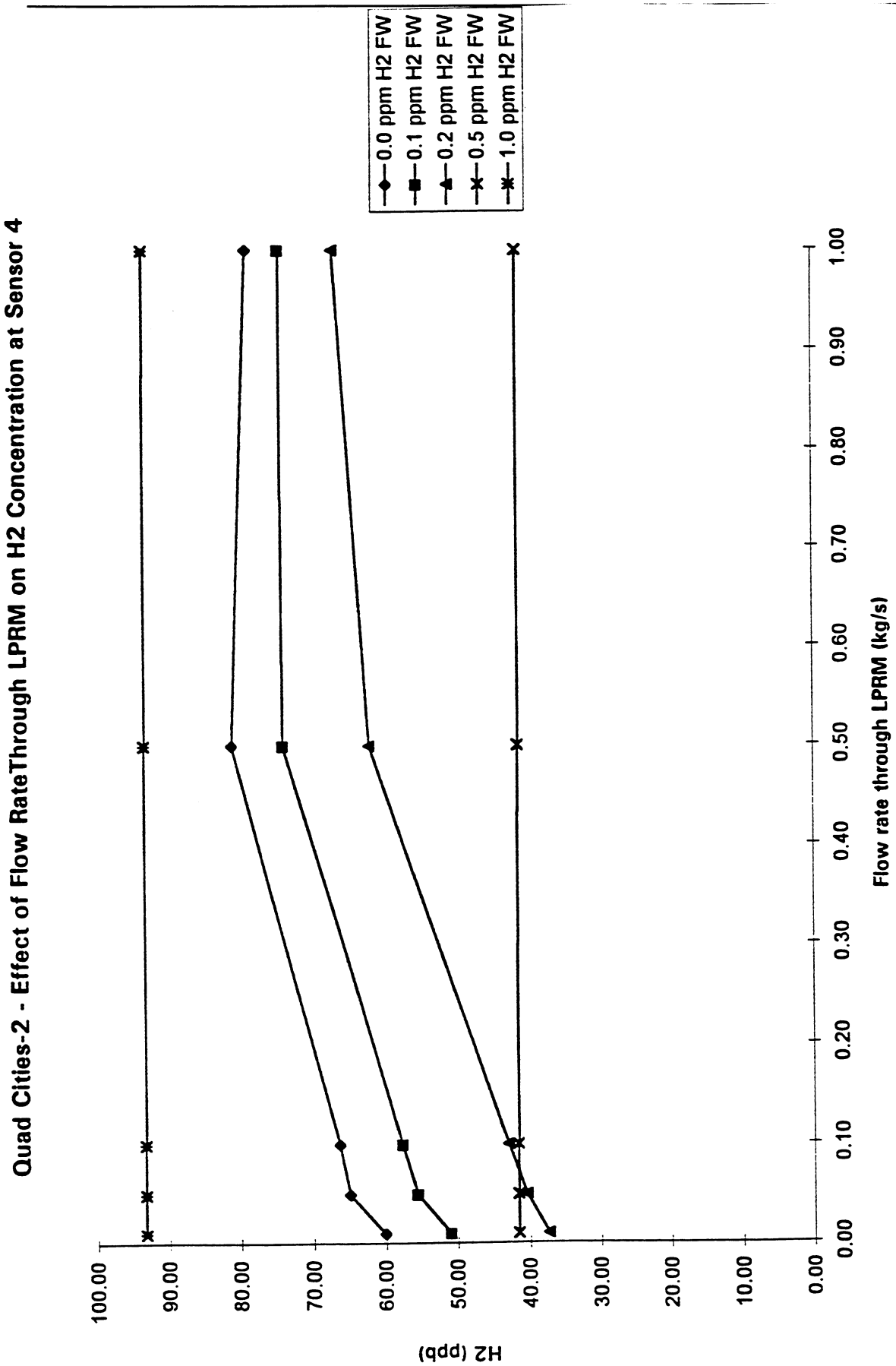
Quad Cities-2 - Effect of Flow RateThrough LPRM on H2 Concentration at Sensor 4
0.0 ppm H2 FW
0.1 ppm H2 FW
0.2 ppm H2 FW
0.5 ppm H2 FW
1.0 ppm H2 FW
H2 (ppb)
100.00
90.00
80.00
70.00
60.00
50.00
40.00
30.00
20.00
10.00
0.00
0.00
0.10
0.20
0.30
0.40
0.50
0.60
0.70
0.80
0.90
1.00
Flow rate through LPRM (kg/s)

Figure B-4

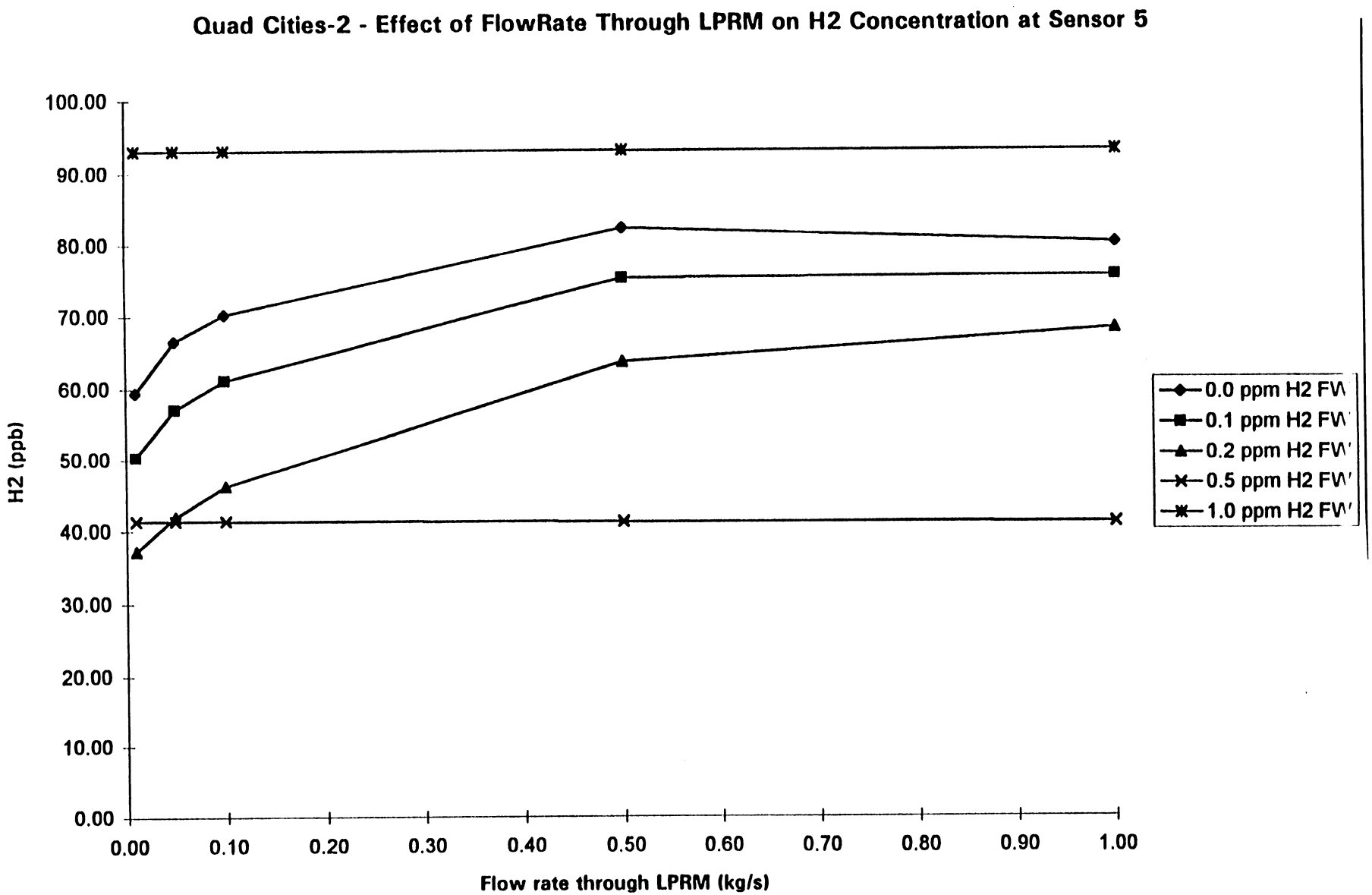

Figure B-5

EPRI Licensed Material

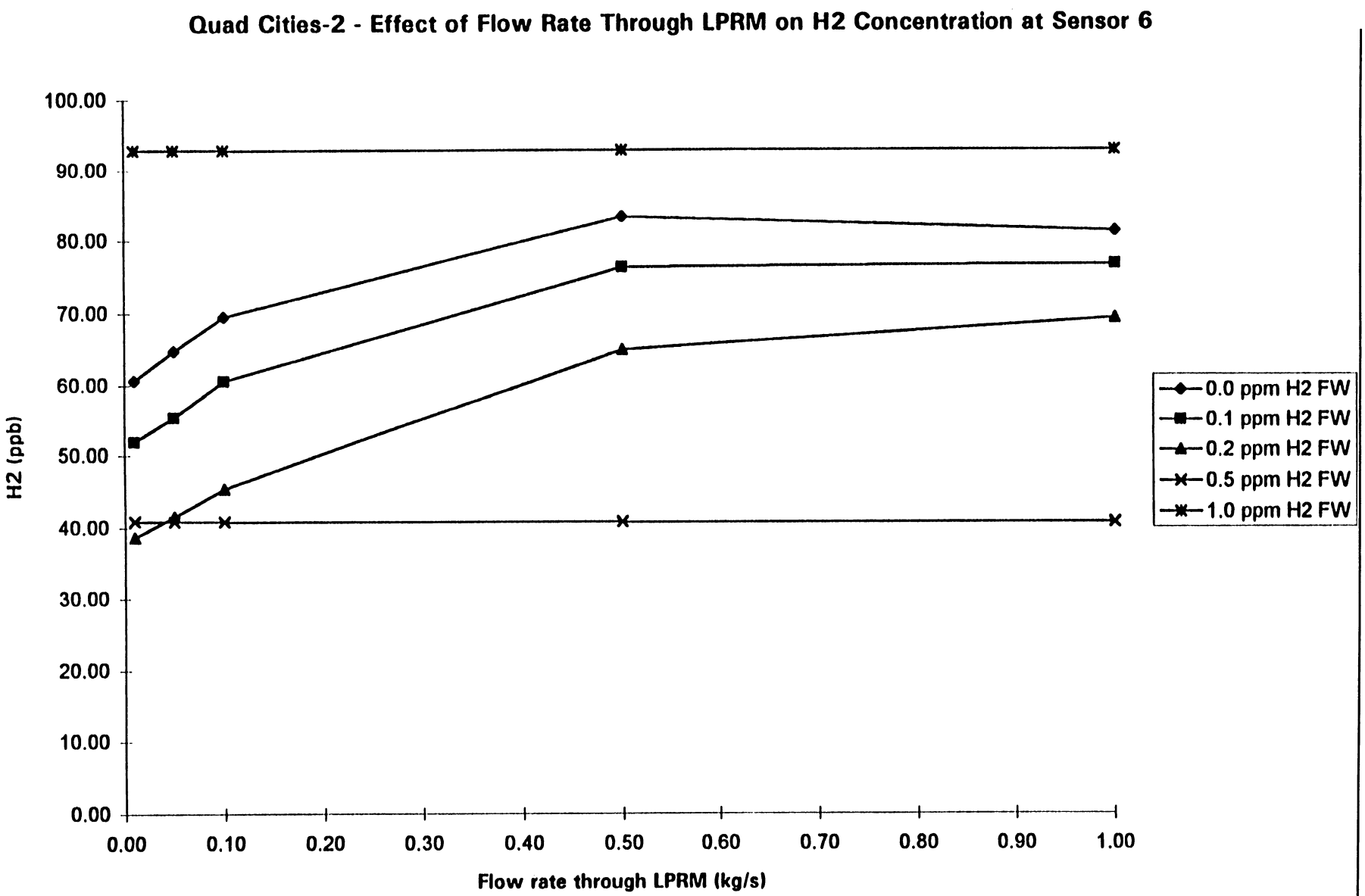

EPRI Licensed Material

Figure B-6

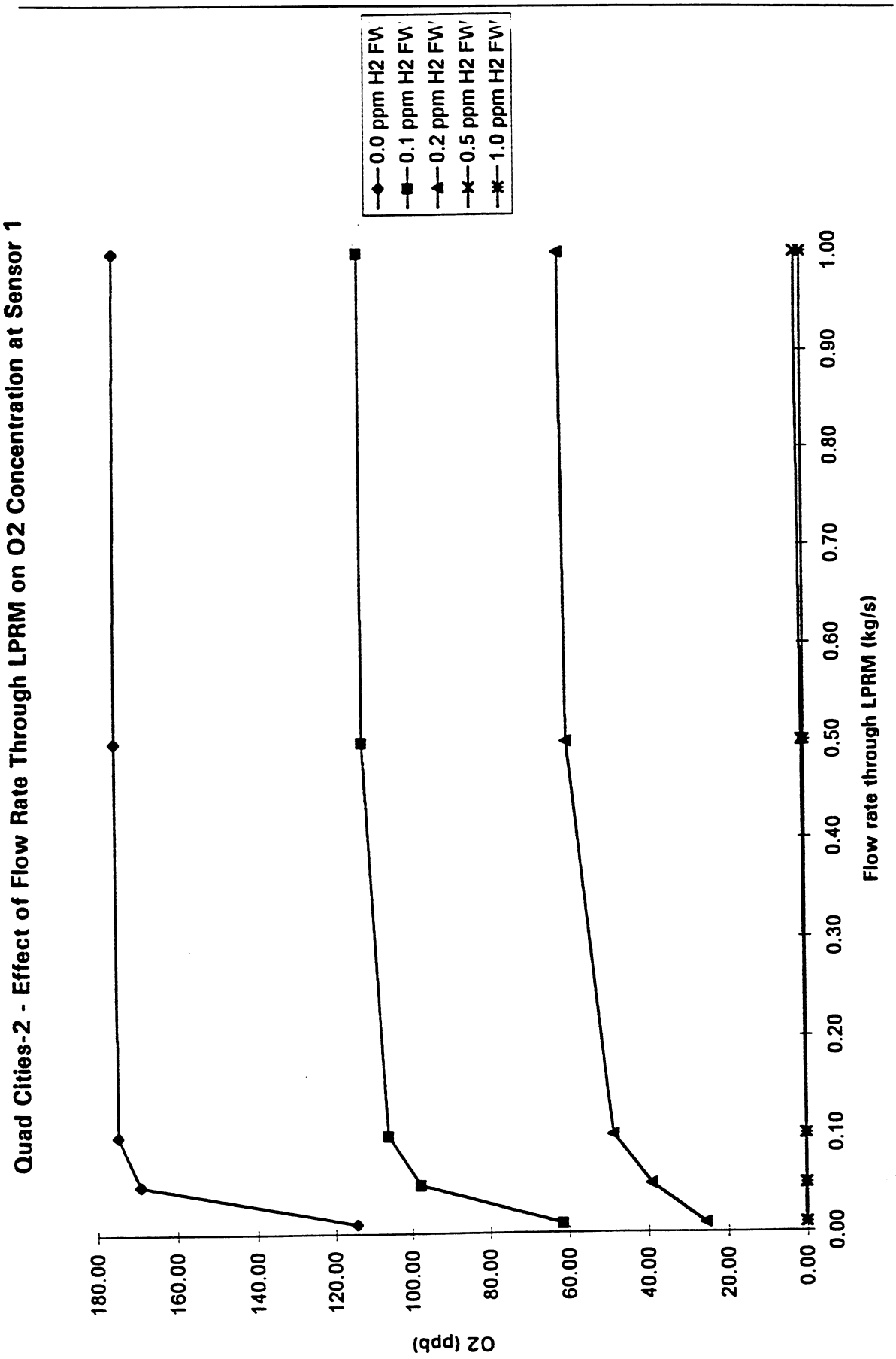
Quad Cities-2 - Effect of Flow Rate Through LPRM on O2 Concentration at Sensor 1
0.0 ppm H2 FW
0.1 ppm H2 FW
0.2 ppm H2 FW
0.5 ppm H2 FW
1.0 ppm H2 FW
O2 (ppb)
180.00
160.00
140.00
120.00
100.00
80.00
60.00
40.00
20.00
0.00
0.00
0.10
0.20
0.30
0.40
0.50
0.60
0.70
0.80
0.90
1.00
Flow rate through LPRM (kg/s)

Figure B-7

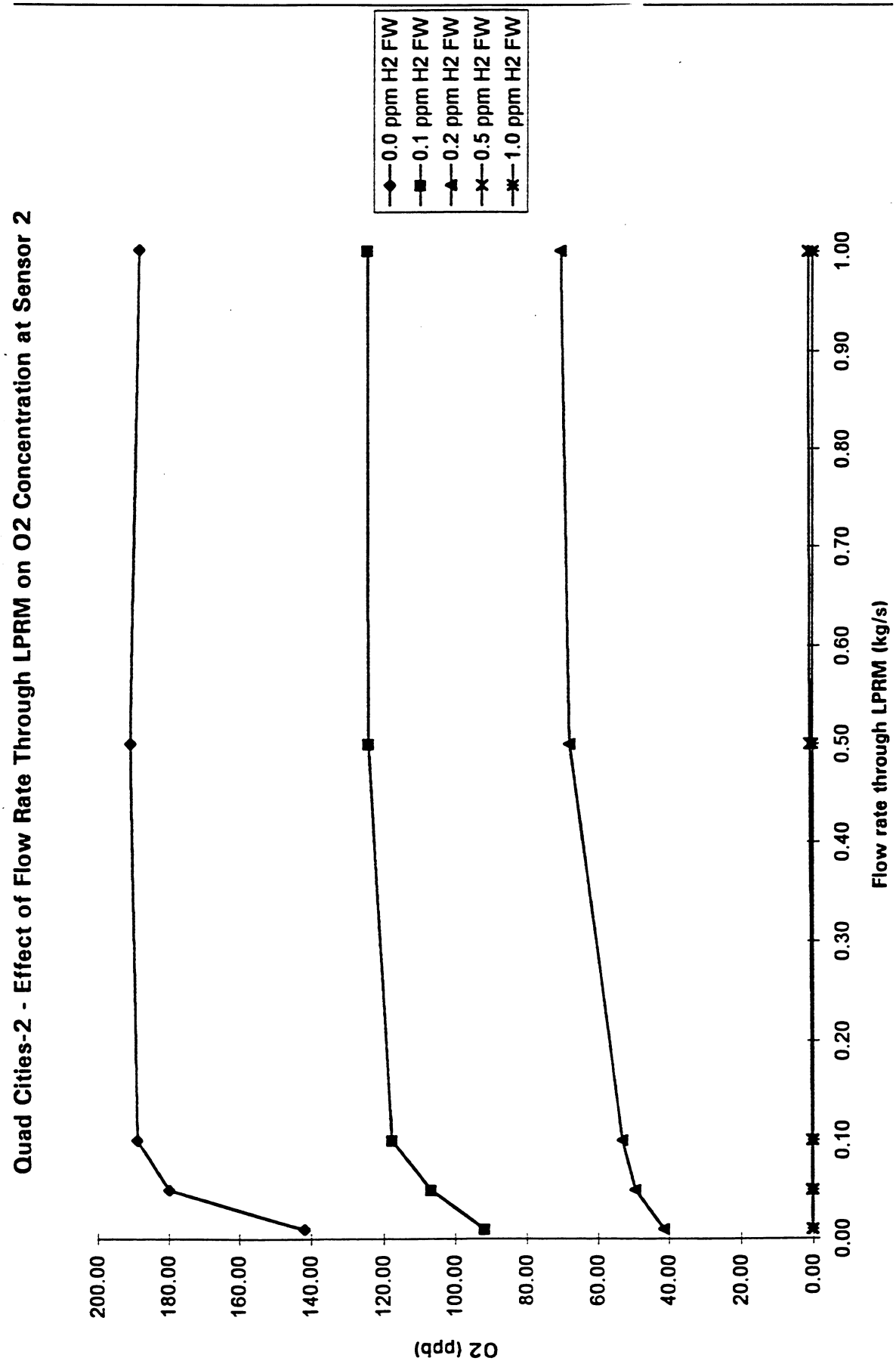
Quad Cities-2 - Effect of Flow Rate Through LPRM on O2 Concentration at Sensor 2
0.0 ppm H2 FW
0.1 ppm H2 FW
0.2 ppm H2 FW
0.5 ppm H2 FW
1.0 ppm H2 FW
O2 (ppb)
200.00
180.00
160.00
140.00
120.00
100.00
80.00
60.00
40.00
20.00
0.00
0.00
0.10
0.20
0.30
0.40
0.50
0.60
0.70
0.80
0.90
1.00
Flow rate through LPRM (kg/s)

Figure B-8

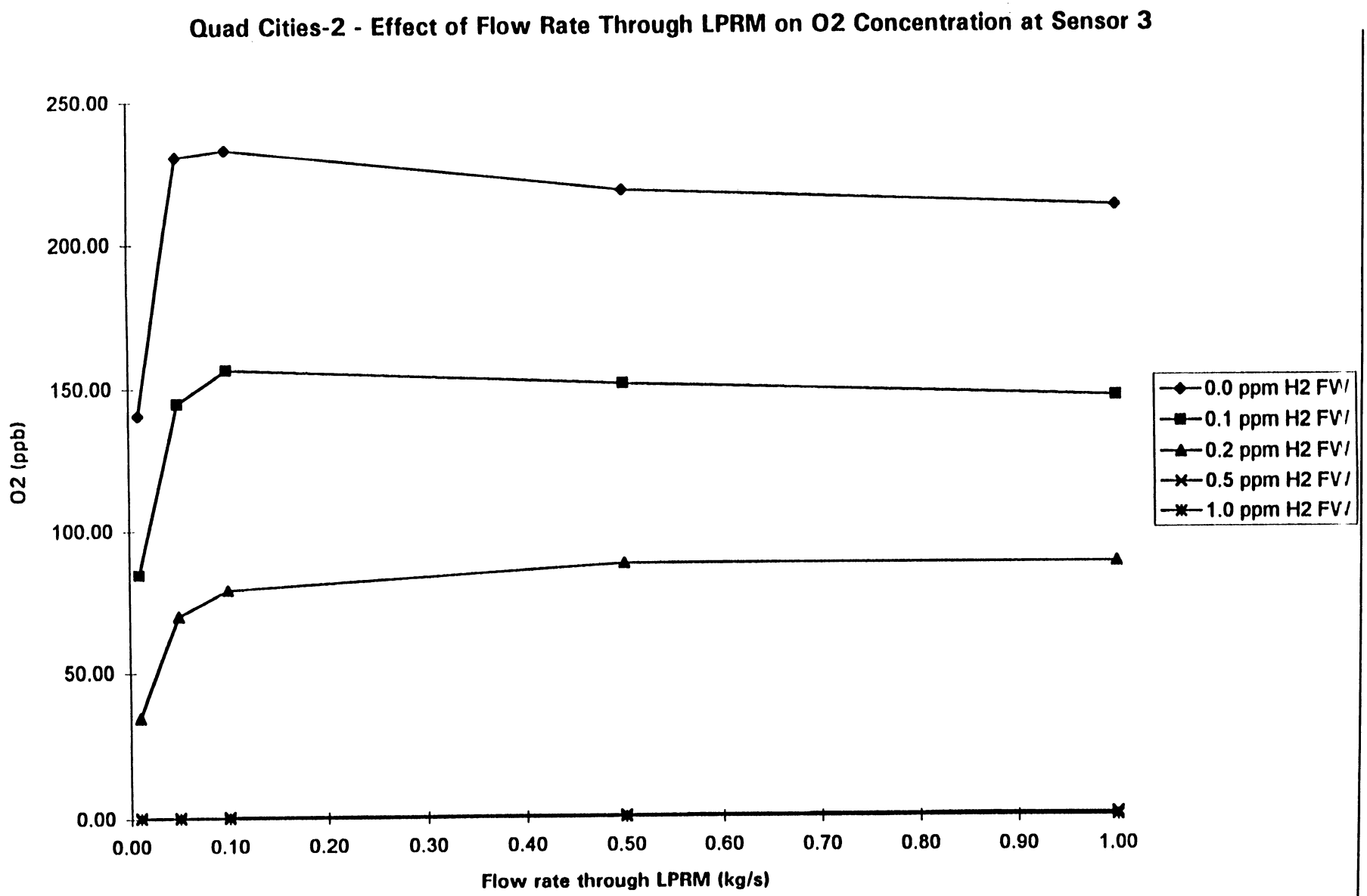

Figure B-9

EPRI Licensed Material

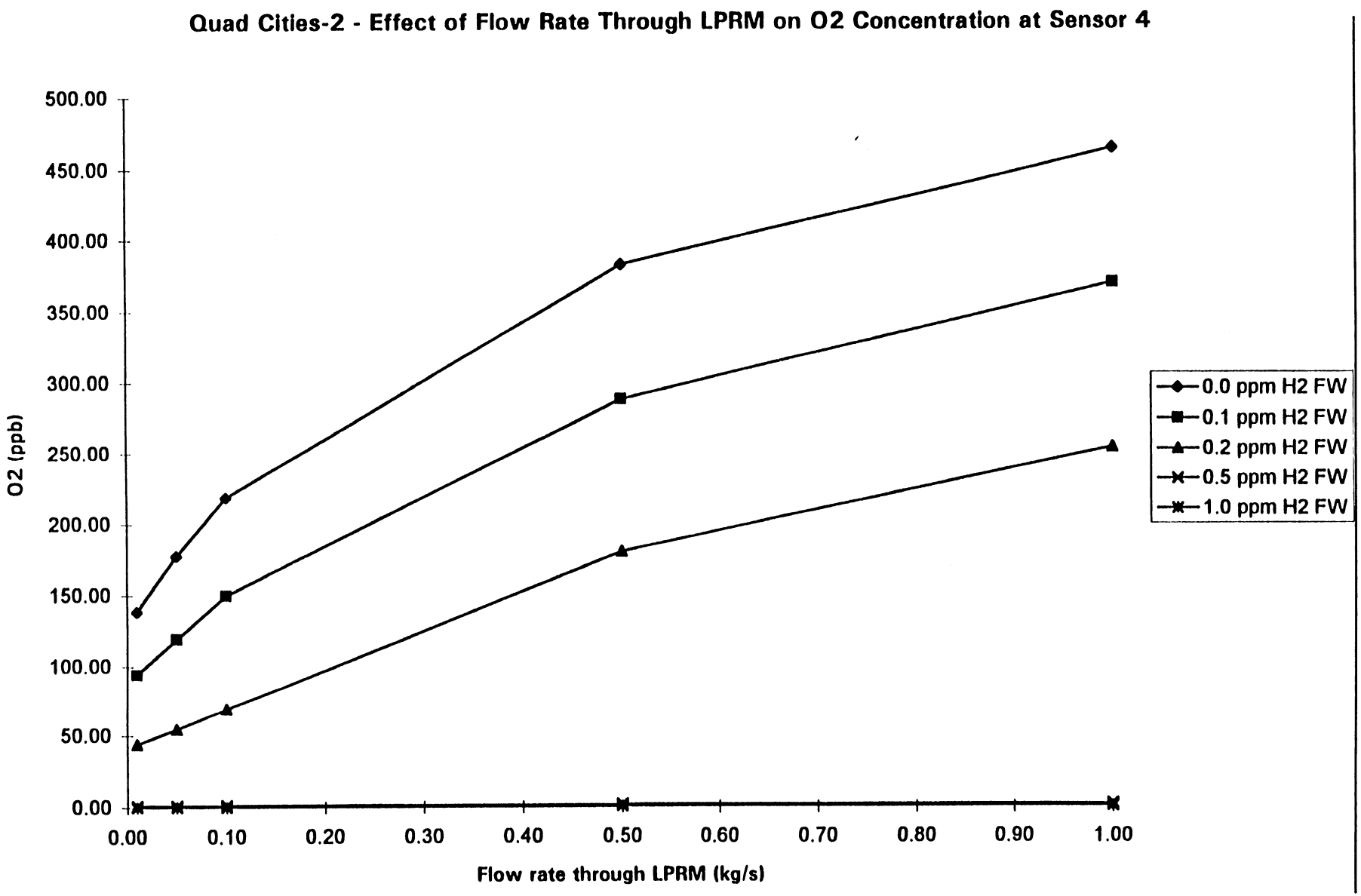

Figure B-10

EPRI Licensed Material

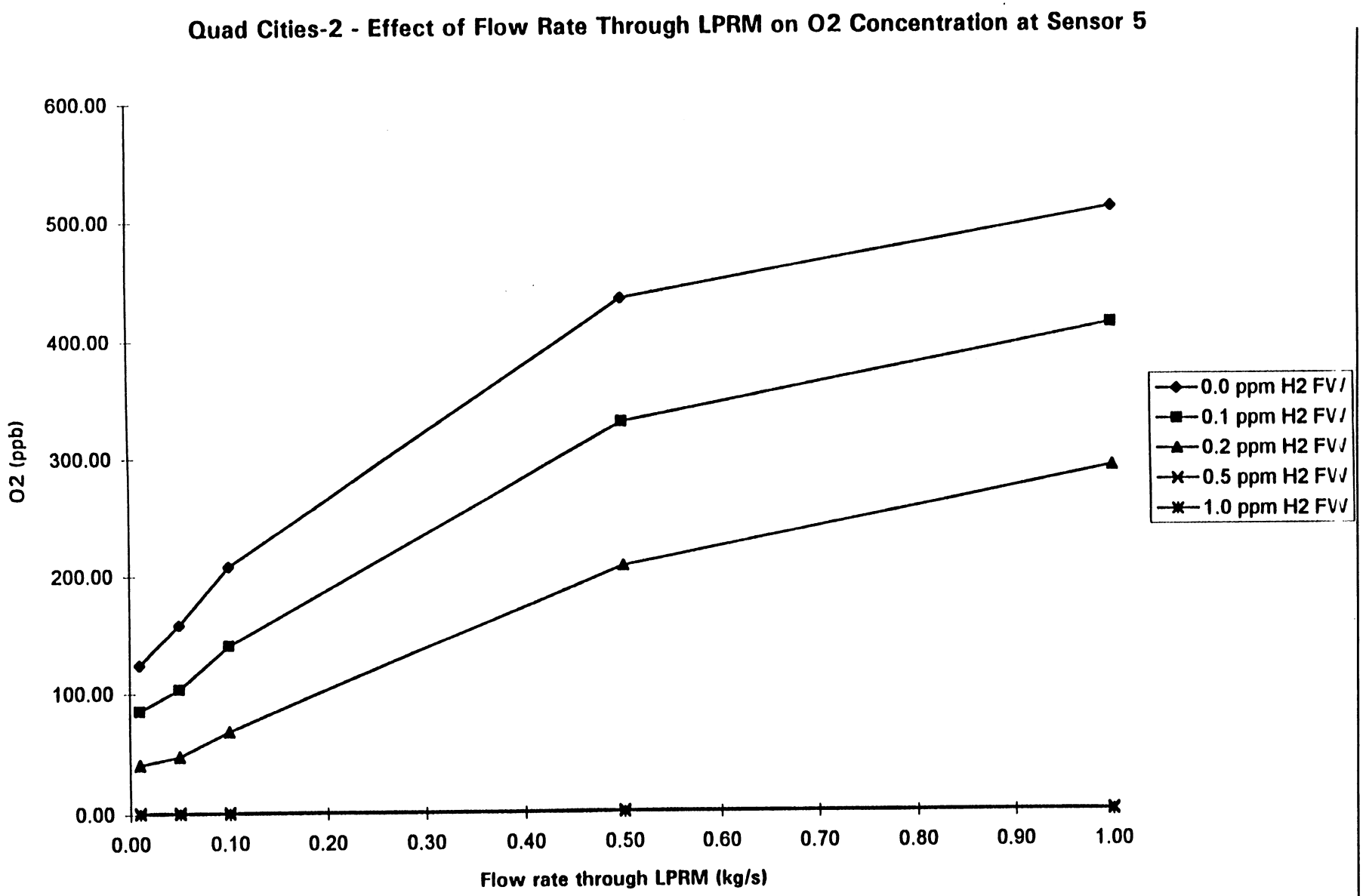

Figure B-11

EPRI Licensed Material

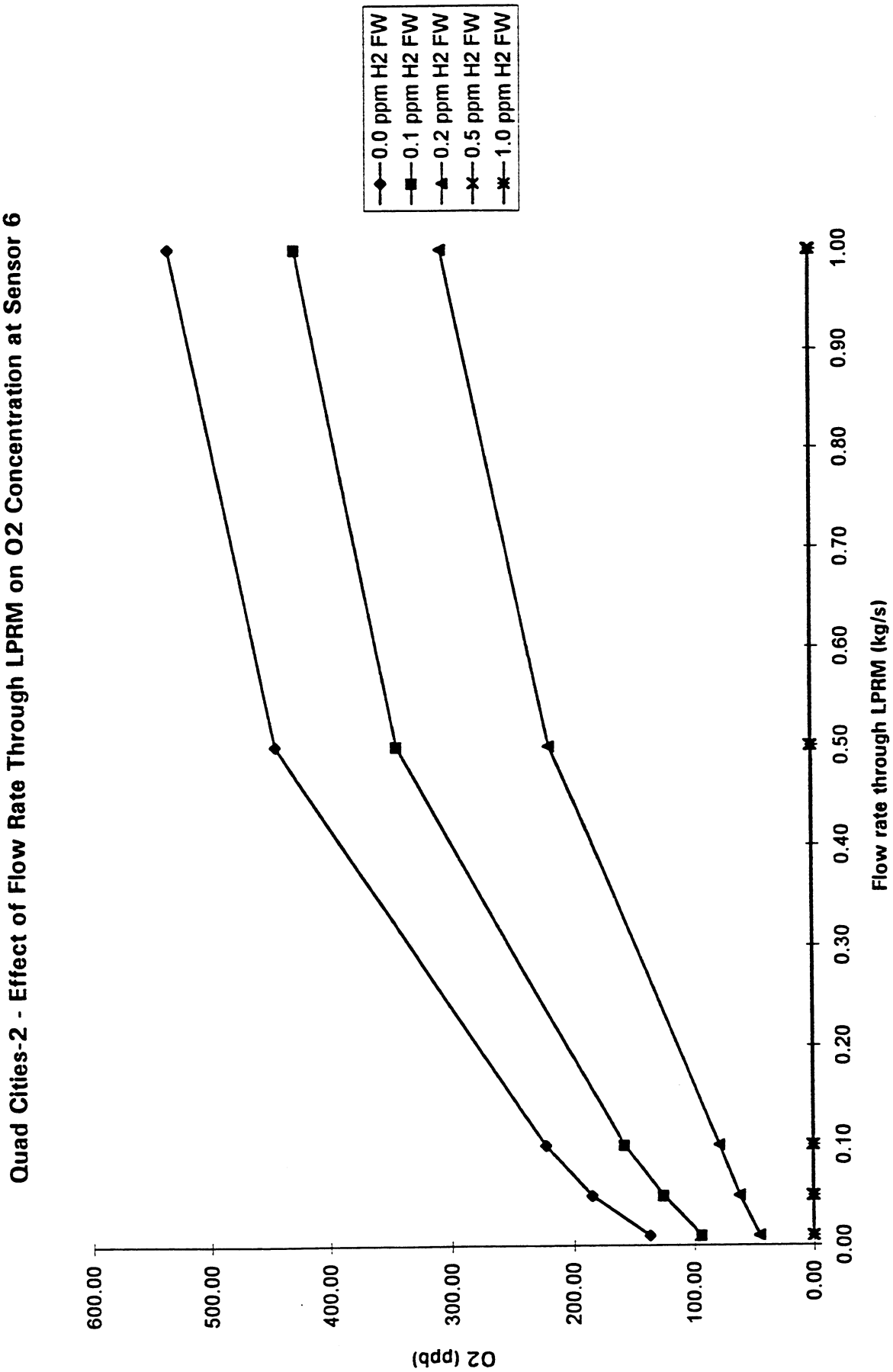
Quad Cities-2 - Effect of Flow Rate Through LPRM on O2 Concentration at Sensor 6
0.0 ppm H2 FW
0.1 ppm H2 FW
0.2 ppm H2 FW
0.5 ppm H2 FW
1.0 ppm H2 FW
O2 (ppb)
600.00
500.00
400.00
300.00
200.00
100.00
0.00
0.00
0.10
0.20
0.30
0.40
0.50
0.60
0.70
0.80
0.90
1.00
Flow rate through LPRM (kg/s)

Figure B-12

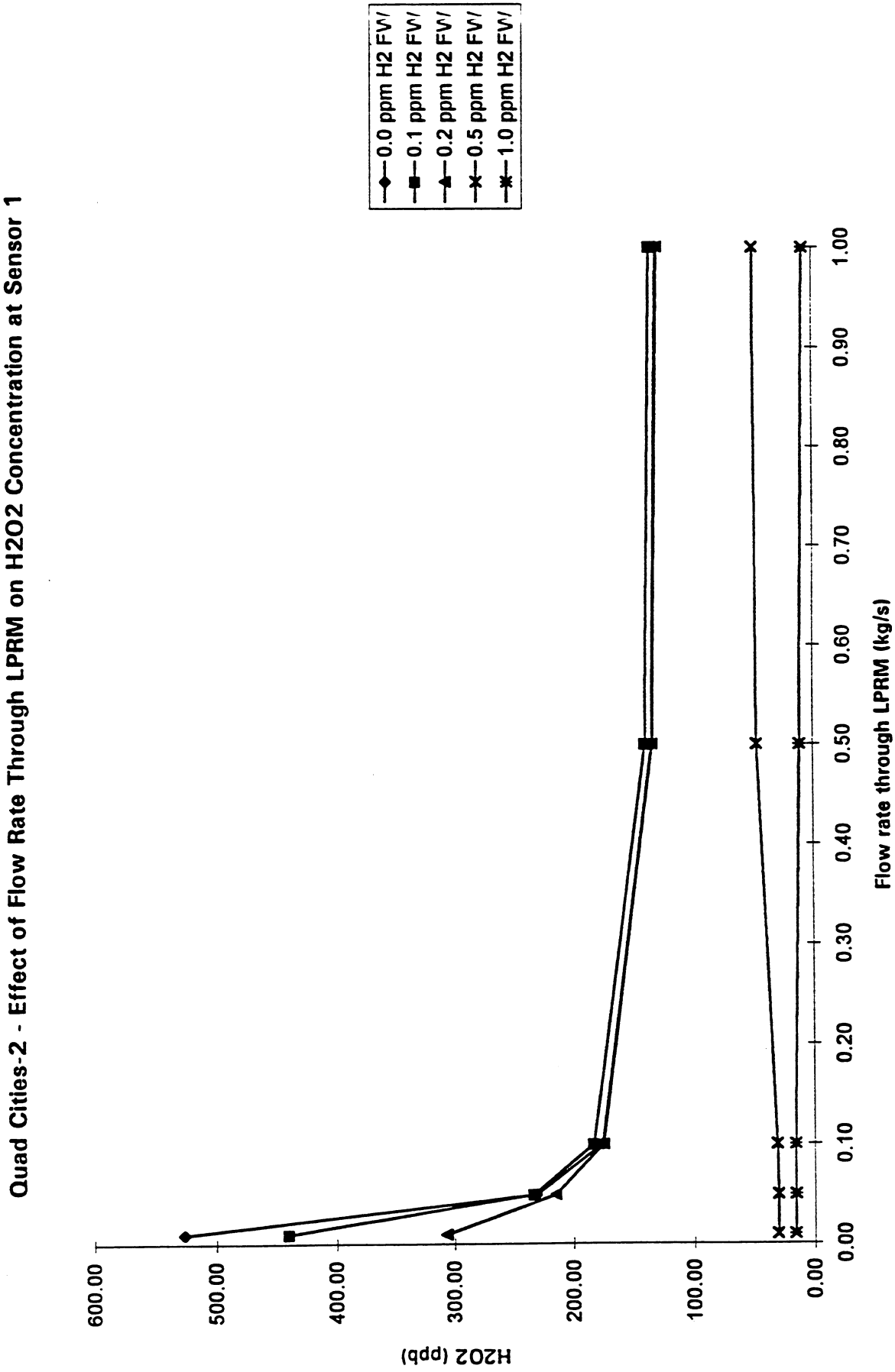
Quad Cities-2 - Effect of Flow Rate Through LPRM on H2O2 Concentration at Sensor 1
0.0 ppm H2 FW
0.1 ppm H2 FW
0.2 ppm H2 FW
0.5 ppm H2 FW
1.0 ppm H2 FW
H2O2 (ppb)
600.00
500.00
400.00
300.00
200.00
100.00
0.00
0.00
0.10
0.20
0.30
0.40
0.50
0.60
0.70
0.80
0.90
1.00
Flow rate through LPRM (kg/s)

Figure B-13

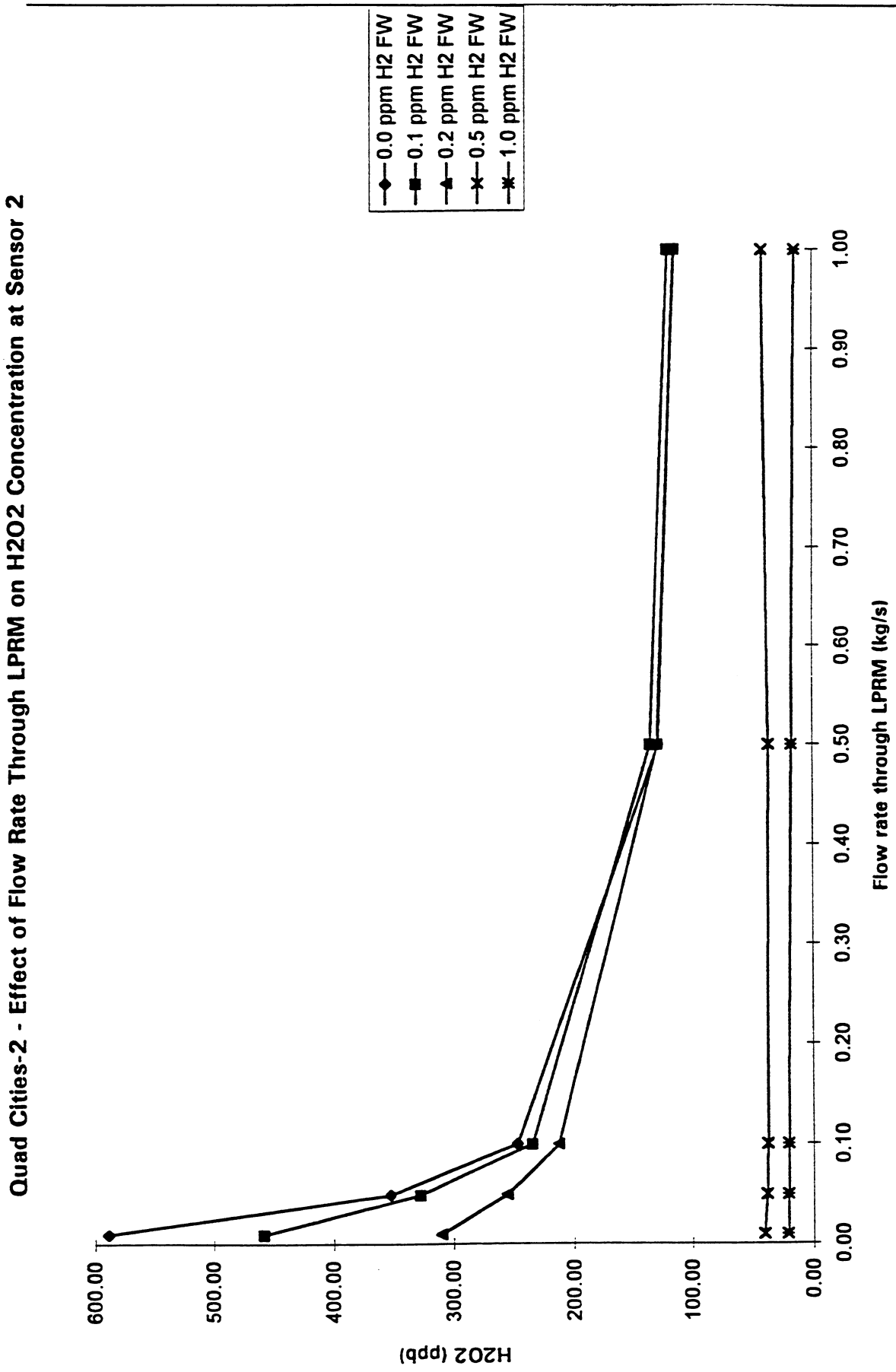
Quad Cities-2 - Effect of Flow Rate Through LPRM on H2O2 Concentration at Sensor 2
0.0 ppm H2 FW
0.1 ppm H2 FW
0.2 ppm H2 FW
0.5 ppm H2 FW
1.0 ppm H2 FW
H2O2 (ppb)
600.00
500.00
400.00
300.00
200.00
100.00
0.00
0.00
0.10
0.20
0.30
0.40
0.50
0.60
0.70
0.80
0.90
1.00
Flow rate through LPRM (kg/s)

Figure B-14

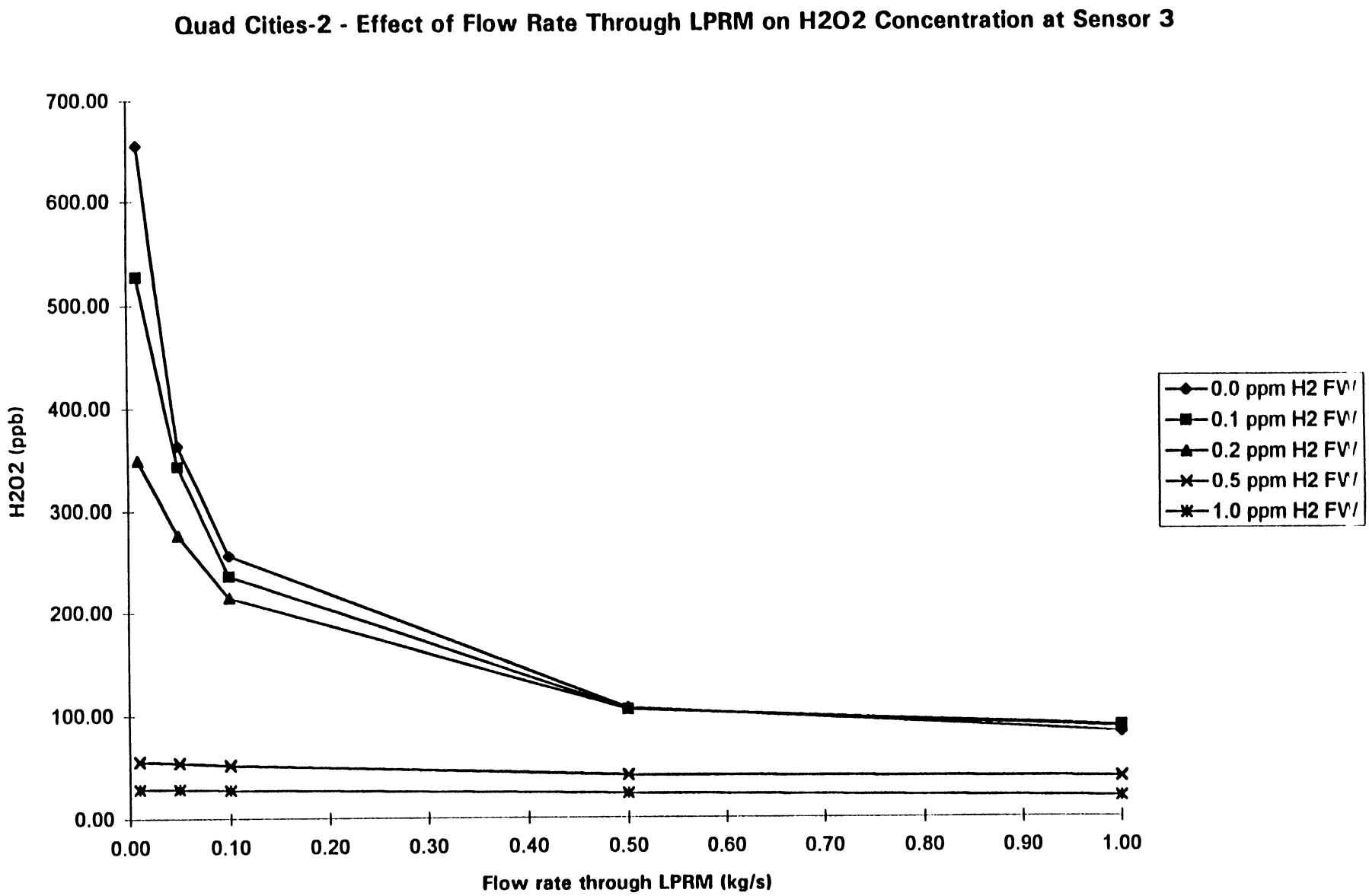

Figure B-15

EPRI Licensed Material

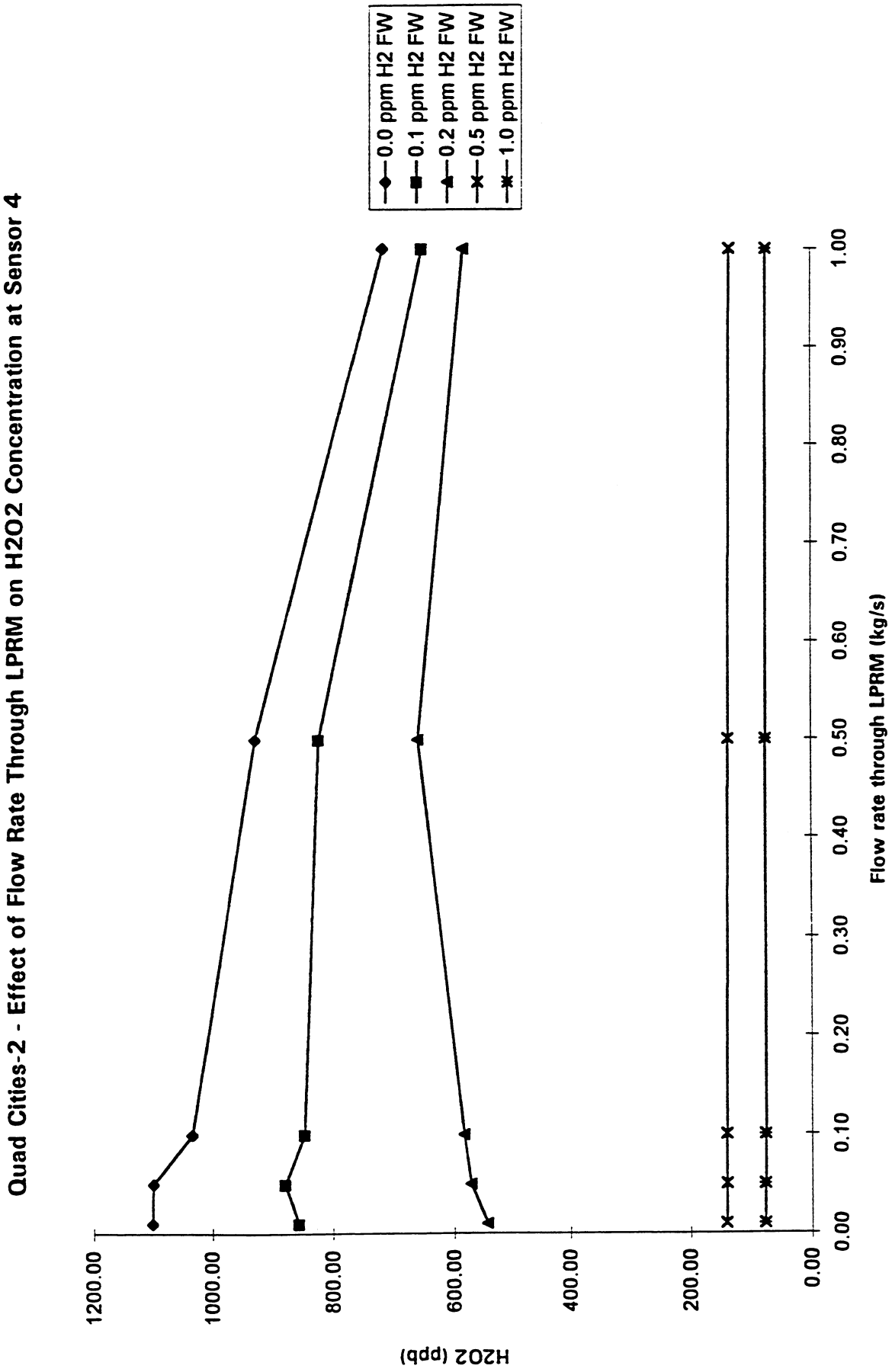
Quad Cities-2 - Effect of Flow Rate Through LPRM on H2O2 Concentration at Sensor 4
0.0 ppm H2 FW
0.1 ppm H2 FW
0.2 ppm H2 FW
0.5 ppm H2 FW
1.0 ppm H2 FW
H2O2 (ppb)
1200.00
1000.00
800.00
600.00
400.00
200.00
0.00
0.00
0.10
0.20
0.30
0.40
0.50
0.60
0.70
0.80
0.90
1.00
Flow rate through LPRM (kg/s)

Figure B-16

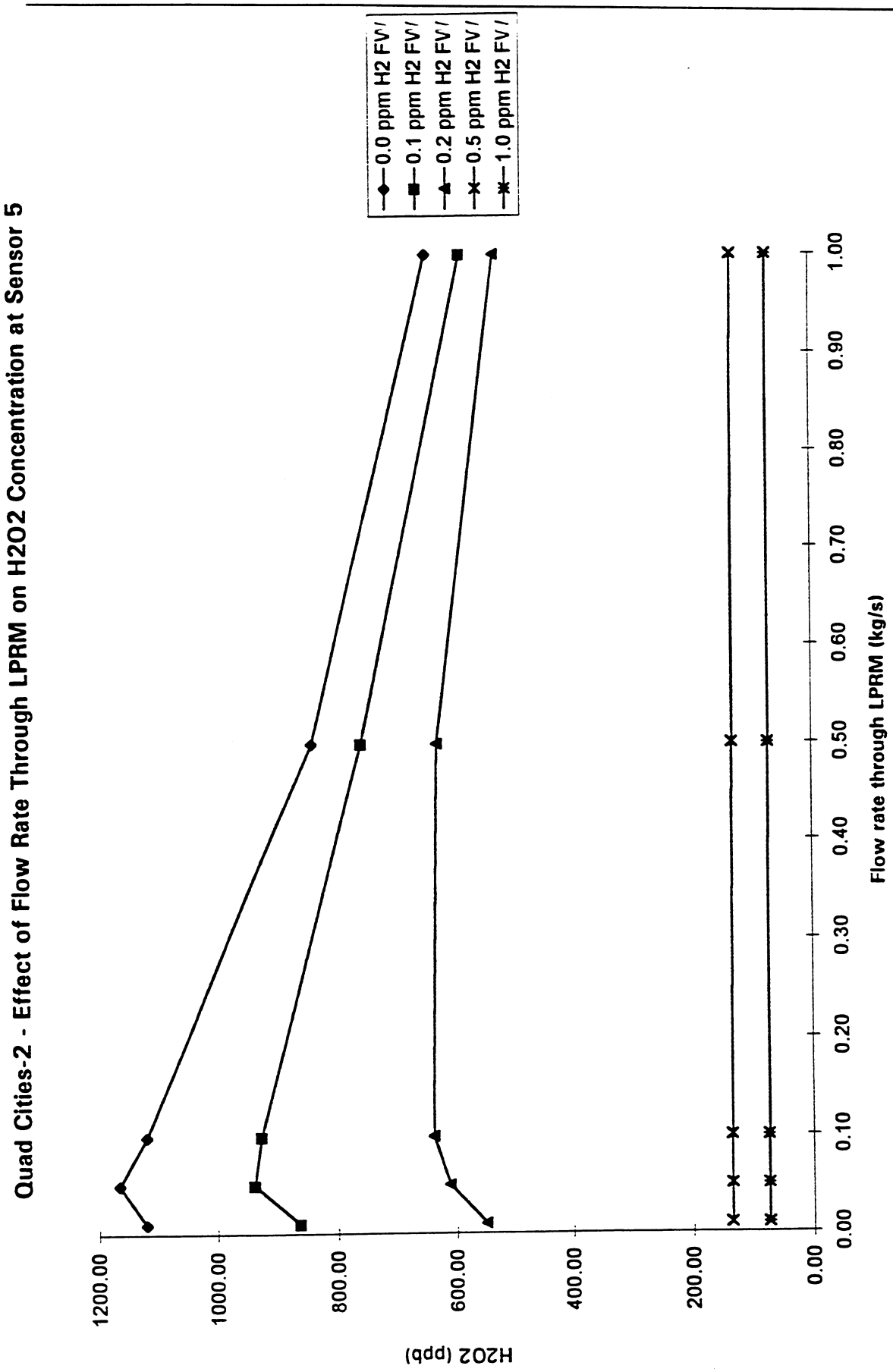
Quad Cities-2 - Effect of Flow Rate Through LPRM on H2O2 Concentration at Sensor 5
0.0 ppm H2 FW
0.1 ppm H2 FW
0.2 ppm H2 FW
0.5 ppm H2 FW
1.0 ppm H2 FW
H2O2 (ppb)
1200.00
1000.00
800.00
600.00
400.00
200.00
0.00
0.00
0.10
0.20
0.30
0.40
0.50
0.60
0.70
0.80
0.90
1.00
Flow rate through LPRM (kg/s)

Figure B-17

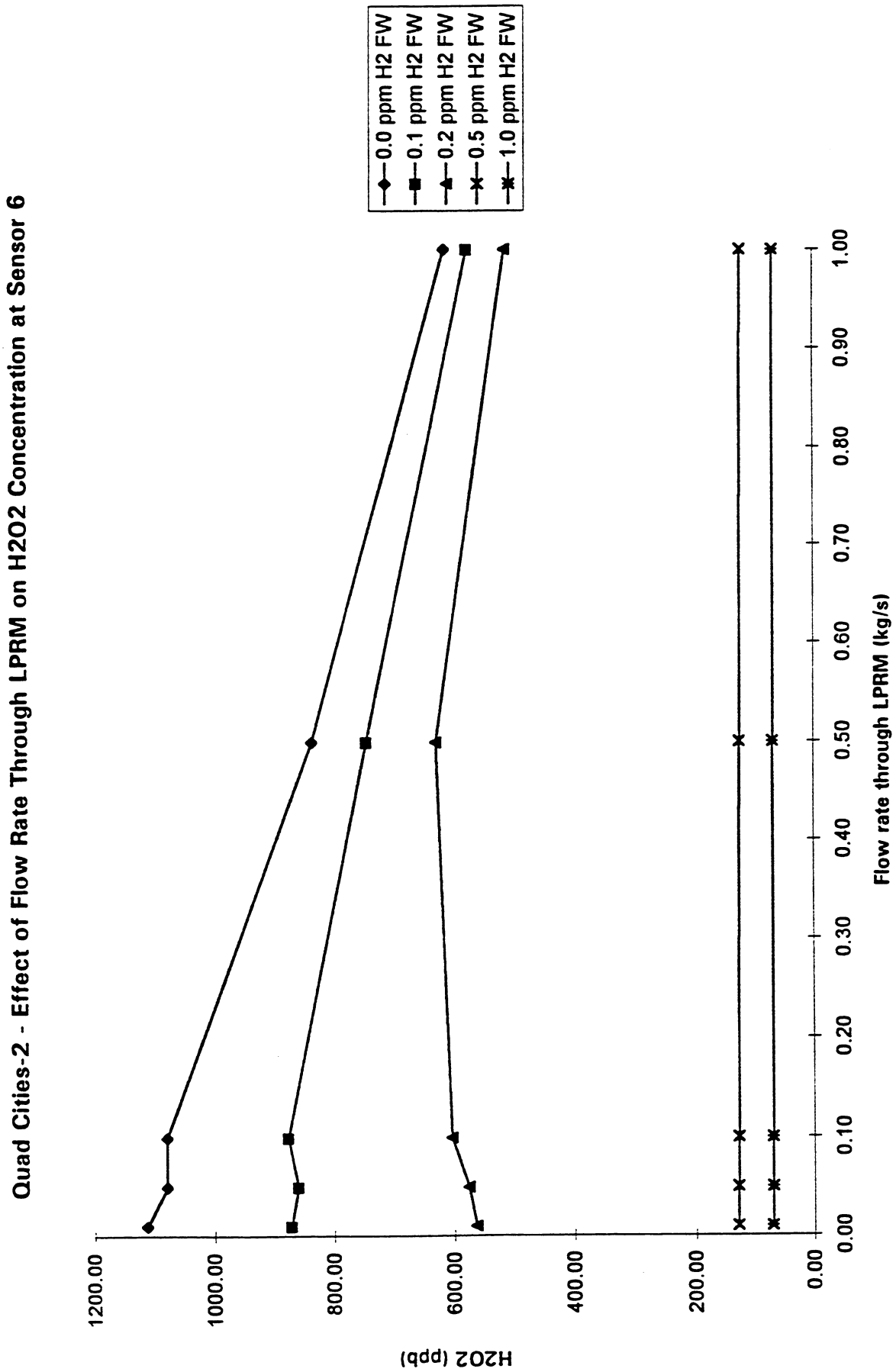
Quad Cities-2 - Effect of Flow Rate Through LPRM on H2O2 Concentration at Sensor 6
0.0 ppm H2 FW
0.1 ppm H2 FW
0.2 ppm H2 FW
0.5 ppm H2 FW
1.0 ppm H2 FW
H2O2 (ppb)
1200.00
1000.00
800.00
600.00
400.00
200.00
0.00
0.00
0.10
0.20
0.30
0.40
0.50
0.60
0.70
0.80
0.90
1.00
Flow rate through LPRM (kg/s)

Figure B-18

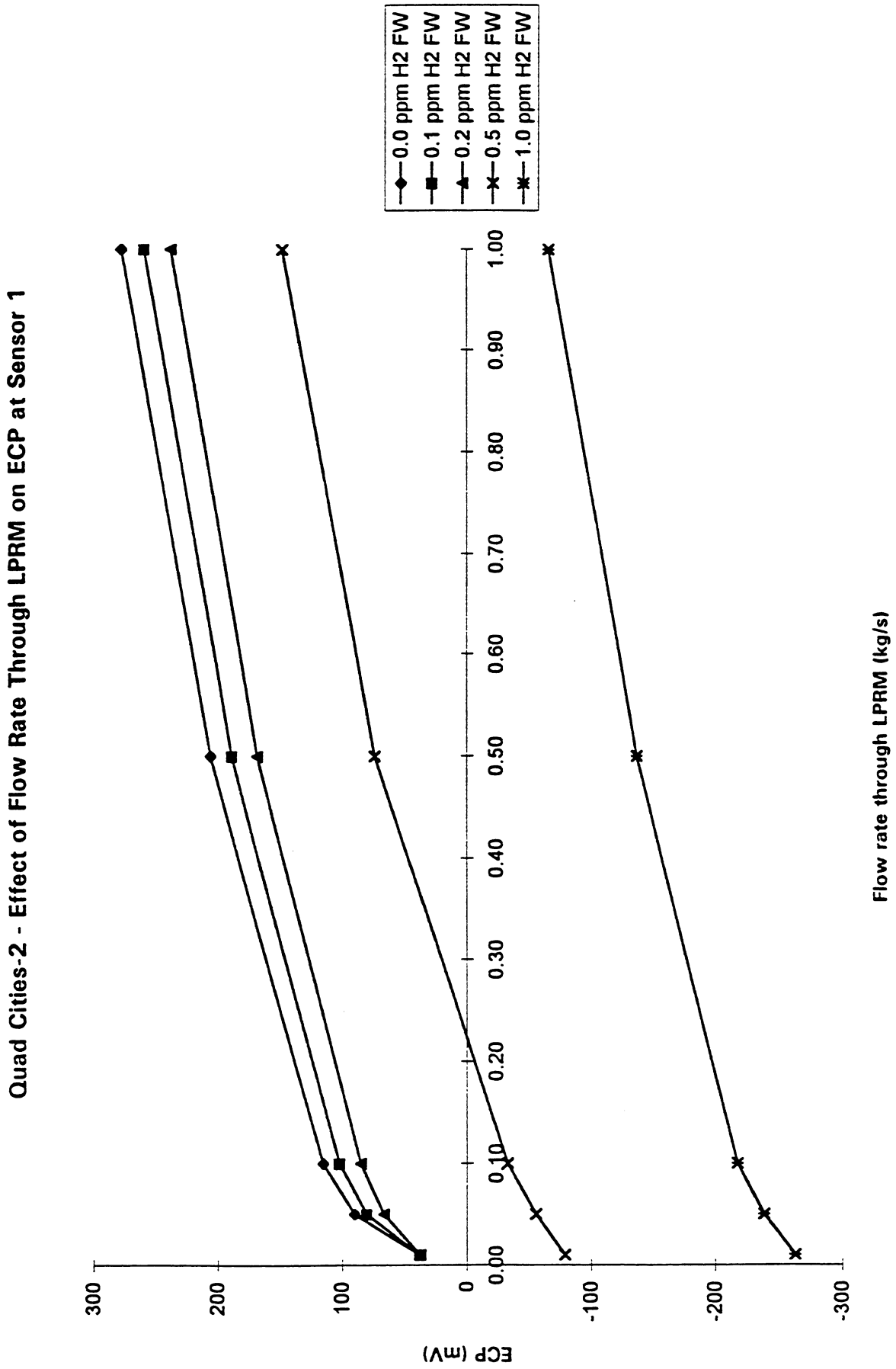
Quad Cities-2 - Effect of Flow Rate Through LPRM on ECP at Sensor 1
0.0 ppm H2 FW
0.1 ppm H2 FW
0.2 ppm H2 FW
0.5 ppm H2 FW
1.0 ppm H2 FW
ECP (mV)
300
200
100
0
-100
-200
-300
0.00
0.10
0.20
0.30
0.40
0.50
0.60
0.70
0.80
0.90
1.00
Flow rate through LPRM (kg/s)

Figure B-19

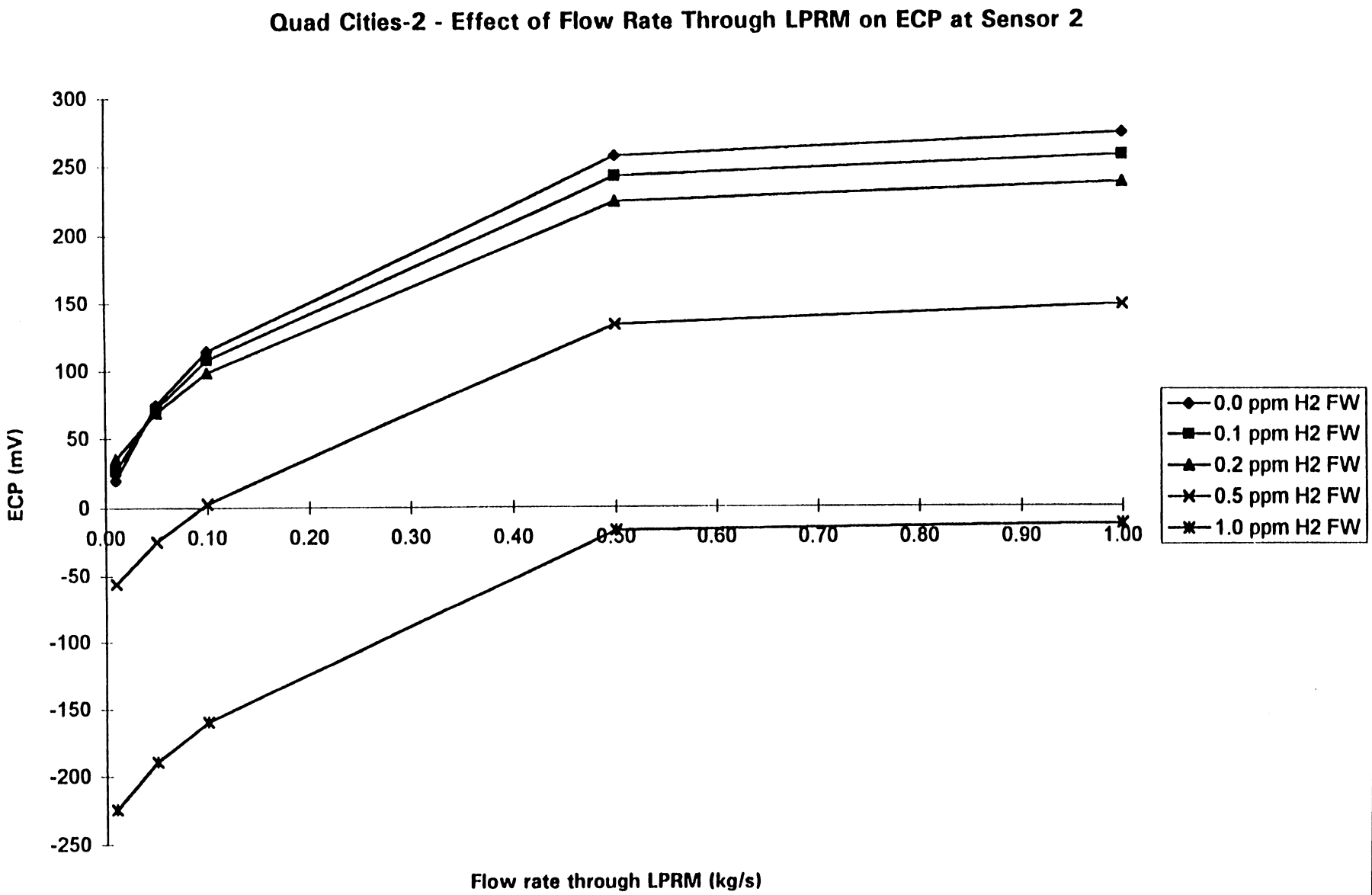

Figure B-20

EPRI Licensed Material

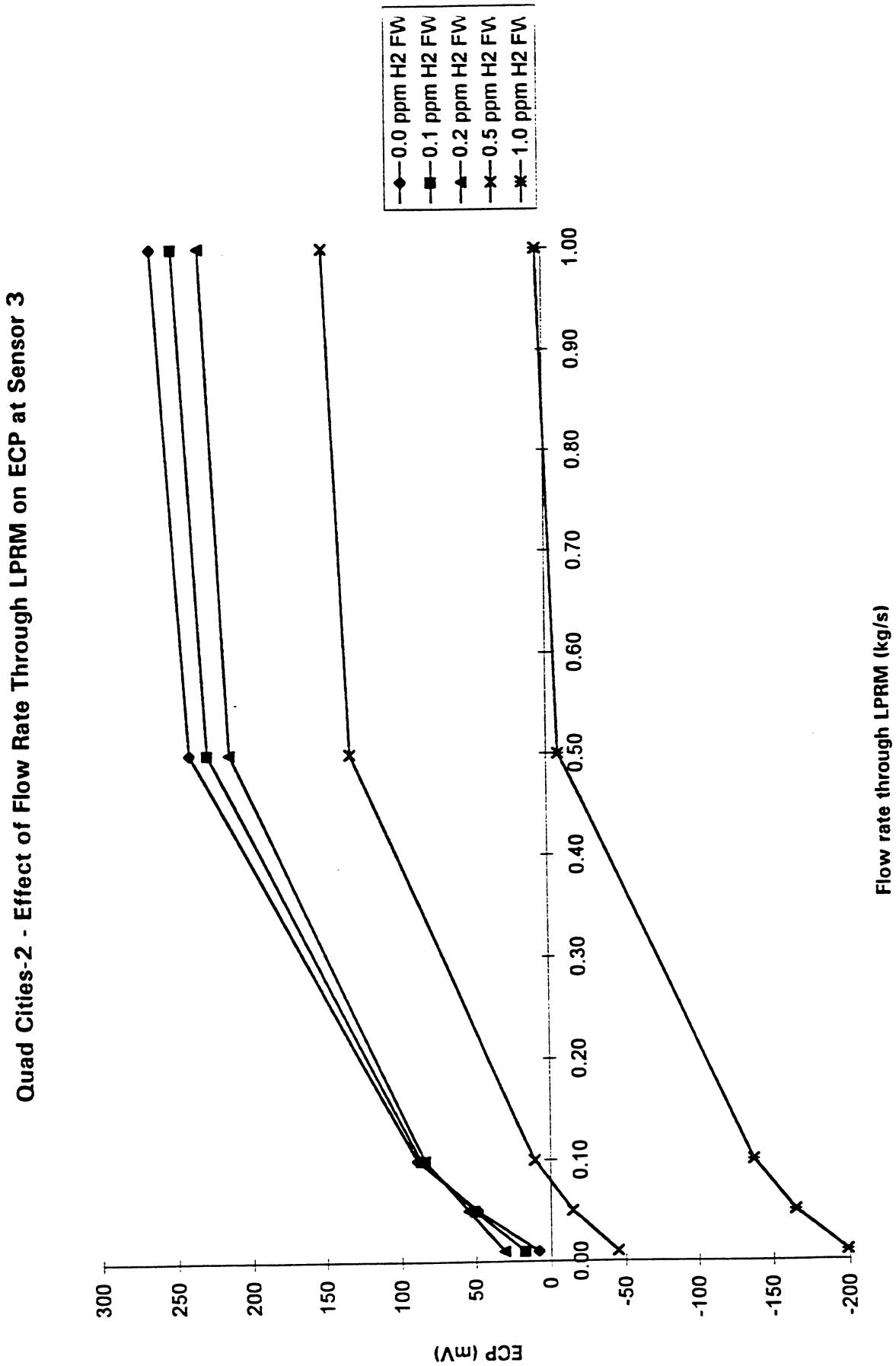
Quad Cities-2 - Effect of Flow Rate Through LPRM on ECP at Sensor 3
0.0 ppm H2 FW
0.1 ppm H2 FW
0.2 ppm H2 FW
0.5 ppm H2 FW
1.0 ppm H2 FW
ECP (mV)
300
250
200
150
100
50
0
-50
-100
-150
-200
0.00
0.10
0.20
0.30
0.40
0.50
0.60
0.70
0.80
0.90
1.00
Flow rate through LPRM (kg/s)

Figure B-21

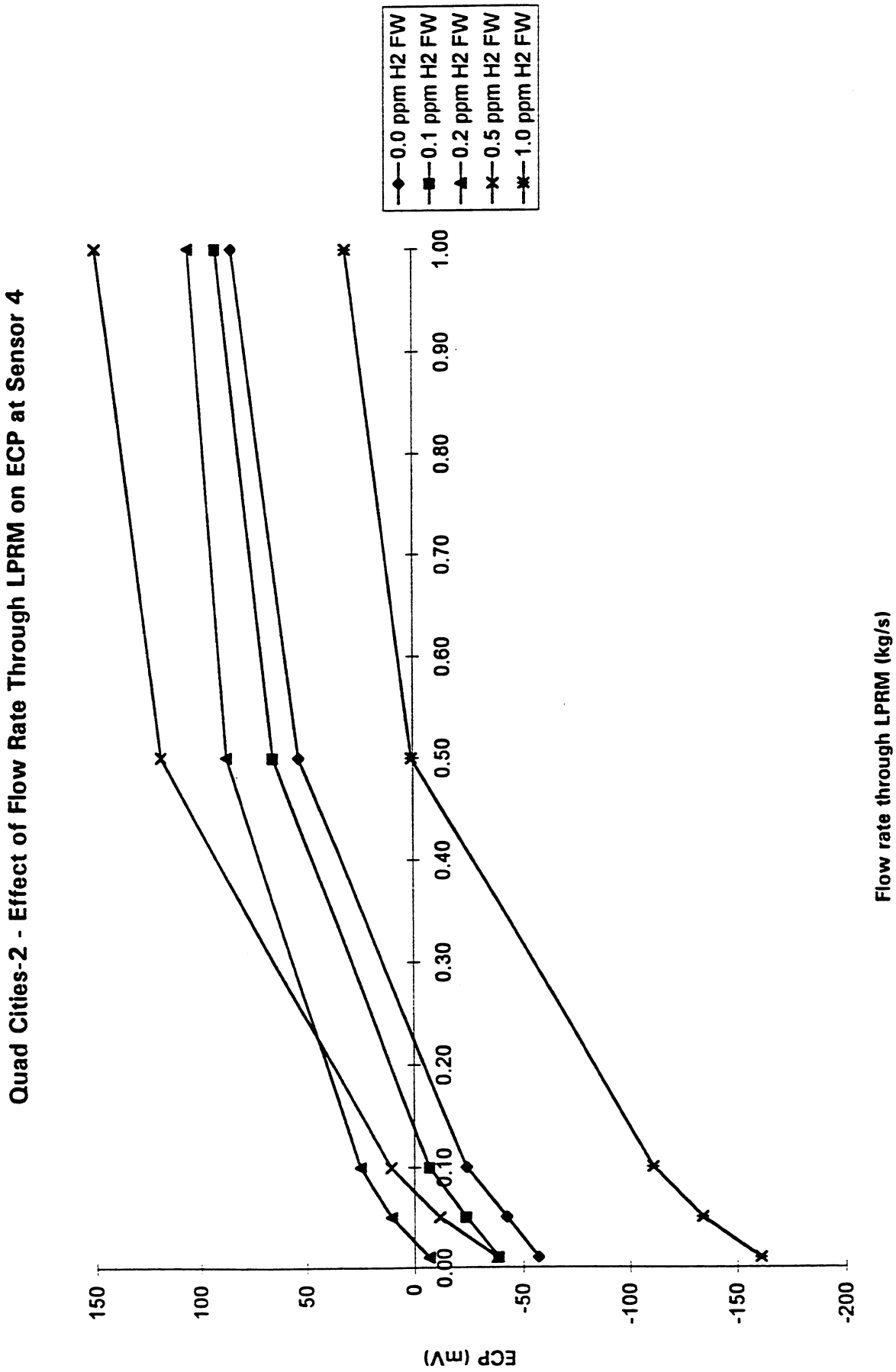
Quad Cities-2 - Effect of Flow Rate Through LPRM on ECP at Sensor 4
0.0 ppm H2 FW
0.1 ppm H2 FW
0.2 ppm H2 FW
0.5 ppm H2 FW
1.0 ppm H2 FW
ECP (mV)
150
100
50
0
-50
-100
-150
-200
0.00
0.10
0.20
0.30
0.40
0.50
0.60
0.70
0.80
0.90
1.00
Flow rate through LPRM (kg/s)

Figure B-22

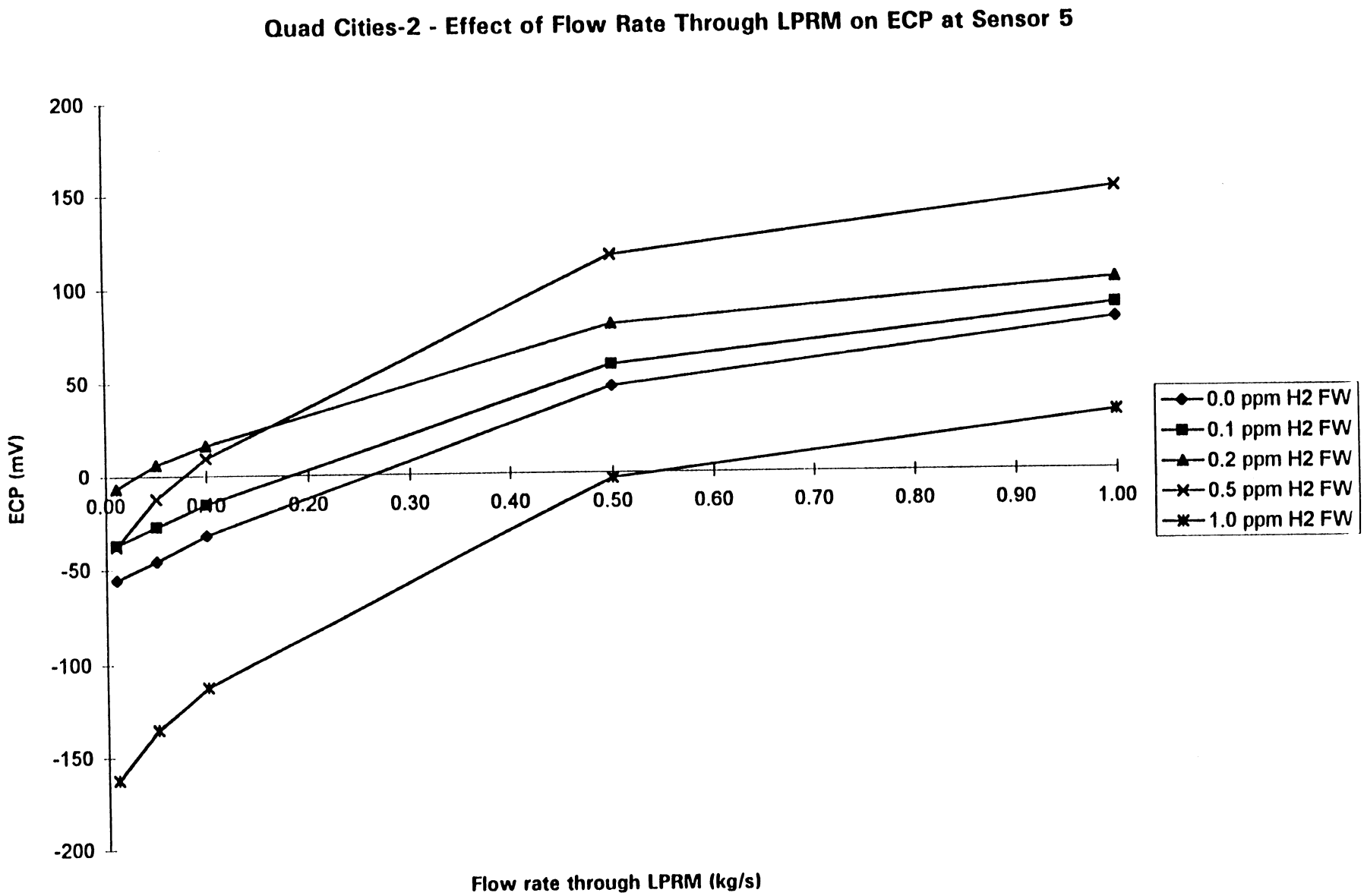

Figure B-23

EPRI Licensed Material

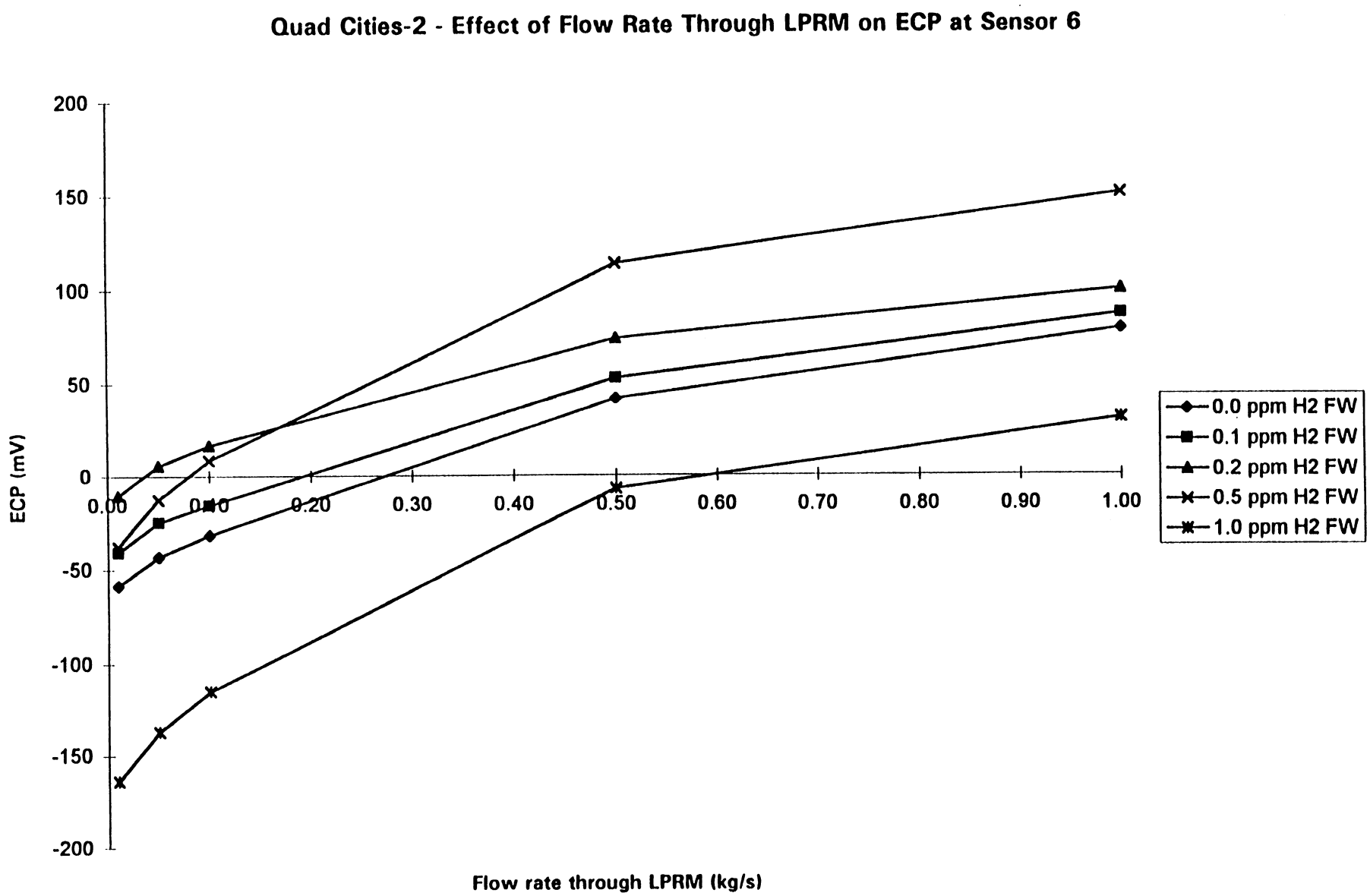

Figure B-24

EPRI Licensed Material

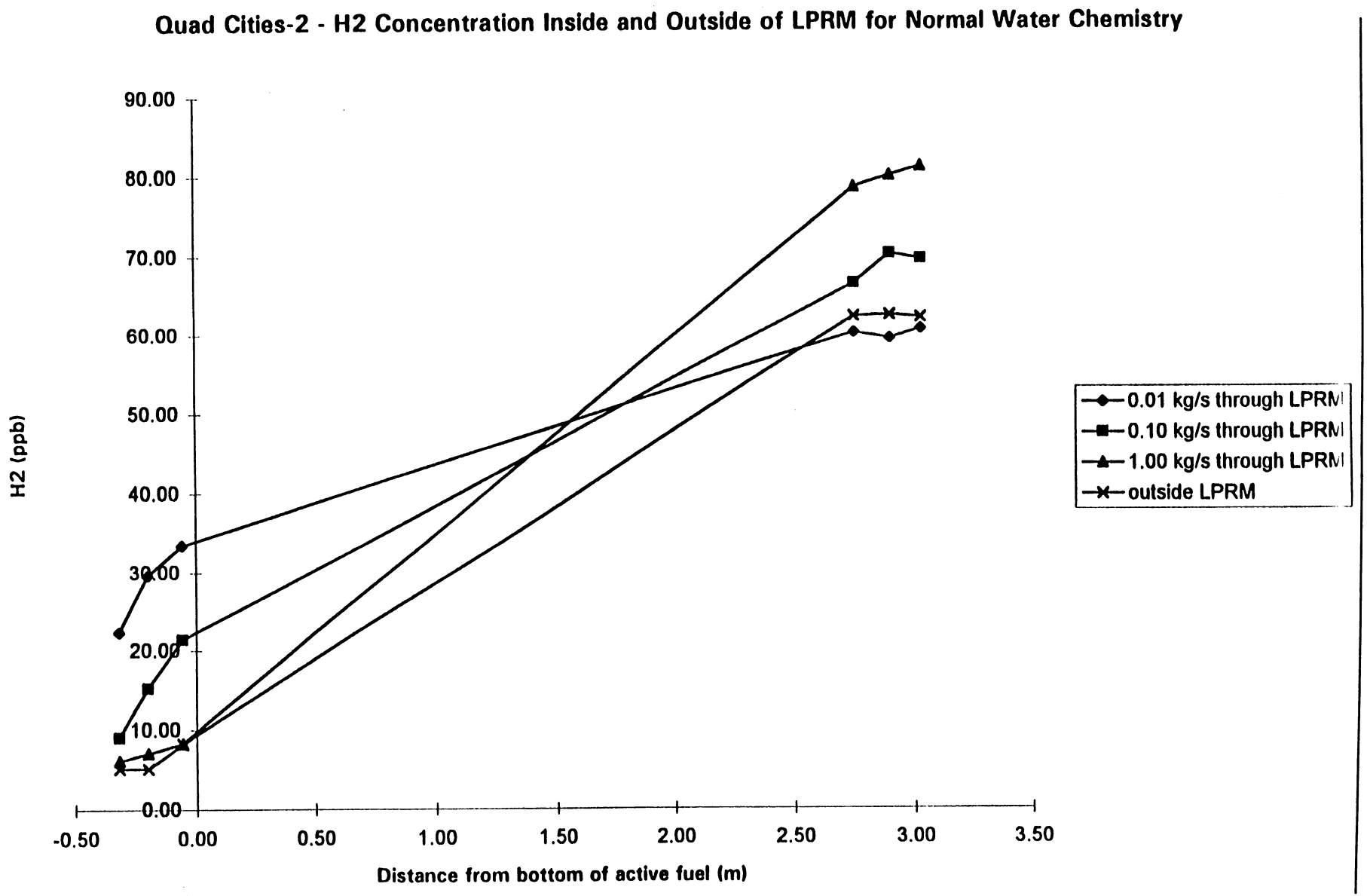

Figure B-25

EPRI Licensed Material

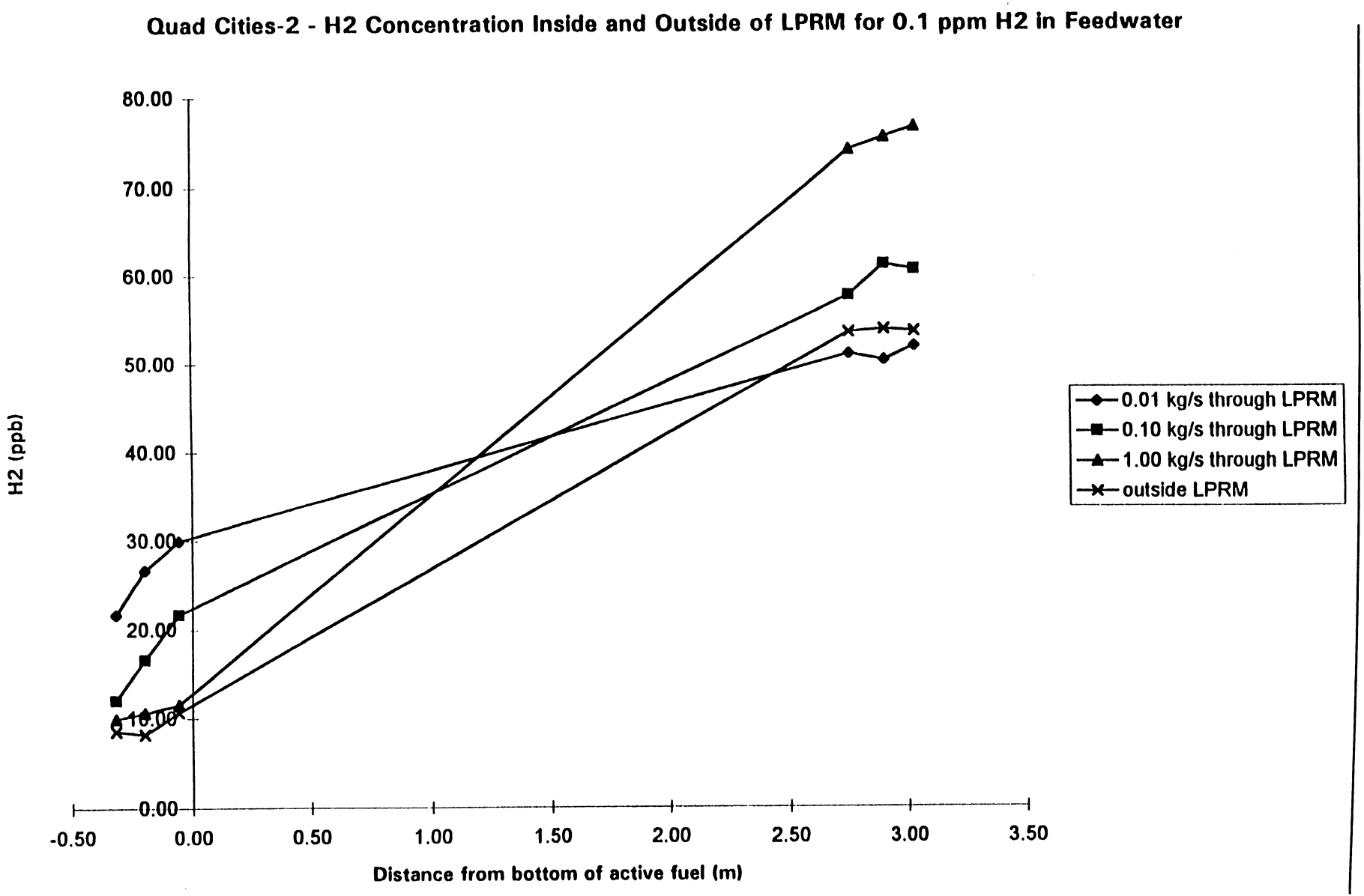

Figure B-26

EPRI Licensed Material

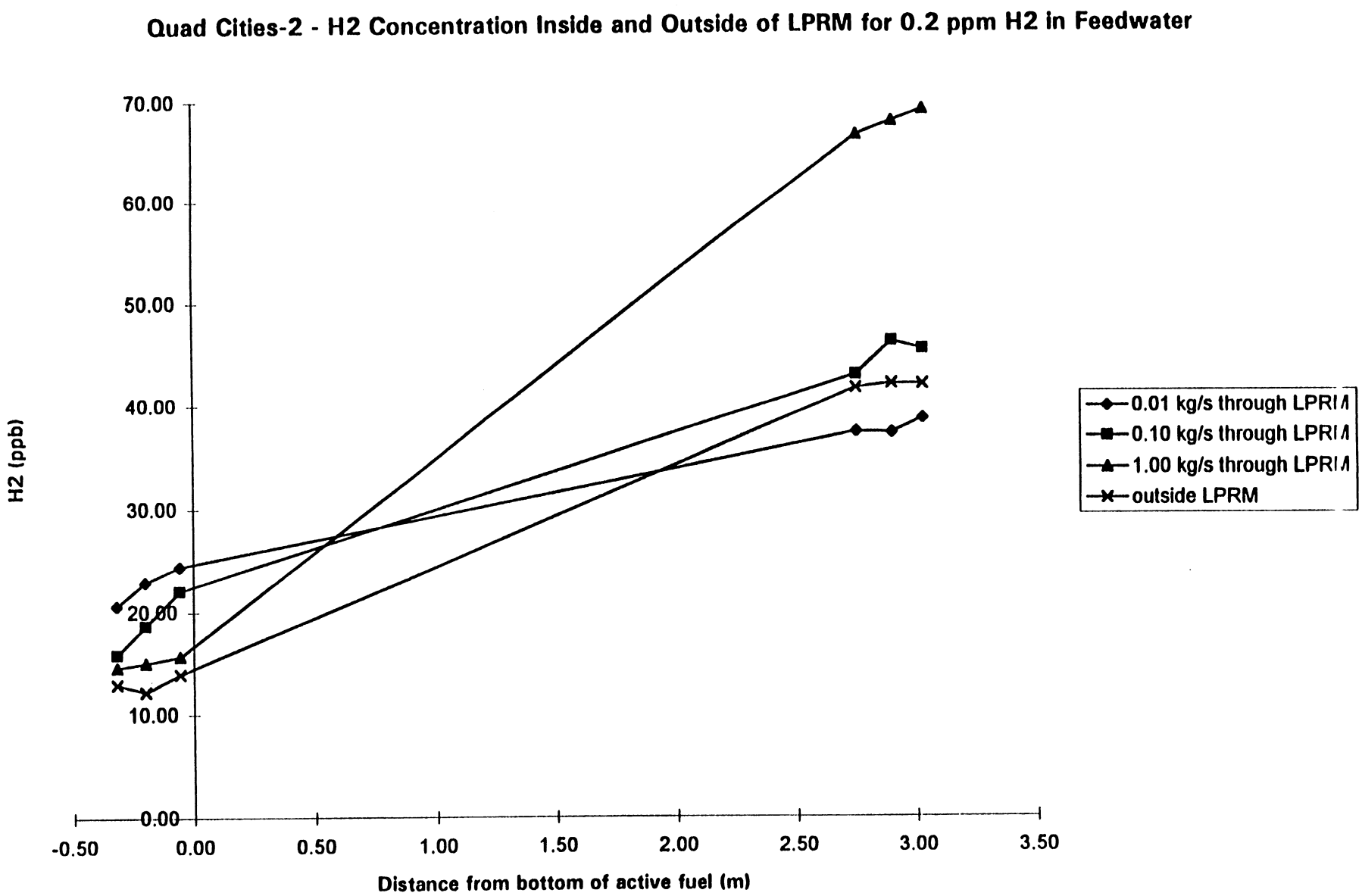

Figure B-27

EPRI Licensed Material

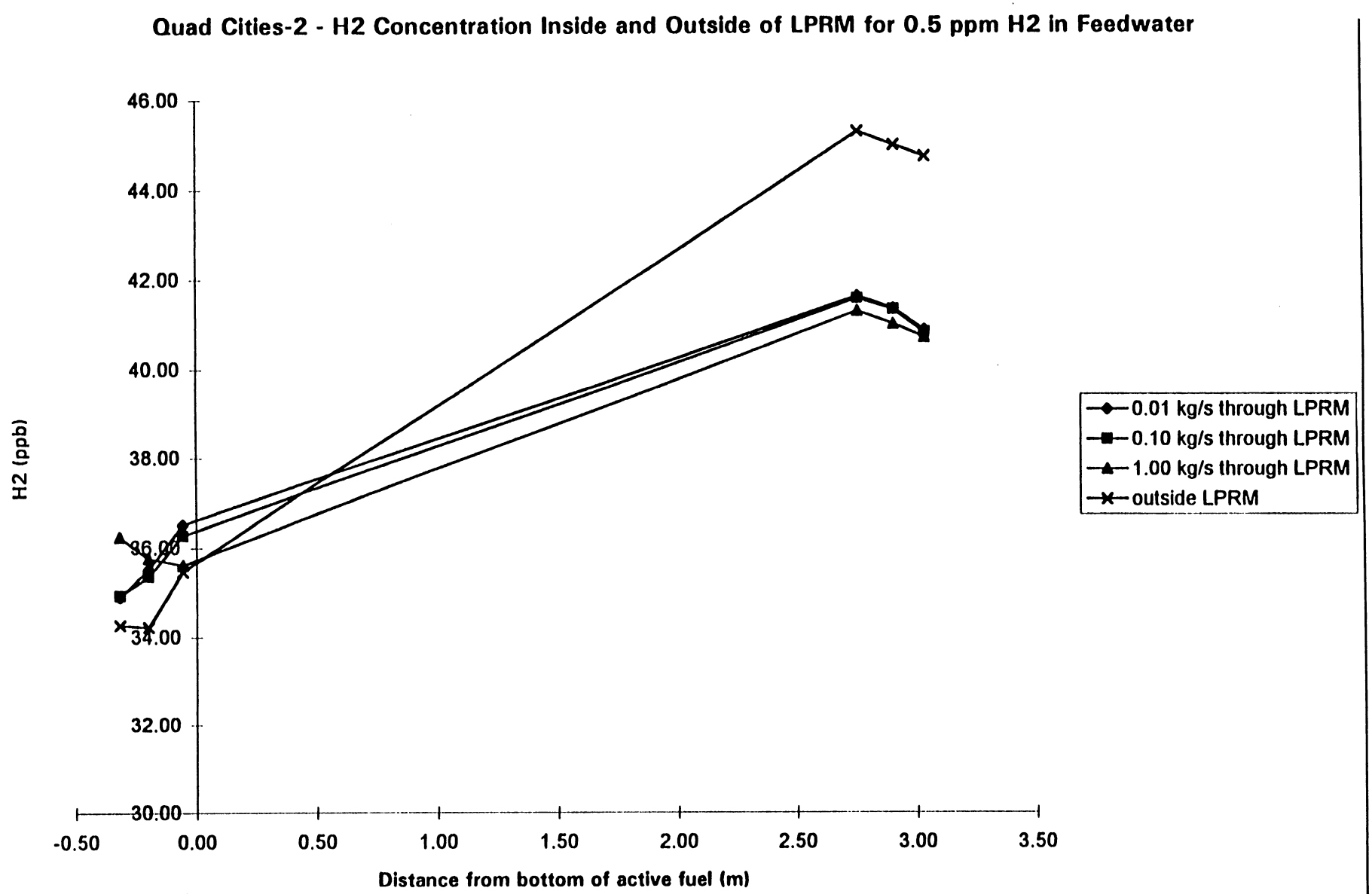

Figure B-28

EPRI Licensed Material

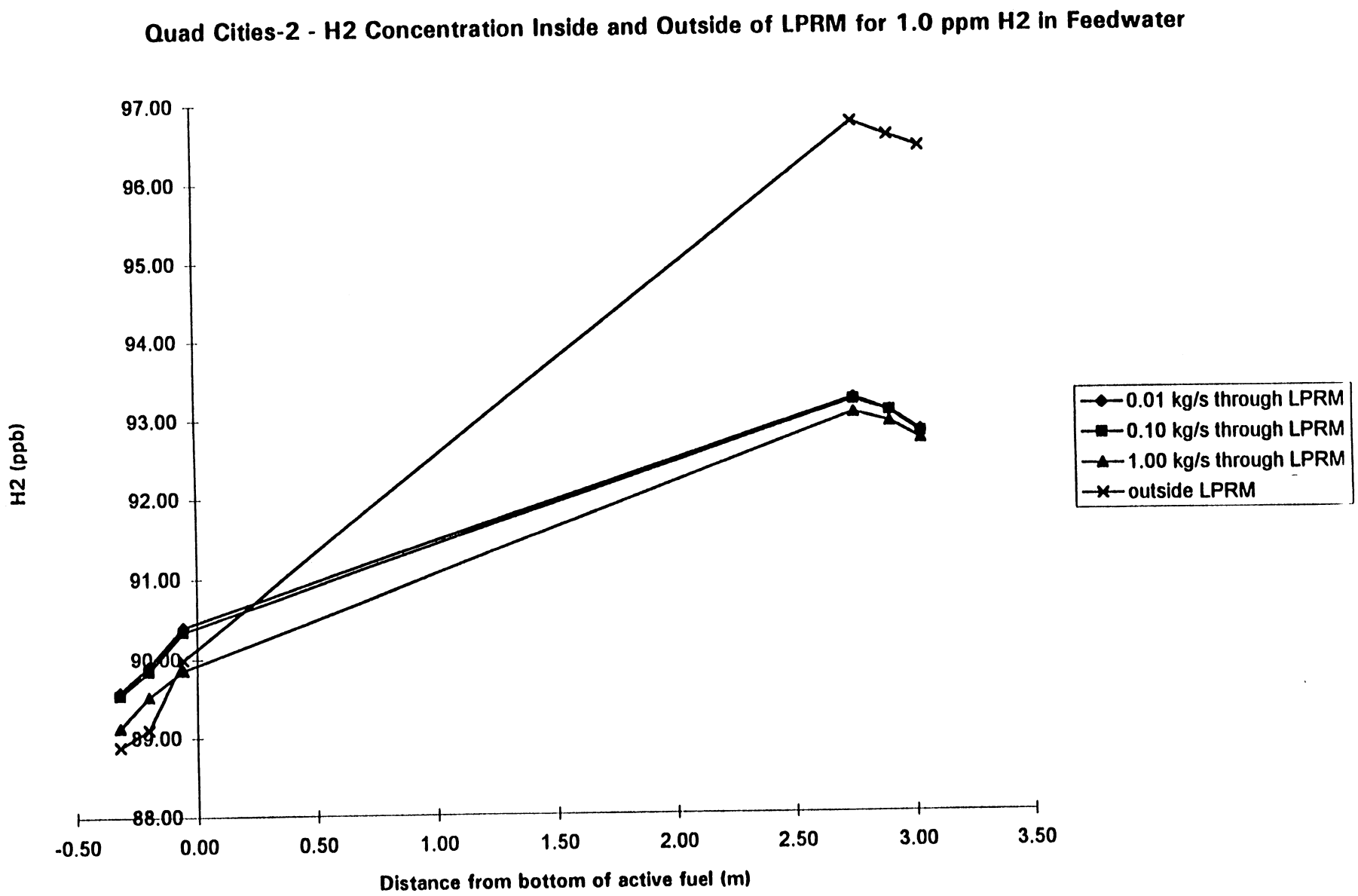

Figure B-29

EPRI Licensed Material

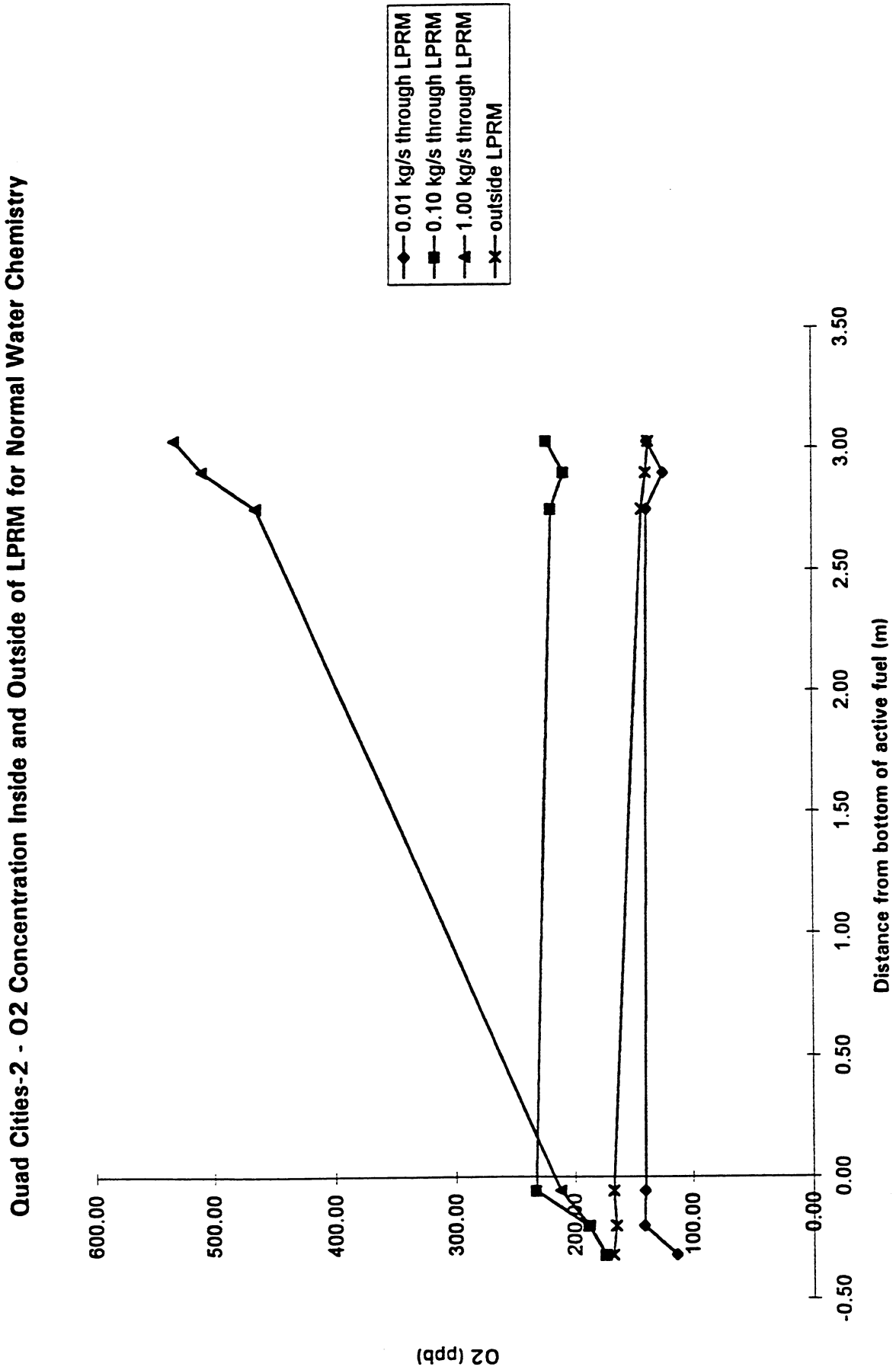
Quad Cities-2 - O2 Concentration Inside and Outside of LPRM for Normal Water Chemistry
0.01 kg/s through LPRM
0.10 kg/s through LPRM
1.00 kg/s through LPRM
outside LPRM
O2 (ppb)
600.00
500.00
400.00
300.00
200.00
100.00
0.00
-0.50
0.00
0.50
1.00
1.50
2.00
2.50
3.00
3.50
Distance from bottom of active fuel (m)

Figure B-30

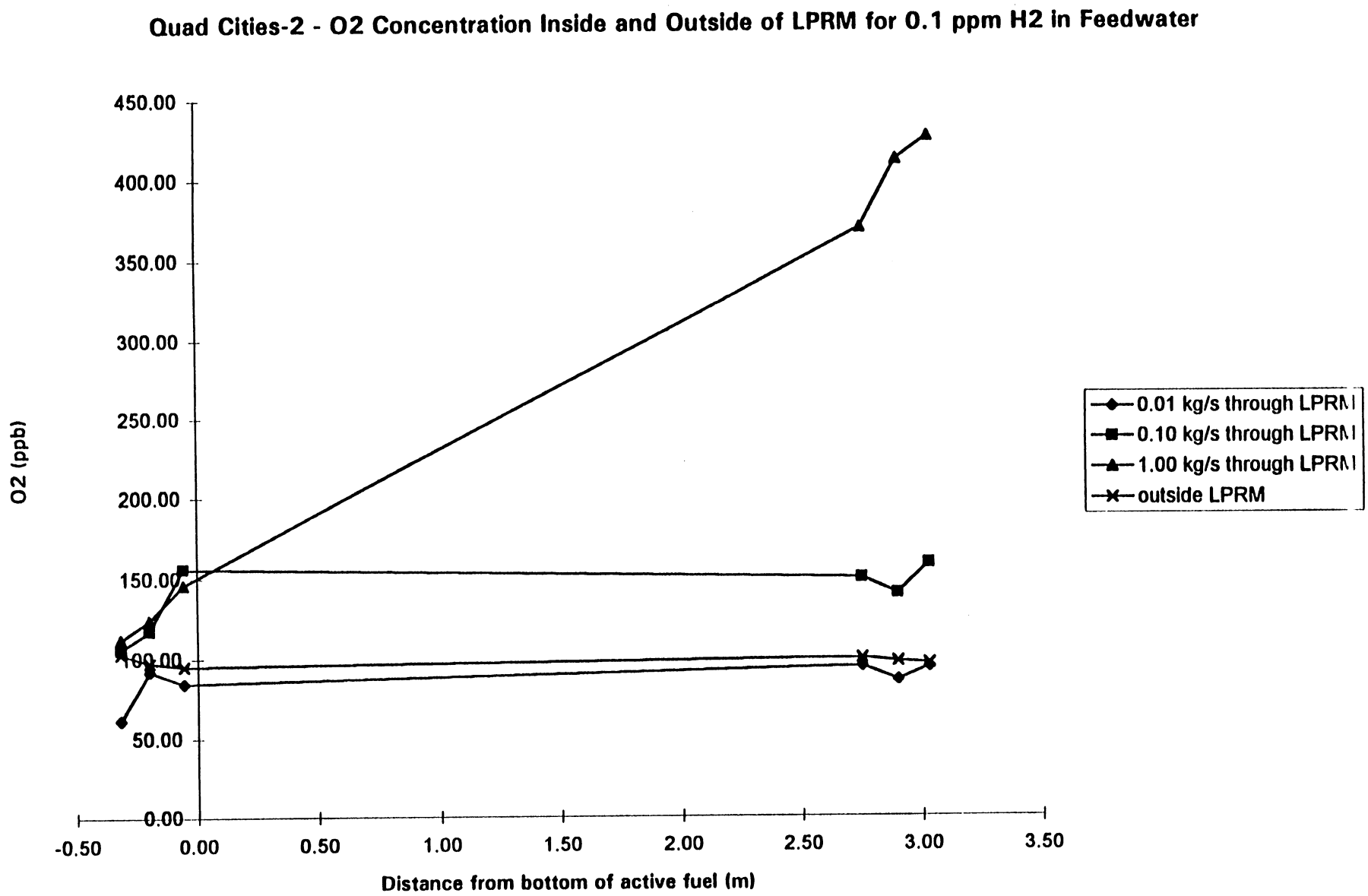

Figure B-31

EPRI Licensed Material

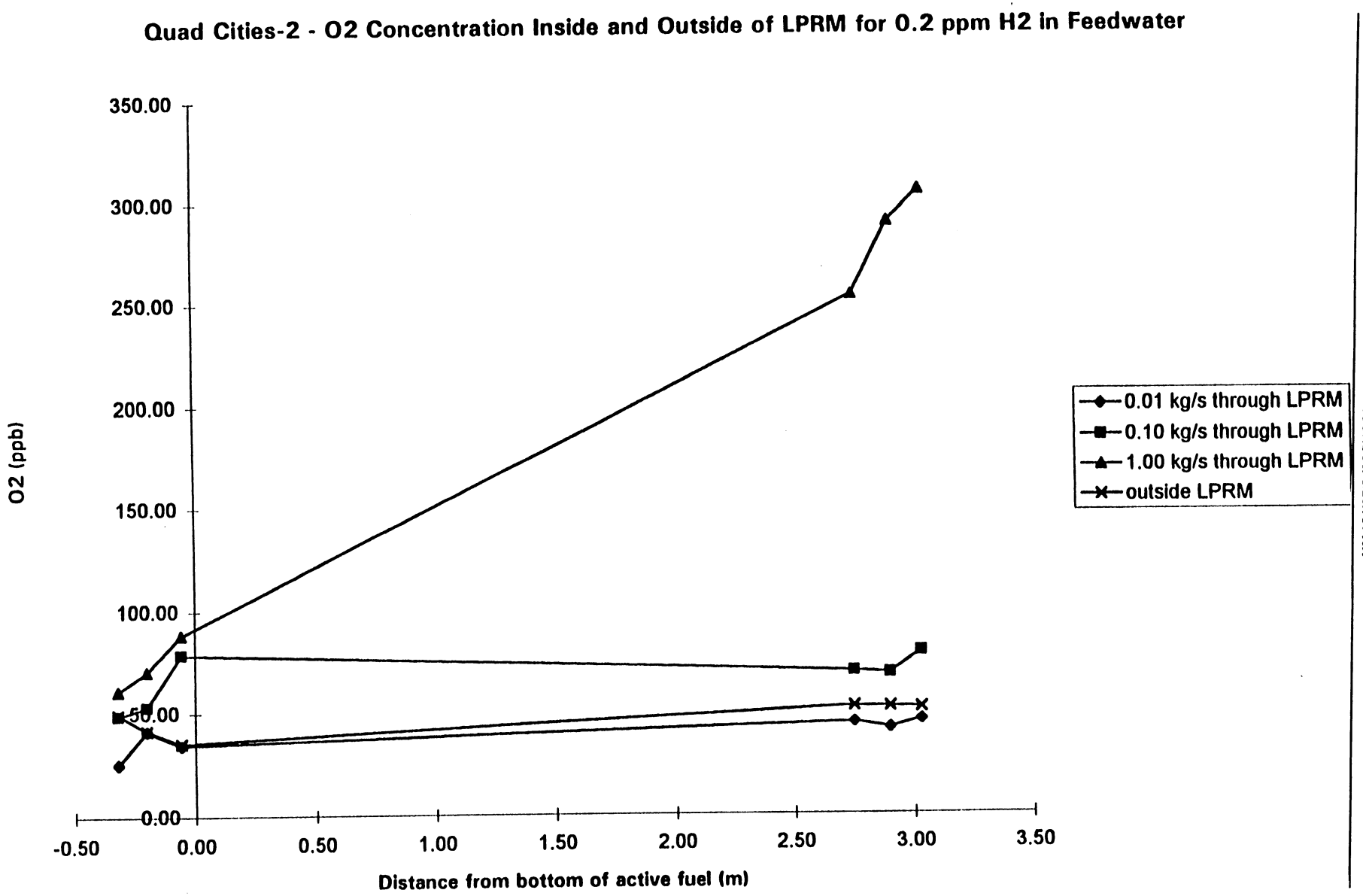

Figure B-32

EPRI Licensed Material

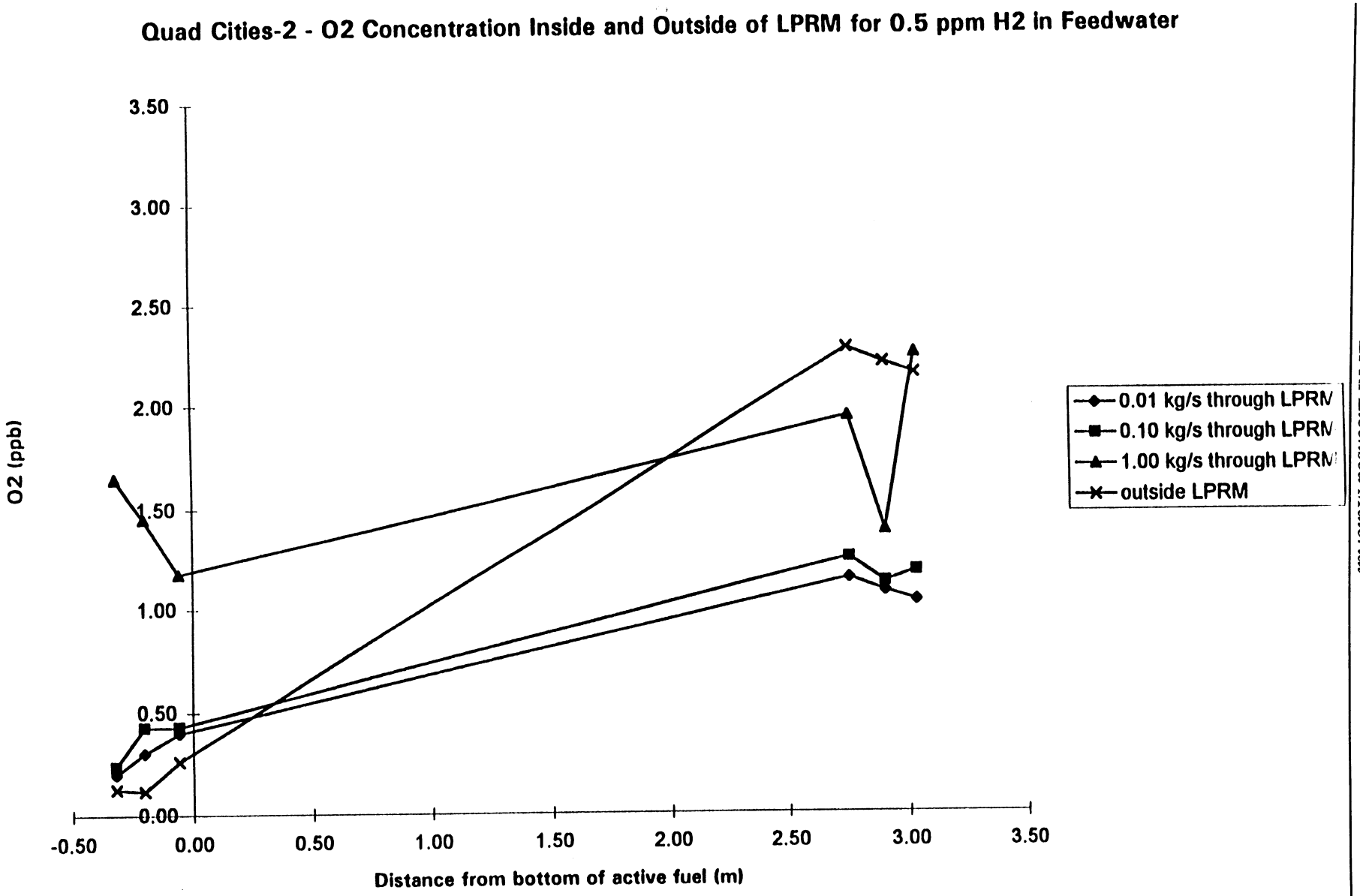

Figure B-33

EPRI Licensed Material

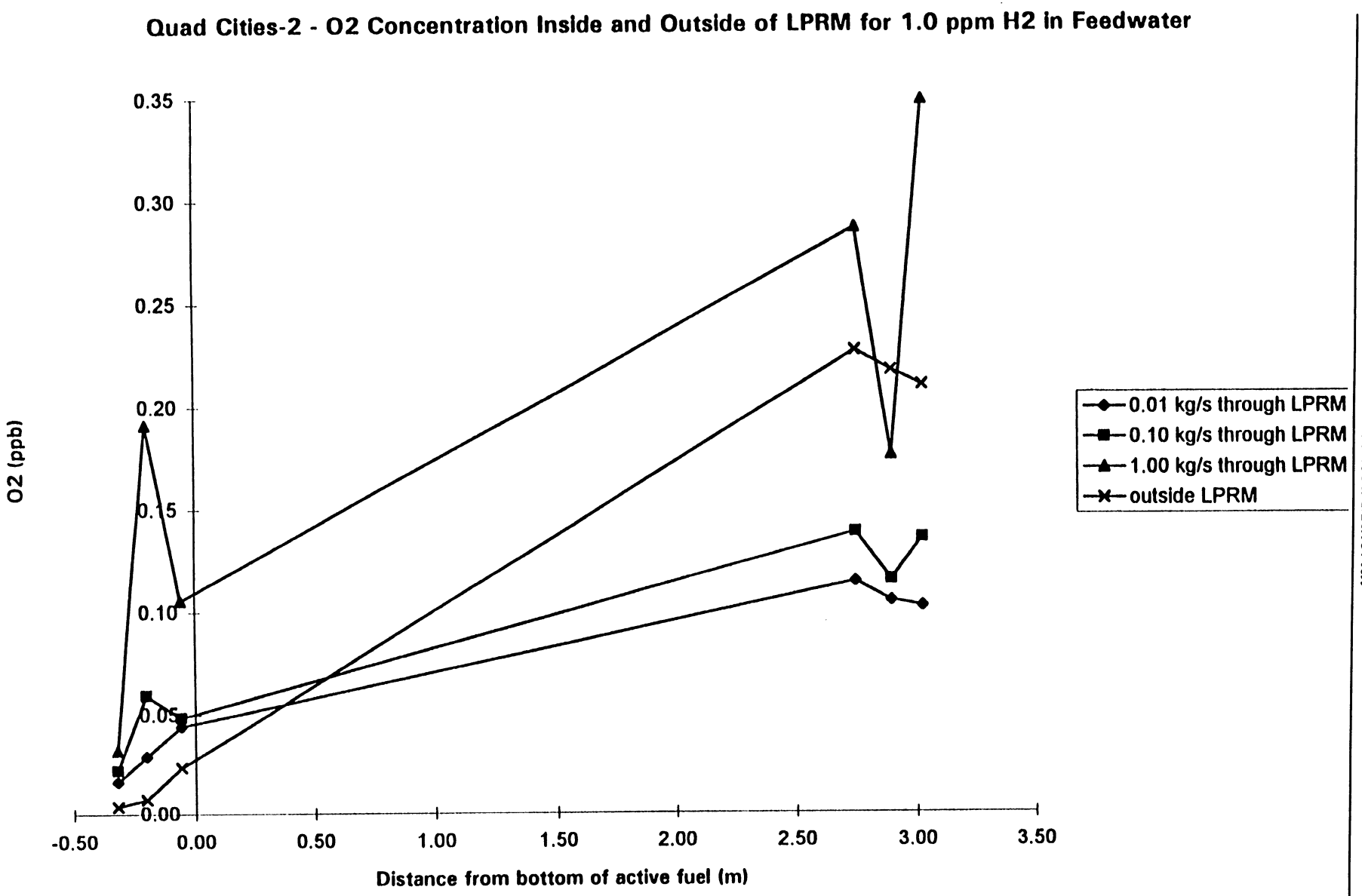

Figure B-34

EPRI Licensed Material

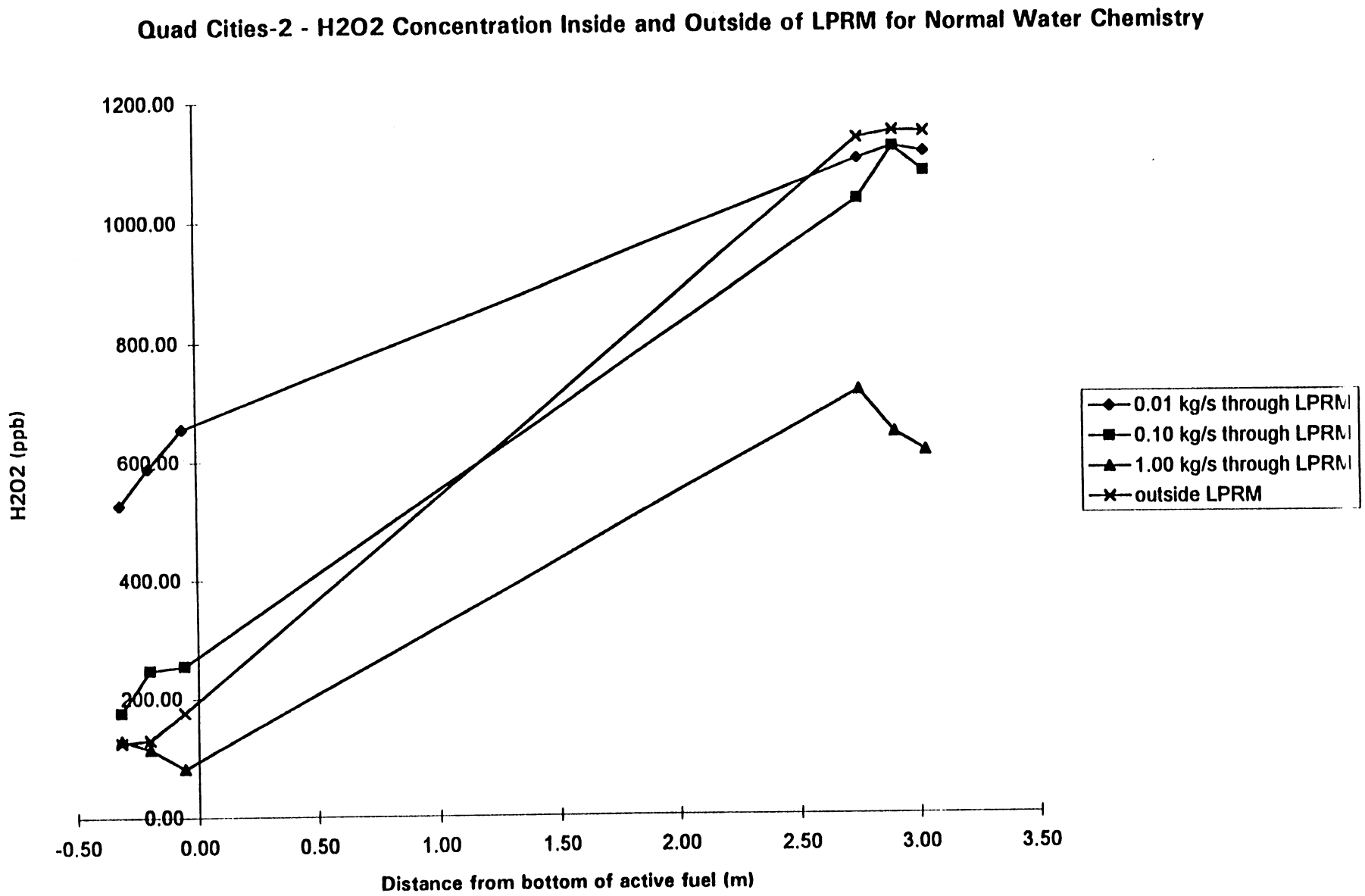

Figure B-35

EPRI Licensed Material

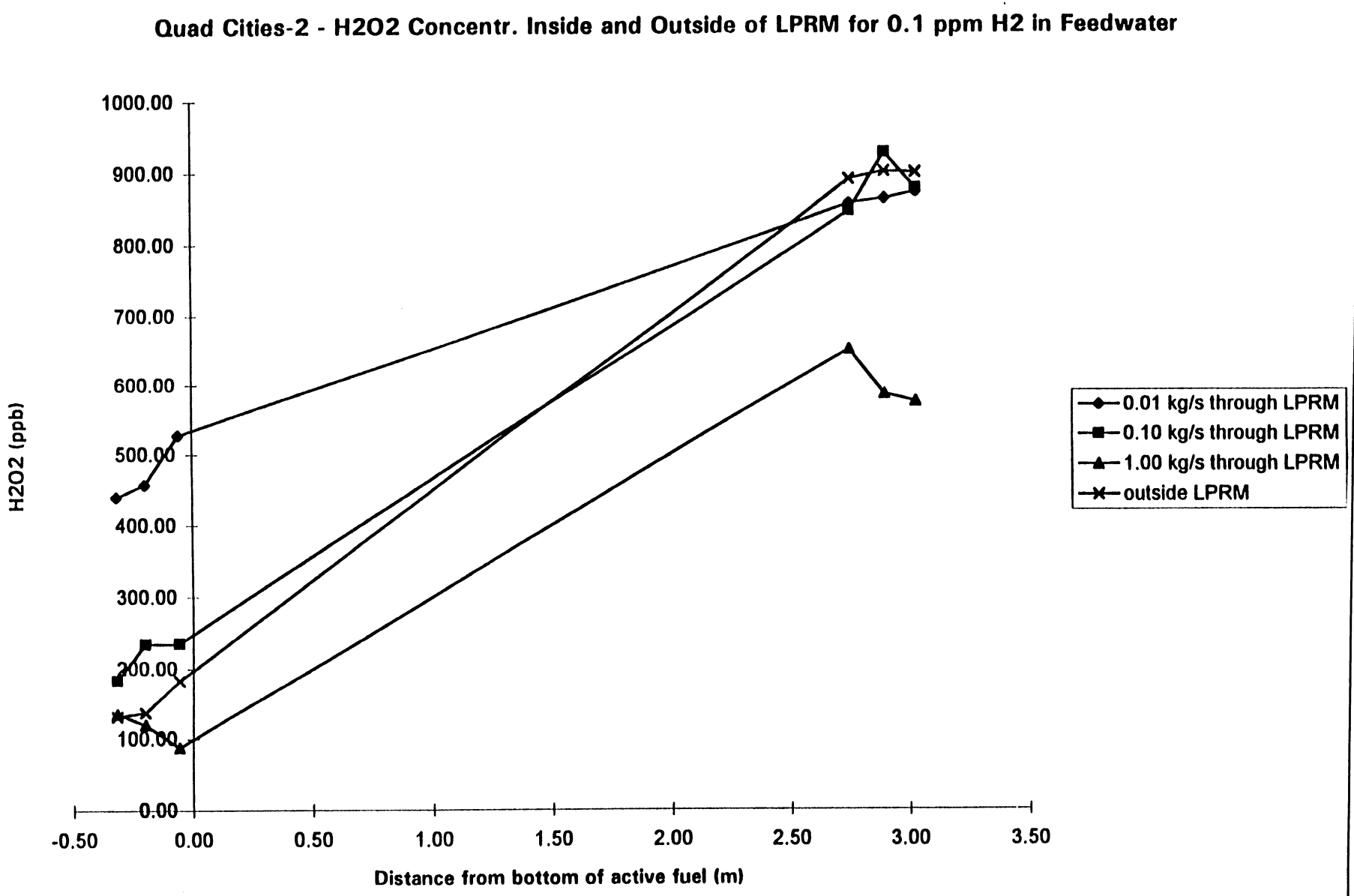

Figure B-36

EPRI Licensed Material

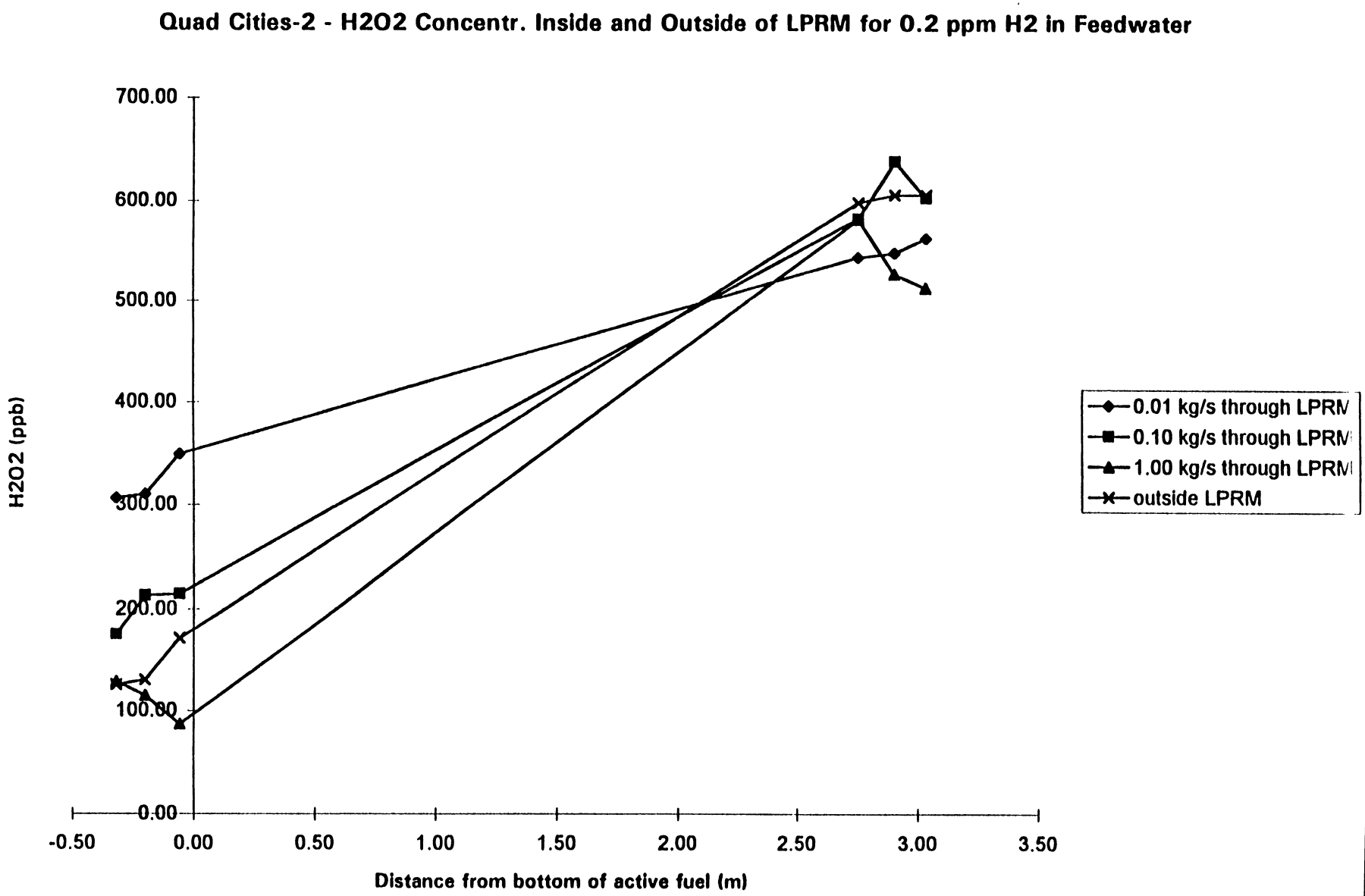

Figure B-37

EPRI Licensed Material

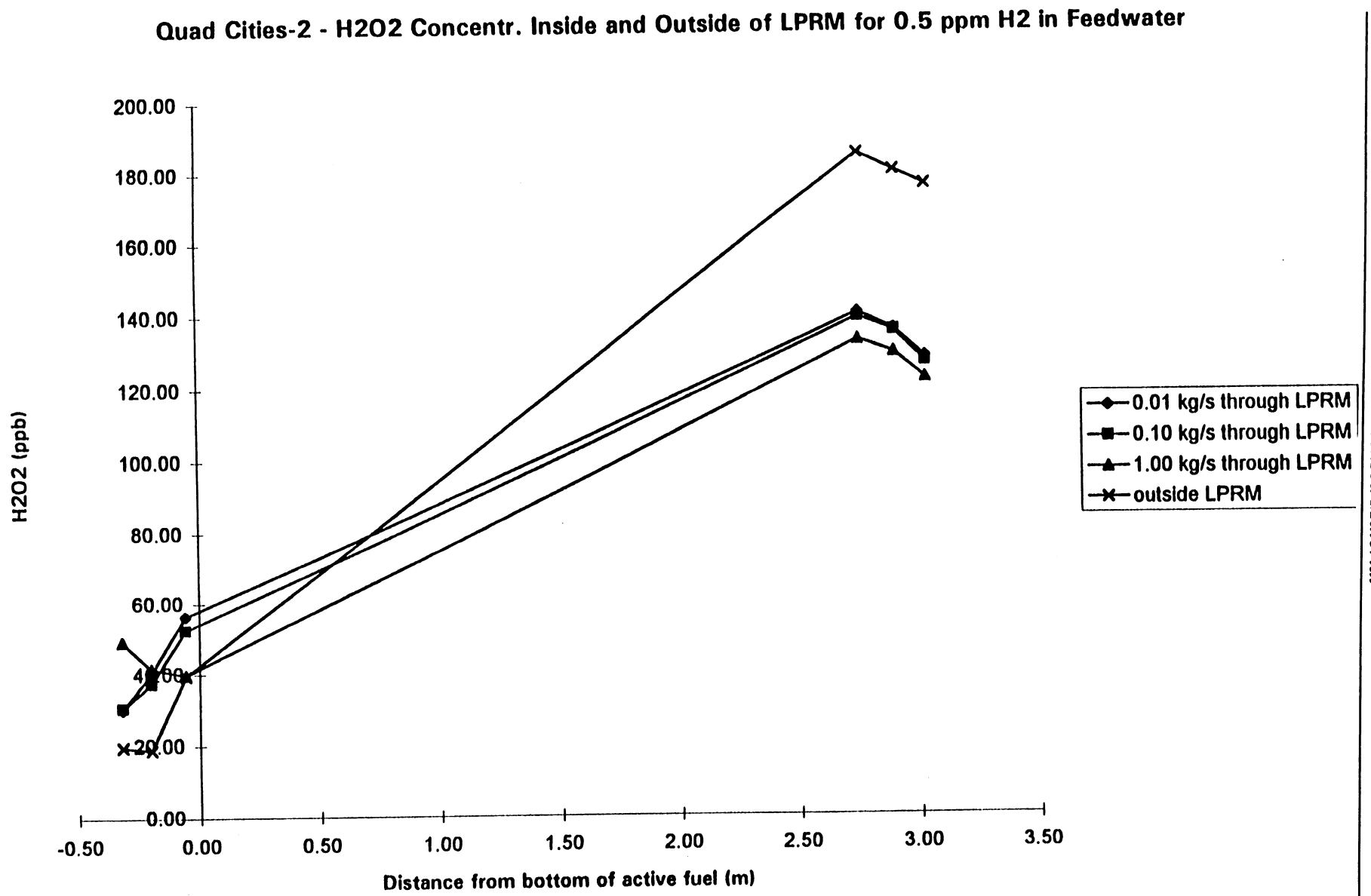

Figure B-38

EPRI Licensed Material

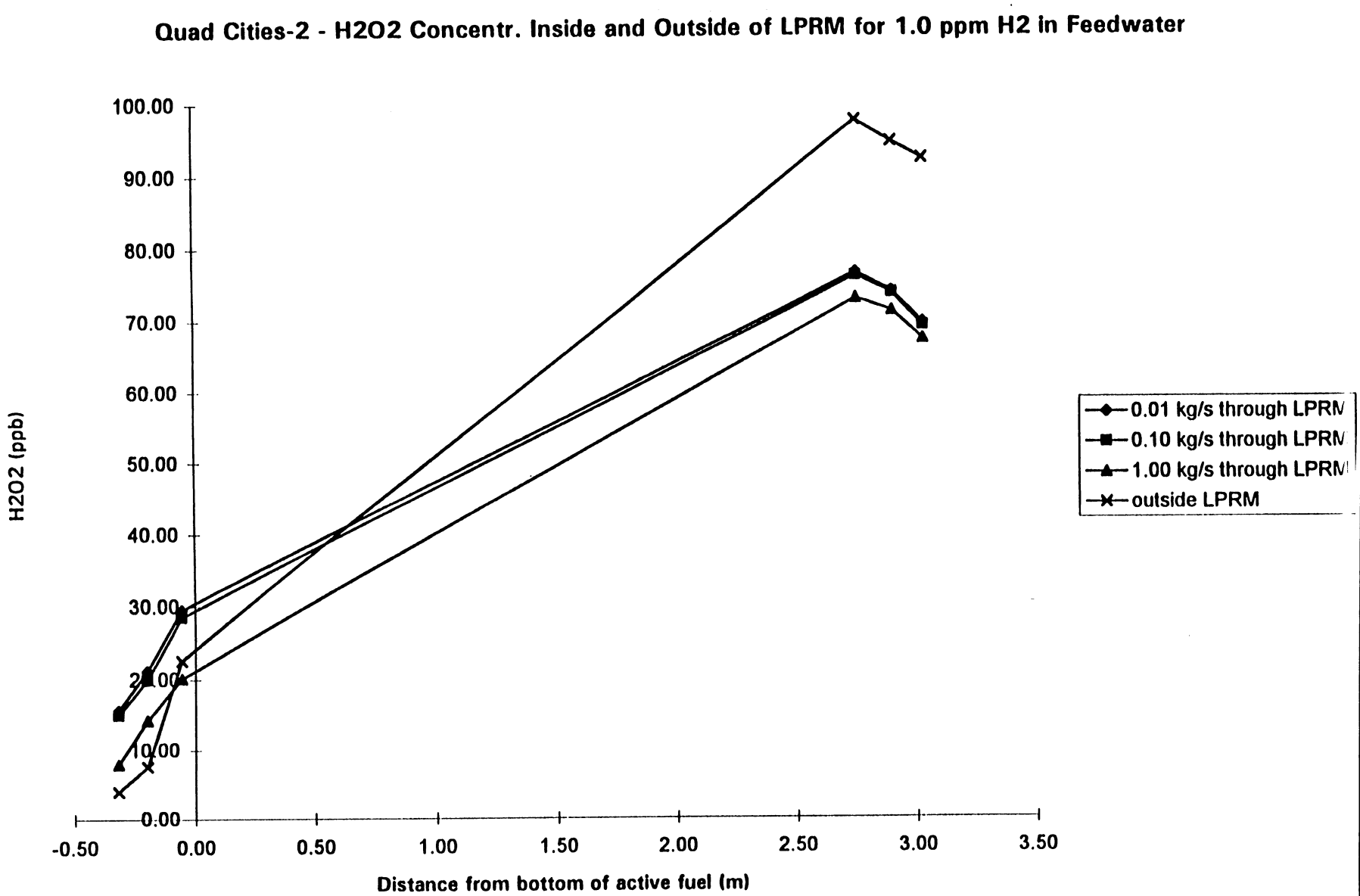

Figure B-39

EPRI Licensed Material

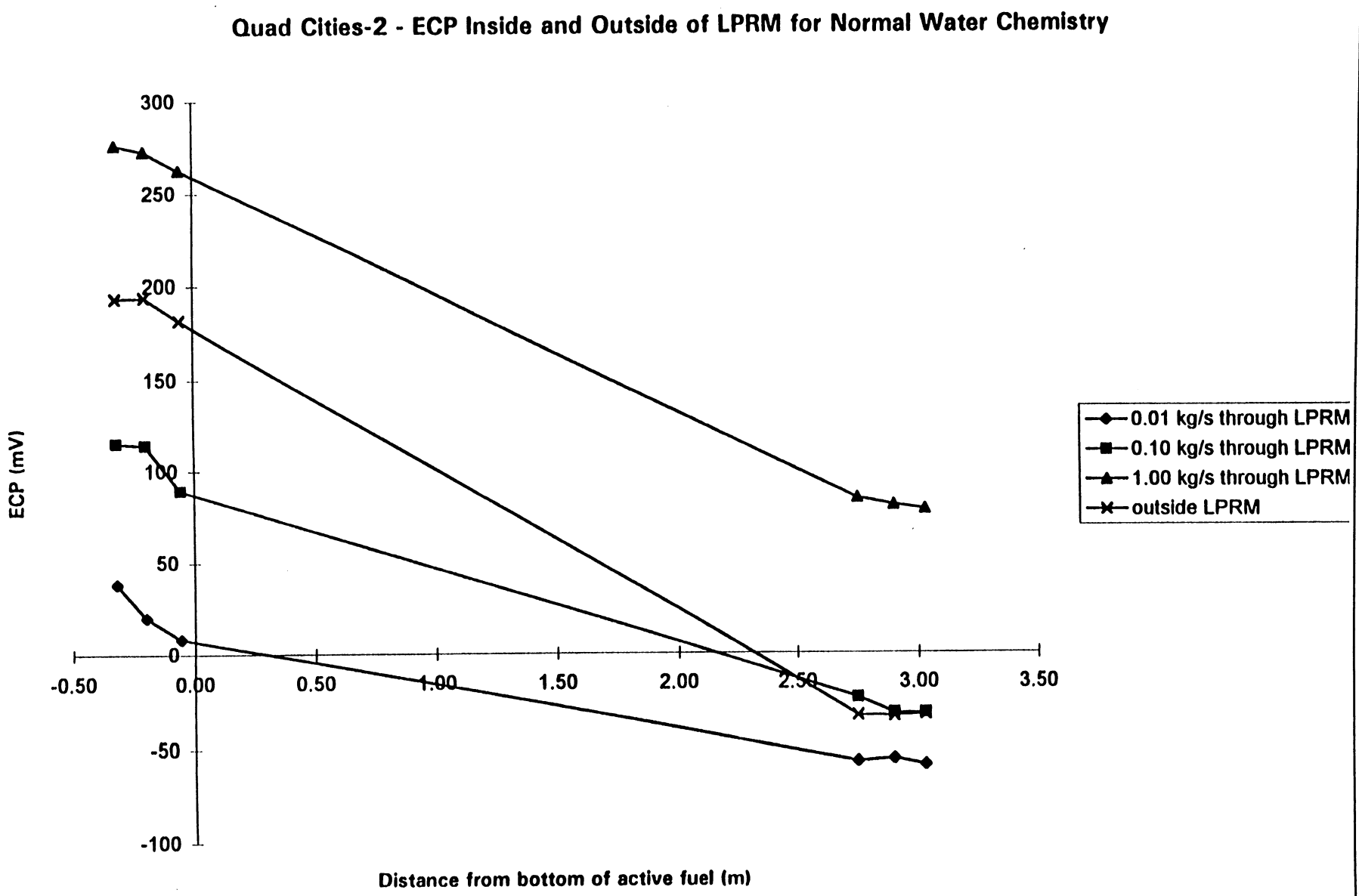

Figure B-40

EPRI Licensed Material

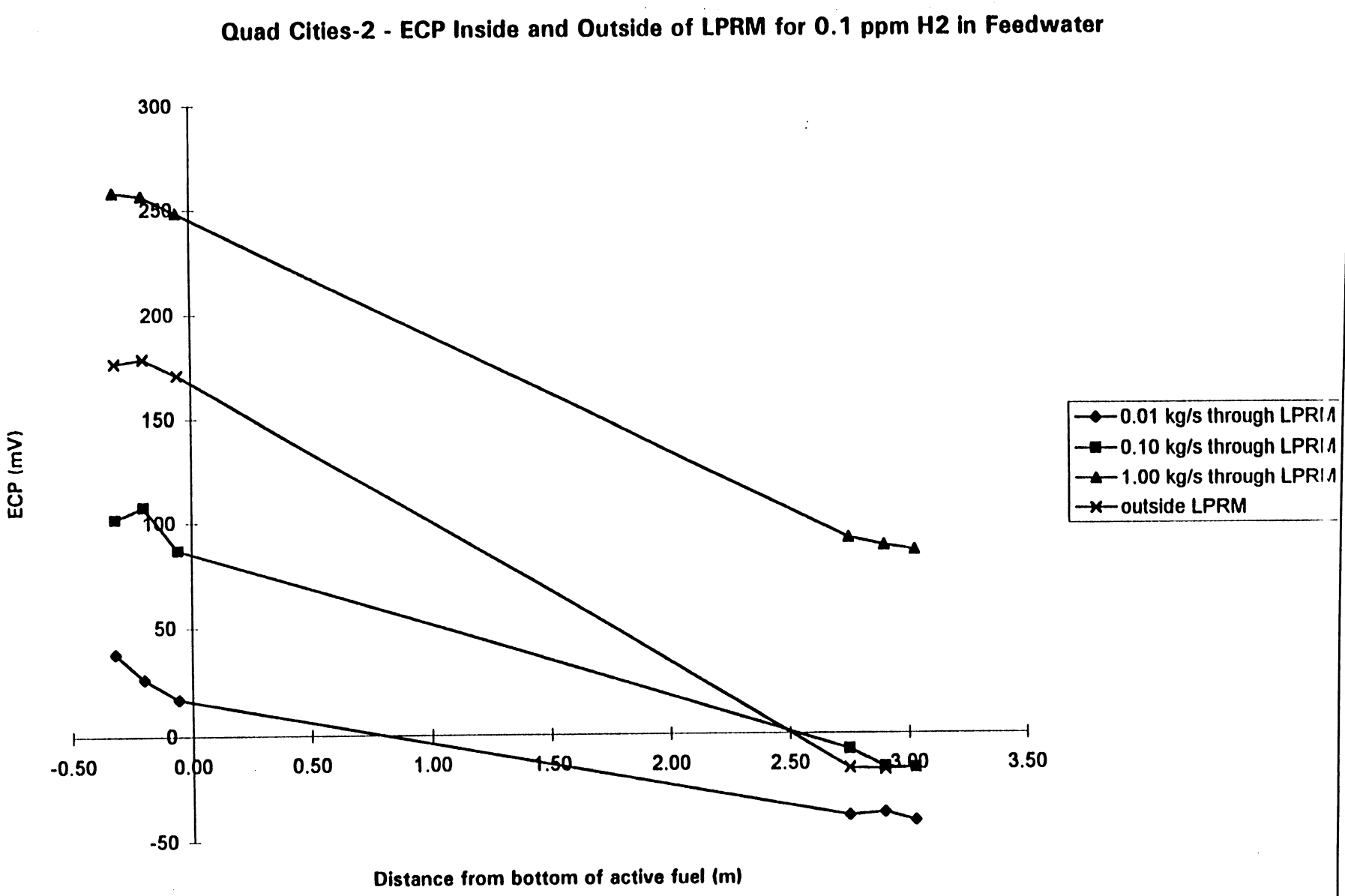

Figure B-41

EPRI Licensed Material

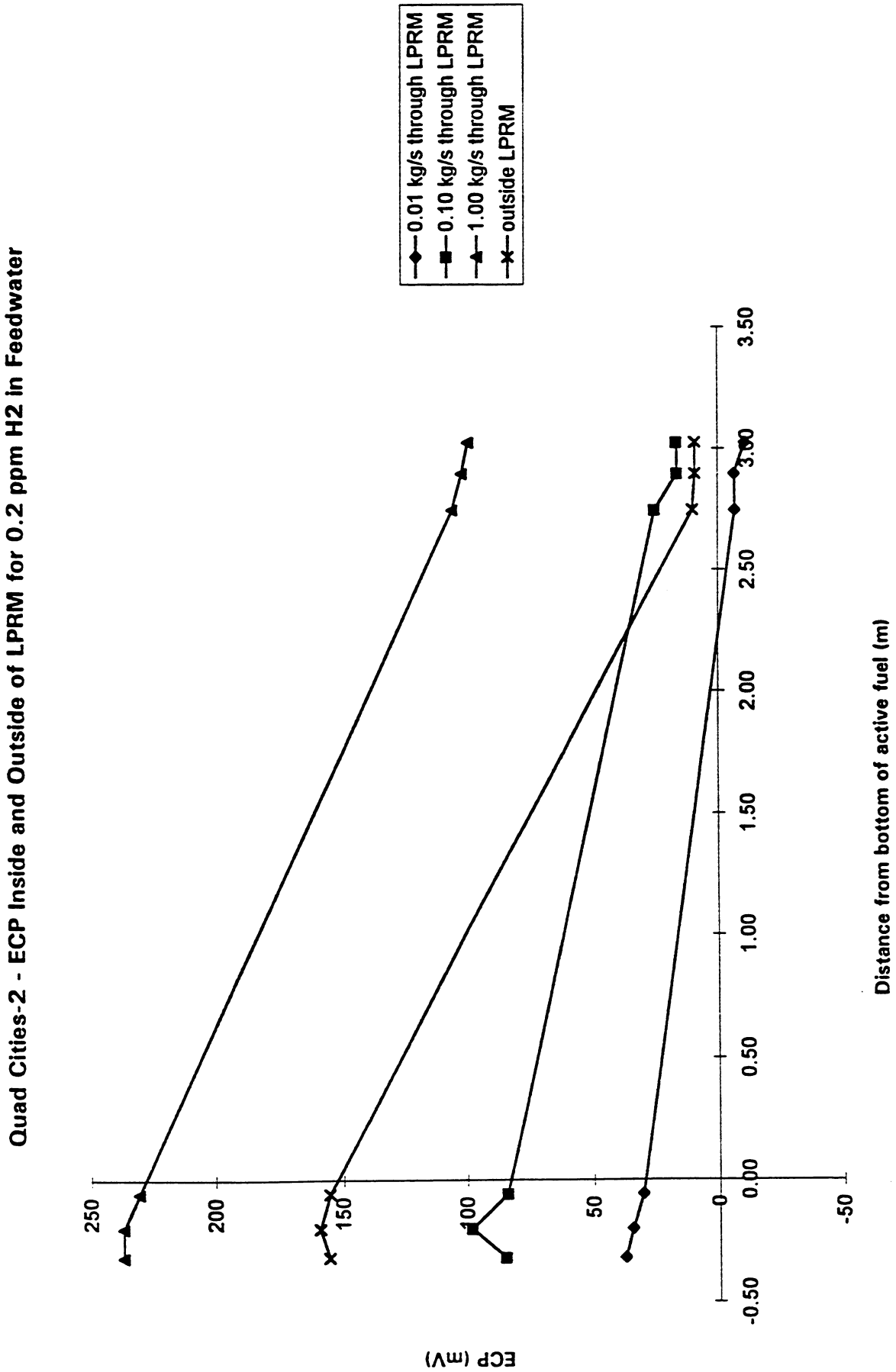
Quad Cities-2 - ECP Inside and Outside of LPRM for 0.2 ppm H2 in Feedwater
0.01 kg/s through LPRM
0.10 kg/s through LPRM
1.00 kg/s through LPRM
outside LPRM
ECP (mV)
250
200
150
100
50
0
-50
-0.50
0.00
0.50
1.00
1.50
2.00
2.50
3.00
3.50
Distance from bottom of active fuel (m)

Figure B-42

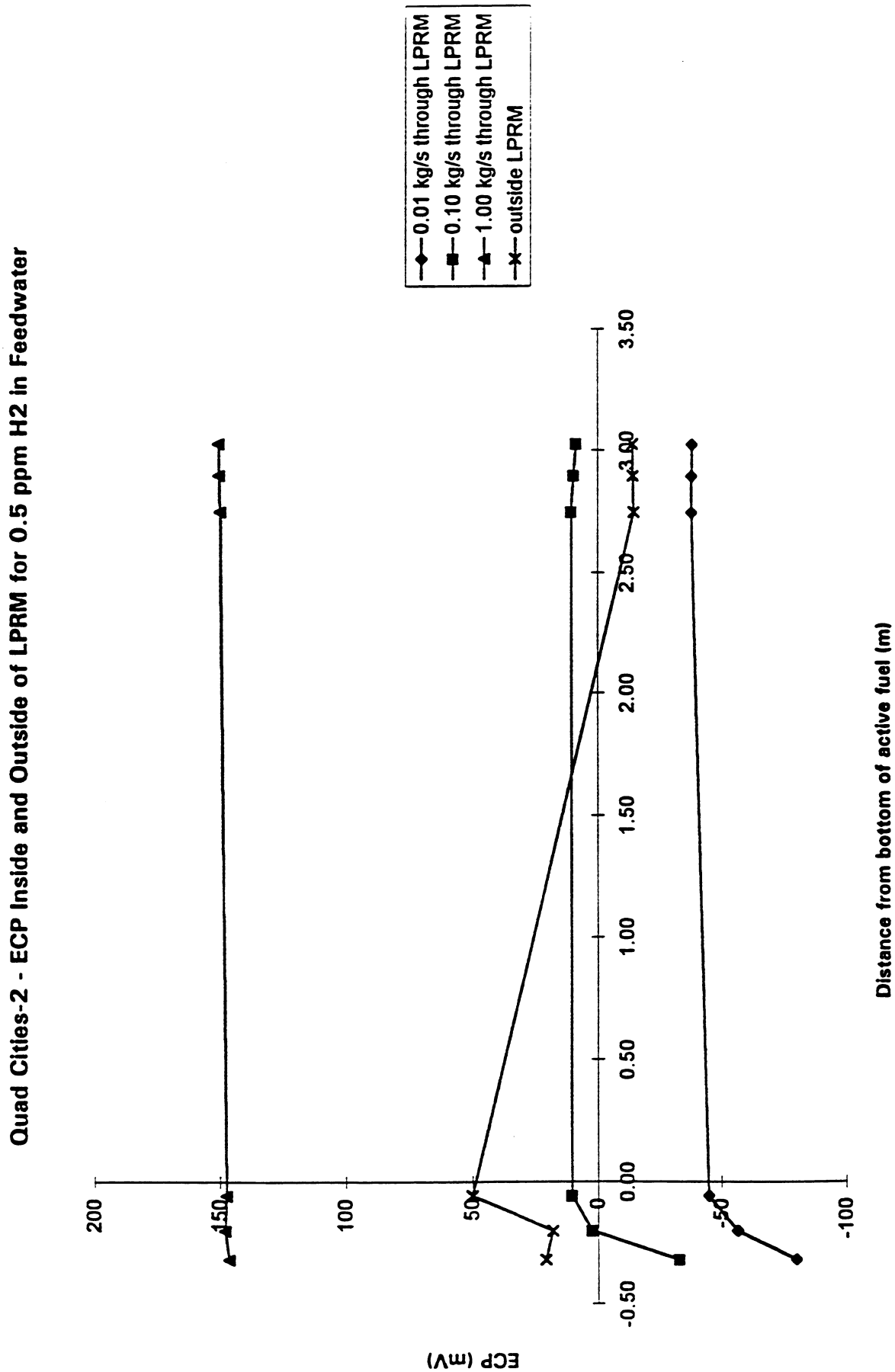
Quad Cities-2 - ECP Inside and Outside of LPRM for 0.5 ppm H2 in Feedwater
0.01 kg/s through LPRM
0.10 kg/s through LPRM
1.00 kg/s through LPRM
outside LPRM
ECP (mV)
200
150
100
50
0
-50
-100
-0.50
0.00
0.50
1.00
1.50
2.00
2.50
3.00
3.50
Distance from bottom of active fuel (m)

Figure B-43

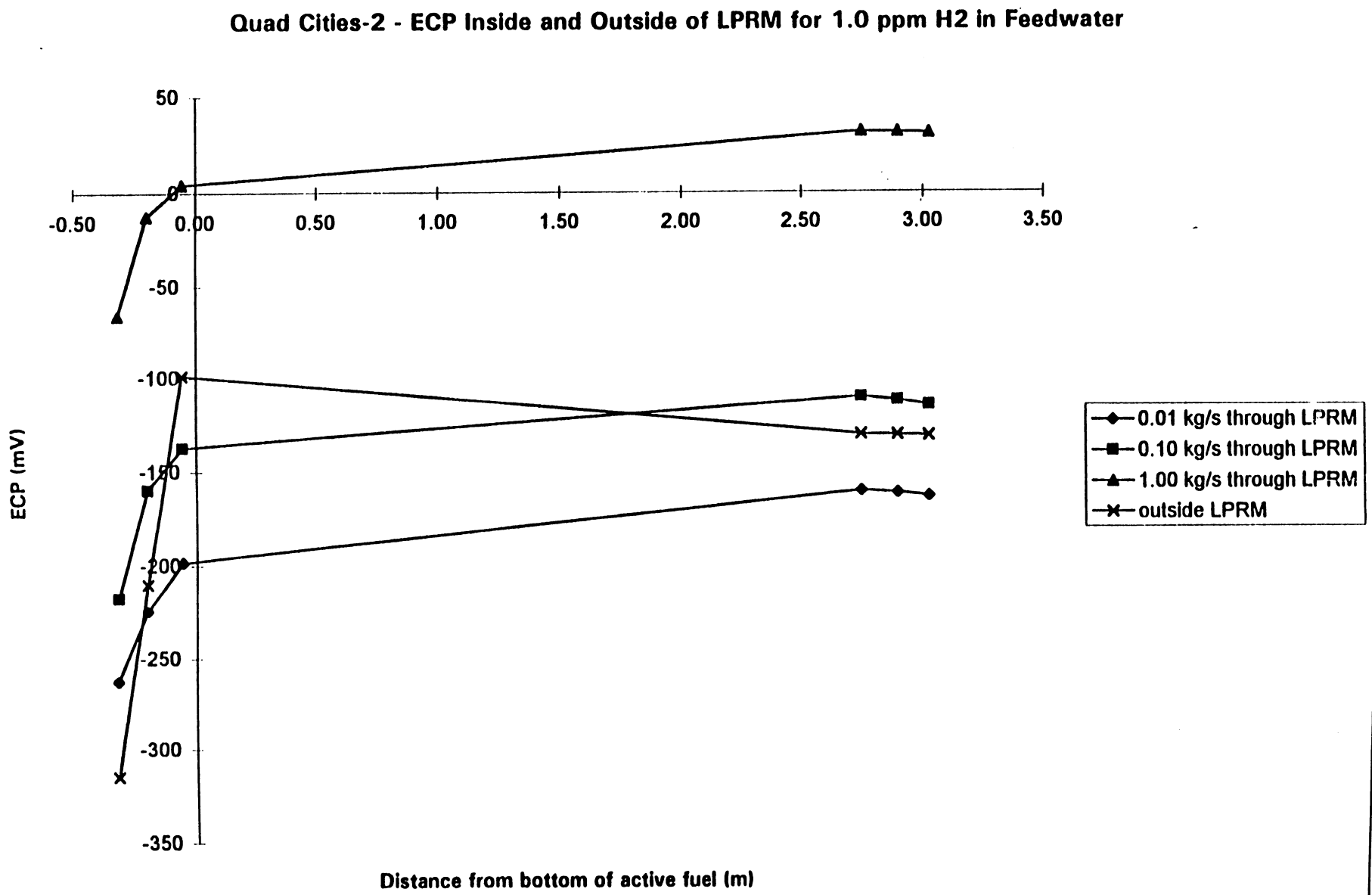

Figure B-44

EPRI Licensed Material

ABOUT BWRVIP

The BWR Vessel and Internals Project (BWRVIP) is an association of utilities owning and operating boiling water reactors. The project is focused exclusively on reactor vessel and vessel internals issues in operating plants. Objectives of the BWRVIP are to lead the BWR industry toward generic resolution of vessel and internals integrity and operability issues; to identify or develop generic, cost-effective strategies from which each operating plant will select the most appropriate alternative; to serve as the focal point for the regulatory interface with the industry on BWR vessel and internals integrity and operability issues; and to share information among members. EPRI manages the technical program on behalf of the utility members of the BWRVIP.

ABOUT EPRI

The mission of the Electric Power Research Institute is to discover, develop, and deliver high value technological advances through networking and partnership with the electricity industry.

Funded through annual membership dues from some 700 member utilities, EPRI's work covers a wide range of technologies related to the generation, delivery, and use of electricity, with special attention paid to cost-effectiveness and environmental concerns.

At EPRI's headquarters in Palo Alto, California, more than 350 scientists and engineers manage some 1600 ongoing projects throughout the world. Benefits accrue in the form of products, services, and information for direct application by the electric utility industry and its customers.

EPRI—*Leadership in Electrification through Global Collaboration*

Printed on recycled paper (50% recycled fiber, including 10% postconsumer waste) in the United States of America.